Advances in Experimental Medicine and Biology 1249

Heung Jae Chun
Rui L. Reis
Antonella Motta
Gilson Khang *Editors*

Bioinspired Biomaterials

Advances in Tissue Engineering and Regenerative Medicine

Springer

Advances in Experimental Medicine and Biology

Volume 1249

Advances in Experimental Medicine and Biology provides a platform for scientific contributions in the main disciplines of the biomedicine and the life sciences. This series publishes thematic volumes on contemporary research in the areas of microbiology, immunology, neurosciences, biochemistry, biomedical engineering, genetics, physiology, and cancer research. Covering emerging topics and techniques in basic and clinical science, it brings together clinicians and researchers from various fields.

Advances in Experimental Medicine and Biology has been publishing exceptional works in the field for over 40 years, and is indexed in SCOPUS, Medline (PubMed), Journal Citation Reports/Science Edition, Science Citation Index Expanded (SciSearch, Web of Science), EMBASE, BIOSIS, Reaxys, EMBiology, the Chemical Abstracts Service (CAS), and Pathway Studio.

2018 Impact Factor: 2.126.

More information about this series at http://www.springer.com/series/5584

Heung Jae Chun
Rui L. Reis • Antonella Motta
Gilson Khang
Editors

Bioinspired Biomaterials

Advances in Tissue Engineering and Regenerative Medicine

Springer

Editors
Heung Jae Chun
Institute of Cell & Tissue Engineering
and College of Medicine
Catholic University of Korea
Seoul, South Korea

Antonella Motta
Department of Industrial Engineering
and BIOtech Research Center
University of Trento
Trento, Italy

Rui L. Reis
3B's Research Group, I3Bs – Research
Institute on Biomaterials, Biodegradables
and Biomimetics, Headquarters of the
European Institute of Excellence on Tissue
Engineering and Regenerative Medicine
University of Minho
Guimarães, Portugal

Gilson Khang
Department of BIN Convergence
Technology, Department of Polymer
Nano Science & Technology and
Polymer BIN Research Center
Jeonbuk National University
Jeonju, South Korea

ISSN 0065-2598 ISSN 2214-8019 (electronic)
Advances in Experimental Medicine and Biology
ISBN 978-981-15-3257-3 ISBN 978-981-15-3258-0 (eBook)
https://doi.org/10.1007/978-981-15-3258-0

This Springer imprint is published by the registered company Springer Nature Singapore Pte Ltd.
The registered company address is: 152 Beach Road, #21-01/04 Gateway East, Singapore 189721, Singapore

Preface

Tissue engineering and regenerative medicine is one of the most active and updating fields with many emerging innovative products, novel techniques, and clinical trials for addressing huge requirements of our society. These advancements make use of bioinspired materials for their application in bone tissue engineering, load-bearing implants, biocompatible tissue engineering materials, 3D printed hydrogels, scaffolds, and stem cell delivery. We are very pleased to launch our next edition of the textbook in two volumes, with the first volume *Bioinspired Biomaterials: Advances in Tissue Engineering and Regenerative Medicine*. We have attempted to maintain the highest standard of excellence, truthfulness, and pedagogy developed by the publishers that address wide audience (including countless students of biological science, medicine, veterinary, dentistry, materials science, engineering, and physics worldwide; bachelor, master, and PhD students; researchers; and company professionals) who intend to update and invent new biomaterials for the tissue engineering and regenerative medicine applications. At the same time, we are very focused on the evolving need of the students and researchers in updating their career in the developing field of bioinspired materials. This book is a continuation of my previously published book *Novel Biomaterials for Regenerative Medicine* and comprehensive reviews on *Cutting-Edge Enabling Technology for Regenerative Medicine*.

The contents of this book are divided into 4 parts with 14 chapters addressing the recent findings and reports being investigated by a prominent researcher in this field from different parts of the world. **The first part of this book consists of three chapters discussing the novel bioinspired biomaterials for regenerative medicine**. Chapters 1, 2, and 3 are focused on the biomaterial natural sources and their application in the field of bone/cartilage tissue engineering and regenerative medicine. **The second part consists of three chapters discussing the bioinspired 3D bioprinting hydrogel for regenerative medicine**. Chapters 4 and 5 deal with the application of 3D bioprinting for the digital light processing and tissue models using bioinks, and Chap. 6 explains the application of visible light curable hydrogels for tissue engineering and drug delivery applications. **The third part consists of three chapters discussing the regulation of stem cell fate by bioinspired biomaterials**. Chapter 7 gives an overview of the scaffolds for cartilage regeneration: to use or not to use? Chap. 8 focuses on the application of inorganic nanomaterials in tissue engineering. Chapter 9 reviews the directional cell migration guide for improved tissue regeneration. **The fourth part consists of five chapters discussing the cutting-edge enabling technology for regenerative medicine**. Chapter 10

reviews the application of extracellular vesicles in drug delivery and regenerative medicine. Chapter 11 discusses the application of tissue engineering and regenerative medicine in maternal-fetal medicine. Chapter 12 gives an overview of fundamentals and current strategies for peripheral nerve repair and regeneration. Finally, Chaps. 13 and 14 discuss brain tumor therapy using protein-based drug delivery and human hair in regenerative medicine.

Acknowledgment We would like to thank the International Research and Development Program (NRF –2017K1A3A7A03089427) that served as sponsor and inspiration for this book. We offer a special thanks to those who enthusiastically invested time, experience, and energy in submitting their impressive research results, being the backbone of this work, and also to the reviewers for their valuable suggestions in maintaining the quality of the book chapters. Finally, we appreciate the efforts of Ms. Emmy Lee, assistant from *Springer Nature*, who publishes Advances in Experimental Medicine and Biology (AEMB), in the timely publication of this book. We would also like to appreciate and thank Mr. Wonchan Lee, Ms. Jeong Eun Song, and Mr. Muthukumar Thangavelu from Gilson's Lab for e-mailing all authors, editing, formatting, pressing, and follow-ups in all technical aspects in publishing this book.

Special Dedication to Professor Claudio Migliaresi in Honor of His Retirement

This book is in honor of the retirement of Professor Claudio Migliaresi, University of Trento, Italy, for his extraordinary career and his great contribution in the development of new strategies and materials in the biomedical field, thanks to his advanced vision, challenging attitude, and curiosity. He is also one of the founders of the Department of Materials Engineering and Industrial Technologies, University of Trento, and leader in the biomedical field. He is professor of composite materials engineering and head of the BIOtech Research Center of the University of Trento. He built an international and multidisciplinary research group, thanks to the numerous projects that he coordinated, creating an inspiring and motivating work environment where people can exchange ideas and build new projects altogether. He is still spending energy for the group. He was also vice-rector for technological transfer and dean of Engineering School in Trento. He has published numerous papers on international journals and is editor of books in the field and international patents.

Heung Jae Chun, Institute of Cell & Tissue Engineering, College of Medicine, The Catholic University of Korea, 222 Banpo-daero, Seocho-gu, Seoul, South Korea.

Antonella Motta, Department of Industrial Engineering and BIOtech Research Center, University of Trento, Via Sommarive 9, 38123 Trento, Italy.

Rui L. Reis, 3B's Research Group - Biomaterials, Biodegradables and Biomimetics, University of Minho, Headquarters of the European Institute of Excellence on Tissue Engineering and Regenerative Medicine, AvePark – Parque de Ciência e Tecnologia, Zona Industrial de Gandra, 4805-017 Barco, Guimarães, Portugal; ICVS/3B's - PT Government Associated Laboratory, Braga/Guimarães, Portugal; The Discoveries Centre for Regenerative and Precision Medicine, Headquarters at University of Minho, Avepark, 4805-017 Barco, Guimarães, Portugal.

Gilson Khang, Department of BIN Convergence Technology, Department of Polymer Nano Science & Technology and Polymer BIN Research Center, Jeonbuk National University, Deokjin-gu, Jeonju-si, Jeollabuk-do, 54896, South Korea.

Contents

Part I

Novel Bioinspired Biomaterials for Regenerative Medicine

1 Natural Sources and Applications of Demineralized Bone Matrix in the Field of Bone and Cartilage Tissue Engineering

Hunhwi Cho, Alessio Bucciarelli, Wonkyung Kim, Yongwoon Jeong, Namyeong Kim, Junjae Jung, Sunjung Yoon, and Gilson Khang

Abstract

Demineralized bone matrix (DBM) is one of the most widely used materials for bone repair. Recently, different strategies in tissue engineering have been used to improve preparation of biomaterials from natural sources suitable for the use in bone regeneration. However, the application of DBM in tissue engineering is still a challenge, because the mechanical properties which are essential to bear tensile and load and the risk of transmission of disease by donor are still a matter of homework. A solution to this problem is to blend natural and synthetic polymers to complement defects and make them ideal biomaterials. An ideal biomaterial improves survival, adhesion, proliferation, induction, and differentiation of cells in the biomaterial after in vivo transplantation. In this review, we will look at the study of DBM made of natural and synthetic materials giving a direction for future research.

Keywords

Demineralized bone matrix (DBM) · Demineralized bone particle (DBP) · Cartilage · Chondrocyte · BMSC · Drug delivery · Bone · Bone morphogenetic protein · Tissue engineering · Scaffold · Natural material · Biomaterial

1.1 Introduction

Bone, a rigid tissue in vivo, is the material that composes the skeleton whose primary function is to provide mechanical support and to sustain the mechanical load due to body movements. It also provides attachment sites for muscle and other tissues, and it produces blood cells [1, 2]. Bone and cartilage damages are primarily caused by traumas, but they can also be caused by genetic disorders, infections, tumors, and other diseases. Critical damages on these tissues could be difficult to self-regenerate; then a surgical treatment is required [3–6]. One among the multiple methods of treating such diseases is the substitution of the

H. Cho · W. Kim · Y. Jeong · N. Kim · J. Jung · G. Khang (✉)
Department of BIN Convergence Technology, Department of Polymer Nano Science & Technology and Polymer BIN Research Center, Jeonbuk National University, Jeonju, South Korea
e-mail: gskhang@jbnu.ac.kr

A. Bucciarelli
Microsystem Technology Group, Fondazione Bruno Kessler, Trento, Italy

Department of Industrial Engineering and BIOtech Research Center, Trento, Italy

S. Yoon
Department of Orthopedic Surgery, Medical School, Chonbuk National University Hospital, Jeonju, Republic of Korea

H. J. Chun et al. (eds.), *Bioinspired Biomaterials*, Advances in Experimental Medicine and Biology 1249, https://doi.org/10.1007/978-981-15-3258-0_1

defective tissue by implantation of biomaterials from natural or synthetic sources [2, 3, 7–10].

In the last decade, tissue engineering and regenerative medicine methods to regenerate and repair injured bones have been studied [11–14]. Due to the extended lifespan and, consequently, the aging of the population, the number of musculoskeletal disorders dramatically increased [5, 6, 15–17]. The use of bone as bio-tissue for transplantation to treat injured bones is reported in millions of cases every year [8, 18]. The surgical procedure is known as bone grafting in the damaged site. In most cases the procedure (autograft) implies the harvesting of bones from another site of the patient skeleton (usually from the hips, legs, or ribs).

Bone is a mineralized connective tissue that is highly dynamic: it is continuously remodeled by the interaction of osteoclast and osteoblast [15]. Therefore, a transplantation therapy should consider not only the loss of structural integrity through but also the circulation of living cells. There are several limitations on the possibility to execute the surgical bone grafting mainly due to harvesting process. These include donor site pain (the most common complication), increased blood loss, increased operative time, and the potential for donor site infection. Additionally, in some cases an inherently limited supply of graft could exist, as example in pediatric patients. Allograft materials can in some cases represent a good alternative whenever the autograft surgical procedure is not possible. Two important aspects need to be considered in the material choice: the mechanical stability and the biological interaction with the site bone to allow the fracture healing.

In general, an ideal bone graft substitute should be biocompatible, bioresorbable, osteoinductive, osteoconductive, structurally similar to the bone, and cost-effective [7, 15, 19]. Here, the strictly needing of resorbability and degradability is due to the fact that bone is a dynamic tissue that undergoes a constant remodeling process. Nonabsorbable or nondegradable biomaterials even if it is able to effectively substitute the bone can cause a delay in the recovery time or other problems in vivo [20]. Implanted biomaterials should also induce, when implanted in vivo, angiogenesis to create new blood vessels [21, 22]. The matching of the mechanical properties of the biomaterial and the natural bone is another critical aspect to take into account into the design of a bone substitution as reported from several in vivo studies [23, 24].

As a result of a number of clinical studies, transplant alternatives of biologically transplantable synthetic and natural materials have been developed. Demineralized bone matrix (DBM) is, nowadays, one of the best biomaterials among the ones used as transplant alternatives. DBM is the collagen matrix that remains from allograft bones after the removal of cells, minerals, and blood. It can serve as scaffold for the growth of new bone tissue. DBM is relatively easy to use for bone treatment due to large availability from commercial supplier. Many typology of DBM have been developed for various purposes, contributing to the development of bone tissue engineering. However, DBMs are commercially manufactured from different producers. There is considerable variability in the available materials as a result of the initial sources and the production methods.

The disinfection and the removal of the organic material can be conducted in several ways, and each company uses a different treatment; then the material, for commercial use, is usually processed with synthetic polymers or incorporated with natural biomaterials to improve its properties. Among the methods of transplantation, different processing procedures for the bones may show considerable variability in post-transplantation effects. Therefore, it is extremely difficult to predict the biological effects in clinical efficacy testing of DBM products based on their composition. Possible side effects due to the chemicals and procedure used to obtain the DBM have not been studied much. As a result, the various clinical effects of commercial DBM are still under evaluation. Studies in laboratory have shown that the implantation of a large amount of DBM is toxic and potentially fatal. For example, the glycerol, used to produce a putty from DBM, resulted to be toxic [25, 26]. The quality of the DBM is also sensitive to the age and health of

animals or humans' donors; this basically affects the protein content of the produced material. The impact of these differences can be evaluated on the bone morphogenesis and formation once DBM is implanted. In many studies, DBM proteins have been reported to regulate cartilage differentiation and osteogenesis from mesenchymal stromal cells (MSCs) [27–30].

DBMs made for different research purposes have different protein contents due to the environment influencing the donors [31, 32]. Therefore, it is possible to have different osteoinductivity and different results in the DBM transplantation. Consequently, it is extremely difficult to have consistent results in the research data. In general, DBM is used clinically as a promoter to assist bone grafting and not as a replacement for the damaged bones. Because of this nature, not all DBMs have the same biological properties so the optimal DBM formulation should be prepared in accordance with the purpose of its use [33–36]. Although bone and cartilage tissue engineering studies have been conducted for decades, there are not many studies that report the use of DBM, especially in vivo. Therefore, a lot of effort will be needed to identify unknown effects of DBM. In this chapter we report a series of research conducted on DBM from natural sources (both and animals). The characteristics of the obtained DBM for each natural material are investigated in the context of a possible future investigation.

1.2 Demineralized Bone Matrix

1.2.1 Composition and Properties of DBM

DBM is what remains from bone after its demineralization and cell and blood removal. Basically, DBMs act as osteoinducer, inducing the cells differentiation into osteocyte encouraging the bone formation [37–39]. The main constituent of the DBM is collagen (above the 93% of the total composition); the rest is composed of proteins called bone morphogenetic proteins (BMP), which act as regulators of bone formation, transforming growth factor-β (TGF-β) proteins, various growth factors, and residual minerals [40]. DBM is biologically more active than non-demineralized bone graft material due to the demineralization process. In fact, the minerals removal from bones also activates biologically bone-forming proteins.

1.2.2 Preparation Methods

As mentioned earlier, the characteristics of DBM prepared according to the different research purposes are different. In particular there is a dependence of these characteristics on the environment in which the bone was taken. Therefore, transplantation treatments and researches that use DBM can significantly differ in their clinical results. DBM is usually bounded to various carriers according to its purpose and is combined with various protein active substances to affect clinical results [41].

1.2.3 Bone Selection

As a general rule, the preparation of DBM for transplantation should avoid the use of bones with diseases or infections. This allows to avoid the transmission of infectious disease from the donor to the patient [42]. Several cases of disease transmission have been reported in DBM research cases used to treat humans. The first preventive measure for these cases is the selection of bone from the donor.

1.2.4 Bone Demineralization

Prior to the demineralization, some passages are performed to remove the organic parts. The blood stain is removed by successive washing with distilled water. The fat residues and impurities are removed using methanol and chloroform, or in alternative the lipids of the desalted powder are extracted, washed with anhydrous

alcohol and acetone and distilled water, and dried [43–45]. Finally, the use of chloridric acid (HCl) allows the removal of the inorganic minerals; then the collagen matrix is left. The resulting fragments are tested for with Fourier-transform infrared spectroscopy (FTIR), X-ray powder diffraction (XRD), and energy-dispersive X-ray spectroscopy (EDX) to check for calcium residuals that can negatively affect the bone induction [46–48].

1.2.5 Sterilization Method

Because there is no way to predict the changes in chemical and physical properties that occur during the sterilization process, it is necessary to compare the different sterilization processes and test the resulting DBMs in others to choose the best sterilization method for the specified purpose. Chemical disinfection methods, which have previously been done with alcohol or using solvents and detergents, are still in use because of the positive clinical results reported in the literature [43, 45]. It has also been confirmed that the sterilization can be conducted through the electrospun [49–52]. Another reported a sterilization method that implies the use of ethylene oxide (EtO) in a procedure [53–55]. EtO sterilization is mainly used to sterilize medical equipment or medicinal products that cannot be sterilized by conventional high-temperature steam. For example, EtO sterilization is useful in case of electronic parts, plastic packages, or equipment where plastic containers are used [56–58]. The advantage of EtO sterilization is that it can deactivate the virus in sterile products. However, there are still controversies about the use of EtO, in particular in DBM sterilization in which it can give adverse effects [59]. EtO is a reactive gas; it cannot be adequately controlled if used in a soft, thermoplastic DBM; and partial loss can occur [60, 61]. Therefore, when conducting sterilization in any way, a careful selection of the method is required to avoid negative effects on the chemical and physical properties of DBM.

1.3 Study of Osteo-cartilage for Various Natural DBMs

1.3.1 Human

Numerous studies of organic and inorganic biomaterials and composites have been carried out, and many have been extensively tested to meet a number of limitations in applying tissue engineering to humans. As a result of various studies, DBM has been improved in material properties and can be applied to tissue engineering more practically, and many clinical studies have confirmed the potential. In this section, we will refer to various research examples applied to tissue engineering for humans using DBM.

1.3.1.1 DBM Scaffold for Cell Adhesion Improvement

The porosity distribution of the scaffold plays a large role in cell proliferation and attachment. As the scaffold porosity increases, more cells may attach giving a fast bone adhesion [62–66]. The surfaces roughness of the scaffold also affects the cell activity and attachment [67]; this was proved by a study in which DBM was only partially demineralized in order to produce surfaces with an enhanced roughness and porosity allowing a better cell proliferation [68]. This study suggests that partially demineralized DBM scaffolds have potential use as bone scaffold.

1.3.1.2 Regulation of Osteogenesis Using Demineralized Bone Powder (DBP)

It has been reported that the calcium factor in the cell periphery affects the activity of the cells [46–48]. In general, the presence of calcium stimulates cells to be more involved in bone formation [69]. As a confirmation method, DBP with a size in the 125–850 μm range was inserted into transwell with pore membrane; hMSCs were cultured on the bottom of the plate. The solubility factors contained in DBP induced the cells regulation improving the expression of the alkaline phosphatase (ALP) [70]. The most abundant solubility factors released by DBP through the

enzyme-linked immunosorbent assay (ELISA) were the insulin-like growth factor binding protein-1 (IGFBP-1), thrombospondin (TSP), and angiostatin [70].

1.3.1.3 Derivation of Biological Properties of DBM

In tissue engineering, the seeding and transplantation of cells in the scaffold is the most important task. To ensure an optimal cell proliferation, the research has been concentrated in the improvement of the functions present in the scaffold. However, some synthetic polymers have been found to cause local acidic environments that interfere with the degradability [71–73]. DBM scaffolds are excellent for cell adhesion, proliferation, and survival due to natural characteristics of bone materials. Therefore, using a bone-based scaffold improves its function as a bone scaffold in standard culture media. In one study, DBM scaffolds were developed using demineralized human epiphyseal bone matrix [74]. The molecules present in this scaffold have been proved to allow a high penetration of the cells inducing the bone formation. These results suggested that the scaffold made of DBM directly affects the attached cells and improves the osteogenic differentiation; therefore, this scaffold can be used as it has a positive potential for implantation for the treatment of lost bone [74].

1.3.1.4 Absorbable Biomaterial DBM

A new approach in tissue engineering therapies is to culture the cells into the matrix before its transplantation to form the cell-matrix complex. This method is used to further increase the bioactivity after the transplantation [75, 76]. Usually to apply this method, the scaffold material should be stable and absorbable in the biological environment [7, 19]. In this context, the use of DBM was evaluated by cell seeding. As a result, DBM had a high-volume expansion and absorptivity, resulting in high penetration and adhesion rates of seeded cells. Cells resulted to be present uniformly in all the matrix from the day 1 after seeding [77]. This property showed the potentiality in the use of DBM in the new tissue engineering approaches.

1.3.1.5 Effect of EtO Sterilization on Human Demineralization Bone

As mentioned earlier, DBM products for commercial are generally sterilized by the use of EtO. One study found that using EtO-sterilized DBM as an autologous bone graft substitute would reduce the bone-inducing potential of bone after transplantation [78]. This is probably due to a chemical change on the exposed surfaces of the scaffold that could interfere with bone induction capabilities of the matrix [79]. The conducted studies suggest that the optimal sterilization via EtO of deionized human bones should stay in the 45–60-minute range [79].

1.3.1.6 DBM for Prevention of Bone Loss in Postmenopausal Women

Estrogen, one of the female hormones, plays an important role in creating and maintaining bones in the human body. In woman, a decreasing in the estrogen hormone due to the menopause is often linked to bone losses and the related diseases. Estrogen has been reported to affect chondrocyte cell not only in the osteochondral tissues but also inside the cartilage. In addition, several studies report that estrogen can play a significant role in bone induction and formation [80–84]. To confirm this phenomenon, gelatin was used to encapsulate human DBM particles and then transplanted [85]. The results of the experiment indicated that estrogen does not participate in the initial bone induction process but instead it regulates the bone growth [85].

1.3.1.7 Relationship Between DBM and Platelet-Rich Plasma (PRP)

Platelet-rich plasma (PRP) is reported to be a favorable biomaterial for osteogenesis because of the presence of the transforming growth factor-β (TGF-β) and the platelet-derived growth factor (PDGF). TGF-β in PRP stimulates osteoblasts and chondrocytes; instead PDGF is reported to promote the angiogenesis and the chondrocyte proliferation [86–89]. Based on these results, the use of PRP in combination with DBM was evaluated on the chlorine osteochondral defects (OCDs) ankle

treatment [90]. The initial assumption was that this combination would decrease the recovery time in comparison with DBM alone. The results showed no significant difference in the treatment groups for osteochondral [90]. The reason of this discrepancy has been suggested by another study, in which the role of thrombin-induced activation of the PRP was carried out in the context of its use in DBM [91]. The osteoconductivity of DBM resulted improved only in the case in which PRP were not activated [91]. However, the optimal concentration of PRP to maximize the effect on the implanted DBM is still unknown [90]. In fact, experiments on PRP were conducted at various concentrations of platelets which vary according to the situation, so there is no consistent data on the results [90]. Therefore, a calibration on the PRP concentration used in combination with DBM should be performed to optimize the in vivo response.

1.3.2 DBM Sources

In addition to commercial DBMs in tissue engineering studies, the use of DBM from animals and human sources have been extensively reported. In these studies, bone-marrow-derived stem cells (BMSCs) have been used to regenerate bone tissue through several animal models [92–94], showing that DBM improves bone formation at the site of loss [43, 44]. The combination of DBM and BMSCs presents several advantages that will be discussed in this chapter.

1.3.2.1 DBM for Improved Scaffold Function

The effect of the degree of demineralization of the DBM scaffold on bone formation capacity of the BMSCs was studied using biomaterials obtained by the bovine femoral bones and cells from humans [95]. The degree of demineralization of the DBM scaffold has been proved to significantly influence the osteogenic differentiation of the BMSC [95]. In particular, the surface of the scaffold changed in accordance with the extent of the demineralization, thereby improving the penetration and adhesion of the cells to the scaffold [68]. By controlling the degree of demineralization, it is therefore possible to control the osteogenic differentiation. These results show a potential usage of animal-derived DBM in combination to human BMSCs in case of transplantation [95]. For a deficient bone therapy, a DBM from a 2-year cow has been tested versus a chitosan control [96]. DBM promoted bone regeneration helping the recovery of the defected part; instead in chitosan the regeneration did not take place. These results suggest that chitosan cannot be used as a biomaterial for promoting bone tissue regeneration alone, but it can be used as matrix in the process of making scaffolds [97, 98]. Scaffolds made by combining chitosan with other materials had a porosity distribution suitable for cell adhesion, low immunological response, and high biodegradability in vivo, when transplanted [99, 100]. Therefore, the combination of chitosan and DBM could be potentially beneficial for the biological response of the scaffolds.

The main issue of the use of DBM applied to tissue engineering is its low mechanical strength [101]. To overcome it, heparin was used to crosslink the collagen matrix in order to improve the mechanical properties of the scaffold. Experimental results showed that the compression modulus of crosslinked DBM increased by a factor 8 in comparison to the uncrosslinked DBM. Due to the demineralization, DBMs are generally soft materials; consequently they do not maintain their initial shape after the transplantation. Crosslinked DBM can be shaped prior to the crosslinking allowing the preservation of shape even after transplantation [101]. The mean pore diameter of crosslinked DBM resulted to be larger in comparison with the uncrosslinked material. This can be explained considering that the crosslinked structure maintained its shape, without any shrinkage during the freeze-drying process [101]. Collagen-based DBM is a useful biomaterial for 3D cell culture, when the same coculture of cells was incubated in 2D and in a 3D DBM, the metabolic activity of the cells was higher in the second case [102]. 3D DBM scaffold had a broader surface area than 2D system and a higher porosity allowing an efficient scaffold-cell interaction and a good diffusion of nutrients [102].

1.3.2.2 Effect of Melanin-Containing DBP on Bone Regeneration

Gallus gallus var. *domesticus* (GD) is a natural mutant black chicken in Korea. It is characterized by a dark blue bone containing melanin that increases ALP activity [43]. To test the effect of melanin on bone regeneration ability, demineralized bone particles (DBP) were produced from GD [43]. GD DBP resulted to reduce the inflammation. The optimal concentration of melanin to favorably induce the bone regeneration was found to be 1% in weight [43]. However, due to the modest amount of bones from GD and the fact that it can only be found in Korea, no so much research has been conducted on it [43].

1.3.2.3 Chitosan-DBM Hybrid Scaffold for Cartilage Regeneration

The pore distribution is one of the main important factors for the cell-scaffold interaction: the porosity should be large enough to consent the cell to enter inside the 3D structure and proliferate. An adverse effect can occur; if the pores size is too large, cells may escape. Chitosan gel was used to fill the larger pores, then maximizing the number of cells entrapped into the scaffold. As a result, in the chitosan-DBM hybrid scaffold, the larger pores were occluded and cells could not escape [103]. The chitosan-DBM hybrid scaffolds are more suitable for cartilage treatment than the single scaffolds. As a positive result of the use of chitosan, the mechanical strength of the scaffold was improved, and the chondrocytes were homogeneously fixed in the defective area [97–100]. These properties of the chitosan-DBM hybrid scaffold in cell attachment and propagation are very important in cartilage tissue engineering [103].

1.3.2.4 DBM for Activation of Cold-Stored Cells

In a recent study, BMSCs were preserved at low temperatures and then activated again, resulting in cell growth and osteogenic differentiation in vitro [104]. The possibility to recover the bone regeneration capabilities of BMSCs already deposited on a 3D scaffold, after cryopreservation, has been recently evaluated [105] on a partial DBM obtained from porcine trabecular bone (pDBM). A vitreous solution (VS442) for cold storage appositely developed was used in combination with the pDBM; cBMSCs cells were seeded in the scaffold and then cryopreserved up to 3 months [105]. The developed VS442 vitreous solution was proved to be more effective in maintaining viability and osteogenesis capability of cells after their reactivation [105].

1.3.2.5 Interaction of DBP Particles with Cells

Some synthetic materials have been used to mimic cartilage morphology and appearance, but from the mechanical point of view, they are generally inferior to the natural tissue [106]. To increase the mechanical strength, a biodegradable joint was prepared by using DBM collected from euthanized mouse distal femur [106]. This bio-joint was a suitable environment for promoting chondrocyte differentiation [106]. The advantage of the use of DBM was the matching of the mechanical properties of the natural cartilage [106]. Two layers of porous collagen were used in combination with DBM to produce a scaffold for in vitro tests. In this case, the use of DBP was proved to induce a strong chemical stimulus to promote the cartilage formation from fibroblasts [107].

1.3.2.6 Demineralized Bone Matrix Gelatin (BMG) in Tissue Engineering

A number of tissue therapies have been developed that can improve the effectiveness of treating cartilage defects locally [108–110]. In particular, several studies have been conducted to identify the process by which bone matrix gelatin (BMG) induces the differentiation of mesenchymal cells into cartilage cells [111–113]. BMG scaffolds are reabsorbed in vivo, releasing growth factors that stimulate the bone formation helping the tissue repair [114]. Based on these reasons, a study reported the development of BMG-based scaffolds using DBM obtained from the distal femur of euthanized white rabbits and evaluated them for osteochondral tissue regeneration [114]. BMG made from a natural DBM resulted to have

no toxicity and to be biocompatible in tests performed in vivo. As an inert material, BMG did not cause any immune or inflammatory reactions. From the mechanical point of view because the support maintains all the mechanical properties, it can be squeezed and fixed to the lost defect area [114]. Therefore, BMG scaffolds resulted was rapidly osteointegrated in vivo due to their excellent mechanical properties [114].

1.3.3 DBM for Drug Delivery

Several studies report the use of DBM as drug delivery system: in fact, the large amount of data available DBM products that allow to select more suitable DBM for a specific drug delivery application and to predict in some extent the result of its usage. DBM has several advantages: its morphology helps the infiltration and adhesion of cells, the biocompatibility is excellent, and it does not cause immune and inflammatory reactions. This allows to load a variety of drugs into the matrix and deliver the drug without side effects to the area to treat. Many studies have been done to improve the effect of using DBM powder through synthetic and natural polymers. Materials developed in this fashion generally show an improved bone growth [115–125].

1.4 Conclusion

With regard to bone grafting, DBM has shown excellent efficacy in many research and treatment outcomes. DBM is based on bone stimulants and has an intensive impact on bone healing. Based on this, various DBM products have been developed for clinical applications and have been successfully used to overcome the shortcomings of synthetic and natural materials in bone therapies or to amplify the effects and apply them to tissue engineering. The efficacy of the DBM was proved to be dependent on isolation/extraction method adopted and on the material synthesized. In addition there is considerable variation in the product obtained from different animal sources. Many studies in literature report the reducing of the DBM effectiveness due to the synthesis with certain substances or disinfecting procedures. These are still challenges that need to be addressed to optimize the DBM usage. In order to enhance the bone and cartilage formation on naturally derived DBM, it is necessary to induce the angiogenesis by seeding cells on it. More studies have to be conducted, on the DBM and its application on bone and cartilage tissue engineering especially to maintain their biological properties.

References

1. Toloue EB, Karbasi S, Salehi H, Rafienia M (2019) Potential of an electrospun composite scaffold of poly (3-hydroxybutyrate)-chitosan/alumina nanowires in bone tissue engineering applications. Mater Sci Eng C Mater Biol Appl 99:1075–1091
2. Behera S (2017) Hydroxyapatite reinforced inherent RGD containing silk fibroin composite scaffolds: promising platform for bone tissue engineering. Nanomedicine 13:1745–1759
3. Chen L, Hu J, Ran J, Shen X, Tong H (2014) Preparation and evaluation of collagen-silk fibroin/hydroxyapatite nanocomposites for bone tissue engineering. Int J Biol Macromol 65:1–7
4. Guex AG (2017) Highly porous scaffolds of PEDOT:PSS for bone tissue engineering. Acta Biomater 62:91–101
5. Ding Z (2016) Silk–hydroxyapatite nanoscale scaffolds with programmable growth factor delivery for bone repair. ACS Appl Mater Interfaces 8:24463–24470
6. Stevens MM (2008) Biomaterials for bone tissue engineering. Mater Today 11:18–25
7. Bao CLM (2013) Regenerative medicine and tissue engineering
8. Fernandez-Yague MA (2015) Biomimetic approaches in bone tissue engineering: integrating biological and physicomechanical strategies. Adv Drug Deliv Rev 84:1–29
9. Chen P (2019) Biomimetic composite scaffold of hydroxyapatite/gelatin-chitosan core-shell nanofibers for bone tissue engineering. Mater Sci Eng C 97:325–335
10. Hassan MN, Mahmoud MM, El-Fattah AA, Kandil S (2016) Microwave-assisted preparation of nanohydroxyapatite for bone substitutes. Ceram Int 42:3725–3744
11. Neel EAA, Chrzanowski W, Salih VM, Kim H-W, Knowles JC (2014) Tissue engineering in dentistry. J Dent 42:915–928
12. Bouët G, Marchat D, Cruel M, Malaval L, Vico L (2014) In vitro three-dimensional bone tissue mod-

els: from cells to controlled and dynamic environment. Tissue Eng Part B Rev 21:133–156
13. Henkel J (2013) Bone regeneration based on tissue engineering conceptions—a 21st century perspective. Bone Res 1:216
14. Atrian M, Kharaziha M, Emadi R, Alihosseini F (2019) Silk-Laponite® fibrous membranes for bone tissue engineering. Appl Clay Sci 174:90–99
15. Zhou J (2017) Improving osteogenesis of three-dimensional porous scaffold based on mineralized recombinant human-like collagen via mussel-inspired polydopamine and effective immobilization of BMP-2-derived peptide. Colloids Surf B: Biointerfaces 152:124–132
16. Blum L (2016) Atypical femur fractures in patients receiving bisphosphonate therapy: etiology and management. Eur J Orthop Surg Traumatol 26:371–377
17. Daruwalla ZJ (2016) Hip fractures, preceding distal radius fractures and screening for osteoporosis: should we be screening earlier? A minimum 10-year retrospective cohort study at a single centre. Osteoporos Int 27:361–366
18. Farokhi M (2018) Silk fibroin/hydroxyapatite composites for bone tissue engineering. Biotechnol Adv 36:68–91
19. Khaled E, Saleh M, Hindocha S, Griffin M, Khan WS (2011) Suppl 2: tissue engineering for bone production-stem cells, gene therapy and scaffolds. Open Orthop J 5:289
20. Acevedo CA (2019) Design of a biodegradable UV-irradiated gelatin-chitosan/nanocomposed membrane with osteogenic ability for application in bone regeneration. Mater Sci Eng C 99:875–886
21. Kusuma S, Dickinson L, Gerecht S (2014) in Cardiac regeneration and repair 350–388
22. Amini AR, Laurencin CT, Nukavarapu SP (2012) Bone tissue engineering: recent advances and challenges. Crit Rev Biomed Eng 40:363
23. Lacroix D, Prendergast PA (2002) Mechano-regulation model for tissue differentiation during fracture healing: analysis of gap size and loading. J Biomech 35:1163–1171
24. Sikavitsas VI, Temenoff JS, Mikos AG (2001) Biomaterials and bone mechanotransduction. Biomaterials 22:2581–2593
25. Wang JC (2001) Dose-dependent toxicity of a commercially available demineralized bone matrix material. Spine 26:1429–1435
26. Bostrom M (2001) An unexpected outcome during testing of commercially available demineralized bone graft materials: how safe are the nonallograft components? Spine 26:1425–1428
27. Billings E (2009) Cartilage resurfacing of the rabbit knee: the use of an allogeneic demineralized bone matrix-autogeneic perichondrium composite implant. Acta Orthop Scand 61:201–206. https://doi.org/10.3109/17453679008993501
28. Chen B (2007) Homogeneous osteogenesis and bone regeneration by demineralized bone matrix loading with collagen-targeting bone morphogenetic protein-2. Biomaterials 28:1027–1035
29. Kiely PD (2014) Evaluation of a new formulation of demineralized bone matrix putty in a rabbit posterolateral spinal fusion model. Spine J 14:2155–2163
30. Jansen EJ (2005) Hydrophobicity as a design criterion for polymer scaffolds in bone tissue engineering. Biomaterials 26:4423–4431
31. Strates BS, Stock AJ, Connolly JF (1988) Skeletal repair in the aged: a preliminary study in rabbits. Am J Med Sci 296:266–269
32. Nishimoto SK, Chang C-H, Gendler E, Stryker WF, Nimni ME (1985) The effect of aging on bone formation in rats: biochemical and histological evidence for decreased bone formation capacity. Calcif Tissue Int 37:617–624
33. Urist MR (1997) Lipids closely associated with bone morphogenetic protein (BMP) – and induced heterotopic bone formation. With preliminary observations of deficiencies in lipid and osteoinduction in lathyrism in rats. Connect Tissue Res 36:9–20
34. Xia W, Chang J (2010) Bioactive glass scaffold with similar structure and mechanical properties of cancellous bone. J Biomed Mater Res B Appl Biomater 95:449–455
35. Kimura I, Wei T, Akazawa T, Murata M (2017) Characterization of demineralization behavior of bovine bone granules related to particulate properties. Adv Powder Technol 28:740–746
36. Dallari D (2012) A prospective, randomised, controlled trial using a Mg-hydroxyapatite-demineralized bone matrix nanocomposite in tibial osteotomy. Biomaterials 33:72–79
37. Berven S, Tay BK, Kleinstueck FS, Bradford DS (2001) Clinical applications of bone graft substitutes in spine surgery: consideration of mineralized and demineralized preparations and growth factor supplementation. Eur Spine J 10:S169–S177
38. Chalmers J, Gray D, Rush J (1975) Observations on the induction of bone in soft tissues. J Bone Joint Surg Br 57:36–45
39. Dahners LE, Jacobs R (1985) Long bone defects treated with demineralized bone. South Med J 78:933–934
40. Aly LAA, Hammouda NI (2017) Evaluation of implant stability simultaneously placed with sinus lift augmented with putty versus powder form of demineralized bone matrix in atrophied posterior maxilla. Future Dent J 3:28–34
41. Tricot M, Deleu P-A, Detrembleur C, Leemrijse T (2017) Clinical assessment of 115 cases of hindfoot fusión with two different types of graft: allograft+ DBM+ bone marrow aspirate versus autograft+ DBM. Orthop Traumatol Surg Res 103:697–702
42. Torres M, Fernandez J, Dellatorre F, Cortizo A, Oberti T (2019) Purification of alginate improves its biocompatibility and eliminates cytotoxicity in matrix for bone tissue engineering. Algal Res 40:101499

43. Kim D (2019) Effect of different concentration of demineralized bone powder with gellan gum porous scaffold for the application of bone tissue regeneration. Int J Biol Macromol 134:749–758
44. Beltrán V (2014) Augmentation of intramembranous bone in rabbit calvaria using an occlusive barrier in combination with demineralized bone matrix (DBM): a pilot study. Int J Surg 12:378–383
45. Sawkins M (2013) Hydrogels derived from demineralized and decellularized bone extracellular matrix. Acta Biomater 9:7865–7873
46. Shi H, Ye X, He F, Ye J (2019) Improving osteogenesis of calcium phosphate bone cement by incorporating with lysine: an in vitro study. Colloids Surf B: Biointerfaces 177:462–469
47. Zhang L, Liu L, Thompson R, Chan C (2014) CREB modulates calcium signaling in cAMP-induced bone marrow stromal cells (BMSCs). Cell Calcium 56:257–268
48. Li D, Li K, Shan H (2019) Improving biocompatibility of titanium alloy scaffolds by calcium incorporated silicalite-1 coatings. Inorg Chem Commun 102:61–65
49. Braghirolli DI (2014) The effect of sterilization methods on electronspun poly(lactide-co-glycolide) and subsequent adhesion efficiency of mesenchymal stem cells. J Biomed Mater Res B Appl Biomater 102:700–708
50. Selim M, Bullock AJ, Blackwood KA, Chapple CR, MacNeil S (2011) Developing biodegradable scaffolds for tissue engineering of the urethra. BJU Int 107:296–302
51. Andrews KD, Hunt JA, Black RA (2007) Effects of sterilisation method on surface topography and in-vitro cell behaviour of electrostatically spun scaffolds. Biomaterials 28:1014–1026
52. Sefat F (2013) Production, sterilisation and storage of biodegradable electrospun PLGA membranes for delivery of limbal stem cells to the cornea. Procedia Eng 59:101–116
53. Horakova J (2018) The effect of ethylene oxide sterilization on electrospun vascular grafts made from biodegradable polyesters. Mater Sci Eng C 92:132–142
54. Funatsu K, Kiminami H, Abe Y, Carpenter JF (2019) Impact of ethylene oxide sterilization of polymer-based prefilled syringes on chemical degradation of a model therapeutic protein during storage. J Pharm Sci 108:770–774
55. Solheim E, Pinholt EM, Bang G, Sudmann E (1995) Ethylene oxide gas sterilization does not reduce the osteoinductive potential of demineralized bone in rats. J Craniofac Surg 6:195–198
56. Gimeno P (2018) Identification and quantification of ethylene oxide in sterilized medical devices using multiple headspace GC/MS measurement. J Pharm Biomed Anal 158:119–127
57. Mendes G, Brandão TR, Silva CL (2012) in Sterilisation of biomaterials and medical devices 71–96
58. Xia X, Wang Y, Cai S, Xie C, Zhu C (2009) Will ethylene oxide sterilization influence the application of novel Cu/LDPE nanocomposite intrauterine devices? Contraception 79:65–70
59. Thomas RZ, Ruben JL, Jaap J, Huysmans M-CD (2007) Effect of ethylene oxide sterilization on enamel and dentin demineralization in vitro. J Dent 35:547–551
60. Hastings C Jr (1990) The effects of ethylene oxide sterilization on the in vitro cytotoxicity of a bone replacement material. Toxicol In Vitro 4:757–762
61. Navarrete L, Hermanson N (1998) The changes in ethylene oxide sterilization and their effect on thermoplastics. In: Medical plastics: degradation resistance & failure analysis. Plastic Design Library, Norwich, p 51
62. Roman M, Haring AP, Bertucio TJ (2019) The growing merits and dwindling limitations of bacterial cellulose-based tissue engineering scaffolds. Curr Opin Chem Eng 24:98–106
63. de Souza RFB (2019) Mechanically-enhanced polysaccharide-based scaffolds for tissue engineering of soft tissues. Mater Sci Eng C 94:364–375
64. Wang S (2019) Pore functionally graded Ti6Al4V scaffolds for bone tissue engineering application. Mater Des 168:107643
65. Du L (2019) Hierarchical macro/micro-porous silk fibroin scaffolds for tissue engineering. Mater Lett 236:1–4
66. Shao H (2019) 3D gel-printing of hydroxyapatite scaffold for bone tissue engineering. Ceram Int 45:1163–1170
67. Dalgic AD, Atila D, Karatas A, Tezcaner A, Keskin D (2019) Diatom shell incorporated PHBV/PCL-pullulan co-electrospun scaffolds for bone tissue engineering. Mater Sci Eng C 100:735–746
68. Mo X-T, Yang Z-M, Qin T-W (2008) Surface configuration properties of partially demineralized bio-derived compact bone scaffolds. Appl Surf Sci 255:449–451
69. Dry H (2013) Effect of calcium on the proliferation kinetics of synovium-derived mesenchymal stromal cells. Cytotherapy 15:805–819
70. Pflum ZE, Palumbo SL, Li W-J (2013) Adverse effect of demineralized bone powder on osteogenesis of human mesenchymal stem cells. Exp Cell Res 319:1942–1955
71. Bergsma EJ, Rozema FR, Bos RR, De Bruijn WC (1993) Foreign body reactions to resorbable poly (L-lactide) bone plates and screws used for the fixation of unstable zygomatic fractures. J Oral Maxillofac Surg 51:666–670
72. Martin C, Winet H, Bao J (1996) Acidity near eroding polylactide-polyglycolide in vitro and in vivo in rabbit tibial bone chambers. Biomaterials 17:2373–2380
73. Middleton JC, Tipton AJ (2000) Synthetic biodegradable polymers as orthopedic devices. Biomaterials 21:2335–2346

74. Abedin E, Lari R, Mahdavi Shahri N, Fereidoni M (2018) Development of a demineralized and decellularized human epiphyseal bone scaffold for tissue engineering: a histological study. Tissue Cell 55:46–52
75. Carvalho MS (2019) Co-culture cell-derived extracellular matrix loaded electrospun microfibrous scaffolds for bone tissue engineering. Mater Sci Eng C 99:479–490
76. Caswell PT, Zech T (2018) Actin-based cell protrusion in a 3D matrix. Trends Cell Biol 28:823–834
77. Kasten P (2003) Comparison of human bone marrow stromal cells seeded on calcium-deficient hydroxyapatite, β-tricalcium phosphate and demineralized bone matrix. Biomaterials 24:2593–2603
78. Aspenberg P, Johnsson E, Thorngren K (1990) Dose-dependent reduction of bone inductive properties by ethylene oxide. J Bone Joint Surg Br 72:1036–1037
79. Doherty MJ, Mollan R, Wilson D (1993) Effect of ethylene oxide sterilization on human demineralized bone. Biomaterials 14:994–998
80. Ikeda K, Tsukui T, Imazawa Y, Horie-Inoue K, Inoue S (2012) Conditional expression of constitutively active estrogen receptor α in chondrocytes impairs longitudinal bone growth in mice. Biochem Biophys Res Commun 425:912–917
81. Li X-F, Wang S-J, Jiang L-S, Dai L-YS (2013) Specific effect of leptin on the expressions of estrogen receptor and extracellular matrix in a model of chondrocyte differentiation. Cytokine 61:876–884
82. Hattori Y (2012) A selective estrogen receptor modulator inhibits tumor necrosis factor-α-induced apoptosis through the ERK1/2 signaling pathway in human chondrocytes. Biochem Biophys Res Commun 421:418–424
83. Talwar RM, Wong BS, Svoboda K, Harper RP (2006) Effects of estrogen on chondrocyte proliferation and collagen synthesis in skeletally mature articular cartilage. J Oral Maxillofac Surg 64:600–609
84. Takano H, Aizawa T, Irie T, Kokubun S, Itoi E (2007) Estrogen deficiency leads to decrease in chondrocyte numbers in the rabbit growth plate. J Orthop Sci 12:366
85. McMillan J (2007) Osteoinductivity of demineralized bone matrix in immunocompromised mice and rats is decreased by ovariectomy and restored by estrogen replacement. Bone 40:111–121
86. Hersant B, La Padula S, SidAhmed-Mezi M, Rodriguez A, Meningaud J (2017) Use of platelet-rich plasma (PRP) in microsurgery. J Stomatol Oral Maxillofac Surg 118:236–237
87. Abdullah BJ, Atasoy N, Omer AK (2019) Evaluate the effects of platelet rich plasma (PRP) and zinc oxide ointment on skin wound healing. Ann Med Surg 37:30–37
88. Atashi F (2019) Does non-activated platelet-rich plasma (PRP) enhance fat graft outcome? An assessment with 3D CT-scan in mice. J Plast Reconst Aesthet Surg 72(4):669–675
89. Dias LP (2018) Effects of intravesical therapy with platelet-rich plasma (PRP) and Bacillus Calmette-Guérin (BCG) in non-muscle invasive bladder cancer. Tissue Cell 52:17–27
90. van Bergen CJ (2013) Demineralized bone matrix and platelet-rich plasma do not improve healing of osteochondral defects of the talus: an experimental goat study. Osteoarthr Cartil 21:1746–1754
91. Han B, Woodell-May J, Ponticiello M, Yang Z, Nimni M (2009) The effect of thrombin activation of platelet-rich plasma on demineralized bone matrix osteoinductivity. J Bone Joint Surg Am 91:1459–1470
92. Xue J (2019) An injectable conductive gelatin-PANI hydrogel system serves as a promising carrier to deliver BMSCs for Parkinson's disease treatment. Mater Sci Eng C 100:584–597
93. Dai Y (2017) The paracrine effect of cobalt chloride on BMSCs during cognitive function rescue in the HIBD rat. Behav Brain Res 332:99–109
94. Man Z (2014) The effects of co-delivery of BMSC-affinity peptide and rhTGF-β1 from coaxial electrospun scaffolds on chondrogenic differentiation. Biomaterials 35:5250–5260
95. Mauney JR (2005) In vitro and in vivo evaluation of differentially demineralized cancellous bone scaffolds combined with human bone marrow stromal cells for tissue engineering. Biomaterials 26:3173–3185
96. Alidadi S, Oryan A, Bigham-Sadegh A, Moshiri A (2017) Comparative study on the healing potential of chitosan, polymethylmethacrylate, and demineralized bone matrix in radial bone defects of rat. Carbohydr Polym 166:236–248
97. Saekhor K, Udomsinprasert W, Honsawek S, Tachaboonyakiat W (2019) Preparation of an injectable modified chitosan-based hydrogel approaching for bone tissue engineering. Int J Biol Macromol 123:167–173
98. Ranganathan S, Balagangadharan K, Selvamurugan N (2019) Chitosan and gelatin-based electrospun fibers for bone tissue engineering. Int J Biol Macromol 133:354
99. Kara A, Tamburaci S, Tihminlioglu F, Havitcioglu H (2019) Bioactive fish scale incorporated chitosan biocomposite scaffolds for bone tissue engineering. Int J Biol Macromol 130:266–279
100. de Souza FCB, de Souza RFB, Drouin B, Mantovani D, Moraes ÂM (2019) Comparative study on complexes formed by chitosan and different polyanions: potential of chitosan-pectin biomaterials as scaffolds in tissue engineering. Int J Biol Macromol 132:178–189
101. Lin H (2008) The effect of crosslinking heparin to demineralized bone matrix on mechanical strength and specific binding to human bone morphogenetic protein-2. Biomaterials 29:1189–1197
102. Ma S (2007) The effect of three-dimensional demineralized bone matrix on in vitro cumulus-free oocyte maturation. Biomaterials 28:3198–3207

103. Man Z (2016) Transplantation of allogenic chondrocytes with chitosan hydrogel-demineralized bone matrix hybrid scaffold to repair rabbit cartilage injury. Biomaterials 108:157–167
104. Bruder SP, Jaiswal N, Haynesworth SE (1997) Growth kinetics, self-renewal, and the osteogenic potential of purified human mesenchymal stem cells during extensive subcultivation and following cryopreservation. J Cell Biochem 64:278–294
105. Yin H, Cui L, Liu G, Cen L, Cao Y (2009) Vitreous cryopreservation of tissue engineered bone composed of bone marrow mesenchymal stem cells and partially demineralized bone matrix. Cryobiology 59:180–187
106. Gong M (2010) Engineered synovial joint condyle using demineralized bone matrix. Mater Sci Eng C 30:531–536
107. Mizuno S, Glowacki J (1996) Three-dimensional composite of demineralized bone powder and collagen for in vitro analysis of chondroinduction of human dermal fibroblasts. Biomaterials 17:1819–1825
108. Van Rossom S, Khatib N, Holt C, Van Assche D, Jonkers I (2018) Subjects with medial and lateral tibiofemoral articular cartilage defects do not alter compartmental loading during walking. Clin Biomech 60:149–156
109. De Bari C, Roelofs AJ (2018) Stem cell-based therapeutic strategies for cartilage defects and osteoarthritis. Curr Opin Pharmacol 40:74–80
110. Jones KJ, Mosich GM, Williams RJ (2018) Fresh precut osteochondral allograft core transplantation for the treatment of femoral cartilage defects. Arthrosc Tech 7:e791–e795
111. Zhong N (2012) MicroRNA-337 is associated with chondrogenesis through regulating TGFBR2 expression. Osteoarthr Cartil 20:593–602
112. Bayat M, Momen-Heravi F, Marjani M, Motahhary PA (2010) Comparison of bone reconstruction following application of bone matrix gelatin and autogenous bone grafts to alveolar defects: an animal study. J Cranio-Maxillofac Surg 38:288–292
113. Nakagawa M, Urist MR (1977) Chondrogenesis in tissue cultures of muscle under the influence of a diffusible component of bone matrix. Proc Soc Exp Biol Med 154:568–572
114. Li X, Jin L, Balian G, Laurencin CT, Greg Anderson D (2006) Demineralized bone matrix gelatin as scaffold for osteochondral tissue engineering. Biomaterials 27:2426–2433
115. Lasa JC, Hollinger J, Drohan W, MacPhee M (1995) Delivery of demineralized bone powder by fibrin sealant. Plast Reconstr Surg 96:1409–1417; discussion 1418
116. Han B, Tang B, Nimni ME (2003) Combined effects of phosphatidylcholine and demineralized bone matrix on bone induction. Connect Tissue Res 44:160–166
117. Pinholt EM, Solheim E, Bang G, Sudmann E (1991) Bone induction by composite of bioerodible polyorthoester and demineralized bone matrix in rats. Acta Orthop Scand 62:476–480
118. Chung Y-M, Simmons KL, Gutowska A, Jeong B (2002) Sol−gel transition temperature of PLGA-g-PEG aqueous solutions. Biomacromolecules 3:511–516
119. Tian M (2012) Delivery of demineralized bone matrix powder using a thermogelling chitosan carrier. Acta Biomater 8:753–762
120. Van Haastert R, Grote J, Van Blitterswijk C, Prewett A (1994) Osteoinduction within PEO/PBT copolymer implants in cranial defects using demineralized bone matrix. J Mater Sci Mater Med 5:764–769
121. Sui S, Wang X, Liu P, Yan Y, Zhang R (2009) Cryopreservation of 3D constructs based on a controlled cell assembling technology. J Bioact Compat Polym 24:473–487
122. Wang X, Liu C (2018) Fibrin hydrogels for endothelialized liver tissue engineering with a predesigned vascular network. Polymers 10:1048
123. Wang X, Liu C (2018) 3D bioprinting of adipose-derived stem cells for organ manufacturing. In: Enabling cutting edge technology for regenerative medicine. Springer, SBM Singapore Pte Ltd., Singapore, pp 3–14
124. Liu F, Chen Q, Liu C, Ao Q, Tian X, Fan J, Tong H, Wang X (2018) Natural polymers for organ 3D bioprinting. Polymers 10:1278
125. Wang X, Ao Q, Tian X, Fan J, Wei Y, Hou W, Tong H, Bai S (2016) 3D bioprinting technologies for hard tissue and organ engineering. Materials 9:802

2 Application of Gellan Gum-Based Scaffold for Regenerative Medicine

Joo Hee Choi, Wonchan Lee, Cheolui Song, Byung Kwan Moon, Sun-jung Yoon, Nuno M. Neves, Rui L. Reis, and Gilson Khang

Abstract

Gellan gum (GG) is a linear microbial exopolysaccharide which is derived naturally by the fermentation process of *Pseudomonas elodea*. Application of GG in tissue engineering and regeneration medicine (TERM) is already over 10 years and has shown great potential. Although this biomaterial has many advantages such as biocompatibility, biodegradability, nontoxic in nature, and physical stability in the presence of cations, a variety of modification methods have been suggested due to some disadvantages such as mechanical properties, high gelation temperature, and lack of attachment sites. In this review, the application of GG-based scaffold for tissue engineering and approaches to improve GG properties are discussed. Furthermore, a recent trend and future perspective of GG-based scaffold are highlighted.

Keywords

Gellan gum · Nature derived · Scaffold · Tissue engineering · Regeneration · Application

J. H. Choi · W. Lee · C. Song · G. Khang (✉)
Department of BIN Convergence Technology, Department of Polymer Nano Science & Technology and Polymer BIN Research Center, Jeonbuk National University, Jeonju, South Korea
e-mail: gskhang@jbnu.ac.kr

B. K. Moon
Department of Polymer Nano Science & Technology, Jeonbuk National University, Jeonju-si, Jeollabuk-do, Republic of Korea

S.-j. Yoon
Department of Orthopedic Surgery, Medical School, Jeonbuk National University, Jeonju-si, Republic of Korea

N. M. Neves · R. L. Reis
3B's Research Group – Biomaterials, Biodegradables and Biomimetics, Headquarters of the European Institute of Excellence on Tissue Engineering and Regenerative Medicine, University of Minho, Guimarães, Portugal

ICVS/3B's – PT Government Associated Laboratory, Braga/Guimarães, Portugal

The Discoveries Centre for Regenerative and Precision Medicine, Headquarters at University of Minho, Guimarães, Portugal

2.1 Introduction: Concept of Tissue Engineering

Tissue engineering (TE) is a combined definition of engineering and natural science that develops biomaterials to regenerate damaged or injured tissues [1]. TE has emerged in the mid-1980s and has continually evolved biological substitutes and materials to reconstruct defective tissues [2, 3]. The general strategies of TE

H. J. Chun et al. (eds.), *Bioinspired Biomaterials*, Advances in Experimental Medicine and Biology 1249, https://doi.org/10.1007/978-981-15-3258-0_2

are (1) transplantation of isolated cells, (2) delivering signals such as growth factors or bioreactors, and (3) implantation of an alternative matrix. The TE field relies extensively on the combination of porous 3D scaffolds, cells, and signals to regenerate tissues. Among these, scaffold design and fabrication are the most important subjects [2, 4].

The scaffold is a three-dimensional (3D) porous biomaterial constructed to perform as a template to support cells and growth factors in vitro or support tissue formation by implanting the matrix in vivo [5–7]. The requirements of scaffold for TE are (1) biocompatibility: The scaffold should promote cell-cell and cell-matrix interaction, cell adhesion, migration, and extracellular matrix (ECM) formation, these factors allow negligible immune reaction in vivo (2) transportation of sufficient nutrients, gases, and signals from regulatory factors for cell viability, growth, and differentiation (3) biodegradability: The scaffold should properly allow cells to proliferate and produce ECM and eventually replace the implanted matrix to tissue engineered construct (4) mechanical properties of the scaffold should be consistent with the target tissue. The scaffold must be tough for surgical implantation [6, 8–10]. In order to process this method, the matrix should be nontoxic and should not interfere with the surrounded organs [6, 11, 12]. An inflammatory response should occur with a control matter with an infusion of cells such as macrophages [2, 6, 13]. In addition to these requirements, porosity, pore size, manufacturing process, and architecture of scaffold are important factors to consider when designing a scaffold [14–18]. The source of scaffolds has been produced from human, animals, insects, plants, or synthetic polymers [18–22].

In this review, we will focus on the nature-derived gellan gum (GG)-based scaffold and its application in TE. In addition, we will describe its merits, disadvantages, recent trends, and challenges of this material.

2.2 Gellan Gum

GG, an FDA-approved food additive, is commonly applied in the food and pharmaceutical industry [23–25]. Recently, it has been also proposed as a new biomaterial for TE application due to its versatility and efficacy for tissue repair strategies [26]. In this section, we will discuss GG properties and their applicability in TE.

2.2.1 Structure

GG is a negatively charged, linear exopolysaccharide. Four repeating units exhibit in the main chain of GG, which consist of two D-glucose carbohydrates, one L-rhamnose, and one D-glucuronic acid. GG is produced from bacterium *Sphingomonas elodea* or *Pseudomonas elodea* by the fermentation process [25, 27, 28]. The type of GG can be divided into high acyl GG (HAGG) or low acyl GG (LAGG), which the latter is the most commonly available form in the market [24].

2.2.2 Gelation and Crosslinking Process

The LAGG and HAGG are capable of gelation depending on the existence and type of cations, temperature, molecular weight, and concentration of polymer [26]. The presence of cations allows GG to form a stable matrix structure by ionic crosslinking. Divalent cations (Ca^{2+}, Mg^{2+}) allow more effective structure compared to monovalent cations (Na^{+}, K^{+}). The gelation process from monovalent cations results from the screening effect of the electrostatic repulsion between negatively charged carboxylate groups on the GG backbone. The divalent cations allow gelation of GG by screening effect and chemical bonding between two ionized carboxylate groups on the glucuronic acid molecules in the GG chains [25]. Furthermore, the crosslinking process can occur by chemically with the chemical

reagents such as 1-ethyl-3-(3-dimethylamino-propyl)carbodiimide (EDC), photoinitiator, etc., such as when GG is chemically modified [29–31]. The temperature is also an important factor in gelation. The physical crosslinking occurs when GG chain forms coiled structure at high temperature (~90 °C) and, when cooled, changes to a double-helix structure due to hydrogen bonds and van der Waals forces between nearby chains which give rise to thermo-reversible gels [25, 26]. Depending on a concentration, degree of deacetylation, and molecular weight, the mechanical property of GG changes [32–35].

2.2.3 Degradation Rate

Degradation of scaffold is an important factor in designing biomaterial in TE. The by-products from degraded material should not diffuse any toxic matter and the time frame of degradation should match the treatment time [8].

Many authors have investigated the degradation behavior of GG in vitro. Especially, *D. Awanthi* et al. showed the mechanical property of swollen LAGG, HAGG, and both blended GG hydrogels incubated in phosphate-buffered saline (PBS, pH 7.4, 37 °C) for up to 168 days and investigated long-term degradation behavior. The results showed maximum mass loss and swelling after 28 days. The mechanical and rheological properties changed because of mass loss. The cytotoxicity test proved that all the hydrogels did not release toxic products which proved appropriate material for TE [36]. *H. Lee* et al. investigated LAGG and LAGG/HAGG blended hydrogel to find the most optimizing GG hydrogel for fibrocartilage TE. The study exhibited that degradation of GG hydrogels which were immersed in cell culture media lost 10–20% of weight over 20 days. In addition, the result suggested that 2% (w/v) LAGG would be most appropriate to apply in fibrocartilage TE [35]. The degradation rate of bone marrow stromal cells encapsulated in alginate, pectin, and GG in cell culture media was studied by *S. H. Jahromi* et al. who presented that GG degradation was the least rapid between these three materials [37]. Furthermore, recent research from *I. Yu* et al. showed the degradation behavior of 3D printed GG scaffolds. The result displayed that the degradation rate was higher when the scaffold had a higher surface area to mass ratio [38].

2.2.4 Biocompatibility and Biodegradability

The definition of biocompatibility in a tissue-engineering concept refers to the ability to support cellular activity, facilitate molecular and mechanical signaling systems, and eventually treat damaged or injured tissue [8, 39]. A toxic effect or an undesirable local or systemic response in the eventual host should not appear in vitro or in vivo which may reduce healing effect or cause immune rejection responses by the body [40]. A biocompatibility test can be performed on mammalian cells in vitro by proceeding viability, proliferation, and protein or gene expression test [5, 41–43]. Once the safety of the material is confirmed, in vivo biological test can be tested by implanting the matrix under subcutaneous or targeted tissue part in the short or long term [44, 45]. Terms for the in vivo study can range from 3 weeks to greater than several months, depending on the specific test data needed [46]. Biodegradability is also an important factor to consider in designing a scaffold [11]. Degradation of scaffold occurs through physical or chemical route in biological processes that are mediated by biological agents, such as enzymes in tissue remodeling [8, 47]. The scaffold should gradually degrade in a predetermined period and be replaced by newly grown tissue from adhered cells. The degraded products should not produce toxic matter. Both biocompatibility and biodegradability should be satisfied with TE material (Table 2.1).

Up to date, a number of researches about GG-based scaffold for TE have been published. In vitro and in vivo study was carried out and

Table 2.1 Summary of the modification and fabrication method of GG-based scaffold and studies

Published year	Composition/modification	Fabrication method	Crosslinking method	Characterization	Cells	In vitro	In vivo	Target of the study	References
2009	Oxidized GG	Blending at 70 °C/ casting (hydrogel)	Physical or PBS	Viscosity, gelation point test	Human epidermis fibroblasts (hEFBs), chondrocytes from porcine articular cartilage	WST-1 assay, live/dead staining, DNA content, glycosaminoglycan (GAG) content, histology (hematoxylin and eosin (H&E), safranin-O, Masson's trichrome, collagen II, collagen I)	X	Cartilage TE	[32]
2010	GG	Blending at 90 °C/ casting (hydrogel)	$CaCl_2$	Compressive stress/ strain measurement, rheological experiments	Human articular cartilage from the femoral head and condyles	Calcein AM staining, histology (H&E, Alcian blue, safranin-O), RT-PCR	Subcutaneous implantation (H&E, dynamic mechanical analysis (DMA), weight measurement)	Cartilage TE	[45]
2010	GG	Blending at 42 °C/ casting (hydrogel)	PBS	X	ASCs and articular chondrocytes from rabbit	X	Injection in rabbit articular cartilage defects (H&E, Alcian blue, histological storing, RT-PCR)	Cartilage TE	[44]
2010	GG	Blending at 85–90 °C/casting (film)	Physical	SEM, water content, tensile strength, weight loss	X	X	Implantation in the bone defect	Bone TE	[87]
2010	Starch/PCL, LAGG	Treatment at 65 °C/ tubular structure (filament)	Physical	SEM, μ-CT, compressive stress/ strain measurement	Mouse lung fibroblast cell line (L929)	MEM extraction test, MTS tests, live/dead staining	Subcutaneous implantation (H&E)	SCI regeneration	[99]
2010	MeGG	Blending at 50 °C/ casting (hydrogel)	Physical or $CaCl_2$ and/or photocrosslink	NMR, FT-IR, swelling kinetics, compressive stress/strain measurement, degradation	NIH-3 T3 fibroblasts	Live/dead staining	X	Wide range of TE	[31]
2011	LAGG, HAGG	Blending at 90 °C/ casting (hydrogel)	$CaCl_2$	DMA, weight loss, gelling temperature, theological measurements	X	X	X	Fibrocartilage TE	[35]

2012	Carboxymethyl chitosan, oxidized GG/ Schiff base reaction	Blending at 90 °C/ casting (hydrogel)	$CaCl_2$	Gelation point test, swelling and degradation kinetics, compressive stress/ strain measurement, SEM	Chondrocytes from articular cartilage of newborn rabbits	MTT, live/dead staining	X	Cartilage TE	[84]
2012	GG	Blending at 85–90 °C/casting (sponge)	EDC	Water content, porosity, compression test, degradation, absorption, and blood clotting test	L929	Cell migration assay	X	Dental filling	[64]
2012	GG, ALP, PDA	Blending at 50 °C/ casting (hydrogel) and incorporation of PDA by coating	$CaCl_2$	Alkaline phosphatase (ALP) release, TGA, FITR, SEM, EDS, XRD, ICP-OES, compressive stress/ strain measurement	Human fibroblastic cell line HFF-1 cells, osteoblastic cell line MC3T3-E1	MTT, live/dead staining, Prestoblue™ assay	X	Bone TE	[88]
2012	Immobilize maleimide-containing GRGDS peptides, furan-modified GG Diels-Alder click chemistry	GGeGRGDS hydrogel in complete medium/ casting (hydrogel)	Medium, physical	NMR, HPLC	NSPC, OEG	Phalloidin/DAPI staining, immunocytochemistry (ICC)	X	SCI regeneration	[53]
2012	MeGG, GelMA	Blending at 50 °C for single network (SN), immersing at 37 °C for double network (DN)/ casting (hydrogel)	Photocrosslink	NMR, diffusion test (FITC), compressive stress/strain measurement, FT-IR	NIH-3 T3 fibroblasts	Live/dead staining	X	Load-bearing (cartilage, bone) TE	[49]
2013	MeGG	Blending at room temperature (RT) casting (hydrogel)	Photocrosslink or PBS	Size exclusion chromatography (SEC), water uptake, weight loss	L929, human intervertebral disc (hIVD)	Calcein-AM staining	Subcutaneous implantation (H&E, quantitative analysis)	Confirm biocompatibility	[48]
2013	LAGG, HAGG	Blending at 80 °C/ casting (hydrogel)	$CaCl_2$	Mass loss, volumetric swelling ratio, circular dichroism (CD) spectroscopy, rheology, compression test	L929	Cell viability analyzer	X	Future application in TE	[36]

(continued)

Table 2.1 (continued)

Published year	Composition/modification	Fabrication method	Crosslinking method	Characterization	Cells	In vitro	In vivo	Target of the study	References
2014	MeGG	Blending at RT/ casting (hydrogel)	Photocrosslink or PBS	X	MSCs, human dermal microvascular endothelial cells (HDMECs)	MTS assay, Elisa, calcein-AM staining, histology (H&E, Alcian blue, Movat's pentachrome staining, collagen II), TUNEL assay, TEM	Subcutaneous implantation (H&E, vimentin, aggrecan, collagen II)	Nucleus pulposus TE	[100]
2014	Gelatin methacrylamide-GG, mesenchymal stromal cell (MSC)-laden polylactic acid microcarriers	Blending at 90 °C/3D printing (hydrogel)	Physical, photocrosslink of GelMA	Compression test, DMA	MSCs from Lewis rats	Phalloidin-FITC staining, lactate dehydrogenase (LDH) activity, ALP activity, osteocalcin (OCN) quantification, live/dead staining, immunofluorescence (actin)	X	Target for bone and osteochondral constructs	[130]
2014	Polyacrylamide (PAAm), GG	Blending at RT/ casting (hydrogel)	$CaCl_2$	Mass loss, swelling ratio, CD spectroscopy, ultraviolet visible (UV-vis) spectroscopy, compression test, cyclic test	L929, PC12	Cell viability analyzer, DNA content	X	Development of tissue engineering applications based on these gel materials	[133]
2014	HA/GG	Blending at 90 °C/ casting (spongy-like hydrogel)	PBS	μ-CT, SEM, Cryo-SEM, water uptake	Human ASCs, human adipose microvascular endothelial cells (hAMECs)	Flow cytometry (CD105, CD73, CD90, CD45, CD34, CD31), Matrigel assay, uptake of acetylated low-density lipoprotein (Dil-Ac-LDL)	Implantation in mouse excisional wound healing model (H&E, Masson's trichrome, immunolabeling-CD31, phalloidin-TRITC, quantification of collagen and non-collagenous proteins), wound closure assessment	Skin TE	[58]
2014	GG	Blending at 90 °C/ casting (spongy-like hydrogel)	$CaCl_2$, PBS, MEM alpha medium	Microscopic analysis, μ-CT, compression test, recovery test, mass loss, water uptake, water content quantification	Human ASCs, hDMECs, hKC, SaOs-2	DNA content, live/dead staining, phalloidin-TRITC staining	X	Engineering cell-compatible scaffold with essential physical and biological features for TE	[60]

2014	LAGG, HAp	Blending at 60 °C/ casting (hydrogel)	PBS	Bioactivity (simulated body quid (SBF)), spectrometer, FTIR, XRD	X	X	X	OCTE	[92]
2014	LAGG, bioactive glasses of type A2, S2, and NBG	Blending at 40 °C/ casting (hydrogel)	$MgCl_2$	Gelation kinetics, degradation, SEM, μ-CT, hydrogel mineralization (SBF), compressive stress/ strain measurement, FT-IR, XRD, ICP-OES, antibacterial test	MG63, MSCs	Live/dead staining, MTT, WST-8 assay, LDH assay, ALP activity	X	Bone TE	[89]
2014	LAGG, G4RGDSY and G4RGESY peptide/ carbodiimide reaction	Blending at 80 °C/ casting (hydrogel)	$CaCl_2$	Atomic absorption spectroscopy (AAS), radiolabelling (chloramine-T), radio-HPLC, Zeba Spin Desalting Columns, viscosity measurement	C2C12, PC12	Calcein-AM, propidium iodide and DAPI staining, MTS assays	X	Improve cell adhesion	[51]
2015	RGD, purified GG/ carbodiimide reaction	Blending at 60 °C/3D printing (hydrogel)	DMEM or $CaCl_2$	SEM, diffusion study	Primary cortical neurons harvested from E18 embryo of BALB/ cArcAusb mice	Live/dead staining, immunofluorescence staining (GFAP, anti-β-III-tubulin)	X	Understanding brain injuries and neurodegenerative diseases	[52]
2015	GGMA	Casting (hydrogel)	Photocrosslink	NMR, compressive elastic modulus measurement	Chondrocytes from human cartilage	Glycosaminoglycan (GAG) content, dsDNA content, RT-PCR, immunofluorescence staining (collagen I, collagen II, aggrecan, DAPI)	X	Cartilage TE	[134]
2016	GG, α-TCP	α-TCP coated with GG at 100 °C	Physical	Compression test, XRD, SEM, immersion test	X	X	X	Bone TE	[55]

(continued)

Table 2.1 (continued)

Published year	Composition/modification	Fabrication method	Crosslinking method	Characterization	Cells	In vitro	In vivo	Target of the study	References
2016	Immobilize maleimide-containing GRGDS peptides, furan-modified GG/Diels-Alder click chemistry	Blending at 40 °C/casting (hydrogel)	$CaCl_2$	X	ASCs, OEG from olfactory bulbs of neonatal Wistar-Hans rat	Immunocytochemistry (ICC) and phalloidin/DAPI staining, DRGs neurite extension analysis	SCI surgery (BBB score, activity box test, immunohistochemistry-IHC, CD 11b/c, GFAP, neurofilament, nuclei antibody)	Lumbar SCI regeneration	[132]
2016	Alginate, GG	Blending at 80 °C/3D printing (hydrogel)	$CaCl_2$	Porosity, swelling, SEM compression test	hMSCs	DNA quantification, ALP activity, immunofluorescence staining (cytoskeleton)	X	Improve biocompatibility	[124]
2016	MeGG, laponite	Blending at 60 °C	Photocrosslink	FT-IR, NMR, rheological experiment, SEM, swelling, diffusion test	The human fibroblast cell line	Neutral red assay	X	Confirm biocompatibility	[122]
2016	LAGG, Ca/Mg microparticle	Blending and gelation at 37 °C/casting (hydrogel)	$CaCl_2$, $MgCl_2$	FT-IR, Raman, XRD, SEM, TEM, AAS, DLS, ICP-OES, gelation speed, μ-CT, 3D analysis	MG-63	Alamar Blue, live/dead staining	X	Bone TE	[71]
2017	Aldehyde-modified GG, hydrazide-modified HA	Blending at RT/casting (hydrogel)	$CaCl_2$	NMR, gelation point test, FT-IR, swelling ratio, enzymatic degradation, storage (G′) and loss (G″) modulus	X	X	X	Soft TE	[135]
2017	GG, Manuka honey	Blending at 70 °C/casting (film)	$CaCl_2$	FTIR, swelling, gel fraction, water vapor transmission rate, tensile strength	X	X	X	Wound dressing application	[129]
2017	GG, eumelanin	Blending at 90 °C/casting (spongy-like hydrogel)	$CaCl_2$	FTIR, UV/Vis absorption, conductivity, μ-CT, compression test, swelling, release study, SEM	hKCs, mouse C3H/connective tissue fibroblast-like cell line (ECCC)	TEM, live/dead staining, immunocytochemistry (K5, K10), DNA content, reactive oxygen species (ROS), reactive nitrogen species (RNS) assay, MTS assay	Subcutaneous implantation (H&E, Masson's trichrome)	Skin TE	[63]

2017	GG, saponin	Blending at 40 °C/ casting (hydrogel)	$CaCl_2$	SEM, FTIR, compressive stress' strain measurement, water uptake, degradation	Chondrocytes from New Zealand white rabbits	SEM, MTT, RT-PCR	X	Cartilage TE	[69]
2017	GRGDS peptides, furan-modified GG/ Diels-Alder click chemistry	Blending at 37 °C7 casting (hydrogel)	Photocrosslink	X	ASCs	MTS, RT-PCR, phalloidin/ DAPI staining, NF staining, DRG analysis	X	SCI regeneration	[56]
2018	WHLPFKC or FF Gen3K (WHLPFKC)16 (unmodified or modified VEGF blocker peptides), MeGG	Blending at 42 °C/ casting (hydrogel)	PBS	X	Human umbilical vascular endothelial cell	EC sprouting 3D tests and qualitative analysis, histology (H&E, lectin), morphometric image analysis	X	An alternative approach to prevent angiogenesis in TE	[136]
2018	Glycidyl methacrylate type I collagen, MeGG	Blending at RT/ casting (hydrogel)	$CaCl_2$, photocrosslink	SEM, swelling, storage (G') and loss (G'') modulus, degradation, NMR	Bone marrow stem cells from SD rats	WST assay, live/dead staining, RT-PCR	X	Vascular TE	[102]
2018	Poly(ethylene glycol) diacrylate (PEGDA), GG	Blending at 37 °C/3D printing (hydrogel)	Photocrosslink	Rheological measurement, shear-thinning and shear-recovery test, compression test, degradation study	Murine bone MSCs	Live/dead staining, histology (F-actin, DAPI)	X	Intervertebral disc TE	[137]
2018	Halloysite nanotubes (HNT), GG, PCL	Injecting hydrogel into 3D printed scaffold	$SrCl_2$ $CaCl_2$	Stereomicroscopy for morphology, X-ray photoelectron spectroscopy (XPS), water uptake, compression test, stress-relaxation test, finite element method (FEM)	TERT-hMSCs, HUVECs	Live/dead staining, presto blue assay, ALP assay, DNA content, OPN and OCN protein expression by ELISA, histology (Alizarin red)	X	Fabricate effective system to study and promote osteogenesis	[131]
2018	TiO2 nanotubes, GG	Blending at 70 °C/ casting (film)	$CaCl_2$	FTIR, XRD, SEM, TEM, EDX	NIH-3 T3 fibroblasts	Acridine orange/propidium iodide, MTT	X	Skin TE	[101]

(continued)

Table 2.1 (continued)

Published year	Composition/modification	Fabrication method	Crosslinking method	Characterization	Cells	In vitro	In vivo	Target of the study	References
2018	GG, HAp	Blending at 60 °C/ casting (spongy-like hydrogel)	$CaCl_2$	Micro-CT, SEM, water uptake, DMA	Bone marrow cells from mice	Tartrate-resistant acid phosphatase (TRAP) staining, live/dead staining, Alamar Blue assay, RT-PCR	X	Bone TE	[59]
2018	GG, polyaniline	Coating at 4 °C casting (spongy-like hydrogel)	$CaCl_2$, PBS	FTIR, SEM, four-point probe technique, compression test	L929, C2C12 myoblast	MTS assay, DNA quantification, immunostaining (myosin)	X	Skeleton muscle TE	[62]
2018	GG, HAp	Blending at 60 °C casting (spongy-like hydrogel)	$CaCl_2$	FTIR, XRD, TGA, SEM, degradation, swelling, DMA, μ-CT, bioactivity (simulated body fluid (SBF))	Human ASCs	Live/dead staining	X	Bone TE	[61]
2018	GG,DC	Coating at RT/ casting (sponge)	$CaCl_2$	Porosity, SEM, compression test, antioxidant ability	NIH/3T3 fibroblasts, RAW 264.7	SEM, MTT, RT-PCR	Subcutaneous implantation (H&E, ED-1)	Improve biocompatibility	[128]
2018	GG, DVS	Blending at 37 °C/ casting (hydrogel)	Bis-thiol crosslinker	Swelling, network sol fraction analysis, storage (G′) and loss (G″) modulus, FRAP, degradation, GPC	HUVECs	Centrifugal cell adhesion assay, cell encapsulation, live/dead staining	X	Vascular TE	[54]
2018	Hap, LAGG, HAGG	Blending at 90 °C/ casting (hydrogel)	PBS	Stereo microscope, μ-CT, DMA, swelling and degradation, bioactivity (simulated body fluid (SBF))	L929, chondrocytes and osteoblasts from New Zealand white rabbit	Proliferation assay, live/ dead staining, DNA content	Subcutaneous implantation (H&E, Masson's trichrome), orthotopic knee model (computed tomography, H&E, safranin-O/light green, Masson's trichrome)	Osteochondral TE	[93]
2018	GG, α-TCP	Blending/casting (hydrogel)	Physical	μ-CT, XRD, FTIR, SEM, ICP-OES, Raman, rheometry analysis, Ca and P release profile	X	X	X	Bone TE	[76]

2018	GG, Ca, Mg	Blending at 90 °C casting (hydrogel) and soaking in calcium/magnesium solution	$CaCl_2$	ATR-FTIR, XRD, SEM, EDS, ICP-OES, TGA, compression test	MC3t3-El	Alamar Blue	X	Bone TE	[77]
2018	HAGG, MeGC, chitosan	Blending different mixture of HAGG and MeGG and injecting inside the chitosan hollow tubes/casting (sponge)	PBS	SEM, μ-CT, water uptake, weight loss	Rat immortalized Schwann cells (iSCs)	Alamar Blue, live/dead staining	10 mm rat sciatic nerve defect (H&E, toluidine blue immunohistochemistry staining – NF200, ED1, CD31, CD34 DAPI)	Nave TE	[34]
2019	GG, poly ethylene glycol (PEG)	Blending at 80 °C/ casting (hydrogel)	$CaCl_2$	FT-IR, porosity, degradation, water uptake	Human retinal pigment epithelium cell line (ARPE-19)	MTT, RT-PCR, histology (H&E)	X	Retinal TE	[66]
2019	GG, poloxamer-heparin (PoH)	Blending at 60 °C/ casting (hydrogel)	$CaCl_2$	NMR, FT-IR, viscosity, TGA, SEM, compression test, swelling ratio, sol fraction, weight loss	Rabbit bone MSCs	SFM, MTT, live/dead staining, dsDNA content, ALP, RT-PCR, histology (H&E, laminin, E-cadherin)	Subcutaneous implantation (H&E, ED-1)	Stem cell delivery	[138]
2019	GG, HA	Blending at 60 °C/ casting (hydrogel)	$CaCl_2$	SEM, FT-IR, swelling ratio, degradation ratio, sol fraction, compression test	Rabbit chondrocytes	MTT, live/dead staining, SEM, dsDNA content, GAG content, RT-PCR	Implantation in rabbit articular cartilage defects (H&E, safranin-O, toluidine blue)	Cartilage TE	[139]

verified biocompatibility and biodegradability by *J.T. Oliveira* et al. with an injectable GG hydrogel for cartilage TE [44, 45]. Another report suggested modified GG hydrogel by oxidation process to provide an optimized gelling point while remaining injectable processability for chondrocyte encapsulation [32]. These reports demonstrated that GG hydrogels can sufficiently support the growth and ECM deposition in vitro and in vivo. Chemically modified GG scaffolds are also reported to be effective in viability, cytotoxicity, proliferation, and differentiation. For example, researches were conducted in vitro and in vivo study with a methacrylate GG (MeGG) [31, 48–50]. *D.F. Coutinho* et al. study showed the physical and mechanical properties of modified GG. The mechanical properties, swelling, and degradation were shown to be tuned by a different crosslinking mechanism. The in vitro study which was performed by cell encapsulation in the modified matrix showed high cell viability which verifies the applicability of the material in TE. Further in vitro and in vivo study was conducted by *J.S. Correia* et al. which showed stability in supporting cells and nontoxic in vivo. Improving mechanical property or encapsulation of stem cells in the modified GG was proceeded by *H. shin* et al. and *M.B. Oliveira* et al., respectively. Biocompatibility of the GG matrix was also enhanced by modifying the surface of GG chain. A peptide-modified GG hydrogel was studied to be effective in providing a microenvironment for anchorage-dependent cells [51–56]. *N.A. Silva* et al. and *E.D. Gomes* et al. respectively proposed a fibronectin-derived synthetic peptide (GRGDS)-modified GG hydrogel for the treatment of spinal cord injury (SCI). The studies displayed highly increased cell survival and proliferation which may be a benefit for SCI TE. *C.J. Ferris* et al. also showed peptide-modified GG. The study modified GG with arginine-glycine-aspartic acid (RGD) and displayed enhanced adhesion, spreading, growth, and differentiation in the modified matrix which verifies the biocompatibility. *R. Lozano* et al. also used RGD-modified GG to fabricate layered brain-like structures with 3D printing. A spongy-like GG is also suggested as an efficient microenvironment for biocompatibility [57–64]. *L.P. Silva* et al. displayed and proposed spongy-like hydrogel for diverse TERM. The study showed an efficient effect on a variety of cells in vitro. Furthermore, incorporation or grafting of bioactive molecules, inorganic materials, polysaccharides, and synthetic polymers in GG or modified GG is reported to be biocompatible and displayed enhanced biological activity [49, 62, 63, 65–77]. To sum up, these researches showed and confirmed the biocompatibility and biodegradability of GG and modified GG. These reports exhibit potential for application in a wide range of TE.

2.3 Application of GG-Based Scaffold

The application of GG-based scaffold in a wide range of TE has been studied in many papers. The GG displayed many merits in TERM due to its abundance in nature, low cost, flexible mechanical properties, easy manufacturing and crosslinking process, thermoresponsive characters, and similar environment to ECM by containing a large amount of water. The most widely used fields of GG-based scaffolds are cartilage, bone, osteochondral, and spinal cord TE. In this section, we will talk more about the most reported area which is cartilage, bone, osteochondral, and spinal cord injury that utilized GG-based scaffold for TE. In addition, other applications will be discussed.

2.3.1 Cartilage TE

Cartilage is a tissue which is composed of 3D microenvironment up to 80% of water and ECM consist of proteins and glycosaminoglycans [78]. The structure and organization of the cartilage tissue can be divided into four different areas based on collagen fiber alignment and composition of proteoglycan. A superficial zone which is the uppermost part of the cartilage has the lowest proteoglycan and the collagen fibers are arranged parallel to the surface. A middle zone is composed of proteoglycan and collagen fibers that are unaligned to the cartilage surface. A deep

zone has the most proteoglycan content and constitutes of radially aligned collagen fibers. A calcified zone does not consist of proteoglycan, has less organized collagen fibers that are branched, and tends to mineralize [79]. Treatment for cartilage defects is still a challenge for clinician and researchers. The cartilage defects which are generated by disease, trauma, or aging are difficult to self-repair due to devoid of blood or lymphatic vessels [80]. A variety of treatment methods have been suggested for the damaged cartilage such as autogenic or allogenic tissue implantation, osteochondral transfer, and arthroscopic repair procedures [81, 82]. One of the most promising techniques to repair the defected cartilage tissue is the tissue-engineering methods based on scaffolds [83].

The GG-based scaffold for the cartilage TE has been proposed as a suitable carrier of drugs and/or cells. Most of the reported researches applied GG as a gel form for cartilage TE. *J.T. Oliveira* et al. reported in vitro and in vivo study of pure GG hydrogels crosslinked with $CaCl_2$. The results represented a potential of the hydrogel for cartilage engineering in mechanical terms. The GG hydrogel displayed appropriate rheological property for cells to homogeneously mix and gel at body temperature which allowed cells to encapsulate within the hydrogels. This property allows noninvasive injection into the defected cartilage. In vitro study which was performed in long term showed an increase in viability, cell number, and cartilage-specific proteins and genes which verifies the biocompatibility of the material. The preliminary in vivo study displayed sustained mechanical stability of the hydrogels after implantation and did not show persistent inflammatory response [45]. An injectable GG hydrogel encapsulated with autologous cells to full-thickness articular cartilage defect was also reported. *J.T. Oliveira* et al. showed that GG hydrogel encapsulated with chondrogenic pre-differentiated rabbit adipose stem cells (ASCs) displayed high regeneration in vivo which allows a promising approach to treat damaged articular cartilage [44]. *Y. Gong* et al. proposed an improved injectable GG hydrogel by lowering the gelling point while maintaining the injectability. The modified GG had an optimized gelation temperature for uniform suspension of chondrocytes in the matrix. The in vitro studies such as biochemical analysis, histology, and immunofluorescent were performed for 150 days to confirm biocompatibility in the long term of the modified gel. The result showed a promising vehicle for chondrocyte delivery to treat injured cartilage tissue [32]. *Y. Tang* et al. showed a double-network hydrogel of GG and carboxymethyl chitosan for chondrocyte encapsulation. The study used an oxidized GG and grafted carboxymethyl chitosan by a Schiff base reaction. The complex gel showed highly improved gelation temperature which was lowered to optimized temperature for chondrocyte encapsulation. The mechanical properties were enhanced with an ability to return to the original form. The in vitro exhibited improved viability of cells which shows a promising material for cartilage TE [84]. *H.Y. Jeon* et al. evaluated saponin-loaded GG hydrogel for cartilage regeneration. The research showed a positive effect of biomolecules in GG hydrogel for the encapsulated chondrocytes in vitro [75]. Furthermore, *H. Lee* et al. suggested a proper GG hydrogel concentration for fibrocartilage TE by displaying mechanical characterizations [35]. These reports confirm the great potential of GG material for application in cartilage TE.

2.3.2 Bone TE

Bone is a highly vascularized and biomineralized connective tissue which plays a vital role in supporting the body. The organization of bone is classified into the macrostructure, microstructure, and nanostructure. The macrostructure of the bone tissue is divided into cortical and cancellous bone. The microstructure is composed of cortical bone which is composed of repeating units of osteon and cancellous bone which is made up of an interconnecting structure of trabeculae that is filled with bone marrow. The nanostructure is constituted with large amounts of collagen fibers, calcium phosphate, and noncollagenous organic proteins. The organization of the bone ECM and specific structure of the

bone tissue is the reason for the high mechanical strength [79]. The bone tissue remodels constantly by processing bone deposition by osteoblasts and bone resorption by osteoclasts [85]. Although bone has native healing potential and most of the damaged bone can regenerate well with conventional therapy or surgery, the critical size of the defect is unlikely to repair completely [86]. The interest in the development of scaffolds has been increasing to reconstruct critical-sized bone defects. The scaffold for bone TE should compose of the similar environment to the native bone tissue ECM which has collagen type I, osteopontin bone sialoprotein, osteonectin, and platelet hydroxyapatite crystals. Furthermore, the mechanical property of the scaffold should match the cancellous bone which has a compressive strength of 2–12 MPa and modulus of 50–500 MPa. The microstructure of the scaffold should be highly porous for vascularization and promote nutrient and oxygen change. Ceramic material is mostly suggested for bone TE due to its similarities to the native bone tissue.

An osteoconductive scaffold which provides cell attachment, proliferation, differentiation, and ECM development has been made with GG-based scaffold. S.J. Chang et al. showed an effect of GG film for guided bone regeneration (GBR). Critical-sized skull defects on Sprague-Dawley (SD) rats were covered with GG film for 2 months. The covered region showed a clear boundary space between connective tissue which shows a promising application in GBR [87]. *T.E.L. Douglas* et al. displayed GG hydrogel loaded with alkaline phosphatase (ALP) to make suitable scaffold for bone TE. Furthermore, the mineralization and mechanical property of the GG hydrogel was enhanced by incorporating polydopamine (PDA). The ALP helped the formation of apatite-like material within GG hydrogel and PDA enhanced enzymatic mineralization, osteoblastic cell adhesion, and proliferation [88]. *T.E.L. Douglas* et al. exhibited GG hydrogel enriched with bioglass particles to improve mechanical properties, antibacterial characters, and microenvironment for bone TE. The study showed GG hydrogel incorporated with different types of bioglasses. The bioglass promoted mineralization of GG hydrogel and mechanical properties, antibacterial properties, and differentiation of rat mesenchymal stem cells (MSCs) were affected depending on the types of the bioglasses [89]. *T.E.L. Douglas* et al. also established an improved injectable GG hydrogel by incorporation of an inorganic phase in particles for bone TE. The results showed that carbonate microparticles with a sufficient amount of Mg in GG hydrogel produced an injectable and cytocompatible hydrogel. *J. W* et al. introduced a porous α-tricalcium phosphate (α-TCP)/GG scaffold for bone repair. The GG was coated on α-TCP and the mechanical properties were adjusted for the bone graft. *F.R. Maia* et al. displayed hydroxyapatite reinforced GG spongy-like hydrogels to observe osteoclastogenesis. The result displayed positive effect in the differentiation of bone marrow cells into pre-osteoclasts which confirm promising scaffold for future bone TE applications [59]. *M.G. Manda* et al. showed GG-hydroxyapatite (HAp) composite spongy-like hydrogels for bone TE. The study exhibited GG scaffolds with or without $CaCl_2$ crosslinker and HAp. The $CaCl_2$ and HAp reinforced mechanical properties of the scaffolds. The bioactivity of the cells was improved with higher adherence and spreading within the biomaterials during 21 days of culture [61]. *M.A. Lopez-Heredia* et al. suggested that alternate soaking in solutions of calcium/magnesium and carbonate ion solution can increase mineralization of GG hydrogels for bone TE [70]. *T.E.L. Douglas* et al. showed that adding α-TCP in GG solution can induce self-gelling injectable hydrogel that can be used in bone TE. The results revealed the inhomogeneous distribution of the inorganic composites in the hydrogels [69].

2.3.3 Osteochondral TE

Osteochondral (OC) TE must take into account the regeneration of both the articular cartilage and the subchondral bone [90]. The OC injury includes degeneration in cartilage, the interface of bone and cartilage, and bone. As the OC tissue has three different tissue layers with each layer

having different characteristics, combinations of multiple factors and delivery methods are required to meet the OC TE [91].

Many efforts have been made by using GG to make a scaffold suitable for the OC region. *D.R. Pereira* et al. reported GG-based hydrogel bilayered scaffolds for OC regeneration. The scaffold was designed by fabricating bilayered hydrogel with LAGG, the cartilage-like layer, and LAGG loaded with HAp, the bone-like layer. The scaffold was tested with in vitro bioactivity analysis. The result displayed promising scaffold for OC TE [92]. The in vitro study with rabbit's chondrocytes and osteoblasts in each layer was also tested from *D.L. Pereira* et al. The cytocompatibility of the scaffold was confirmed and biocompatibility was further analyzed with an in vivo study. The scaffold was implanted under subcutaneous part in mice which exhibited a weak immune response after 4 weeks. The in vivo study was also carried out by injecting the acellular scaffold in the osteochondral defects in the rabbit's knee for 4 weeks. The results showed successful in vitro and in vivo performance which leads the scaffold to further advanced platforms to treat the osteochondral defects [93].

2.3.4 Spinal Cord Injury (SCI) Regeneration

SCI which results in paraplegia or quadriplegia is a challenging task to be solved for clinicians and researchers as there is no effective therapeutic method so far. The SCI can be divided into primary and secondary injury. The primary injury results from direct damage of the spinal cord tissue from the initial mechanical force. This injury causes neural cell death, breakage of nerve fiber, and hemorrhagic necrosis and edema. The secondary injuries are ischemia and hypoxia in the spinal cord, immune and inflammation response, excitotoxicity, and formation of glial scar and cavity [94–96]. The focuses of current research on SCI are related to the secondary. The aims include reducing the neuronal cells death, inhibiting immune and inflammatory reactions, and promoting the growth of axons to build up synapses [97, 98].

There have been researches on GG-based scaffold for treating SCI. *N.A. Silva* et al. represented 3D tubular structures to regenerate SCI regions. The tubular structure was constructed by using 3D bioplotting with a biodegradable blend of starch. The GG hydrogel was injected in the center of the structures. The characterization of the scaffolds, biocompatibility, and bioactivity of the material all matched the TE standards. The in vivo study within the rat SCI model showed well-integrated scaffold and tissue and did not cause chronic inflammatory response [99]. The investigation of peptide-modified GG hydrogel for SCI regeneration was carried out by *N.A. Silva* et al. The GG hydrogel was grafted with a fibronectin-derived synthetic peptide (GRGDS) by Diels-Alder click chemistry. The modified GG hydrogel presented enhanced adhesion, survival, proliferation, and morphology of a neural stem/progenitor cell (NSPC). Furthermore, the study displayed that co-culture of NSPC and olfactory ensheathing glia (OEG) in the modified GG can enhance the survival and outgrowth of NSPC which demonstrate a therapeutic benefit for SCI repair [53]. *E.D. Gomes* et al. also used GG hydrogel modified with the GRGDS for SCI regeneration. The GRGDS-modified GG hydrogel was combined with ASCs and OEG. The in vitro resulted with high neurite outgrowth and the in vivo study in a hemisection SCI rat model transplanted with ASCs and OEG encapsulated in a GRGDS-modified GG hydrogel showed a low infiltration of inflammatory cells and astrocytes and increased neurofilament. *E. Oliveira* et al. compared different ECM-like hydrogels and studied neurite outgrowth. The GRGDS-modified GG hydrogel, collagen, and a hydrogel rich in laminin epitopes (NVR-gel) were used for the study. The results showed that all the hydrogels supported cell survival and viability but showed different gene expression levels [56].

2.3.5 Other Applications

Besides the applications that are mentioned above, researches in various TE have been carried out. *R. Tsaryk* et al. tested the effect of

MeGG hydrogel for nucleus pulposus regeneration. The nasal chondrocytes and MSCs were used to investigate the MeGG hydrogel in vitro which resulted in non-cytotoxicity in extraction assays and did not induce pro-inflammatory responses in endothelial cells. The in vivo study was also studied and exhibited that the material induced chondrogenesis in subcutaneous implantation [100]. *R. Lozano* et al. developed an in vitro model of the brain with 3D printing by using the GG modified with a short peptide GGGGRGDSY (RGD). The bioink was printed by combining the modified GG with primary cortical neurons. The modified GG showed a positive effect on primary cell proliferation and network formation. Many types of research on skin TE have also been performed [52]. *L.P. da Silva* et al. exhibited eumelanin-releasing spongy-like hydrogels for skin reepithelialization. The in vitro with human keratinocytes and in vivo under subcutaneous part in mice were well performed and showed promising material for skin regeneration [63]. *N.A. Ismail* et al. evaluated GG film loaded with TiO_2 nanotubes for skin TE. The chemical and mechanical properties of the novel film were appropriate for skin TE and in vitro studies showed non-cytotoxicity and proliferation of the cells [101]. In addition, the GG was used in promoting vascularization. *M.T. Cerqueira* et al. proposed a cell-adhesive GG-hyaluronic acid (HA) spongy-like hydrogel for neovascularization in skin wounds. The matrix allowed cell entrapment and encapsulation by interactions between a cell and polymer. The in vivo study was conducted by implanting the polymeric network into mice full-thickness excisional wounds. The GG-HA spongy-like hydrogel showed biocompatibility, successful tissue formation, and reepithelialization [58]. *H. Chen* et al. also suggested GG-based scaffold for effective vascularization. The MeGG and type I collagen was ion/photo dual crosslinked and evaluated physicochemical properties and biological activity of MSCs for effective vascularization. The results of the study show the potential for future material for bioink [102].

2.4 Fabrication of GG-Based Scaffold

The architecture and manufacturing method of scaffolds used for TE is significant. In all multicellular organisms, a complex and bioactive matrix, which is called the ECM, structurally supports cells [6, 8, 103]. The ECM is an organization of proteins and polysaccharides that plays a critical role in deriving migration, differentiation, and growth of cells [103]. Therefore, scaffolds should contain microenvironment for cells to produce ECM. An interconnected pore structure and high porosity is a critical factor to consider as these structures lead to penetration of cells and adequate diffusion of gases and nutrients to cells within the matrix and eventually ECM can be formed by these cells [18, 19, 104]. Although a critical range of pore sizes may differ depending on the target tissue, the pores need to be large enough to allow cells to migrate into the structure, but small enough to establish a sufficiently high specific surface [105–107]. In addition, a porous interconnected structure allows removal of the waste product by diffusion from the scaffold but it is important that the diffused products are not toxic in vivo and interfere with the surrounded tissue [18]. Furthermore, since most cells are anchorage dependent, it is important for the scaffold to provide an attachment site on the material [51, 53]. To sum up, the goal of the scaffold in TE is to promote ECM production, cell adhesion, proliferation, and differentiation.

Herein, we will talk more about the types of GG-based scaffold that had been reported.

2.4.1 Hydrogel

Hydrogels have obtained many attentions in the field of TE. The backbone of hydrogels is composed of hydrophilic moieties (carboxyl, amino, amide, hydroxyl groups) which are crosslinked physically or chemically [16]. The main merit of hydrogels is similar microenvironment to natural ECM. This property is due to the ability to retain

large quantities of water [108, 109]. The equilibrium swollen state of hydrogels is reached through a balance between osmotic driving forces. This process is encouraged by the entrance of water and biological saline into the hydrogels and the cohesive forces exerted by the polymers [16, 110]. The number of hydrophilic polymers in the chain or the extent of crosslinking affects the swelling ratio of the hydrogel [111]. Furthermore, hydrogels have advantages to treat tissue in a minimally invasive method which allowed extensive studies on drug delivery, cell carrier, and TE [16, 112, 113].

GG has been widely applied in TE as hydrogel form due to its attractive characteristics such as structural similarity with native glycosaminoglycans and elastic moduli similar to common soft tissue [25]. As we discussed earlier in the GG structure section, the gelation is greatly affected by external temperature and presence of cations in which divalent cations make stronger physical properties of GG hydrogel. The injectable GG hydrogel which is crosslinked with cations has been investigated for tissue regeneration [32, 44, 65, 68, 75, 84, 92, 93, 114–123]. The target tissues include cartilage, bone, osteochondral, and retinal pigment epithelium. However, GG hydrogels which are crosslinked with cations have low stability due to the exchange process of divalent cations and monovalent ones that are presented in higher concentrations in the physiological environment. Mechanical properties of physically crosslinked GG hydrogels are also weak. Thus, MeGG and double network with other polymers have been suggested to enhance mechanical and degradation properties that can match the native tissues [31, 48–50, 102, 124, 125]. Researches of MeGG confirmed its safety in vitro and in vivo. Another critical limitation of GG hydrogels is the lack of specific attachment sites. Chemical modification of grafting peptide to GG chains has been proceeded to overcome this limitation. The modified GG hydrogel showed the successful result in biocompatibility and exhibited various applications such as brain-like structure and matrix for neural stem/progenitor cell, endothelial cell, lumbar spinal cold, and ASCs [51–56].

2.4.2 Sponge

Sponge scaffold refers to a porous 3D structure which provides proper microenvironments for cultured cells [8, 126]. The porosity and pore size of sponge scaffold affect cell growth, function, migration, and transportation of nutrient and diffusion of waste. In addition, the pores assist and promote new tissue formation in vivo [18, 105, 106, 127]. There are various methods to fabricate 3D porous scaffold. Typical techniques are freeze-drying, phase separation, salt leaching, and gas foaming [18].

GG-based sponge scaffolds have been characterized and in vitro and in vivo was proceeded to confirm its application in TE. Most of the GG-based sponge scaffolds were fabricated by the freeze-drying method. A spongy-like GG hydrogel was introduced and reported improved mechanical and physical properties when compared to GG hydrogel. This research also showed improved adhesion of human ASCs, dermal microvascular endothelial cells (hDMECs) and human keratinocytes (hKC), and human osteoblast-like cells (Saos-2) in spongy-like GG hydrogel [60]. Composite of spongy-like GG hydrogel with biomolecules or other types of polysaccharide was also reported to be effective in skin wound healing purpose [58, 63]. Furthermore, it was reported that the inflammatory response of GG sponge scaffold can be enhanced by duck's feet-derived collagen (DC) [128]. Application of GG sponge scaffold is also suggested for dental filling or for bone TE [59, 61].

2.4.3 Other Fabrications

A number of researches on various biofabrication have been introduced for manufacturing GG-based scaffold. A film structure of GG was reported for bone TE. The result exhibited that 2% GG film was suitable for guiding bone regeneration [87]. Incorporation of other bioactive materials in GG was investigated for skin TE [101, 129]. Furthermore, GG-based scaffolds

manufactured by 3D printing method are reported. A study on pure GG material is only reported on the mechanical and physical concept [38]. A peptide-modified GG hydrogel was applied in manufacturing brain-like structures with 3D printing [52]. GG material was used to optimize other types of polymers for 3D printing. GG was applied in methacrylated gelatin (GelMA) to optimize the material as a bioink for 3D printing [130]. GG was also used to encapsulate cells to optimize poly(ε-caprolactone) (PCL) bioink for osteogenic model [131]. Composite of alginate and GG was also introduced to be effective in mechanical properties in which GG had shown to enhance fidelity and lower the swelling in cell culture media. In addition, the composite scaffold allowed higher proliferation and differentiation of human MSCs [132].

Nowadays, many types of biofabrication techniques such as extrusion printing, inkjet printing, wet spinning, or electrospinning have been presented and applied in TE [24]. However, compared to other types of biopolymers, biofabrication of GG is mostly reported by applying casting method. The attention in biofabrication of GG is very low. This signifies that applying various types of fabrication technique with GG is necessary. It is only a matter of time to supplement the characteristics of GG such as mechanical, physical, and microenvironment for cells and apply it to a wide field because the biofabrication method is already reported widely that may be readily applied to GG.

2.5 Conclusion

Over time, biomaterial is one of the most actively studied fields in TERM. Researchers have actively sought the materials and supplemented them with several techniques to further develop these materials. The improved biomaterials were then applied as a polymeric scaffold for a wide range of TE.

This book chapter focuses on informing readers about GG-based scaffold in various types of TE. The biocompatibility of the GG itself was confirmed in vitro and in vivo and showed a promising application in TE [45]. Many papers displayed the importance of blending with other biopolymers or biomolecules and chemical modification of GG to improve biofunctional properties such as mechanical strength, degradation characters, biocompatibility, attachment site, and gelation temperature for cell encapsulation [30, 68, 76, 77, 101, 102, 120, 125, 128, 131]. These modifications allowed GG to possess viable substrate for diverse application in tissue engineering. As we have discussed earlier, the GG-based scaffolds may be applied in cartilage TE, bone TE, osteochondral TE, disc TE, skin TE, muscle TE, neural TE, and brain TE. Considering that GG has considerable competency for modification and optimization to suit particular applications, it is expected that many avenues of application of the material are yet to be discovered. Design parameters of scaffold have been standardized over time. However, the requirement for alternative solutions to meet the requirement for substitution of organs and tissue parts will continue to guide advances in TE.

Acknowledgments This research was supported by Basic Science Research Program through the National Research Foundation of Korea (NRF) funded by the Ministry of Science, ICT & Future Planning (NRF-2017R1A2B3010270) and Korea Health Technology R&D Project through the Korea Health Industry Development Institute (KHIDI), funded by the Ministry of Health and Welfare, Republic of Korea (HI15C2996).

References

1. Groll J, Boland T, Blunk T et al (2016) Biofabrication: reappraising the definition of an evolving field. Biofabrication 8(1):013001
2. Dhandayuthapani B, Yoshida Y, Maekawa T et al (2011) Polymeric scaffolds in tissue engineering application: a review. Int J Polym Sci 2011:1–19
3. Chan BP, Leong KW (2008) Scaffolding in tissue engineering: general approaches and tissue-specific considerations. Eur Spine J 17(4):467–479
4. Wu GH, Hsu SH (2015) Review: polymeric-based 3D printing for tissue engineering. J Med Biol Eng 35(3):285–292
5. Stratton S, Shelke NB, Hoshino K et al (2016) Bioactive polymeric scaffolds for tissue engineering. Bioact Mater 1(2):93–108
6. O'Brien FJ (2011) Biomaterials & scaffolds for tissue engineering. Mater Today 14(3):88–95
7. Shoichet MS (2010) Polymer scaffolds for biomaterials applications. Macromolecules 42(2):581–591

8. Choi JH, Kim DK, Song JE et al (2018) Silk fibroin-based scaffold for bone tissue engineering. In: Chun H, Park K, Kim CH, Khang G (eds) Novel biomaterials for regenerative medicine, Advances in experimental medicine and biology, vol 1077. Springer, Singapore, pp 371–387
9. Drury JR, Mooney DJ (2003) Hydrogels for tissue engineering: scaffold design variables and applications. Biomaterials 24(24):4337–4351
10. Chen G, Ushida T, Tateishi T (2002) Scaffold design for tissue engineering. Macromol Biosci 2(2):67–77
11. Polo-Corrales L, Latorre-Esteves M, Ramirez-Vick JE (2014) Scaffold design for bone regeneration. J Nanosci Nanotechnol 14(1):15–56
12. Chun HJ, Kim GW, Kim CH (2008) Fabrication of porous chitosan scaffold in order to improve biocompatibility. J Phys Chem Solids 69(5–6):1573–1576
13. Howard D, Buttery LD, Shakesheff KM et al (2008) Tissue engineering: strategies, stem cells and scaffolds. J Anat 213(1):66–72
14. Carletti E, Motta A, Migliaresi C (2011) Scaffolds for tissue engineering and 3D cell culture methods. Mol Biol 695:17–39
15. Seo NM, Ko JH, Park YH et al (2011) In vitro biocompatibility of PLGA-HA nano-hybrid scaffold. Tissue Eng Regen Med 8(1):16–22
16. Yang DH, Lee DW, Kwon YD et al (2015) Surface modification of titanium with hydroxyapatite-heparin-BMP-2 enhances the efficacy of bone formation and osseointegration in vitro and in vivo. J Tissue Eng Regen Med 9(9):1067–1077
17. Kim MS, Park S, Chun HJ (2011) Thermosensitive hydrogels for tissue engineering. Tissue Eng Regen Med 8(2):117–123
18. Loh QL, Choong C (2013) Three-dimensional scaffolds for tissue engineering applications: role of porosity and pore size. Tissue Eng Part B Rev 19(6):485–502
19. Yoo JJ, Park YJ, Rhee SH et al (2012) Synthetic peptide-conjugated titanium allow for enhanced bone formation in vivo. Connect Tissue Res 53(5):359–365
20. Sachlos E, Czernuszka JT, Gogolewski S (2003) Making tissue engineering scaffolds work. Review: the application of solid freeform fabrication technology to the production of tissue engineering scaffolds. Eur Cells Mater 30(5):29–39
21. Hollister SJ, Maddox RD, Taboas JM (2002) Optimal design and fabrication of scaffolds to mimic tissue properties and satisfy biological constraints. Biomaterials 23(20):4095–4103
22. Lam CXF, Mo XM, Teoh SH et al (2002) Scaffold development using 3D printing with a starch-based polymer. Mater Sci Eng C 20(1–2):49–56
23. Osmałek T, Froelich A, Tasarek S (2014) In vitro study of polyoxyethylene alkyl ether niosomes for delivery of insulin. Int J Pharm 466(1–2):328–340
24. Stevens LR, Gilmore KJ, Wallace GG et al (2016) Tissue engineering with gellan gum. Biomater Sci 4(9):1276–1290
25. Bacelar AH, Silva-Correia J, Oliveira JM et al (2016) Recent progress in gellan gum hydrogels provided by functionalization strategies. J Mater Chem B 37(4):6164–6174
26. Zia KM, Tabasum S, Khan MF et al (2018) Recent trends on gellan gum blends with natural and synthetic polymers: a review. Int J Biol Macromol 109:1068–1087
27. Prajapati VD, Jani GK, Zala BS et al (2013) An insight into the emerging exopolysaccharide gellan gum as a novel polymer. Carbohydr Polym 93(2):670–678
28. Oliveira JT, Martins L, Picciochi R (2010) Gellan gum: a new biomaterial for cartilage tissue engineering applications. J Biomed Mater Res Part A 93(3):852–863
29. Lee MW, Chen HJ, Tsao SW (2010) Preparation, characterization and biological properties of gellan gum films with 1-ethyl-3-(3-dimethylaminopropyl) carbodiimide cross-linker. Carbohydr Polym 82(3):920–926
30. Koivisto JT, Joki T, Parraga JE et al (2017) Bioamine-crosslinked gellan gum hydrogel for neural tissue engineering. Biomed Mater 12(2):025014
31. Coutinho DF, Sant SV, Shin H et al (2010) Modified gellan gum hydrogels with tunable physical and mechanical properties. Biomaterials 31(29):7494–7502
32. Gong Y, Wang C, Lai RC et al (2009) An improved injectable polysaccharide hydrogel: modified gellan gum for long-term cartilage regeneration in vitro. J Mater Chem 19(14):1925–2088
33. Caggioni M, Spicer PT, Blair DL et al (2007) Rheology and microrheology of a microstructured fluid: the gellan gum case. J Rheol 51(5):851–865
34. Carvalho CR, Wrobel S, Meyer C et al (2018) Gellan gum-based mineralization of gellan gum for peripheral nerve regeneration: an in vivo study in the rat sciatic nerve repair model. Biomater Sci 6(5):1059–1075
35. Lee H, Fisher S, Kallos MS et al (2011) Optimizing gelling parameters of gellan gum for fibrocartilage tissue engineering. J Biomed Mater Res B Appl Biomater 98(2):238–245
36. De Silva DA, Poole-Warren LA, Martens PJ et al (2013) Mechanical characteristics of swollen gellan gum hydrogels. J Appl Polym Sci 130(5):3374
37. Jahromi SH, Grover LM, Paxton JZ et al (2011) Degradation of polysaccharide hydrogels seeded with bone marrow stromal cells. J Mech Behav Biomed Mater 4(7):1157–1166
38. Yu I, Kaonis S, Chen R (2017) A study on degradation behavior of 3D printed gellan gum scaffolds. Procedia CIRP 65(2017):78–83
39. Parenteau-Bareil R, Gauvin R, Berthod F (2010) Collagen-based biomaterials for tissue engineering applications. Materials (Basel) 3(3):1863–1887
40. Naahidi S, Jafari M, Logan M et al (2017) Biocompatibility of hydrogel-based scaffolds for tissue engineering applications. Biotechnol Adv 35(5):530–544

41. Wang H, Li Y, Zuo Y et al (2007) Biocompatibility and osteogenesis of biomimetic nano-hydroxyapatite/polyamide composite scaffolds for bone tissue engineering. Biomaterials 28(22):3338–3348
42. Kim DK, Kim JI, Hwang TI et al (2017) Bioengineered osteoinductive broussonetia kazinoki/silk fibroin composite scaffolds for bone tissue regeneration. ACS Appl Mater Interfaces 9(2):1384–1394
43. Lee DH, Tripathy N, Shin JH et al (2017) Enhanced osteogenesis of β-tricalcium phosphate reinforced silk fibroin scaffold for bone tissue biofabrication. Int J Biol Macromol 95:14–23
44. Oliveira JT, Gardel LS, Rada T et al (2010) Injectable gellan gum hydrogels with autologous cells for the treatment of rabbit articular cartilage defects. J Orthop Res 28(9):1193–1199
45. Oliveira JT, Santos TC, Martins L et al (2010) Gellan gum injectable hydrogels for cartilage tissue engineering applications: in vitro studies and preliminary in vivo evaluation. Tissue Eng Part A 16(1):343–353
46. Patrick CW, Uthamanthil R, Beahm E et al (2008) Animal models for adipose tissue engineering. Tissue Eng Part B Rev 14(2):167–178
47. Wang Y, Rudym DD, Walsh A et al (2008) In vivo degradation of three-dimensional silk fibroin scaffolds. Biomaterials 29(24–25):3415–3428
48. Silva-Correia J, Zavan B, Vindigni V et al (2013) Biocompatibility evaluation of ionic- and photocrosslinked methacrylated gellan gum hydrogels: in vitro and in vivo study. Adv Healthc Mater 2(4):568–575
49. Shin H, Olsen BD, Khademhosseini A et al (2012) The mechanical properties and cytotoxicity of cell-laden double-network hydrogels based on photocrosslinkable gelatin and gellan gum biomacromolecules. Biomaterials 33(11):3143–3152
50. Oliveira MB, Custódio CA, Gasperini L et al (2016) Recent progress in gellan gum hydrogels provided by functionalization strategies. Acta Biomater 41(1):119–132
51. Ferris CJ, Stevens LR, Gilmore KJ et al (2015) Peptide modification of purified gellan gum. J Mater Chem B 3:1106–1115
52. Lozano R, Stevens L, Thompson BC et al (2015) 3D printing of layered brain-like structures using peptide modified gellan gum substrates. Biomaterials 67:264–273
53. Silva NA, Cooke MJ, Tam RY et al (2012) The effects of peptide modified gellan gum and olfactory ensheathing glia cells on neural stem/progenitor cell fate. Biomaterials 33(27):6345–6354
54. Da Silva LP, Jha AK, Correlo VM et al (2018) Gellan gum hydrogels with enzyme-sensitive biodegradation and endothelial cell biorecognition sites. Adv Healthc Mater 7(5):1700686
55. Gomes ED, Mendes SS, Leite-Almeida H et al (2016) Combination of a peptide-modified gellan gum hydrogel with cell therapy in a lumbar spinal cord injury animal model. Biomaterials 105:38–51
56. Oliveira E, Assunção-Silva RC, Ziv-Polat O et al (2017) Influence of different ECM-like hydrogels on neurite outgrowth induced by adipose tissue-derived stem cells. Stem Cells Int 2017:6319129
57. Gantar A, Da Silva LP, Oliveira JM et al (2014) Nanoparticulate bioactive-glass-reinforced gellan-gum hydrogels for bone-tissue engineering. Mater Sci Eng C 43:27–36
58. Cerqueira MT, Da Silva LP, Santos RC et al (2014) Gellan gum-hyaluronic acid spongy-like hydrogels and cells from adipose tissue synergize promoting neoskin vascularization. ACS Appl Mater Interfaces 6(22):19668–19679
59. Maia FR, Musson DS, Naot D et al (2018) Differentiation of osteoclast precursors on gellan gum-based spongy-like hydrogels for bone tissue engineering. Biomed Mater 13(3):035012
60. Da Silva LP, Cerqueira MT, Sousa RA et al (2014) Engineering cell-adhesive gellan gum spongy-like hydrogels for regenerative medicine purposes. Acta Biomater 10(11):4787–4797
61. Manda MG, Da Silva LP, Cerqueira MT et al (2018) Gellan gum-hydroxyapatite composite spongy-like hydrogels for bone tissue engineering. J Biomed Mater Res Part A 106(2):479–490
62. Srisuk P, Berti FV, Da Silva LP et al (2018) Electroactive gellan gum/polyaniline spongy-like hydrogels. ACS Biomater Sci Eng 4(5):1779–1787
63. Da Silva LP, Oliveira S, Pirraco RP et al (2017) Eumelanin-releasing spongy-like hydrogels for skin re-epithelialization purposes. Biomed Mater 12(2):025010
64. Chang SJ, Huang YT, Yang SC et al (2012) In vitro properties of gellan gum sponge as the dental filling to maintain alveolar space. Carbohydr Polym 88(2):684–689
65. Cerqueira MT, Da Silva LP, Santos TC et al (2014) Human skin cell fractions fail to self-organize within a gellan gum/hyaluronic acid matrix but positively influence wound healing. Tissue Eng Part A 20(9–10):1369–1378
66. Kim HS, Kim D, Jeong YW et al (2019) Engineering retinal pigment epithelial cells regeneration for transplantation in regenerative medicine using PEG/gellan gum hydrogels. Int J Biol Macromol 130:220–228
67. Da Silva LP, Pirraco RP, Santos TC et al (2016) Neovascularization induced by the hyaluronic acid-based spongy-like hydrogels degradation products. ACS Appl Mater Interfaces 8(49):33464–33474
68. Posadowska U, Parizek M, Filova E et al (2015) Injectable nanoparticle-loaded hydrogel system for local delivery of sodium alendronate. Int J Pharm 485(1–2):31–40
69. Jeon HY, Shin EY, Choi JH et al (2018) Evaluation of saponin loaded gellan gum hydrogel scaffold for cartilage regeneration. Macromol Res 26(8):724–729
70. Duarte Pereira HM, Silva-Correia J, Yan LP et al (2013) Silk-fibroin/methacrylated gellan gum hydrogel as an novel scaffold for application in meniscus

cell-based tissue engineering. Arthrosc J Arthrosc Relat Surg 29(10):e53–e55
71. Wen J, Kim IY, Kikuta K et al (2016) Fabrication of porous α-TCP/gellan gum scaffold for bone tissue engineering. J Nanosci Nanotechnol 16(3):3077–3083
72. Song JE, Song YS, Jeon SH et al (2017) Evaluation of gelatin and gellan gum blended hydrogel for cartilage regeneration. Polymer (Korea) 41(4):619–623
73. Douglas TEL, Pilarz M, Lopez-Heredia M et al (2015) Composites of gellan gum hydrogel enzymatically mineralized with calcium-zinc phosphate for bone regeneration with antibacterial activity. J Tissue Eng Regen Med 11(5):1610–1618
74. Wen C, Lu L, Li X (2014) An interpenetrating network biohydrogel of gelatin and gellan gum by using a combination of enzymatic and ionic crosslinking approaches. Polym Int 63(9):1643
75. Choi I, Kim C, Song JE et al (2017) A comprehensive study on cartilage regeneration using gellan-gum/chondroitin sulfate hybrid hydrogels. Polymer (Korea) 41(6):962–966
76. Douglas TEL, Schietse J, Zima A et al (2017) Novel self-gelling injectable hydrogel/alpha-tricalcium phosphate composites for bone regeneration: physiochemical and microcomputer tomographical characterization. J Biomed Mater Res A 106A(3):822–828
77. Lopez-Heredia MA, Łapa A, Reczyńska K et al (2018) Mineralization of gellan gum hydrogels with calcium and magnesium carbonates by alternate soaking for bone regeneration applications. J Tissue Eng Regen Med 12(8):1825–1834
78. Temenoff JS, Mikos AG (2000) Review: tissue engineering for regeneration of articular cartilage. Biomaterials 21(5):431–440
79. Amini AA, Nair LS (2012) Injectable hydrogels for bone and cartilage repair. Biomed Mater 7(2):024105
80. Armiento AR, Stoddart MJ, Alini M et al (2018) Biomaterials for articular cartilage tissue engineering: learning from biology. Acta Biomater 65:1–20
81. Buckwalter JA (1998) Articular cartilage: injuries and potential for healing. J Orthop Sports Phys Ther 28(4):192–202
82. Makris EA, Gomoll AH, Malizos KN et al (2015) Repair and tissue engineering techniques for articular cartilage. Nat Rev Rheumatol 11(1):21–34
83. Iwasa J, Engebretsen L, Shima Y et al (2009) Clinical application of scaffolds for cartilage tissue engineering. Knee Surg Sports Traumatol Arthrosc 17(6):561–577
84. Tang Y, Sun J, Fan H et al (2012) An improved complex gel of modified gellan gum and carboxymethyl chitosan for chondrocytes encapsulation. Carbohydr Polym 88(1):46–53
85. Li JJ, Kaplan DL, Zreiqat H (2014) Scaffold-based regeneration of skeletal tissues to meet clinical challenges. J Mater Chem B 42(2):7272–7306
86. Stevens MM (2008) Biomaterials for bone tissue engineering. Mater Today 11(5):18–25
87. Chang SJ, Kuo SM, Liu WT et al (2010) Gellan gum films for effective guided bone regeneration. J Med Biol Eng 30(2):99–103
88. Douglas TEL, Wlodarczyk M, Pamula E et al (2014) Enzymatic mineralization of gellan gum hydrogel for bone tissue-engineering applications and its enhancement by polydopamine. J Tissue Eng Regen Mat 8:906–918
89. Douglas TEL, Wlodarczyk M, Pamula E et al (2014) Injectable self-gelling composites for bone tissue engineering based on gellan gum hydrogel enriched with different bioglasses. Biomed Mater 9(4):045014
90. Iulian A, Dan L, Camelia T et al (2018) Synthetic materials for osteochodnral tissue engineering. In: Oliveira J, Pina S, Reis R, San RJ (eds) Osteochondral tissue engineering, Advances in experimental medicine and biology, vol 1058. Springer, Cham, pp 31–52
91. Chen G, Kawazoe N (2018) Porous scaffolds for regeneration of cartilage, bone and osteochondral tissue. In: Oliveira J, Pina S, Reis R, San Roman J (eds) Osteochondral tissue engineering, Advances in experimental medicine and biology, vol 1058. Springer, Cham, pp 171–191
92. Pereira DR, Canadas RF, Silva-Correia J et al (2013) Gellan gum-based hydrogel bilayered scaffolds for osteochondral tissue engineering. Key Eng Mater 587:255–260
93. Pereira DR, Canadas RF, Silva-Correia J et al (2018) Injectable gellan-gum/hydroxyapatite-based bilayered hydrogel composites for osteochondral tissue regeneration. Appl Mater Today 12:309–321
94. Hejčl A, Lesný P, Přádný M et al (2008) Biocompatible hydrogels in spinal cord injury repair. Physiol Res 57(3):S121–S132
95. Tukmachev D, Forostyak S, Koci Z et al (2016) Injectable extracellular matrix hydrogels as scaffolds for spinal cord injury repair. Tissue Eng Part A 22(3–4):306–317
96. Gelain F, Panseri S, Antonini S et al (2011) Transplantation of nanostructured composite scaffolds results in the regeneration of chronically injured spinal cords. ACS Nano 5(1):227–236
97. Muheremu A, Peng J, Ao Q (2016) Stem cell based therapies for spinal cord injury. Tissue Cell 48(4):328–333
98. Coutts M, Keirstead HS (2008) Stem cells for the treatment of spinal cord injury. Exp Neurol 209(2):368–377
99. Silva NA, Salgado AJ, Sousa RA et al (2010) Development and characterization of a novel hybrid tissue engineering-based scaffold for spinal cord injury repair. Tissue Eng Part A 16(1):45–54
100. Tsaryk R, Silva-Correia J, Oliveira JM et al (2017) Biological performance of cell-encapsulated methacrylated gellan gum-based hydrogels for nucleus pulposus regeneration. J Tissue Eng Regen Med 11(3):637–648

101. Ismail NA, Mat Amin KA, Razali MH (2018) Novel gellan gum incorporated TiO_2 nanotubes film for skin tissue engineering. Mater Lett 228:116–120
102. Chen H, Zhang Y, Ding P et al (2018) Bone marrow-derived mesenchymal stem cells encapsulated in functionalized gellan gum/collagen hydrogel for effective vascularization. ACS Appl Bio Mater 1(5):1408–1415
103. Badylak SF (2007) The extracellular matrix as a biologic scaffold material. Biomaterials 28(25):3587–3593
104. Mastrogiacomo M, Scaglione S, Martinetti R et al (2006) Role of scaffold internal structure on in vivo bone formation in macroporous calcium phosphate bioceramics. Biomaterials 27(17):3230–3237
105. O'Brien FJ, Harley BA, Yannas IV et al (2005) The effect of pore size on cell adhesion in collagen-GAG scaffolds. Biomaterials 26(4):433–441
106. Murphy CM, Haugh MG, O'Brien FJ (2010) The effect of mean pore size on cell attachment, proliferation and migration in collagen-glycosaminoglycan scaffolds for bone tissue engineering. Biomaterials 31(3):461–466
107. O'Brien FJ, Harley BA, Waller MA et al (2007) The effect of pore size on permeability and cell attachment in collagen scaffolds for tissue engineering. Technol Health Care 15(1):3–17
108. Nicodemus GD, Bryant SJ (2008) Cell encapsulation in biodegradable hydrogels for tissue engineering applications. Tissue Eng Part B Rev 14(2):149–165
109. Tseng KY, Wang HC, Chang LL et al (2018) Advances in experimental medicine and biology: intrafascicular local anesthetic injection damages peripheral nerve-induced neuropathic pain. In: Shyu BC, Tominaga M (eds) Advances in pain research: mechanisms and modulation of chronic pain, Advances in experimental medicine and biology, vol 1099. Springer, Singapore, pp 65–76
110. Sundelacruz S, Kaplan DL (2009) Stem cell- and scaffold-based tissue engineering approaches to ostochondral regenerative medicine. Semin Cell Dev Biol 20(6):646–655
111. Gulrez SKH, Al-Assaf S, Phillips GO (2011) Hydrogels: methods of preparation, characterisation and applications. In: Carpi A (ed) Progress in molecular and environmental bioengineering – from analysis and modeling to technology applications. IntechOpen, London, pp 117–150. https://www.intechopen.com/books/progress-in-molecular-and-environmental-bioengineering-from-analysis-and-modeling-to-technology-applications/hydrogels-methods-of-preparation-characterisation-and-applications
112. Hoare TR, Kohane DS (2008) Hydrogels in drug delivery: Progress and challenges. Polymer 49(8):1993–2007
113. Yoon SJ, Yoo Y, Nam SE et al (2018) The cocktail effect of BMP-2 and TGF-β1 loaded in visible light-cured glycol chitosan hydrogels for the enhancement of bone formation in a rat tibial defect model. Mar Drugs 16(10):351
114. Jeon SH, Lee WT, Song JE et al (2017) Cartilage regeneration using hesperidin-containing gellan gum saffolds. Polymer (Korea) 41(4):670–674
115. Baek JS, Carlomagno C, Muthukumar T et al (2019) Evaluation of cartilage regeneration in gellan gum/agar blended hydrogel with improved injectability. Macromol Res 27(6):558–564
116. Park JH, Jeon HY, Jeon YS et al (2018) Effect of cartilage regeneration on gellan gum and silk fibroin. Polymer (Korea) 42(2):298–302
117. Oliveira JT, Santos TC, Martins L et al (2009) Performance of new gellan gum hydrogels combined with human articular chondrocytes for cartilage regeneration when subcutaneously implanted in nude mice. J Tissue Eng Regen Med 3(7):493–500
118. Canadas RF, Marques AP, Reis RL et al (2017) Osteochondral tissue engineering and regenerative strategies. In: Regenerative strategies for the treatment of knee joint disabilities, Studies in mechanobiology, tissue engineering and biomaterials, vol 21. Springer, Cham, pp 213–233
119. Costa L, Silva-Correia J, Oliveira JM et al (2018) Gellan gum-based hydrogels for osteochondral repair. Adv Exp Med Biol 1058:281–304
120. Vilela CA, Correia C, Da Silva MA et al (2018) In vitro and in vivo performance of methacrylated gellan gum hydrogel formulations for cartilage repair. J Biomed Mater Res Part A 106(7):1987–1996
121. Timothy D, Wojciech P, Jana L et al (2014) Injectable self-gelling composites for bone tissue engineering based on gellan gum hydrogel enriched with different bioglasses. Biomed Mater 9(4):045014
122. Douglas TEL, Łapa A, Reczyńska K et al (2016) Novel injectable, self-gelling hydrogel-microparticle composites for bone regeneration consisting of gellan gum and calcium and magnesium carbonate microparticles. Biomed Mater 11(6):065011
123. Bongjo M, van den Beucken JJ, Nejadnik MR et al (2011) Biomimetic modification of synthetic hydrogels by incorporation of adhesive peptides and calcium phosphate nanoparticles: in vitro evaluation of cell behavior. Eur Cell Mater 22:350–376
124. Pacelli S, Paolicelli P, Moretti G et al (2016) Gellan gum methacrylate and laponite as an innovative nanocomposite hydrogel for biomedical applications. Eur Polym J 77:114–123
125. Xu Z, Li Z, Jiang S et al (2016) Chemically modified gellan gum hydrogels with tunable properties for use as tissue engineering scaffolds. ACS Omega 3(6):6998–7007
126. Hollister SJ (2005) Porous scaffold design for tissue engineering. Nat Mater 4:518–524
127. Perez RA, Mestres G (2016) Role of pore size and morphology in musculo-skeletal tissue regeneration. Mater Sci Eng C Mater Biol Appl 61:922–939
128. Song JE, Lee SE, Cha SR et al (2016) Inflammatory response study of gellan gum impregnated duck's

feet derived collagen sponges. Sci Polym Ed 27(15):1495–1506
129. Mohd Azam NAN, Amin KAM (2017) The physical and mechanical properties of gellan gum films incorporated manuka honey as wound dressing materials. IOP Conf Ser Mater Sci Eng 209:012027
130. Levato R, Visser J, Planell JA et al (2014) Biofabrication of tissue constructs by 3D bioprinting of cell-laden microcarriers. Biofabrication 6(3):035020
131. De Giglio E, Bonifacio MA, Ferreira AM et al (2018) Multi-compartment scaffold fabricated via 3D-printing as in vitro co-culture osteogenic model. Sci Rep 8(1):15130
132. Akkineni A, Mhlfeld T, Funk A et al (2016) Highly concentrated alginate-gellan gum composites for 3D plotting of complex tissue engineering scaffolds. Polymers 8(5):170
133. De Silva DA, Martens PJ, Gilmore KJ et al (2014) Degradation behavior of ionic-covalent entanglement hydrogels. J Appl Polym Sci 132(1):1–10
134. Bartnikowski M, Bartnikowski NJ, Woodruff MA et al (2015) Protective effects of reactive functional groups on chondrocytes in photocrosslinkable hydrogel systems. Acta Biomater 27:66–76
135. Karvinen J, Koivisto JT, Jönkkäri I et al (2017) The production of injectable hydrazone crosslinked gellan gum-hyaluronan-hydrogels with tunable mechanical and physical properties. J Mech Behav Biomed Mater 71:383–391
136. Perugini V, Guildford AL, Silva-Correia J et al (2018) Anti-angiogenic potential of VEGF blocker dendron loaded on to gellan gum hydrogels for tissue engineering applications. J Tissue Eng Regen Med 12(2):e669–e678
137. Hu D, Wu D, Huang L et al (2018) 3D bioprinting of cell-laden scaffolds for intervertebral disc regeneration. Mater Lett 223:219–222
138. Choi JH, Choi OK, Lee J et al (2019) Evaluation of double network hydrogel of poloxamer-heparin/gellan gum for bone marrow stem cells delivery carrier. Colloids Surf B Biointerfaces 181:879–889
139. Kim WK, Choi JH, Shin ME et al (2019) Evaluation of cartilage regeneration of chondrocyte encapsulated gellan gum-based hyaluronic acid blended hydrogel. Int J Biol Macromol 141:51–59

3 Natural Fibrous Protein for Advanced Tissue Engineering Applications: Focusing on Silk Fibroin and Keratin

Yuejiao Yang, Jie Chen, Claudio Migliaresi, and Antonella Motta

Abstract

As one of the important branches of natural biopolymer, natural fibrous protein has a lot of advantages including good mechanical properties, excellent biocompatibility, controllable biodegradability, renewability, abundant sources, and so on. Moreover, natural fibrous protein is also a protein that could only be used for structure supporting without any bioactivities, which attracts a lot of attentions in the field of tissue engineering scaffold. This chapter is taking silk fibroin and keratin as model materials of natural fibrous protein, focusing on their protein structure, chemical compositions, processing and extraction methods, chemical modification methods, and their applications in tissue engineering through advanced manufacturing.

Keywords

Natural fibrous protein · Silk fibroin · Keratin · Processing · Extraction · Chemical modification · Tissue engineering

Y. Yang · C. Migliaresi · A. Motta (✉)
Department of Industrial Engineering and BIOtech Research Center, University of Trento, Trento, Italy
e-mail: Antonella.motta@unitn.it

J. Chen
School of Environmental and Chemical Engineering, Shanghai University, Shanghai, China

3.1 General Introduction of Natural Fibrous Protein

With the development of technology, the draining away of sources of materials and energy is becoming a serious topic all over the world. As a sequence, producing synthesized polymers with lower cost of resources is facing the challenge [1]. Over the past half century, explorations and applications of advanced technologies provide the possibilities to approach new materials, and natural polymers are becoming more and more popular. As a sustainable material, because of its rich resources, wide varieties, and degradability, natural polymer is showing an important position. A large number of different kinds of natural polymers are classified as natural biopolymers, because of good biocompatibility and biodegradability, like alginate, cellulose, collagen, starch, and chitosan. These materials are already well studied and applied widely in biomedical and biomaterial fields.

The main study subjects of natural biopolymers are sugar, nucleic acid, and protein. Proteins are formed by polymerization of amino acids according to the sequence of genetic code in mRNA. As one of the most important macromolecules in organisms, protein takes part in almost all the physiological activities and functions. Proteins can be classified into many categories based on different criterions. According to different structures of the molecules, there are two

H. J. Chun et al. (eds.), *Bioinspired Biomaterials*, Advances in Experimental Medicine and Biology 1249, https://doi.org/10.1007/978-981-15-3258-0_3

main classes: globular protein and fibrous protein. Globular proteins are normally spherical or globular in shape, with good water solubility and specific biological activities referring to the environment (e.g., catalysis, molecule recognition, etc.). Most of the proteins belong to globular proteins, while fibrous proteins are linear in shape and forming long fibers or sheaths. Some of fibrous proteins are water-soluble, like myosin and fibrin. Most of fibrous proteins are insoluble, like keratin, collagen, elastin, and silk fibroin.

Generally, fibrous proteins are composed of highly repetitive amino acid sequences that primarily provide mechanical and architectural functions but without biological activities [2]. There are mainly three secondary structures of fibrous protein: α-helix, β-sheet, and random coil. Especially, for collagen, there is a unique "super helix" structure, twisted by three left-handed helices together into a right-handed triple helix. Among all the secondary structures, β-sheet is the main structure that provides outstanding strength and rigidity of fibrous proteins. It is folding by relatively extended polypeptide chains with the cooperative hydrogen bonds interactions.

Studies with fibrous proteins are often directed to understand structure-function relationships and to understand nature's ability to optimize protein-based biomaterials with functional attributes for survival, such as protective enclosures, mechanical support, or energy conversion [3–5]. Among fibrous protein materials, silk fibroin and keratin are already deep studied and widely used in biomedical and bioengineering fields.

3.2 Silk Fibroin

3.2.1 General Information of Silk Fibroin

The application of silk was first developed in ancient China at 3500 B.C. and spread gradually to other regions over the world. Among varieties of silk, domestic *Bombyx mori* silk is the widely used one. There is a current interest in the development of composites containing silkworm silk for biomedical application.

3.2.2 The Structure of Cocoon Silk, Sericin, and Silk Fibroin

Silkworm silk is a protein polymer that is produced from specialized glands where proteins are stored and spun into fibers by silkworm. The structure of silk fiber is mainly constructed with two different protein-based materials: silk fibroin filaments (75 wt% of total silk fiber) and sericin coating (25 wt% of total silk fiber). Both the fibroin and sericin proteins contain the same 18 amino acids. Silk fibroin contains highly repetitive β-sheet crystalline or semicrystalline structure, which provides silk excellent mechanical properties. Sericin is an amorphous gumlike coating material in the outer layer of silk to conglutinate fibroin filaments together and maintains the overall structural integrity of the cocoon. It can be removed by soaking cocoon in hot or boiling water due to its hydrophilic properties, which is called degumming. However, the removal of sericin could cause the altering of mechanical, chemical, and biological performances of degummed fibers.

3.2.3 Chemical Composition of Silk Fibroin

Silk fibroin consisted of two major fibroin proteins with the ration of 1:1, named light chain (L-chain, 28 kDa) and heavy chain (H-chain, 391 kDa), respectively. The light-chain fibroin, a short protein of 262 residues, is linked to the heavy-chain fibroin, a long protein of 5263 residues. The third protein, named P25, exists every six H-chain-L-chain arrangement. It is a short glycosylated protein of 220 amino acids and a molecular weight of 25 kDa. The primary structure of silk fibroin is made of a few predominant amino acids, mainly accounted for in the heavy-chain protein whose molecular weight is 14 times that of the light chain. Four amino acids account for 93% of the heavy chain's 5239 residues, with 46% of glycine (G), 30% of alanine (A), 12% of serine (S), and 5% of tyrosine (Y). The H-chain primary structure is composed of the main hexapeptide repeats GAGAGS which form highly

crystalline regions due to the small side chains of these amino acids. In addition, tyrosine-coating blocks (such as GAGAGY or GAGAGVGY) form semicrystalline regions. The H-chain is thus made of 12 hydrophobic crystalline regions (~GAGAGS~/~GY~~~GY~) separated by 11 amorphous hydrophilic regions (~GT~~~GT~) containing residues with large side chain and hydrophilic head and tail. These amorphous regions form turns to allow the antiparallel β-pleated sheet secondary structure where protein chains are held together by non-covalent interactions, notably hydrogen bonding. The H-chain is linked in the tertiary structure to the small globular L-chain fibroin by a disulfide bridge between Cys-20 (H-chain) and Cys-172 (L-chain) and to the glycoprotein P25 through hydrophobic interactions.

3.2.4 Secondary Structure of Silk Fibroin

In the solid state, SF exhibits two crystalline polymorphs known as Silk I and Silk II. Early studies [6, 7] about SF solution, directly extracted from the posterior division of the silkworm gland, identified the parameters involved in the conformational changes between the random coil form and the crystalline polymorphs.

The random coil state of SF is clearly metastable since it readily transforms in either Silk I or Silk II polymorphs by subjecting the native SF solution to heat or shearing. The crystal structures proposed for the crystalline polymorphs of SF concern mainly the molecular structure of the aforementioned crystalline domains of SF H-chain, since the L-chain lacks sufficient regularity in the primary structure to crystallize to a significant extent. Silk II, or β-form, is the stable crystalline form of SF found in the fibers, which was first described by the Marsh-Pauling-Corey model of polar-antiparallel β-sheet elaborated upon by Crick and Kendrew in 1957. The crystal structure was successively resolved with the antipolar-antiparallel model by Takahashi and coworkers [8].

The model was recently refined by considering the GA peptide as the base of the amino acid sequence of SF crystalline region5. The refined model proposes a statistical crystal structure in which two antipolar-antiparallel β-sheet structures with different orientations occupy a crystal site with a ratio 2:1. Actually the antiparallel β-sheet structure of Silk II is isomorphous with poly(AG) I, for which a similar X-rays diffraction pattern was early observed.

Some different secondary structures of silk fibroin are reported: α-helical (silk I) and β-sheet (silk II) structures in crystalline areas and disordered conformation of random globules in amorphous areas. The Silk I structure is stabilized by intramolecular hydrogen bonds, with the hydrophobic fragments displaced to the periphery. Silk I is a water-soluble state (can be obtained in vitro in aqueous conditions) and easily converts to the Silk II structure when exposed to physical stresses or heating. The β-sheet structures are asymmetrical with one side occupied with hydrogen side chains from glycine and the other occupied with the methyl side chains from the alanines. Antiparallel β-sheets of silk fibroin are packed in the face-to-face, back-to-back mode. The Silk II structure is water-insoluble in several solvents including alkaline conditions, mild acid, and several chaotropes [9, 10].

3.2.5 Processing of Silk Fibroin

Native SF water solutions are obtained by diluting the content of the posterior division of the silkworm silk gland where SF is still separated from sericin. Regenerated SF in water is obtained from "degummed" silk fibers by dissolving them in concentrated saline solution and subsequent salt removal by dialysis.

3.2.5.1 Degumming

Degumming is the conventional name for sericin removal from cocoon shells and can be performed in different ways [11]. In the standard method, cocoon shells or raw silk are kept in 50 times v/w of boiling aqueous 0.05% Na_2CO_3 for 60 min. Usually, this treatment is repeated twice.

Alternatively various concentrations of Na_2CO_3 and heating time can be used, depending on the desired degree of sericin removal. Traditional soap degumming is performed in 100 times v/w of 0.5% Marseille soap for 30 min at 100 °C. Enzymatic degumming [12–14] is also possible, e.g., by alkalase solution. Degumming by urea is carried out by 8 M aqueous urea containing 0.04 M Tris-SO_4 (pH 7) and 0.5 M mercaptoethanol, under various conditions of time and temperature. Even hot water alone can be used for degumming either boiling at atmospheric pressure (100 °C) or in an autoclave (about 120 °C). After the above degumming treatments, the resulting silk mats are washed in water repeatedly and then air-dried. The differences in the aforementioned production methods are in the degree of sericin removal and in the associated damage produced both at microscopic and molecular levels in the resulting SF.

3.2.5.2 Dissolution

Effectively dissolving agents for SF are formic acid [15], $Ca(NO_3)_2$/MeOH solutions [16], N-methyl morpholine N-oxide [17], N-methylpyrrolidone, and dimethyl sulfoxide [18]. Other dissolving media are LiSCN, LiBr, $CaCl_2$, or $Ca(NO_3)_2$ aqueous or alcoholic solutions [11, 18, 19]. Since the solubility equilibrium of SF in the pure organic solvent is quite critical, regenerated SF water solutions are preferentially prepared from the so-called mixed solvents consisting of saline solution and alcohols or just from concentrated saline solutions. A frequently used mixed solvent is the so-called Ajisawa's reagent [20] consisting of a mixture of $CaCl_2$/ethanol/water (111/92/144 by weight), while common organics-free saline solutions are lithium thiocyanate (LiSCN aq 9 M) and lithium bromide (LiBr aq 9–9.5 M). A common feature of all the aforementioned solvents is their hydrogen bonding ability which is necessary to loosen the strongly H-bonded crystalline structures in SF fibers which are first swollen and subsequently dissolved obtaining solutions in which the salvation degree of SF differs depending on the specific dissolving medium used [19].

3.2.5.3 Dialysis

After complete dissolution the dissolving medium is exchanged by dialysis against distilled water through a selectively permeable membrane; the structure of regenerated SF in diluted water solution at room temperature is mainly the random coil one, but the system must be preferably regarded as (metastable) colloidal suspension with the formation of micellar structures due to the primary structure of SF molecule. In fact on examination of the primary sequence for the native SF H-chain, a pattern of hydrophobic and hydrophilic blocks was identified [21]; that suggests the possible formation of micellar structures in water. A model of SF assembly in water was proposed [22]. SF molecules act as hydrophobic-hydrophilic block copolymers with the formation of irregular-sized micelles depending on chain folding and hydrophobic interactions. The small hydrophilic blocks present along the protein chain maintain solubility in water and prevent premature β-sheet formation. Extensive interactions are present, however, among the blocks (hydrogen bonds and hydrophobic interactions), and the assembly in the hydrophobic clusters becomes tighter and eventually local crystalline order tends to develop; this would be also confirmed by the fact that regenerated SF is water-soluble only just after dialysis from LiBr [23]. Increasing concentration and temperature promotes micelles coalescence into globules which could finally yield a gel state.

3.3 Keratin

3.3.1 General Information of Keratin

Keratin is the most important biopolymer which exists in the skin, hair, and nails of humans and animals (also hooves, horns, and feathers) [24]. According to the Ashby map, keratin refers to the most rigid biological materials having high toughness and high modulus, although it consists exclusively of polymer components and rarely contains minerals [25].

Keratin can be classified into three types: α, β, and γ. α-Keratin is the prevalent group and provides structural support for the hair shaft, while β-keratin serves as protection and forms a cuticle. γ-Keratins play a role of disulfide (-S-S-) cross-linking agent and also retain the hair shaft structure. α-Keratin can be found in mammals (there is one mammal, a pangolin, which is according to research has both α and β), and this is the principal component of wool, hair, nails, hooves, horns, and layer corneum (outer layer of skin). β-Keratin is the main component of hard materials such as feathers, claws, and beaks of birds and scales and claws of reptiles.

3.3.2 Secondary Structure of Keratin

α-Keratin proteins are organized in the form of spiral coils. This conformation was defined as α-helical conformation. The naturally occurring α-helices found in proteins are right-handed. The helical structure is stabilized by hydrogen bonds and disulfide bonds. It has the 0.51 nm pitch [26]. The helical chain forms a protofilament (about 2 nm in diameter); two protofilaments crosswise with protofibril to stabilize into dimer; four protofibrils combine in a circular or spiral intermediate filament (IF) with a diameter of about 7 nm. The IFs are then packed in a super-configured conformation and bound to matrix proteins. An amorphous keratin matrix is rich in sulfur containing a large amount of cysteine residues or a large number of residues of glycine, tyrosine, and phenylalanine amino acids [27].

β-Keratin has the pleated sheet structure, which consists of side-packaged β-yarns that can be parallel or antiparallel (that are more stable). The structure of the pleated sheet is stabilized by two factors: hydrogen bonds between beta chains that are in charge of the formation of leaf and planarity of the peptide bonds that causes the β-sheet to be corrugated [28]. The formation of the β-keratin filament includes the following: the central region of one polypeptide chain is added to form four lateral beta bonds, connected by a hydrogen bond, resulting in a corrugated shaped sheet; then the sheet is distorted to lie on the left screw ruled surface; each residue is represented by as a sphere in the model; two sheets are connected by a horizontal dyad, overlapping and moving in opposite directions, forming a 4 nm diameter thread (9.5 nm and 4 turns per unit). The end portions of the peptide chains flow around the β-keratin filaments and form a matrix. So, keratin can be considered as some sort of composite that has a polymer-polymer constraint that is formed by crystalline filaments intruded in an amorphous matrix [29].

3.3.3 Chemical Properties of Keratin

The presence of numerous cell adhesion sequences, RGD (Arg-Gly-Asp) and LDV (Leu-Asp-Val), which occur in proteins of extracellular matrices such as fibronectin, has been reported in keratin of such materials as wool, silk, and human hair as well as glutamic acid-aspartic acid-serine (EDS), which is capable of supporting cellular attachment [30]. Together, these properties create an appropriate three-dimensional matrix that allows cellular infiltration, attachment, and proliferation of cells that is making keratin so favorable to be used to develop tissue engineering constructs. The biomaterials from keratin have been under a spotlight of the researchers for many decades, but at the present time, there are no biomaterials made of keratin in clinical application.

3.3.4 Processing of Keratin

Hair dissolution and extracting keratin from hairs are not easy to approach because a large amount of disulfide bond, hydrogen bond, and hydrophobic amino acid exist in hair. Chemical methods, microbial and enzymatic treatment, supercritical water and steam explosion, and microwave radiation are main methods for keratin extraction, which are already well explored and studied. Among them, chemical methods are the ones well developed and widely used.

3.3.4.1 Traditional Chemical Methods for Keratin Extraction

The traditional chemical methods for keratin extraction are oxidation, reduction, and hydrolysis. The mechanism of oxidation method is to oxidize the disulfide bond into a sulfonic acid group by using an oxidizing agent. This reaction will produce keratin with hydrophilic groups, so dissolving the hair. Due to the strong effect of oxidation method, peptide chains could be degraded during the procedure. The average molecular weight of keratin extracted by this method is usually around 3000 Da, which may have some limitations for applications. Reduction method, the most well studied, is utilizing micelles in surfactant as a protector to keep extracted keratin stable, avoiding oxidation and precipitation during procedure. Keratin obtained from this method usually has a larger molecular weight and with a higher dissolubility. Hydrolysis method is using a strong base (e.g., sodium hydroxide) solution to break the disulfide bond between macromolecules and decompose the peptide chain in the hair. The extractions are mainly polypeptide with a low molecular weight.

3.3.4.2 Environmental-Friendly Method: Ionic Liquids

Due to its three-dimensional polypeptide structure which consists of a triple helix of protein chains held together by a range of covalent (disulfide bonds) and noncovalent interactions [31, 32], keratin is stable to most solvents. Water-soluble keratin from wool, hair, and feathers can be partially extracted by the methods mentioned above. However, some of the reagents used in these methods are toxic, difficult to remove from the substrates, or difficult to recycle. Recently, the use of ionic liquid (IL) solvents showed improvements in the dissolution process, with a higher yield of keratin from feathers [33, 34] and wool [35, 36]. IL solvents provide a unique combination of properties, including low vapor pressure and high thermal stability [37]. ILs containing chloride such as 1-butyl-3-methylimidazolium chloride ([BMIM]Cl) as anion were shown to dissolve wool better than other ILs (BF4, PF6, and Br). [BMIM]Cl itself has been proposed as an effective solvent for extracting keratin from duck [36] and turkey feathers [33] when treated at 100–180 °C for several hours. [BMIM]Cl was also used to prepare wool keratin/cellulose composite materials which displayed a homogeneous structure without any residual fibers [36].

3.4 Engineering Natural Fibrous Protein Materials Through Advanced Manufacturing

Natural fibrous protein materials have the great potential to be applied in tissue engineering and regenerative medicine. Bio-recognition ability of fibrous protein is the basic contribution to induce regeneration of various mammalian tissues. Taking silk fibroin as an example, two different active sequences VITTDSDGNE and NINDFDED, recognized by the integrin promoting fibroblast growth, were localized in the N-terminal region of the heavy chain [38]. Besides, fibrous protein could be processed into many different kinds of materials which enable its extensive application in tissue engineering and regenerative medicine. All these diverse kinds of materials start from the protocol to obtain aqueous solution [39]. Then, this solution can be prepared into films, sponges, fibers, and gels [22, 40, 41]. Depending on the procedure of processing and the source, fibrous protein could have different secondary conformation and molecule assembling, which result in different mechanical and biological functions [40].

3.4.1 Chemical Modification of Natural Fibrous Protein

As a biopolymer in general, silk fibroin and keratin are popular due to their advanced properties. Besides biocompatibility and biodegradability, tunable conformations obtained from different processing methods make them easy to match different fabrication methods, which extend the use of silk fibroin into different fields, especially in biomedical applications. It is already well known that with physical modification methods,

silk fibroin and keratin could have various tunable microstructures and mechanical properties affecting biological abilities [42]. With further improvements and optimizations of the applications of these fibrous proteins, the requirements of modification are moving to the molecular level. Thus, chemical modifications are explored to expand the utility of fibrous protein with enhanced physicochemical properties and added functionalities [43, 44]. The amino acid compositions of fibrous protein showed that it contains several reactive groups, including serine, tyrosine, threonine, glycine, and aspartic acid [45]. As an improved applicability in tissue engineering, peptides, enzymes, drugs, and polymers are immobilized on these active groups via different chemical functionalization methods, to altered fast cell adhesion and proliferation and controllable cell differentiation, and responsive to specific conditions. Therefore, chemical modifications provide the possibility to fabricate fibrous protein-based materials with designed chemical, physical, and biological properties. Compared with silk fibroin, chemical modification on keratin is not so well studied. And all the methods employed on keratin are the same ones for silk fibroin. Thus, silk fibroin is taken as an example to present different methods that can be carried out on different reactive groups on silk fibroin.

From chemical point of view, the frequently used chemical modification methods of silk fibroin are coupling reactions [45] (e.g., cyanuric chloride, carbodiimide), amino acid modification (e.g., arginine masking, sulfation, and azo-modified of tyrosine), and grafting reaction (e.g., tyrosinase-catalyzed grafting and polymethacrylate grafting). Cyanuric chloride and carbodiimide coupling are the mainly used reactions. The biggest advantage of cyanuric chloride reaction is the basic pH condition, which makes it compatible with silk. Carbodiimide coupling is already widely used in many proteins which contain carboxylic acids reacting with primary amines to form an amide bond. For amino acid modification, there are several methods using different amino acids. A small amount of arginine residues, existing in silk fibroin, can react with 1,2-cyclohexandione under basic aqueous conditions to form an uncharged imidazolidinone product [46, 47]. However, due to the low amount of arginine, the final product is not easy to be characterized. Sulfation of tyrosine can be treated directly on degummed silk fibers [43]. Azo-modified tyrosine can be carried out by treating dissolved silk fibroin in borate buffer (pH 9.0) or soaking solid silk fibroin films and scaffolds into the buffer and then followed by treatment with diazonium salt [45]. Considering silk fibroin is a biopolymer, tyrosinase-catalyzed grafting is applied as an enzyme-catalyzed method which can be carried out on aqueous solution of SF in phosphate buffer. Attachment of acrylate monomers to silk followed by radical polymerization is another polymer grafting approach used to modify the surface of silk fibroin fibers.

3.4.2 Engineering Natural Fibrous Protein in Tissue Engineering

3.4.2.1 Reconstruction and Repair in Bone Tissue

Most of the research on silk fibroin has been carried out for bone tissue engineering. Films, electrospun scaffolds, and salt-leaching 3D porous scaffolds are processed in bone tissue engineering [18, 48, 49]. Some previous work showed that silk fibroin hydrogels and membranes/nets without pre-seeded cells have been used for guided bone regeneration [23, 50]. However, recently 3D porous silk fibroin scaffolds combined with MSCs resulted in advance bone formation for the repair of critical-sized bone defects [14]. Furthermore, the silk fibroin scaffold is also modified with RGD to increase the cell attachment and slow down the degradation in bone tissue engineering. RGD-silk scaffolds were demonstrated to be suitable for autologous bone tissue engineering, probably because of their stable macroporous structure, tailorable mechanical properties matching those of native bone, and slow degradation [13].

In 2005, Meinel et al. [14] first used silk fibroin as a scaffold for bone tissue engineering and applied it to the study of mouse skull trauma

model, which proved that silk fibroin has good biocompatibility and mechanical stability, suggesting it can be used as a potential material for bone tissue reconstruction. Rajkhowa et al. [51] prepared a porous silk fibroin scaffold in aqueous solution and hexafluoroisopropanol (HFIP) and then mixed silk fibroin particles into it, which improved the mechanical properties of the sponge by nearly 40 times, increasing compression modulus from less than 50 kPa to 2.2 MPa. Subsequently, they modified the silk fibroin microparticles into microfilament fibers and mixed them with the silk fibroin porous scaffold [52] to obtain a material with a modulus of elasticity of 13 MPa. In addition to a certain degree of mechanical strength, silk fibroin materials can be processed to achieve the desired mechanical requirements for bone tissue that requires compression. Kuboyama et al. [53] separately prepared a porous scaffold prepared by aqueous silk fibroin preparation and silk fibroin hexafluoroisopropanol (HFIP) into rabbit leg bones, and new bones grew after 4 weeks. And the material prepared by the aqueous silk fibroin solution is more effective.

In addition, the blending of silk fibroin with a variety of materials can not only enhance the mechanical and biological properties of the material but also broadens its application in bone tissue engineering. Vachiraroj et al. [54] used a silk fibroin-based and chitosan-based material mixed with gelatin and hydroxyapatite to obtain a hybrid scaffold. With the comparison of different base materials, protein-based materials are more effective in improving osteogenic differentiation of rat osteoblasts and rat bone marrow stem cells. Wang et al. [55] used the porous silk fibroin/graphene composite as a drug-loaded scaffold for bone tissue engineering, and the results confirmed that the scaffold has a good application prospect in promoting bone regeneration.

3.4.2.2 Repairing Nerve Gap

In neural tissue engineering, especially in the peripheral nervous system, the dorsal root ganglia and Schwann cells cultured on silk fibroin maintain their viability and keep their normal phenotype or functionality without any cytotoxic effects [56]. Silk-carbon nanotubes composite scaffolds were able to improve the neuron differentiation of human embryonic stem cells, which is applicable for efficient supporting matrices for stem cell-derived neuronal transplants [57]. Human hair keratin has good properties in promoting regeneration and functional recovery of nerve tissue. This repairing can be realized by activating Schwann cells. Human hair keratin has the ability to activate Schwann cells through chemotaxis, as well as enhance cell adhesion and proliferation, and at the same time, improve the expression of some important genes [58]. Human hair keratin is an excellent nerve repair inducer and achieves a therapeutic effect comparable to autologous nerve transplantation in an animal model of nerve injury [59].

Sierpinski et al. [59] found that besides the abilities mentioned above, human hair keratin can be passed to a biological model that improves neurological resuscitation, suggesting that human hair keratin biomaterials are a neural reactor that can be modeled as a neural injury similar to an autologous. Apel et al. [60] used a keratin-inducing nerve-inducing catheter to achieve a nerve regeneration rate of 100% at 6 weeks, whereas only 50% of the rats in the blank group were observed to have nerve regeneration. The nerve pulse rate and signal level of the keratin group were significantly higher than those without keratin. The study showed that keratin scaffolds can promote nerve regeneration in surrounding tissues, and keratin hydrogel can improve physiological repair and increase axonal density, thereby promoting nerve regeneration.

3.4.2.3 Wound Healing and Hemostatic

Silk fibroin can be mixed with a variety of materials to prepare a composite membrane, which has the advantages of preventing bacterial infection, good wound adhesion, low irritation, good softness, and promoting wound cell growth [61]. For skin wound healing, fibroin films and fibroin-alginate sponges have been reported to enhance skin wound healing in vivo compared to clinically used materials [62, 63]. Oral keratinocytes also

proliferate on woven fibroin meshes [20], a form that is likely to be used for wound healing applications. Both studies concluded that fibroin-based materials promoted epithelialization. Moriyama et al. [64] added an active ingredient of aloe vera gel into silk fibroin solution to prepare silk fibroin/aloe vera gel membrane, which was used to repair full-thickness skin lesions of diabetic model mice, and obtained obvious effects. A mixed film of silk fibroin/polylactide-glycolide (PLGA) prepared by Shahverdi et al. [65] can be used as a chronic wound hemostatic material. Shan et al. [66] prepared silk fibroin and gelatin as a double-layer hemostatic material and compared it with commercially available hemostatic materials. The results showed that the new hemostatic material can significantly reduce the wound area and promote wound healing and formation. Kanokpanont et al. [53] performed wax coating modification on the surface of silk fibroin to prepare a nonadhesive hemostatic material. The results showed that this material can effectively stop bleeding, reduce wound pain, and reduce the risk of wound reinjury.

Keratin is the major structural protein of various types of epithelial cells and plays an important role in wound healing. Li Pengfei et al. prepared a keratin nanofiber membrane to promote wound healing. Keraplast company (in the United States) has made human hair keratin into a skin wound covering material and commercialized it, which has a positive impact on the treatment of full-thickness skin defects and non-thick skin defects. Lee et al. [67] mixed silk fibroin and keratin to form a silk fibroin/keratin membrane, which improved anticoagulant and biocompatibility. Aboushwareb et al. [68] found that keratin hydrogels have hemostatic properties and are expected to be effective hemostatic agents. Compared with other common hemostatic agents, keratin hemostatic gel can improve survival rate. Chen Yinghua et al. found human hair keratin/collagen sponge membrane has good physical and biological properties, good histocompatibility, and strong vascularization ability, can stimulate cell proliferation, can promote the healing of damaged skin, and can be used as a substitute for the dermis.

3.5 Conclusions and Perspectives

In this chapter, silk fibroin and keratin are well introduced through protein structures, chemical properties, and applications according to their different biological properties. It is also proved that by using advanced manufacturing methods, the properties of silk fibroin and keratin can be designed as required to match more complex conditions. More natural fibrous proteins should be explored, processed, modified, and applied into biomedical field with multifunction.

References

1. Raza F, Zafar H, Zhu Y, Ren Y, Ullah A, Khan A, He X, Han H, Aquib M, Boakye-Yiadom K (2018) A review on recent advances in stabilizing peptides/proteins upon fabrication in hydrogels from biodegradable polymers. Pharmaceutics 10:16
2. Wang X, Kim HJ, Wong C, Vepari C, Matsumoto A, Kaplan DL (2006) Fibrous proteins and tissue engineering. Mater Today 9:44–53
3. McGrath K, Kaplan D (1997) Protein-based materials. Springer, Heidelberg
4. Shewry PR, Tatham AS, Bailey AJ (2003) Elastomeric proteins: structures, biomechanical properties, and biological roles. Cambridge University Press, Cambridge
5. Steinbüchel A (2001) Biopolymers: polyamides and complex proteinaceous materials II. Wiley-VCH, Weinheim
6. Angelova N, Hunkeler D (1999) Rationalizing the design of polymeric biomaterials. Trends Biotechnol 17:409–421
7. Park H, Park K, Shalaby WS (2011) Biodegradable hydrogels for drug delivery. CRC Press, Boca Raton
8. Gutowska A, Jeong B, Jasionowski M (2001) Injectable gels for tissue engineering. Anat Rec 263:342–349
9. Vepari C, Kaplan DL (2007) Silk as a biomaterial. Prog Polym Sci 32:991–1007
10. Sashina E, Bochek A, Novoselov N, Kirichenko D (2006) Structure and solubility of natural silk fibroin. Russ J Appl Chem 79:869–876
11. Altman GH, Horan RL, Lu HH, Moreau J, Martin I, Richmond JC, Kaplan DL (2002) Silk matrix for tissue engineered anterior cruciate ligaments. Biomaterials 23:4131–4141
12. Meinel L, Karageorgiou V, Fajardo R, Snyder B, Shinde-Patil V, Zichner L, Kaplan D, Langer R, Vunjak-Novakovic G (2004) Bone tissue engineering using human mesenchymal stem cells: effects of scaffold material and medium flow. Ann Biomed Eng 32:112–122

13. Meinel L, Karageorgiou V, Hofmann S, Fajardo R, Snyder B, Li C, Zichner L, Langer R, Vunjak-Novakovic G, Kaplan DL (2004) Engineering bone-like tissue in vitro using human bone marrow stem cells and silk scaffolds. J Biomed Mater Res Part A 71:25–34
14. Meinel L, Fajardo R, Hofmann S, Langer R, Chen J, Snyder B, Vunjak-Novakovic G, Kaplan D (2005) Silk implants for the healing of critical size bone defects. Bone 37:688–698
15. Unger RE, Wolf M, Peters K, Motta A, Migliaresi C, Kirkpatrick CJ (2004) Growth of human cells on a non-woven silk fibroin net: a potential for use in tissue engineering. Biomaterials 25:1069–1075
16. Chiarini A, Petrini P, Bozzini S, Dal Pra I, Armato U (2003) Silk fibroin/poly (carbonate)-urethane as a substrate for cell growth: in vitro interactions with human cells. Biomaterials 24:789–799
17. Gotoh Y, Niimi S, Hayakawa T, Miyashita T (2004) Preparation of lactose–silk fibroin conjugates and their application as a scaffold for hepatocyte attachment. Biomaterials 25:1131–1140
18. Li C, Vepari C, Jin H-J, Kim HJ, Kaplan DL (2006) Electrospun silk-BMP-2 scaffolds for bone tissue engineering. Biomaterials 27:3115–3124
19. Cai K, Yao K, Lin S, Yang Z, Li X, Xie H, Qing T, Gao L (2002) Poly (D, L-lactic acid) surfaces modified by silk fibroin: effects on the culture of osteoblast in vitro. Biomaterials 23:1153–1160
20. Min B-M, Lee G, Kim SH, Nam YS, Lee TS, Park WH (2004) Electrospinning of silk fibroin nanofibers and its effect on the adhesion and spreading of normal human keratinocytes and fibroblasts in vitro. Biomaterials 25:1289–1297
21. Wise DL (2000) Biomaterials and bioengineering handbook. Marcel Dekker, New York
22. Motta A, Migliaresi C, Faccioni F, Torricelli P, Fini M, Giardino R (2004) Fibroin hydrogels for biomedical applications: preparation, characterization and in vitro cell culture studies. J Biomater Sci Polym Ed 15:851–864
23. Fini M, Motta A, Torricelli P, Giavaresi G, Aldini NN, Tschon M, Giardino R, Migliaresi C (2005) The healing of confined critical size cancellous defects in the presence of silk fibroin hydrogel. Biomaterials 26:3527–3536
24. McKittrick J, Chen P-Y, Bodde S, Yang W, Novitskaya E, Meyers M (2012) The structure, functions and mechanical properties of keratin. JOM 64:449–468
25. Wegst U, Ashby M (2004) The mechanical efficiency of natural materials. Philos Mag 84:2167–2186
26. Chou C-C, Buehler MJ (2012) Structure and mechanical properties of human trichocyte keratin intermediate filament protein. Biomacromolecules 13:3522–3532
27. Fraser R, MacRae TP, Sparrow LG, Parry D (1988) Disulphide bonding in α-keratin. Int J Biol Macromol 10:106–112
28. Lodish H, Berk A, Zipursky SL, Matsudaira P, Baltimore D, Darnell J (2000) Molecular cell biology, 4th edn. National Center for Biotechnology Information, Bookshelf
29. Fraser RB, Parry DA (2011) The structural basis of the filament-matrix texture in the avian/reptilian group of hard β-keratins. J Struct Biol 173:391–405
30. Makarem R, Humphries MJ (1991) LDV: a novel cell adhesion motif recognized by the integrin α4β1. Portland Press
31. Wong WCV, Narkevicius A, Chow WY, Reid DG, Rajan R, Brooks RA, Green M, Duer MJ (2016) Solid state NMR of isotope labelled murine fur: a powerful tool to study atomic level keratin structure and treatment effects. J Biomol NMR 66:93–98
32. Wang B, Yang W, McKittrick J, Meyers MA (2016) Keratin: structure, mechanical properties, occurrence in biological organisms, and efforts at bioinspiration. Prog Mater Sci 76:229–318
33. Idris A, Vijayaraghavan R, Rana UA, Fredericks D, Patti AF, D.R. (2013) Macfarlane, dissolution of feather keratin in ionic liquids. Green Chem 15:525–534
34. Idris A, Vijayaraghavan R, Patti AF, Macfarlane DR (2014) Distillable protic ionic liquids for keratin dissolution and recovery. ACS Sustain Chem Eng 2:1888–1894
35. Idris A, Vijayaraghavan R, Rana UA, Patti AF, Macfarlane DR (2014) Dissolution and regeneration of wool keratin in ionic liquids. Green Chem 16:2857–2864
36. Xie H, Li S, Zhang S (2005) Ionic liquids as novel solvents for the dissolution and blending of wool keratin fibers. Green Chem 7:606–608
37. Yoo CG, Pu Y, Ragauskas AJ (2017) Ionic liquids: promising green solvents for lignocellulosic biomass utilization. Curr Opin Green Sustain Chem 5:5–11
38. Yamada H, Igarashi Y, Takasu Y, Saito H, Tsubouchi K (2004) Identification of fibroin-derived peptides enhancing the proliferation of cultured human skin fibroblasts. Biomaterials 25:467–472
39. Rockwood DN, Preda RC, Yücel T, Wang X, Lovett ML, Kaplan DL (2011) Materials fabrication from Bombyx mori silk fibroin. Nat Protoc 6:1612
40. Motta A, Maniglio D, Migliaresi C, Kim H-J, Wan X, Hu X, Kaplan DL (2009) Silk fibroin processing and thrombogenic responses. J Biomater Sci Polym Ed 20:1875–1897
41. Foss C, Merzari E, Migliaresi C, Motta A (2012) Silk fibroin/hyaluronic acid 3D matrices for cartilage tissue engineering. Biomacromolecules 14:38–47
42. Dong X, Zhao Q, Xiao L, Lu Q, Kaplan DL (2016) Amorphous silk nanofiber solutions for fabricating silk-based functional materials. Biomacromolecules 17:3000–3006
43. Murphy AR, John PS, Kaplan DL (2008) Modification of silk fibroin using diazonium coupling chemistry and the effects on hMSC proliferation and differentiation. Biomaterials 29:2829–2838
44. Ai C, Cai J, Zhu J, Zhou J, Jiang J, Chen S (2017) Effect of PET graft coated with silk fibroin via EDC/

NHS crosslink on graft-bone healing in ACL reconstruction. RSC Adv 7:51303–51312
45. Murphy AR, Kaplan DL (2009) Biomedical applications of chemically-modified silk fibroin. J Mater Chem 19:6443–6450
46. Gotoh Y, Tsukada M, Minoura N (1996) Chemical modification of the arginyl residue in silk fibroin: 2. Reaction of 1, 2-cyclohexanedione in aqueous alkaline medium. Int J Biol Macromol 19:41–44
47. Gotoh Y, Tsukada M, Minoura N (1992) Chemical modification of arginyl residues in silk fibroin: 1. Reaction of 1, 2-cyclohexanedione in borate buffer. Int J Biol Macromol 14:198–200
48. Sofia S, McCarthy MB, Gronowicz G, Kaplan DL (2001) Functionalized silk-based biomaterials for bone formation. J Biomed Mater Res 54:139–148
49. Hofmann S, Hagenmüller H, Koch AM, Müller R, Vunjak-Novakovic G, Kaplan DL, Merkle HP, Meinel L (2007) Control of in vitro tissue-engineered bone-like structures using human mesenchymal stem cells and porous silk scaffolds. Biomaterials 28:1152–1162
50. Kim K-H, Jeong L, Park H-N, Shin S-Y, Park W-H, Lee S-C, Kim T-I, Park Y-J, Seol Y-J, Lee Y-M (2005) Biological efficacy of silk fibroin nanofiber membranes for guided bone regeneration. J Biotechnol 120:327–339
51. Rajkhowa R, Gil ES, Kluge J, Numata K, Wang L, Wang X, Kaplan DL (2010) Reinforcing silk scaffolds with silk particles. Macromol Biosci 10:599–611
52. Mandal BB, Grinberg A, Gil ES, Panilaitis B, Kaplan DL (2012) High-strength silk protein scaffolds for bone repair. Proc Natl Acad Sci 109:7699–7704
53. Kanokpanont S, Damrongsakkul S, Ratanavaraporn J, Aramwit P (2013) Physico-chemical properties and efficacy of silk fibroin fabric coated with different waxes as wound dressing. Int J Biol Macromol 55:88–97
54. Vachiraroj N, Ratanavaraporn J, Damrongsakkul S, Pichyangkura R, Banaprasert T, Kanokpanont S (2009) A comparison of Thai silk fibroin-based and chitosan-based materials on in vitro biocompatibility for bone substitutes. Int J Biol Macromol 45:470–477
55. Wang L, Lu C, Li Y, Wu F, Zhao B, Dong X (2015) Green fabrication of porous silk fibroin/graphene oxide hybrid scaffolds for bone tissue engineering. RSC Adv 5:78660–78668
56. Yang Y, Chen X, Ding F, Zhang P, Liu J, Gu X (2007) Biocompatibility evaluation of silk fibroin with peripheral nerve tissues and cells in vitro. Biomaterials 28:1643–1652
57. Chen C-S, Soni S, Le C, Biasca M, Farr E, Chen EY, Chin W-C (2012) Human stem cell neuronal differentiation on silk-carbon nanotube composite. Nanoscale Res Lett 7:126
58. Hill PS, Apel PJ, Barnwell J, Smith T, Koman LA, Atala A, Van Dyke M (2011) Repair of peripheral nerve defects in rabbits using keratin hydrogel scaffolds. Tissue Eng A 17:1499–1505
59. Sierpinski P, Garrett J, Ma J, Apel P, Klorig D, Smith T, Koman LA, Atala A, Van Dyke M (2008) The use of keratin biomaterials derived from human hair for the promotion of rapid regeneration of peripheral nerves. Biomaterials 29:118–128
60. Apel PJ, Garrett JP, Sierpinski P, Ma J, Atala A, Smith TL, Koman LA, Van Dyke ME (2008) Peripheral nerve regeneration using a keratin-based scaffold: long-term functional and histological outcomes in a mouse model. J Hand Surg Am 33:1541–1547
61. Zhang W, Chen L, Chen J, Wang L, Gui X, Ran J, Xu G, Zhao H, Zeng M, Ji J (2017) Silk fibroin biomaterial shows safe and effective wound healing in animal models and a randomized controlled clinical trial. Adv Healthc Mater 6:1700121
62. Sugihara A, Sugiura K, Morita H, Ninagawa T, Tubouchi K, Tobe R, Izumiya M, Horio T, Abraham NG, Ikehara S (2000) Promotive effects of a silk film on epidermal recovery from full-thickness skin wounds (44552). Proc Soc Exp Biol Med 225:58–64
63. Roh D-H, Kang S-Y, Kim J-Y, Kwon Y-B, Kweon HY, Lee K-G, Park Y-H, Baek R-M, Heo C-Y, Choe J (2006) Wound healing effect of silk fibroin/alginate-blended sponge in full thickness skin defect of rat. J Mater Sci Mater Med 17:547–552
64. Moriyama M, Kubo H, Nakajima Y, Goto A, Akaki J, Yoshida I, Nakamura Y, Hayakawa T, Moriyama H (2016) Mechanism of Aloe vera gel on wound healing in human epidermis. J Dermatol Sci 84:e150–e151
65. Shahverdi S, Hajimiri M, Esfandiari MA, Larijani B, Atyabi F, Rajabiani A, Dehpour AR, Gharehaghaji AA, Dinarvand R (2014) Fabrication and structure analysis of poly (lactide-co-glycolic acid)/silk fibroin hybrid scaffold for wound dressing applications. Int J Pharm 473:345–355
66. Shan Y-H, Peng L-H, Liu X, Chen X, Xiong J, Gao J-Q (2015) Silk fibroin/gelatin electrospun nanofibrous dressing functionalized with astragaloside IV induces healing and anti-scar effects on burn wound. Int J Pharm 479:291–301
67. Lee KY, Kong S, Park W, Ha W, Kwon IC (1998) Effect of surface properties on the antithrombogenicity of silk fibroin/S-carboxymethyl kerateine blend films. J Biomater Sci Polym Ed 9:905–914
68. Aboushwareb T, Eberli D, Ward C, Broda C, Holcomb J, Atala A, Van Dyke M (2009) A keratin biomaterial gel hemostat derived from human hair: evaluation in a rabbit model of lethal liver injury. J Biomed Mater Res B Appl Biomater 90:45–54

Part II

Bioinspired 3D Bioprinting Hydrogel for Regenerative Medicine

4 Silk Fibroin Bioinks for Digital Light Processing (DLP) 3D Bioprinting

Soon Hee Kim, Do Yeon Kim, Tae Hyeon Lim, and Chan Hum Park

Abstract

Three-dimensional (3D) bioprinting has been a highly influential technology in the field of tissue engineering to enable speedy and precise spatial patterning of cells, growth factors, and biomaterials. Bioink is one of the main factors in 3D bioprinting, and hydrogels are excellent matrix type by means of bioinks for 3D bioprinting. Recently, stereolithographic bioprinting via digital light processing (DLP) that allows high spatial resolution and rapid printing time of complex structures has attracted many studies. However, a small number of bioinks have been applied to DLP bioprinting in comparison with bioinks for other bioprinters. We developed a novel bioink based on silk fibroin that has been extensively used in biomedical fields due to its positive biological and biochemical properties as biomaterials. In this chapter, we summarized the silk fibroin basics and various applications of silk fibroin as printing material. Also, fabrication and performance of silk-based bioink for DLP bioprinter were discussed.

Keywords

Digital light processing · 3D bioprinting · Photo-crosslinking · Silk Fibroin · Tissue engineering · Scaffold fabrication · Modeling · Rheological property · Bioink · 3D structure

4.1 Introduction

Tissue engineering is rapidly advancing in the field of regenerative medicine as a realistic alternative to solve problems on tissue damages by aging, trauma, or diseases. It is conservative to say that the progress in tissue engineering has been largely due to three-dimensional (3D) bioprinting. 3D bioprinting is defined as an additive layer-by-layer manufacturing of cell-laden biomaterials and bioactive molecules in a structure designed by computer-aided design (CAD). However, deposition of bio-

The original version of this chapter was revised: An earlier version of this chapter was published with an incorrect Acknowledgements text which has been updated now. The correction to this chapter is available at https://doi.org/10.1007/978-981-15-3258-0_15

S. H. Kim · D. Y. Kim · T. H. Lim
Nano-Bio Regenerative Medical Institute, College of Medicine, Hallym University, Chuncheon, Republic of Korea

C. H. Park (✉)
Nano-Bio Regenerative Medical Institute, College of Medicine, Hallym University, Chuncheon, Republic of Korea

Departments of Otorhinolaryngology-Head and Neck Surgery, Chuncheon Sacred Heart Hospital, School of Medicine, Hallym University, Chuncheon, Republic of Korea
e-mail: hlpch@paran.com

H. J. Chun et al. (eds.), *Bioinspired Biomaterials*, Advances in Experimental Medicine and Biology 1249, https://doi.org/10.1007/978-981-15-3258-0_4

logical factors in a 3D structure remains still many problems to be solved to make a complete organ.

Bioink plays a significant role for loading cells and biomolecules, and it also substantially contributes to the final shape fidelity. Hydrogels are recommended as bioink material; several hydrogel biomaterials based on alginate, collagen, gelatin, hyaluronic acid, Pluronic®, and poly(ethylene glycol) form the basis of commercial bioinks (Table 4.1). However, bioink materials are needed to be continuously developed because these are not clinically available and not fully satisfied to requirements of bioink.

Various bioprinting strategies have been applied to fabricate cell-laden 3D structures including inkjet, extrusion-based, laser-assisted, and stereolithography-based printing [1–3]. Among these strategies, digital light processing (DLP) printing (digital micro-mirror device (DMD)-based stereolithography) developed by Lu et al. [4] has been magnified as a high-throughput technique which gives high spatial resolution and great biocompatibility. DLP printer requires photosensitive polymers as bioink; however, a limited number of materials such as polyethylene glycol diacrylate (PEGDA), gly-

Table 4.1 Commercial bioinks [68] (referred company homepage)

Company	Trade name	Material
CELLINK (Sweden)	CELLINK A	Alginate
	CELLINK A-RGD	Alginate/RGD
	CELLINK bioink	Alginate and nanofibrillar cellulose
	CELLINK bone	CELLINK and tricalcium phosphate
	CELLINK FIBRIN	CELLINK and fibrinogen
	CELLINK LAMININ	CELLINK and laminin
	CELLINK RGD	CELLINK and alginate coupled with L-arginine-glycine-L-aspartic acid peptide
	Coll 1	Collagen type 1
	ColMA	Collagen methacrylate
	Bio Conductink	Gelatin methacrylate and carbon nanotubes
	GelMA	Gelatin methacrylate
	GelMA A	Gelatin methacrylate and alginate
	GelMA C	Gelatin methacrylate, nanofibrillar cellulose, and alginate
	GelMA HA	Gelatin methacrylate and methacrylated hyaluronic acid
	GelMA HIGH	High-concentration gelatin methacrylate
	GelXA	Gelatin methacrylate, xanthan gum, and alginate
	GelXA BONE	Gelatin methacrylate, xanthan gum, alginate, tricalcium phosphate, and hydroxyapatite
	GelXA FIBRIN	Gelatin methacrylate, xanthan gum, alginate, and fibrinogen
	GelXA LAMININ	Gelatin methacrylate, xanthan gum, alginate, and laminin
	GelXG	Gelatin methacrylate and xanthan gum
Bioink solution (Korea)	Gel4Cell®	Gelatin methacryloyl
	Gel4Cell®⁻Peptides	Gel4Cell® conjugated with growth factor mimetic peptides (BMP, VEGF, or TGF)
	TGel-S	Extracellular matrix extracted from small intestinal submucosa
regenHU (Swiss)	ECM-BioInk™	Human relevant synthetic ECM
	BioInk™	PEG/gelatin/hyaluronic acid
BioBots (USA)	Bio127	Pluronic® F127 base
	BioGel	GelMA
Aladdin (China)	GelMA25%	Gelatin methacryloyl (25~125% degree of methacrylation)
	GelMA50%	
	GelMA75%	
	GelMA100%	
	GelMA125%	

cidyl methacrylate-modified hyaluronic acid (GM-HA), and gelatin methacrylate (GelMA) have been applied for DLP printing (Table 4.2).

Silk fibroin (SF), a natural fibrous protein produced by *Bombyx mori* (*B. mori*), approved as a biomaterial by the FDA in 1993 has extensively been used in biomedical fields due to its excellent biocompatibility, adjustable biodegradability, good mechanical properties, and produceableness into various scaffold types [5–7]. Considering SF's versatility, it is not surprised that SF can be promising materials for bioink. However, low concentration and low viscosity of single SF are obstacles for common 3D printing application. Therefore, the 3D bioprinting using SF is now being processed by blending with other high viscosity materials to increase its printability [8–10].

In our laboratory, SF- or SF-blended biomaterials have been fabricated to sponge, powder, membrane, film, hydrogel, etc. for biomedical application during the last 10 years. Recently, in an effort to use SF as a bioink, our team developed a novel photopolymerizable bioink consisting of solely SF (Sil-MA) for DLP printing. In this chapter, we will mainly discuss the fabrication of Sil-MA bioink and its performance via DLP printer. Before this, we summarized the SF basics and various studies of SF as a 3D bioprinting material.

4.2 Silk Fibroin Basic and Rheological Property

Silk produced from *B. mori* is composed of SF as fibrous protein and sericin as glue-like protein that surrounds the fibroin threads. H-chain (hydrophobic domains) of SF contains a repetitive polypeptide sequence of Gly-Ala-Gly-Ala-Gly-Ser and Gly-Ala/Ser/Tyr dipeptides, which can build stable antiparallel β-sheet crystallites [7]. SF is more stable and stronger than other common natural materials due to its hydrophobicity, substantial hydrogen bonding, and high protein crystallinity by β-sheet crystals, which prolongs degradation time of the engineered product. Established aqueous processing such as lithium bromide treatment, calcium chloride treatment, etc. results in aqueous solutions of regenerated SF (RSF) [11, 12]. Hydrophobic segments (β-sheet) and hydrophilic segments (random coils) are dispersed randomly in a fresh RSF aqueous solution; it can be easily aggregated through physical or chemical stimuli to form a β-sheet [13] and be a hydrogel [5, 14]. Besides hydrogel, RSF can be different forms including film, membrane [15], powder [16], nanofibers [17, 18], and porous sponges [19, 20], which are suitable for regeneration field. RSF-based products show excellent biocompatibility, low immunogenicity, enzymatic degradability, and controllable biodegradability [21]. In addition, RSF-derived products can be a modified molecular weight distribution, protein conformation, and degree of crystallinity through processing condition [22–25]. With these merits, it has been applied for biomedical field such as cartilage regeneration [26], drug delivery [27], ridge preservation [28], bone regeneration [29–32], tympanic membrane perforation [33], intervertebral disc [34], wound dressing [35, 36], enzyme immobilization matrix [37], vascular prosthesis and structural implant [19, 38], etc.

Bioink should be thorough, including cytocompatibility, applicable mechanical properties, cell encapsulation ability, printability, biomimicry, etc., to meet both 3D cell culture and printing process. In this respect, hydrogels are recommended as bioink material due to its ability to encapsulate living cells and controllable mechanical-, degradable-, and chemical properties [39]. The main parameters determining the printability of bioinks are viscosity, density and surface tension, and nozzle diameter [40]. The printability of single RSF is low, reflecting its original environment in which SF coexists with sericin in silk. It has insufficient rheological properties (a low concentration (6%) and a low viscosity (46.5 mPa·s at 16%, 71 mPa·s at 24%, 200–800 mPa·s at 10%) [41, 42] for 3D printing. SF bioinks show shear thinning behavior (decreasing viscosity with increasing shear stress) below 20 wt% and represents a typical Newtonian fluid behavior (constant viscosity

Table 4.2 Bioinks used for DLP (= DMD μSL, projection micro-stereolithography)

Research title	Research objects	Materials	Application	Cell type	Photoinitiator	Note
A simple and high-resolution stereolithography-based 3D bioprinting system using visible light cross-linkable bioinks [69]	The use of commercial projector with a simple water filter (a low-cost printing system) for visible light	2.5–10% PEGDA, 5–7.5% GelMA	Microscale cell patterning Tissue engineering (broad)	NIH/3T3 fibroblasts	Eosin Y-based photoinitiator (visible light initiated)	
A novel bioprinting method and system for forming hybrid tissue engineering constructs [70]	Hybrid bioprinter composed of DLP-SLA module to print rigid scaffolds and soft hydrogel at the same time	15% PEGDA and PCL	Broad tissue engineering	HUVECs suspended in the PEGDA	0.25% w/v LAP	Hybrid printer of DLP-SLA
Rapid fabrication of complex 3D extracellular microenvironments by dynamic optical projection Stereolithography [71]	A novel DLP, called dynamic optical projection stereolithography to study cell interactions with microenvironments	20% PEGDA, 15% GelMA	Chip-based cell research platform	HUVECs and NIH-3T3	1% I2959	
Digital microfabrication of user-defined 3D microstructures in cell-laden hydrogels [72]	Development of a flexible platform to evaluate cell interactions with complex 3D micro-features	15% GelMA	3D cell research platform	NIH/3T3 cells 10T1/2 cells	0.3% w/v, I2959	
A digital micro-mirror device-based system for the microfabrication of complex, spatially patterned tissue engineering scaffolds [4]	Development of a system to create precise, predesigned, spatially patterned biochemical and physical microenvironments inside polymer scaffolds	100% PEGDA	Scaffold for osteogenic differentiation of stem cells	Murine mesenchymal stem cell	0.1% I2959	DLP printing pioneer
Thiol-ene clickable gelatin: a platform bioink for multiple 3D biofabrication technologies [73]	To make wider biofabrication window than common GelMA by introduction of flexible network via thiol-ene clickable bioink	10–20 wt% allylated gelatin (GelAGE)	Broad tissue engineering	Human articular chondrocytes (HACs)	$0.5/5 \times 10^{-3}$ M, Ru/SPS	Allyl:SH allyl glycidyl ether (AGE)
Bio-resin for high-resolution lithography-based biofabrication of complex cell-laden constructs [74]	Development of a new bio-resin based on PVA-MA and GelMA and a transition metal-based visible light photoinitiator	10 wt% PVA-MA/ 1 wt% gelatin methacryloyl (GelMA)	Broad tissue engineering	Human mesenchymal stromal cells (MSCs) and articular cartilage-derived progenitor cells (ACPCs)	0.2 mM/2 mM Ru/SPS	1 wt% photo-absorber (Ponceau 4R):

Precisely printable and biocompatible silk fibroin bioink for digital light processing 3D printing [45]	Development of silk-based DLP bioink for complex tissue engineered products	10–30% methacrylated silk fibroin (Sil-MA)	Broad tissue engineering	NIH/3T3 fibroblasts, human chondrocyte	0.3% LAP	
Scanningless and continuous 3D bioprinting of human tissues with decellularized extracellular matrix [75]	Development of rapidly DLP bioprintable dECM bioinks with accurate tissue-scale design for human tissue available in regenerative medicine	5% decellularized liver or heart left ventricle (HdECM) + 5% GelMA	Broad tissue engineering	Human-induced pluripotent stem cell (hiPSC)-derived cardiomyocytes and hepatocytes	0.25% LAP	
Vascularized bone-mimetic hydrogel constructs by 3D bioprinting to promote osteogenesis and angiogenesis [76]	Development of cell-loaded hydrogel-based bone structure with a biomimetic dual-ring structure	7.5% GelMA for vascular formation, 7.5%GelMA+5%octacalcium phosphate (OCP) for bone formation	Bone tissue engineering	Vascular formation: HUVEC spheroids Bone formation: mouse mesenchymal C3H10T1/2 cells	Vascular formation: 0.5% LAP, bone formation: 1% LAP	Bone formation: visible light projection SLA (DLP-based SLA)
Microfluidics-enabled multi-material maskless stereolithographic bioprinting [77]	A pattern of PEGDA frame and three different concentrations of GelMA, loaded with vascular endothelial growth factor, are further assessed for its neovascularization potential in a rat model	35% v/v PEGDA for frame, 5%, 10%, and 15% gelatin methacryloyl (GelMA) for bioprinting	Broad tissue engineering	Angiogenesis: breast cancer cells (MCF7), HUVECs Musculoskeletal system: NIH/3T3 fibroblasts and C2C12 skeletal muscle cells Tendon-to-bone insertion model: osteoblasts, human MSCs, fibroblasts	TEMPO (0.01% w/v) and LAP (1.0% w/v)	
Photopolymerizable gelatin and hyaluronic acid for stereolithographic 3D bioprinting of tissue-engineered cartilage [78]	To make articular cartilage niche resemble tissue using GelMA and HAMA via DLP	5 wt%GelMA or 1 wt%HAMA	Cartilage tissue engineering	Porcine chondrocytes	0.1% LAP	

Abbreviation: *PEGDA* poly(ethylene glycol diacrylate), *GelMA* gelatin methacrylate, *PCL* poly-(ε-caprolactone), *I2959 (UV initiated)* 2-hydroxy-1-[4-(hydroxyethoxy)-phenyl]-2-methyl-1-propanon, *Ru/SPS (metal-based visible light photoinitiator)* tris(2,2′-bipyridyl)dichlororuthenium(II) hexahydrate with sodium persulfate, *LAP (UV-visible light initiated)* lithium phenyl(2,4,6-trimethylbenzoyl) phosphinate, *PVA-MA* methacrylated poly(vinyl alcohol), *HAMA* methacrylated hyaluronic acid, *TEMPO (mitigator of free radical migration)* 2,2,6,6-tetramethylpiperdine 1-oxyl

with increasing shear stress) more than 20 wt% because of reduced chain mobility [43]. RSF is slowly gelated by enzyme (e.g., HRP), and common gelation processes being applied for SF (e.g., low pH, high temperature, additives) are not suitable for cell viability [9, 44]. However, the rheological properties of SF can be improved by adjusting the molecular weight of the SF (by degumming time and degumming temperature) and the final concentration of SF solution [40]. Nevertheless, quite a few studies have been conducted to apply SF to 3D bioprinting, and here are some examples on how SF was used as bioink depending on the printing technology in the below section.

4.3 Silk Fibroin-Based Materials for 3D Printing

4.3.1 The Use of SF in Inkjet Bioprinting

Inkjet bioprinting motivated from conventional 2D inkjet printing has advantages, such as relatively low cost, ease of use, and moderate printing speed ($mm \cdot s^{-1}$), and disadvantages that high viscosity materials and high cell density cannot be applied due to nozzle clogging. This feature ultimately brings restrictions on the fabrication of thick 3D structure [45]. For inkjet bioprinting, the bioinks with dilatant behavior and rheopectic (a time-dependent dilatant) behavior are suited. In this property, the polymer's viscosity increases with an increment of shear stress; therefore, droplets are formed by the increased viscosity following ejection during printing. Inkjet bioprinting ideally adopts a low-viscosity bioink (3.5–12 mPa·s) for easy flow without the nozzle clogging.

SF that can form solution drops (pL~nL) due to the amphiphilic nature of SF chains enables application to inkjet printing by itself. Tao et al. fabricated 3 wt% SF (90–350 kDa) solution in DW which could make stable droplets with suitable surface tension (0.046 N/m) and dynamic viscosity (3 mPa·s) [40]. They generated 20 μm spots through BMP added SF solution and commercial inkjet printer, which can be used for osteoblastic differentiation of h-MSC. In addition, they fabricated several functional silk inks including gold nanoparticles (Au-NP)-silk inks, horseradish peroxidase (HRP)-silk inks, antibiotic-silk inks, and silk ink mixed with polydiacetylene/IgG for colorimetric bacterial sensing.

Compaan et al. developed a two-step gelation process for the printing of SF, which uses alginate as a sacrificial hydrogel during an inkjetting-based printing to realize SF freeform fabrication [46]. First, alginate in NIH/3T3 laden SF/alginate solution is cross-linked by calcium chloride, and then tyrosine residues of SF were cross-linked by HRP. Finally, the calcium alginate is removed by sodium citrate treatment, and only cross-linked SF gel was remained. The SF hydrogel through this system showed excellent cell adhesion and no noticeable change in the shape integrity for 42 days. The considering side effect of the sodium citrate treatment on cell metabolic activity can be overcome by using biodegradable alginate.

4.3.2 The Use of SF in Extrusion-Based Bioprinting

Extrusion-based bioprinter developed by modifying the inkjet printer uses a screw plunger or an air pump to extrude bioink. Hydrogels with high viscosity are applicable to extrusion-based bioprinter. However, cells encapsulated in bioink receive large mechanical stress when they pass the nozzle. Also relatively higher viscosity of bioink and longer printing time than others can reduce cell viability by 40–80% [45]. Generally, bioinks with shear thinning and thixotropic behavior are commensurate with the extrusion-based bioprinting. In shear thinning bioinks, the polymer chain aligns to facilitate ejection when shear stress is applied to the hydrogel. Also, thixotropic hydrogels show a time-dependent shear thinning behavior, result to a low viscosity in the nozzle tip during printing, and recover its stability after printing. The ideal viscosity of extrusion bioprinting is from 30 mPa·s to 60 × 10^7 mPa·s [47]. Zhong et al. fabricated silk

fibroin/hydroxypropyl methyl cellulose (30 wt%SF/10 wt%HPMC) thixotropic hydrogel using an extrusion printer (Regenovo 3D bioprinter) and seeded normal human bronchial epithelial cell line (BEAS-2B) on the scaffold. They degummed SF solution using sodium carbonate to be concentrated to a high concentration [48]. Rodriguez et al. printed SF solution within a printing medium composed of synthetic nanoclay (laponite, 2.5%w/v) and polyethylene glycol (PEG, 40%v/v) using pneumatic extrusion printer (CELLINK INKREDIBLE+bioprinter) [49]. They degummed SF in sodium bicarbonate to make a high concentration of SF solution (> 30%). PEG contributed to cross-link the SF bioink and laponite supported structures while printing through thixotropic properties. They seeded primary human skeletal muscle myoblasts on the cross-linked SF hydrogel after removal of nanoclay. This method gives in situ physical cross-linking of SF into arbitrary geometries fabricated by freeform 3D printing.

Yeon et al. developed a less invasive, patient-specific, mechanically stable, and high biocompatible 3D printed bone clip as an internal fixation device. This contains 94% polylactide, 3% hydroxyapatite, and 3% SF (PLA/HA/SF) [50]. SF particles with 500–800 nm were obtained from freeze-dried 6% SF solution. Cell-free PLA/HA/SF bioink was printed through extrusion printing. This composite bone clip showed similar mechanical property with and superior biocompatibility to PLA and PLA/HA bone clip. In addition, excellent alignment of the bony segments across the femur fracture site was observed under the bone clip in a rat animal study.

4.3.3 The Use of SF in Laser-Assisted Bioprinting

Laser-assisted bioprinting is the principle using a laser beam for cell transfer. Laser-induced forward transfer (LIFT) printer composes of a pulsed laser source, glass slides that are composed of a thin layer of laser-absorbing material and a layer of biomaterial to be transferred (donor ribbon), and a receiving layer. The laser is focused toward laser-absorbing layer, which generates local heating and creates a vapor bubble in the underlying bioink in the donor layer. Finally, bioink droplets reach the receiving layer. For laser-assisted bioprinting, the bioink should have properties such as sufficient adhesion and low surface tension for even spreading and good adhesion on the donor slide. In addition, the bioink should have high viscoelasticity, rapid gelation ability, and easy transfer of thermal energy into kinetic energy. Generally, the bioink for laser-assisted printing adopts viscosity with ranges 1–300 mPa·s. Until now, SF bioink has not applied to this LIFT-type printer.

As another laser method, laser-guided direct writing system is the principle that laser-irradiated bioink is deposited on the target surface, and the bioink is drawn while moving the target surface. Ghosh et al. described the formation of 3D microperiodic scaffolds by laser-based direct writing of SF (Aerotech Inc.) [43]. The 29 wt%SF bioink had low shear viscosity (~2.9 Pa) which is similar to the synthetic polyelectrolyte complexes developed initially for direct writing. They printed SF solution into scaffolds with small feature sizes (diameter 5 μm). The SF ink resulted in minimized dimensional shrinkage in the scaffolds. Human bone marrow-derived mesenchymal stem cells (hMSCs) seeded on this scaffold were differentiated under chondrogenic conditions. However, they met frequent choking of nozzles due to shear-induced β-sheet crystallization and shortage of cell adhesion motifs on SF as demerit. Therefore, in their further study, they optimized viscoelastic property of SF by mixing gelatin in the various ratio [51]. This SF-gelatin blended bioink facilitated the flow through nozzles and supported redifferentiation of chondrocyte.

4.3.4 The Use of SF Bioink in DLP Bioprinting

Digital light projection (DLP) technology as stereolithography is an emerging technology recently. This printing method works in the top-down or bottom-up setups. DLP technology has

many advantages as compared to the techniques mentioned above. First of all, projection technology allows the polymerization in layer-by-layer fashion. Therefore, the building time is faster (~30 min, $mm^3 \cdot s^{-1}$) than other printers with line-by-line fashion (extrusion, inject, laser micro-stereolithography). The printing time of each layer is the same regardless of the complexity or size and only depends on the thickness of the structure. These fast printing time and nozzle-free way result in very high cell viability (85–95%). Especially, numerous mirrors in digital micro-mirror device (DMD) tilt separately in an on/off state, which play a role as a dynamic mask [45, 52] and result in resolution down to 200 μm. Shin et al. reduced the transparency of poly(ethylene glycol)-tetraacrylate (PEG4A) solution by adding SF incorporated with melanin (SFM) nanoparticles for DLP printing [53]. This blend enabled complex features including hollow blood vessels or tubes to be fabricated. Also, the elastic modulus of the hydrogel printed by this mixture increased 2.5-fold higher than the PEG4A hydrogel. Cell-encapsulated PEG4A/SFM bioink showed superior biocompatibility than PEG4A. Zhao et al. fabricated composite polypyrrole and 13%SF (PPy/SF) scaffolds with subsequent electrochemical deposition of PPy and stereolithography printing (or electrospinning) of SF for application into neuronal tissue engineering [54]. This scaffold has aligned construct and nanofiber structures. Schwann cells and L929 cells seeded onto scaffold showed good cytocompatibility. Na et al. printed a bioink composed of gelatin methacrylate/silk fibroin-encapsulated fibroblasts using DLP printing. SF raised the viscosity of gelatin methacrylate and contributed to avoid cells' precipitation. In addition, SF helped to increase cell dispersion and viability [55]. As a strategy to make the bone fixation system, Kim et al. fabricated SF plate and screw through a centrifugal casting technique incorporated 3D DLP printing technology [56]. Reverse-image casting molds as templates for the bone fixation system were printed by 3D DLP printer. These casting molds were put into a centrifuge, and 30%SF solution was filled in the molds. Finally, mechanically and structurally stable plates and screws were completed after centrifugation at 3000 rpm for 4 h. In vivo study, the devices resulted in new bone formation maintaining well in the fixed location. Lastly, we developed precisely printable and biocompatible 10–30%SF bioink for DLP bioprinting through SF methacrylation and proved their performance as fabricating complex structures with high resolution and biocompatibility [45]. This is discussed in the below section in more detail.

4.4 Methacrylated Silk Fibroin Solution for 3D DLP Printer

Although DLP printer has advantages of rapid printing time, high resolution and biocompatible by nozzle-free printing, etc., DLP printing is not widely used because of the limited light sensitive biomaterials to be applied. Table 4.2 provides an overview of the photopolymerized bioinks (including material, concentration, cell type, and concept of study) used for 3D DLP bioprinting. Materials being applied for DLP printing are based on gelatin or hyaluronic acid (HA) as natural polymer and polyvinyl alcohol and polyethylene glycol as synthetic polymer. We are going to mention only the natural polymer that has superior biocompatibility compared to synthetic polymer.

Gelatin has advantages including biocompatibility, biodegradability, low antigenicity, exist of intrinsic Arg-Gly-Asp (RGD) motifs, etc. However, gelatin belongs to the thermo-responsive, UCST (upper critical solution temperature) hydrogel, that is, gelatin can be dissolved in water (sol state) above a specific temperature threshold of about 40 °C and it can be gel below the temperature [57]. Therefore, temperature control is needed during printing to inhibit gelation in a bath.

HA belonging to a polysaccharide is non-immunogenic and non-thrombogenic and can be cross-linked via various mechanisms to form hydrogels. HA has been proven in angiogenesis [58], wound healing [59], tendon regeneration [60], cartilage regeneration [61, 62], etc. Because of one of the significant drawbacks, the weak of

water, HA is used as being blended with other materials or being modified chemically [63]. Nevertheless, HA has still a short degradation time (within 2 days, methacrylated HA) [64]. In addition, HA with high viscosity (at least 500 mPa·s by high molecular weight (20~1500 kDa) appears to be more suitable for extrusion-based bioprinter [65] than DLP.

In the absence of suitable bioink for DLP printer, it is important to develop a novel bioink satisfied with biodegradable, biocompatible, bioprintable, and mechanically stable properties. Therefore, Kim et al. have reported that methacrylated SF is synthesized as bioink (for cell encapsulation) for DLP bioprinter [45]. SF can be incorporated with various materials through chemical modifications including coupling reactions, amino acid modifications, and grafting reactions. Like gelatin, SF can be modified with photopolymerizable methacryloyl groups through amine-containing side groups, enabling covalent cross-linking by UV light following the DLP bioprinting process. In addition, SF has a suitable viscosity for DLP printing.

As degumming process, 40 g of sliced *B. mori* cocoons were boiled in 1 L of 0.05 M sodium carbonate (Na_2CO_3) solution for 30 min at 100 °C. Degummed silk was dried at RT, and 20 g of it was dissolved in 100 mL of 9.3 M lithium bromide (LiBr) solution at 60 °C for 1 h. Right after SF was solved by LiBr, glycidyl methacrylate solution (GMA) (final concentration 141–705 mM) was added to the mixture stirring with a speed of 300 rpm for 3 h at 60 °C to create a high yield reaction between GMA and SF. Then, the resulting solution was dialyzed against distilled water using 12–14 kDa cutoff dialysis tubes for 4–7 days. Finally, methacrylated SF solutions (Sil-MA) were freeze-dried for 48 h. The methacrylation's success or failure and the degree of methacrylation were confirmed using NMR and FT-IR. Usually, gelatin [66] and HA [67] were modified by methacrylic anhydride (MA) to give methacryloyl groups. However, GMA reagent is more recommended to SF modification than MA because GMA rarely produces an acidic by-product (which can crystalize SF at unwanted steps) primarily through the epoxide ring-opening mechanism.

To make Sil-MA bioink, 0.2%w/v lithium phenyl (2,4,6-trimethylbenzoyl) phosphinate (LAP) was added to the solution of 10–30% Sil-MA and printed with DLP bioprinter of high resolution. LAP that is initiated at 365 nm UV light has a higher water solubility and lower cell cytotoxicity than Irgacure 2959. The absorbance of LAP at 400 nm allows for polymerization with visible light. Applegate et al. used riboflavin (vitamin B2) as a photoinitiator and visible light as a light source for SF polymerization via tyrosine in SF protein. The visible light is safe to cells; however, the high penetration ratio and long cross-linking time that affects the final structure of construct are not preferred to DLP printer.

The Sil-MA hydrogel printed by DLP printer showed suitable properties for use in tissue engineering. Through rheometer, Sil-MA hydrogel showed a typical viscoelastic character of hydrogels. The hydrogel (30% Sil-MA) has a compressive strength (910 kPa) and a good tensile strength, and it endured a weight of kettle bell (7 kg) with elastic resilience. These high mechanical properties of Sil-MA enabled the hydrogel to be sutured and especially made it possible to perform dog's tracheal end-to-end anastomosis.

We tested the printability of Sil-MA by printing various types of objects or organs such as porous scaffold and the Eiffel Tower, ear and brain, trachea, heart, lung, and vessel. DLP printing using Sil-MA bioink produced successfully these complex structures including micro vein, artery, folds, and small holes (700 μm~) (Fig. 4.1).

In order to evaluate Sil-MA biocompatibility, we printed NIH/3T3-encapsulated Sil-MA hydrogel and carried out a live/dead assay and CCK-8 assay. Sil-MA hydrogel showed good cytocompatibility at even high concentration. Especially, it was shown that alive cells were distributed evenly over the printed constructs regardless of the size and complexity of the construct (HL logo and the brain and trachea with different cell-type layers) through single plane illumination microscopy (SPIM). To see the possibility to specific targeted tissue engineering on this sys-

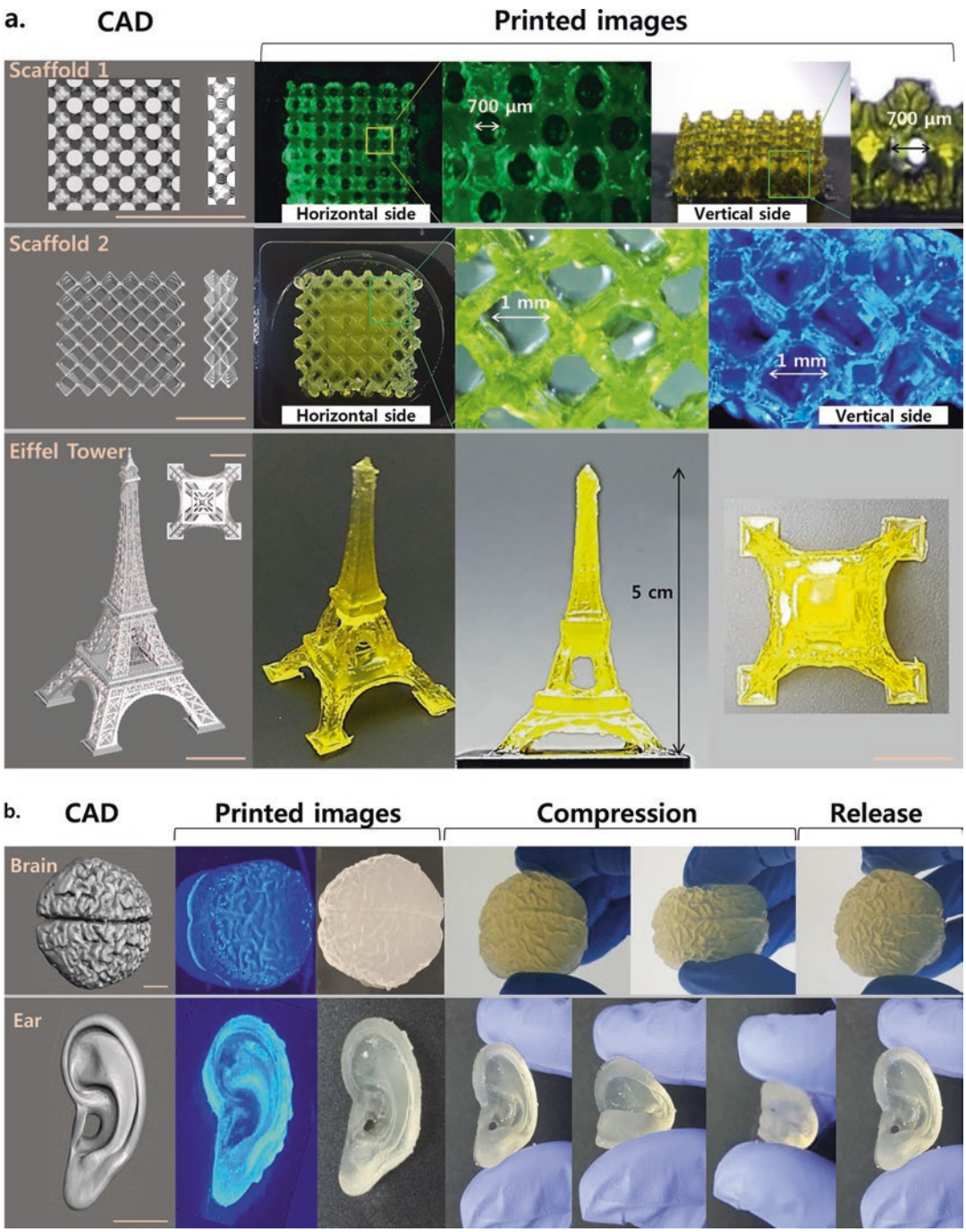

Fig. 4.1 Printability of 30%Sil-MA using DLP printer. (**a**) Porous scaffold and Eiffel Tower imitation; (l) CAD images depicting scaffolds and the Eiffel Tower and (r) printed images. Printed scaffolds had small pores around ~700 μm, and the Eiffel Tower had small holes and grid on the surface. (**b**) Ear and brain mimicked shape; (l) CAD images depicting the ear and brain and (r) printed images. Printed products were not damaged when they were compressed by fingers tightly, and they were back to their original shape when fingers were relaxed. (**c**) Trachea, heart, lung, and vessel mimicked shape; (l) CAD images depicting the trachea, heart, lung, and vessel and (r) printed images at various angles. Printed products by DLP using Sil-MA showed complex structure reflecting their CAD images, including veins, arteries, folds, and holes. Scale bar indicates 1 cm. [45] Copyright: Nature publishing group

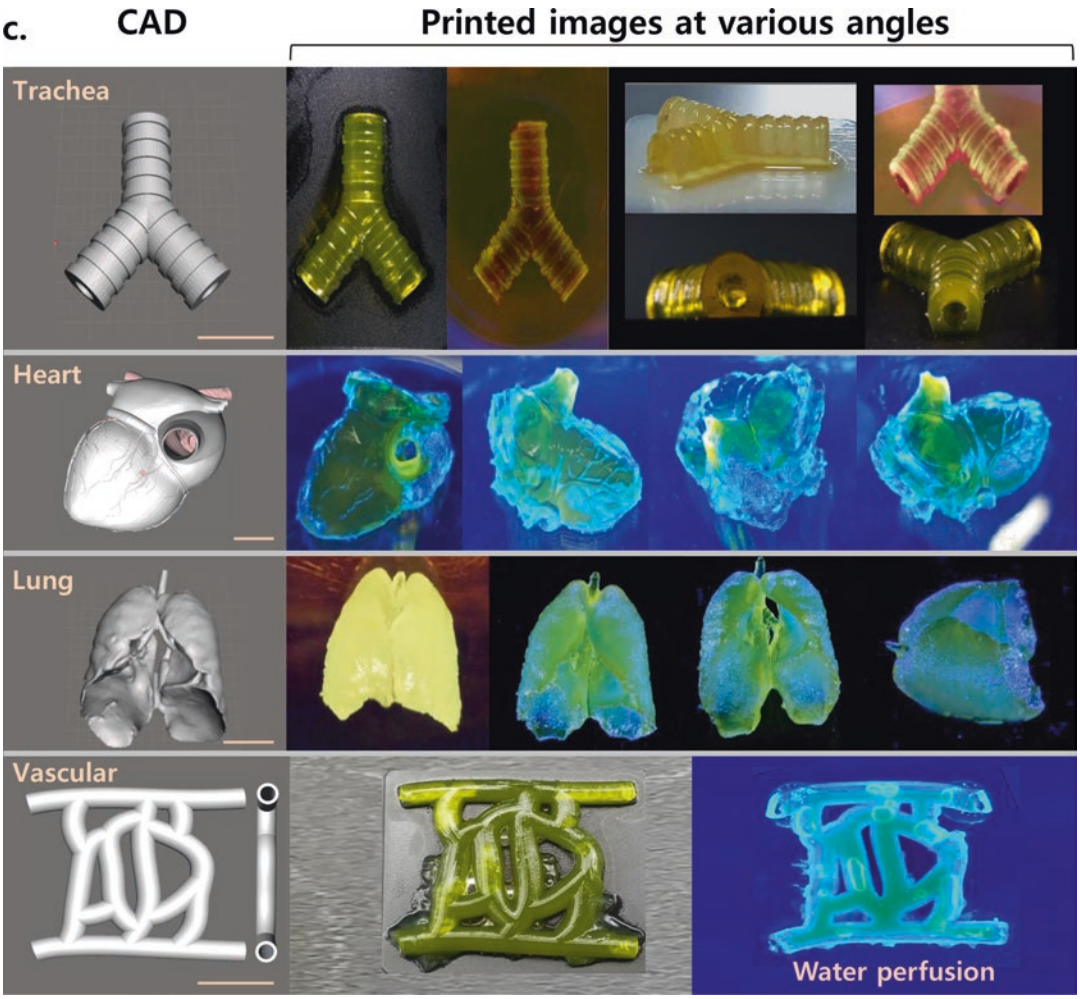

Fig. 4.1 (continued)

tem, human chondrocytes were encapsulated in Sil-MA hydrogel and cultivated in vitro. This cell-laden Sil-MA hydrogel showed a great cartilage tissue formation in them. Our study suggests that Sil-MA bioink can actively play as a promising material combined with DLP bioprinter in tissue engineering field.

4.5 Conclusions

Silk fibroin (SF) has been utilized in a variety of tissue engineering applications. With biological advantages of SF, SF is also attractive as a bioink material. However, SF's unique characters (such as amphiphilicity, β-sheet self-assembly by various stimuli, intrinsic low viscosity, changeable rheological property depending on concentration, etc.) are things that should be considered for applications into general bioprinting technology as a bioink. Several studies have been reported on the utilization of SF to various 3D bioprinting modalities. The printing performance of SF can be improved by lowering the density of the silk for inkjet printing and by mixing with other biomaterials (e.g., gelatin) for extrusion printing. The sole SF was used in a small number of studies; however, important issues to be solved were remained. Most of the studies using silk bioink until now have proceeded by seeding cells after

printing, not cell encapsulation in bioink. Studies using DLP printing dealt with cell-laden SF bioink, but blended bioink with other materials for photocross-linking was used. Methacrylated SF was developed with a suitable rheological property and obtained printability for DLP printing as well as cell encapsulation property with biocompatibility.

We expect that this methacrylated SF can play a role in tissue engineering being in harmony with DLP bioprinter. However, there are many issues to be solved for the actual application of this system. For examples, the use of UV light in polymerization, chemical reagent for the introduction of photocross-linkable group, and photoinitiator are cell unfriendly causing cytotoxicity. The lack of cell binding motif in silk is also a problem to be overcome. In terms of printability using DLP printer, the transparency of the SF is needed to be considered because of shape fidelity. For further valuable study of SF bioink application to various printing modalities including DLP, it is important to have a deep understanding of SF as well as printer to be applied.

Acknowledgments This work was supported by the National Research Foundation of Korea (NRF) grant funded by the Korea government (MSIP) (grant No.: 2016R1E1A1A01942120), Republic of Korea and by the Hallym University Research Fund.

References

1. Derakhshanfar S, Mbeleck R, Xu K, Zhang X, Zhong W, Xing M (2018) 3D bioprinting for biomedical devices and tissue engineering: a review of recent trends and advances. Bioactive Mater 3(2):144–156
2. Liu F, Liu C, Chen Q, Ao Q, Tian X, Fan J, Tong H, Wang X (2018) Progress in organ 3D bioprinting. Int J Bioprint 4:1–15
3. Kačarević ŽP, Rider PM, Alkildani S, Retnasingh S, Smeets R, Jung O, Barbeck M (2018) An introduction to 3D bioprinting: possibilities, challenges and future aspects. Materials 11(11):2199
4. Lu Y, Mapili G, Suhali G, Chen S, Roy K (2006) A digital micro-mirror device-based system for the microfabrication of complex, spatially patterned tissue engineering scaffolds. J Biomed Mater Res Part A 77(2):396–405
5. Ju HW, Lee OJ, Moon BM, Sheikh FA, Lee JM, Kim JH, Park CH (2014) Silk fibroin based hydrogel for regeneration of burn induced wounds. Tissue Eng Regen Med 11(3):203–210
6. Melke J, Midha S, Ghosh S, Ito K, Hofmann S (2016) Silk fibroin as biomaterial for bone tissue engineering. Acta Biomater 31:1–16
7. Qi Y, Wang H, Wei K, Yang Y, Zheng RY, Kim IS, Zhang KQ (2017) A review of structure construction of silk fibroin biomaterials from single structures to multi-level structures. Int J Mol Sci 18(3):237
8. Das S, Pati F, Choi YJ, Rijal G, Shim JH, Kim SW, Ghosh S (2015) Bioprintable, cell-laden silk fibroin–gelatin hydrogel supporting multilineage differentiation of stem cells for fabrication of three-dimensional tissue constructs. Acta Biomater 11:233–246
9. Lee H, Yang GH, Kim M, Lee J, Huh J, Kim G (2018) Fabrication of micro/nanoporous collagen/dECM/silk-fibroin biocomposite scaffolds using a low temperature 3D printing process for bone tissue regeneration. Mater Sci Eng C 84:140–147
10. Shi W, Sun M, Hu X, Ren B, Cheng J, Li C, Ao Y (2017) Structurally and functionally optimized silk-fibroin–gelatin scaffold using 3D printing to repair cartilage injury in vitro and in vivo. Adv Mater 29(29):1701089
11. Miyaguchi Y, Hu J (2005) Physicochemical properties of silk fibroin after solubilization using calcium chloride with or without ethanol. Food Sci Technol Res 11(1):37–42
12. Zhang X, Reagan MR, Kaplan DL (2009) Electrospun silk biomaterial scaffolds for regenerative medicine. Adv Drug Deliv Rev 61(12):988–1006
13. Cao Z, Chen X, Yao J, Huang L, Shao Z (2007) The preparation of regenerated silk fibroin microspheres. Soft Matter 3(7):910–915
14. Lee J, Sultan M, Kim S, Kumar V, Yeon Y, Lee O, Park C (2017) Artificial auricular cartilage using silk fibroin and polyvinyl alcohol hydrogel. Int J Mol Sci 18(8):1707
15. Lee OJ, Lee JM, Kim JH, Kim J, Kweon H, Jo YY, Park CH (2012) Biodegradation behavior of silk fibroin membranes in repairing tympanic membrane perforations. J Biomed Mater Res A 100(8):2018–2026
16. Yoshimizu H, Asakura T (1990) Preparation and characterization of silk fibroin powder and its application to enzyme immobilization. J Appl Polym Sci 40(1–2):127–134
17. Park YR, Ju HW, Lee JM, Kim DK, Lee OJ, Moon BM, Park CH (2016) Three-dimensional electrospun silk-fibroin nanofiber for skin tissue engineering. Int J Biol Macromol 93:1567–1574
18. Sheikh FA, Ju HW, Lee JM, Moon BM, Park HJ, Lee OJ, Park CH (2015) 3D electrospun silk fibroin nanofibers for fabrication of artificial skin. Nanomedicine 11(3):681–691
19. Park HJ, Lee OJ, Lee MC, Moon BM, Ju HW, min Lee J, Park CH (2015) Fabrication of 3D porous silk scaffolds by particulate (salt/sucrose) leaching for bone tissue reconstruction. Int J Biol Macromol 78:215–223

20. Irawan V, Sung TC, Higuchi A, Ikoma T (2018) Collagen scaffolds in cartilage tissue engineering and relevant approaches for future development. Tissue Eng Regen Med 15(6):673–697
21. Dickerson MB, Dennis PB, Tondiglia VP, Nadeau LJ, Singh KM, Drummy LF, Naik RR (2017) 3D printing of regenerated silk fibroin and antibody-containing microstructures via multiphoton lithography. ACS Biomater Sci Eng 3(9):2064–2075
22. Tao H, Kaplan DL, Omenetto FG (2012) Silk materials–a road to sustainable high technology. Adv Mater 24(21):2824–2837
23. Pereira RF, Silva MM, de Zea Bermudez V (2015) Bombyx mori silk fibers: an outstanding family of materials. Macromol Mater Eng 300(12):1171–1198
24. Rockwood DN, Preda RC, Yücel T, Wang X, Lovett ML, Kaplan DL (2011) Materials fabrication from Bombyx mori silk fibroin. Nat Protoc 6(10):1612
25. Wray LS, Hu X, Gallego J, Georgakoudi I, Omenetto FG, Schmidt D, Kaplan DL (2011) Effect of processing on silk-based biomaterials: reproducibility and biocompatibility. J Biomed Mater Res B Appl Biomater 99(1):89–101
26. Jung CS, Kim BK, Lee J, Min BH, Park SH (2018) Development of printable natural cartilage matrix bioink for 3D printing of irregular tissue shape. Tissue Eng Regen Med 15(2):155–162
27. Shera SS, Sahu S, Banik RM (2018) Preparation of drug eluting natural composite scaffold using response surface methodology and artificial neural network approach. Tissue Eng Regen Med 15(2):131–143
28. Seok H, Jo YY, Kweon H, Kim SG, Kim MK, Chae WS (2017) Comparison of bio-degradation for ridge preservation using silk fibroin-based grafts and a collagen plug. Tissue Eng Regen Med 14(3):221–231
29. Kashte S, Jaiswal AK, Kadam S (2017) Artificial bone via bone tissue engineering: current scenario and challenges. Tissue Eng Regen Med 14(1):1–14
30. Chen L, Hu J, Ran J, Shen X, Tong H (2014) Preparation and evaluation of collagen-silk fibroin/hydroxyapatite nanocomposites for bone tissue engineering. Int J Biol Macromol 65:1–7
31. Sanosh KP, Gervaso F, Sannino A, Licciulli A (2014) Preparation and characterization of collagen/hydroxyapatite microsphere composite scaffold for bone regeneration. Key Eng Mater 587:239–244. Trans Tech Publications
32. Paşcu EI, Stokes J, McGuinness GB (2013) Electrospun composites of PHBV, silk fibroin and nano-hydroxyapatite for bone tissue engineering. Mater Sci Eng C 33(8):4905–4916
33. Kim SH, Jeong JY, Park HJ, Moon BM, Park YR, Lee OJ, Park CH (2017) Application of a collagen patch derived from duck feet in acute tympanic membrane perforation. Tissue Eng Regen Med 14(3):233–241
34. Tavakoli J (2017) Tissue engineering of the intervertebral disc's annulus fibrosus: a scaffold-based review study. Tissue Eng Regen Med 14(2):81–91
35. Lee JM, Chae T, Sheikh FA, Ju HW, Moon BM, Park HJ, Park CH (2016) Three dimensional poly (ε-caprolactone) and silk fibroin nanocomposite fibrous matrix for artificial dermis. Mater Sci Eng C 68:758–767
36. Lee OJ, Kim JH, Moon BM, Chao JR, Yoon J, Ju HW, Park HS (2016) Fabrication and characterization of hydrocolloid dressing with silk fibroin nanoparticles for wound healing. Tissue Eng Regen Med 13(3):218–226
37. Moon BM, Choi MJ, Sultan MT, Yang JW, Ju HW, Lee JM, Lee MC (2017) Novel fabrication method of the peritoneal dialysis filter using silk fibroin with urease fixation system. J Biomed Mater Res B Appl Biomater 105(7):2136–2144
38. Dal Pra I, Freddi G, Minic J, Chiarini A, Armato U (2005) De novo engineering of reticular connective tissue in vivo by silk fibroin nonwoven materials. Biomaterials 26(14):1987–1999
39. Gopinathan J, Noh I (2018) Recent trends in bioinks for 3D printing. Biomater Res 22(1):11
40. Tao H, Marelli B, Yang M, An B, Onses MS, Rogers JA, Omenetto FG (2015) Inkjet printing of regenerated silk fibroin: from printable forms to printable functions. Adv Mater 27(29):4273–4279
41. Li X, Zhang Q, Feng Y, Yan S, Qu J, You R (2016) Preparation of Antheraea pernyi silk fibroin microparticles through a facile electrospinning method. Adv Mater Sci Eng 2016:1–7
42. Kim HH, Kim MK, Lee KH, Park YH, Um IC (2015) Effects of different Bombyx mori silkworm varieties on the structural characteristics and properties of silk. Int J Biol Macromol 79:943–951
43. Ghosh S, Parker ST, Wang X, Kaplan DL, Lewis JA (2008) Direct-write assembly of microperiodic silk fibroin scaffolds for tissue engineering applications. Adv Funct Mater 18(13):1883–1889
44. Wang X, Kluge JA, Leisk GG, Kaplan DL (2008) Sonication-induced gelation of silk fibroin for cell encapsulation. Biomaterials 29(8):1054–1064
45. Kim SH, Yeon YK, Lee JM, Chao JR, Lee YJ, Seo YB, Hong IS (2018) Precisely printable and biocompatible silk fibroin bioink for digital light processing 3D printing. Nat Commun 9(1):1620
46. Compaan AM, Christensen K, Huang Y (2016) Inkjet bioprinting of 3D silk fibroin cellular constructs using sacrificial alginate. ACS Biomater Sci Eng 3(8):1519–1526
47. Mandrycky C, Wang Z, Kim K, Kim DH (2016) 3D bioprinting for engineering complex tissues. Biotechnol Adv 34(4):422–434
48. Zhong N, Dong T, Chen Z, Guo Y, Shao Z, Zhao X (2019) A novel 3D-printed silk fibroin-based scaffold facilitates tracheal epithelium proliferation in vitro. J Biomater Appl 34(1):3–11. 0885328219845092
49. Rodriguez MJ, Dixon TA, Cohen E, Huang W, Omenetto FG, Kaplan DL (2018) 3D freeform printing of silk fibroin. Acta Biomater 71:379–387
50. Yeon YK, Park HS, Lee JM, Lee JS, Lee YJ, Sultan MT, Park CH (2018) New concept of 3D printed bone clip (polylactic acid/hydroxyapatite/silk composite)

for internal fixation of bone fractures. J Biomater Sci Polym Ed 29(7–9):894–906
51. Zhou M, Lee BH, Tan LP (2017) A dual crosslinking strategy to tailor rheological properties of gelatin methacryloyl. Int J Bioprint 3(2):130–137
52. Billiet T, Vandenhaute M, Schelfhout J, Van Vlierberghe S, Dubruel P (2012) A review of trends and limitations in hydrogel-rapid prototyping for tissue engineering. Biomaterials 33(26):6020–6041
53. Shin S, Kwak H, Hyun J (2018) Melanin nanoparticle-incorporated silk fibroin hydrogels for the enhancement of printing resolution in 3D-projection Stereolithography of poly (ethylene glycol)-Tetraacrylate bio-ink. ACS Appl Mater Interfaces 10(28):23573–23582
54. Zhao YH, Niu CM, Shi JQ, Wang YY, Yang YM, Wang HB (2018) Novel conductive polypyrrole/silk fibroin scaffold for neural tissue repair. Neural Regen Res 13(8):1455
55. Na K, Shin S, Lee H, Shin D, Baek J, Kwak H, Hyun J (2018) Effect of solution viscosity on retardation of cell sedimentation in DLP 3D printing of gelatin methacrylate/silk fibroin bioink. J Ind Eng Chem 61:340–347
56. Kim DK, Lee JM, Jeong JY, Park HJ, Lee OJ, Chao J, Park CH (2018) New fabrication method of silk fibroin plate and screw based on a centrifugal casting technique. J Tissue Eng Regen Med 12(11):2221–2229
57. Salamon A, Van Vlierberghe S, Van Nieuwenhove I, Baudisch F, Graulus GJ, Benecke V, Dubruel P (2014) Gelatin-based hydrogels promote chondrogenic differentiation of human adipose tissue-derived mesenchymal stem cells in vitro. Materials 7(2):1342–1359
58. West DC, Hampson IN, Arnold F, Kumar S (1985) Angiogenesis induced by degradation products of hyaluronic acid. Science 228(4705):1324–1326
59. Chen WJ, Abatangelo G (1999) Functions of hyaluronan in wound repair. Wound Repair Regen 7(2):79–89
60. Majima T, Irie T, Sawaguchi N, Funakoshi T, Iwasaki N, Harada K, Nishimura SI (2007) Chitosan-based hyaluronan hybrid polymer fibre scaffold for ligament and tendon tissue engineering. Proc Inst Mech Eng H J Eng Med 221(5):537–546
61. Kim TH, Yun YP, Shim KS, Kim HJ, Kim SE, Park K, Song HR (2018) In vitro anti-inflammation and Chondrogenic differentiation effects of inclusion Nanocomplexes of hyaluronic acid-Beta Cyclodextrin and simvastatin. Tissue Eng Regen Med 15(3):263–274
62. Kang SW, Bada LP, Kang CS, Lee JS, Kim CH, Park JH, Kim BS (2008) Articular cartilage regeneration with microfracture and hyaluronic acid. Biotechnol Lett 30(3):435–439
63. Leach JB, Schmidt CE (2005) Characterization of protein release from photocrosslinkable hyaluronic acid-polyethylene glycol hydrogel tissue engineering scaffolds. Biomaterials 26(2):125–135
64. Masters KS, Shah DN, Leinwand LA, Anseth KS (2005) Crosslinked hyaluronan scaffolds as a biologically active carrier for valvular interstitial cells. Biomaterials 26(15):2517–2525
65. Perale G, Hilborn J (eds) (2016) Bioresorbable polymers for biomedical applications: from fundamentals to translational medicine. Woodhead Publishing, Sawston
66. Van Den Bulcke AI, Bogdanov B, De Rooze N, Schacht EH, Cornelissen M, Berghmans H (2000) Structural and rheological properties of methacrylamide modified gelatin hydrogels. Biomacromolecules 1(1):31–38
67. Smeds KA, Grinstaff MW (2001) Photocrosslinkable polysaccharides for in situ hydrogel formation. J Biomed Mater Res 54(1):115–121
68. Hospodiuk M, Dey M, Sosnoski D, Ozbolat IT (2017) The bioink: a comprehensive review on bioprintable materials. Biotechnol Adv 35(2):217–239
69. Wang Z, Abdulla R, Parker B, Samanipour R, Ghosh S, Kim K (2015) A simple and high-resolution stereolithography-based 3D bioprinting system using visible light crosslinkable bioinks. Biofabrication 7(4):045009
70. Shanjani Y, Pan CC, Elomaa L, Yang Y (2015) A novel bioprinting method and system for forming hybrid tissue engineering constructs. Biofabrication 7(4):045008
71. Zhang AP, Qu X, Soman P, Hribar KC, Lee JW, Chen S, He S (2012) Rapid fabrication of complex 3D extracellular microenvironments by dynamic optical projection stereolithography. Adv Mater 24(31):4266–4270
72. Soman P, Chung PH, Zhang AP, Chen S (2013) Digital microfabrication of user-defined 3D microstructures in cell-laden hydrogels. Biotechnol Bioeng 110(11):3038–3047
73. Bertlein S, Brown G, Lim KS, Jungst T, Boeck T, Blunk T, Groll J (2017) Thiol–ene clickable gelatin: a platform bioink for multiple 3D biofabrication technologies. Adv Mater 29(44):1703404
74. Lim KS, Levato R, Costa PF, Castilho MD, Alcala-Orozco CR, van Dorenmalen KM, Woodfield TB (2018) Bio-resin for high resolution lithography-based biofabrication of complex cell-laden constructs. Biofabrication 10(3):034101
75. Yu C, Ma X, Zhu W, Wang P, Miller KL, Stupin J, Chen S (2019) Scanningless and continuous 3D bioprinting of human tissues with decellularized extracellular matrix. Biomaterials 194:1–13
76. Anada T, Pan CC, Stahl AM, Mori S, Fukuda J, Suzuki O, Yang Y (2019) Vascularized bone-mimetic hydrogel constructs by 3D bioprinting to promote osteogenesis and angiogenesis. Int J Mol Sci 20(5):1096
77. Miri AK, Nieto D, Iglesias L, Goodarzi Hosseinabadi H, Maharjan S, Ruiz-Esparza GU, Shin SR (2018) Microfluidics-enabled multimaterial Maskless stereolithographic bioprinting. Adv Mater 30(27):1800242
78. Lam T, Dehne T, Krüger JP, Hondke S, Endres M, Thomas A, Kloke L (2019) Photopolymerizable gelatin and hyaluronic acid for stereolithographic 3D bioprinting of tissue-engineered cartilage. J Biomed Mater Res Part B Appl Biomater 107(8):2649–2657

5 3D Bioprinting of Tissue Models with Customized Bioinks

Murat Taner Vurat, Can Ergun, Ayşe Eser Elçin, and Yaşar Murat Elçin

Abstract

The ordered assembly of multicellular structures mimicking native tissues has lately come into prominence for various applications of biomedicine. In this respect, three-dimensional bioprinting (3DP) of cells and other biologics through additive manufacturing techniques has brought the possibility to develop functional in vitro tissue models and perhaps creating de novo transplantable tissues or organs in time. Bioinks, which can be defined as the printable analogues of the extracellular matrix, represent the foremost component of 3DP. In this chapter, we attempt to elaborate the major classes of bioinks which are prevalently being evaluated for the 3DP of a wide range of tissue models.

Keywords

Three-dimensional (3D) bioprinting · Bioink · Tissue model · Tissue engineering · Organ manufacturing · Drug testing platform · Organ-on-a-chip · Biomaterials · In vitro tissue model · Microphysiological system · Personalized medicine · Viable construct

M. T. Vurat · C. Ergun · Y. M. Elçin (✉)
Biovalda Health Technologies, Inc., Ankara, Turkey

Tissue Engineering, Biomaterials and Nanobiotechnology Laboratory, Ankara University Faculty of Science, Ankara, Turkey

A. E. Elçin
Tissue Engineering, Biomaterials and Nanobiotechnology Laboratory, Ankara University Faculty of Science, and Ankara University Stem Cell Institute, Ankara, Turkey

Abbreviations

3DP	Three-dimensional bioprinting
A1AT	Alpha-1 antitrypsin
ACCs	Articular cartilage chondrocytes
AChR	Acetylcholine receptor
Alg	Calcium alginate
ALI	Air-liquid interface
ALP	Alkaline phosphatase
APAP	Acetaminophen
ASCs	Adipose stem cells
$BaCl_2$	Barium chloride
BM-MSCs	Bone marrow-derived mesenchymal stem cells
$CaCl_2$	Calcium chloride
CECs	Corneal epithelial cells
CKCs	Corneal keratocytes
CMA	Collagen methacrylamide
CMPCs	Cardiac-derived cardiomyocyte progenitor cells
CMs	Cardiomyocytes
CYP	Cytochrome P450
dECM	Decellularized extracellular matrix
DLP	Digital light processing

H. J. Chun et al. (eds.), *Bioinspired Biomaterials*, Advances in Experimental Medicine and Biology 1249, https://doi.org/10.1007/978-981-15-3258-0_5

DVS	Divinyl sulfone
EBB	Extrusion-based bioprinting
EDC	1-Ethyl-(3-3-dimethylaminopropyl) hydrochloride
ESC-LESCs	Embryonic stem cell-derived limbal epithelial stem cells
FBs	Fibroblasts
FDM	Fused deposition modeling
Gel-MA	Gelatin methacrylate
Gel-AGE	Allylated gelatin
GRGDS	Cell binding domain of osteopontin
HA	Hyaluronic acid
HAGM	Hyaluronic acid glycidyl methacrylate
HUVECs	Human umbilical vein endothelial cells
iPSCs	Induced pluripotent stem cells
LAB	Laser-assisted bioprinting
LAP	Lithium phenyl-2,4,6-trimethylbenzoylphosphinate
LBB	Laser-based bioprinting
MBB	Microvalve-based bioprinting
MCs	Melanocytes
MMP	Matrix metalloproteinase
MPCs	Muscle progenitor cells
MRI	Magnetic resonance imaging
MSCs	Mesenchymal stem cells
$NaHCO_3$	Sodium bicarbonate
nHAp	Nanohydroxyapatite
NSCs	Neural stem cells
PCL	Poly(caprolactone)
PCNs	Primary cortical neurons
PDMS	Poly(dimethylsiloxane)
PEGDE	Poly(ethylene glycol) diglycidyl ether
PEGDMA	Poly(ethylene glycol) dimethacrylate
PEGDVS	Poly(ethylene glycol) divinyl sulfone
PHCs	Primary hepatocytes
PMMA	Poly(methyl methacrylate)
PU	Poly(urethane)
RGD	Arginylglycylaspartic acid peptide
RT	Room temperature
s.c.	Subcutaneous
sGAGs	Sulfated glycosaminoglycans
TA	Tibialis anterior
μCOP	Micro-continuous optical printing
μCT	X-ray micro-tomography

5.1 Introduction

Tissue engineering has emerged as a field to overcome limitations encountered in tissue and organ transplants about three decades ago [64]. In the course of time, several cellular and acellular approaches have been evaluated [98]. Biomaterial scaffolds have been used to provide structural support for the adhesion, migration, and proliferation of seeded cells. They have been fabricated by means of numerous techniques, such as phase separation, freeze drying, solution casting, gas foaming, melt molding, solvent casting, electrospinning, and others [13, 14, 31, 63, 82]. Scaffolds made up of such techniques usually have limitations in positioning different cell types, forming the cell gradients, and providing necessary cell concentrations in order to simulate the histotypic and/or organotypic arrangements [27, 47].

Three-dimensional (3D) printing also known as the "additive manufacturing" is a rapidly growing technology which is applied to numerous fields [30]. The approach of 3D printing together with viable cells (3D bioprinting) and extracellular matrix (ECM) analogues has attracted great attention in the last decade and is presented as the technology which will revolutionize tissue engineering, regenerative medicine, reconstructive surgery, and personalized medicine in the near future [68]. It is anticipated that 3D bioprinting will overcome challenges with conventional tissue engineering methods, such as manual cell seeding heterogeneity and neovascularization.

In the future, it is expected that the patient's individual treatment could be performed by using customized compatible and functional 3D-bioprinted tissues or organs. Briefly, printable form and size will be customized by computer-

aided design combined with medical imaging (e.g., CT or MRI) to fabricate viable neografts with precise anatomical shape to mimic exactly the patient's disease and/or defect requirements with microscale structural integrity and architecture hereafter [54].

Bioinks are printable ECM-like fluids which can be processed under mild and cell-friendly conditions, without damaging the living cells and bioactive macromolecules [40]. They differ from traditional additive manufacturing materials, e.g., thermoplastics, ceramics, and metals which necessitate the use of harsh solvents, high temperatures, and/or crosslinking methods for printing. The most commonly used bioinks are the functionalized [90] and/or composite forms of alginate [3], collagen, [79], methacrylated gelatin [105], hyaluronic acid [86], decellularized extracellular matrices (dECMs) [12, 53], silk [9], fibrin, agarose hydrogels, etc. which are natural hydrogels responsive to environmental processing conditions (Fig. 5.1).

While 3D bioprinting of transplantable functional tissues and organs will be the main objective of this technology, for today it is more realistic to state that it is possible to fabricate a variety of in vitro tissue models (Tables 5.1, 5.2, 5.3, and 5.4) for studying organogenesis and modeling diseases with current printable bioinks in hand [41, 66]. This chapter briefly discusses on the current state of bioinks and gives examples of the 3D-bioprinted tissue models.

5.2 Alginate-Based Bioinks

Alginate (Alg) is a natural anionic polysaccharide having (1,4)-linked β-D-mannuronate (M) and C-5 epimer α-L-guluronate (G) consecutive residues. Related to its biocompatibility and mild gelation properties, this biopolymer has been widely used for various biotechnological applications, such as for immobilization of enzymes [24], as biological control matrix [25, 26], bioartificial liver systems [22], tissue engineering scaffold [52, 104], drug delivery vehicles [50], wound dressings [1], etc.

Alginates, with a great number of variations, can be extracted from different brown seaweed sources such as *Laminaria hyperborea* and *Ascophyllum nodosum*; thus the physicochemical and mechanical properties of alginates are largely affected by their molecular weights, G-block lengths, and copolymer compositions (M/G ratio) [69]. Thus, the carboxylic acid groups of G residues are crosslinked through bivalent cations, such as Ca^{2+}, Mg^{2+}, Ba^{2+}, and Sr^{2+}. Besides, methacrylated forms of alginate can be photocrosslinked in the presence of eosin triethanolamine [100]. Increasing the MW of alginate can improve the physical properties of the resultant gels; nevertheless, high MW alginate solutions are very viscous making it needless for processing [72] and bring the risk of cell damage through forces generated during mixing [61] and perhaps in the course of bioprinting. Therefore, there is a diffi-

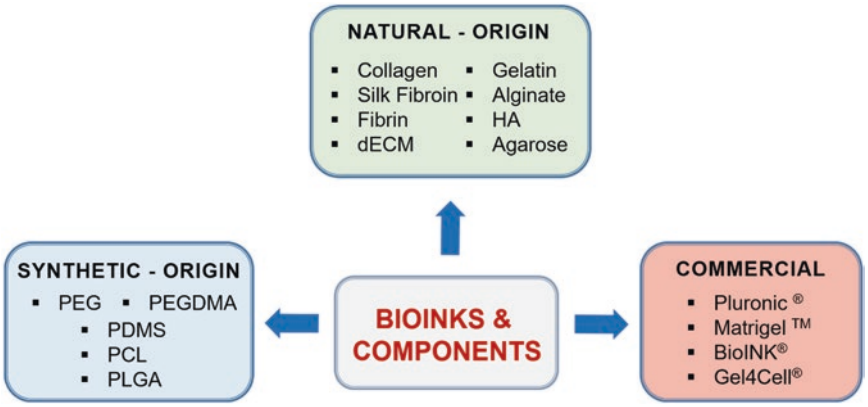

Fig. 5.1 Types of bioinks and components prevalently used in 3DP studies

Table 5.1 Representative examples of bioinks used for 3D-bioprinting bone/cartilage tissue models

Bioinks, components	Bioprinting method, conditions	Cell type, density	Outcomes, determinants	References
Bone models				
Collagen (2 mg/mL), nHAp (1.2 wt.%) composite gel	LAB; nozzle-free; 300 μm/s speed, 1 kHz frequency, 27.5 μJ energy	Mouse Luc + D1 BM-MSCs (1.2×10^8/mL gel)	Bone regeneration efficiency of in situ bioprinted construct evaluated in mouse calvaria defect model. Mature bone formation observed in the center of the defects assessed by μCT, in vivo luminescence imaging, and histology after 2 months	[56]
PEGDMA (10 wt.%); GRGDS and MMP-sensitive acrylated peptides (1 mM); crosslinked by Irgacure 2959 photoinitiator (0.05%)	Inkjet bioprinting; 300 dpi resolution with 3.6 kHz firing frequency; 50 staggered nozzles on printhead compensated for firing order	Human BM-MSCs (6×10^6/mL gel); 18 μm layer thickness; construct had 222 printed layers	Bioprinted MSCs with acrylated peptides and PEG promoted robust bone and cartilage formation with minimal printhead clogging during long-term culture. Cell viability ~88% at day 0	[37]
Collagen (4 mg/mL), agarose (3 wt.%)	Inkjet bioprinting; electromagnetic microvalve coupled to a heatable syringe, 600 μm nozzle ∅, 0.5 bar pressure	Human BM-MSCs (1.6×10^6/mL gel)	Bioprinted MSCs in thermosensitive hydrogel supported osteogenic differentiation of MSCs as confirmed by ALP activity and osteogenic mRNA expressions. Cell viability 98% after 21 days	[21]
Cartilage models				
Rat tail collagen (7.5–20 mg/mL)	EBB; deposition surface heated	Bovine meniscal fibrochondrocytes (10×10^6/mL gel)	Post-printing viability ~90%; resolution accuracy ~5 mm; geometric printing fidelity achieved	[94]
Gel-MA (20 wt%); PCL reinforcing framework	Inkjet printing, microextrusion, and FDM; printing scalable arrays of spheroids within framework	Porcine BM-MSCs (20×10^6/mL gel); porcine ACCs (3×10^6/mL gel); MSC:CC ratio 3:1	Osteochondral tissue modeling; static/bioreactor culture up to 10 weeks, evaluation by sGAG, total collagen, and calcium content and mechanical analysis	[16]
Cartilage dECM (3%; w/v); Alg (2 wt.%); dECM crosslinked by tyrosinase; Alg crosslinked by $CaCl_2$; PCL scaffold framework	Projection-based micro-stereolithography	Human ASCs (1×10^7/mL gel)	Post-printing viability >87%; in vitro chondrogenesis evaluation up to 21 days; in vivo neocartilage formation (s.c.) evaluated up to 12 weeks in Balb/c mouse	[112]

Abbreviations: ∅ nozzle diameter, *ACCs* articular cartilage chondrocytes, *ASCs* adipose stem cells, *Alg* calcium alginate, *ALP* alkaline phosphatase, *BM-MSCs* bone marrow-derived mesenchymal stromal cells, *$CaCl_2$* calcium chloride, *dECM* decellularized extracellular matrix, *EBB* extrusion-based bioprinting, *EDC* 1-ethyl-(3-3-dimethylaminopropyl) hydrochloride, *FDM* fused deposition modeling, *Irgacure 2959* 2-hydroxy-1-(4-(hydroxyethoxy)phenyl)-2-methyl-1-propanone, *LAB* laser-assisted bioprinting, *μCT* X-ray micro-tomography, *MSCs* mesenchymal stem cells, *nHAp* nanohydroxyapatite, *PCL* poly(caprolactone), *PEGDMA* poly(ethylene glycol) dimethacrylate, *s.c.* subcutaneous, *sGAGs* sulfated glycosaminoglycans, *RT* room temperature

Table 5.2 Representative examples of bioinks used for 3D-bioprinting skin/cornea models

Bioinks, components	Bioprinting method, conditions	Cell type, density	Outcomes, determinants	References
Skin models				
Collagen I (3 mg/mL; rat tail); blend of Alg (4 wt%) and blood plasma; collagen neutralized and gelled by $NaHCO_3$; Alg crosslinked by $CaCl_2$	LBB layer-by-layer using Nd:YAG laser (1064 nm)	Mouse NIH-3T3 dermal FBs; human HaCaT KCs (1.5×10^6/mL gel)	Evaluation of 3D-cell arrangement and proliferation up to 10 days as potential multicellular skin graft model; analysis of adherens and gap junctions	[60]
Collagen (2 mg/mL gel), neutralized and gelled by $NaHCO_3$; bioprinting on a PDMS mold	3D-freeform fabrication; electromechanical microvalve-based printing in layer-by-layer fashion; 1.2 and 2 psi pressures	Human dermal FBs; human epidermal KCs (1×10^6/mL gel)	Organotypic 3D-skin tissue model; post-printing viability of 95% (FBs), 85% (KCs)	[71]
Collagen (3 mg/mL), neutralized and gelled by nebulized $NaHCO_3$ vapor	Microvalve-based bioprinting; higher printing pressure applied for viscous collagen precursor than cell suspensions	Human HFF-1 FBs (2.3×10^5/mL); human HaCaT KCs (1.4×10^6/mL gel)	Post-printing viability of >95%; cultures grown at the ALI transwells up to 14 days; multilayered epithelium formation shown by histology	[70]
Collagen I (6 mg/mL; bovine), neutralized and gelled by nebulized $NaHCO_3$ vapor	Microvalve-based printing directly onto transwell membrane inserts; 2.0 and 2.5 psi pressures	Human dermal FBs (1×10^6/mL), MCs (2×10^7/mL gel), KCs (7×10^6/mL gel)	Full-thickness skin model containing pigmentation at the dermal-epidermal junction; formation of the stratum corneum	[80]
Hyaluronic acid (3 mg/mL), glycerol (10% v/v), gelatin (30 mg/mL), and fibrinogen (20 mg/mL), crosslinked by thrombin	EBB; for cell-laden hydrogel printing, 300 μm nozzle ∅, 60 kPa pressure; for PU, 200 μm nozzle ∅, 1500 kPa pressure, 160 °C temperature; for PCL, 200 μm nozzle ∅, 800 kPa pressure	Human epidermal KCs (1×10^7/mL gel); human dermal FBs (5×10^6/mL gel). PU wound dressing layer and printed PCL scaffold used for in vivo study	FBs proliferated after 7 days, while KCs did not in culture; application to an athymic mice skin wound resulted in skin contraction and regeneration of skin tissue consisting of epidermis and dermis layers	[97]
Collagen I (2 wt%; porcine); PCL framework and sacrificial gelatin (25%)	EBB for FBs, and inkjet-based dispensing for KCs	Human dermal FBs (2.5×10^5/mL gel); human epidermal KCs (1×10^6/mL gel)	Skin model with stabilized fibroblast-stretched dermis and stratified epidermis layers after 14 days in ALI	[57]
Cornea models				
Alginate (3 wt.%), collagen (6, 8 mg/mL), crosslinked by $CaCl_2$	EBB; 200 μm nozzle ∅, 10–180 kPa pressure	Human CKCs (2×10^6/mL gel)	Proof-of-concept study for the use of 3DP corneal stroma equivalent using collagen-based bioink containing encapsulated CKCs. Cell viability >90% at day 1 and 83% at day 7	[49]

(continued)

Table 5.2 (continued)

Bioinks, components	Bioprinting method, conditions	Cell type, density	Outcomes, determinants	References
Laminin-521 (0.1 mg/mL), collagen I (human; 3 mg/mL), HA (1 wt.%), human plasma and thrombin	LBB; Nd:YAG laser (λ:1064 nm; 20 Hz, 10 ns pulse) for single cell type; for multicellular construction, Er:YAG laser (λ:2940 nm; pulse, 500 Hz, 3 μs, 500 kHz, 18 μJ; 5000 mm/s speed)	Human ESC-LESCs (30×10^6/mL/gel); human ASCs (30×10^6/mL gel) for constructing layered stroma	Construction of three types of corneal tissue equivalents; i.e., stratified corneal epithelium, lamellar corneal stroma, and both were evaluated. hESC-LESCs formed a stratified epithelium with apical expression of CK3 and basal expression of the progenitor markers. Col I+ neostroma organized horizontally. Constructs attached to host tissue when implanted in porcine corneal organ cultures	[101]
Alginate (1 wt.%), gelatin (10 wt.%), collagen I (0.5–1 mg/), crosslinked by $CaCl_2$	EBB	Human CECs (1×10^6/mL gel); eight-layered construct	Citrate-mediated, degradation-controllable CEC-laden corneal tissue equivalent. Cell viability ~95% at day 0	[110]

Abbreviations: *Alg* alginate, *ALI* air-liquid interface, *ASCs* adipose tissue-derived stem cells, *$CaCl_2$* calcium chloride, *CECs* corneal epithelial cells, *CKCs* corneal keratocytes, *EBB* extrusion-based bioprinting, *ESC-LESCs* embryonic stem cell-derived limbal epithelial stem cells, *FBs* fibroblasts, *HA* hyaluronic acid, *KCs* keratinocytes, *LBB* laser-based bioprinting, *PDMS* poly(dimethylsiloxane), *MCs* melanocytes, *$NaHCO_3$* sodium bicarbonate, *PCL* poly(caprolactone), *PU* poly(urethane)

culty in balancing gels with beneficial features for bioprinting and acceptable features for culturing cells (i.e., low modulus).

In 3DP applications, Alg has been commonly employed to form a variety of tissue constructs, generally using Ca^{2+} as the divalent cation for ionic crosslinking related to the ease of creating 3D structures [3]. However, the majority of alginate-bioprinting processes last for short periods of time (e.g., 7–10 days) due to degradation-related issues post-bioprinting under both in vitro and in vivo conditions. For this reason, bioprinted constructs in some cases are strengthened by further crosslinking. Extrusion-based bioprinting is prevalently used for bioprinting alginates (usually 2–4 wt.% gels), while droplet-based bioprinting is also applicable if the concentration permits the formation of droplets [42].

The lack of signaling molecules for cell adhesion may be considered as a limitation of alginate in cellular interactions. On the other hand, it is possible to introduce molecular binding sites to Alg by modifying with peptides (e.g., RGD, IKVAV) [69]. For example, thiol-ene alginate hydrogels were developed which allowed 3D bioprinting of multiple cell types, adjustment of mechanical properties, and the introduction of RGD functional groups to Alg hydrogels [87].

Moreover, Alg has been blended with numerous hydrogels possessing inherent signaling molecules, for example, with cartilage dECM and hASCs using the projection-based microstereolithography to create neocartilage constructs [Table 5.1; 112]; with collagen, blood plasma, and dermal fibroblasts by LBB to develop a multicellular skin graft model [Table 5.2; 60]; with collagen and corneal keratocytes by EBB for a corneal stroma equivalent [Table 5.2; 49]; with collagen, gelatin, and corneal epithelial cells by EBB for generating a corneal tissue equivalent

Table 5.3 Representative examples of bioinks used for 3D-bioprinting skeletal muscle and cardiac muscle models

Bioinks, components	Bioprinting method, conditions	Cell type, density	Outcomes, determinants	References
Skeletal muscle models				
Fibrinogen (20 mg/mL), hyaluronic acid (3 mg/mL), gelatin (35 mg/mL) composite crosslinked by thrombin (20 UI/ml); acellular sacrificial gel without fibrinogen; supporting PCL pillar	EBB at 18 °C; for cell-laden hydrogel printing, 50–70 kPa pressure, 90 mm/min speed; for PCL, 300 μm nozzle ∅, 780 kPa pressure, 75 mm/min speed, 95 °C temperature; for sacrificial gelatin, 50–80 kPa pressure, 160 mm/min speed	Human primary MPCs; bioprinted muscle constructs ($10 \times 10 \times 3$ mm^3) with different cell densities (10, 20, 30, and 50×10^6/mL gel)	Post-printing viability ~86%; in vivo study presented that bioprinted muscle constructs reached 82% functional recovery and integration with host vascular and neural networks in the rodent TA defect model after 8 weeks	[58]
Hyaluronic acid (3 mg/mL), fibrinogen (20–30 mg/mL) composite hydrogel crosslinked by thrombin; sacrificial gelatin (35–45 mg/mL) and pluronic F-127; supporting PCL pillar	EBB; for hydrogel, 300 μm nozzle ∅, 50–80 kPa; for pluronic F127, 250 μm nozzle ∅, 200–300 kPa pressure; for PCL, 250 μm nozzle ∅, 800 kPa pressure	Mouse C2C12 myoblasts (3×10^6/mL gel); bioprinted muscle constructs ($15 \times 5 \times 1$ mm^3)	Post-printing viability ~97%; 7-day differentiated models implanted (s.c.) in nude rats for 2 weeks showed formation of muscle fiber-like structures, with presence of AChR clusters, neurofilament contacts, and neovascularization	[54]
Heart muscle models				
Alginate and RGD-modified alginate (5–10 wt.%) (1:1) crosslinked by $CaCl_2$	EBB, with resolution of 5 mm/step	Human fetal CMPCs (30×10^6/mL gel); 2 × 2 cm construct final size	Post-printing cell viability ~92% at day; ~89% at day 7. Enhanced gene expression of early cardiac transcription factors and troponin T. Printed cells migrated into adjacent Matrigel and formed tubular-like structures	[35]
Gel-MA (5 wt.%), crosslinked by LAP photoinitiator (0.1 wt.%); sacrificial HAGM slab (2 wt.%)	Light-based μCOP; system consisting of a UV light source, projection optics, and a digital micromirror device	Human ESCs-derived CMs (40×10^6/mL gel)	Post-printing cell viability: ~90% at day 3. Cardiac model for drug screening and evaluation of cardiac tissue maturation with the ability to assess cardiac force and calcium transient	[73]
PEGMA-fibrinogen (1 wt.%) and sacrificial alginate (4 wt.%), crosslinked by Irgacure 2959 photoinitiator (0.01 wt.%) and $CaCl_2$	EBB; with microfluidic-based printing head; 25G nozzle ∅; 10-layer-thick constructs printed with consecutive layers perpendicular to each other	Mouse iPSCs-derived CMs (8 and 40×10^6/mL gel); HUVECs (6×10^6/mL gel) Multicellular final construct size: $8 \times 8 \times 1$ mm^3	Post-printing cell viability: 80–90% at day 14; a 3D cardiac tissue model with high orientation index imposed by different defined geometries and blood vessel-like shapes generated by HUVECs in a NOD-SCID mice	[78]

(continued)

Table 5.3 (continued)

Bioinks, components	Bioprinting method, conditions	Cell type, density	Outcomes, determinants	References
Fibrinogen (20 mg/mL), gelatin (30 mg/mL), aprotinin (20 mg/mL), hyaluronic acid (3 mg/mL) hydrogel crosslinked by thrombin; sacrificial hydrogel of gelatin and HA	EBB; for cell-laden hydrogel, 200 μm nozzle ∅, 100 kPa pressure, 18 °C temperature; for PCL, 300 μm nozzle ∅, 750 kPa pressure, 98 °C temperature; for sacrificial hydrogel, 100 mm/min printing speed	Rat ventricular CMs (10×10^6/mL gel)	Constructs maintained 55% of initial tissue size for up to 9 weeks of culture. Spontaneous synchronous contraction observed in culture. Progressive cardiac tissue development confirmed by α-actinin and connexin 43. Notch signaling blockade significantly accelerated development and maturation of bioprinted cardiac tissues	[106]
Fibrinogen (30 mg/mL), gelatin (35 mg/mL), crosslinked by thrombin	EBB; 20 kPa pressure; 300 mm/min speed	Cardiac organoids composed of iPSCs-derived CMs (90%) and primary cardiac FBs (10%)	Multi-tissue interactions in an integrated three-tissue (heart, liver, and lung) organ-on-a-chip platform. Cardiac organoids demonstrated both normal cardiac biomarker expression and maintenance of long-term viability. Propranolol prevented epinephrine-induced increases in beating rates	[99]

Abbreviations: *AChR* acetylcholine receptor, *Alg* alginate, *$CaCl_2$* calcium chloride, *CMs* cardiomyocytes, *CMPCs* cardiac-derived cardiomyocyte progenitor cells, *EBB* extrusion-based bioprinting, *ESCs* embryonic stem cells, *FBs* fibroblasts, *Gel-MA* gelatin methacrylate, *HUVECs* human umbilical vein endothelial cells, *HAGM* hyaluronic acid glycidyl methacrylate, *iPSCs* induced pluripotent stem cells, *μCOP* micro-continuous optical printing, *MPCs* muscle progenitor cells, *LAP* lithium phenyl-2,4,6-trimethylbenzoylphosphinate, *PCL* poly(caprolactone), *PEGMA* polyethylene glycol monoacrylate, *TA* tibialis anterior

Table 5.4 Representative examples of bioinks used for 3D-bioprinting liver and neural models

Bioinks, components	Bioprinting method, conditions	Cell type, density	Outcomes, determinants	References
Liver models				
Alginate (2%); cellulose nanocrystals (4%) crosslinked by $CaCl_2$	EBB; 100 μm nozzle ∅, 5–25 psi pressure, 25 mm/s speed	Mouse NIH/3T3 FBs (1×10^6/mL gel); human HCs (1×10^6/mL gel); 3D honeycomb structure bioprinted with FBs and HCs	Bioink rheological properties optimized. Post-printing cell viability: ~59% (FBs) and ~50% (HCs) at day 3. This decline is interpreted to the lack of cell-binding sites in the hydrogel	[109]
Alginate (3 wt.%), crosslinked by $CaCl_2$; PDMS substrate with indented chambers	MBB; 250 μm nozzle ∅	Human HepG2 cells ($1–4 \times 10^6$/mL gel)	A preliminary study based on testing the construct as an in vitro drug metabolism model by evaluating the metabolization of EFC into the drug product HFC	[8]

(continued)

Table 5.4 (continued)

Bioinks, components	Bioprinting method, conditions	Cell type, density	Outcomes, determinants	References
RGD-coupled alginate (1.5 wt.%), crosslinked by $CaCl_2$ or $BaCl_2$	MBB; 102 μm nozzle ∅; 1.0 bar (Alg) and 0.5 bar ($CaCl_2$) pressure, 400 μs pulse time	Human iPSCs-derived HLCs; human ESCs-derived HLCs (1×10^7/mL gel); 20 and 40 layers of 3D-bioprinted construct	Post-printing cell viability: >84% for the short nozzle and > 71% for the long nozzle at day 1; bioprinted HLCs derived from iPSCs or ESCs examined in vitro for the presence of hepatic marker albumin	[34]
Gel-MA (5 wt.%) and GMHA (2 wt.%); crosslinked by LAP photoinitiator (0.45%)	DLP-based 3DB; two-step bioprinting process: printing hepatic cell layer followed by a second complementary layer of supporting cells that fits in the empty space of the first layer	Triculture model composed of human iPSCs-derived HLCs (40×10^6/mL gel), HUVECs (40×10^6/mL gel), and ASCs (8×10^5/mL gel) as supporting cells	Triculture model led to improved morphological organization, higher liver-specific gene expression levels, increased metabolic product secretion, and enhanced CYP induction	[77]
Gelatin (3% w/v), collagen type I (2% w/v). PCL housing material	EBB; 200 μm nozzle ∅; for PCL: 200 μm nozzle ∅; 500 kPa pressure, 200 mm/min speed	Human HepG2 cells ($1–2 \times 10^7$/mL gel); HUVECs (5×10^4/mL gel); 400 μm-thick bioprinted constructs	3D bioprinting technology applied for fabricating a liver-on-a-chip system having basic hepatic functions, i.e., albumin and urea synthesis for up to 6 days	[68]
Gel-MA (10 wt.%), crosslinked by Irgacure 2959 photoinitiator; PDMS and PMMA as housing materials	Microextrusion bioprinting; bioprinted GelMA dot size ~800 μm	Human HepG2/C3A cell-based spheroids (4×10^4 spheroids/mL gel; spheroid size ˂200 μm)	A liver-on-a-chip platform with bioprinted hepatic spheroids. Thirty-day functionality achieved in terms of albumin, A1AT, transferrin, and ceruloplasmin secretion under perfusion (200 μL/h) culture. APAP-induced hepatotoxicity tested	[5]
Thiolated HA (1.5 mg/mL); thiolated gelatin (30 mg/mL); liver dECM; PEG-based crosslinkers	EBB; 20 kPa pressure; 300 mm/min speed	Hepatic organoids composed of human PHCs (80%), HStCs (10%), and Kupffer cells (10%)	Multi-tissue interactions in an integrated three-tissue (liver, heart, and lung) organ-on-a-chip platform. Liver unit demonstrated functional outputs of urea and albumin and the presence of key CYP enzymatic activities. APAP-induced hepatotoxicity tested	[99]

(continued)

Table 5.4 (continued)

Bioinks, components	Bioprinting method, conditions	Cell type, density	Outcomes, determinants	References
Neural models				
Alginate (2%), fibrin (10–40 mg/mL), hyaluronic acid (1%), RGD-coupled alginate (1%); crosslinked by $CaCl_2$ and thrombin	EBB; 200 μm nozzle ∅, 20–60 kPa pressure, 1–11 mm/s speed, 22 °C temperature	Schwann cells (1 × 10^6/mL gel)	Post-printing cell viability: >95% at day 10. Bioprinting process supports Schwann cell viability, elongation and directional growth of neurites, and cellular protein expression	[85]
PU (25, 30%), 4:1 of PCL diol, and poly(L-lactide) diol or poly(D,L-lactide) diol	FDM; 250 μm nozzle ∅, 55 kPa pressure, 1–11 mm/s speed, 37 °C temperature	Mouse NSCs (4 × 10^6/mL gel); 3D-printed construct of 1.5 cm × 1.5 cm × 1.5 mm	Post-printing cell viability: ~100% at 72 h. NSCs-laden PU hydrogels support cell proliferation and gene expression in vitro. Constructs rescue impaired nervous system function in zebrafish embryo neural injury model	[44]
RGD-modified gellan gum (0.5 wt.%); crosslinked by $CaCl_2$	EBB; 200 μm nozzle ∅	Mouse PCNs (1 × 10^6/mL gel)	Post-printing cell viability: ~73% at day 5. Bioprinted PCNs encapsulated in RGD-coupled hydrogels supported survival and networking of PCNs	[75]
Alginate (5 wt.%), carboxymethyl chitosan (5 wt.%), agarose (1.5 wt.%); crosslinked by $CaCl_2$	EBB; 200 μm nozzle ∅; ~8.5 N extrusion force	Human iPSCs-derived neural cells (4 × 10^7/mL gel)	A proof-of-concept study evaluating the bioprintability and survival of a number of cell types (neural and nonneural) derived from iPSCs using the composite hydrogel	[39]

Abbreviations: *3DP* three-dimensional bioprinting, *A1AT* alpha-1 antitrypsin, *APAP* acetaminophen, *Alg* alginate, *ASCs* adipose-derived stem cells, *$BaCl_2$* barium chloride, *$CaCl_2$* calcium chloride, *CYP* cytochrome P450, *dECM* decellularized extracellular matrix, *DLP* digital light processing, *EBB* extrusion-based bioprinting, *EFC* 7-ethoxy-4-trifluoromethyl coumarin, *ESCs* embryonic stem cells, *FBs* fibroblasts, *FDM* fused deposition manufacturing, *Gel-MA* gelatin methacrylate, *GMHA* glycidyl methacrylate-hyaluronic acid, *HCs* hepatoma cells, *HepG2* hepatocellular carcinoma cells, *HFC* 7-hydroxy-4-trifluoromethyl coumarin, *HLCs* hepatocyte-like cells, *HStCs* hepatic stellate cells, *HUVECs* human umbilical vein endothelial cells, *iPSCs* induced pluripotent stem cells, *Irgacure 2959* 2-hydroxy-1-(4-(hydroxyethoxy) phenyl)-2-methyl-1-propanone, *LAP* lithium phenyl-2,4,6-trimethylbenzoylphosphinate, *MBB* microvalve-based bioprinting, *NSCs* neural stem cells, *PCL* poly(ε-caprolactone), *PCNs* primary cortical neurons, *PDMS* poly(dimethylsiloxane), *PHCs* primary hepatocytes, *PMMA* poly(methyl methacrylate), *PU* poly(urethane), *RGD* arginylglycylaspartic acid peptide, the binding motif of fibronectin to cell adhesion molecules

[Table 5.2; 110]; with RGD-modified alginate and cardiac-derived cardiomyocyte progenitor cells by EBB to create a cardiac tissue model [Table 5.3; 35]; with RGD-coupled alginate and human iPSCs-derived HLCs by microvalve-based bioprinting for developing a hepatic model [Table 5.4; 34]; and with fibrin, hyaluronic acid, RGD-coupled alginate, and Schwann cells by EBB to form a neural model [Table 5.4; 85].

5.3 Collagen-Based Bioinks

Collagen is the primary structural component of mammalian ECM which provides strength and structural stability to the tissues [32]. There are about 29 different types of collagen; however type I is the most abundant among all. Collagen is organized in a triple-helix polypeptide conformation and possesses cell-interactive binding domains [95]. Collagen forms a hydrogel at physiological conditions, has excellent biocompatibility, and retains full integrity during engraftment. For these reasons, it can be considered as a suitable material for biomedical, cell encapsulation, and bioprinting applications [23, 43]. For example, bovine meniscal fibrochondrocytes-laden collagen was bioprinted by EBB to create an in vitro cartilage model [Table 5.1; 94]. In another study, epidermal keratinocytes/dermal fibroblasts-laden collagen was fabricated by 3D free-form to create an organotypic skin graft model [Table 5.2; 71]. A multicellular combination of human dermal fibroblasts, melanocytes, and keratinocytes-laden collagen was bioprinted using the microvalve-based printing to form a full-thickness skin model containing pigmentation at the dermal-epidermal junction [Table 5.2; 80].

On the other hand, pure collagen hydrogels have weak mechanical properties compared to crosslinked synthetic polymer gels. Another limitation is the low shape fidelity of bioprinted collagen materials. Complete gelation of collagen bioink can take up about half an hour, which can hamper the homogenous distribution of the cells within the hydrogel [42]. Additional stabilization by chemical crosslinking (e.g., with riboflavin or genipin) can be an option; however it could lessen the biocompatibility and induce antigenicity of the resulting biomaterial [76]. Nevertheless, the photocrosslinkable collagen methacrylamide (CMA) has been developed as a bioink for 3DP [7, 20]. CMA can be printed in high resolution and photocrosslinked with UV light in the presence of a radical photoinitiator (such as 2-hydroxy-1-(4-(hydroxyethoxy)phenyl)-2-methyl-1-propanone; Irgacure 2959). CMA exhibits quite similar properties to collagen in terms of biocompatibility. Gaudet et al. (2012) reported that cells interacting with CMA showed more than 80% vitality after 72 h despite UV exposure due to photocrosslinking [38]. On the other hand, there is an ongoing effort to develop concentrated, but soluble collagen solutions which can support shape fidelity after extrusion by optimizing the processes [88].

Blending of collagen with faster-setting hydrogels or components (such as alginate, fibrin, nHAp) has also been proposed to surpass the existing mechanical limitations of collagen [48, 81]. For example, mouse BM-MSCs-laden collagen/nHAp composite gel was in situ bioprinted in a mouse calvaria defect model using LAB which led to the formation of mature bone within 2 months [Table 5.1; 56]. Human BM-MSC in a thermosensitive collagen/agarose hydrogel was inkjet-bioprinted to develop an in vitro osteogenic model [Table 5.1; 21]. Dermal fibroblasts encapsulated in a collagen/alginate/blood plasma blend were bioprinted by using LBB to develop a skin graft model [Table 5.2; 60]. In a recent study by Sorkio et al. (2018), collagen enriched with laminin-521 and human plasma was blended with hESC-derived limbal epithelial cells for bioprinting through LBB to construct a stratified corneal epithelium and a lamellar corneal stroma equivalent [Table 5.2; 101].

5.4 Methacrylated Gelatin-Based Bioinks

Gelatin, also called the hydrolyzed collagen, is a fibrous, water-soluble protein/peptide mixture derived through the chemical or physical degradation (reduction of the protein fibrils and triple-helical structure) of collagen into smaller units

[108]. Gelatins can be either obtained via acidic or alkaline processes, resulting in type A or type B gelatin, respectively. Gelatin has the same amino acid content of collagen and resembles the structural properties of collagen [29, 84].

As a biomaterial gelatin has versatile properties such as amphoteric behavior, solubility in polar solvents, nonimmunogenicity, high cellular compatibility, bioactivity, and low toxicity [28, 51, 83]. Also gelatin contains the linear RGD peptides, responsible from cell adhesion, migration, and proliferation [45]. Since gelatin is soluble at physiological temperatures, this hydrogel can only be used as a bioink after suitable modifications which can ensure the shape fidelity and mechanical strength of the resultant 3D-bioprinted constructs. A commonly used chemical crosslinking agent, glutaraldehyde, is highly toxic to cells and cannot be harnessed for developing cell-containing bioinks [103]. To overcome the limitations, gelatin can be blended with easily crosslinkable hydrogels, such as with alginate, silk fibroin, or fibrin [89, 111]. For example, Das et al. (2015) have demonstrated the successful bioprinting of cells using a bioink composed of gelatin and silk fibroin with high retention of cell viability [18].

The prevalent approach of using gelatin as a bioink is through methacrylation. Semisynthetic gelatin methacryloyl (Gel-MA), the photocrosslinkable form of gelatin, has been shown to possess favorable bioprintability features (i.e., shape fidelity and thermal stability), while incorporating most of the biological properties of gelatin (such as high cellular compatibility and low antigenicity). For example, a composition of PEGDMA-, GRGDS-, and MMP-sensitive acrylated peptides containing human BM-MSCs was inkjet-bioprinted to develop an in vitro osteogenic model [Table 5.1; 37]. Porcine BM-MSCs and ACCs (with the ratio of 3:1) containing Gel-MA hydrogel was inkjet-printed to create an osteochondral tissue model which was then evaluated for up to 10 weeks, both under static and bioreactor culture conditions [Table 5.1; 16]. Human ESCs-derived cardiomyocytes were bioprinted with Gel-MA hydrogel by using the light-based micro-continuous optical printing (μCOP) method to create a cardiac model for drug screening and evaluation of cardiac tissue maturation with the ability to assess cardiac force and calcium transient [Table 5.3; 73].

Gel-MA forms hydrogels with tunable mechanical properties when crosslinked by exposing to UV light in the presence of a radical photoinitiator [84, 113]. Moreover, the mechanical and rheological properties of Gel-MA bioinks can be easily controlled [74, 92, 102, 107]. Bertlein et al. (2017) reported the allylated gelatin (Gel-AGE) as a thiol-ene clickable bioink for distinct biofabrication applications [4]. More recently, AnilKumar et al. (2019) proposed furfuryl-gelatin as a visible-light crosslinkable bioink for fabricating cell-laden structures with high cell viability [2].

5.5 Hyaluronic Acid-Based Bioinks

Hyaluronic acid or hyaluronan (HA) is a non-sulfated glycosaminoglycan with N-acetyl-D-glucosamine and glucuronic acid [α-1,4-D-glucuronic acid-β-1,3-N-acetyl-D-glucosamine] repeating units [65]. HA is mostly found in the connective tissues, cartilage, synovial fluid, vitreous fluid, and umbilical cord. The polysaccharide has long linear high molecular weight carbohydrate chains providing viscoelastic properties to the biopolymer. As one of the main components of the ECM, HA plays a vital role in cellular signaling activity, cell surface receptor interactions, wound repair, morphogenesis, and matrix organization [33]. HA has high water retention capacity; it is basically biocompatible, nonimmunogenic, and biodegradable. HA and its derivatives have been used in a variety of biomedical applications till now [6, 10, 19]. Besides, the poor mechanical properties and rapid degradation features are the major limitations of HA when considering the bioprinting conditions. Like most other natural biopolymers, it is chemically modified for altering inadequate physicochemical properties or is used as a bioactive component in polymer blends having fast-setting properties.

The bioprintability of HA blends with fast-setting hydrogel components has been evaluated

in a number of studies based on static in vitro, microfluidic organ-on-a-chip, and in vivo platforms. Human epidermal keratinocytes and dermal fibroblasts suspended in HA blended with fibrinogen and gelatin were bioprinted using EBB to create a double-layered skin model and were applied to the skin wounds of athymic mice. The constructs led to skin contraction and regeneration of skin tissue consisting of epidermis and dermis layers [Table 5.2; 97]. Human primary muscle progenitor cells-laden HA/fibrinogen/gelatin hydrogel was bioprinted using EBB to develop a skeletal muscle model and was tested on rodent tibialis anterior defects. Findings showed functional recovery and integration of the construct with host vascular and neural networks after 8 weeks [Table 5.3; 58]. In a study to develop a cardiac muscle model, HA was used as a secondary component in a fibrinogen/aprotinin hydrogel to bioprint rat ventricular CMs using EBB. The construct maintained 55% of initial tissue size for up to 9 weeks of culture with spontaneous synchronous contraction [Table 5.3; 106]. In a study by Skardal et al. (2017), thiolated hyaluronic acid, blended with thiolated gelatin and liver dECM, was used to bioprint hepatic organoids composed of human primary hepatocytes, stellate cells, and Kupffer cells by the EBB technique. The hepatic component of the integrated three-tissue organ-on-a-chip platform demonstrated functional outputs of urea and albumin and the presence of key CYP enzymatic activities [Table 5.4; 99]. Hyaluronic acid has also been used as a component of bioinks to develop neural models. For example, Ning et al. (2018) have evaluated the bioprintability of such a hydrogel blend using Schwann cells [Table 5.4; 85].

The modification and crosslinking parameters of HA-based hydrogels have been reported by Kenne et al. (2013) [55]. Esterification is known to reduce the water solubility and degradation properties of HA. The mechanical features can be improved by covalent crosslinking of the HA polymer chains into a 3D network (e.g., hydrazide modification, auto-crosslinking, or crosslinking by glutaraldehyde, carbodiimide, or genipin) [15, 62]. Divinyl sulfone, poly(ethylene glycol) diglycidyl ether (PEGDE), and poly(ethylene glycol) divinyl sulfone (PEGDVS) have also been used to crosslink HA hydrogels [36]. Both the rheological and cell-interaction properties are jointly critical for 3D bioprinting with cells. Photocrosslinking method has allowed the use of HA as a suitable bioink (i.e., methacrylated and diacrylated forms of HA). For example, Paldervaart et al. (2017) have reported the photocrosslinking of HA by introducing the methacrylate groups under UV light in the presence of a photoinitiator [93]. In addition, Kiyotake et al. (2019) have bioprinted rat BM-MSCs and neural stem cells through a pentenoate-functionalized HA bioink crosslinked with dithiothreitol and a photoinitiator [59] hybrid bioink, based on acrylated HA for immobilizing bioactive peptides and tyramine-conjugated HAs for fast gelation [67].

5.6 Decellularized Extracellular Matrix-Based Bioinks

Decellularization is the process of removing the cellular components from tissues and organs by using physical, chemical, and/or enzymatic methods. Decellularized ECM (dECM) hydrogels or scaffolds preserve some of the biological properties of the tissues of which they are derived from [91, 96]. A dECM processed through an optimized protocol should retain collagen, glycosaminoglycans, glycoproteins, and certain levels of cell-recognition peptides and growth factors [46, 91].

Thus, bioactive dECM is attracting interest for use as a bioink in the recent years [12, 53]. However, despite its cell-friendly features, single utilization of dECMs for 3D bioprinting has limitations, such as low shape fidelity and low resolution accuracy due to its low viscosity, weak mechanical integrity, and rapid biodegradation rates [89]. Crosslinking of dECM using genipin or 1-ethyl-3-(3-dimethylaminopropyl) carbodiimide does not seem to be applicable for cell bioprinting. For that reason, the use of milder reactives (such as vitamin B2) or hydrogel blends with fast-setting properties is currently being evaluated. For example, Skardal et al. (2017)

employed the liver dECM as the hepato-inducing component for modifying a hydrogel blend to develop a liver model [Table 5.4; 99].

Das et al. (2019) recently reported the use of cardiac dECM, together with gelatin as a bioink to bioprint cardiomyocytes for creating a cardiac tissue model [17]. Here, a poly(ethylene/vinyl acetate) frame was also used to support the shape fidelity of the bioprinted cell-laden hydrogel. Yi and co-workers (2019) reported a bioink composed of cartilage dECM blended with alginate for bioprinting adipose stem cells to develop a construct amenable to in vivo neocartilage formation in the mouse ectopic site [Table 5.1; 112]. In another recent study, Choi et al. (2019) described a novel VML treatment with dECM bioink using the 3D cell bioprinting technology. Volumetric muscle constructs made up of cell-laden dECM bioinks were formed using a granule-based printing reservoir. In vivo findings demonstrated ~85% functional recovery at the wound site [11].

5.7 Conclusions and Perspectives

There is great interest in three-dimensional bioprinting technology and its potential for the future of biomedicine (i.e., for drug development and transplantation medicine). Prevalently used bioinks are quite limited and are far from being optimal from several aspects, for example, the ability to support different printing modalities and cell viability, printing resolution, elasticity and scalability during the 3DP process, and the ability to support cell proliferation, fusion of layers, and desirable mechanical and degradation properties of the maturating tissue equivalent, after 3DP. Nevertheless, studies thoroughly devoted to the refinement of functional bioinks are still limited. As the foremost component of 3DP, there seems to be a need for developing all-purpose bioinks which are suitable for specific modifications with certain features meeting the needs of each designated tissue type to be developed.

Acknowledgments The work was supported by grants from TUBITAK, the Scientific and Technological Research Council of Turkey (117M281 and 216S575).

References

1. Aderibigbe BA, Buyana B (2018) Alginate in wound dressings. Pharmaceutics 10(2):42
2. AnilKumar S, Allen SC, Tasnim N, Akter T, Park S, Kumar A, Chattopadhyay M, Ito Y, Suggs LJ, Joddar B (2019) The applicability of furfuryl-gelatin as a novel bioink for tissue engineering applications. J Biomed Mater Res B Appl Biomater 107(2):314–323
3. Axpe E, Oyen ML (2016) Applications of alginate-based bioinks in 3D bioprinting. Int J Mol Sci 17(12):1976
4. Bertlein S, Brown G, Lim KS, Jungst T, Boeck T, Blunk T, Tessmar J, Hooper GJ, Woodfield TBF, Groll J (2017) Thiol–ene clickable gelatin: a platform bioink for multiple 3D biofabrication technologies. Adv Mater 29(44):1703404
5. Bhise NS, Manoharan V, Massa S, Tamayol A, Ghaderi M, Miscuglio M, Lang Q, Shrike Zhang Y, Shin SR, Calzone G, Annabi N, Shupe TD, Bishop CE, Atala A, Dokmeci MR, Khademhosseini A (2016) A liver-on-a-chip platform with bioprinted hepatic spheroids. Biofabrication 8(1):014101
6. Bian S, He M, Sui J, Cai H, Sun Y, Liang J, Fan Y, Zhang X (2016) The self-crosslinking smart hyaluronic acid hydrogels as injectable three-dimensional scaffolds for cells culture. Colloids Surf B: Biointerfaces 140:392–402
7. Brinkman WT, Nagapudi K, Thomas BS, Chaikof EL (2003) Photo-cross-linking of type I collagen gels in the presence of smooth muscle cells: mechanical properties, cell viability, and function. Biomacromolecules 4(4):890–895
8. Chang R, Emami K, Wu H, Sun W (2010) Biofabrication of a three-dimensional liver microorgan as an in vitro drug metabolism model. Biofabrication 2(4):045004
9. Chawla S, Midha S, Sharma A, Ghosh S (2018) Silk-based bioinks for 3D bioprinting. Adv Healthc Mater 7(8):1701204
10. Chircov C, Grumezescu AM, Bejenaru LE (2018) Hyaluronic acid-based scaffolds for tissue engineering. Romanian J Morphol Embryol 59:71–76
11. Choi YJ, Jun YJ, Kim DY, Yi HG, Chae SH, Kang J, Lee J, Gao G, Kong JS, Jang J, Chung WK, Rhie JW, Cho DW (2019) A 3D cell printed muscle construct with tissue-derived bioink for the treatment of volumetric muscle loss. Biomaterials 206:160–169
12. Choudhury D, Tun HW, Wang T, Naing MW (2018) Organ-derived decellularized extracellular matrix: a game changer for bioink manufacturing? Trends Biotechnol 36(8):787–805

13. Chun HJ, Park CH, Kwon IK, Khang G (2018) Cutting-edge enabling technologies for regenerative medicine, vol 1078. Springer, Singapore
14. Chun HJ, Park K, Kim C-H, Khang G (2018) Novel biomaterials for regenerative medicine, vol 1077. Springer, Singapore
15. Collins MN, Birkinshaw C (2013) Hyaluronic acid based scaffolds for tissue engineering—a review. Carbohydr Polym 92(2):1262–1279
16. Daly AC, Kelly DJ (2019) Biofabrication of spatially organised tissues by directing the growth of cellular spheroids within 3D printed polymeric microchambers. Biomaterials 197:194–206
17. Das S, Kim SW, Choi YJ, Lee S, Lee SH, Kong JS, Park HJ, Cho DW, Jang J (2019) Decellularized extracellular matrix bioinks and the external stimuli to enhance cardiac tissue development in vitro. Acta Biomater 95:188
18. Das S, Pati F, Choi YJ, Rijal G, Shim JH, Kim SW, Ray AR, Cho DW, Ghosh S (2015) Bioprintable, cell-laden silk fibroin–gelatin hydrogel supporting multilineage differentiation of stem cells for fabrication of three-dimensional tissue constructs. Acta Biomater 11:233–246
19. Demirdogen B, Elçin AE, Elçin YM (2010) Neovascularization by bFGF releasing hyaluronic acid–gelatin microspheres: in vitro and in vivo studies. Growth Factors 28(6):426–436
20. Drzewiecki KE, Malavade JN, Ahmed I, Lowe CJ, Shreiber DI (2017) A thermoreversible, photocrosslinkable collagen bio-ink for free-form fabrication of scaffolds for regenerative medicine. Technology 5(04):185–195
21. Duarte Campos DF, Blaeser A, Buellesbach K, Sen KS, Xun W, Tillmann W, Fischer H (2016) Bioprinting organotypic hydrogels with improved mesenchymal stem cell remodeling and mineralization properties for bone tissue engineering. Adv Healthc Mater 5(11):1336–1345
22. Durkut S, Elçin AE, Elçin YM (2015) In vitro evaluation of encapsulated primary rat hepatocytes pre-and post-cryopreservation at −80° C and in liquid nitrogen. Artif Cells Nanomed Biotechnol 43(1):50–61
23. Durkut S, Elçin YM (2017) Synthesis and characterization of thermosensitive poly (N-vinylcaprolactam)-g-collagen. Artif Cells Nanomed Biotechnol 45(8):1665–1674
24. Elçin YM (1995) Encapsulation of urease enzyme in xanthan-alginate spheres. Biomaterials 16(15):1157–1161
25. Elçin YM (1995) Bacillus sphaericus 2362-calcium alginate microcapsules for mosquito control. Enzym Microb Technol 17(7):587–591
26. Elçin YM (1995) Control of mosquito larvae by encapsulated pathogen Bacillus thuringiensis var. israelensis. J Microencapsul 12(5):515–523
27. Elçin YM (2004) Stem cells and tissue engineering, In biomaterials (pp. 301–316). Springer, Boston
28. Elçin YM, Akbulut U (1992) Polyester film strips coated with photographic gelatin containing immobilized glucose oxidase hardened by chromium (III) sulphate. Biomaterials 13(3):156–161
29. Elçin YM, Vurat MT, Elçin AE, Parmaksiz M, Seker S, Lalegul-Ulker O (2018) Printable composite bioink for periodontal tissue engineering. In: Brevini T, Fazeli A, Katusic A, Vidos A, May G (eds) In vitro 3D total cell guidance and fitness. School of Medicine University of Zagreb, Zagreb, pp 28–29
30. Elçin YM (2017) Organs-on-chips & 3D-bioprinting technologies for personalized medicine. Stem Cell Rev Rep 13(3):319–320
31. Ercan H, Durkut S, Koc-Demir A, Elçin AE, Elçin YM (2018) Clinical applications of injectable biomaterials. In: Novel biomaterials for regenerative medicine. Springer, Singapore, pp 163–182
32. Exposito JY, Cluzel C, Garrone R, Lethias C (2002) Evolution of collagens. Anat Rec 268(3):302–316
33. Fallacara A, Baldini E, Manfredini S, Vertuani S (2018) Hyaluronic acid in the third millennium. Polymers 10(7):701
34. Faulkner-Jones A, Fyfe C, Cornelissen DJ, Gardner J, King J, Courtney A, Shu W (2015) Bioprinting of human pluripotent stem cells and their directed differentiation into hepatocyte-like cells for the generation of mini-livers in 3D. Biofabrication 7(4):044102
35. Gaetani R, Doevendans PA, Metz CH, Alblas J, Messina E, Giacomello A, Sluijter JP (2012) Cardiac tissue engineering using tissue printing technology and human cardiac progenitor cells. Biomaterials 33(6):1782–1790
36. Gallo N, Nasser H, Salvatore L, Natali ML, Campa L, Mahmoud M, Capobiancod L, Sanninoa A, Madaghiele M (2019) Hyaluronic acid for advanced therapies: promises and challenges. Eur Polym J 117:134–147
37. Gao G, Yonezawa T, Hubbell K, Dai G, Cui X (2015) Inkjet-bioprinted acrylated peptides and PEG hydrogel with human mesenchymal stem cells promote robust bone and cartilage formation with minimal printhead clogging. Biotechnol J 10(10):1568–1577
38. Gaudet ID, Shreiber DI (2012) Characterization of methacrylated type-I collagen as a dynamic, photoactive hydrogel. Biointerphases 7(1):25
39. Gu Q, Tomaskovic Crook E, Wallace GG, Crook JM (2017) 3D bioprinting human induced pluripotent stem cell constructs for in situ cell proliferation and successive multilineage differentiation. Adv Healthc Mater 6(17):1700175
40. Guvendiren M, Molde J, Soares RM, Kohn J (2016) Designing biomaterials for 3D printing. ACS Biomater Sci Eng 2(10):1679–1693
41. Hardwick RN, Viergever C, Chen AE, Nguyen DG (2017) 3D bioengineered tissues: from advancements in in vitro safety to new horizons in disease modeling. Clin Pharmacol Ther 101(4):453–457
42. Hospodiuk M, Dey M, Sosnoski D, Ozbolat IT (2017) The bioink: a comprehensive review on bioprintable materials. Biotechnol Adv 35(2):217–239
43. Hölzl K, Lin S, Tytgat L, Van Vlierberghe S, Gu L, Ovsianikov A (2016) Bioink properties before,

during and after 3D bioprinting. Biofabrication 8(3):032002
44. Hsieh FY, Lin HH, Hsu SH (2015) 3D bioprinting of neural stem cell-laden thermoresponsive biodegradable polyurethane hydrogel and potential in central nervous system repair. Biomaterials 71:48–57
45. Hutson CB, Nichol JW, Aubin H, Bae H, Yamanlar S, Al-Haque S, Koshy ST, Khademhosseini A (2011) Synthesis and characterization of tunable poly (ethylene glycol): gelatin methacrylate composite hydrogels. Tissue Eng A 17(13–14):1713–1723
46. Ibsirlioglu T, Elçin AE, Elçin YM (2019) Decellularized biological scaffold and stem cells from autologous human adipose tissue for cartilage tissue engineering. Methods S1046-2023(18):30435-3
47. Inanc B, Elçin AE, Elçin YM (2008) Human embryonic stem cell differentiation on tissue engineering scaffolds: effects of NGF and retinoic acid induction. Tissue Eng A 14(6):955–964
48. Irvin SA, Venkatraman SS (2016) Bioprinting and differentiation of stem cells. Molecules 21(9):1188
49. Isaacson A, Swioklo S, Connon CJ (2018) 3D bioprinting of a corneal stroma equivalent. Exp Eye Res 173:188–193
50. Jain D, Bar-Shalom D (2014) Alginate drug delivery systems: application in context of pharmaceutical and biomedical research. Drug Dev Ind Pharm 40(12):1576–1584
51. Jaipan P, Nguyen A, Narayan RJ (2017) Gelatin-based hydrogels for biomedical applications. MRS Commun 7(3):416–426
52. Jeong SM, Kim EY, Hwang JH, Lee GY, Cho SJ, Bae JY, Song JE, Yoon KH, Joo CK, Lee D, Khang G (2011) A study on proliferation and behavior of retinal pigment epithelial cells on purified alginate films. Int J Stem Cells 4(2):105
53. Kabirian F, Mozafari M (2019) Decellularized ECM-derived bioinks: prospects for the future. Methods S1046-2023(18):30437–30437
54. Kang HW, Lee SJ, Ko IK, Kengla C, Yoo JJ, Atala A (2016) A 3D bioprinting system to produce human-scale tissue constructs with structural integrity. Nat Biotechnol 34(3):312
55. Kenne L, Gohil S, Nilsson EM, Karlsson A, Ericsson D, Helander Kenne A, Nord LI (2013) Modification and cross-linking parameters in hyaluronic acid hydrogels—definitions and analytical methods. Carbohydr Polym 91(1):410–418
56. Keriquel V, Oliveira H, Rémy M, Ziane S, Delmond S, Rousseau B, Rey S, Catros S, Amedee J, Guillemot F, Fricain JC (2017) In situ printing of mesenchymal stromal cells, by laser-assisted bioprinting, for in vivo bone regeneration applications. Sci Rep 7(1):1778
57. Kim BS, Lee JS, Gao G, Cho DW (2017) Direct 3D cell-printing of human skin with functional transwell system. Biofabrication 9(2):025034
58. Kim JH, Seol YJ, Ko IK, Kang HW, Lee YK, Yoo JJ, Atala A, Lee SJ (2018) 3D bioprinted human skeletal muscle constructs for muscle function restoration. Sci Rep 8(1):12307
59. Kiyotake EA, Douglas AW, Thomas EE, Nimmo SL, Detamore MS (2019) Development and quantitative characterization of the precursor rheology of hyaluronic acid hydrogels for bioprinting. Acta Biomater 95:176
60. Koch L, Deiwick A, Schlie S, Michael S, Gruene M, Coger V, Zychlinski D, Schambach A, Reimers K, Vogt PM, Chichkov B (2012) Skin tissue generation by laser cell printing. Biotechnol Bioeng 109(7):1855–1863
61. Kong HJ, Smith MK, Mooney DJ (2003) Designing alginate hydrogels to maintain viability of immobilized cells. Biomaterials 24(22):4023–4029
62. La Gatta A, Schiraldi C, Papa A, De Rosa M (2011) Comparative analysis of commercial dermal fillers based on crosslinked hyaluronan: physical characterization and in vitro enzymatic degradation. Polym Degrad Stab 96(4):630–636
63. Lalegül-Ülker Ö, Elçin AE, Elçin YM (2018) Intrinsically conductive polymer nanocomposites for cellular applications. In: Cutting-edge enabling technologies for regenerative medicine. Springer, Singapore, pp 135–153
64. Lanza R, Langer R, Vacanti J, Atala A (2020) Principles of tissue engineering, 5th edn. Academic Press, Cambridge, MA. ISBN: 9780128184226
65. Laurent TC, Fraser JR (1992) Hyaluronan. FASEB J 6(7):2397–2404
66. Lee H, Cho DW (2016) One-step fabrication of an organ-on-a-chip with spatial heterogeneity using a 3D bioprinting technology. Lab Chip 16(14):2618–2625
67. Lee J, Lee SH, Kim BS, Cho YS, Park Y (2018) Development and evaluation of hyaluronic acid-based hybrid bio-ink for tissue regeneration. Tissue Eng Regen Med 15(6):761–769
68. Lee JM, Yeong WY (2016) Design and printing strategies in 3D bioprinting of cell-hydrogels: a review. Adv Healthc Mater 5(22):2856–2865
69. Lee KY, Mooney DJ (2012) Alginate: properties and biomedical applications. Prog Polym Sci 37(1):106–126
70. Lee V, Singh G, Trasatti JP, Bjornsson C, Xu X, Tran TN, Yoo SS, Dai G, Karande P (2013) Design and fabrication of human skin by three-dimensional bioprinting. Tissue Eng Part C Methods 20(6):473–484
71. Lee W, Debasitis JC, Lee VK, Lee JH, Fischer K, Edminster K, Park JK, Yoo SS (2009) Multi-layered culture of human skin fibroblasts and keratinocytes through three-dimensional freeform fabrication. Biomaterials 30(8):1587–1595
72. LeRoux MA, Guilak F, Setton LA (1999) Compressive and shear properties of alginate gel: effects of sodium ions and alginate concentration. J Biomed Mater Res 47(1):46–53
73. Liu J, He J, Liu J, Ma X, Chen Q, Lawrence N, Zhu W, Xu Y, Chen S (2019) Rapid 3D bioprinting of in vitro cardiac tissue models using human embry-

onic stem cell-derived cardiomyocytes. Bioprinting 13:e00040
74. Liu W, Zhong Z, Hu N, Zhou Y, Maggio L, Miri AK, Fragasso A, Jin X, Khademhosseini A, Zhang YS (2018) Coaxial extrusion bioprinting of 3D microfibrous constructs with cell-favorable gelatin methacryloyl microenvironments. Biofabrication 10(2):024102
75. Lozano R, Stevens L, Thompson BC, Gilmore KJ, Gorkin R, Stewart EM, in het Panhuis M, Romero-Ortega M, Wallace GG (2015) 3D printing of layered brain-like structures using peptide modified gellan gum substrates. Biomaterials 67:264–273
76. Lynn AK, Yannas IV, Bonfield W (2004) Antigenicity and immunogenicity of collagen. J Biomed Mater Res B Appl Biomater 71(2):343–354
77. Ma X, Qu X, Zhu W, Li YS, Yuan S, Zhang H, Liu J, Wang P, Lai CS, Zanella F, Feng GS, Sheikh F, Chien S, Chen S (2016) Deterministically patterned biomimetic human iPSC-derived hepatic model via rapid 3D bioprinting. Proc Natl Acad Sci 113(8):2206–2211
78. Maiullari F, Costantini M, Milan M, Pace V, Chirivì M, Maiullari S, Rainer A, Baci D, Marei HE, Seliktar D, Gargioli C, Bearzi C, Rizzi R (2018) A multi-cellular 3D bioprinting approach for vascularized heart tissue engineering based on HUVECs and iPSC-derived cardiomyocytes. Sci Rep 8(1):13532
79. Marques CF, Diogo GS, Pina S, Oliveira JM, Silva TH, Reis RL (2019) Collagen-based bioinks for hard tissue engineering applications: a comprehensive review. J Mater Sci Mater Med 30(3):32
80. Min D, Lee W, Bae IH, Lee TR, Croce P, Yoo SS (2018) Bioprinting of biomimetic skin containing melanocytes. Exp Dermatol 27(5):453–459
81. Moncal KK, Ozbolat V, Datta P, Heo DN, Ozbolat IT (2019) Thermally-controlled extrusion-based bioprinting of collagen. J Mater Sci Mater Med 30(5):55
82. Moroni L, Boland T, Burdick JA, De Maria C, Derby B, Forgacs G, Groll J, Li Q, Malda J, Mironov VA, Mota C, Nakamura M, Shu W, Takeuchi S, Woodfield TBF, Xu T, Yoo JJ, Vozzi G (2018) Biofabrication: a guide to technology and terminology. Trends Biotechnol 36(4):384–402
83. Neumann PM, Zur B, Ehrenreich Y (1981) Gelatin-based sprayable foam as a skin substitute. J Biomed Mater Res 15(1):9–18
84. Nikoo BM, Benjakul S, Ocen D, Yang N, Xu B, Zhhang L, Xu X (2013) Physical and chemical properties of gelatin from the skin of cultured Amur sturgeon (Acipenser schrenckii). J Appl Ichthyol 29(5):943–950
85. Ning L, Sun H, Lelong T, Guilloteau R, Zhu N, Schreyer DJ, Chen DX (2018) 3D bioprinting of scaffolds with living Schwann cells for potential nerve tissue engineering applications. Biofabrication 10(3):035014
86. Noh I, Kim N, Tran HN, Lee J, Lee C (2019) 3D printable hyaluronic acid-based hydrogel for its potential application as a bioink in tissue engineering. Biomater Res 23(1):3
87. Ooi HW, Mota C, Ten Cate AT, Calore A, Moroni L, Baker MB (2018) Thiol–Ene alginate hydrogels as versatile bioinks for bioprinting. Biomacromolecules 19(8):3390–3400
88. Osidak EO, Karalkin PA, Osidak MS, Parfenov VA, Sivogrivov DE, Pereira FDAS, Gryadunova AA, Koudan EV, Khesuani YD, Kasyanov VA, Belousov SI, Krasheninnikov SV, Grigoriev TE, Chvalun SN, Bulanova EA, Mironov VA, Domogatsky SP (2019) Viscoll collagen solution as a novel bioink for direct 3D bioprinting. J Mater Sci Mater Med 30(3):31
89. Panwar A, Tan L (2016) Current status of bioinks for micro-extrusion-based 3D bioprinting. Molecules 21(6):685
90. Parak A, Pradeep P, du Toit LC, Kumar P, Choonara YE, Pillay V (2019) Functionalizing bioinks for 3D bioprinting applications. Drug Discov Today 24(1):198–205
91. Parmaksiz M, Dogan A, Odabas S, Elcin AE, Elcin YM (2016) Clinical applications of decellularized extracellular matrices for tissue engineering and regenerative medicine. Biomed Mater 11(2):022003
92. Pepelanova I, Kruppa K, Scheper T, Lavrentieva A (2018) Gelatin-Methacryloyl (GelMA) hydrogels with defined degree of functionalization as a versatile toolkit for 3D cell culture and extrusion bioprinting. Bioengineering 5(3):55
93. Poldervaart MT, Goversen B, De Ruijter M, Abbadessa A, Melchels FP, Öner FC, Dhert WJA, Vermondent AJ (2017) 3D bioprinting of methacrylated hyaluronic acid (MeHA) hydrogel with intrinsic osteogenicity. PLoS One 12(6):e0177628
94. Rhee S, Puetzer JL, Mason BN, Reinhart-King CA, Bonassar LJ (2016) 3D bioprinting of spatially heterogeneous collagen constructs for cartilage tissue engineering. ACS Biomater Sci Eng 2(10):1800–1805
95. Ricard-Blum S (2011) The collagen family. Cold Spring Harb Perspect Biol 3(1):a004978
96. Saldin LT, Cramer MC, Velankar SC, White LJ, Badylak SF (2017) Extracellular matrix hydrogels from decellularized tissues: structure and function. Acta Biomater 49:1–15
97. Seol YJ, Lee H, Copus JS, Kang HW, Cho DW, Atala A, Lee SJ, Yoo JJ (2018) 3D bioprinted biomask for facial skin reconstruction. Bioprinting 10:e00028
98. Shafiee A, Atala A (2017) Tissue engineering: toward a new era of medicine. Annu Rev Med 68:29–40
99. Skardal A, Murphy SV, Devarasetty M, Mead I, Kang HW, Seol YJ, Shrike Zhang Y, Shin SR, Zhao L, Aleman J, Hall AR, Shupe TD, Kleensang A, Dokmeci MR, Jin Lee S, Jackson JD, Yoo JJ, Hartung T, Khademhosseini A, Soker S, Bishop CE, Atala A (2017) Multi-tissue interactions in an integrated three-tissue organ-on-a-chip platform. Sci Rep 7(1):8837

100. Smeds KA, Pfister-Serres A, Miki D, Dastgheib K, Inoue M, Hatchell DL, Grinstaff MW (2001) Photocrosslinkable polysaccharides for in situ hydrogel formation. J Biomed Mater Res 54(1):115–121
101. Sorkio A, Koch L, Koivusalo L, Deiwick A, Miettinen S, Chichkov B, Skottman H (2018) Human stem cell based corneal tissue mimicking structures using laser-assisted 3D bioprinting and functional bioinks. Biomaterials 171:57–71
102. Stratesteffen H, Köpf M, Kreimendahl F, Blaeser A, Jockenhoevel S, Fischer H (2017) GelMA-collagen blends enable drop-on-demand 3D printability and promote angiogenesis. Biofabrication 9(4):045002
103. Van Den Bulcke AI, Bogdanov B, De Rooze N, Schacht EH, Cornelissen M, Berghmans H (2000) Structural and rheological properties of methacrylamide modified gelatin hydrogels. Biomacromolecules 1(1):31–38
104. Venkatesan J, Bhatnagar I, Manivasagan P, Kang K-H, Kim S-K (2015) Alginate composites for bone tissue engineering: a review. Int J Biol Macromol 72:269–281
105. Wang X, Ao Q, Tian X, Fan J, Tong H, Hou W, Bai S (2017) Gelatin-based hydrogels for organ 3D bioprinting. Polymers 9(9):401
106. Wang Z, Lee SJ, Cheng HJ, Yoo JJ, Atala A (2018) 3D bioprinted functional and contractile cardiac tissue constructs. Acta Biomater 70:48–56
107. Wang Z, Tian Z, Menard F, Kim K (2017) Comparative study of gelatin methacrylate hydrogels from different sources for biofabrication applications. Biofabrication 9(4):044101
108. Ward AG, Courts A (1977) The science and technology of gelatin. Academic, New York
109. Wu Y, Lin ZYW, Wenger AC, Tam KC, Tang XS (2018) 3D bioprinting of liver-mimetic construct with alginate/cellulose nanocrystal hybrid bioink. Bioprinting 9:1–6
110. Wu Z, Su X, Xu Y, Kong B, Sun W, Mi S (2016) Bioprinting three-dimensional cell-laden tissue constructs with controllable degradation. Sci Rep 6:24474
111. Xu W, Zhang Molino B, Cheng F, Molino PJ, Yue Z, Su D, Wang X, Willför S, Xu C, Wallace GG (2019) On low-concentration inks formulated by nanocellulose assisted with gelatin methacrylate (gelma) for 3D printing toward wound healing application. ACS Appl Mater Interfaces 11(9):8838–8848
112. Yi HG, Choi YJ, Jung JW, Jang J, Song TH, Chae S, Ahn M, Choi TH, Rhie JW, Cho DW (2019) Three-dimensional printing of a patient-specific engineered nasal cartilage for augmentative rhinoplasty. J Tissue Eng 10:2041731418824797
113. Yue K, Santiago GT, Alvarez MM, Tamayol A, Annabi N, Khademhosseini A (2015) Synthesis, properties, and biomedical applications of gelatin methacryloyl (GelMA) hydrogels. Biomaterials 73:254–271

6 Visible Light-Curable Hydrogel Systems for Tissue Engineering and Drug Delivery

Dae Hyeok Yang and Heung Jae Chun

Abstract

Visible light-curable hydrogels have been investigated as tissue engineering scaffolds and drug delivery carriers due to their physicochemical and biological properties such as porosity, reservoirs for drugs/growth factors, and similarity to living tissue. The physical properties of hydrogels used in biomedical applications can be controlled by polymer concentration, cross-linking density, and light irradiation time. The aim of this review chapter is to outline the results of previous research on visible light-curable hydrogel systems. In the first section, we will introduce photo-initiators and mechanisms for visible light curing. In the next section, hydrogel applications as drug delivery carriers will be emphasized. Finally, cellular interactions and applications in tissue engineering will be discussed.

Keywords

Visible light-curable hydrogels · Photo initiator · Riboflavin · Tissue engineering scaffolds · Drug delivery carriers · Physicochemical properties · Biological properties · Polymer concentration · Cross-linking density · Light irradiation time

6.1 Light-Curable Hydrogels

Light-curable hydrogels have hydrophilic three-dimensional (3D) polymer networks with porosity and soft consistencies, and these structures are capable of absorbing many water molecules and biological fluids. Due to these unique characteristics, the hydrogels can closely simulate living tissue [1, 2]. In addition, cells can be transplanted and proliferated in the hydrogels because the polymer matrices have enough porosity for cell survival, and the cell-laded hydrogels with injectability are known to have potential as tissue engineering scaffolds [3]. Another biomedical application of porous hydrogels is as drug delivery carriers [4, 5]. Their porous structure allows for drug loading and controlled release.

Ultraviolet (UV) and visible irradiation are generally used as light sources for preparing light-curable hydrogels. UV irradiation produces more chemical bonds among light-curable polymer precursor chains than visible irradiation, because the

D. H. Yang · H. J. Chun (✉)
Institute of Cell & Tissue Engineering and College of Medicine, Catholic University of Korea, Seoul, South Korea
e-mail: yangdh@catholic.ac.kr; chunhj@catholic.ac.kr

H. J. Chun et al. (eds.), *Bioinspired Biomaterials*, Advances in Experimental Medicine and Biology 1249, https://doi.org/10.1007/978-981-15-3258-0_6

photons of the former carry more energy than do the latter [6]. Therefore, UV light-curing systems are more popular than visible ones in industrial applications. However, in biomedical applications, the UV system has limited utility, because the overexposure of skin to UV causes sunburn and some types of skin cancers such as malignant melanoma. UV irradiation also results in indirect DNA damage by the free radicals and oxidative stress produced by the light [6]. Compared to UV, visible irradiation not only minimizes the drawbacks of UV but also provides lots of advantages in biomedicine by hydrogel formation in situ and simple environmental control [7]. Additionally, visible light has more benefits for hydrogel formation when the precursor solution is injected subcutaneously, since its wavelength has better transmission across skin [8].

6.2 Cytocompatible Visible Light Photo-initiators

Photo-initiators are required for interconnectively cross-linking among polymer chains with photoreactive groups, in which radicals or ions produced by absorbed visible light energy lead to photo-curing [8–10]. Some factors that should be considered for biomedical applications of photo-initiators include biocompatibility, water solubility, stability, and cytotoxicity [11, 12]. Given these conditions, there have been reports regarding the preparation of visible light-curable hydrogels for biomedical applications on two main kinds of photo-initiators: eosin Y (EY) and riboflavin (Figs. 6.1 and 6.2).

EY is one of the most widely used visible light photo-initiators in radical photopolymerization systems in biological environments [13]. EY, a xanthene dye photosensitizer, initiates radical photopolymerization when used with a triethanolamine (TEA) during excitation in green light that is a cytocompatible wavelength (λ_{max} = 510 nm) [14–17]. Visible light irradiation induces the excited triplet state of EY and abstracts hydrogen from TEA to produce two kinds of protonated eosin and TEA radicals. However, the cytotoxic TEA coactivator results in limited compatibility with cells; therefore, Shih and his colleagues have used EY as the only photo-initiator without a coactivator to prepare visible light-curable PEG hydrogels [17].

A naturally extracted vitamin B_2 from various plants, (-)-riboflavin, has been widely used in biomedical applications due to its water solubility and biocompatibility [18–24]. It absorbs light strongly at the wavelengths of 330–470 nm and produces superoxide radicals (O_2^-) that initiate photo-curing [18–24]. It has no side effects, because most of the compounds are excreted in the urine within a few hours after ingestion [19]. In addition, a small amount of (-)-riboflavin (<5 mg/1 g hydrogel precursor solution) is required to prepare visible light-curable hydrogel; therefore, it is almost harmless. Generally, (-)-riboflavin is commonly used with amine groups as electron donors to produce radicals during visible light irradiation [18].

6.3 Tissue Engineering

6.3.1 Scaffolds for Tissue Regeneration

For chronic wound management, conventional therapeutic methods such as autologous, natural, and synthetic skin substitutes have been developed; however, they often cause the incomplete restoration of tissue homeostasis, leading to necrosis and sepsis [25–27]. Hydrogels with appropriated mechanical and adhesive properties on wound sites can promote fibroblast proliferation, keratinocyte migration, and reepithelialization by absorbing wound exudates [28]. A visible light-curing system allows for the modulation of the mechanical adhesive properties of hydrogels by controlling irradiation time and photo-initiator concentration [29]. Based on this, some researchers have designed various types of visible light-curable hydrogels as wound dressings.

Visible light-curable glycol chitosan (GC) hydrogel systems have been investigated by some researchers for wound healing applications. It is known that several growth factors including epidermal growth factor (EGF), vascular endothelial growth factor (VEGF), transforming growth factor-α (TGF-α), platelet-derived growth factor

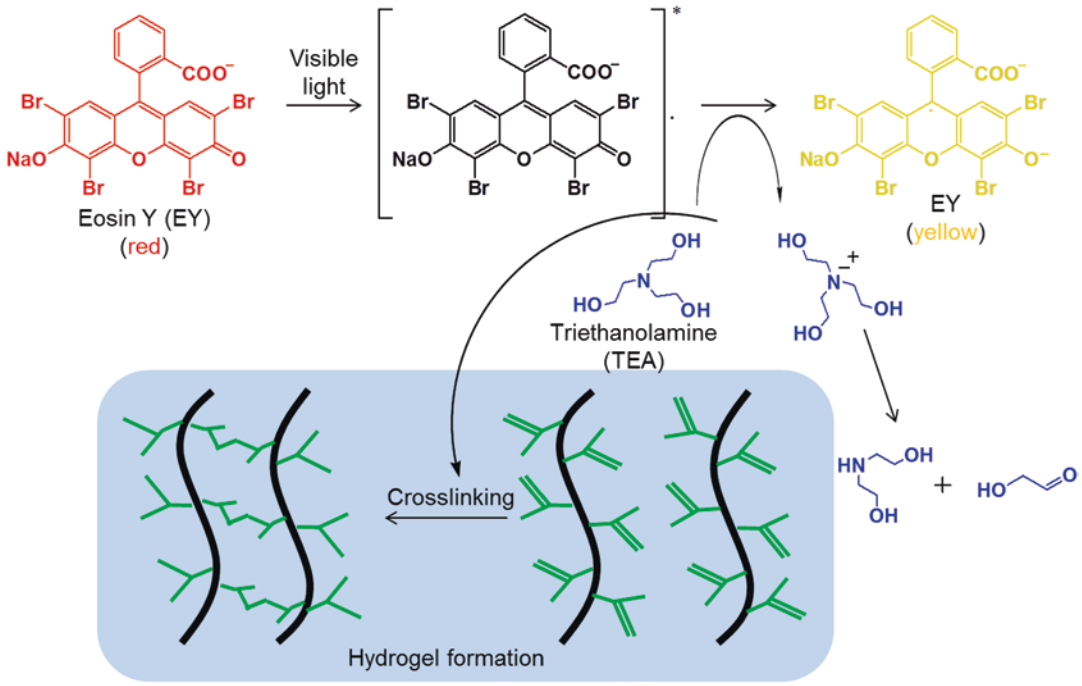

Fig. 6.1 Scheme for the hydrogel formation of methacrylated polymers initiated by EY

(PDGF), and transforming growth factor-β (TGF-β) have important influences on wound healing acceleration [30]. Based on these factors, Yang et al. [31] have reported the potential of a GC hydrogel containing two kinds of growth factors as a wound dressing agent. To accelerate wound healing, they used two kinds of growth factors, VEGF and platelet-derived growth factor-BB (PDGF-BB), because these factors play important roles in neo-vasculature [32] and the migration and proliferation of fibroblasts [33], respectively. Methoxy poly(ethylene glycol) (MPEG) was coupled to the amine groups of GC to enhance the plasticity of a GC hydrogel [34]. The researchers prepared three kinds of growth factor-incorporated GC hydrogels including VEGF/MPEG-g-GC, PDGF/MPEG-g-GC, and VEGF/PDGF/MPEG-g-GC, and their wound healing efficacies were investigated using a mouse model of wound healing, which was compared to the results of a commercial DuoDERM® and GC hydrogel. The results demonstrated that VEGF/PDGF/MPEG-g-GC had a superior wound healing effect due to the improved angiogenesis from VEGF and the increased cell proliferation rate from PDGF-BB [48]. Yoo et al. [35] have used visible light-curable GC hydrogels containing EGF and basic FGF (bFGF) for wound healing acceleration. In their study, EGF and bFGF were chosen for wound healing acceleration because they improve epidermal regeneration at the donor sites of split-thickness skin grafts and second-degree burn sites and stimulate the proliferation of cutaneous fibroblasts, respectively [36–38]. Through in vivo animal tests, the researchers found that the combination of EGF and bFGF contributed to the improvement of reepithelialization, granulation tissue formation, and collagen formation in the proliferation phase. Some specific plant-derived extracts are known to accelerate wound healing. Curcumin is a natural polyphenol extracted from the rhizome of *Curcuma longa* (turmeric). It has antioxidant, anti-inflammatory, and detoxification effects [39] and accelerates cutaneous wound healing by tissue remodeling, granulation tissue formation, and collagen deposition [40]. However, its clinical applications are limited due to its poor water

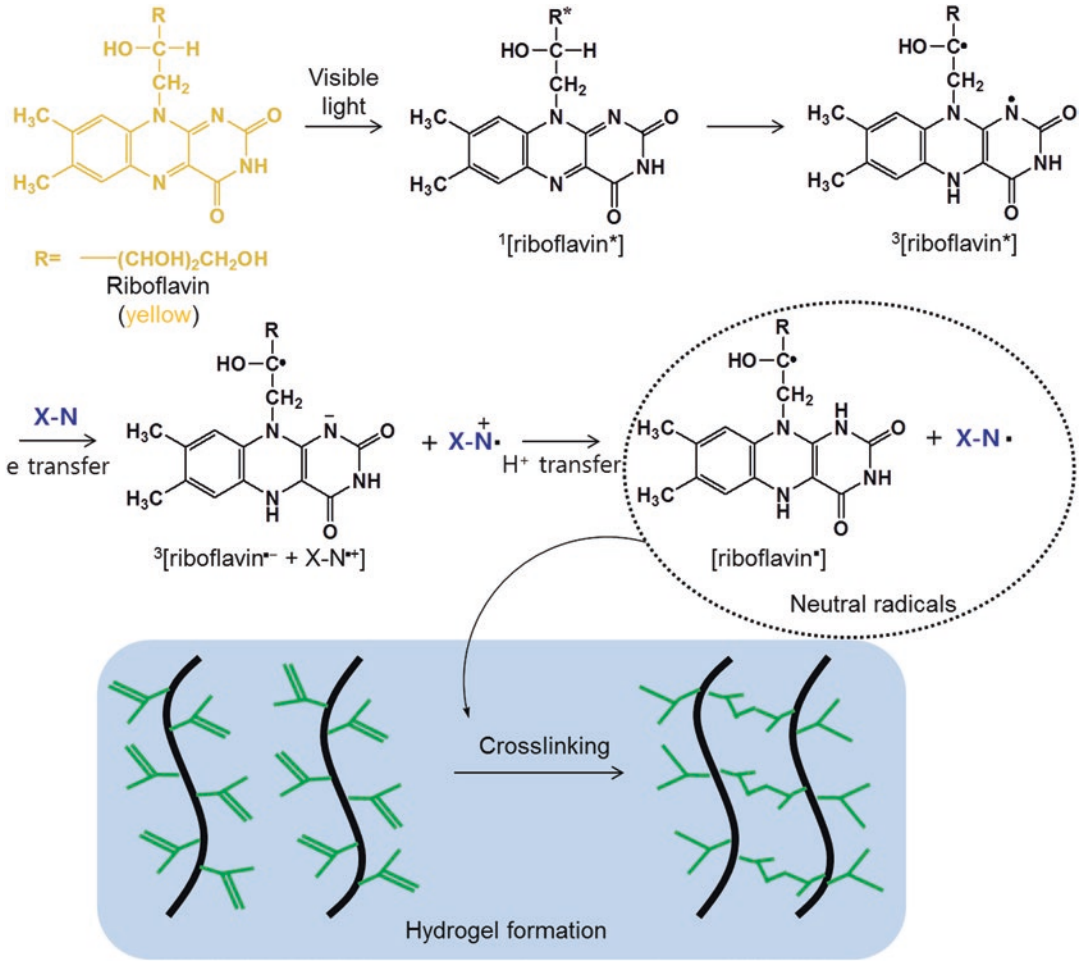

Fig. 6.2 Scheme for the hydrogel formation of methacrylated polymers initiated by riboflavin

solubility [41]. Beta-cyclodextrin (β-CD) can improve the water solubility of curcumin by inclusion complex formation [42]. The wound healing potential of visible light-curable GC containing a β-CD/curcumin complex (β-CD-c-CUR/GC) has been investigated by Yoon and his colleagues [43]. The results of in vivo animal tests demonstrated that β-CD-c-CUR/GC accelerates wound healing by a controlled release of curcumin in a sustained manner.

As another tissue engineering application, Yoon et al. [44] investigated the feasibility of a growth factor-loaded visible light-curable GC hydrogel as a bone tissue engineering scaffold in vitro and in vivo. To improve bone formation, bone morphogenetic protein-2 (BMP-2) and transforming growth factor-beta1 (TGF-β1) were loaded into the GC hydrogel prior to photo-curing (GC/BMP-2/TGF-β1), because BMP-2 and TGF-β1 are known to facilitate superior bone repair [45–47]. They found that two factors, including the cocktail effect and the controlled release of BMP-2 and TGF-β1, increased the mRNA expressions of alkaline phosphatase (ALP), type I collagen (COL 1), and osteocalcin (OCN) in vitro and also increased bone volume (BV) and bone mineral density (BMD) in vitro.

A visible light-curable hydrogel based on an interpenetrated polymer network (IPN) composed of biodegradable silanized hydroxypropylmethylcellulose (Si-HPMC) and photo-curable methacrylated carboxymethyl chitosan (MA-CMCS) has

been identified as a potential material for guided tissue regeneration (GTR), as reported by Chichiricco and his colleagues [48]. MA-CMCS was used as a matrix for a visible light-curable hydrogel, and the precursor solution was cured with visible light irradiation (420–480 nm). GTR in oral diseases including dental caries and periodontitis is a significant surgical procedure to recover periodontium [48]. It is used to prevent the migration of soft tissue that presents a faster proliferation rate than bone and ligament cells, followed by complete regeneration of periodontal tissue [48]. The researchers found that Si-HPMC/MA-CMCS has an appropriate storage modulus for clinical applications in dentistry and prohibits cell invasion in periodontal defects [48].

Hu et al. have designed a suitable hydrogel system using visible light irradiation for regenerating focal osteochondral and chondral defects [49]. Three types of hydrogels were prepared using methacrylated GC and three visible lights: camphorquinone (CQ), fluorescein (FR), and riboflavin. They found that the cell viability of primary articular chondrocytes was between 80% and 90% when the cells were encapsulated into the GC hydrogel cured with riboflavin for 40 s [49]. To further investigate the feasibility of GC hydrogels cured with riboflavin as cartilage tissue engineering scaffolds, the hydrogels were prepared using three different irradiation times: 40, 120, and 300 s. The results demonstrated that the GC hydrogels cured with riboflavin for 120 and 300 s remained stable on the defect sites for at least 2 weeks by integrating the hydrogels with surrounding native tissues [49].

6.3.2 Tissue Sealants

Biocompatible tissue sealants are essential materials for soft tissue repair to prevent the leakage of blood, air, and body fluids. Compared with synthetic adhesives, natural polymer-based sealants have some advantages including biocompatibility, degradability, sustainable derivation, and intrinsic bioactive qualities [50, 51]. Therefore, Charron et al. prepared visible light-curable alginate-based tissue sealants [52]. In this study, they observed the formation of covalent bonds between amine groups present on extracellular matrix (ECM) and aldehyde groups produced by the oxidation of alginate backbone chains (i.e., imine reactions) for a strong sealant [53, 54]. As a result, an appropriate oxidation degree (1~5%) was found to maintain adhesion between hydrogel and tissue.

6.3.3 Three-Dimensional Culture of Cells

Cells actually live in 3D environments with biophysical and biomechanical signals that have effects on cell migration, adhesion, proliferation, and gene expression [55, 56]. Therefore, analyzing the behaviors of cells in 3D matrices is an important consideration for clinical applications as tissue engineering scaffolds. Lee et al. have designed visible light-curable in situ-forming hyaluronic acid (HA) hydrogels as cytocompatible tissue engineering scaffolds [57]. This hydrogel system was prepared by light-induced thiol-ene reactions between methacrylated HA (MA-HA) and thiolated HA (SH-HA) using blue light for 40 s in the presence of riboflavin phosphate (RFP). The cytocompatibility test using corneal fibroblasts revealed no cytotoxic effects, suggesting that this hydrogel may be used as a tissue engineering scaffold. Hao et al. [58] have developed visible light-curable PEG hydrogel systems with tunable degradation for 3D cell culture of human mesenchymal stem cells (hMSCs), because the polymer is known as a suitable biomaterial for tissue engineering applications such as controlled drug delivery and stem cell differentiation [58, 59]. The hydrogel system was prepared by thiol-vinyl reaction between acrylated PEG and di-thiol peptide in the presence of photo-initiator EY, and this system revealed an hMSC survival rate of over 90% and osteogenic differentiation achieved by controlling the hydrolytic degradation [58].

Photo-cured gelatin methacryloyl (GelMA) with two- and three-dimensional networks can lead to good attachment and proliferation [60, 61]. Based on these previous studies, a stereolithography (SLA) 3D bioprinting process using

cell adhesive GelMA cured with EY with various concentrations was developed by Wang and his colleagues [62]. Bioprinting has been widely used in tissue engineering applications, because it can make various artificial tissues, such as cartilage, blood vessel, bone, and complex heterogeneous tissues containing different cell types and ECM [63, 64]. They suggested that an EY-GelMA hydrogel with specific concentrations (2× EY and 15% GelMA) has great potential as a bioink for tissue engineering applications, because the polymer network can improve the proliferation of NIH-3T3 fibroblast cells.

6.3.4 Drug Delivery Carriers

Visible light-curable hydrogels were developed as local drug delivery carriers for cancer therapy, because the systems can be directly injected around cancers, and anticancer drugs can be delivered to the tissues. Chitosan can be a candidate as a drug delivery carrier, because it is a deacetylated chitin that is similar to the glycosaminoglycans (GAGs) found in connective tissue [65], biodegradability, antimicrobial activity, low toxicity, and immunogenicity [66, 67]. Despite these merits, the poor water solubility of chitosan limits its biomedical applications. Glycol chitosan (GC) can substitute for chitosan, because it has water solubility along with the inherent properties of chitosan. The application of a visible light-curable GC hydrogel as a local drug delivery carrier for breast cancer therapy has been reported by Hyun and his colleagues [68]. They conducted in vitro MCF-7 cell viability tests to compare the antitumor effects of GC hydrogels containing doxorubicin·hydrochloride (DOX·HCl) as a function of storage modulus. The results showed that the GC hydrogel cured for 10 s containing DOX·HCl (GC_{10}/DOX) had a greater antitumor effect than GC_{60}/DOX. In addition, in vivo animal tests indicated that the local drug delivery of GC_{10}/DOX noticeably decreased tumor volume for 7 days [69]. The potential of visible light-curable GC hydrogels as local drug delivery systems for cancer therapy has been expanded by Yoo and his colleagues [69]. They investigated the efficacy of the hydrogel containing DOX·HCl on thyroid cancer treatment using a thyroid cancer-bearing mouse model. The intravenous injection of free DOX·HCl is harmful to heart tissue, causing side effects including the appearance of inflammatory cells, disorganization of myocardium, and increased cytoplasmic vacuolization and myofibrillar fragmentation in the heart tissue [70]. In addition, this conditional therapeutic method has little influence on decreasing tumor size [69]. These researchers found that the drug-loaded hydrogel injected near the tumor led to a decrease in tumor size along with minimized cardiotoxicity [69]. Hyun et al. [71] also demonstrated the feasibility of a visible light-curable GC hydrogel containing paclitaxel (PTX) for ovarian cancer therapy. In this study, β-CD was used to improve the water solubility of PTX, because the poor solubility of the drug leads to low bioavailability [72–74]. To examine the potential of β-CD in injectable hydrogel-based drug delivery, the researchers prepared two types of GC hydrogel systems: a GC hydrogel containing PTX (GC/PTX) and a GC hydrogel containing a β-CD/PTX complex (GC/CD/PTX). In in vitro and in vivo tests, GC/CD/PTX resulted in a lower cell viability percentage and tumor volume than GC/PTX. From these results, they suggested that the GC/CD platform has clinical potential as a drug carrier for ovarian cancer therapy [71].

In another application as drug delivery carriers, visible light-curable hydrogels have been applied to direct pulp capping treatment. For successful treatment of direct pulp capping in dentistry, appropriate drug carriers for delivering calcium hydroxide, steroids, osteogenic protein-1, and transforming growth factor-beta are required [75–78]. Komabayashi et al. [79] have developed PEG-maleate-citrate (PEGMC) hydrogels composed of PEGMC (45% w/v), acrylic acid (AA) (5% w/v), and 2,2′-azobis(2-methylpropionamidine) dihydrochloride (AAPH) (0.1% w/v) as an endodontic drug delivery vehicle for direct pulp capping. They have demonstrated the feasibility of the visible light-curable PEGMC hydrogel as a drug carrier, confirming

that the matrix results in the controlled release of $Ca2^{+}$ and is cytocompatible against the L-929 fibroblast cell line [79].

6.4 Future Perspectives

The three-dimensional structures of hydrogels are controlled by cross-linking density, porosity, and degradation time, which contribute to the maintenance of drug concentrations in vivo by controlling the drug release rate in a sustained manner. In addition, hydrogels have been attractive options as tissue engineering scaffolds because they are similar to the physical environment of the body and can be prepared similarly to the biochemical factors of target tissues. Generally known hydrogel preparation methods include use of physical factors (ions, temperature, and pH) and chemical cross-linking agents (formaldehyde and glutaraldehyde); however, these have drawbacks such as weak physical properties, agent toxicity, and the difficulty in controlling cross-linking tempo-spatially. In contrast, visible light-curable hydrogels have gained much attention as biomaterials in biomedical applications due to the simple control of their physical properties and the use of biocompatible photo-initiators and cytocompatible visible light. However, despite these merits, there have been limited clinical applications due to insufficient information on the biocompatibility and toxicity of hydrogels. So, the safety evaluation of visible light-curable hydrogels should be sufficiently conducted. If sufficient safety data is available, visible light-curable hydrogels are expected to be developed as smart drug delivery carriers and tissue engineering scaffolds in the future.

References

1. Peppas NA, Bures P, Leobandung W et al (2000) Hydrogels in pharmaceutical formulations. Eur J Pharm Biopharm 50(1):27–46
2. Caló E, Khutoryanskiy VV (2015) Biomedical applications of hydrogels: a review of patents and commercial products. Eur Polym J 65:252–267
3. Liu M, Zeng X, Ma C et al (2017) Injectable hydrogels for cartilage and bone tissue engineering. Bone Res 5:17014
4. Hoare TR, Kohane DS (2008) Hydrogels in drug delivery: progress and challenges. Polymer 49(8):1993–2007
5. Vashist A, Vashist A, Gupta YK et al (2014) Recent advances in hydrogel based drug delivery systems for the human body. J Mater Chem B 2:147–166
6. Davies H, Bignell GR, Cox C et al (2002) Mutations of the BRAF gene in human cancer. Nature 417(6892):949–954
7. Lindahl T (1993) Instability and decay of the primary structure of DNA. Nature 362:709–715
8. Nguyen KT, West JL (2002) Photopolymerizable hydrogels for tissue engineering applications. Biomaterials 23:4307–4314
9. Allen NS (1996) Photoinitiators for UV and visible curing of coatings: mechanisms and properties. J Photochem Photobiol A 100(1–3):101–107
10. Gómez ML, Previtali CM, Montejano HA (2012) Two-and three-component visible light photoinitiating systems for radical polymerization based on onium salts: an overview of mechanistic and laser flash photolysis studies. Int J Photoenergy 2012:260728
11. Scranton AB, Bowman CN, Peiffer RW (1997) Photopolymerization: fundamentals and applications. American Chemical Society, Washington, DC
12. Purbrick MD (1995) Photoinitiation, photopolymerization and photocuring. Gardner Publications, New York. https://doi.org/10.1002/(SICI)1097-0126(199608)40:4<315::AID-PI566>3.0.CO;2-T
13. Kaastrup K, Sikes HD (2015) Investigation of dendrimers functionalized with eosin as macrophotoinitiators for polymerization-based signal amplification reactions. RSC Adv 5:15652–15659
14. Bahney CS, Lujan TJ, Hsu CW et al (2011) Visible light photoinitiation of mesenchymal stem cell-laden bioresponsive hydrogels. Eur Cell Mater 22:43–55
15. Cruise GM, Gegre OD, Scharp DS et al (1998) A sensitivity study of the key parameters in the interfacial photopolymerization of poly(ethylene glycol) diacrylate upon porcine islets. Biotechnol Bioeng 57(6):655–665
16. Kizilel S, Pérez-Luna VH, Teymour F (2004) Photopolymerization of poly(ethylene glycol) diacrylate on eosin-functionalized surfaces. Langmuir 20(20):8652–8658
17. Shih H, Lin CC (2013) Visible-light-mediated thiol-ene hydrogelation using eosin-Y as the only photoinitiator. Macromol Rapid Commun 34(3):269–273
18. Kim S-H, Chu C-C (2009) Visible light induced dextran-methacrylate hydrogel formation using (-)-riboflavin vitamin B2 as a photoinitiator and L-arginine as a co-initiator. Fibers Polym 10(1):14–20
19. Unna K, Greslin JG (1942) Studies on the toxicity and pharmacology of riboflavin. J Pharmacol Exp Ther 76(1):75–80

20. Bajpai SK, Dubey S (2004) Modulation of dynamic release of vitamin B2 from a model pH-sensitive terpolymeric hydrogel system. Polym Int 53(12):2178–2187
21. Ramu A, Mehta MM, Liu J et al (2000) The riboflavin-mediated photooxidation of doxorubicin. Cancer Chemother Pharmacol 46(6):449–458
22. Wasylewski M (2000) Binding study of riboflavin-binding protein with riboflavin and its analogues by differential scanning calorimetry. J Protein Chem 19(6):523–528
23. Ramu A, Mehta MM, Leaseburg T et al (2001) The enhancement of riboflavin-mediated photo-oxidation of doxorubicin by histidine and urocanic acid. Cancer Chemother Pharmacol 47(4):338–346
24. Baldursdottir SG, Kjoniksen A-L (2005) Rheological characterization and turbidity of riboflavin-photosensitized changes in alginate/GDL systems. Eur J Pharm Biopharm 59(3):501–501
25. Annabi N, Rana D, Shirzaei Sani E et al (2017) Engineering a sprayable and elastic hydrogel adhesive with antimicrobial properties for wound healing. Biomaterials 139:229–243
26. Werdin F, Tenenhaus M, Rennekampff HO (2008) Chronic wound care. Lancet 372(9653):1860–1862
27. Ng VW, Chan JM, Sardon H et al (2014) Antimicrobial hydrogels: a new weapon in the arsenal against multidrug-resistant infections. Adv Drug Deliv Rev 78:46–62
28. Ghobril C, Grinstaff MW (2015) The chemistry and engineering of polymeric hydrogel adhesives for wound closure: a tutorial. Chem Soc Rev 44(7):820–1835
29. Kamoun E, El-Betany A, Menzel H et al (2018) Influence of photoinitiator concentration and irradiation time on the crosslinking performance of visible-light-activated pullulan-HEMA hydrogels. Int J Biol Macromol 120:1884–1892
30. Dijke P, Iwata KK (1989) Growth factors wound healing. Nat Biotechnol 7:793–798
31. Yang DH, Seo DI, Lee D-W et al (2017) Preparation and evaluation of visible-light cured glycol chitosan hydrogel dressing containing dual growth factors for accelerated wound healing. J Ind Eng Chem 53:360–370
32. Bao P, Kodra A, Tomic-Canic M et al (2009) The role of vascular endothelial growth factor in wound healing. J Surg Res 153(2):347–358
33. Rajkumar VS, Shiwen X, Bostrom M et al (2006) Platelet-derived growth factor-β receptor activation is essential for fibroblast and pericyte recruitment during cutaneous wound healing. Am J Pathol 169(6):2254–2265
34. Kolhe P, Kannan RM (2003) Improvement of ductility of chitosan through blending and copolymerization with PEG: FTIR investigation of molecular interactions. Biomacromolecules 4(1):173–180
35. Yoo Y, Hyun H, Yoon S-J et al (2018) Visible light-cured glycol chitosan hydrogel dressing containing endothelial growth factor and basic fibroblast growth factor accelerates wound healing in vivo. J Ind Eng Chem 67:365–372
36. Brown GL, Nanney LB, Griffen J et al (1989) Enhancement of wound healing by topical treatment with epidermal growth factor. N Engl J Med 321:76–79
37. Shi H-X, Lin C, Lin B-B et al (2013) The anti-scar effects of basic fibroblast growth factor on the wound repair in vitro and in vivo. PLoS One 8(4):e59966
38. Akita S, Akino K, Hirano A (2013) Basic fibroblast growth factor in scarless wound healing. Adv Wound Care 2:44
39. Akbik D, Ghadiri M, Chrzanowski W et al (2014) Curcumin as a wound healing agent. Life Sci 116(1):1–7
40. Joe B, Vijaykumar M, Lokesh BR (2010) Biological properties of curcumin-cellular and molecular mechanisms of action. Crit Rev Food Sci Nutr 44(2):97–111
41. Prasad S, Tyagi AK, Aggarwal BB (2014) Recent developments in delivery, bioavailability, absorption and metabolism of curcumin: the golden pigment from golden spice. Cancer Res Treat 46(1):2–18
42. Rachmawati H, Edityaningrum CA, Mauludin R (2013) Molecular inclusion complex of curcumin-beta-cyclodextrin nanoparticle to enhance curcumin skin permeability from hydrophilic matrix gel. AAPS PharmSciTech 14:1303–1312
43. Yoon S-J, Hyun H, Lee D-W et al (2017) Visible light-cured glycol chitosan hydrogel containing a beta-cyclodextrin-curcumin inclusion complex improves wound healing in vivo. Molecules 22:1513
44. Yoon S-J, Yoo Y, Nam SE et al (2018) The cocktail effect of BMP-2 and TGF-β1 loaded in visible light-cured glycol chitosan hydrogels for the enhancement of bone formation in a rat tibial defect model. Mar Drugs 16:351
45. Yang DH, Moon SW, Lee D-W (2017) Surface modification of titanium with BMP-2/GDF-5 by a heparin linker and its efficacy as a dental implant. Int J Mol Sci 18(1):229
46. Kasagi S, Chen W (2012) TGF-beta 1 on osteoimmunology and the bone component cells. Cell Biosci 3(1):4
47. Ogasawara T, Kawaguchi H, Jinno S et al (2004) Bone morphogenetic protein 2-induced osteoblast differentiation requires Smad-mediated down-regulation of Cdk6. Mol Cell Biol 24(15):6560–6568
48. Chichiricco PM, Riva R, Thomassin JM et al (2018) In situ photochemical crosslinking of hydrogel membrane for guided tissue regeneration. Dent Mater 34(12):1769–1782
49. Hu J, Hou Y, Park H et al (2012) Visible light cross-linkable chitosan hydrogels for tissue engineering. Acta Biomater 8(5):1730–1738
50. Draget KI, Taylor C (2011) Chemical, physical and biological properties of alginates and their biomedical implications. Food Hydrocoll 5(2):251–256
51. Lee KY, Mooney DJ (2012) Alginate: properties and biomedical applications. Prog Polym Sci 37(1):106–126

52. Charron PN, Fenn SL, Poniz A et al (2016) Mechanical properties and failure analysis of visible light crosslinked alginate-based tissue sealants. J Mech Behav Biomed Mater 59:314–321
53. Balakrishnan B, Lesieur S, Labarre D et al (2005) Periodate oxidation of sodium alginate in water and in ethanol-water mixture: a comparative study. Carbohydr Res 340(7):1425–1429
54. Jeon O, Alt DS, Ahmed SM, Alsberg E (2012) The effect of oxidation on the degradation of photocrosslinkable alginate hydrogels. Biomaterials 33(13):3503–3514. https://10.1016/j.biomaterials.2012.01.041
55. Ayala P, Lopez JI, Desai TA (2010) Microtopographical cues in 3D attenuate fibrotic phenotype and extracellular matrix deposition: implications for tissue regeneration. Tissue Eng Part A 16:19–27
56. Bott K, Upton Z, Schrobback K et al (2010) The effects of matrix characteristics on fibroblast proliferation in 3D gels. Biomaterials 31(32):8454–8464
57. Lee HJ, Fernandes-Cunha GM, Myung D (2018) In situ-forming hyaluronic acid hydrogel through visible light-induced thiol-ene reaction. React Funct Polym 131:29–35. https://doi.org/10.1016/j.reactfunctpolym.2018.06.010
58. Hao Y, Shih H, Muňoz Z et al (2014) Visible light cured thiol-vinyl hydrogels with tunable degradation for 3D cell culture. Acta Biomater 10(1):104–114
59. Cushing MC, Anseth KS (2007) Hydrogel cell culture. Science 316(5828):1133–1134
60. Wang Z, Tian Z, Menard F et al (2017) Comparative study of gelatin methacrylate hydrogels from different sources for biofabrication applications. Biofabrication 9(4):044101
61. Yoon HJ, Shin SR, Cha JM et al (2016) Cold water fish gelatin methacryloyl hydrogel for tissue engineering application. PLoS One 11(10):e0163902
62. Wang Z, Kumar H, Tian Z et al (2018) Visible light photoinitiation of cell-adhesive gelatin methacryloyl hydrogels for stereolithography 3D bioprinting. ACS Appl Mater Interfaces 10(32):26859–26869
63. Cui X, Breitenkamp K, Finn MG et al (2012) Direct human cartilage repair using three-dimensional bioprinting technology. Tissue Eng Part A 18(11–12):1304–1312
64. Kolesky DB, Truby RL, Gladman AS et al (2014) 3D bioprinting of vascularized, heterogeneous cell-laden tissue constructs. Adv Mater 26(19):3124–3130
65. Kim C-H, Park SJ, Yang DH et al (2018) Chitosan for tissue engineering. In: Chun HJ, Park K, Kim C-H, Khang GS (eds) Novel biomaterials for regenerative medicine, vol 1077. Springer, Singapore, pp 475–485
66. Khor E, Lm LY (2003) Implantable applications of chitin and chitosan. Biomaterials 24(13):2339–2349
67. Shahidi F, Abuzaytoun R (2005) Chitin, chitosan, and co-products: chemistry, production, applications, and health effects. Adv Food Nurt Res 49:93–135
68. Hyun H, Park MH, Lim W et al (2018) Injectable visible light-cured glycol chitosan hydrogels with controlled release of anticancer drugs for local cancer therapy in vivo: a feasible study. Artif Cells Nanomed Biotechnol 46(Suppl 2):874–882
69. Yoo Y, Yoon S-J, Kim SY et al (2018) A local drug delivery system based on visible light-cured glycol chitosan and doxorubicin·hydrochloride for thyroid cancer treatment in vitro and in vivo. Drug Deliv 25(1):1664–1671
70. Volkova M, Russell R III (2011) Anthracycline cardiotoxicity: prevalence, pathogenesis and treatment. Curr Cardiol Rev 7(4):214–220
71. Hyun H, Park MH, Jo G et al (2019) Photo-cured glycol chitosan hydrogel for ovarian cancer drug delivery. Mar Drugs 17:41
72. Namgung R, Lee YM, Kim J et al (2014) Polycyclodextrin and poly-paclitaxel nano-assembly for anticancer therapy. Nat Commun 5:3702
73. Chen Y, Huang Y, Qin D et al (2016) β-Cyclodextrin-based inclusion complexation bridged biodegradable self-assembly macromolecular micelle for the delivery of paclitaxel. PLoS One 11(3):e0150877
74. Liu Y, Chen G-S, Yuan Y (2003) Inclusion complexation and solubilization of paclitaxel by bridged bis(beta-cyclodextrin)s containing a tetraethylenepentaamino spacer. J Med Chem 46(22):4634–4637
75. Schroder U (1985) Effects of calcium hydroxide-containing pulp-capping agents on pulp cell migration, proliferation, and differentiation. J Dent Res 64:541–548
76. Watts A, Paterson RC (1988) The response of the mechanically exposed pulp to prednisolone and triamcinolone acetonide. Int Endod J 21:9–16
77. Rutherford RB, Spångberg L, Tucker M et al (1994) The time-course of the induction of reparative dentine formation in monkeys by recombinant human osteogenic protein-1. Arch Oral Biol 39(10):833–838
78. Zhang W, Walboomers XF, Jansen JA (2008) The formation of tertiary dentin after pulp capping with a calcium phosphate cement, loaded with PLGA microparticles containing RGF-beta 1. J Biomed Mater Res A 85(2):439–444
79. Komabayashi T, Wadajkar A, Santimano S et al (2016) Preliminary study of light-cured hydrogel for endodontic drug delivery vehicle. J Investig Clin Dent 7:87–92

Part III

Regulation of Stem Cell Fate by Bioinspired Biomaterials

7 Scaffolds for Cartilage Regeneration: *To Use or Not to Use?*

Munirah Sha'ban
and Muhammad Aa'zamuddin Ahmad Radzi

Abstract

Joint cartilage has been a significant focus on the field of tissue engineering and regenerative medicine (TERM) since its inception in the 1980s. Represented by only one cell type, cartilage has been a simple tissue that is thought to be straightforward to deal with. After three decades, engineering cartilage has proven to be anything but easy. With the demographic shift in the distribution of world population towards ageing, it is expected that there is a growing need for more effective options for joint restoration and repair. Despite the increasing understanding of the factors governing cartilage development, there is still a lot to do to bridge the gap from bench to bedside. Dedicated methods to regenerate reliable articular cartilage that would be equivalent to the original tissue are still lacking. The use of cells, scaffolds and signalling factors has always been central to the TERM. However, without denying the importance of cells and signalling factors, the question posed in this chapter is whether the answer would come from the methods to use or not to use scaffold for cartilage TERM. This paper presents some efforts in TERM area and proposes a solution that will transpire from the ongoing attempts to understand certain aspects of cartilage development, degeneration and regeneration. While an ideal formulation for cartilage regeneration has yet to be resolved, it is felt that scaffold is still needed for cartilage TERM for years to come.

Keywords

Biomaterial · Cartilage · Chondrocytes · Development · Regeneration · Regenerative medicine · Scaffolds · Tissue engineering

7.1 Introduction

Joint cartilage has been a significant focus in the field of tissue engineering and regenerative medicine (TERM) since its inception in the 1980s. When "tissue engineering" is combined with "regenerative medicine", these two subjects form a broad advanced scientific field. This advanced field is encompassing principles from various disciplines, in which no single subject may deal

M. Sha'ban (✉)
Department of Physical Rehabilitation Sciences, Kulliyyah of Allied Health Sciences, International Islamic University Malaysia, Kuantan, Pahang, Malaysia
e-mail: munirahshaban@iium.edu.my

M. A. Ahmad Radzi
Department of Biomedical Science, Kulliyyah of Allied Health Sciences, International Islamic University Malaysia, Kuantan, Pahang, Malaysia

H. J. Chun et al. (eds.), *Bioinspired Biomaterials*, Advances in Experimental Medicine and Biology 1249, https://doi.org/10.1007/978-981-15-3258-0_7

with its all aspects in a meaningful depth. After three decades of research, the TERM is still immature and contributes insignificantly to the actual healthcare settings. Various tissue-engineered medical products (TEMPs) such as cartilage, bone, skin, bladders, small arteries and even a full trachea have been implanted in patients. However, those TEMPs are still considered experimental and not cost-effective. Although some researchers have successfully formed complex tissues or organs, these tissues or organs are still far from being fully reproducible and ready to be implanted into patients. Despite all the uncertainties surrounding these laboratory-grown TEMPs, the TERM field continues to grow.

Represented by only one cell type, cartilage has been a simple tissue that is thought to be straightforward to deal with. After many years, engineering functional cartilage has proven to be anything but easy. With the demographic shift in the distribution of world population towards ageing [1], it is expected that there is a growing need for more effective options for joint restoration and repair. The WHO report outlined some key facts including:

- *The ratio of the world's population over 60 years old will nearly double from 12% in 2015 to 22% in 2050.*
- *The number of people aged between 60 years and above will be more than children younger than five years old by 2020.*
- *Approximately 80% of older people will be living in low- and middle-income countries in 2050.*
- *The leap of population ageing is much faster than in the past.*
- *All countries across the globe will face significant challenges to ensure that their health and social care systems are ready to make the most of this demographic shift.*

The above facts have a direct relation with the readiness of the global healthcare system in managing or dealing with degenerative diseases. Degeneration naturally occurs among the ageing population. Despite the increasing understanding of the factors governing cartilage development and degeneration, there is still a lot to do to bridge the gap from bench to bedside. Dedicated methods to regenerate reliable articular cartilage that would be equivalent to the original tissue are still lacking.

The use of proper cells source, biomaterial scaffolds and signalling factors has always been central to the TERM field. However, without denying the importance of cells and signalling factors, in this chapter, the authors aimed to emphasise on the use of biomaterial scaffolds in regenerating the articular cartilage. Ideal scaffolds for cartilage TERM should meet some requirements related but not limited to safety, biocompatibility, biodegradability and adequate mechanical properties. Numerous studies and characterisations on scaffolds for articular cartilage tissue engineering have been ongoing and evolving in many forms of the physical aspect, ranging from chemically and biologically cross-linked hydrogel, sponge, fibre, micro-/nanoparticles and 3D printing.

On the one hand, a quick search on currently available literature indicated that the following scaffolds are among the most versatile scaffolds which remain viable and relevant in the field of TERM. They include but not limited to:

- Decellularised tissue-derived scaffolds [2–5]
- Chitosan [6–8]
- Platelet-rich plasma scaffold [9]
- Gelatin and poly(lactic-*co*-glycolic acid) (PLGA) [10, 11]
- Hydrogel [12, 13]
- Collagen hydrogel and polyhydroxyalkanoate [14]
- Alginate [15, 16]
- Silk fibroin [17]
- Gelatin/hyaluronic acid [18]
- Poly-ε-caprolactone (PCL) [19]

On the other hand, the scaffold-free approach has been studied equally for cartilage tissue engineering by some researchers in some part of the world which include:

- Chondrocytes and their self-produced extracellular matrix (ECM) [20]
- Glutamic acid-based dendritic peptides [21]
- 3D bioprinting microtissues, spheroid using a high-throughput microwell system [22]
- Cellular spheroids using 3D bioprinting technology (Regenova Bio 3D Printer) [23]
- "Osteo-chondro" constructs using a scaffold-free bioprinter [24]
- Cell sheet technology [25]

Information given in this chapter is not meant to be comprehensive but to present some efforts in TERM and proposes a solution that will transpire from the ongoing attempts to understand certain aspects of cartilage development, degeneration and regeneration. The question is whether the answer would come from the methods to use or not to use scaffolds for cartilage regeneration.

7.2 Cartilage Structure and Function

Cartilage (*chondral*) is made up of one cell type, i.e. chondrocyte (*chondros* = cartilage; *cyte* = cell). By physical properties, cartilage is categorised as a supporting connective tissue. Cartilage and bone, another supporting connective tissue type, work together and make up the human skeleton to protect soft tissues and organs and support the weight of part or all of the body. Supporting connective tissues vary from connective tissue proper (e.g. adipose tissue and tendon) and fluid connective tissue (e.g. blood and lymph). They have a lesser diverse cell population and a matrix containing much more densely packed fibres than the connective tissue proper and the fluid connective tissue. The ECM of cartilage is a gel with characteristics that vary with the predominant type of fibre [26].

The ECM of cartilage is a firm gel that contains polysaccharide derivatives known as chondroitin sulphate. Chondroitin sulphates and proteins form complexes producing proteoglycans in the ground substance. The only cells in the cartilage ECM, i.e. chondrocytes, occupy small chambers known as lacunae. The proteoglycans of the ECM, as well as the type and abundance of extracellular fibres, determine the physical characteristics of cartilage [27].

Unlike bone and other connective tissues, cartilage is avascular, aneural and alymphatic, so all nutrients and waste products exchange take place by diffusion through the ECM. Because of this situation, cartilage cannot heal efficiently. There is no blood vessels growth in cartilage because chondrocytes produce a chemical known as an antiangiogenetic factor that inhibits their formation. Other angiogenesis inhibitors have also been identified and developed as drugs to treat cancer. The inhibitors discourage the formation of new blood vessels to tumours, thus decelerating the growth [28].

Cartilage is separated from its surrounding tissues by a fibrous perichondrium. The perichondrium consists of two distinct layers, i.e. an outer fibrous layer comprising dense irregular connective tissue and an inner layer consisting the cellular component. The fibrous region gives mechanical support and protection. The layer also attaches the cartilage to other structures. The cellular layer is essential to cartilage growth and maintenance. The presence of blood vessels in the perichondrium is essential in order to provide oxygen and nutrients to the underlying chondrocytes [29].

The three main types of cartilage in the human body are hyaline, elastic and fibrocartilage. Hyaline cartilage (*hyalos* = glass) is the most common type of cartilage. The examples of hyaline cartilage in adults include the nasal cartilages, the connections between the ribs and the sternum, the supporting C-shaped rings cartilages along the trachea and the articular cartilages, which cover the end of bone surfaces within many synovial joints, e.g. the elbow and knee. A dense perichondrium surrounds hyaline cartilages except inside the synovial joint cavities. Hyaline cartilage is a tough tissue but relatively flexible because its ECM has tightly packed collagen fibres. Since these fibres are not in large bundles and do not stain darkly, they are not always seen under the light microscope [26].

Elastic cartilage is exceptionally resilient and flexible because it has numerous elastic fibres.

These cartilages usually have a yellowish colour macroscopically. Examples of elastic cartilage include the auricle or, the external flap of the outer ear, the epiglottis at the opening of the windpipe which prevents food and liquids from entering the trachea when swallowing, the auditory passageway and the cuneiform cartilages in the larynx or voice box [27].

Fibrocartilage is a sturdy and extremely durable tissue because it contains little ground substance and its ECM is dominated by densely interwoven collagen fibres. This tissue can be found as fibrocartilage pads, e.g. in the intervertebral discs which lie between the spinal vertebrae, around tendons and within or around joints and between the pubic bones of the pelvis. In these positions, fibrocartilage absorbs shocks, resists compression, limits movement and helps prevent damaging bone-to-bone contact [28].

7.3 Cartilage Development, Degeneration and Regeneration

In embryogenesis, the skeletal system is derived from the mesodermal layer. Cartilage development (or also known as chondrogenesis or chondrification) is a process by which cartilage is formed from condensed mesenchyme tissue. The mesenchymal cells will differentiate into chondrocytes and begin secreting molecules and substances to form the cartilaginous ECM. Early in foetal development, a major part of the skeleton is cartilaginous in nature. This temporary cartilage is replaced gradually by bone through endochondral ossification, which usually ends at puberty. Nonetheless, the cartilage in the joints remains unossified throughout life and is, therefore, permanent.

Cartilage develops through interstitial and appositional growth. Interstitial growth expands the cartilage from inside. Chondrocytes in the cartilage ECM divide and the daughter cells produce additional ECM. Interstitial growth is an essential process during cartilage development. The process begins early during embryonic development and continues through adolescence. Appositional growth increases the size of the cartilage gradually by adding to its outer surface. During this process, the inner layer cells of the perichondrium divide repeatedly and become chondroblasts [26].

Chondroblasts are immature chondrocytes. The cells begin producing the cartilage ECM. As they are surrounded by and embedded in a new ECM, the chondroblasts differentiate into mature chondrocytes. They now become part of the cartilage and continue to grow. Both interstitial and appositional growth occurs during cartilage developmental stage, but interstitial growth contributes more to the mass of adult cartilage. Neither interstitial nor appositional cartilage growth occurs in healthy adults. However, appositional growth may take place in rare conditions, e.g. after the cartilage has been damaged or stimulated by growth hormone from the pituitary gland excessively. Insignificant cartilage damage can be regenerated and repaired by appositional growth at the affected surface. If the damage has become more severe than the above condition, a dense fibrous patch will develop and substitute the injured portion of the cartilage [29].

In the human body, there are several complex joints, including the knee joints that consist of both hyaline cartilage and fibrocartilage. The hyaline cartilage articulates the end of bone surfaces, while the fibrocartilage pads the joint to prevent friction between bones during movement. Any injuries to these pads can interfere with regular movements because they do not heal spontaneously. After repeated or severe damage, joint mobility is significantly reduced. Although surgery may be prescribed to overcome joint mobility issue, it usually gives only a temporary or incomplete repair. Unlike cartilage, complete bone regeneration and repair can be achieved even after severe damage to the structure [26, 27]. It is because the bone is rich in vascularisation, but the cartilage is not.

A compelling argument in TERM field is that *is developmental process* equivalent with *regeneration*? In a recent review article on cellular senescence in development, regeneration and disease, Muriel et al. [30] indicated that although many studies have exposed beneficial effects of

senescence, especially in the context of embryonic development, tissue repair and regeneration and cellular reprogramming, the understanding of the biological functions of the senescence process is still lacking. Perhaps a thorough comparison of senescent cells in each stage will help to understand their real biological significance.

Myohara [31] has suggested previously that comparisons between development (or embryogenesis) and regeneration can give information about the steps essential to regeneration. The knowledge would help the scientist to gain better insight into how much reactivation of developmental processes might help improve regeneration capacity in higher vertebrates. By using an example of the in vivo osteogenesis potential of mesenchymal-like cells derived from human embryonic stem cells (hESC-MCs) study, Kuhn et al. [32] suggested that the implanted hESC-MCs differentiated to chondrocytes and bone-forming cells and tissue via an endochondral ossification pathway. Interestingly, no osteogenic or chondrogenic differentiation protocols were introduced to the cells before implantation. According to Kuhn et al. [32], this developmental-like bone regeneration study represents a crucial step forward for tissue engineering because of the reproducibility of new bone formation without preimplantation differentiation to osteo- or chondroprogenitors or having to over-commit the hESC-MCs to a particular lineage before implantation.

Nevertheless, from the analyses conducted on annelids or segmented worms, Myohara [31] stated that the alkaline phosphatase (ALP) expression patterns and central nervous system (CNS) development differ between embryogenesis and the regeneration. Although annelids are invertebrates, the results serve as an indication that regeneration is not a simple replication of embryogenesis but involves different regulatory mechanisms, especially in higher vertebrates. In another study on a stepwise model system for limb regeneration, Tetsuya et al. [33] suggested that although the later phase of limb regeneration is equivalent to its development, the early phase involving blastema genesis is unique to regeneration that perhaps would enhance regenerative processes in humans. There are many other examples, but the above initiatives give a basis for the exposition of unique and crucial mechanisms to regeneration which remains underexplored in cartilage tissue engineering.

7.4 Cartilage Disorders and Management

Findings of a Global Burden of Disease (GBD) 2017 study show that human life expectancy is 73 years, but healthy life expectancy is only 63 years [34]. From the two figures, on average, 10 years of life were spent in poor health globally. Another GBD study indicated that musculoskeletal injury and degeneration are leading causes of disability in 2010, with osteoarthritis (OA) as the most common cause of disability in older adults [35]. With a demographic shift in the distribution of world population towards ageing as per stated in the [1] report, it is expected that there is a growing need for more effective options for joint restoration and repair [1].

Osteoarthritis is a long-term chronic disease characterised by the deterioration of the cartilage in joints. Other than related to ageing, OA is also associated with various modifiable and non-modifiable risk factors, e.g. obesity, lack of exercise, bone density, occupational injury, trauma, gender and genetic predisposition (Table 7.1). These examples are based on the assessment in the context of the Malaysian population. The OA symptoms include joint pain, stiffness, joint swelling and decreased range of motion. If the vertebrae or backbone is affected, numbness and weakness of the arms and legs will indeed affect work and alter daily activities.

Table 7.1 Risk factors

Non-modifiable	Modifiable
Advancing age Female Genetic Heberden's nodes in hand OA	Body mass index (BMI) >25 kg/m^2 Previous knee injury Joint malalignment

Adopted from the Malaysia Health Technology Assessment Section, MaHTAS [36]

Osteoarthritis can be classified into primary (idiopathic) and secondary OA based on the joint involved, i.e. hand, hip or knee, or by aetiology. The primary OA includes generalised OA, a condition associated with Heberden's nodes and polyarticular disease which occurs mainly in the hand, with a female preponderance and has a high prevalence in first-degree relatives. As for the secondary OA, it can be due to several factors: (1) metabolic disorders such as acromegaly, haemochromatosis and chondrocalcinosis; (2) anatomic such as slipped femoral epiphysis, Legg-Perthes disease, congenital dislocation of the hip, leg length inequality, hypermobility syndromes and avascular necrosis; (3) trauma such as joint injury and fracture through a joint or osteonecrosis; and (4) inflammatory such as rheumatoid arthritis, psoriatic arthropathy and septic arthritis.

As indicated in the earlier section, mature cartilage tissue has minimal capacity for self-repair. If the cartilage is injured and left untreated, it can lead to early degeneration and progress into OA. As far as this paper is written, there is no known cure for OA. Pharmacotherapy, physical rehabilitation, strengthening exercise, interventional therapy, complementary medicine and surgery help to improve patient's outcome. However, the available therapies do not treat or address the underlying issues. Although current surgical interventions to cartilage repair are clinically useful, they are unable to restore the structurally and functionally normal articular cartilage surface. In the case of Malaysia, the algorithm on the management of knee and hip OA is summarised in Fig. 7.1.

As of 2013, because of the lack of available evidence, the Clinical Practice Guidelines (CPG) and Quick Reference (QR) for the Management of Osteoarthritis (Second Edition) issued by the Ministry of Health (MOH) Malaysia were unable to recommend the use of intraarticular stem cells, autologous chondrocyte implantation, platelet-rich plasma or even any recent advances in orthopaedic tissue engineering approaches in the treatment of OA [36, 37]. It was indicated in the 2013 CPG document that it would be reviewed if new evidence in the treatment of OA becomes available, which is not the case, as of 2019. It is felt that the outcome of TERM research, if successful, may have an impact on the Malaysian CPG. Relevant scientific evidence for OA management will be disclosed based on the best cartilage TERM approaches. The information perhaps can shed some light and give some insight into OA holistic healthcare model and be included in the CPG, MOH Malaysia, as one of the viable benchmarks for OA management.

7.5 Cartilage Tissue Engineering

7.5.1 Cells Source

Cells can be taken from autologous, allogeneic or xenogeneic cells sources. Autologous cells are harvested from the same individual (donor = recipient), while allogeneic and xenogeneic cells are harvested from a different person and a different species, respectively. The types of cell can be divided into differentiated and undifferentiated cells. These two cell types vary in that the differentiated cells (or also known as adult progenitor cells, specialised cells or committed cells) perform a specific function in the tissue, while the undifferentiated cells are uncommitted cells (or also known as stem cells) that will remain uncommitted until appropriate signals stimulate the stem cells to differentiate into committed cells.

It has been well-documented that the triggering needs for stem cells in TERM are because of the inadequate supply of committed cells so far. Other unresolved issues include morbidity at the harvested donor site as well as lack proliferative and biosynthetic activities of the committed cells. Stem cells have been known for their ability to self-renew and to divide actively in the monolayer in vitro culture. Stem cells can differentiate into multiple specialised cell types in the body. This criterion makes them as a suitable candidate for tissue regeneration and repair, especially for tissues that are unable to regenerate spontaneously after injuries.

Stem cells can be isolated from a human embryo, foetal or relevant adult tissues. Other

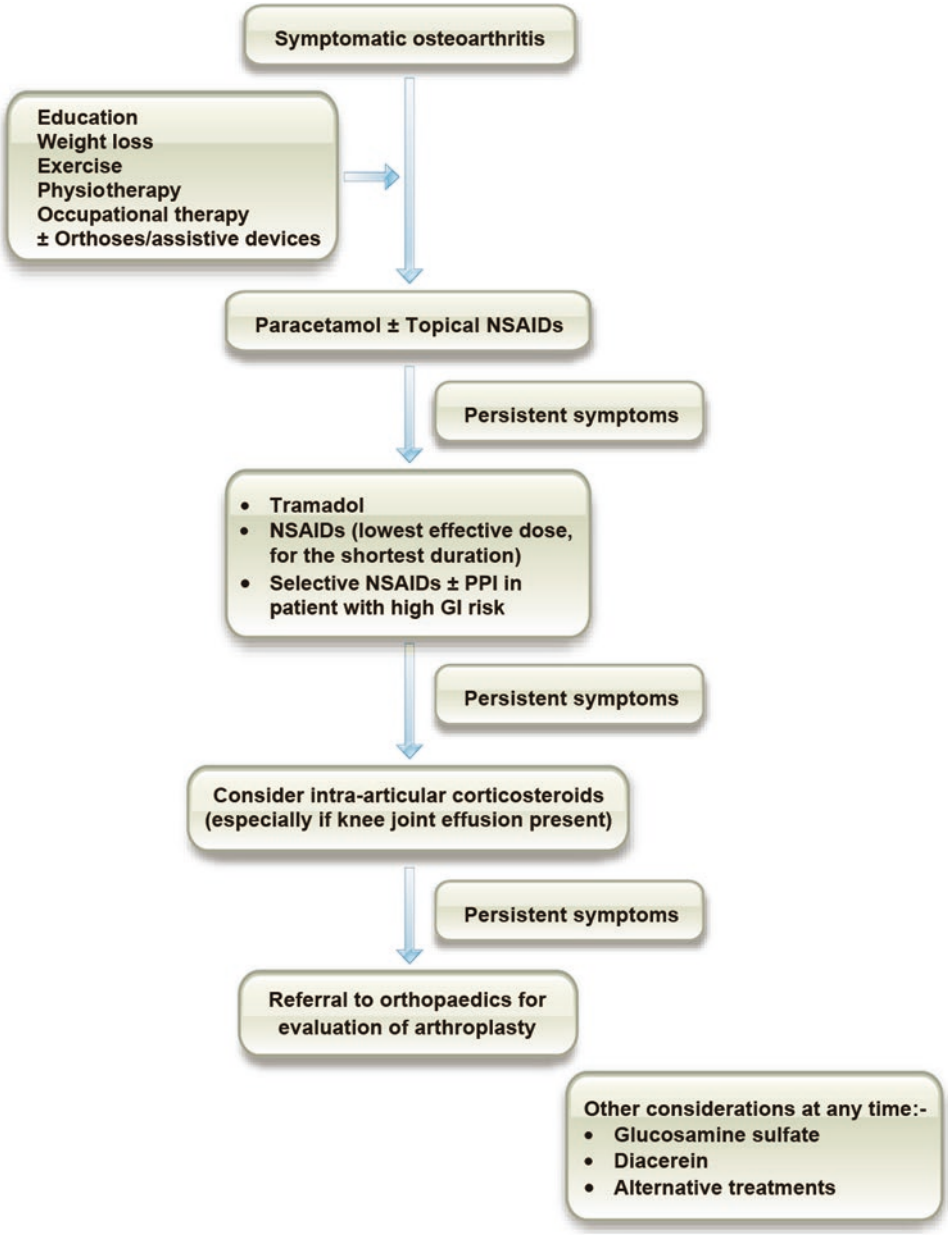

Fig. 7.1 Algorithm on the management of knee and hip osteoarthritis based on the CPG and QR, Management of OA, MOH Malaysia (Adopted from Refs. [36, 37])

than isolating cells from the inner cell mass of the blastocyst, the pluripotent embryonic stem cells (ESCs) can also be harvested from foetal tissue from terminated pregnancies. To date, TERM researchers are still investigating whether the differentiated cells and the undifferentiated stem cells (from adult tissues) have equivalent potential to that of the ESCs [12, 19, 38]. In terms of development potential, ESCs have been reported to have a more significant differentiation potential than the differentiated cells and adult stem cells (ASCs) [39]. While the ESCs can differentiate into almost every cells lineage, the ASCs may only develop into limited cell types. However, the

ASCs have shown to have greater plasticity than they were initially thought [9, 40]. The remaining challenge is that *which cells source holds advantages for tissue regeneration*?

From the above arguments, both the differentiated cells and the ASCs hold a unique advantage. In a fully autologous system, a patient's cells will be harvested, cultured and reimplanted or transplanted back into the same patient. It can be appreciated that there shall be no issues on immune rejection since the autologous cells are compatible with the patient's own body. Nevertheless, for ESCs, the recipient may require lifelong immune-suppressive drugs to overcome rejection of the newly transplanted cells. The differentiated cells and ASCs are adult tissues and obtained with consent from the patient. Technically, there may be little if any ethical issue on the ASCs therapies compared to the ESCs.

7.5.2 Signalling Factors

The governing principle of this part is that cell fate is influenced by cells' interactions with components of their microenvironment. Cell fate is believed to have a strong association with culture conditions. Cell differentiation requires optimum physiological conditions such as temperature, pH, oxygen, 3D environment and adequate cell-to-cell contact. Biochemical factors (e.g. nutrients and growth factors) and physical stimulation (e.g. compression and tension) are essential to direct proper cell growth and differentiation. Insufficient signalling factors will lead to loss of specific function, cells senescence or ageing and, eventually, cell death. The signalling factors may include soluble and immobilised factors, the ECM (*see* biomaterial scaffolds) and signals presented by adjacent cells. In cell culture basis, defined culture media induce cell differentiation by providing vital regulatory factors.

Dynamic culture system such as bioreactors improves cell seeding and functional tissue development by providing mixing, mass transport and biophysical stimulation. This microenvironment simulation is critical for proper expansion of cells in vitro and particularly significant for both primary and translational research in TERM.

Gene transfer approaches have been introduced for TERM applications due to inefficiencies of protein delivery in vitro ([41]; Md Ali@ [42]). The difficulties of protein delivery include short biological half-life, ineffective localisation, rapid withdrawal from the application site, the higher dosage required, unwanted side effects and very costly. In overcoming these issues, gene transfer offers more efficient management of protein delivery through independent protein regulation [43]. The advantages of gene transfer include the ability to sustain and regulate the endogenous synthesis of a gene product, efficient localisation and higher biological potency with multiple gene transfer [44]. In practical, gene transfer can be done in situ with minimal scaffolds requirement.

Genetic engineering is one of the most significant discoveries in modern science nowadays. Its applications (e.g. cloning and recombinant technology) enable us to synthesise growth factors or its gene and hormones (e.g. insulin that was taken from pig previously) for both research and clinical treatments. Gene transfer involves cloning and thus part of genetic engineering. If the combination of gene transfer and tissue engineering approaches is successful, a simple, cost-effective, expedited tissue restoration may be achieved using a single intraoperative procedure, as indicated in Fig. 7.2.

Figure 7.2 illustrates the hypothetical impression to use the gene transfection procedure using the identified vector into the harvested mesenchymal stem cells for osteochondral treatment. The transfecting cells will be then incorporated with a suitable biomaterial scaffold and transplanted into the defect. It is anticipated that the resulting cells-scaffold complex will be able to regenerate and achieve full tissue reparation. It is also believed that this single intraoperative procedure will reduce harm to the patient [46].

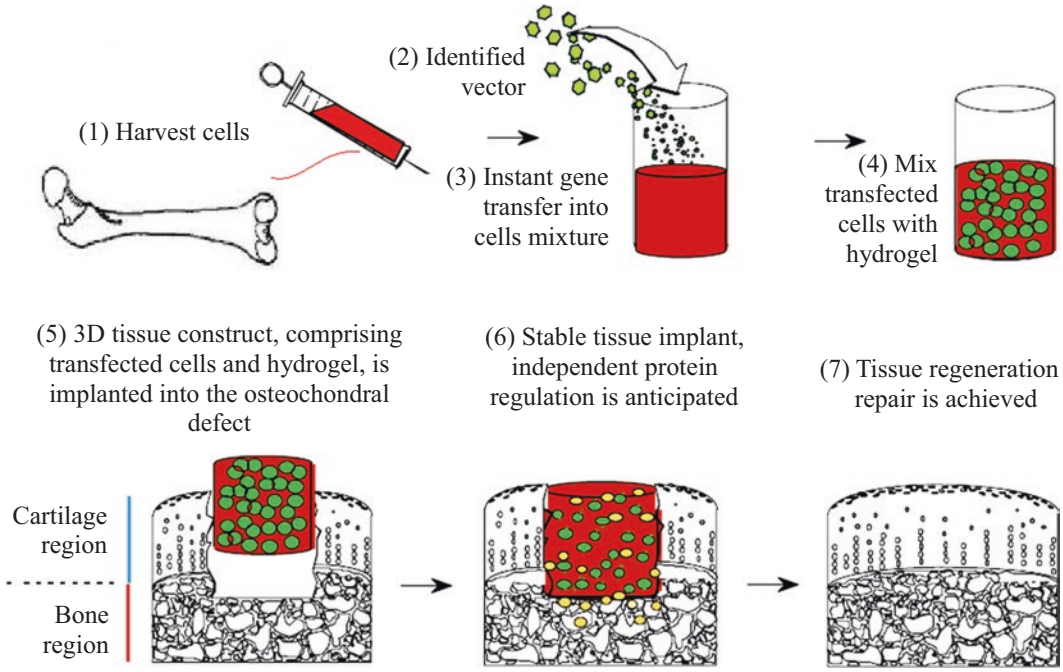

Fig. 7.2 A stepwise gene transfer approach for cartilage TERM based on the osteochondral defect model (Adopted and adapted from Ref. [45])

7.5.3 Biomaterial Scaffolds

The use of cells and growth factors are quite specific in TERM experiments. However, the use of biomaterial scaffolds may vary depending on the needs or design of a tissue. It is believed that "nature" is the best designer for tissue or organ development. It has never been easy to manufacture scaffolds since the suitable design for biomaterial scaffolds should bear a resemblance to the actual extracellular matrix of the tissue [47].

Biomaterial scaffolds can be either natural or synthetic. The natural and synthetic biomaterials can be used individually or in combination to produce functional scaffolds. Suitable scaffolds will direct cell growth and regenerate 3D tissue [48]. The naturally derived biomaterials include protein- and polysaccharide-based materials. Proteins and polysaccharides hold significant advantages and meet the requirements for TERM applications based on their multitude of functions in the human body. Natural biomaterials usually have suitable sites for cellular adhesion and biocompatible to the human body. However, the composition of natural biomaterials can be varied and uncertain. The purity of the protein-based biomaterials (e.g. collagen, silk and fibrin) or polysaccharide-based biomaterials (e.g. agarose, alginate, hyaluronan and chitosan-based scaffolds) must be appropriately identified to avoid potential post-implantation activation of the immune response. In terms of mechanical properties, usually the naturally derived scaffolds lack mechanical strength [49] and thus need to be optimised accordingly.

Polymer-, peptide- and ceramic-based biomaterials are the most common synthetic biomaterials used in TERM. As an alternative to the natural biomaterials, these synthetic biomaterials have well-defined chemicals and biomechanical compositions. The synthetic biomaterial scaffolds can be tailor-made to meet specifications at the injury or implantation site. The properties are essential to determine cell differentiation and facilitate reproducibility of the scaffolds in that the mechanical properties, shape and degradation

rate can be controlled based on the intended requirement. In drug developments, the specific degradation rate is more critical as it controls the release (rate) of drugs incorporated into scaffolds. Unlike natural biomaterials, the synthetic biomaterials lack sites for cell adhesion. The sites must be altered chemically to allow appropriate signals for cell adhesion and proliferation.

The suitability for in vivo implantation is subjected to the biocompatibility of the materials [50]. Therefore, biocompatibility assessment of the materials and its by-product is essential to avoid any harms or complications such as unwanted immune responses that may be triggered in the host-recipient after implantation [51]. Biocompatibility testing can be done based on the US Food and Drug Administration (FDA) guideline to ensure a thorough safety assessment. Other than safety issues, the origin of the materials should be observed and must not contain prohibited materials.

7.5.4 Scaffold-Based and Scaffold-Free Approaches: *Current Trend and Way Forward*

It can be appreciated that the current methods in TERM employed two different yet interrelated strategies, i.e. scaffold-based and scaffold-free approaches. A systematic search on cartilage tissue engineering study between 1994 and 2017 using Web of Science (WoS) and Scopus databases yielded 4071 articles after the removal of duplicate items in both databases amounting to 1393 articles. All data were extracted between January and March 2018, and the thematic analysis was completed on 30 May 2019. After the exclusion of 189 non-English articles, 1361 non-original research articles, 138 unavailable full-text articles and 594 indirectly related articles, a total of 1789 articles included for the analyses with 1645 articles are directly related to "biomaterials". Although Martin-Martin et al. [52] suggested that in all areas, Google Scholar database citation data is *a superset of WoS and Scopus, with substantial additional coverage*, the selection of the two later databases is enough for the review of this paper.

Out of 1645 articles, 706 studies involved natural biomaterials, 363 studies used synthetic biomaterials, 242 studies used combination of the natural-synthetic biomaterials, 183 studies aimed at scaffold-free approach, 115 studies did not specify the types of biomaterials or scaffold they used and 36 studies used either natural or synthetic biomaterials in their articles (Fig. 7.3). From the results, the scaffold-based approach (89%) is more popular than the scaffold-free approach (11%) across the TERM field worldwide. Nonetheless, Ovsianikov et al. [53] opined that the rapidly emerging synergetic TERM strat-

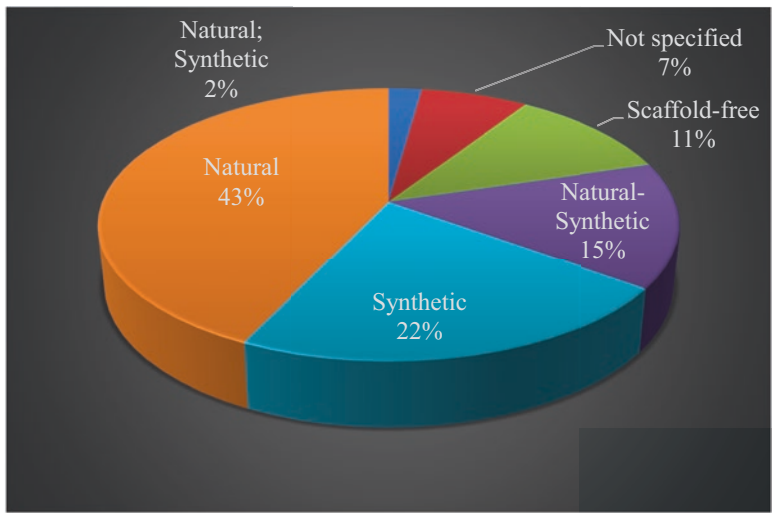

Fig. 7.3 The distribution of scaffold-based and scaffold-free approach based on 1645 articles

egy, integrating scaffold-based and scaffold-free approaches, represents a new, genuinely convergent research direction with strong potential for enabling disruptive solutions and advancing the fields of TERM.

The focal point of scaffold-based approach is on the use of appropriate transient 3D template, skeleton or framework to support cellular attachment, proliferation and formation of new tissue and organ. The essence of the vital functions of the scaffold should be adequately designed to match the degradation profile of the scaffold to the formation of new ECM by the cells. This aspect must be balanced and is always necessary to maintain the compliance of the TEMPs, particularly for weight-bearing tissues such as cartilage [9]. Durable 3D scaffolds can protect cells from possible damage by external factors. Another aspect of design that must be taken into consideration is that the scaffolds should be able to equip a biomimetic microenvironment for cells as well as the delivery and controlled release of signalling molecules to facilitate new tissue formation [54].

With 89% coverage of research worldwide, the scaffold-based approach is seen as a popular and advantageous method, especially in addressing the mechanical properties and degradation profile of TEMPs. The choices of biomaterial scaffolds are many, and they can be tailored to suit the TERM applications (Appendix). There is also an option to deliver signalling molecules either by controlled release from the materials or by immobilizing them on the surface [55, 56]. In addition, rapidly progressing 3D printing technologies offer a wide range of possibilities from using bioinspired composites to the realisation of multiphasic TEMPs and shape-morphing systems [22–24].

The scaffold-free approach is a bottom-up strategy using cell sheet engineering [57, 58], spheroids [10, 11, 59] or tissue strands [60, 61] as building blocks. This approach depends on the intrinsic ability of these cellular materials to assemble and fuse to form larger tissue constructs or TEMPs. Unlike the scaffold-based approach, scaffold-free TEMPs need a high initial cell density. In this case, the proliferation and migration of cells are not absolute factors, so the time needed for new tissue formation can be reduced significantly. A notable advantage of this scaffold-free approach is its ability to address the structure or architecture of the multifaceted tissues or organs by the controlled assembly of various cellular sources [53].

However, one critical disadvantage of this scaffold-free approach is the inferior mechanical properties of the cellular sources in that the materials of the cell may break during the manipulation in vitro. In addition, the holding time needed to obtain a reliable TEMP may be longer than the scaffold-based approach because the scaffold-free cellular materials sometimes need to fuse themselves and prompt the ECM to deposit and thus develop the tissue. Despite lingering uncertainties concerning the above facts, "cell sheet engineering" perhaps is the most successful scaffold-free approach, developed using temperature-responsive culture dishes by a Japanese research team. This method is explored to overcome the limitations of tissue reconstruction using biodegradable scaffolds or single-cell suspension injection. Popularised by Yamato and Okano [62], the resulted cell sheets have been applied clinically for various tissue reconstructions, including ocular surfaces, periodontal ligaments, cardiac patches and bladder augmentation.

7.6 Conclusion

Basic research and scientific development reveal the potential of TERM applications. However, a significant number of unanswered questions about the actual requirements for tissue regeneration, the mechanisms associated with its pathophysiology and the unresolved ethical issues remain as challenges to the field. While an ideal formulation for cartilage regeneration has yet to be resolved, it is felt that the scaffold-based approach is still needed for cartilage TERM for years to come.

Acknowledgement The authors thanked the Ministry of Education (MOE) Malaysia Transdisciplinary Research

Grant Scheme TRGS/1/2016/UIAM/02/8/2 (TRGS16-02-002-0002) under TRGS/1/2016/UIAM/02/8 programme and the Ministry of Energy, Science, Technology, Environment and Climate Change (MESTECC, formerly known as MOSTI) Malaysia Science Fund (SF14-012-0062/06-01-08-SF0238); the Kulliyyah of Allied Health Sciences, International Islamic University Malaysia (IIUM), Kuantan Campus, Pahang, Malaysia; and Tissue Engineering and Regenerative Medicine Research Team, IIUM, for their support.

Appendix

List of biomaterial scaffolds used as an individual or in combination in cartilage tissue engineering experimentation based on 1645 studies starting 1994 to 2017. Note Table (A) natural biomaterials and (B) synthetic biomaterials.

(A) Natural biomaterials
1. Agarose
2. Collagen type I (Integra®) commercial
3. Hyaluronic acid (HYAFF®-11)
4. Fibrin
5. Alginate
6. Collagen I
7. Collagen I/GAG
8. Gelatin
9. Calcium phosphate tribasic
10. Collagen type I
11. Collagen II
12. Hyaluronic acid, alginate (NS) [NS]
13. Silicone rubber membranes coated with type I collagen; ~agarose
14. Atelocollagen I
15. Silk fibroin
16. Calcium polyphosphate
17. Chitosan
18. HYAFF-11; HYAFF-11-S
19. Sodium alginate
20. Methacrylated form of hyaluronan (HA-MA) (hydrogel, cylindrical) [Photocross-linking]
21. Collagen type I (Cellagen™) commercial
22. Self-assembling collagen type I
23. Alginate; agarose; gelatin; fibrin
24. Agarose; alginate; gelatin
25. B-TCP
26. Cartilage ECM
27. Hyaluronic acid methacrylated
28. Bacterial cellulose; collagen type II; alginate
29. Hyaluronan
30. Self-assembled (collagen type II-coated; aggrecan-coated); ~agarose
31. Collagen I; II; III
32. Pellet; ~atelocollagen
33. Fibrinogen
34. Hyaluronic acid;{atelocollagen}
35. Hyaluronic acid (HA) hydrogels (2 wt% 1100 kDa, 2 wt% 350 kDa, 5 wt% 350 kDa, 2 wt% 50 kDa, 5 wt% 50 kDa, 10 wt% 50 kDa; 20 wt% 50 kDa)
36. Pellet; ~collagen
37. Macroporous gelatin-coated microcarrier beads CultiSpher
38. Gelatin (photopolymerisable styrenated gelatin)
39. Alginate beads; agarose
40. CaReS (rat-tail collagen type I); atelocollagen (bovine collagen type I); dermal regeneration template (bovine collagen type I); Chondro-Gide (bovine collagen type I/III); atelocollagen honeycomb small (bovine collagen type I); atelocollagen honeycomb large (bovine collagen type I)
41. Human amniotic membrane (epithelial side of intact HAM (IHE), basement side of denuded HAM (DHB) and stromal side of denuded HAM (DHS))
42. Collagen type I (Resorba®) commercial
43. Collagen
44. ECM (cell-derived)
45. Pellets vitro and vivo; ~alginate gel vivo
46. Micromass; collagen honeycomb
47. Osteochondral cores (cylindrical) [NS]
48. Collagen I (Antema®) commercial
49. Pellet → engineered ECM
50. Collagen type II
51. Alginate hydrogel; agarose hydrogel
52. Hyaluronan biomaterial (HYAFF-11, Fidia) {cylinder} [NS]
53. Alginate bead → coralline hydroxyapatite
54. Hyaluronic acid {hydrogels}
55. Decellularised (cartilage ECM)
56. Collagen I (Helistat®) commercial
57. Chitosan + Arg-Gly-Asp (RGD); chitosan + epidermal growth factor (EGF)
58. Coral
59. Whole blood, agarose
60. Cell sheet → cell plate in culture insert; ~atelocollagen honeycomb-shaped
61. Chitin (di-butyryl-chitin)
62. Alginate beads → calcium phosphate Calcibon®
63. Cellulose
64. Gellan gum
65. Hyaluronic acid HA (0.5, 1 and 2 g)
66. Aragonite matrix
67. Layered agarose hydrogel

(continued)

(A) Natural biomaterials
68. Chondron ECM
69. Cross-linked methacrylated hyaluronic acid hydrogels (MeHA);{agarose}
70. HA; agarose {gel}
71. Collagen II (recombinant human)
72. Calcium alginate
73. Gelatin, chitosan (cylindrical) [NS]
74. Gellan um;{agarose}
75. Alginate (hydrogel) [NS]; demineralised bone matrix (NS) [3D printing]
76. Atelocollagen
77. Hyaluronic acid (nonwoven mesh) [NS]
78. Decellularised (osteochondral graft)
79. Demineralised joint condyle
80. Alginate beads; ~hydroxyapatite (HA) carrier
81. Collagen type I (CaRes®)
82. Collagen I (CaReS®)
83. Hydroxyapatite, chitin, chitosan (NS) [NS]
84. Collagen type I (Arthro Kinetics Biotechnology)
85. Collagen (Chondro-Gide®)
86. Pellet; cross-linkable hyaluronan hydrogel
87. Decellularised osteochondral explant
88. Gelatin; chitosan
89. Silk fibroin;{hyaluronic acid (HYAFF®-11)}
90. Fibrin glue hydrogel; platelet-rich fibrin glue hydrogel; fibrin glue hydrogel containing heparin-binding delivery system; platelet-rich fibrin glue hydrogel containing heparin-binding delivery system
91. Nonbiomedical and biomedical grade alginates
92. Collagen I (Porcogen™)
93. Sodium alginate (Sea Matrix®)
94. Methacrylated glycol chitosan
95. Collagen type I, collagen type III (disc) [NS]
96. Self-assembled; fibrin
97. Collagen I (Ultrafoam®) commercial
98. Pellet culture; agarose
99. Hyaluronic acid (HA) hydrogel; agarose hydrogel
100. Hyaluronic acid methacrylated; agarose
101. κ-Carrageenan
102. "Hydrogel: (1) soluble rat-tail type I collagen (0.2% w/v) (BD Biosciences, San Jose, CA, USA); (2) type I collagen (0.2%) incorporating transglutaminase (TG)-2 (100 lgml–1) (Sigma); (3) type I collagen (0.2%) incorporating microbial transglutaminase (mTG; 100 lg ml–1) (Ajinomoto Food Ingredients LLC, Chicago, IL); (4) type I collagen (0.2%) incorporating genipin (GP, 0.25 mM) (Wako, Richmond, VA, USA); (5) type I collagen (0.2%) incorporating GP (0.25 mM) and control agarose beads (without heparin) (Sigma); and (6) type I collagen (0.2%) incorporating GP (0.25 mM) and heparin-agarose type I beads (10% weight of heparin/ weight of collagen) (Sigma)

(A) Natural biomaterials
103. Sponge-like scaffolds were prepared: (1) porcine type I/III collagen (CI) (0.5% w/v) (Geistlich Biomaterials, Wolhusen, Switzerland); (2) CI (0.5%) additionally supplemented with CS (7% w/w relative to CI) (Sigma Chemical Co., St Louis, MO, USA); and (3) CI (0.5%) additionally supplemented with HS (7% w/w relative to CI) (Sigma)"
104. Cell pellet – collagen type II nanoarchitectured molecules; collagen fibrils (CNFs); collagen spheres (CNPs)
105. Gelatin; chitosan; agarose
106. Decellularised (dermal ECM)
107. Hyaluronic acid (HYAFF®-11); collagen (Bio-Gide®) commercial
108. Self-assembled (agarose mould) → collagen cross-linking via lysyl oxidase (timing)
109. Collagen type I (PureCol®) commercial
110. Bacterial cellulose
111. Pellet culture (aggregate);~micromass (self-assembled) in plate; ~collagen II
112. Devitalised cartilage explant
113. Alginate (beads) [NS]; cell pellet (NS) [NS]; collagen, chitosan (NS) [NS]
114. Alginate bead → scaffold free on b-tricalcium phosphate carriers []
115. Fibrin hydrogel in agarose well; agarose well only
116. Osteochondral cores, agarose (disc) [NS]
117. Extracellular matrix (ECM) by ASCs; ECM by synovium-derived stem cells (SDSCs). The cell in pellet condition
118. TCP
119. Glycerol phosphate
120. Decalcified bone matrix
121. Hyaluronic acid hydrogel
122. Recombinant human collagen type II (Fibrinogen Europe, Helsinki, Finland)
123. PRP
124. Micromass; pellet culture model; vivo~fibrin gel
125. Injectable hydroxypropylmethylcellulose (HPMC) hydrogel
126. Hyaluronic acid methacrylate (HA-MA), chondroitin sulphate methacrylate (CS-MA); (hydrogel) [NS]
127. Collagen type I, collagen type III (NS) [NS]
128. Sulphated alginate
129. Agarose; plasma; whole blood
130. Photocross-linkable gelatin-methacrylamide (Gel-MA); varying concentrations (0–2%) of hyaluronic acid methacrylate (HA-MA)
131. Human acellular cartilage matrix powders
132. Self-assembled (polyethylene terephthalate (PET)-coated); agarose hydrogel encapsulation
133. Methacrylated gelatin

(continued)

(A) Natural biomaterials
134. ECM (MSC-derived)
135. Demineralised bone matrix
136. Hybrid organic-inorganic (HOI) material photopolymer ORMOSIL SZ2080; ∗collagen type I membrane
137. Decellularised (meniscus ECM)
138. Alginate; chitosan; fibrin
139. Heparin-conjugated fibrin (gel) [NS]
140. Microcavitary alginate hydrogel (microsphere)
141. Chondroitin sulphate methacrylate
142. Micromass cell pellets; alginate hydrogels
143. 45S5 Bioglass®
144. Graphene oxide (NS) [NS]
145. Amniotic membrane
146. Hyaluronic acid (NS) [NS]
147. Collagen type I, collagen type II, hydroxyapatite (cylindrical) [NS]
148. Porcine articular cartilage extracellular matrix (ACECM) (disc) [directional crystallisation and freeze-drying]
149. Cartilage ECM powder
150. Self-assembled; ~alginate
151. Pellet; ECM hydrogel
152. RGD-immobilised microcavitary alginate hydrogels; microcavitary alginate hydrogel
153. Gelatin methacryloyl
154. Gelatin methacrylamide (GelMA), hyaluronic acid methacrylate (HAMA), alginate (ALG), hydroxyapatite paste (HAP) (hydrogel) [3D printing]
155. Chitosan; alginate; collagen I
156. Demineralised cancellous bone
157. Human dermal fibroblast-derived ECM (hECM)
158. Decellularised (cartilage ECM) and methacrylated; methacrylated gelatin
159. Calcium-cobalt alginate
160. Devitalised cartilage
161. Transglutaminase-cross-linked hyaluronan hydrogels (HA-TG); alginate
162. Pellet; alginate bead; {monolayer}
163. ECM
164. Alginate; agarose
165. Decellularised (bone matrix) and demineralised
166. Gelatin methacrylamide; polyacrylamide
167. Pellets; agarose
168. Monomeric type I and type II collagen
169. Sodium alginate, collagen type I, collagen type II, chondroitin sulphate (hydrogel) [NS]

(B) Synthetic biomaterials
1. 2-Hydroxyethyl methacrylate-L-lactate–dextran (HEMA–LLA–D)
2. B-TCP
3. Calcium carbonate (Calcibon®)
4. Calcium polyphosphate
5. Cell pellet; ~PLGA
6. Collagen-like proteins
7. Compact polyelectrolyte complexes (CoPECs)
8. Elastin-like polypeptide (ELP)
9. Hyaluronan benzyl ester (disc) [NS]
10. Injectable PLGA microsphere
11. Macromers of PEG-caprolactone (PEG-CAP) endcapped with norbornene (PEG-CAP-NOR)
12. Nonporous microcarriers poly(lactic-co-glycolic acid) (PLGA); porous PLGA; amine-functionalised PLGA-NH2
13. Nonwoven PGA fibres
14. Nonwoven polyethylene terephthalate fibre
15. NS polycarbonate membrane
16. Oligo(trimethylene carbonate)-poly(ethylene glycol)-oligo (trimethylene carbonate) diacrylate (TPT-DA)
17. OPF
18. PBT
19. PCL
20. PEG
21. PEG hydrogel; PLGA microfibers
22. PEGDA
23. PEGDM
24. PEG–oligo(lactic acid) dimethacrylate PEG–LA-DM
25. Peptide-modified PEGDA (hydrogel) [NS]
26. PGA
27. PGA; PLGA (disc) [NS]
28. PGA; PLLA; PDLLA; PLGA; PCL
29. PGA-PLA (Ethisorb 210); poly-L-lactic acid
30. PGLA (polyglycollic-co-lactic acid)
31. PHBV (3-hydroxybutrate-co-3-hydroxyvalerate)
32. PLA
33. PLA (OPLA®)
34. PLA; PGA; PLGA
35. PLAG
36. PLCL
37. PLG
38. PLGA
39. PLGA, poly(ethy1ene oxide)-dimethacrylate, poly(ethy-1-ene glycol) (NS) [double emulsion]

(continued)

(B) Synthetic biomaterials
40. PLGA; polydioxanone (PDO)
41. PLGA-fleece (darts) [NS]
42. PLLA
43. PLLA (NS) [electrospinning]
44. PLLA (RESOMERL207S)
45. PLLA; PLGA(L); PLGA(H); PLA/CL; PDLA
46. PLLA; PGA; PLGA; PLAO3
47. Poly(1,8-octanediol citrate)
48. Poly(2-acrylamido-2-methyl-1-propanesulfonic acid (NaAMPS)-co-N,N-dimethylacrylamide(DMAAm))
49. Poly(2-hydroxyethyl methacrylate)
50. Poly(3-hydroxybutyrate-co-3-hydroxyhexanoate) (PHBHHx)
51. Poly(3-hydroxybutyrate-co-4-hydroxybutyrate) (P3HB4HB)
52. Poly(ethyl acrylate-co-hydroxyethyl acrylate) [P(EA-co-HEA)]
53. Poly(ethylene oxide) dimethacrylate (PEODM)
54. Poly(ethylene terephthalate) (PET)
55. Poly(glycerol sebacate) (PGS)
56. Poly(hydroxybutyrate-co-hydroxyvalerate) (PHBV)
57. Poly(lactic-glycolic acid) (PLGA)
58. Poly(L-lactide-co-e-caprolactone) (PLCL) (NS) [supercritical fluid foaming; solvent-casting and salt leaching method]
59. Poly(L-lactide-co-e-caprolactone) (PLCL) {sponge} [supercritical fluid foaming; solvent-casting and salt leaching method]
60. Poly(L-lactide-co-e-caprolactone) (PLCL); articular cartilage explant (control)
61. Poly(N-isopropylacrylamide)-g-methylcellulose (PNIPAAm-g-MC) thermoreversible hydrogel
62. Poly(N-isopropylacrylamide-co-acrylic acid) (p(NiPAAm-co-AAc)) (hydrogel) [NS]
63. Poly(N-isopropylacryl-amide-co-acrylic acid) thermoreversible gel
64. Poly(propylene fumarate-co-ethylene glycol) [P(PF-co-EG)]; {agarose}; {alginate}
65. Poly(urethane urea) Artelon®
66. Poly(γ-benzyl-L-glutamate) (PBLG)
67. Poly(ε-caprolactone) (PCL) nanofibrous electrospinning
68. Poly3-hydroxybutyrate4-hydroxybutyrate (P34HB)
69. Polycaprolactone; poly(L-lactide); poly(lactic-co-glycolic acid); polyurethane
70. Polydimethylsiloxane (PDMS)

(B) Synthetic biomaterials
71. Polydimethylsiloxane (PDMS) concave microwells
72. Polyester poly(3-hydroxybutyrate) (PHB) film
73. Polyethylene glycol diacrylate
74. Polyglycolic acid (PGA)
75. Polyglycolic acid (PGA); cartilage explant
76. Polyglycolic acid (PGA); poly(glycolic acid-e-caprolactone) (PGCL); poly(l-lactic acid-glycolic acid) (PLGA), poly(l-lactic acid-e-caprolactone;75:25 (w/w)) [P(LA-CL)25]; poly-e-caprolactone (tetrabutoxy titanium) [PCL(Ti)]; fullerene C-60 dimalonic acid (DMA)
77. PolyHIPE polymer (PHP)
78. Polyhydroxyalkanoate (PHA) = poly[(R)-3-hydroxybutyrate-co-(R)-3-hydroxy-10-38 undecenoate] (PHBU)
79. Poly-L,D-lactic acid (PLDLA)
80. Polylactic acid (PLA); Acrylonitrile butadiene styrene (ABS) (NS) [3D printing]
81. Polylactic acid poly-e-caprolactone (PLCL)
82. Polylactic acid-polyglycolic acid (PLGA)
83. Polylactic glycolic acid (PLGA)
84. Polylactic glycolic acid (PLGA)
85. "Polylactic glycolic
86. acid (3D-PLGA) (NS) [NS]"
87. Polylactide-polyglycolic acid (PLGA)
88. Polylactide-co-glycolide (PLGA) 85:15 microspheres/biodegradable hydrogel
89. Poly-L-lactic acid (PLLA)
90. Poly-L-lactic acid (PLLA) microsphere; poly-L-lactic acid (PLLA) microsphere + tripeptide Arg-Gly-Asp
91. Polymer solutions of poly(ethylene) oxide diacrylate
92. Polyurethane
93. Polyurethane (PU); poly(L/DL-lactide) (PLA)-control
94. Polyurethane/poly(L-lactide-co-D, llactide) (PU/PLDL) [6:4; 5:5; 8:2]
95. Poly-ε-caprolactone (NS) [electrospinning]
96. PuraMatrix (hydrogel) [NS]
97. PVA
98. Recombinant streptococcal collagen-like 2 (Scl2) protein with heparin-binding, integrin-binding and hyaluronic acid-binding peptide sequences (HIHA) [nonviral bacteria]. ScrMMP7-HIHA-Scl2, MMP7-HIHAScl2, MMP7:ACAN(75:25)-HIHA-Scl2, MMP7:ACAN(50:50)-HIHAScl2, MMP7:ACAN(25:75)-HIHA-Scl2 and ACAN-HIHA-Scl2 hydrogels.

(continued)

(B) Synthetic biomaterials
99. Self-assembling peptide (KLD) AcN-(KLDL)3-CNH2
100. Self-assembling peptide (KLD); cartilage explants
101. Self-assembling peptide (KLDL)
102. Self-assembling peptide (RADA)4
103. Self-assembling peptide AcN–(KLDL)3–CNH2 hydrogels;{agarose}
104. Self-assembly aggrecan (0.6% w/w), aggrecan–HA (0.6% w/w) and HA (1% w/w) solutions; ~type II collagen/aggrecan; ~PVA hydrogel
105. Silanised hydroxypropyl methylcellulose (Si-HPMC) hydrogel [E4M®]
106. Silated hydroxypropyl methylcellulose (hydrogel) [NS]
107. Silk; collagen; gelatin
108. Silk-elastin-like-protein polymer SELP-47 K
109. Sodium cellulose sulphate; polydiallyl dimethyl ammonium chloride (NS) [NS]
110. Tantalum
111. Tetramethacrylate prepolymer
112. Thermoreversible gelation polymer [poly(N-isopropylacrylamide-co-n-butyl methacrylate) (poly(NIPAAm-co-BMA))]
113. Titanium

References

1. WHO (2018) The WHO register. https://www.who.int/news-room/fact-sheets/detail/ageing-and-health. Accessed 11 Dec 2019
2. Benders KE, Terpstra ML, Levato R et al (2019) Fabrication of decellularized cartilage-derived matrix scaffolds. JoVE 143:e58656
3. Hazwani A, Sha'Ban M, Azhim A (2019) Characterization and in vivo study of decellularized aortic scaffolds using closed sonication system. Organogenesis 15(4):120–136
4. Wiggenhauser PS, Schwarz S, Koerber L et al (2019) Addition of decellularized extracellular matrix of porcine nasal cartilage improves cartilage regenerative capacities of PCL-based scaffolds in vitro. J Mater Sci Mater Med 30(11):121
5. Yusof F, Sha'ban M, Azhim A (2019) Development of decellularized meniscus using closed sonication treatment system: potential scaffolds for orthopedics tissue engineering applications. Int Nanomed 14:5491–5502
6. Ahmad M, Manzoor K, Ikram S (2019) Chitosan nanocomposites for bone and cartilage regeneration. In: Jamia MI (ed) Applications of nanocomposite materials in dentistry. Woodhead Publishing, New Delhi, pp 307–317
7. Izzo D, Palazzo B, Scalera F et al (2019) Chitosan scaffolds for cartilage regeneration: influence of different ionic crosslinkers on biomaterial properties. Int J Polym Mater Polym Biomater 68(15):936–945
8. Roffi A, Kon E, Perdisa F (2019) A composite chitosan-reinforced scaffold fails to provide osteochondral regeneration. Int J Mol Sci 20(9):2227
9. Wang K, Li J, Li Z et al (2019) Chondrogenic progenitor cells exhibit superiority over mesenchymal stem cells and chondrocytes in platelet-rich plasma scaffold-based cartilage regeneration. Am J Sports Med 47(9):2200–2215
10. Chen K, Li X, Li N et al (2019) Spontaneously formed spheroids from mouse compact bone-derived cells retain highly potent stem cells with enhanced differentiation capability. Stem Cells 2019:1–13
11. Chen W, Xu Y, Liu Y, Wang Z et al (2019) Three-dimensional printed electrospun fiber-based scaffold for cartilage regeneration. Mater Des 179:1–13
12. Li J, Chen G, Xu X et al (2019a) Advances of injectable hydrogel-based scaffolds for cartilage regeneration. Regen Biomater 6(3):129–140
13. Rogan H, Ilagan F, Yang F (2019) Comparing single cell versus pellet encapsulation of mesenchymal stem cells in three-dimensional hydrogels for cartilage regeneration. Tissue Eng Part A 25:1–27
14. De Pascale C, Marcello E, Getting SJ et al (2019) Populated collagen hydrogel and polyhydroxyalkanoate composites: novel matrices for cartilage repair and regeneration? Osteoarthr Cartil 27:S432–S433
15. Baena JM, Jiménez G, López-Ruiz E, Antich C et al (2019) Volume-by-volume bioprinting of chondrocytes-alginate bioinks in high-temperature thermoplastic scaffolds for cartilage regeneration. Exp Biol Med 244(1):13–21
16. Farokhi M, Jonidi Shariatzadeh F, Solouk A (2019) Alginate based scaffolds for cartilage tissue engineering: a review. Int J Polym Mater Polym Biomater 69:1–18
17. Farokhi M, Mottaghitalab F, Fatahi Y et al (2019) Silk fibroin scaffolds for common cartilage injuries: possibilities for future clinical applications. Eur Polym J 115:251–267
18. Lin H, Beck AM, Shimomura K (2019) Optimization of photocrosslinked gelatin/hyaluronic acid hybrid scaffold for the repair of cartilage defect. J Tissue Eng Regen Med 2019:1–12
19. Li J, Yao Q, Xu Y (2019b) Lithium chloride-releasing 3D printed scaffold for enhanced cartilage regeneration. Med Sci Monit 25:4041
20. Park IS, Jin RL, Oh HJ et al (2019) Sizable scaffold-free tissue-engineered articular cartilage construct for cartilage defect repair. Artif Organs 43(3):278–287
21. Sivadas VP, Dhawan S, Babu J (2019) Glutamic acid-based dendritic peptides for scaffold-free cartilage tissue engineering. Acta Biomater 99:196–210
22. De Moor L, Beyls E, Declercq H (2019) Scaffold free microtissue formation for enhanced cartilage repair. Ann Biomed Eng 48:1–14
23. Aguilar IN, Olivos DJ III, Brinker A et al (2019) Scaffold-free bioprinting of mesenchymal stem cells

using the Regenova printer: spheroid characterization and osteogenic differentiation. Bioprinting 15:e00050
24. Breathwaite EK, Weaver JR, Murchison AC et al (2019) Scaffold-free bioprinted osteogenic and chondrogenic systems to model osteochondral physiology. Biomed Mater 14(6):065010
25. Lu Y, Zhang W, Wang J et al (2019) Recent advances in cell sheet technology for bone and cartilage regeneration: from preparation to application. Int J Oral Sci 11(2):1–13
26. Martini FH, Nath JL, Bartholomew EF (2018) Fundamentals of anatomy & physiology, 11th edn. Pearson Education, Inc, New York
27. Tortora GJ, Derrickson B (2017) Principles of human anatomy & physiology, 15th edn. Wiley, Milton
28. Saladin KS, Gan CA, Cushman HN (2018) Anatomy & physiology: the unity of form and function, 8th edn. McGraw-Hill Education, New York
29. Shier D, Butler J, Lewis R (2016) Hole's human anatomy & physiology, 14th edn. McGraw-Hill Education, New York
30. Muriel R, Birgit R, William MK (2019) Cellular senescence in development, regeneration and disease. Development 146:dev151837
31. Myohara M (2004) Differential tissue development during embryogenesis and regeneration in an annelid. Dev Dyn 231:349–358
32. Kuhn LT, Liu Y, Boyd NL et al (2014) Developmental-like bone regeneration by human embryonic stem cell-derived mesenchymal cells. Tissue Eng Part A 20(1–2):365–377
33. Tetsuya E, Susan VB, David M (2004) A stepwise model system for limb regeneration. Dev Biol 270(1):135–145
34. Angela YC, Vegard FS, Stefanos T et al (2019) Measuring population ageing: an analysis of the global burden of disease study 2017. Lancet Public Health 4(3):e159–e167
35. Theo V, Abraham DF, Mohsen N et al (2012) Years lived with disability (YLDs) for 1160 sequelae of 289 diseases and injuries 1990–2010: a systematic analysis for the global burden of disease study 2010. Lancet 380(9859):2163–2196
36. Malaysia health technology assessment section (MaHTAS) (2013) Quick reference (QR): management of osteoarthritis, 2nd edn. Ministry of Health (MOH), Malaysia
37. Malaysia Health Technology Assessment Section (MaHTAS) (2013) Clinical practice guidelines (CPG): management of osteoarthritis, 2nd edn. Ministry of Health (MOH), Malaysia
38. Francis SL, Di Bella C, Wallace GG (2018) Cartilage tissue engineering using stem cells and bioprinting technology–barriers to clinical translation. Front Surg 5:70
39. Xue K, Zhang X, Gao Z (2019) Cartilage progenitor cells combined with PHBV in cartilage tissue engineering. J Transl Med 17(1):104
40. Catacchio I, Berardi S, Reale A et al (2013) Evidence for bone marrow adult stem cell plasticity. In: Prancla R(ed) properties, molecular mechanisms, negative aspects, and clinical applications of hematopoietic and mesenchymal stem cells transdifferentiation. Stem Cells Int 2013:1–11
41. Md Nazir N, Zulkifly AH, Khalid KA et al (2019) Matrix production in chondrocytes transfected with sex determining region Y-box 9 and telomerase reverse transcriptase genes: an in vitro evaluation from monolayer culture to three-dimensional culture. Tissue Eng Regen Med 16:285
42. Tahir AH, Azhim A, Sha'ban M et al (2017) Chondrocytes-induced SOX5/6/9 and TERT genes for articular cartilage tissue engineering: HYPE or Hope? Trans Persatuan Genetik Malaysia 7:151–160
43. Ahmad R, Muhammad A, Abdulahi H et al (2017) The application of gene transfer technology in articular cartilage tissue engineering: an insight. TPGM 7:211–216
44. Mohamed Amin MAI, Azhim A, Mohamed Sideek MA et al (2017) Current trends in gene-enhanced tissue engineering for articular cartilage regeneration in the animal model. Trans Persatuan Genetik Malaysia (TPGM) 7:201–210
45. Munirah S, Zainul Ibrahim Z, Rozlin AR et al (2014) Exploring the islamic perspective on tissue engineering principles and practice. Comm Publ Ethics 4(2):29–40
46. Nazir NM, Sha'ban M (2018) Overview of safety and efficacy of non-viral gene transfer in cartilage tissue engineering from the worldview of Islam. Int Med J Malaysia 17:115–123
47. Willerth SM, Sakiyama-Elbert SE (2008) Combining stem cells and biomaterial scaffolds for constructing tissues and cell delivery. StemBook, Washington University
48. Tahir AHMA, Amin MAIM, Azhim A (2018) Evaluation of cartilaginous extracellular matrix production in in vitro "cell-scaffold" construct. In: 2018 IEEE-EMBS Conference on Biomedical Engineering and Sciences (IECBES), pp 500–504
49. Munirah S, Samsudin OC, Chen HC et al (2007) Articular cartilage restoration in load-bearing osteochondral defects by autologous chondrocytes-fibrin constructs implantation: an experimental study in sheep. J Bone Joint Surg (Br) 89B:1099–1109
50. Hazwani A, Sha'ban M, Azhim A (2017) Inflammatory response of bioscaffolds decellularized by sonication treatment. In: International conference for innovation in biomedical engineering and life sciences 2017, pp 183–185
51. Mohamed Amin MAI, Tahir AHMA, Azhim A et al (2018) Physical properties and biocompatibility of 3D hybrid PLGA based scaffolds. In: 2018 IEEE-EMBS Conference on Biomedical Engineering and Sciences (IECBES), pp 480–484
52. Martín-Martín A, Orduna-Malea E, Thelwall M et al (2018) Google scholar, web of science, and scopus: a systematic comparison of citations in 252 subject categories. J Informet 12(4):1160–1177

53. Ovsianikov A, Khademhosseini A, Mironov V (2018) The synergy of scaffold-based and scaffold-free tissue engineering strategies. Trends Biotechnol 36(4):348–357
54. He D, Zhao AS, Su H et al (2019) An injectable scaffold based on temperature-responsive hydrogel and factor-loaded nanoparticles for application in vascularization in tissue engineering. J Biomed Mater Res A 107(A):2123–2134
55. Kelly DC, Raftery RM, Curtin CM et al (2019) Scaffold-based delivery of nucleic acid therapeutics for enhanced bone and cartilage repair. J Orthop Res 37:1671–1680
56. Wen YT, Dai NT, Hsu SH (2019) Biodegradable water-based polyurethane scaffolds with a sequential release function for cell-free cartilage tissue engineering. Acta Biomater 88:301–313
57. Kobayashi J, Kikuchi A, Aoyagi T (2019) Cell sheet tissue engineering: cell sheet preparation, harvesting/manipulation, and transplantation. J Biomed Mater Res A 107(5):955–967
58. Takahashi H, Okano T (2015) Cell sheet-based tissue engineering for organizing anisotropic TEMPs produced using microfabricated thermoresponsive substrates. Adv Healthc Mater 4(16):2388–2407
59. Antunes J, Gaspar VM, Ferreira L et al (2019) In-air production of 3D co-culture tumor spheroid hydrogels for expedited drug screening. Acta Biomater 94:392–409
60. Akkouch A, Yu Y, Ozbolat IT (2015) Microfabrication of scaffold-free tissue strands for three-dimensional tissue engineering. Biofabrication 7(3):031002
61. Yu Y, Moncal KK, Li J et al (2016) Three-dimensional bioprinting using self-assembling scalable scaffold-free "tissue strands" as a new bioink. Sci Rep 6(1):28714
62. Yamato M, Okano T (2004) Cell sheet engineering. Mater Today 7(5):42–47

8 Bio-application of Inorganic Nanomaterials in Tissue Engineering

Sung-Won Kim, Gwang-Bum Im, Yu-Jin Kim, Yeong Hwan Kim, Tae-Jin Lee, and Suk Ho Bhang

Abstract

Inorganic nanomaterials or nanoparticles (INPs) have drawn high attention for their usage in the biomedical field. In addition to the facile synthetic and modifiable property of INPs, INPs have various unique properties that originate from the components of the INPs, such as metal ions that are essential for the human body. Apart from their roles as components of the human body, inorganic materials have unique properties, such as magnetic, antibacterial, and piezoelectric, so that INPs have been widely used as either carriers or inducers. However, most of the bio-applicable INPs, especially those consisting of metal, can cause cytotoxicity. Therefore, INPs require modification to alleviate the harmful effect toward the cells by controlling the release of metal ions from INPs. Even though many attempts have been made to modify INPs, many things, including the side effects of INPs, still remain as obstacles in the bio-application, which need to be elucidated. In this chapter, we introduce novel INPs in terms of their synthetic method and bio-application in tissue engineering.

S.-W. Kim · G.-B. Im · Y.-J. Kim · Y. H. Kim · T.-J. Lee · S. H. Bhang (✉)
School of Chemical Engineering, Sungkyunkwan University, Suwon, Gyeonggi, Republic of Korea
e-mail: sukhobhang@skku.edu

Keywords

Biocompatibility · Cancer therapy · Controlled release · Cytotoxicity · Differentiation · INPs · Metal ions · Stem cells · Synthesis · Tissue regeneration

8.1 Introduction

Nanoparticles (NPs) have been widely used in medical treatment and biomedical research [1–3]. Since NPs have high surface area to volume ratio, which meets the dimension of biological compounds, nanoscale materials can easily interact with their biological surroundings [4]. For example, NPs can stimulate cellular pathway by binding ligands on the surface of the cells. NPs are also able to penetrate the cell membrane by either active or passive transport, resulting in the change of cellular activity. Therefore, researchers have developed various NPs to improve therapeutic efficacy by controlling the shape, size, and components of the NPs [5, 6]. Among the various NPs, inorganic nanoparticles (INPs) have drawn high attention for their unique property. INPs are normally synthesized by inorganic salt crystallization forming atoms' binding. Based on metallic and covalent bindings, which are major bindings in INPs, INPs can have high rigidity and order. Therefore, it is relatively easy to modify

H. J. Chun et al. (eds.), *Bioinspired Biomaterials*, Advances in Experimental Medicine and Biology 1249, https://doi.org/10.1007/978-981-15-3258-0_8

and synthesize uniform INPs to achieve the duties of biomedical application [7, 8]. For example, INPs can be used for drug delivery systems (DDS), antibody labeling, bio-imaging, and tissue regeneration [9–12]. Among the applicable INPs, gold nanoparticles (AuNPs) and magnetic nanoparticles (MNPs) are normally used as carriers for drug and gene delivery. Brust et al. discovered a simple step to synthesize colloidal AuNPs [13], and numerous studies to develop AuNPs have been conducted [14–16]. With the introduction of synthetic technology to exchange ligands on the surface of AuNPs, it is possible to detect target areas with the active targeting property of AuNPs [16]. AuNPs also have advantages of tunable size and surface modification that result in various effects on biomedical application [17, 18]. MNPs are also widely known candidates for DDS research, due to their magnetic responsiveness properties with biocompatibility and reactional functional groups on the surface of the MNPs [19, 20]. The MNPs are usually composited with materials such as metallic, ferrite, and magnetic element-doped ferrites. Widely used MNPs include iron oxide nanoparticles (IONPs) and superparamagnetic iron oxide nanoparticles, not only for their magnetic properties but also for their good biocompatibility, which is an important issue for bio-application. Under a magnetic field, MNP carriers can be delivered to the targeted area effectively, even under liquid biological environments [21, 22].

Apart from their roles as tools in DDS, INPs are used as the main factors for inducing tissue regeneration. As aforementioned, biocompatibility is a crucial issue for bio-application. Therefore, INPs consisting of biocompatible metal components have been chosen for the candidates. Since there are many receptors that can correlate with various metals on the cell surface, some metal ions, usually degraded from the INPs in the cell, were discovered to increase tissue regenerative efficacy by inducing cellular behavior change, such as cell differentiation by means of the stimulation of the ligand-receptor pathway [23]. Moreover, other unique properties of the INPs, such as antimicrobial ability and piezoelectricity, have also been discovered as factors to stimulate tissue regeneration [24, 25]. In this chapter, we introduce some novel INPs that mainly consist of metal derivatives that have been widely used in tissue engineering, with regard to their synthetic methods and therapeutic results.

8.2 INPs as Carriers

8.2.1 Gold

AuNPs are one of the most promising tools that can serve as great carriers for drug, gene, and even other bio-applicable materials [26–28]. One of the representative properties of AuNPs used for DDS is their stability, especially in pH responsiveness, as compared with other metal materials. Bhang et al. developed manganese-incorporated AuNPs (MnAuNPs), where they utilized AuNPs as nanocarriers for manganese [29]. The MnAuNPs were fabricated by reducing both Mn^{2+} and Au^{3+} with sodium borohydride ($NaBH_4$) in the presence of polyvinylpyrrolidone. As they treated pheochromocytoma 12 (PC12) cells with MnAuNPs, MnAuNPs could be delivered to the PC12 cells via endocytosis, followed by the release of Mn^{2+} ions into the endosome (Fig. 8.1a). Mn can relatively easy react with hydrogen, as compared with Au, due to its low standard reduction potential of −1.18 V, in contrast to that of Au of +0.7 V [30]. Therefore, Mn^{2+} can be released from the MnAuNPs while in the endosomes, which have low pH conditions. Controlled Mn^{2+} release allowed PC12 cells to have enhanced neuronal differentiative efficacy without cytotoxicity (Fig. 8.1b, c), because this system prohibits the overdose of Mn^{2+} release and ATP depletion in preventing active transport, which cause PC12 cells' apoptosis [31, 32]. In conclusion, Au in MnAuNPs served as carriers for the pH-triggered, intracellular delivery of Mn ions to stimulate neuronal differentiation of PC12 cells (Fig. 8.1d).

Tian et al. invented functionalized AuNPs as delivery carriers for cancer therapy by exploiting the properties of Au, which can retain its stability in acidic pH condition, including photothermal therapeutic efficacy [33]. In this study, gold nanostars (GNS) were incorporated into the pH

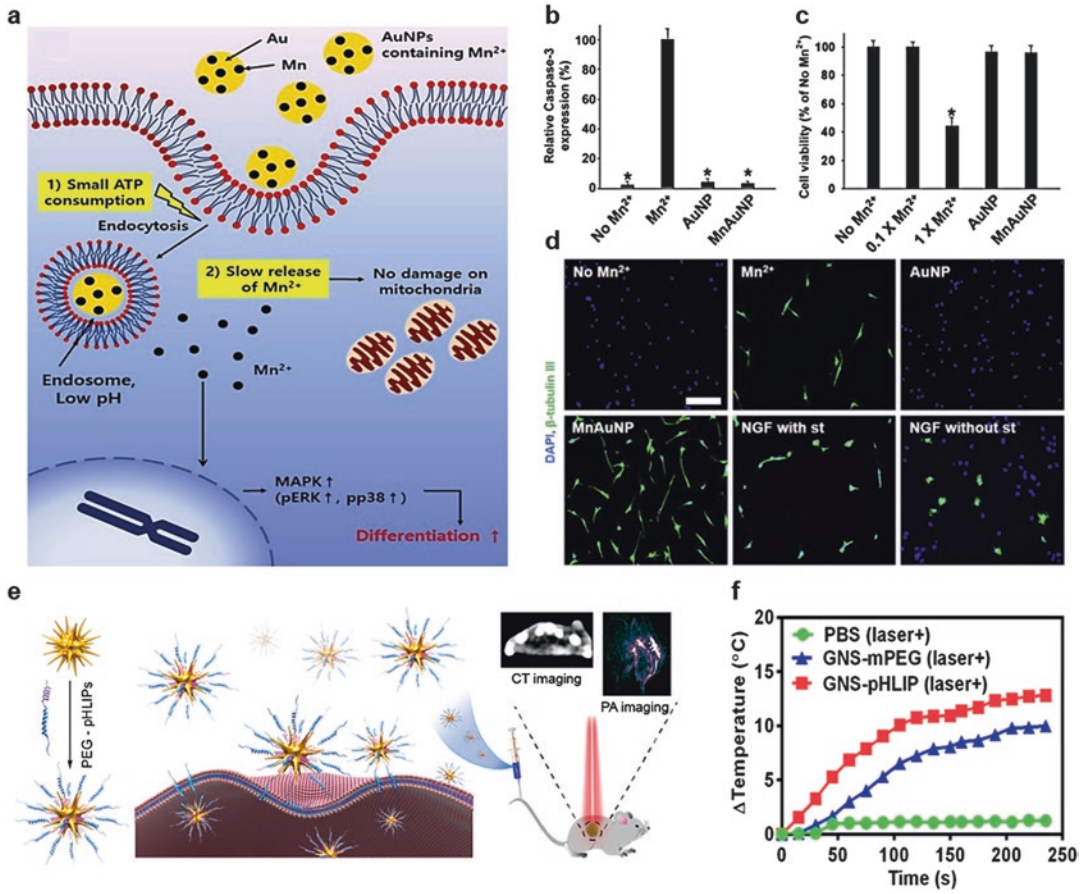

Fig. 8.1 Applications of novel modified AuNPs for bio-application. Schematics of (**a**) pH-triggered intracellular delivery of Mn^{2+} through MnAuNPs for the neuronal differentiation of PC12 cells. (**b**) Western blot analysis for caspase-3 protein expression, which is a representative apoptotic marker, and its quantification at 24 h ($n = 5$, $*p < 0.01$ versus Mn^{2+} group). (**c**) Neutral red assay for cell viability of PC12 cells at 24 h ($n = 5$, $*p < 0.01$ versus no-Mn^{2+} group). (**d**) Neuronal differentiation of PC12 cells evaluated by immunocytochemistry for β-tubulin III (green) and nucleus (blue). (Reprinted from Biomaterials, 55, Bhang et al., pH-triggered release of manganese from MnAu nanoparticles that enables cellular neuronal differentiation without cellular toxicity, 39, 2015, with permission from Elsevier). (**e**) Scheme of GNS-pHLIP for enhanced cancer therapy with CT and PA imaging. (**f**) The tumor temperature variance during the irradiation of laser in each group in vivo. (Reprinted with permission from Tian et al., ACS applied materials & interfaces, 9 (3) pp. 2114–2122)

(low) insertion peptides (pHLIPs) by mixing amine-PEG-thiol with maleimide-PEG2000-pHLIPs, followed by adding bare GNS solution (Fig. 8.1e). The fabricated product was named GNS-pHLIP. In acidic conditions, the pHLIPs are protonated to increase the hydrophobicity of the peptides that inserts the GNS-pHLIP into tumor cells [34, 35]. GNS are one of the contrast agents for computed tomography (CT) and photoacoustic (PA) imaging, in addition to their photothermal therapeutic effect [36]. Therefore when irradiated with NIR light, GNS-pHLIPs could effectively target and decrease the volume of MCF-7 breast tumor in vivo (Fig. 8.1f). Simultaneously, GNS-pHLIPs presented enhanced signals through CT and PA imaging. This study demonstrated that the GNS-pHLIPs can be used as dual platforms for cancer therapy, by targeting and imaging the tumor at the same time.

Au can easily incorporate with thiol-modified DNA using Au-thiol chemistry [16, 37]. Because of the stable and strong covalent bonding between

AuNPs and thiol-modified DNA, many efforts have been made to develop AuNPs as carriers for gene therapy [38–40]. AuNPs have also stimulated tremendous efforts due to their inherent surface plasmon resonance (SPR) effect [41, 42]. Aside from cancer-eliminating tools for the photothermal effect of AuNPs, their unique SPR bands have been utilized for gene-releasing platform in DDS. As the shape and size of AuNPs are changed, the SPR bands of AuNPs are also changed. For example, Au nanorods are known to enhance photothermal capability under NIR light irradiation by the shifting of SPR band toward the longer-wavelength light region [6]. Tian et al. used the GNS to allow SPR band to shift toward the NIR region for effective phototherapy [33]. Vankayla et al. also utilized GNS for in vivo fluorescence imaging with NIR light-activated photodynamic therapy [43]. Recently, Han et al. utilized these two unique properties of AuNPs, represented by Au-thiol chemistry and SPR band shift, for imaging and in vivo drug delivery [44]. The research group designed stabilized up-conversion nanoparticles based on the coupling of very tiny AuNPs (=2 nm) and thiol-modified hairpin DNA (hpDNA). By using coprecipitation process, $NaYF_4$ nanoparticles were co-doped with Yb^{3+} and Tm^{3+}. Thereafter, the research group coated $NaYF_4$:Yb/Tm nanoparticles with thin layer of silica, followed by attaching AuNPs to silica shell. The resultant $NaYF_4@SiO_2$-Au nanoparticles showed increased photothermal effect. Since AuNPs attached to up-conversion particles quenched up-conversion emission under NIR light, $NaYF_4@SiO_2$-Au showed the best photothermal efficacy among the other experimental groups. This is because the quenched light was mostly absorbed by AuNPs and that of the absorbed light energy was mostly released as heat. Since hpDNA has high thermal sensitivity and ability to encapsulate drug, the released heat stimulated the release of doxorubicin from $NaYF_4@SiO_2$-Au by means of photothermal effect. Furthermore, it was observed that the tumor size of tumor-bearing mice was significantly decreased, as compared with all three control experiments. Up-converted NIR emission was also detected from the tumor site.

Lei et al. invented a small interfering RNA (siRNA) of nerve growth factor (NGF)-incorporated gold nanoclusters, to increase the therapeutic efficacy of cancer therapy [45]. Aside from the effect of NGF inhibition for pancreatic cancer, the research group used gold nanocluster-shaped AuNPs to enhance the stability of NGF siRNA. First, the GNS was synthesized by one-step reduction of Au^{3+} (Fig. 8.2a). After that, the NGF siRNA was absorbed onto cationic GNC through electrostatic interaction (Fig. 8.2b). The resultant GNC-siRNA complex structure allowed siRNA to hide its negative charge in the spacer. The GNC-siRNA-treated group showed increased stability in serum nuclease and cellular uptake, compared to that of free siRNA. For therapeutic effect of cancer therapy, the GNC-siRNA downregulated the NGF expression in Panc-1 cells with about 75% downregulation of NGF mRNA expression, as compared to the no-treated group. The antitumor and gene knockdown effects were investigated in three different pancreatic models: subcutaneous model, orthotopic model, and patient-derived xenograft model. It was confirmed that weight and tumor size were also decreased in the GNC-siRNA complex-treated group (Fig. 8.2c, d). The gene knockdown effect was also discovered in three different pancreatic models by detecting NGF mRNA and protein expression.

8.2.2 Magnetic Materials

MNPs have emerged as a promising tool in biomedical fields that include gene delivery and biosensors [46–48]. Representatively, IONPs have been investigated for their magnetic targeting efficacy. Wu et al. illustrated natural killer (NK) cell-based anticancer treatment using the magnetic delivery of polydopamine (PDA)-capped iron oxide (Fe_3O_4) NPs [49]. They manufactured Fe_3O_4 NPs with thermal decomposition method, before sequentially capping with sodium dodecyl sulfate and dopamine monomer to fabricate PDA-capped Fe_3O_4 NPs. PDA shells have been commonly used to increase biocompatibility and biodegradability [50–52]. The NK cells were

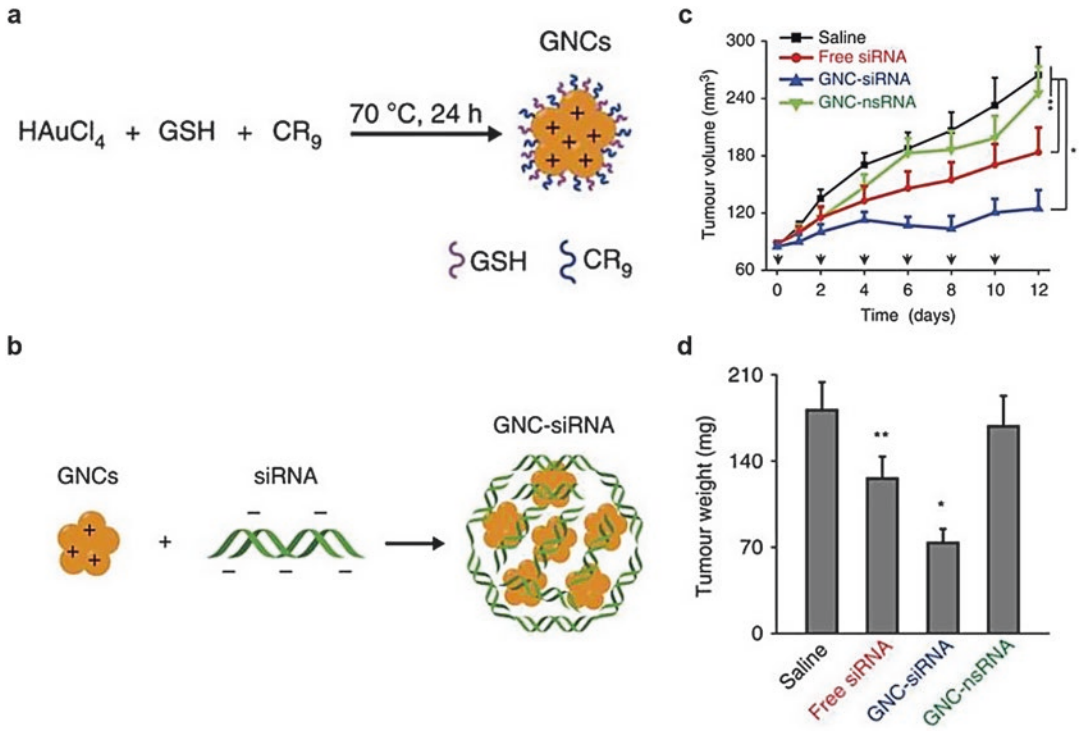

Fig. 8.2 Synthetic method of GNC-siRNA complex and its cancer therapeutic efficacy. (**a**) Scheme of the positively charged GNCs. (**b**) Scheme of the synthetic method of GNC-siRNA complex. Electrostatic interaction between cationic GNCs and negatively charged siRNA, which was condensed onto the GNCs. (**c**) Tumor growth curve during the GNC-siRNA treatments, where the black arrows indicate the injection time. (**d**) Tumor weight at the end of experiment. (This work is licensed under the Creative Commons Attribution 4.0 International License. To view a copy of this license, visit http://creativecommons.org/licenses/by/4.0/, or send a letter to Creative Commons, PO Box 1866, Mountain View, CA 94042, USA)

treated with PDA-capped Fe_3O_4 NPs, which had no significant effect on NK cells' viability and cytokine production, such as tumor necrosis factor alpha, and interferon gamma. PDA-capped Fe_3O_4 NP-loaded NK cells (NP-NK) showed high toxicity against A549 cancer cell under magnetic traction in vitro. Additionally, the researchers investigated increased accumulation of NP-NK in the tumor microenvironment and decreased tumor volume, after treatment with PDA-capped Fe_3O_4 NPs.

Magnetic hyperthermia generates heat in response to a magnetic field. The properties of MNPs vary with the size, structure, and composition, which were discovered to affect the characteristics of magnetic hyperthermia and heating efficacy [53]. Therefore, various MNPs have been investigated regarding cancer treatment [54–56]. Tsai et al. examined truncated octahedral IONPs that have a double layer of Au/Ag alloy for magnetic targeting with hyperthermia and photothermal cancer therapy [57]. In this study, IONPs were dispersed in oleic acid solution adding each of $AgNO_3$ and $HAuCl_4$ solution twice, to make shell-in-shell structure (Fig. 8.3a). They performed photothermal ablation of U87 cells, after treating with IONP@shell-in-shell NPs. Compared to U87 cells with only laser irradiation, most of the U87 cells died when treated with laser irradiation and magnetic attraction together. Similarly, in vivo test established with human-brain-tumor mouse model showed that the IONP@shell-in-shell NPs could penetrate the blood-brain barrier and were gathered at the tumor site. Therefore, IONP@shell-in-shell NPs

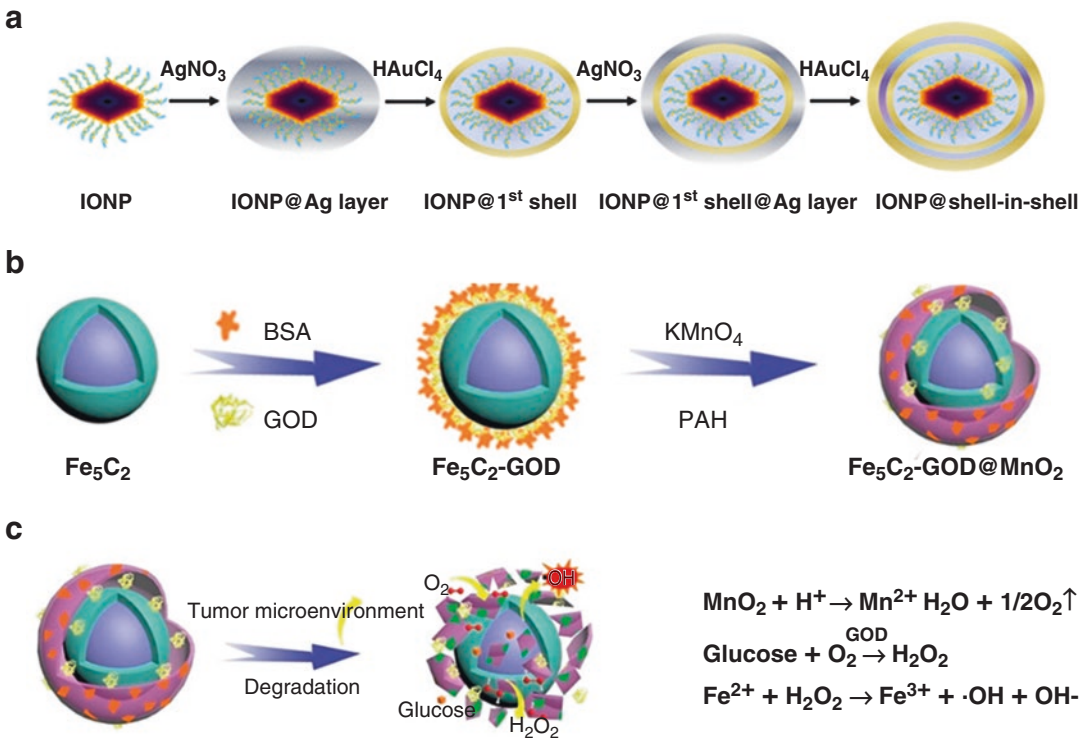

Fig. 8.3 Applications of various novel MNPs as carriers for DDS. (**a**) Schematic of preparation for the IONP@shell-in-shell complex. (Reprinted with permission from (Yun et al., ACS applied materials & interfaces, 18 (2), pp. 838–845.) Copyright (2018) American Chemical Society). (**b**) Scheme of synthetic procedure of Fe_5C_2-GOD@MnO_2 nanocatalysts. (**c**) Biodegradation behavior of Fe_5C_2-GOD@MnO_2 nanocatalysts and the mechanism of Fe_5C_2-GOD@MnO_2 generating hydroxyl radicals following the Fenton reaction. (Reprinted with permission from (Feng et al., ACS Nano, 12(11):11000–11012.) Copyright (2018) American Chemical Society). (**d**) Description of force that a Mag-Cell having ZnMNPs has to overcome, when moving toward the tissues with magnetic assistance. (**e**) Bioluminescence images of various material-treated cell migrations. (Mag-Cell-1 indicated neural stem cell (NSC) with 15 nm ZnMNPs, Mag-Cell-2 indicated NSC with 15 nm Fe_3O_4, and Mag-Cell-3 indicated NSC with Feridex.) (**f**) 60-fold more live magnetically targeted Mag-Cells-1 were delivered than non-targeted ones. (Reprinted with permission from (Yun et al., Nano Letters, 18 (2), pp. 838–845.) Copyright (2018) American Chemical Society). (**g**) Schematic illustrating the fabrication of magnetic nanospear arrays. Polystyrene (PS) nanospheres are first assembled on a silicon (Si) wafer, followed by size reduction via oxygen plasma etching. Dry etching is then applied to etch the Si and nanospheres simultaneously to generate Si nanospear arrays. Next, layers of nickel (Ni, 40 nm) and gold (Au, 10 nm) are evaporated on the Si nanospear arrays. Schemes of control of the nanospear mechanical motions using magnet, including orientation control in the (**h**) vertical and (**i**) horizontal plane. (Reprinted with permission from (Xu et al., ACS Nano, 12 (5), p. 4503–4511.) Copyright (2018) American Chemical Society)

had better photothermal inhibition of tumor growth, compared to other experimental groups.

When the Fe^{2+} ion of IONPs reacts with H_2O_2, highly reactive hydroxyl radicals (OH•) come out, which reaction is called the Fenton reaction [58]. Therefore, treatment of IONPs can generate intracellular hydroxyl radicals from the cells, which affect cell viability and function [59, 60]. Feng et al. combined the magnetic property of IONPs with the Fenton reaction for cancer therapy [61]. They designed manganese dioxide (MnO_2)-encapsulated and glucose oxidase (GOD)-loaded magnetic iron carbide (Fe_5C_2) core-shell structured nanoparticles (Fe_5C_2-GOD@MnO_2 NPs) to enhance tumor ablation. The Fe_5C_2-GOD@MnO_2 was fabricated by

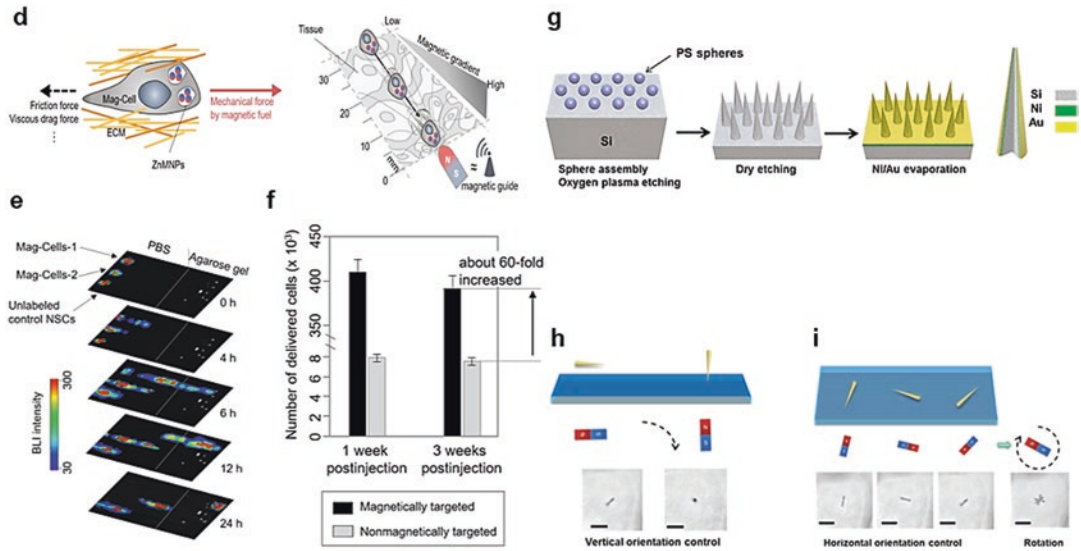

Fig. 8.3 (continued)

loading the GOD onto the surface of Fe_5C_2 nanoparticles, followed by reducing $KMnO_4$ in the presence of poly(allylamine hydrochloride) (Fig. 8.3b). Tumor acidic microenvironment generates Mn^{2+} and O_2 caused by each decomposition of MnO_2 and release of GOD. Thereafter, the GOD generated H_2O_2, which consumes glucose in tumor cells. The Fe_5C_2 could also induce H_2O_2 into tumor cells through the Fenton reaction with enhanced tumor targeting at magnetic field (Fig. 8.3c). Fe_5C_2-GOD@MnO_2 NPs showed glucose degradation at pH 6.0 condition, similar to the pH at tumor microenvironment. The cytotoxicity of HeLa cells was the highest in the treatment of Fe_5C_2-GOD@MnO_2 NPs in magnetic field, among the experimental groups. Furthermore, Fe_5C_2-GOD@MnO_2 NPs with magnetic field promoted in vivo cancer therapeutic efficacy as well. Yun et al. demonstrated that zinc-doped ferrite MNPs (ZnMNPs) can control stem cell migration and differentiation (Fig. 8.3d) [62]. The ZnMNPs were synthesized by a one-pot thermal decomposition method using $ZnCl_2$ and $Fe(acac)_3$. The fabricated ZnMNPs showed higher magnetization than both typical ferrite MNPs and commercial ferrite MNPs, so that ZnMNPs could increase stem cell migration efficacy, along with the largest magnetic gradient in ZnMNP-transfected neural stem cells (MNP-NSCs) (Fig. 8.3e). In neurodegenerative brain injury model, the number of magnetic MNP-NSCs in the brain was about 60-fold larger than that of non-magnetically moved NSCs (Fig. 8.3f). Furthermore, zinc ions released from ZnMNPs enhanced neuronal differentiation and neurotrophic factor secretion of NSCs, by activating Wnt signaling pathway. Xu et al. introduced novel nanospears having magnetic property induced by nickel [63]. Polystyrene nanospheres are assembled on a silicon wafer, followed by size reduction with oxygen plasma etching. Thereafter, dry etching is applied to the nanospheres to generate Si nanospear arrays. Finally, both Ni and gold layers were evaporated on the Si nanospear (Fig. 8.3g). The resultant nanospears were controlled vertically (Fig. 8.3h) or horizontally by magnet (Fig. 8.3i). This study showed that the targeted cells were transfected with enhanced green fluorescent protein (eGFP) expression through eGFP expression plasmid-modified Au/Ni/Si nanospears. Consequently, Au/Ni/Si nanospears were introduced to be used as gene-editing tools for immunology and stem cell biology.

8.3 INPs as Inducers

8.3.1 Zinc

Zinc (Zn) is one of the most abundant essential elements for our human body. It can be observed in all body tissues, such as muscle, bone, and skin tissue. In particular, Zn is an important element for a healthy brain, because it influences regulatory, structural, and signaling processes in the neuronal system. However, the cytotoxicity of neuronal cells can result from abnormally high concentration of Zn. Therefore, the level of Zn in the central nervous system (CNS) has to be regulated in the therapeutic application [64, 65]. Previous study showed that the Zn level is controlled during embryogenesis, so that Zn deficiencies can contribute to the occurrence of human birth defects involving CNS malformation [64, 65]. Zn is also an essential component of RNA and DNA polymerases and histone deacetylases for both cellular proliferation and DNA replication [66]. In addition, Zn-dependent enzyme metalloproteinases and Zn-biding proteins like metallothioneins are responsible for Zn signaling and metabolism [67]. Specifically, transcription factors such as ZIC1 and ZIC2, which regulate key genes regarding neurogenesis and cellular proliferation, are controlled by Zn finger motifs [68, 69]. Presumably, Zn plays an important role as a cell differentiation inducer. Sabbatini et al. applied Zn-doped bioactive glasses to undifferentiated SKNBE neuronal cell lines to stimulate adhesion and differentiation [70]. Pfaender et al. confirmed adequate concentration of Zn for better differentiation efficiency of human-induced pluripotent stem cells [71]. Another intriguing aspect of Zn is its antimicrobial and wound regenerative efficacy [24, 72–74]. It is important to keep wound sites from microbial complications, because microbial complications, including overt and local infection, delay healing of the wound site [75]. For example, biofilm, commonly described as microbial colony, colonizes the damaged wound area by attaching to it. As biofilm attaches to the wound site, it starts to product destructive toxins and enzymes that increase the inflammatory state of the wound [76]. Therefore, various attempts have been made to use Zn^{2+} for wound recovery by inhibiting microorganisms. Ali et al. synthesized Zn peroxide nanoparticles (ZnO_2 NPs) for increased wound healing application [77]. ZnO_2 NPs were shown to display as significant anti-proteinase activity as aspirin. In addition, it was discovered that Zn^{2+} promotes the production of fibroblasts that stimulate skin wound regeneration [78, 79]. Mao et al. developed hydrogel embedded with Ag/Ag@AgCl/ZnO nanostructures to promote wound healing with simultaneous exploitation of antimicrobial and wound regenerative properties [24]. The Ag/Ag@AgCl/ZnO hydrogels were fabricated by a simple synthetic technique. First, Ag@AgCl was made by adding $AgNO_3$ to carboxymethyl cellulose and kept the synthetic hydrogel swollen in water for 12 h. The Ag@AgCl was irradiated with ultraviolet light to form the Ag-incorporated Ag@AgCl (Ag/Ag@AgCl). Thereafter, $Zn(NO_3)_2$ and NaOH were added to the Ag/Ag@AgCl, to incorporate ZnO with the Ag/Ag@AgCl. The resultant Ag/Ag@AgCl was used as photocatalysis stimulated by visible light, resulting in the release of both reactive oxygen species (ROS) and Ag^+ (Fig. 8.4a). As a result, Ag/Ag@AgCl could stimulate the antibacterial activity of ZnO. The hydrogel can regulate the release rate of ions by means of its reversible swelling-shrinking transition, which varies, depending on pH conditions. Released Ag^+ and Zn^{2+} can penetrate the membrane of bacteria, so that treated *E. coli* and *S. aureus* were leaked and condensed (Fig. 8.4b, c). The research group confirmed the antibacterial and therapeutic effect of the Ag/Ag@AgC/ZnO hydrogel by applying various hydrogels to rat skin wound infected with *S. Aureus*. Dermal fibroblasts and newborn blood vessels were observed 4 days after treatment. In addition, it was observed that the released Ag^+ and Zn^{2+} promoted immune functions with increasing amount of neutrophil as well.

Zn can also be used for wound regeneration through its piezoelectricity. It is known that electrical fields (EF) enhance skin wound healing by stimulating and controlling cellular behaviors in wound site [80, 81]. The EF stimulation not only helps the fibroblast differentiate into

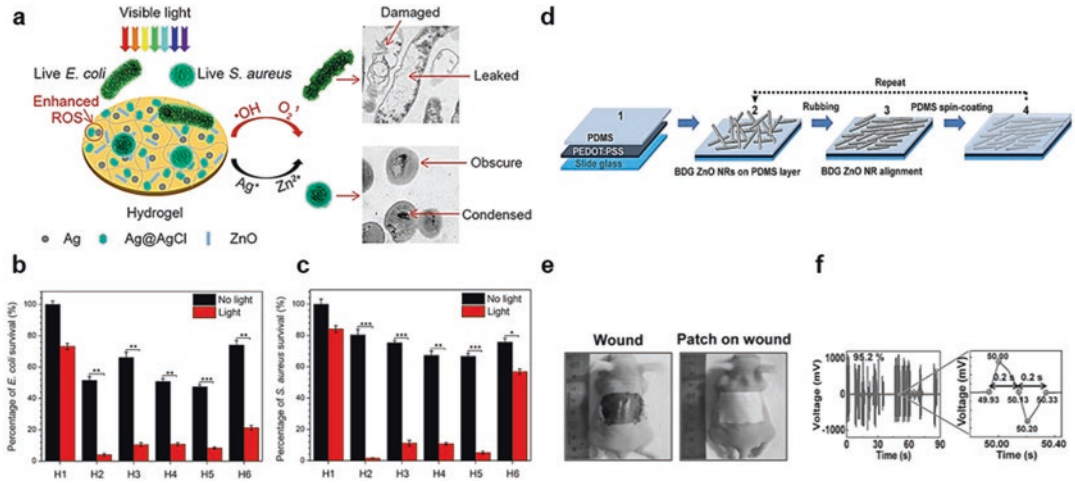

Fig. 8.4 (**a**) Overall scheme of the antibacterial effect of Ag/Ag@AgCl/ZnO hybrid nanostructures toward live *S. aureus* and *E. coli*. Killing ability of hydrogel against (**b**) *E. coli* and (**c**) *S. aureus*. (H1, control hydrogel; H2, Ag/Ag@AgCl hydrogel; H3, H4, and H5, Ag/Ag@AgCl/ZnO hydrogels, and H4 for representative; H6, ZnO hydrogel, $n = 3$) (Reprinted with permission from (Mao et al., ACS Nano, 11 (9) pp. 9010–9021.) Copyright (2017) American Chemical Society). (**d**) Schematic of the BDG ZnO NR-based PZP making process. BDG ZNO NRs are put on the PDMS layer with rubbing for alignment order. (**e**) In vivo application of a nine-layered PZP. The skin wound was induced on the back of a mouse. A nine-layered PZP was placed on the wound, and the PZP was fixed by dressing a transparent film over the PZP. (**f**) The piezoelectric voltage generated upon animal motion from the nine-layered PZPs applied on the mouse wound at 95.2% BDG ZnO NR filling density. (Reprinted by permission from John Wiley & Sons, Inc: [Advanced Functional Materials] (Bhang et al. 2016), copyright (2016))

myofibroblast but also increases angiogenesis and keratinocyte migration and proliferation [82–84]. Bhang et al. invented a bidirectionally grown ZnO nanorod-based piezoelectric patch (BDG ZnO NR PZP) to enhance wound recovery [25]. The research group utilized a poly(3,4-ethylened ioxythiophene):poly(styrenesulfonate) for anti-adhesive layer with thermal annealing. Then they put BDG ZNO NRs on the PDMS layer with rubbing for alignment order (Fig. 8.4d). The fabricated BDG ZnO NR PZP patch was placed on the wound site of mouse (Fig. 8.4e). In this research, BDG ZnO NR PZP generated sufficient EF required for wound recovery, generating about 900 mV of electric potential, which was in the range of 150–1000 mV that was discovered as adequate range of voltage for wound healing (Fig. 8.4f) [85]. When dermal fibroblasts were cultured on the BDG ZnO NR PZP, no cytotoxic effect was observed, which was attributed to the biocompatible properties of ZnO. Human dermal fibroblasts cultured on BDG ZnO NR PZP showed increased angiogenic protein expression and migration efficacy. In further in vivo test, the BDG ZnO NR PZP patched mouse showed the best wound recovery, as compared with that of other experimental groups.

8.3.2 Copper

In Earth's crust, copper (Cu) is present at 0.00007% as a trace element, and adult males have ~100 mg of Cu [86]. However, Cu is an important catalytic and structural cofactor that activates biochemical events that are essential for life. In biological systems, Cu ions exist in two oxidation states: one is reduced (Cu^{+}), while the other is oxidized (Cu^{2+}) state [87]. These Cu^{+} showed affinity to thiol and thioether groups (such as cysteine or methionine), and Cu^{2+} prefers coordination with oxygen or imidazole nitrogen group (such as glutamate or aspartate) [87] Therefore, Cu ions can easily interact with

various proteins and biochemical reactions [87]. In particular, it is known that Cu is correlated with the wound healing process [88]. Cu ions were known to stimulate tissue regeneration by promoting angiogenesis in the presence of the upregulation of angiogenic growth factors, such as vascular endothelial growth factor (VEGF) [89], known as the most popular, effective, and long-term signal that induces angiogenesis in the wound recovery process [90]. VEGF promoted angiogenesis by enhancing both the migration and proliferation of endothelial cells [91]. Furthermore, Cu was discovered to enhance the expression and stabilization of keratin and collagen components of extracellular skin proteins [92], and upregulated Cu-mediated enzymes and polysaccharides are used for matrix remodeling, cell proliferation, and re-epithelization [93]. However, the excess amount of Cu ions would be harmful, because Cu ions can induce ROS generation. It is important to control the amount of Cu ions to inhibit an excess amount of ROS generation [94]. Xiao et al. invented folic acid-modified Cu-based metal-organic framework nanoparticles (F-HKUST-1) to stimulate wound healing with alleviated toxicity by regulating the release rates of Cu^{2+} [95]. F-HKUST-1 was synthesized by the addition of Cu acetate monohydrate aqueous solution dropwise into a mixture of 1,3,5-benzenetricarboxylic acid. Thereafter, gel-like green suspension was fabricated after stirring at room temperature (RT) for 40 min. When biocompatible folic acid is incorporated into HKUST-1, folic acid blocks most of the pores of HKUST-1, increasing hydrophobicity and decreasing the internal surface area of the nanoparticles. As a result, the stability of the nanoparticles and the diffusion rate of ions in the protein solution could be increased and controlled. F-HKUST-1 below the 0.5 mM concentration showed low toxicity against both human epithelial keratinocytes and human dermal fibroblasts (HDFs). In addition, dermal splinted wound healing of diabetic mice was accelerated (Fig. 8.5a). It was observed that more new vessels were formed after treatment with F-HKUST-1 hydrogel, as compared with that of other hydrogels, in the dermal tissue of diabetic mouse (Fig. 8.5b, c). This result showed that controlled release of Cu^{2+} from F-HKUST can improve the therapeutic effect of wound healing without toxicity.

As mentioned earlier, antimicrobial efficacy is also an important factor for wound recovery. Nanostructured-based Cu materials showed antimicrobial activity toward microorganism [96]. Li et al. fabricated Cu-containing bioactive glass/eggshell membrane nanocomposites to promote wound healing, inducing angiogenesis and antibacterial activity [97]. They first made Cu-containing bioactive silicate glass-ceramic powders with different Cu contents of 0, 2, and 5 mol. % by using a sol-gel method via tetraethyl orthosilicate (TEOS, 98%), triethyl phosphate (TEP, 99.8%), $Ca(NO_3)_2{\cdot}4H_2O$, and $Cu(NO_3)_2{\cdot}3H_2O$ as primary materials. Thereafter, Cu-containing glass-ceramic disc was ablated by focused laser to coat previously prepared eggshell film (ESM) in the pulsed laser deposition chamber. The resultant Cu nanomaterials were named xCu-BG/ESM films (where x indicates the concentration of Cu in the BG/ESM films). The human umbilical vein endothelial cells (HUVEC) were cultured on the various concentrations of xCu-BG/ESM films. Angiogenic gene expressions were upregulated in the 5Cu-BG/ESM films, as compared with that of no ESM, 0Cu-BG/ESM films, and 2Cu-BG/ESM films. 5Cu-BG/ESM film group showed the best antimicrobial effect against *E. coli*. Moreover, 5Cu-BG/ESM group showed the best therapeutic improvement among the experimental groups, even in the mouse wound model.

8.3.3 Iron

Iron (Fe) is an essential nutrient in the body. It plays important roles in homeostasis, such as several enzyme synthesis, DNA synthesis, and oxygen transport. In the human body, about 65–75% of Fe is in red blood cell, in the form of hemoglobin [98]. Despite the importance in life conservation of Fe, a large amount of Fe can cause harmful effect toward the human body. Dixon and Stockwell reported that Fe acts as a catalyst,

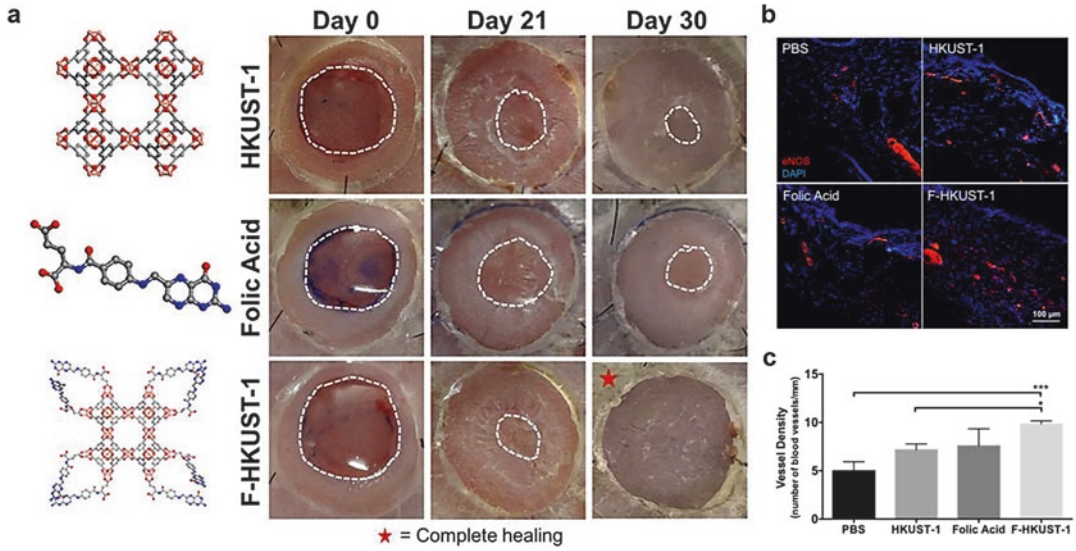

Fig. 8.5 (**a**) Dermal wound healing of diabetic mice treated with HKUST-1, folic acid, and F-HKUST-1. (**b**) Analysis of wound recovery with blood vessels visualized by eNOS immunofluorescence staining (blue, nucleus; red, eNOS). (Reprinted with permission from (Xiao et al., ACS Nano, 12 (2) pp. 1023–1032). Copyright (2018) American Chemical Society). (**c**) Quantification of the positive eNOS immunofluorescence staining ($n = 3$, $*P < 0.05$, $***P < 0.001$)

changing hydrogen peroxides to ROS [99]. As generated ROS induce mitochondrial damage, in consequence, Fe-exposed cells can undergo apoptosis. This pathway is called ferroptosis. Zanganeh et al. utilized the toxic effect of Fe for cancer therapy [100]. In the research, the Food and Drug Administration-approved Fe_3O_4 nanoparticle compound, called ferumoxytol, was applied to cancer therapy by inducing pro-inflammatory macrophage polarization. It was already reported that ferumoxytol attracts macrophages and induces the polarization of macrophage into M1 macrophages. Moreover, pro-inflammatory M1 macrophages are widely known to release OH• through the Fenton reaction [101, 102]. They found that the administration of ferumoxytol may attract more macrophages and then induce the macrophages to be polarized toward M1 macrophage, which causes cancer suppression. They found that implanted ferumoxytol also showed inhibition of metastases in the liver and lungs in mouse cancer model.

Fe has also been discovered to have therapeutic potency toward stem cell. Huang et al. controlled cellular behavior through Fe-based magnetic nanoparticles [103]. Iron oxide magnetic nanoparticle (IO-MNP)-treated bone marrow-derived mesenchymal stem cells (MSCs) showed enhanced C-X-C chemokine receptor type 4 (CXCR4). CXCR4 is a receptor for stromal-derived factor 1α (SDF-1α) known as representative stem cell homing factor, so that IO-MNP-treated MSCs easily moved to the designated area, consequently enhancing therapeutic efficacy. Han et al. increased the therapeutic efficacy of MSCs in myocardial infarction (MI) by introducing IONPs [104]. Previous studies have shown that both paracrine factor and the electrophysical phenotype development of MSCs are crucial for MI treatment [105, 106]. In this respect, coculture of cardiomyocytes or cardiomyoblasts with MSCs was introduced for priming MSCs (Fig. 8.6a) [107]. Active gap junctional crosstalk of MSCs with cardiac cells in coculture has been known to play a key role in the MSC modification. IONPs were treated to

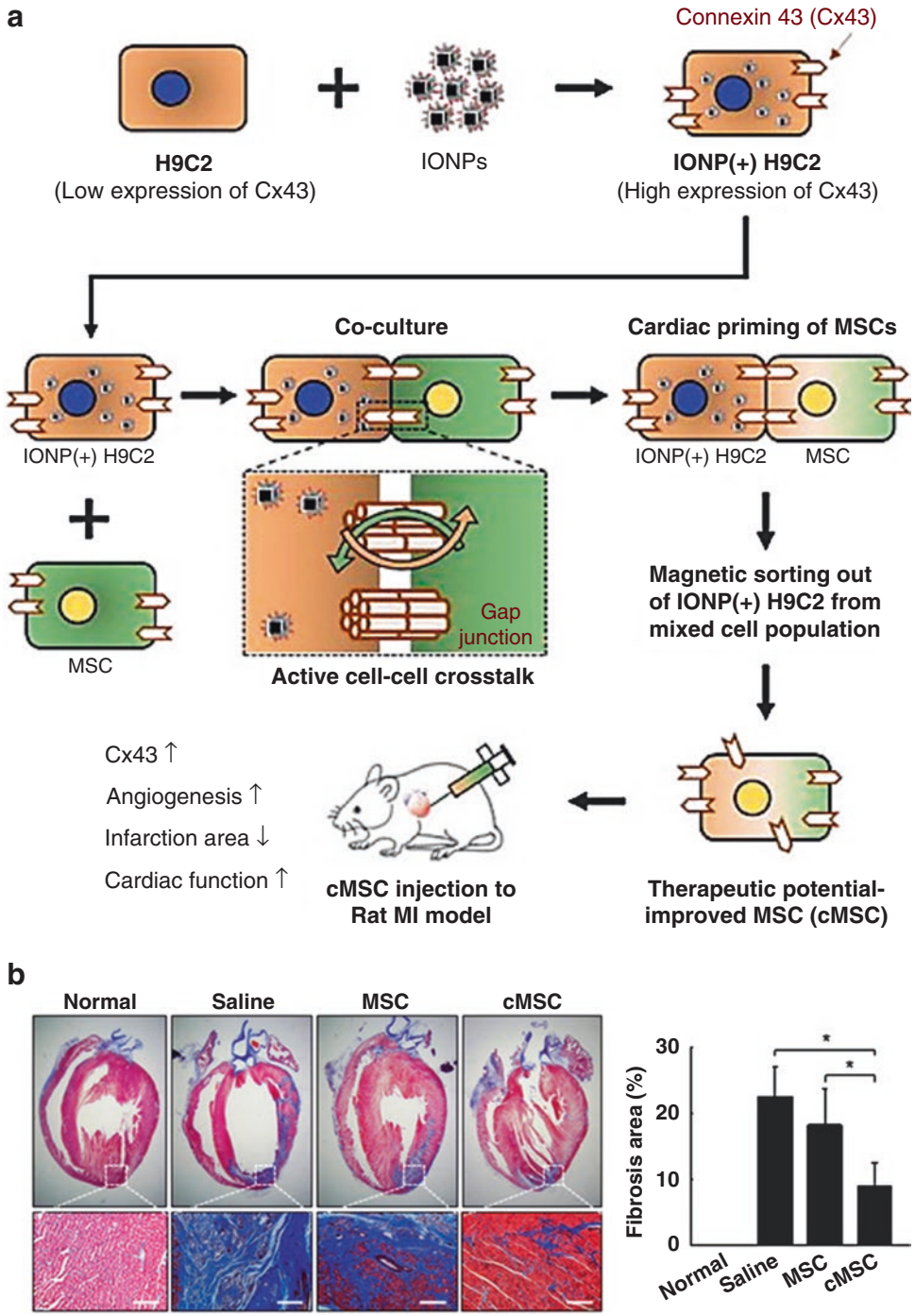

Fig. 8.6 (**a**) Schematic of IONP-induced Cx43 expression increment in H9C2 and its effect on coculture with MSCs, including in vivo therapeutic efficacy of the cMSCs. (**b**) Histology of myocardium stained with Masson's trichrome staining and their quantitative analysis (n = 4 animals, $*P < 0.05$, scale bars = 200 μm). (Reprinted with permission from (Han et al., ACS Nano, 9 (3) pp. 2805–2819) Copyright (2015) American Chemical Society)

cardiomyoblast (H9C2) and confirmed higher expression of connexin 43 (Cx43) in H9C2 (Fig. 8.6a). MSCs cocultured with IONP-treated H9C2 (cMSCs) displayed significantly higher level of cardiac repair-favorable paracrine profile among the other experimental groups. As a result, cMSC-injected rat MI improved animal survival and heart function, compared with the unmodified MSC-injected MI models (Fig. 8.6b).

8.4 Conclusion

With increasing interests in INPs, numerous studies regarding INPs have been discovered [1–3]. For bio-application, biocompatibility is one of the most important issues [19, 20]. Therefore, recent novel INPs have been shown to have their own unique characteristics that originate from their metal components with increased biocompatibility. In this chapter, we introduced novel INPs that serve as either carriers or inducers for tissue regeneration. For the DDS carriers, widely used materials include AuNPs and MNPs. In the case of Au, they showed various results for cancer therapy through photodynamic, phototherapy, and bio-imaging efficacy with low responsiveness. It was also discovered that MNPs showed good carriers for delivering several materials to designated areas with magnetic assistance.

Apart from their roles as carriers, modified INPs were introduced to increase tissue regeneration. Zn has both antimicrobial effect and piezoelectricity, so that Zn-derivative INPs showed increased therapeutic effect on tissue generation, especially in the wound healing process. Zn also served as a motif for nerve regeneration. Since Cu has antimicrobial effect and angiogenic property, Cu could be used to help wound recovery. Fe also has toxicity against the biological organelles, so that Fe was utilized as a cancer-killing element in cancer therapy. It was also discovered that Fe-treated stem cells showed increased therapeutic efficacy for stem cell therapy.

Various inorganic materials have been discovered to influence their biological surroundings. However, little is known about the effect of the various INPs in bio-application. This chapter can help to comprehend the synthetic methods of recent novel INPs and their bio-application. It can also suggest directions for novel INP application to tissue engineering.

References

1. Del Pozo-Rodríguez A, Solinís MÁ, Rodríguez-Gascón A (2016) Applications of lipid nanoparticles in gene therapy. Eur J Pharm Biopharm 109:184–193
2. Kim K, Oh KS, Park DY et al (2016) Doxorubicin/gold-loaded core/shell nanoparticles for combination therapy to treat cancer through the enhanced tumor targeting. J Control Release 228:141–149
3. Detappe A, Kunjachan S, Sancey L et al (2016) Advanced multimodal nanoparticles delay tumor progression with clinical radiation therapy. J Control Release 238:103–113
4. Krpetić Z, Anguissola S, Garry D et al (2014) Nanomaterials: impact on cells and cell organelles. Adv Exp Med Biol 811:135–156
5. Huang X, Teng X, Chen D et al (2010) The effect of the shape of mesoporous silica nanoparticles on cellular uptake and cell function. Biomaterials 31(3):438–448
6. Li Z, Huang H, Tang S et al (2016) Small gold nanorods laden macrophages for enhanced tumor coverage in photothermal therapy. Biomaterials 74:144–154
7. Park SJ, Kim S, Lee S et al (2000) Synthesis and magnetic studies of uniform iron nanorods and nanospheres. J Am Chem Soc 122(35):8581–8582
8. Vallhov H, Gabrielsson S, Stromme M et al (2007) Mesoporous silica particles induce size dependent effects on human dendritic cells. Nano Lett 7:3576–3582
9. Cheng Y, Meyers JD, Broome AM et al (2011) Deep penetration of a PDT drug into tumors by noncovalent drug-gold nanoparticle conjugates. J Am Chem Soc 133(8):2583–2591
10. Kim KS, Hur W, Park SJ et al (2010) Bioimaging for targeted delivery of hyaluronic acid derivatives to the livers in cirrhotic mice using quantum dots. ACS Nano 4(6):3005–3014
11. Nie LB, Wang XL, Li S et al (2009) Amplification of fluorescence detection of DNA based on magnetic separation. Anal Sci 25(11):1327–1331
12. Kim T, Hyeon T (2013) Applications of inorganic nanoparticles as therapeutic agents. Nanotechnology 25(1):012001
13. Brust M, Walker M, Bethell D et al (1994) Synthesis of thiol-derivatised gold nanoparticles in a two-phase liquid–liquid system. J Chem Soc Chem Commun 0(7):801–802
14. Jana NR, Gearheart L, Murphy CJ (2001) Evidence for seed-mediated nucleation in the chemical reduc-

tion of gold salts to gold nanoparticles. Chem Mat 13:2313
15. Sakamoto M, Fujistuka M, Majima T (2009) Light as a construction tool of metal nanoparticles: synthesis and mechanism. J Photochem Photobiol C 10:33–56
16. Ding Y, Jiang Z, Saha K et al (2014) Gold nanoparticles for nucleic acid delivery. Mol Ther 22:1075–1083
17. Jang B, Park JY, Tung CH et al (2011) Gold-nanorod-photosensitizer complex for near-infrared fluorescence imaging and photodynamic/photothermal therapy in vivo. ACS Nano 5(2):1086–1094
18. Liu Y, Ai K, Cheng X et al (2010) Gold-nanocluster-based fluorescent sensors for highly sensitive and selective detection of cyanide in water. Adv Funct Mater 20:951–956
19. Huang J, Li Y, Orza A et al (2016) Magnetic nanoparticle facilitated drug delivery for cancer therapy with targeted and image-guided approaches. Adv Funct Mater 26(22):3818–3836
20. Kang YS, Risbud S, Rabolt JF et al (1996) Synthesis and characterization of nanometer-size Fe_3O_4 and γ-Fe_2O_3 particles. Chem Mater 8(9):2209–2211
21. Riegler J, Liew A, Hynes SO et al (2013) Superparamagnetic iron oxide nanoparticle targeting of MSCs in vascular injury. Biomaterials 34(8):1987–1994
22. Landazuri N, Tong S, Suo J et al (2013) Magnetic targeting of human mesenchymal stem cells with internalized superparamagnetic iron oxide nanoparticles. Small 9:4017–4026
23. He M, Chen X, Cheng K et al (2018) Enhanced cellular osteogenic differentiation on Zn-containing bioglass incorporated TiO_2 nanorod films. J Mater Sci Mater Med 29(9):136
24. Mao C, Xiang Y, Liu X et al (2017) Photo-inspired antibacterial activity and wound healing acceleration by hydrogel embedded with Ag/Ag@AgCl/ZnO nanostructures. ACS Nano 11(9):9010–9021
25. Bhang SH, Jang WS, Han J et al (2017) Zinc oxide nanorod-based piezoelectric dermal patch for wound healing. Adv Func Mater 27(1):1603497
26. Wang F, Wang YC, Dou S et al (2011) Doxorubicin-tethered responsive gold nanoparticles facilitate intracellular drug delivery for overcoming multidrug resistance in cancer cells. ACS Nano 5(5):3679–3692
27. Guo S, Huang Y, Jiang Q et al (2010) Enhanced gene delivery and sirna silencing by gold nanoparticles coated with charge-reversal polyelectrolyte. ACS Nano 4(9):5505–5511
28. Tang J, Jiang X, Wang L et al (2014) Au@Pt nanostructures: a novel photothermal conversion agent for cancer therapy. Nanoscale 6:3670
29. Bhang SH, Han J, Jang HK et al (2015) pH-triggered release of manganese from MnAu nanoparticles that enables cellular neuronal differentiation without cellular toxicity. Biomaterials 55:33–43
30. Haynes WM (2012) CRC handbook of chemistry and physics, vol 93. CRC Press, Boca Raton, pp 8–25
31. Hernandez RB, Farina M, Esposito BP et al (2011) Mechanisms of manganese-induced neurotoxicity in primary neuronal cultures: the role of manganese speciation and cell type. Toxicol Sci 124(2):414–423
32. Lieberthal W, Menza SA, Levine JS (1998) Graded ATP depletion can cause necrosis or apoptosis of cultured mouse proximal tubular cells. Am J Phys 274:F315–F327
33. Tian Y, Zhang Y, Teng Z et al (2017) pH-dependent transmembrane activity of peptide-functionalized gold nanostars for computed tomography/photoacoustic imaging and photothermal therapy. ACS Appl Mater Interfaces 9(3):2114–2122
34. Tapmeier TT, Moshnikova A, Beech J et al (2015) The pH low insertion peptide pHLIP variant 3 as a novel marker of acidic malignant lesions. Proc Natl Acad Sci. U S A 112:9710–9715
35. Yu M, Guo F, Wang J et al (2015) Photosensitizer-loaded pH-responsive hollow gold nanospheres for single light-induced photothermal/photodynamic therapy. ACS Appl Mater Interfaces 7(32):17592–17597
36. Cheheltani R, Ezzibdeh RM, Chhour P (2016) Tunable, biodegradable gold nanoparticles as contrast agents for computed tomography and photoacoustic imaging. Biomaterials 102:87–97
37. Pensa E, Cortés E, Corthey G et al (2012) The chemistry of the sulfur-gold interface: in search of a unified model. Acc Chem Res 45(8):1183–1192
38. Pissuwan D, Niidome T, Cortie MB (2011) The forthcoming applications of gold nanoparticles in drug and gene delivery systems. J Control Release 149(1):65–71
39. Bishop CJ, Tzeng SY, Green JJ (2014) Degradable polymer-coated gold nanoparticles for co-delivery of DNA and siRNA. Acta Biomater 11:393–403
40. Chang CC, Chen CY, Chuang TL et al (2016) Aptamer-based colorimetric detection of proteins using a branched DNA cascade amplification strategy and unmodified gold nanoparticles. Biosens Bioelectron 78:200–205
41. Huang P, Lin J, Wang S et al (2013) Photosensitizer-conjugated silica-coated gold nanoclusters for fluorescence imaging-guided photodynamic therapy. Biomaterials 34(19):4643–4654
42. Kang S, Bhang SH, Hwang S et al (2015) Mesenchymal stem cells aggregate and deliver gold nanoparticles to tumors for photothermal therapy. ACS Nano 9(10):9678–9690
43. Vankayala R, Kuo CL, Nuthalapati K et al (2015) Nucleus-targeting gold nanoclusters for simultaneous in vivo fluorescence imaging, gene delivery, and NIR-light activated photodynamic therapy. Adv Func Mater 25(37):5934–5945
44. Han S, Samanta A, Xie X et al (2017) Gold and hairpin DNA functionalization of upconversion

nanocrystals for imaging and in vivo drug delivery. Adv Mater 29(40):201704811
45. Lei Y, Tang L, Xie Y et al (2017) Gold nanoclusters-assisted delivery of NGF siRNA for effective treatment of pancreatic cancer. Nat Commun 25(8):15130
46. McBain SC, Yiu HH, Dobson J (2008) Magnetic nanoparticles for gene and drug delivery. Int J Nanomed 3(2):169–180
47. Liang YC, Chang L, Qiu W et al (2017) Ultrasensitive magnetic nanoparticle detector for biosensor applications. Sensors (Basel) 17(6):1296
48. Chemla YR, Grossman HL, Poon Y et al (2000) Ultrasensitive magnetic biosensor for homogeneous immunoassay. Proc Natl Acad Sci U S A 97(26):14268–14272
49. Wu L, Zhang F, Wei Z et al (2018) Magnetic delivery of Fe_3O_4@polydopamine nanoparticle-loaded natural killer cells suggest a promising anticancer treatment. Biomater Sci 6(10):2714–2725
50. Waite JH, Qin X (2001) Polyphosphoprotein from the adhesive pads of mytilus edulis. Biochemistry 40(9):2887–2893
51. Jiang J, Zhu L, Zhu L et al (2011) Surface characteristics of a self-polymerized dopamine coating deposited on hydrophobic polymer films. Langmuir 27(23):14180–14187
52. Bettinger CJ, Bruggeman JP, Misra A (2009) Biocompatibility of biodegradable semiconducting melanin films for nerve tissue engineering. Biomaterials 30(17):3050–3057
53. Eric CA, Sameera W, Jesbaniris BC et al (2016) Structural effects on the magnetic hyperthermia properties of iron oxide nanoparticles. Prog Nat Sci-Mater 26(5):440–448
54. Huang HS, Hainfeld JF (2013) Intravenous magnetic nanoparticle cancer hyperthermia. Int J Nanomedicine 8:2521–2532
55. Bañobre-López M, Teijeiro A, Rivas J (2013) Magnetic nanoparticle-based hyperthermia for cancer treatment. Rep Pract Oncol Radiother 18(6):397–400
56. Hervault A, Thanh NT (2014) Magnetic nanoparticle-based therapeutic agents for thermo-chemotherapy treatment of cancer. Nanoscale 6(20):11553–11573
57. Tsai MF, Hsu C, Yeh CS et al (2018) Tuning the distance of rattle-shaped ionp@shell-in-shell nanoparticles for magnetically-targeted photothermal therapy in the second near-infrared window. Acs Appl Mater Inter 10(2):1508–1519
58. Winterbourn CC (1995) Toxicity of iron and hydrogen peroxide: the Fenton reaction. Toxicol Lett 82–83:969–974
59. Voinov MA, Sosa Pagán JO, Morrison E et al (2011) Surface-mediated production of hydroxyl radicals as a mechanism of iron oxide nanoparticle biotoxicity. J Am Chem Soc 133(1):35–41
60. Lee KT, Lu YJ, Chiu SC et al (2018) Heterogeneous Fenton reaction enabled selective colon cancerous cell treatment. Sci Rep 8(1):16580
61. Feng L, Xie R, Wang C et al (2018) Magnetic targeting, tumor microenvironment-responsive intelligent nanocatalysts for enhanced tumor ablation. ACS Nano 12(11):11000–11012
62. Yun S, Shin TH, Lee JH et al (2018) Design of magnetically labeled cells (Mag-Cells) for in vivo control of stem cell migration and differentiation. Nano Lett 18(2):838–845
63. Xu X, Hou S, Wattanatorn N et al (2018) Precision-guided nanospears for targeted and high-throughput intracellular gene delivery. ACS Nano 12(5):4503–4511
64. Chowanadisai W, Graham DM, Keen CL et al (2013) A zinc transporter gene required for development of the nervous system. Commun Integr Biol 6(6):e26207
65. Morris DR, Levenson CW (2013) Zinc regulation of transcriptional activity during retinoic acid-induced neuronal differentiation. J Nutr Biochem 24(11):1940–1944
66. Marks PA (2010) Histone deacetylase inhibitors: a chemical genetics approach to understanding cellular functions. Biochim Biophys Acta 1799(10–12):717–725
67. Tapiero H, Tew KD (2003) Trace elements in human physiology and pathology: zinc and metallothioneins. Biomed Pharmacother 57(9):399–411
68. Merzdorf CS, Sive HL (2006) The zic1 gene is an activator of Wnt signaling. Int J Dev Biol 50(7):611–617
69. Kim SU, Lee HJ, Kim YB (2013) Neural stem cell-based treatment for neurodegenerative diseases. Neuropathology 33(5):491–504
70. Sabbatini M, Boccafoschi F, Bosetti M et al (2014) Adhesion and differentiation of neuronal cells on Zn-doped bioactive glasses. J Biomater Appl 28(5):708–718
71. Pfaender S, Föhr K, Lutz AK et al (2016) Cellular zinc homeostasis contributes to neuronal differentiation in human induced pluripotent stem cells. Neural Plast 2016:3790702
72. Zheng K, Setyawati MI, Lim TP et al (2016) Antimicrobial cluster bombs: silver nanoclusters packed with daptomycin. ACS Nano 10(8):7934–7942
73. Sirelkhatim A, Mahmud S, Seeni A et al (2015) Review on zinc oxide nanoparticles: antibacterial activity and toxicity mechanism. Nanomicro Letters 7(3):219–242
74. Meyer K, Rajanahalli P, Ahamed M et al (2011) ZnO nanoparticles induce apoptosis in human dermal fibroblasts via p53 and p38 pathways. Toxicol In Vitro 25(8):1721–1726
75. Daeschlein G (2013) Antimicrobial and antiseptic strategies in wound management. Int Wound J 1:9–14
76. Davey ME, O'toole GA (2000) Microbial biofilms: from ecology to molecular genetics. Microbiol Mol Biol Rev 64(4):847–867

77. Ali SS, Morsy R, El-Zawawy NA et al (2017) Synthesized zinc peroxide nanoparticles (ZnO_2-NPs): a novel antimicrobial, anti-elastase, anti-keratinase, and anti-inflammatory approach toward polymicrobial burn wounds. Int J Nanomedicine 12:6059–6073
78. Rouabhia M, Park H, Meng S et al (2013) Electrical stimulation promotes wound healing by enhancing dermal fibroblast activity and promoting myofibroblast transdifferentiation. PLoS One 8(8):e71660
79. Ninan N, Forget A, Shastri VP et al (2016) Antibacterial and anti-inflammatory pH-responsive tannic acid-carboxylated agarose composite hydrogels for wound healing. ACS Appl Mater Interfaces 8(42):28511–28521
80. Song B, Gu Y, Pu J et al (2007) Application of direct current electric fields to cells and tissues in vitro and modulation of wound electric field in vivo. Nat Protoc 2(6):1479–1489
81. Moulin VJ, Dubé J, Rochette-Drouin O et al (2012) Adv Wound Care (New Rochelle) 1(2):81–87
82. Li X, Kolega J (2002) Effects of direct current electric fields on cell migration and actin filament distribution in bovine vascular endothelial cells. J Vasc Res 39(5):391–404
83. Trollinger DR, Isseroff RR, Nuccitelli R (2002) Calcium channel blockers inhibit galvanotaxis in human keratinocytes. J Cell Physiol 193(1):1–9
84. Goldman R, Pollack S (1996) Electric fields and proliferation in a chronic wound model. Bioelectromagnetics 17(6):450–457
85. Assimacopoulos D (1968) Wound healing promotion by the use of negative electric current. Am Surg 34(6):423–431
86. Linder MC, Goode CA (1991) Biochemistry of copper. Springer, New York
87. Kim BE, Nevitt T, Thiele DJ (2008) Mechanisms for copper acquisition, distribution and regulation. Nat Chem Biol 4(3):176–185
88. Gopal A, Kant V, Gopalakrishnan A et al (2014) Chitosan-based copper nanocomposite accelerates healing in excision wound model in rats. Eur J Pharmacol 731:8–19
89. Dioufa N, Schally AV, Chatzistamou I et al (2010) Acceleration of wound healing by growth hormone-releasing hormone and its agonists. Proc Natl Acad Sci U S A 107(43):18611–18615
90. Nissen NN, Polverini PJ, Koch AE et al (1998) Vascular endothelial growth factor mediates angiogenic activity during the proliferative phase of wound healing. Am J Pathol 152(6):1445–1452
91. Inoue M, Itoh H, Ueda M et al (1998) Vascular endothelial growth factor (VEGF) expression in human coronary atherosclerotic lesions: possible pathophysiological significance of VEGF in progression of atherosclerosis. Circulation 98(20):2108–2116
92. Marelli B, Le Nihouannen D, Hacking SA et al (2015) Newly identified interfibrillar collagen cross-linking suppresses cell proliferation and remodelling. Biomaterials 54:126–135
93. Rucker RB, Kosonen T, Clegg MS et al (1998) Copper, lysyl oxidase, and extracellular matrix protein cross-linking. Am J Clin Nutr 67(5):996S–1002S
94. Chen Z, Meng H, Xing G et al (2006) Acute toxicological effects of copper nanoparticles in vivo. Toxicol Lett 163(2):109–120
95. Xiao J, Zhu Y, Huddleston S et al (2018) Copper metal-organic framework nanoparticles stabilized with folic acid improve wound healing in diabetes. ACS Nano 12(2):1023–1032
96. Ramyadevi J, Jeyasubramanian K, Marilani A et al (2012) Synthesis and antimicrobial activity of copper nanoparticles. Mat Lett 71:114–116
97. Li J, Zhai D, Lv F et al (2016) Preparation of copper-containing bioactive glass/eggshell membrane nanocomposites for improving angiogenesis, antibacterial activity and wound healing. Acta Biomater 36:254–266
98. Anderson J, Fitzgerald C (2010) Iron: an essential nutrient. Food and nutrition series. Health; no 9.356
99. Dixon SJ, Stockwell BR (2014) The role of iron and reactive oxygen species in cell death. Nat Chem Biol 10(1):9–17
100. Zanganeh S, Hutter G, Spitler R et al (2016) Iron oxide nanoparticles inhibit tumour growth by inducing pro-inflammatory macrophage polarization in tumour tissues. Nat Nanotechnol 11(11):986–994
101. Richards JM, Shaw CA, Lang NN et al (2012) In vivo mononuclear cell tracking using superparamagnetic particles of iron oxide: feasibility and safety in humans. Circ Cardiovasc Imaging 5(4):509–517
102. Sindrilaru A, Peters T, Wieschalka S et al (2011) An unrestrained proinflammatory M1 macrophage population induced by iron impairs wound healing in humans and mice. J Clin Invest 121(3):985–997
103. Huang X, Zhang F, Wang Y et al (2014) Design considerations of iron-based nanoclusters for noninvasive tracking of mesenchymal stem cell homing. ACS Nano 8(5):4403–4414
104. Han J, Kim B, Shin JY et al (2015) Iron oxide nanoparticle-mediated development of cellular gap junction crosstalk to improve mesenchymal stem cells' therapeutic efficacy for myocardial infarction. ACS Nano 9(3):2805–2819
105. Song H, Hwang HJ, Chang W et al (2011) Cardiomyocytes from phorbol myristate acetate-activated mesenchymal stem cells restore electromechanical function in infarcted rat hearts. Proc Natl Acad Sci U S A 108(1):296–301
106. Ranganath SH, Levy O, Inamdar MS et al (2012) Harnessing the mesenchymal stem cell secretome for the treatment of cardiovascular disease. Cell Stem Cell 10(3):244–258
107. Fukuhara S, Tomita S, Yamashiro S et al (2003) Direct cell-cell interaction of cardiomyocytes is key for bone marrow stromal cells to go into cardiac lineage in vitro. J Thorac Cardiovasc Surg 125(6):1470–1480

9 Directional Cell Migration Guide for Improved Tissue Regeneration

Young Min Shin, Hee Seok Yang, and Heung Jae Chun

Abstract

The field of tissue regeneration has seen a paradigm shift after one wave of technological innovation after another, which has notably made significant contributions to basic cellular response control and overall tissue regeneration. One particular area that is seeing rekindled interest after technological innovation is managing cell migration toward defects because successful host cell migration from adjacent tissue can accelerate overall regeneration time in tissue defects that are either large in size or irregular in shape. This chapter surveys significant advances on directed cell migration upon topological cues. First, we introduce several examples of patterning and electrospinning technology for guiding directed cell migration, followed by a discussion on approaches to influencing radially aligned topography in pattern or electrospun sheet for overall tissue regeneration.

Y. M. Shin · H. S. Yang
Department of Nanobiomedical science, Dankook University, Cheonan-si, Chungnam, Republic of Korea

H. J. Chun (✉)
Institute of Cell & Tissue Engineering and College of Medicine, Catholic University of Korea, Seoul, South Korea
e-mail: chunhj@catholic.ac.kr

Keywords

Cell migration · Contact guidance · Electrospinning · Patterning · Radially aligned · Topographical cue

9.1 Introduction

The previous two decades have seen many breakthroughs in tissue engineering and regenerative medicine. In the earlier days, tissue engineering studies have been performed to facilitate regeneration of injured tissue mostly by simply implanting various forms of scaffolds or hydrogel with cells [1]. However, their structure only has a simple porous structure and led to incomplete tissue regeneration. Tissue engineers soon began to look into other various biomedical fields including material science, polymers, cell biology, molecular biology, pathology, and so on [2]. One interesting approach tried in in-depth studies is to rebuild an artificial microenvironment similar to native tissue to help cells survive [3]. Native cell-surrounding environments (extracellular matrix or ECM) consist of multiple bioactive molecules, whose basic backbone is fibers. In this environment, cells can attach to these fibrous microstructures through integrin binding and interact with various water-soluble factors to multiply or differentiate into specific tissues [4].

H. J. Chun et al. (eds.), *Bioinspired Biomaterials*, Advances in Experimental Medicine and Biology 1249, https://doi.org/10.1007/978-981-15-3258-0_9

Inspired by how the native environment works, the engineers have made attempts to artificially reconstruct microenvironments and to connect new scaffolds with a real healing process that occurs within the tissue.

These attempts showcased that the trend was developing basic techniques that regulate certain cellular behaviors, not necessarily overall tissue regeneration [5–9]. For example, synthetic material-based scaffolds have been modified with arginine-glycine-aspartic acid (RGD) peptide just to mimic the cell-adhesive property of native ECM [10]. In some studies, several growth factors such as vascular endothelial cell growth factor (VEGF) and bone morphogenetic protein-2 (BMP-2) are frequently delivered to the damaged tissues to induce angiogenesis and bone formation, respectively [11, 12]. Other studies have demonstrated effectiveness of deploying multiple cues, e.g., both fibrous architecture/growth factor and peptide/growth factors, for controlling cellular behaviors [13, 14]. The implication is that overall tissue healing process is highly complex and various basic techniques should be combined in order to develop highly effective tools for tissue regeneration [15–18]. While many papers have been written for these individual goals, similar attention has not been paid to the topic of inducing cell migration toward tissue defects. This needs remedy because host cell recovery can accelerate overall healing time. This is our justification for including in our discussion the trend in developing cell migration guiding techniques, especially "directed migration toward the defect via contact guidance." How we can prepare the substrates or scaffolds and what kind of modifications can be effective to promote the migration will be introduced in this chapter.

9.2 Basic Cell Migration and Contact Guidance

9.2.1 Cell Migration

Cell migration is commonly controlled with several cues including chemoattractants, ECM gradient, and growth factor gradient [19]. These mechanisms have been extensively studied in cancer biology because it could shed light on cancer metastasis and invasion [20]. One should note however that in general studies on tissue regeneration have the goals of accelerating healing of damaged tissue and directing host cells from normal tissue to be relocated to damaged tissue, whereas oncology has a different perspective. Cell movement can be defined with the following factors: durotaxis (rigidity of extracellular molecules), haptotaxis (gradient of cell adhesion molecules), chemotaxis (chemoattractant gradient), galvanotaxis (electrical potential gradient), or mechanotaxis (external stimuli) [21]. However, these key factors present technical difficulties for regenerating damaged tissues because they cannot be simply applied in fabricating the scaffolds. In response, novel techniques, which we describe in the following section, have been attempted to promote cell migration, especially contact guidance.

9.2.2 Contact Guidance

Contact guidance drives cell migration with underlying topological cues. In tissue engineering, a scaffold-based contact with topological cues is preferred as an alternative strategy because technical issues render general cell migration theories inapplicable to scaffold design. Two notable examples based on this feature are patterned surface and electrospinning. First, in the patterned surface approach, a pattern is prepared via micro-contact printing or soft lithography [22]. The type of technique used determines various factors: the scale of pattern between nanometers and micrometers, the distance between the patterns and height, and cell orientation and migration. Laser ablation is also used in producing highly ordered patterns for carving metals, ceramics, and polymers, all of which are popularly used in tissue engineering [23]. Second, electrospinning is one of the more popular methods for manufacturing scaffolds during the last decade [24]. In this approach, three-dimensional (3D) fibrous scaffolds like the native ECM were prepared, and it has generated

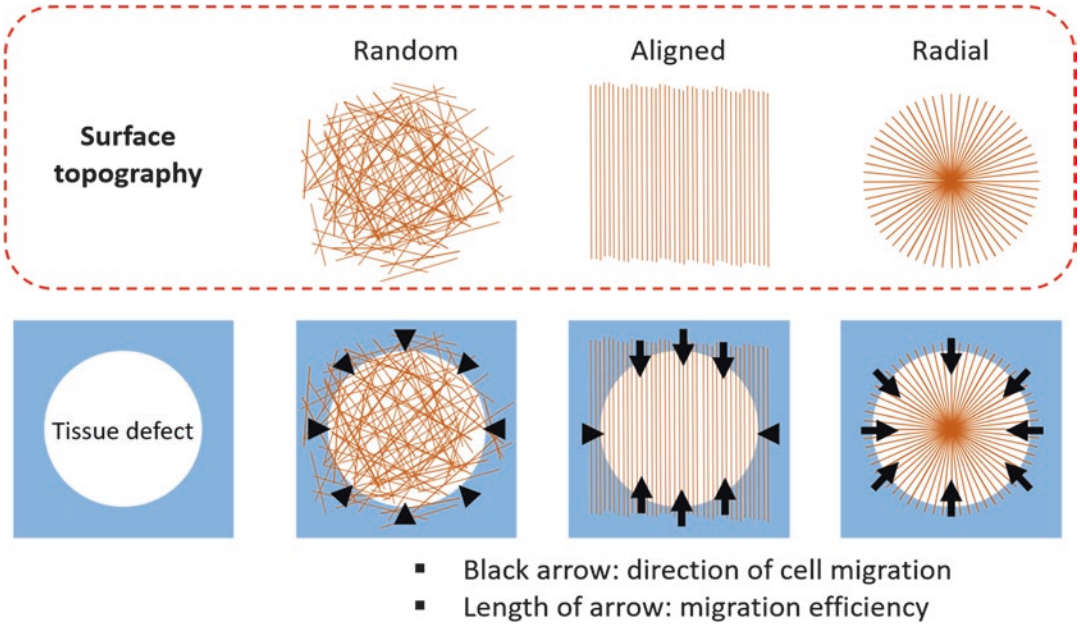

Fig. 9.1 Designs of underlying topography for tissue regeneration. Several designs prepared by patterning or electrospinning technology are tried to recruit adjacent host cells toward the defect. Random fibrous or flat patterns do not clearly provide path for cell guiding toward the core of the defect, and overall cell migration directing the core is restricted. However, aligned or highly ordered patterns generate transversal or longitudinal guiding path for the cells, and adjacent cells at the edge of the defect can move the defect along the pattern or fiber direction. As an ideal design, radial pattern can manage the directed cell migration from all front of border toward the center in a large or irregular shaped defect

aligned nanofibers by using specific collector or adjusting the collector rotation speed [25]. Both the patterned substrates and the aligned fibrous sheets present transverse or longitudinal topological signals ranging from a few nanometers to a few micrometers to the cells, and many cells sense these topographical cues and successfully response by showing cell orientation and directed migration through the patterns and fiber directions (Fig. 9.1).

9.3 Fabrication of Underlying Topography for Regulating Directed Cell Migration

9.3.1 Micro-/Nano-patterns

For controlling cell migration, the growth factor gradient has been a popular approach as reported by Irmeli Barkefors and her colleagues. They generated a gradient of VEGF and fibroblast growth factor-2 (FGF-2) and demonstrated endothelial cell migration responding to the gradients [26]. Unlike these traditional factors, geometrical microfeature successfully modulated migration of various cells [27–29]. For example, Lei et al. fabricated line micropatterns (10, 50, and 100 μm width) using a photolithography and modified with GDSVVYGLR peptide. When human umbilical vein endothelial cells (HUVEC) were cultured on the surface, directed cell orientation was observed on a narrow pattern (10 and 50 μm), whereas a wide pattern and unpatterned groups exhibited random orientation. It was observed that the patterns guided bidirectional cell movement, while unpattern group showed random migration toward all directions (Fig. 9.2a) [30]. Narrower pattern also regulates migration of fibroblasts. Kim et al. prepared PUA micro- and nano-pattern arrays which have a gradient pattern spacing (~100 nm increments in groove width

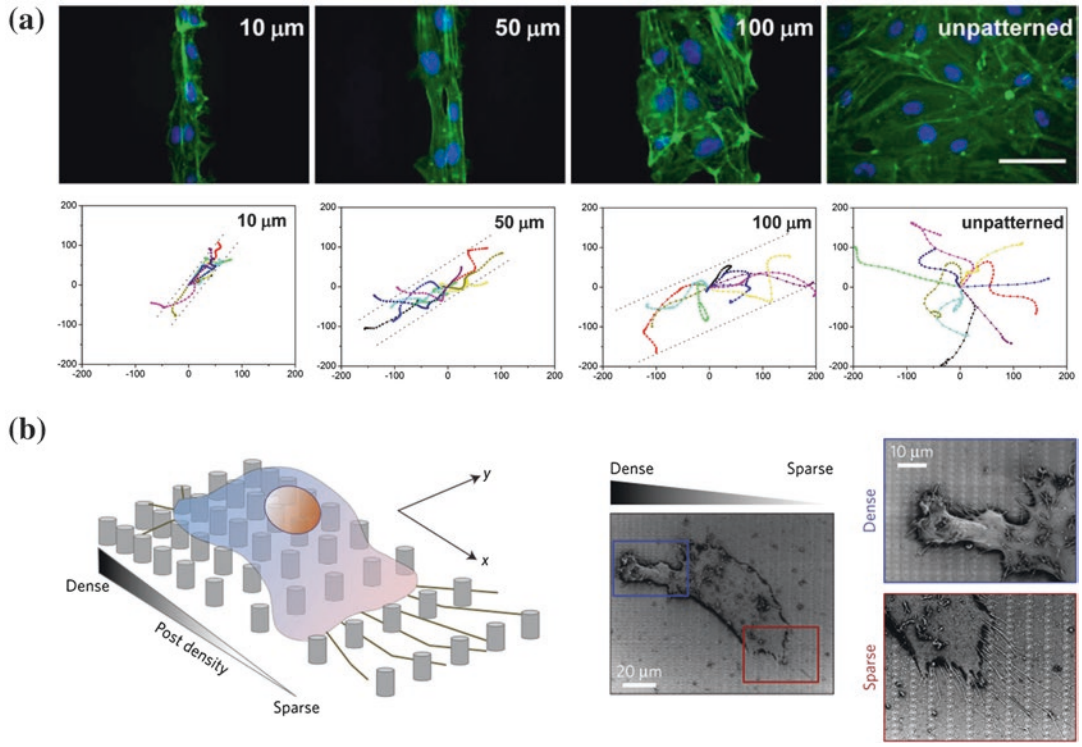

Fig. 9.2 Surface patterning for directing cell migration. (**a**) Lei et al. prepared GDSVVYGLR peptide-modified line micropatterns (10, 50, and 100 μm width) using a photolithography to investigate an orientation and migration of HUVEC. In the results, directed cell orientation was observed on a narrow pattern (10 and 50 μm), and the patterns successfully guided bidirectional cell movement (reprinted by permission from Public Library of Science: PLoS One, copyright. [2012] Lei et al. [30]), and (**b**) a graded post pattern prepared by Park et al. influenced directional migration of melanoma cells on the substrates, and it was found that it depends on the local topographical cue, which was correlated with the phosphoinositide 3-kinase (PI(3)K) and ROCK signaling. (Reprinted by permission from Springer Nature Ltd.: Nat Mater, copyright. [2016] Park et al. [33])

between neighboring ridges) [31]. The fibroblasts cultured on the pattern arrays not only had a morphology that varied depending on the density of the underlying patterns but also a differential migration speed that varied on different positions. Direction of migration is also regulated by the pattern, in which dense pattern allowed bidirectional cell movement than those on the sparse patterns.

Ordered cell alignment and directed migration are crucial in nervous tissue regeneration, and a notable work using the micropattern for nerve regeneration was reported by Joo et al. [32]. They developed laminin (stripe) and poly-D-lysine (background) micropatterns (30 μm of width and 30, 70, 120, and 170 μm of spacing, respectively) using a polydimethylsiloxane (PDMS) stamp. When adult neural stem cells were seeded on the substrates, the cells homogeneously were attached to the entire surface. However, after 6 days of differentiation, astrocytes were observed on the laminin stripe, while the neurons were only positioned at the poly-D-lysine-coated background. In addition, the astrocytes located on the laminin stripe mainly migrated following the pattern, whereas the neurons randomly moved on the poly-D-lysine-coated background. The authors claimed that the patterned ECM proteins can be used to guide neural cell movement and determine the interaction between astrocyte and neuron for neural tissue engineering.

Recently, an interesting pattern was introduced for directed migration of cancer cells. Park et al. fabricated an underlying matrix using a

photolithography which has a graded post pattern (Fig. 9.2b) [33]. The post density was varied from 0.3 and 4.2 μm (constant spacing 600 nm), and each post was 600 nm in diameter. After fibronectin coating, melanoma cells were seeded, and they observed migration of the cell on the substrates. In the results, the cancer cells widely moved than those from flat surface. They found that the directionality of migration depends on the local topographical cue, which was correlated with the phosphoinositide 3-kinase (PI(3)K) and ROCK signaling. It can be useful to determine the cancer cell behaviors or cell migration for tissue regeneration.

9.3.2 Electrospinning

Electrospinning is a popular fiber manufacturing technology that has been around for quite some time, and it has been applied to fabricate fibrous scaffolds such as extracellular matrices. This method enables to use various biocompatible polymers such as natural and synthetic polymers, and the diameter of fabricated fibers can be from several tens of nanometers to several micrometers in scale. In its early days, electrospun fibrous sheets featured random fiber orientation similar to the topography of ECM, which promoted cell adhesion and proliferation in contrast to flat surfaces because the fabricated sheets provided multiple cell attachment points. In addition, it was possible to align fibers with the advent of high-speed collectors, which were effectively used for regeneration of tissues with directionality, e.g., nerve and muscle tissues [34–37]. In tissue repair, aligned fibrous sheet has been gaining attention since Patel et al. introduced their experimental results [38]. To develop a highly effective fibrous scaffold, they fabricated an aligned poly-L-lactic acid (PLLA) fibrous sheet, which was then modified with laminin and FGF-2. The product showed fiber distribution that was bidirectional and a potential bio-component for cell migration. When compared to the sheets that were identical except alignment, neurite extension from dorsal root ganglion increased approximately fourfold, and migration of dermal fibroblast was 1.5 times higher. However, horizontal alignment of fibers and cells were observed to inhibit cell migration, and this highlights the significance of fiber orientation in cell migration. Lee et al. introduced one of the earlier applications of aligned fibrous sheets [39]. In their approach, aligned PLLA nanofiber was prepared with a high-speed collector (2000 rpm). After polydopamine modification, the migration speed of mesenchymal stem cell was 10 times faster in vitro in the direction of the fiber. When this scaffold was implanted in a mouse calvarial defect model, the recovery speed of the defects in the host cells was 3 times faster than scaffolds with fibers that were not aligned. In short, aligned fibrous sheets have been demonstrated to accelerate overall tissue regeneration by guiding recruitment of host cells toward defect. The significance of aligned fibrous sheet in defect healing was once again emphasized by Liu et al. [40]. In their experiment, they observed the behavior of annulus fibrosus-derived stem cells on aligned fibrous sheets. The results showed that aligned fibrous sheets allowed higher gene and protein expression as compared to non-aligned fibrous sheets, and the produced collagen-I was oriented in the direction of the electrospun fiber. Thus, they concluded that the fiber orientation can influence the differentiation of the stem cells as well as migration.

9.4 Radially Aligned Underlying Structures for Inducing Directed Migration from All Fronts of the Defect Boundary Toward the Center

Many reports have been produced applicable for tissue regeneration promoted via patterned surfaces or nanofibrous platform, and the application may be limited in practice particularly in recruiting host cells to the defect. Bidirectional migration with one-way guidance has been observed only through linear patterns and aligned nanofibers [41–44]. As like the calvarial defect, even though it is just a defect model, bidirectional recruitment of the host cells is not enough to cover the wide or irregular defect. An innova-

tive design can significantly expedite overall healing process if it can recruit host cells from all fronts of the boundary toward the center. A radial topographical design has been proposed with a substrate where the surface structure is oriented toward the substrate center. Considering the results of previous studies, the alignment and migration of cells are influenced by underlying surface topography. Therefore, the designed pattern can guide the movement of cells from the distal end of the scaffold to the center and finally can suggest great scenarios for shortening the recovery time of a defect. Several studies have demonstrated the usefulness of this design for tissue regeneration.

9.4.1 Radially Aligned Nanofibers

A radially aligned nanofiber structure proposed by Xie et al. may be a great option for addressing the concerns we have discussed so far because it recruits host cells from all directions at the edge of defects to the center of scaffolds [45]. In the structure, an electrospinning collector was reconstructed with a core electrode (metal pin) and an edge electrode (metal ring) in consideration of electric fields. During electrospinning, flying electrospun polycaprolactone (PCL) fibers were stacked over the metal and the metal ring in high electrical conductivity, which resulted in a PCL nanofiber sheet with radially and evenly aligned fibers. When fibroblasts were seeded at the peripheral region of the scaffold, cells migrated toward the center following the direction of the fibers. The authors argued that their radially aligned fibrous sheets accelerate overall tissue regeneration through enhanced cell migration.

In addition, radially aligned nanofibers were used to create gradient of growth factors. As discussed in the previous section, radially aligned electrospun sheets promote cell migration toward the core region of defects, and its effect may compound if a gradient of growth factors is integrated into the system. This combination system was tried by Li et al. [46]. They fabricated radially aligned collagen/PCL nanofibers in a manner like Xie et al. and found that the density of fibers at the center and at the end was different. This led them to hypothesize that a gradient of growth factors emerges starting from the center toward the outer edge when the same amount of growth factor was introduced. They reported that the density of stromal cell-derived factor 1α (SDF1α) and the released amount of SDF1α were higher if closer to the center of scaffold. This radially aligned system with growth factor gradient exhibited their potential in regulating the migration of neural stem cells. Radially aligned sheet was successful in promoting the cell migration as compared to the random fiber. This migration was re-accelerated by the introduced SDF1α gradient. The radially aligned nanofiber with the growth factor gradient prepared in this way was able to control the migration of the cell toward the center part more rapidly before and after the introduction of the growth factor that was occurred by synergistic effect of the underlying structure and the growth factor gradient.

There were still further improvements to radially aligned fibrous sheets. Shin et al. addressed an issue of scaffold handling that rendered radially aligned fibrous sheets less practical (Fig. 9.3a) [47]. They increased the thickness of radially aligned fibrous sheets by adjusting the spinning condition so that the structure of the scaffolds would remain even when soaked in water. The increased thickness improved the mechanical property of the scaffolds, enabling to be useful for bone regeneration. Their scaffold was further modified with polydopamine to enhance cell affinity, which promoted overall cell adhesion and proliferation. Migration of human mesenchymal stem cell (hMSC) toward the center of the scaffolds was accelerated by both underlying topography and polydopamine modification. The manufacturing system for radially aligned fibrous sheet was utilized to develop transparent hemispherical 3D nanofibrous scaffolds for cornea regeneration. As demonstrated by Kim et al., this modified collector could generate radially aligned and hemispherical 3D nanofibrous structures. Along the fiber, the scaffold could align rabbit corneal cells, the migration of which was promoted toward the core (Fig. 9.3b) [48].

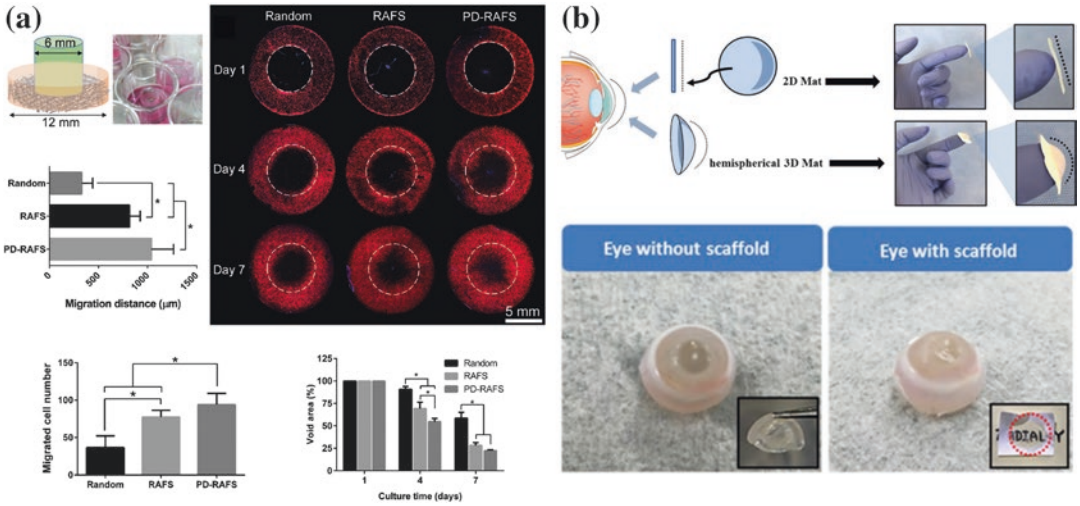

Fig. 9.3 Radially aligned fibrous scaffolds for guiding cell migration. (**a**) Radially aligned PLLA fibrous scaffolds provided a guiding path for the cells seeded at the border of the scaffolds. A cell-free void area was generated using a PDMS cylinder (6 mm diameter and 10 mm height) and traced the cell-free void areas following 7 days of culturing (F-actin-stained cells were scanned over the entire surface with a confocal laser scanning microscope). Directional cell migration (migrated cell number, migration distance, and void area) toward the center of the scaffolds was accelerated depending on the underlying topography and modification (reprinted by permission from Royal Society of Chemistry: Journal of Materials Chemistry B, copyright. [2017] Shin et al. [47]), and (**b**) radially aligned and hemispherical 3D nanofibrous structures were considerably fitted the curvature of the eyeball and allowed the alignment and migration of rabbit corneal cells toward the core the scaffolds. (Reprinted by permission from Springer Nature Ltd.: Scientific Reports, copyright. [2018] Kim et al. [48])

9.4.2 Radially Aligned Patterns

Patterning technique is another method for fabricating radial structures. Yoon et al. fabricated topographically defined implants with micropatterns (line and radial with 5 μm of width and depth) for bone tissue regeneration and evaluated the direction of cell migration (Fig. 9.4). The calcium phosphate-coated patterns regulated the orientation of MC3T3-E1 osteoblast following the pattern direction. The migration rates with the radial, line, and flat patterns were approximately 30, 20, and 5 μm/h, respectively, as observed for 2 days. The effectiveness of the patterned implant in recruiting host cells was evaluated in the mouse calvarial defect model. Then the radial pattern was implanted, and a 4 millimeter bone defect was completely recovered with a new bone in 7 weeks. In contrast, the flat and line patterns accomplished only partial healing, suggesting that radial structure can promote the regeneration of bone defect by allowing the directed cell migration toward the center of the scaffold [49].

9.5 Conclusions

Over the past two decades, tissue engineering and regenerative medicine research has continued to evolve to reach the larger goal of improving the quality of human lives. Various basic technologies developed for organ regeneration from theoretical stages to in vivo trials can be contributive. In this chapter, we discussed a few modern tissue engineering methods that control directional migration of cells among several techniques. Patterning and electrospinning have made it possible to control directed cell migration, which was not possible when we hand only the early 3D porous scaffolds. In addition, radially aligned topological cues for rapid reconstruction of irregularly shaped defects are thought to accelerate host cell migration at all front of the bound-

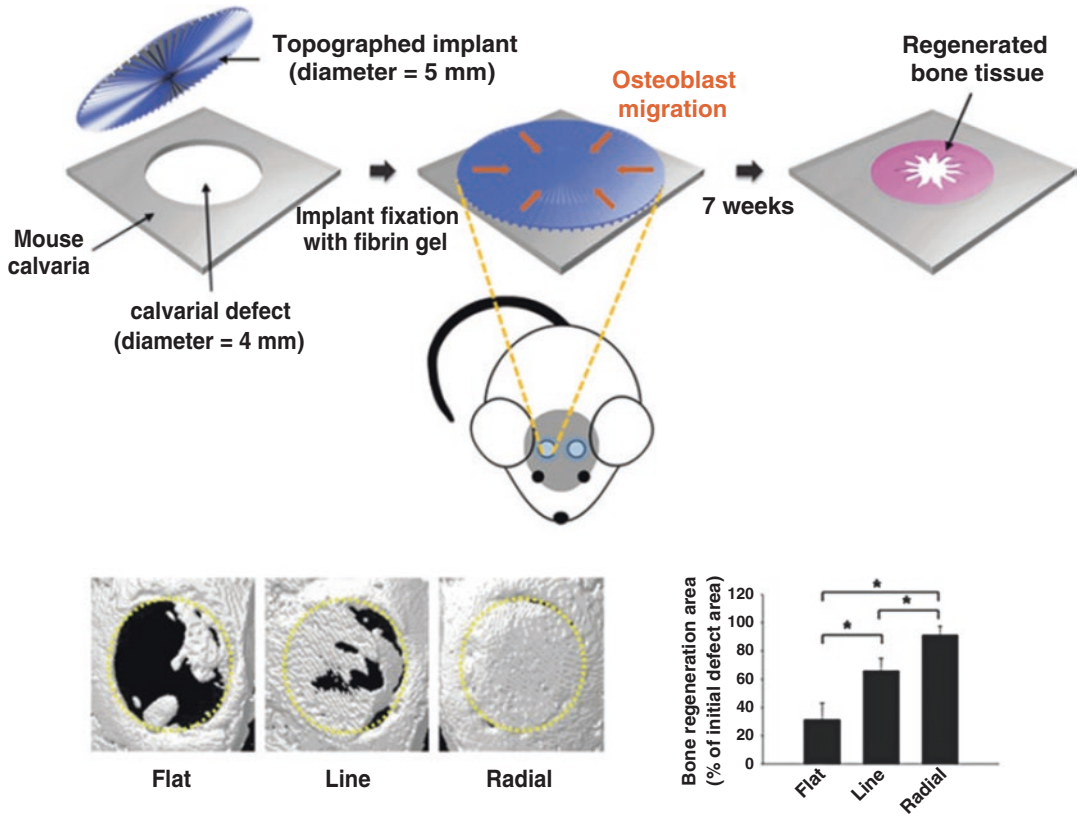

Fig. 9.4 Radial pattern for regenerating the bone defect. Yoon and his colleagues investigated the regenerating efficiency of the micropatterned substrates using a mouse calvarial defect model. Even though line pattern improved the migration of seeded MC3T3-E1 unidirectionally, radial pattern enabled the seeded cells at the periphery migrate faster toward the core of the scaffolds at every location, and almost complete recovery of the defect was achieved within 7 weeks after the implantation of the scaffolds. (Reprinted by permission from Mary Ann Liebert, Inc.: Tissue engineering A, copyright. [2016] Yoon et al. [49])

ary to accelerate tissue regeneration. It can be helpful for achieving the ultimate goal as a fundamental technology.

Acknowledgment This work was supported by a grant from the National Research Foundation (NRF) of Korea, which is supported by the Korean government (MEST) (NRF-2017R1D1A1B03031656 to Y.M.S.), and a grant from the Ministry of Trade, Industry and Energy (MOTIE) (Grant No. 10047811 to H.J.C).

References

1. Chan BP, Leong KW (2008) Scaffolding in tissue engineering: general approaches and tissue-specific considerations. Eur Spine J 17(4):467–479
2. Ikada Y (2006) Challenges in tissue engineering. J R Soc Interface 3(10):589–601
3. Kim TG, Shin H, Lim DW (2012) Biomimetic scaffolds for tissue engineering. Adv Funct Mater 22(12):2446–2468
4. Daley WP, Peters SB, Larsen M (2008) Extracellular matrix dynamics in development and regenerative medicine. J Cell Sci 121(3):255–264
5. Richert L, Boulmedais F, Lavalle P et al (2004) Improvement of stability and cell adhesion properties of polyelectrolyte multilayer films by chemical cross-linking. Biomacromolecules 5(2):284–294

6. Matsuoka M, Akasaka T, Hashimoto T et al (2009) Improvement in cell proliferation on silicone rubber by carbon nanotube coating. Biomed Mater Eng 19(2–3):155–162
7. Zhang Y, He Y, Bharadwaj S et al (2009) Tissue-specific extracellular matrix coatings for the promotion of cell proliferation and maintenance of cell phenotype. Biomaterials 30(23):4021–4028
8. Ren YJ, Zhang S, Mi R et al (2013) Enhanced differentiation of human neural crest stem cells towards the Schwann cell lineage by aligned electrospun fiber matrix. Acta Biomater 9(8):7727–7736
9. Kheradmandfard M, Kashani-Bozorg SF, Jungsung L et al (2018) Significant improvement in cell adhesion and wear resistance of biomedical β-type titanium alloy through ultrasonic nanocrystal surface modification. J Alloys Compd 762:941–949
10. Kim TG, Park TG (2006) Biomimicking Extracellular Matrix: Cell adhesive RGD peptide modified electrospun poly(D,L-lactic-co-glycolic acid) nanofiber mesh. Tissue Eng 12(2):221–233
11. Shin YM, La WG, Lee MS et al (2015) Extracellular matrix-inspired BMP-2-delivering biodegradable fibrous particles for bone tissue engineering. J Mater Chem B 3(42):8375–8382
12. Moulisová V, Gonzalez-García C, Cantini M et al (2017) Engineered microenvironments for synergistic VEGF – integrin signalling during vascularization. Biomaterials 126:61–74
13. Lee YB, Shin YM, Lee J et al (2012) Polydopamine-mediated immobilization of multiple bioactive molecules for the development of functional vascular graft materials. Biomaterials 33(33):8343–8352
14. Xie Z, Paras CB, Weng H et al (2013) Dual growth factor releasing multi-functional nanofibers for wound healing. Acta Biomater 9(12):9351–9359
15. Ku SH, Lee SH, Park CB (2012) Synergic effects of nanofiber alignment and electroactivity on myoblast differentiation. Biomaterials 33(26):6098–6104
16. Feng J, Zhang D, Zhu M, Gao C (2017) Poly(L-lactide) melt spun fiber-aligned scaffolds coated with collagen or chitosan for guiding the directional migration of osteoblasts in vitro. J Mater Chem B 5(26):5176–5188
17. Shin YM, Shin HJ, Heo Y et al (2017) Engineering an aligned endothelial monolayer on a topologically modified nanofibrous platform with a micropatterned structure produced by femtosecond laser ablation. J Mater Chem B 5:318–328
18. Slater JH, Boyce PJ, Jancaitis MP et al (2015) Modulation of endothelial cell migration via manipulation of adhesion site growth using nanopatterned surfaces. ACS Appl Mater Interfaces 7:4390–4400
19. Vicente-Manzanares M, Webb DJ, Horwitz AR (2005) Cell migration at a glance. J Cell Sci 118(21):4917–4919
20. Paul CD, Mistriotis P, Konstantopoulos K (2016) Cancer cell motility: lessons from migration in confined spaces. Nat Rev Cancer 17:131–140
21. Rodriguez LL, Schneider IC (2013) Directed cell migration in multi-cue environments. Integr Biol 5:1306–1323
22. Ermis M, Antmen E, Hasirci V (2018) Micro and nanofabrication methods to control cell-substrate interactions and cell behavior: a review from the tissue engineering perspective. Bioact Mater 3(3):355–369
23. Jeon H, Koo S, Reese WM et al (2015) Directing cell migration and organization via nanocrater-patterned cell-repellent interfaces. Nat Mater 14:918–923
24. Jun I, Han H-S, Edwards JR et al (2018) Electrospun fibrous scaffolds for tissue engineering: viewpoints on architecture and fabrication. Int J Mol Sci 19(3):745
25. Sajeesh KMP, Lee J, Ahmad T et al (2015) Effects of immobilized BMP-2 and nanofiber morphology on in vitro osteogenic differentiation of hMSCs and in vivo collagen assembly of regenerated bone. ACS Appl Mater Interfaces 7(16):8798–8808
26. Barkefors I, Le Jan S, Jakobsson L et al (2008) Endothelial cell migration in stable gradients of vascular endothelial growth factor a and fibroblast growth factor 2: Effects on chemotaxis and chemokinesis. J Biol Chem 283:13905–13912
27. Hu B, Leow WR, Amini S et al (2017) Orientational coupling locally orchestrates a cell migration pattern for re-epithelialization. Adv Mater 29(29):1700145
28. Nam K-H, Kim P, Wood DK et al (2016) Multiscale cues drive collective cell migration. Sci Rep 6:29749
29. Raghavan S, Desai RA, Kwon Y et al (2010) Micropatterned dynamically adhesive substrates for cell migration. Langmuir 26:17733–17738
30. Lei Y, Zouani OF, Rémy M et al (2012) Geometrical microfeature cues for directing tubulogenesis of endothelial cells. PLoS One 7(7):e41163
31. Kim DH, Han KR, Gupta K et al (2009) Mechanosensitivity of fibroblast cell shape and movement to anisotropic substratum topography gradients. Biomaterials 30(29):5433–5444
32. Joo SH, Kim JY, Lee ES et al (2015) Effects of ECM protein micropatterns on the migration and differentiation of adult neural stem cells. Sci Rep 5:13043
33. Park JS, Kim DH, Kim HN et al (2016) Directed migration of cancer cells guided by the graded texture of the underlying matrix. Nat Mater 15:792–801
34. Jun I, Chung YW, Heo YH et al (2016) Creating hierarchical topographies on fibrous platforms using femtosecond laser ablation for directing myoblasts behavior. ACS Appl Mater Interfaces 8:3407–3417
35. Jun I, Kim KS, Chung YW (2018) Effect of spatial arrangement and structure of hierarchically patterned fibrous scaffolds generated by a femtosecond laser on cardiomyoblast behavior. J Biomed Mater Res A 106(6):1732–1742
36. Peng SW, Li CW, Chiu IM et al (2017) Nerve guidance conduit with a hybrid structure of a PLGA microfibrous bundle wrapped in a micro/nanostructured membrane. Int J Nanomed 12:421–432
37. Xie J, Liu W, Macewan MR (2014) Neurite outgrowth on electrospun nanofibers with uniaxial alignment:

the effects of fiber density, surface coating, and supporting substrate. ACS Nano 8(2):1878–1885
38. Patel S, Kurpinski K, Quigley R et al (2007) Bioactive nanofibers: synergistic effects of nanotopography and chemical signaling on cell guidance. Nano Lett 7:2122–2128
39. Lee J, Lee YJ, Hj C et al (2014) Guidance of in vitro migration of human mesenchymal stem cells and in vivo guided bone regeneration using aligned electrospun fibers. Tissue Eng Part A 20(15–16):2031–2042
40. Liu C, Zhu C, Li J et al (2015) The effect of the fibre orientation of electrospun scaffolds on the matrix production of rabbit annulus fibrosus-derived stem cells. Bone Res 3:15012
41. Ahmed M, Ramos T, Wieringa P et al (2018) Geometric constraints of endothelial cell migration on electrospun fibres. Sci Rep 8:6386
42. Kwon CG, Kim YJ, Jeon HJ (2017) Collective migration of lens epithelial cell induced by differential microscale groove patterns. J Funct Biomater 8(3):34
43. Luo B, Tian L, Chen N et al (2018) Electrospun nanofibers facilitate better alignment, differentiation, and long-term culture in an in vitro model of the neuromuscular junction (NMJ). Biomater Sci 6:3262–3272
44. Ottosson M, Jakobsson A, Johansson F (2017) Accelerated wound closure – differently organized nanofibers affect cell migration and hence the closure of artificial wounds in a cell based in vitro model. PLoS One 12:e0169419
45. Xie J, MacEwan MR, Ray WZ et al (2010) Radially aligned, electrospun nanofibers as dural substitutes for wound closure and tissue regeneration applications. ACS Nano 4:5027–5036
46. Li X, Li M, Sun J et al (2016) Radially aligned electrospun fibers with continuous gradient of SDF1 for the guidance of neural stem cells. Small 12(36):5009–5018
47. Shin YM, Shin HJ, Yang DH et al (2017) Advanced capability of radially aligned fibrous scaffolds coated with polydopamine for guiding directional migration of human mesenchymal stem cells. J Mater Chem B 5:8725–8737
48. Kim JI, Kim JY, Park CH (2018) Fabrication of transparent hemispherical 3D nanofibrous scaffolds with radially aligned patterns via a novel electrospinning method. Sci Rep 8:1–13
49. Yoon JK, Kim HN, Bhang SH et al (2016) Enhanced bone repair by guided osteoblast recruitment using topographically defined implant. Tissue Eng Part A 22(7–8):654–664

Part IV

Cutting-Edge Enabling Technology for Regenerative Medicine

10 Extracellular Vesicles: The Next Frontier in Regenerative Medicine and Drug Delivery

Md. Asadujjaman, Dong-Jin Jang, Kwan Hyung Cho, Seung Rim Hwang, and Jun-Pil Jee

Abstract

Extracellular vesicles (EVs) are nanosized membrane particles secreted by cells to convey intercellular information. In recent years, EVs have enticed scientists owing to their prevalent distribution, enormous possibility as therapeutic aspirants, and probable roles as disease biomarkers. As natural transporters in the endogenous communication system, they play a role in protein, lipid, miRNA, mRNA, and DNA transport. In this chapter, we recapitulate the roles of EVs in the vast field of regenerative medicine. This summary mainly describes the potential roles of EVs in the regeneration of extensively studied organs or tissues, such as the heart, kidney, lung, liver, skin, and hair. Furthermore, EV can also transport drugs and corroborate their uptake by target cells through endocytosis; therefore, this chapter also highlights the use of EVs in the field of drug delivery.

Keywords

Drug delivery · Endocytosis · Extracellular vesicles (EVs) · Regenerative medicine · Target cells · Therapeutic agents

Abbreviations

ALIX	ALG-2-interacting protein X
APP	Amyloid precursor protein
ARF6	ADP-ribosylation factor 6
ARMMs	Arrestin domain-containing protein 1-mediated microvesicles
CXCR4	CXC chemokine receptor 4
GAPDH	Glyceraldehyde 3-phosphate dehydrogenase
HSP70	Heat shock 70 kDa protein
HSPG	Heparan sulfate proteoglycan
ICAM	Intercellular adhesion molecule
LBPA	Lyso-bis-phosphatidyl acid
LFA1	Lymphocyte function-associated antigen 1
MHC	Major histocompatibility complex
PECAM1	Platelet-endothelial cell adhesion molecule
PLD	Phospholipase D
PrP	Prion protein

Authors Md. Asadujjaman and Dong-Jin Jang have equally contributed to this chapter

Md. Asadujjaman · S. R. Hwang · J.-P. Jee (✉)
College of Pharmacy, Chosun University, Gwangju, Republic of Korea
e-mail: jee@chosun.ac.kr

D.-J. Jang
Department of Pharmaceutical Engineering, Inje University, Gimhae, Republic of Korea

K. H. Cho
Department of Pharmacy, College of Pharmacy, Inje University, Gimhae, Republic of Korea

H. J. Chun et al. (eds.), *Bioinspired Biomaterials*, Advances in Experimental Medicine and Biology 1249, https://doi.org/10.1007/978-981-15-3258-0_10

ROCK	RHO-associated protein kinase
TCR	T cell receptor
TDP43	TAR DNA-binding protein 43
TFR	Transferrin receptor
TSG101	Tumor susceptibility gene 101 protein
TSPAN	Tetraspanin
VPS	Vacuolar protein sorting

10.1 Background

All cells except specialized cells secrete numerous kinds of membrane vesicles. These vesicles are categorized as extracellular vesicles (EVs) [1]. Initially, EV secretion was considered an elimination process of unnecessary compounds from the cells [2]. Nowadays, EVs are no longer considered carriers of only waste. They can exchange the components of nucleic acids, lipids, and proteins within cells. EVs also act as signaling vehicles in the homeostatic processes of normal cells or under pathological changes [3, 4]. Although all secreted membrane vesicles are known by the generic term "EV," they are, in fact, vastly heterogeneous (Fig. 10.1). Transmission electron microscopy, immune electron microscopy, and biochemical assays have provided insights into the biogenesis of secreted vesicles. Currently, membrane vesicles are broadly divided into two main categories: microvesicles and exosomes (Fig. 10.1a).

At first, the vesicles released by cultured cells were termed exosomes which later embraced to refer to reticulocytes that released membrane vesicles during the period of differentiation [2]. Exosomes are 30–150 nm-sized cup-shaped vesicles originating from fusion between the multivesicular body (MVB) and plasma membrane, releasing exosomes to the extracellular space (Fig. 10.1a–c) [5, 6]. At present, it is assumed that various types of cells secrete exosomes; however, in the mid-1990s, it was reported that only dendritic cells [7] and B lymphocytes [8] secrete exosomes. Microvesicles were once touted as "platelet dust" because they are secreted by platelets to normal plasma and serum [9]. In the past, microvesicles were considered mainly for their role in blood coagulation; however, at present, they are thought to play a role in the intercellular communication of several cell types. Usually, microvesicles range from 50 to 1000 nm in diameter. It is evident now that specific composition defines the fate and role of each type of EVs (Fig. 10.1d).

The endosomal system serves as the starting place of exosome biogenesis (Fig. 10.2). Endocytosis of plasma membrane-bound cargo leads to formation of early endosomes. MVBs, the mature form of early endosomes, fuse with lysosomes to vitiate their content. MVBs can also release their substances as exosomes by fusing with the cell plasma membrane in an exocytotic manner. A wide array of cells can secrete exosomes under normal and pathological conditions [11]. Rab GTPase regulates the fusion of MVBs with the cell membrane and regulates the spatiotemporal traffic of vesicles. Moreover, exosome formation at the endosomes requires the endosomal sorting complex required for transport (ESCRT) machinery [12].

It has been suggested that ESCRT-dependent and ESCRT-independent signals determine exosome sorting. Exosome formation is carried out by syndecan heparin sulfate proteoglycans and their cytoplasmic adaptor, syntenin. The mechanisms mediating exosome uptake involve fusion of vesicles with the cellular membrane of recipient cells, juxtacrine signaling via receptor-ligand interactions, and phagocytosis-induced endocytosis. Although the specific receptors involved are still unclear, intercellular adhesion molecule 1 (ICAM-1) protein and transmembrane protein and Tim 1/4 are considered potential receptors for exosomal uptake [14].

Cell type and cell microenvironment determine the molecular composition of exosomes. Topography, mechanical properties, and secreted exosome's protein cargo regulator naming biochemical stimuli are the component of microenvironment. Nanosized exosomes are enriched in

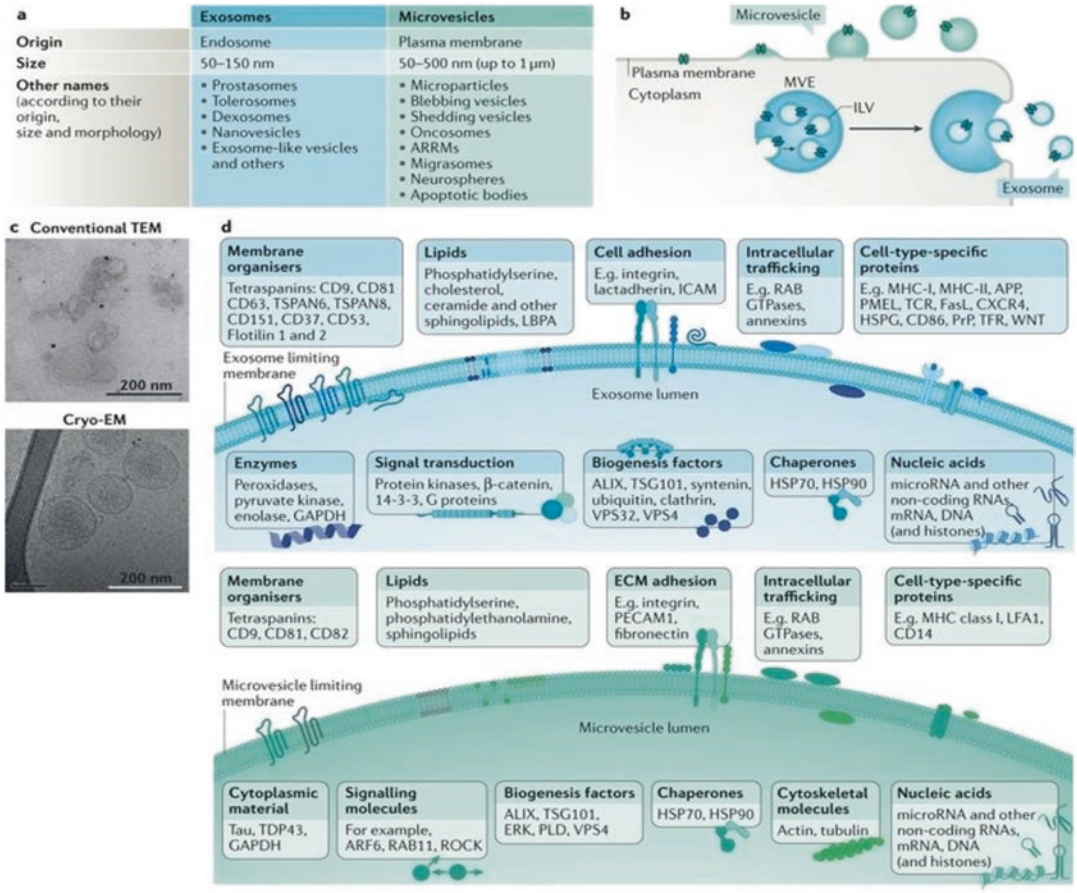

Fig. 10.1 Extracellular vesicle main features. (**a**) Extracellular vesicles: two distinct classes – exosomes and microvesicles. (**b**) Formation of extracellular vesicles. (**c**) Cup-shaped morphology (top panel) by conventional transmission electron microscopy (TEM). Round structures by cryo-electron microscopy (cryo-EM). (**d**) Extracellular vesicle composition [10]

bilayer lipids, proteins, and nucleic acids. These lipid bilayer particles contain different lipid content than the parent cell. Most exosomes include tetraspanins (CD9, CD63, and CD81), which are the commonly used marker; adhesion molecules; heat shock proteins (HSP); and the endosomal sorting complexes required for transport (ESCRT) pathway markers, namely, ALIX and TSG101 (Fig. 10.3).

All body fluids, namely, blood, bronchial lavage, cerebrospinal fluid, lymph, mucus, tears, semen, ascites, milk, urine, sweat, and even saliva, can be a source of exosomes in vivo [16–29].

At present, several methods, namely, differential centrifugation, filtration, immunomagnetic isolation, size exclusion chromatography, and polymer precipitation, are being used to isolate exosomes (Fig. 10.4). All methods have some advantages and limitations. Among these methods, differential centrifugation is the widely used and gold standard method for isolation of exosomes from biological fluids [30, 31]. However, the immunomagnetic isolation method can be used to obtain ultrapure exosomes or to isolate a subpopulation of exosomes by targeting exosomal markers [32].

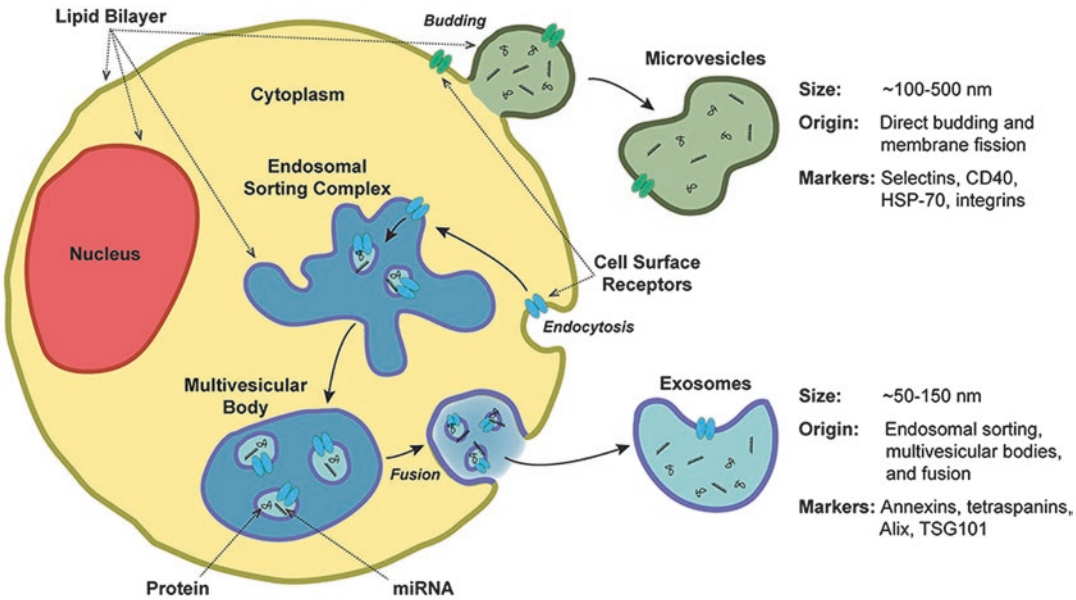

Fig. 10.2 Release of extracellular vesicles, their structure, and composition [13]

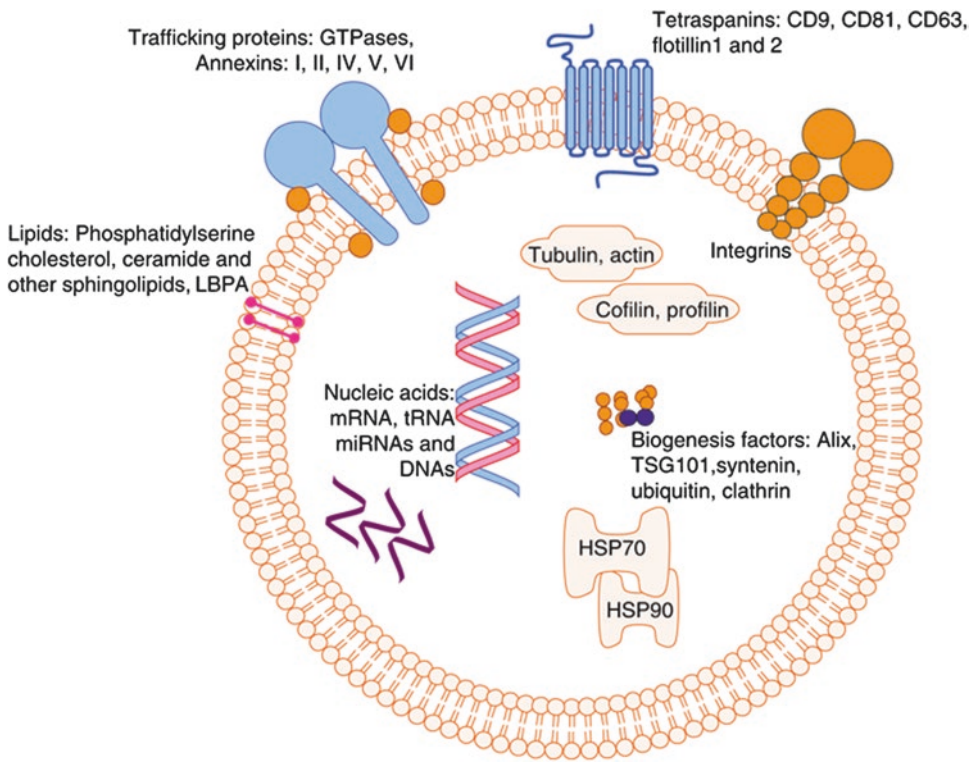

Fig. 10.3 Schematic presentation of exosome's molecular composition [15]

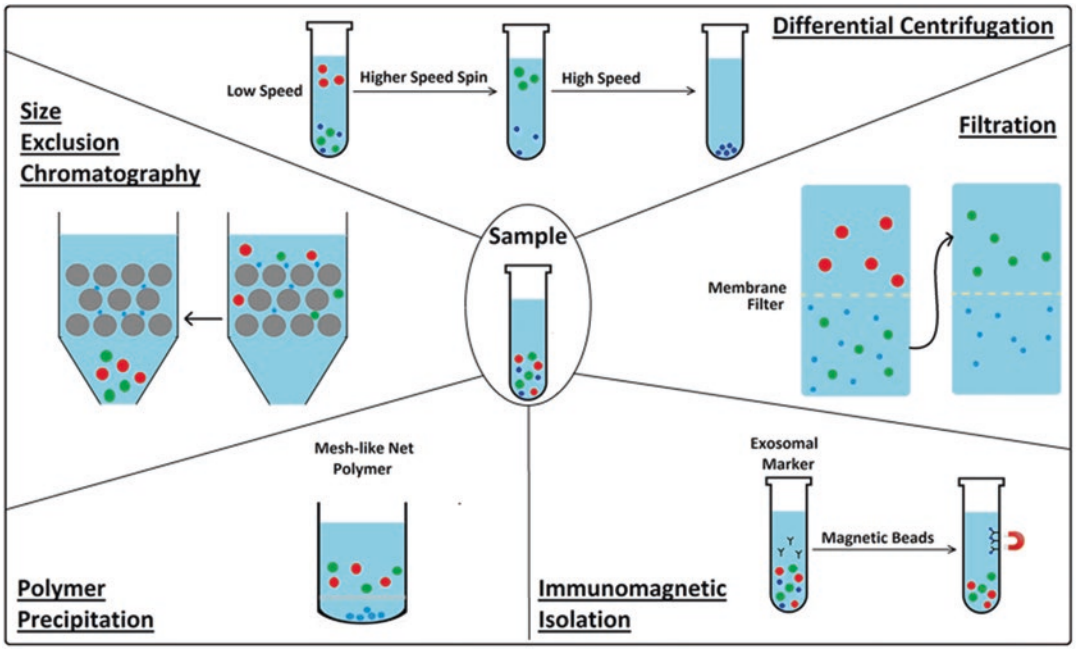

Fig. 10.4 Schematic diagram of exosome isolation [33]

10.2 Therapeutic Activities of EVs

10.2.1 EVs in Regenerative Medicine

Although the scrutiny of EVs has an eon of historical standing, the number of comprehensive studies on EVs was limited because the procedures to study nanosized vesicles are poorly developed. However, along with technical advancements in EV studies, their importance has been revealed, attracting the attention of many researchers.

10.2.1.1 Lung Regeneration

Studies have revealed that the respiratory system can lead to regeneration of lost or damaged cells. Usually, the adult lung is remarkably calm in unperturbed condition. However, any injury to the lung activates the populations of progenitor cells or other cells to re-enter the cell cycle [34]. In several experimental models, mesenchymal stem cells (MSCs) have been found to protect against lung injury. However, as the number of donor cells is low, it is assumed that paracrine mechanisms facilitate these beneficial effects [35]. In addition, the lung is unique to other organs or tissues because it allows both intravenous and inhalation deliveries of stem cells [36]. In 2007, Gupta and colleagues reported intratracheal MSCs have comparable effectiveness to that of intravenous MSCs in alleviating acute lung injury in mice [37]. This was one of the earliest studies comparing intratracheal and intravenous delivery of MSCs. After that, many studies have used and compared these two routes for other deliveries. However, the route with the highest efficacy is still debatable [38–42]. Most studies showed that stem cell-derived extracellular vesicles act as paracrine factors that support and enhance lung regeneration rate, irrespective of delivery route. Recently, it was shown that human MSC-derived microvesicles have similar efficacy as that of stem cells in ameliorating bacterial pneumonia-induced lung inflammation and in improving survival from *E. coli* pneumonia in a murine model [43].

Wills et al. showed that MSC-derived exosomes also alleviate bronchopulmonary dysplasia, improve lung function, decrease fibrosis, and ameliorate pulmonary hypertension [44]. They

also reported that these exosomes, even at a single dose, restore normal lung architecture, providing long-term beneficial effects on lung function in a hyperoxia-induced pulmonary hypertension and bronchopulmonary dysplasia mouse model. They also assumed that immunomodulatory effects help them achieve this efficacy. Several studies revealed that specific miRNAs from EVs are vital to lung repair in vivo, mainly in hypoxia-induced pulmonary hypertension [45], influenza [46], and ventilator-induced lung injury [47].

In another study, miRNA regulations during the early and late stages of repair were analyzed in an influenza-infected mouse model [46]. miR-21, miR-290, let-7, and miR-200 were identified as the most important miRNAs that start the regeneration process. miR-21 and let-7 also exert anti-inflammatory properties, providing prominent beneficial effects against uncontrolled inflammation in the regenerating lung. Pulmonary inflammation and hypertension are associated with activation of hypoxic signaling, which can be prevented by exosomes. Lee and coworkers used exosomes originating from umbilical cord-derived MSCs in a hypoxia-induced pulmonary hypertensive mice model and found that the treatment suppressed hypoxia-induced pulmonary inflammation and promoted vascular remodeling in a dose-dependent manner; they also showed that mouse lung fibroblast-derived exosomes, compared to exosomes derived from MSCs, have no protective activity against pulmonary hypertension [45]. This action was attributed to the presence of miR-16 and miR-21 in MSC-derived exosomes. Serotonin transporter (SERT) expression is reduced by miR-16 protein, which is needed to treat pulmonary edema [48]. Exosomes derived from MSC reduce the expression of pro-inflammatory cytokine IL-6. By suppressing the hyperproliferative pathways, including STAT3-mediated signaling and hypoxia-induced activation of the STAT3 gene, MSC-derived exosomes inhibit pulmonary hypertension [45].

Moreover, specific mRNAs are effective against acute lung injury induced by endotoxin. In *Escherichia coli* endotoxin-induced acute lung injury mouse models, intratracheal administration of microvesicles reduced inflammation and prevented pulmonary edema formation in the injured alveoli. Human bone marrow-derived MSCs were used to generate microvesicles containing the mRNA of keratinocyte growth factor (KGF), which was then found to be a key factor in the repair process; thus, the mRNA expression of KGF played a key role in ameliorating alveolus injury [49].

A recent study revealed that in a sepsis mouse model, the immunomodulatory effects of human umbilical cord MSC-derived exosomes are highly dependent on the role of miR-146a protein [50]. In a ventilator-induced lung injury mouse model, inhibition of IRAK-1 and TRAF-6 of miR-146 suppresses the expression of alveolar macrophages IL-1β, IL-6, and TNF-α [47]. Moreover, miR-146a reduces the expression of inflammatory genes and deters inflammation induced by endotoxin in mice [51]. Through the toll-like receptor signaling pathway, miR-146a also reduces microbial and mechanical inflammations in lung epithelia [52]. To improve lung regeneration after injury with exosomes, exosomes must be enriched with miR-146a protein. Precise and prudent enrichment of exosomes with miR-146a protein will define the fate of exosomes as a treatment for lung regeneration in the near future.

10.2.1.2 Cardiac Regeneration

Exosomes have great potential in the treatment of myocardial ischemia. Exosomes from cardiosphere-derived cells were injected into the hearts of mouse suffering from ischemia injury, and they were shown to prevent apoptosis and stimulate the proliferation of cardiomyocytes [53]. The authors also summarized that these positive properties are closely associated with miR-146a content in exosomes. Teng and colleagues used exosomes from bone marrow mesenchymal stem cells (BMSCs). They found that these exosomes significantly enhance tube formation of human umbilical vein endothelial cells and subdue the T cell proliferation in vitro. They also observed infarct size reduction and well-maintained cardiac function in rats induced with acute myocardial infarction following treatment

with mesenchymal stem cell (MSC)-derived exosomes [54]. Khan et al. used exosomes (mES-Ex) derived from mouse embryonic stem cells. They found that these exosomes contribute to endogenous myocardial repair and improve cardiac function post-myocardial infarction. They found that neovascularization and cardiomyocyte survival were improved in mice after intramyocardial administration of mES-Ex at the onset of myocardial infarction and then used microRNA array analysis to investigate the mechanisms associated with these beneficial effects. The results showed that the regenerative potential of mES-Exis related to the delivery of embryonic stem cell-specific miR-294 to cardiac progenitor cells (CPCs) [55].

Zhao and coworkers showed that exosomes from human umbilical cord mesenchymal stem cells (hUCMSCs) protect myocardial cells from apoptosis and stimulate angiogenesis, thereby restoring the cardiac systolic function in acute myocardial infarction rat models. These effects are possibly associated with modifications in the expression of Bcl-2 family proteins [56].

Agarwal et al. reported that factors such as donor age and hypoxia level affect the efficacy of human CPC-derived exosomes. They investigated the regenerative character of exosomes derived from human CPCs in a rat model with myocardial ischemia-reperfusion injury. In their experiment, human CPCs from children of various ages were isolated and then cultured under normal and hypoxic conditions. Exosomes were then isolated from the conditioned media and administered to rats. The results showed that, regardless of oxygen level in the culture, exosomes from neonate CPCs improve cardiac function by improving angiogenesis and decreasing fibrosis. On the contrary, exosomes from the CPCs of older children and cultured in hypoxic condition only exert ameliorative effects [57].

10.2.1.3 Renal Regeneration

Vinas et al. found that endothelial colony-forming cell (ECFC)-derived exosomes are rich in miR-486-5p. ECFCs were derived from human umbilical cord blood. They found that delivery of PTEN-targeting exosomes derived from ECFCs led to reduction of ischemic acute kidney injuries [58].

Borges and colleagues reported that hypoxic conditions help tubular epithelial cells to produce exosomes that are rich in transforming growth factor β1 (TGF-β1) mRNA. These exosomes can trigger fibroblasts to initiate the response needed for fibrotic repair. This result suggested that TGF-β1 mRNA delivery by exosomes induces a prompt response to trigger tissue regeneration following hypoxia injury. The authors also reported the potential of exosome-targeted treatments in protecting against tissue fibrosis [59]. Tomasoni et al. found that hBMSC-released exosomes promote the proliferation of proximal tubular epithelial cells damaged by cisplatin via horizontal transfer of IGF-1 receptor mRNA [60]. Zhou et al. reported that hUCMSC-derived exosomes ameliorate cisplatin-induced acute kidney injuries in rats by decreasing apoptosis and renal oxidative stress and increasing renal epithelial cell proliferation [61].

Jiang and colleagues showed that kidney injury induced by streptozotocin is alleviated by weekly intravenous injection of exosomes from urine-derived stem cells (USCs-Exo) via the tail. They also suggested that this treatment obviously prevents podocyte apoptosis as well as stimulates vascular regeneration and cell survival [62].

10.2.1.4 Hepatic Regeneration

Before Momen-Heravi and coworkers found that alcoholic hepatitis patients contain higher plasma levels of exosomes than the healthy population, Tan and colleagues investigated the potential of MSC-derived exosomes in liver regeneration in mouse models of liver injury induced by carbon tetrachloride. They found that treatment with MSC exosomes significantly attenuates liver injury induced by CCl_4. It was assumed that the activation of proliferative and regenerative reactions helps achieve this effect [63, 64]. Other groups of researchers have tried to elucidate the role of exosomes in liver regeneration. Nojima et al. reported that in acute liver injury, exosomes derived from hepatocytes promote in vitro proliferation of hepatocytes and in vivo liver regeneration [65]. The mechanism may involve targeting

of hepatocytes by neutral ceramidase and sphingosine kinase 2 (SK2) exosomal transfer. They reported that the circulating levels of exosomes post-liver injury also increased along with the proliferation-promoting effects.

More recently, Yan et al. reported that systemic administration of exosomes derived from hUCMSCs (hUCMSC-Ex) effectively rescues mice from liver failure induced by CCl_4. It was assumed that this effect was closely related with glutathione peroxidase 1 derived from hUCMSC-Ex [66]. Nong and coworkers also studied the potential of mesenchymal stromal cell-derived exosomes in regeneration. They used MSC exosomes (hiPSC-MSCs-Exo) from human-induced pluripotent stem cells of hepatic ischemia-reperfusion injury [67]. Although the molecular mechanism is not clear, it was assumed that these exosomes exert their regenerative effect by mitigating oxidative stress responses, suppressing inflammatory reactions, and preventing cellular apoptosis.

10.2.1.5 Neural Regeneration

Research on EVs has led to development in the research field of neural regeneration. Several regenerative effects of exosomes on the nerves and neurons have been reported. Frohlich and coworkers found that glutamate-stimulated oligodendrocyte-derived exosomes promote the survival of oxygen- and glucose-deprived neurons [68]. Xin and colleagues were the first to mention a communication between MSCs and brain parenchymal cells. They stated that exosomes from multipotent mesenchymal stromal cells enhance neurite outgrowth by delivering miRNA-133b to neural cells [69]. Takeda et al. found that exosomes from differentiating neuronal cells induce neuronal differentiation in human MSCs [70]. The authors also suggested that these exosomes comprise miRNAs, which subsequently stimulate neuronal differentiation.

El Bassit et al. also reported the pro-regenerative effect of exosomes on injured HT22 neuronal cells [71]. They used human adipose-derived stem cell (hASC)-derived exosomes. The results showed that hASC-derived exosomes enhance neuronal survival and proliferation by elevating the expression of PKCδII in HT22 cells. In another study, MALAT1, a long noncoding RNA obtained from hASC-derived exosomes, was reported to mediate splicing of PKCδII, thereby increasing its expression; this study also concluded that insulin stimulation further enhances the regenerative effect of hASC-derived exosomes. Recently, Mead and coworkers found that BMSC-originated exosomes significantly promote the survival of retinal ganglion cells and the regeneration of their axons. They also reported that these effects might be correlated with the miRNA effector molecule argonaute-2 [72].

Without axonal regeneration, spinal cord injuries may lead to permanent damage. Schwann cells (SCs) mainly support axonal regeneration in the peripheral nervous system. SCs can dedifferentiate and proliferate in response to nervous damage. They can also efficiently direct axons to their original target tissues. Lopez-Verrilli et al. treated nerve injury rat models with exosomes from dedifferentiated SCs [73]. They reported that these exosomes are specifically internalized by axons, consequently increasing axonal regeneration in vitro. The authors also found increasing regeneration of sciatic nerve injury in a Sprague Dawley rats, although the underlying molecular mechanism remains unknown. However, they reported that exosomes derived from SCs trigger axon regeneration. It was believed that RhoA, a GTPase, could hinder axon elongation and stimulate growth cone collapse. The agonist of retinoic acid receptor β (RARβ) could recover the locomotor and sensory responses of rat cervical avulsion models [74]. Further, cytoplasmic phosphorylation decreases the activity of major negative regulators of neuronal regeneration, such as PTEN, in RARβ agonist-treated neurons. Furthermore, neurons treated with an RARβ agonist secrete higher exosomes than nontreated neurons. These exosomes prevent scar formation by reducing the proliferation of astrocytes. RARβ signaling by neuronal and neuronal-glial regenerative effects ultimately leads to axonal regeneration in the spinal cord.

Zhang and coworkers also investigated the regenerative potential of exosomes on traumatic

brain injury in rats. They used systemic administration of human bone marrow mesenchymal stem cell (hBMSC)-derived exosomes [75]. The results showed enhanced endogenous angiogenesis and neurogenesis in rats, as well as attenuation of neuroinflammation, suggesting that exosomes from hBMSCs improve functional recovery in rats suffering from traumatic brain injury. Zhang et al. in another experiment found that compared to native MSC exosomes, tailored MSC exosomes carrying elevated miR-17-92 cluster lead to more enhanced axonal growth [76]. They reported increased individual members of this cluster and that tailored MSC exosomes activate the PTEN/mTOR signaling pathway in the recipient neurons. They concluded that tailored exosomes can transport their selective payload of miRNAs into target signals and activate it in the recipient neurons.

10.2.1.6 Cutaneous Regeneration

The skin frequently suffers from acute and chronic wounds. Extensive burns or diabetic skin ulcerations are one of them. These wounds incur physical and mental distresses in the affected individuals. Numerous scientists have attempted to accelerate the process of wound healing, but still there is no definitive solution. Treatment of traumatized soft tissue faces two major challenges in the form of prolonged healing and scar formation. In tissue regeneration, adipose mesenchymal stem cells (ASCs) play a fundamental role. Several recent studies have reported that stem cell-secreted exosomes may contribute to paracrine signaling. Hu et al. investigated ASC-derived exosomes (ASCs-Exos) and their functions in cutaneous wound healing. Their research provides a new insight to the use of ASCs-Exos in repairing soft tissues [77]. After being internalized by fibroblasts, ASCs-Exos stimulate cell migration and proliferation and collagen synthesis in a dose-dependent manner. The authors also found significant acceleration in cutaneous wound healing in vivo in mouse models of skin wound, suggesting that ASCs-Exos can accelerate cutaneous wound healing by optimizing the characteristics of fibroblasts.

Liang et al. found that human adipose-derived MSC (adMSC) exosomes considerably promote angiogenesis of endothelial cells in vitro and in vivo [78]. Furthermore, these exosomes relocate miR-125a to endothelial cells, thereby downregulating angiogenic inhibitor delta-like 4.

Zhao and coworkers tested the effect of human amniotic epithelial stem cell-derived exosomes on the healing of full-thickness skin defects in rats [79]. After isolation, different concentrations of exosomes were injected subcutaneously around the wound site. The results showed that human amniotic epithelial stem cell-released exosomes promote the migration and proliferation of fibroblasts. They also found that the accelerating effect on the healing of full-thickness skin defect was dose-dependent. Zhang and colleagues found robust proangiogenic and wound healing activities of exosomes in diabetic rat models. They used endothelial progenitor cell exosomes derived from human umbilical cord blood [80]. Guo et al. reported that platelet-rich plasma-derived exosomes effectively induce the proliferation and migration of endothelial cells and fibroblasts, subsequently triggering angiogenesis and re-epithelialization in chronic cutaneous wound for treatment of chronic ulcer [81].

In 2014, Zhang et al. developed second-degree burn injury rat models to investigate the role of EVs in wound healing. Following subcutaneous injection at three sites, treatment with both human umbilical cord MSC (hucMSC)-derived EVs (200 μg) and hucMSC (1×10^6 cells suspended in 200 μl phosphate buffer solution (PBS)) leads to tremendous re-epithelialization, compared to treatment with human lung fibroblasts (HFL1) or exosomes from human lung fibroblasts (HFL1-Ex) [82]. Shabbir et al. (2015) reported that treatment with MSC-EVs leads to a dose-dependent increase in the growth of normal fibroblast cells. During treatment with MSC-EVs, improved migration of normal and diabetic wound fibroblasts was observed [83].

Burn injury is a predominant cause of cutaneous damage. Following burn injury, interleukin-1β (IL-1β) and tumor necrosis factor α (TNF-α) levels increase, whereas IL-10 level decreases significantly [84–86]. Li and

coworkers reported that hUCMSC exosomes effectively reverse the inflammatory reaction induced by burn injury [84]. Moreover, miR-181c in hUCMSC exosomes downregulates the TLR4 signaling pathway to alleviate inflammation associated with burn injury, thereby reducing excessive inflammation and enhancing tissue repair. Exosomes can also lead to controlled cutaneous regeneration in a bipolar manner. Zhang and coworkers found that hUC-MSC-derived exosomes repair damaged skin tissue by stimulating the Wnt/β-catenin signaling pathway during the initial healing stages of deep second-degree burn [87].

Han and coworkers revealed that corneal epithelial cell exosomes fuse with keratocytes and induce myofibroblast transformation in corneal wound [88]. Moreover, these exosomes can stimulate proliferation of endothelial cells and sprouting of aortic ring in vitro. Exosomes derived from epithelial cell might be involved in neovascularization processes and corneal wound healing, suggesting their potential as useful therapeutic interventions.

Timely and efficient repair of intestinal mucosal wound and alleviation of inflammation are very important in maintaining mucosal homeostasis. Intestinal epithelial cell (IEC)-derived exosomes have an important content, namely, annexin A1 (ANXA1). These exosomes enhance wound repair in IECs. These exosomes, which initiate repair of epithelial wound, can also be obtained from leukocytes after injury [89]. Zhang et al. reported that exosomes from human-induced pluripotent stem cells accelerate cutaneous wound healing by promoting collagen synthesis and angiogenesis in a dose-dependent manner (50 and 100 μg/ml) [90].

10.2.1.7 Hair Growth

Hair loss is a common medical problem with detrimental consequences on the quality of life of both men and women. In the treatment of hair loss, drug treatment provides short-term improvement, whereas hair follicle transplantation is costly, and the number of donors is low. Thus, an efficient and innovative treatment method is required urgently. Rajendran et al. explored the effects of EV treatment on the proliferation, migration, and growth factor expression in human dermal papilla (DP) cells. The authors used the EVs derived from mesenchymal stem cell (MSC-EVs). Treatment with MSC-EV increases the proliferation and migration of DP cell and elevated the expression of Bcl-2, phosphorylated Akt, and ERK levels in the cells. MSC-EV-treated DP cells also showed increased expression and secretion of IGF-1 and VEGF. Further, the authors intradermally injected MSC-EVs to mice, and the results showed enhanced conversion of telogen to anagen, as well as increased expression of versican, wnt3a, and wnt5a [91]. The results of this research suggested that MSC-EVs activate DP cells, prolong their survival, and induce growth factor activation in vitro, as well as promote hair growth in vivo.

Zhou and coworkers cutaneously injected exosomes derived from dermal papilla cells (DPC-Exos) into hair follicles at different stages of hair follicle cycle. DPC-Exos accelerates the onset of hair follicle anagen and delays catagen in mice. Furthermore, treatment with DPC-Exos enhances the proliferation and migration of outer root sheath cells, as well as stimulates expression of β-catenin protein and Sonic hedgehog (Shh) in vitro [92]. Thus, DPC-Exos play an important role in regulating and accelerating hair follicle growth, providing new insight to hair loss treatment.

10.2.1.8 EVs in Drug Delivery

EVs can transfer and circulate various active agents in the intercellular environment for a long period of time. EVs have high stability and specificity to the recipient, making them a promising therapeutic agent delivery system [93] that may replace polymer nanoparticles and liposomes, the current most prominent delivery systems. EVs can protect their load from deterioration, which is an important phenomenon in protein and RNA delivery within cells. In addition, EVs have low immunogenicity, no toxicity, and high tolerability by the host [94]. More importantly, they can deliver proteins, lipid, peptides, and nucleic acids, suggesting that therapeutic entities with diverse chemical nature can be delivered using EVs [95].

Usually, small interfering RNAs (siRNAs) are used in genetic therapy for genetic disorders. However, its use is limited owing to its low stability and tendency to degrade quickly in the systemic circulation. Interestingly, exosomes can act as delivery vehicles that protect and deliver siRNA to the target cells. Several experiments have assessed the potential of exosomes as candidate delivery vehicles to transport exogenous genetic materials, as well as the function of exosomes after the transport. Alvarez-Erviti et al. successfully utilized exosomes to deliver siRNA to mouse brain [96]. In another study, human exosomes were used to deliver siRNA to T cells and monocytes [97]; siRNA was introduced to exosomes isolated from different cell types, including the peripheral blood of healthy donors, TB-177 lung cancer cells, and HeLa cells, and then effective delivery of siRNA into peripheral blood mononuclear cells (PBMC) was confirmed by flow cytometry. It was observed that exosomal siRNA led to a decrease in MAPK-1 expression, indicating successful gene silencing. Although further investigation and consideration are needed to elucidate the function of exosomes in exogenous siRNA delivery, the result of this study clearly proves the proficiency of exosomes as a delivery system of genetic therapy.

Eukaryote gene protein RAD51 assists in repairing DNA double-strand breaks. This protein has been revealed as a potential target to repress the progression of abnormally proliferating cells in cancers [98]. The effect of exosome-delivered siRNA in knocking down RAD51 upon delivery to human cells was shown in vitro. Further, exosomes were isolated from HeLa cells and loaded with Alexa Fluor 488-labeled siRNA using chemical treatment. Flow cytometry and confocal microscopy revealed successful delivery of siRNA by the exosomes after co-culture with recipient cells (HeLa and HT1080 cells). The study also reported that the protein levels of RAD51 and RAD52 were decreased, which indicates their downregulation [99]. Exosomes derived from endothelial cells are associated with atherosclerosis and vascular inflammation. Exosomes loaded with siRNA were incubated with luciferase-expressing endothelial cells. Compared to the control groups, the cells treated with endothelial exosomes carrying siRNA showed lower luciferase expression. Taken together, these results showed that exosomes of endothelial origin have the potential to deliver exogenous agents to cells in vitro and remain functional at the targeted site [100].

miRNAs, a short form of noncoding RNA, bind to complementary sequences on targeted mRNAs and regulate post-transcriptional gene expression [101, 102]. Because exosomes are known to carry miRNAs naturally, exosomes may be potential as a therapeutic vehicle for miRNA delivery to targeted cells. Ohno et al. [103] used exosomes to deliver miRNA targeting the epidermal growth factor receptor (EGFR) of breast cancer cells. The elevated EGFR expression level in epithelial human tumors suggested the prospect of EGFR ligand as a cancer drug target [104]. miRNAs, such as lethal-7 gene (let-7a), act as a tumor suppressor. They impede cancer growth by decreasing the expression of RAS and high-mobility group AT-hook protein (HMGA2). To deliver let-7a to EGFR-expressing cancer tissues, epidermal growth factor (EGF) and EGFR-specific peptide (GE11) were fused onto the surfaces of let-7a-carrying exosomes [103]. GE11 or EGF was transfected into HEK-293 cells to generate GE11- and EPF-positive exosomes. Several experiments verified the ability of GE11- or EGF-positive exosomes to bind to EGFR in various breast cancer cell lines, including HCC70, HCC1954, and MCF-7. In addition, the researchers hypothesized that GE11-positive exosomes might be more suitable than EGF-positive exosomes for treating breast cancer in terms of inhibiting cancer cell proliferation.

In another study, the lipofection method was used to incorporate *let-7a* into GE11 exosomes, which was then intravenously injected to tumor-bearing mice. The results exhibited strong inhibition in the expression of HMGA2 in cancer cells, indicating that exosomes effectively transported their cargo to the target cells [103].

Recently, c(RGDyK)-engineered and curcumin-loaded exosomes were administered intravenously into an ischemic brain. By target-

ing the lesion area, the exosomes reduce inflammatory response and cellular apoptosis [105]. Furthermore, specific targeting of particular receptors or cell surface antigens can be realized by coupling the exosomes with a biological recognition factor [106].

Microvesicles (MVs) can also act as unique, cell-originated "liposomes" for disease treatment by effectively delivering therapeutic mRNA/proteins. Mizrak et al. generated microvesicles containing protein-cytosine deaminase (CD), which were fused with uracil phosphoribosyltransferase (UPRT) by transducing donor cells with CD-UPRT-EGFP (enhanced green fluorescent protein). Simultaneous injection of the prodrug 5-fluorocytosine and microvesicles containing CD-UPRT-mRNA/protein led to reduced tumor size and growth. The reason may be that 5-fluorocytosine is converted to 5-fluorouracil within tumor cells [107].

Epithelial-originated human tumors possess epidermal growth factor receptor (EGFR). GE11 peptide can bind to EGFR. Ohno and coworkers isolated tumor cells targeting GE11-positive exosomes and showed that let-7a-containing exosomes inhibit tumor development by targeting the tumor in mice models. Cells were transfected with let-7a miRNA to generate let-7a-containing exosomes [103]. miR-146b decreases glioma cell invasion and motility and decreases EGFR expression. Katakowski and coworkers isolated exosomes from MSCs, which were then transfected with miR-146b. Delivery of miR-146b-loaded exosomes reduced the growth of 9L glioma cells in vitro. It was also observed that 9L tumor volume was reduced in a primary brain tumor rat model [108].

Nanoparticles or liposomes are promising noninvasive drug delivery systems to the brain [109, 110]. However, owing to their immunogenicity, insufficient specificity, limited half-life, and post-penetration efficiency in the blood-brain barrier (BBB), these strategies are not extensively used in medical practice [111]. EVs are a potential strategy for delivery of therapeutic agents to the brain, in terms noninvasiveness [112].

EVs can penetrate the BBB; although the mechanisms of interaction between the BBB and exosomes are still unclear, there is evidence of exosome penetration to the BBB. Furthermore, exosomes can carry numerous elements to the brain, and BBB penetration by EVs is mainly facilitated through active endocytosis [113]. Models are being developed to elucidate drug delivery to the brain by EVs through the BBB, such as virus protein-originated, brain-specific peptides [96, 114]. Macrophage-derived exosomes are highly prospective as nanocarriers of therapeutic proteins to the brain for treating central nervous system diseases. Macrophage-derived exosomes can deliver brain-derived neurotrophic factor (BDNF), a cargo protein, through the BBB after intravenous administration. Interestingly, this delivery is facilitated by brain inflammation, a typical condition presented in central nervous system diseases [115].

Alzheimer's disease (AD) is the disease responsible for dementia. It is an age-related neurodegenerative disease characterized by diminishing cognitive response function and progressive loss of memory. Exosomes have been used as a delivery platform for the treatment of this disease [96]. Curcumin or BACE1 siRNA-containing exosomes were injected to mice to ameliorate AD-like pathology in the brain. With advancements in nanotechnological strategies, these efficient exosomes or exosome-mimicking liposomes, or even fusion of them, may be useful to restore brain capacity in patients with AD [116–118]. In familial AD, genetic mutations cause increased production of Aβ [119]. In common irregular cases, generation of Aβ is normal, but its clearance is decreased [120]. Exosomes administered intracerebrally can function as powerful Aβ scavengers by binding to Aβ through enriched glycans on the glycosphingolipids on the exosome surface, suggesting that exosomes play an important role in Aβ clearance in the central nervous system [121]. Therefore, a novel therapeutic intervention for AD was obtained.

The developed world is challenged with Parkinson's disease (PD), one of the fastest developing neurological disorders. Inflammation of the brain, activation of microglia, and neurotoxic secretions, including reactive oxygen species, are the most common phenomena in PD

[122, 123]. Decreased levels of catalase, superoxide dismutase, and redox enzymes are commonly found in the brain samples of patients with PD. These conditions may lead to neurodegeneration and oxidative stress in PD patients [124]. In this perspective, delivery of catalase to the brain can be an effective strategy to treat PD. Haney et al. have shown that exosomes can be potent transporters of catalase and therapeutic proteins inhibiting microglia activation and secretion of active oxygen species [125]. Another pathological feature in the brain of PD patients is the ubiquitous presence of Lewy bodies. Aggregates of alpha-synuclein (α-Syn) are the main element of Lewy bodies. Therefore, attenuating α-Syn expression is considerably an attractive process to halt or delay PD progression. In 2014, Cooper and coworkers have described decreases in the aggregation and expression of α-Syn following delivery of α-Syn siRNA with the help of exosomes derived from dendritic cells [126].

10.3 Obstacles

Although EVs possess many enthralling features, we still cannot straightforwardly use them. Some commercially utilized synthetic vectors, such as liposomes, can be used in many amenable approaches and be scaled up in a large magnitude. On the contrary, EVs require many more steps to be used for therapeutic purposes, and these steps can negatively affect EVs or their parent cells [127]. More importantly, until now, it is difficult to generate EVs in sufficient amounts without using an enormous number of cells. Thus, large-scale production of EVs is still a foremost challenge for researchers in this field [128].

The purity and intactness of EVs also pose a challenge to researchers. Interestingly, many widely used protocols fail to generate particles that typically eluted with EVs [129]. In fact, isolation and purification of EVs are difficult tasks in the development of EVs [130, 131]. Multistep ultracentrifugation is the most frequently used strategy to isolate EVs. However, this method requires a long time, obtains poor yields [118, 132], and requires skilled operators and expensive equipment [133]. By contrast, density gradient separation techniques afford high-purity yields and good recovery rate, but they require complex sample processing and longer process time [134]. In addition, compared to physical property-based isolation methods, immunoaffinity-based isolation and immunomagnetic isolation can obtain higher-purity EVs, despite also affording low yield and causing damage to vesicles [128]. Currently, there are commercial reagents in the market for isolating exosomes using a polymer precipitation method, which can afford high yield of EVs within a short time, but with low purity.

It is also noticeable numerous exogenous EVs can hamper the communication of endogenous EVs within cells. Furthermore, a timely understood or not understood at all mechanism could bring to disasters for the hosts. EVs can induce signaling cascades by binding with cell surface receptors, thereby releasing intraluminal contents into the cytoplasm by fusing with the cytoplasmic membrane. Endocytosis can internalize them; otherwise they remain docked on cell surface [135]. These different modes of interactions will affect the efficacy of the delivered therapeutics. It is important to establish protocols with robust purification capacity and implement safety measures to overcome these difficulties in in vitro and in vivo experiments.

10.4 Conclusion

In the last decade, scientists mainly studied the vesicles originating from animal cells. However, in recent times, other vesicles originating from other sources, such as milk and vegetables, have gained interest. Their lack of toxicity and possibility of large-scale production may lead to consideration of milk- and plant-derived vesicles for therapeutic applications. However, to understand the intrinsic properties and possible biotechnological applications of these vesicles, in-depth studies are required to characterize these vesicles and their bioactive contents. EVs, especially exosomes, have provided new insight into the fields

of regenerative medicine and drug delivery. Currently, scientists are focusing on noncoding RNAs, such as miRNAs, which promote regeneration of organ tissues. Thus, the application of EVs will certainly continue to swell. However, the development of EVs for therapeutic purpose faces limitations in the generation, isolation, and purification of EVs in large quantity. Overcoming these difficulties will certainly be useful in almost every sphere of therapeutic application of EVs.

Acknowledgments This work was supported by the Basic Science Research Program of the National Research Foundation of Korea (NRF) funded by the Ministry of Education (NRF-2018R1D1A1B07045240).

References

1. Schorey JS, Cheng Y, Singh PP et al (2015) Exosomes and other extracellular vesicles in host–pathogen interactions. EMBO Rep 16(1):24–43
2. Johnstone RM, Adam M, Hammond JR et al (1987) Vesicle formation during reticulocyte maturation. Association of plasma membrane activities with released vesicles (exosomes). J Biol Chem 262(19):9412–9420
3. YáñezMó M, Siljander PRM, Andreu Z et al (2015) Biological properties of extracellular vesicles and their physiological functions. J Extracell Vesicles 4(1):27066
4. Colombo M, Raposo G, Théry C (2014) Biogenesis, secretion, and intercellular interactions of exosomes and other extracellular vesicles. Annu Rev Cell Dev Biol 30(1):255–289
5. György B, Szabó TG, Pásztói M et al (2011) Membrane vesicles, current state-of-the-art: emerging role of extracellular vesicles. Cell Mol Life Sci 68(16):2667–2688
6. Keller S, Sanderson MP, Stoeck A et al (2006) Exosomes: from biogenesis and secretion to biological function. Immunol Lett 107(2):102–108
7. Zitvogel L, Regnault A, Lozier A et al (1998) Eradication of established murine tumors using a novel cell-free vaccine: dendritic cell derived exosomes. Nat Med 4(5):594–600
8. Raposo G, Nijman HW, Stoorvogel W et al (1996) B lymphocytes secrete antigen-presenting vesicles. J Exp Med 183(3):1161–1172
9. Wolf P (1967) The nature and significance of platelet products in human plasma. Br J Haematol 13(3):269–288
10. Niel GV, Angelo GD, Raposo G (2018) Shedding light on the cell biology of extracellular vesicles. Nat Rev Mol Cell Biol 19(4):213–228
11. Beach A, Zhang HG, Ratajczak MZ et al (2014) Exosomes: an overview of biogenesis, composition and role in ovarian cancer. J Ovarian Res 7(1):14
12. Barile L, Vassalli G (2017) Exosomes: therapy delivery tools and biomarkers of diseases. Pharmacol Ther 174:63–78
13. Blaser MC, Aikawa E (2018) Roles and regulation of extracellular vesicles in cardiovascular mineral metabolism. Front Cardiovasc Med 5:187
14. Li W, Li C, Zhou T et al (2017) Role of exosomal proteins in cancer diagnosis. Mol Cancer 16(1):145
15. Gao M, Gao W, Papadimitriou JM et al (2018) Exosomes-the enigmatic regulators of bone homeostasis. Bone Res 6(1):36
16. Chen C, Skog J, Hsu C-H et al (2010) Microfluidic isolation and transcriptome analysis of serum microvesicles. Lab Chip 10(4):505–511
17. Levänen B, Bhakta NR, Torregrosa Paredes P et al (2013) Altered microRNA profiles in bronchoalveolar lavage fluid exosomes in asthmatic patients. J Allergy Clin Immunol 131(3):894–903
18. Street JM, Barran PE, Mackay CL et al (2012) Identification and proteomic profiling of exosomes in human cerebrospinal fluid. J Transl Med 10(1):5
19. Brown M, Johnson LA, Leone DA et al (2018) Lymphatic exosomes promote dendritic cell migration along guidance cues. J Cell Biol 217(6):2205–2221
20. Kesimer M, Scull M, Brighton B et al (2009) Characterization of exosome-like vesicles released from human tracheobronchial ciliated epithelium: a possible role in innate defense. FASEB J 23(6):1858–1868
21. Grigor'eva AE, Tamkovich SN, Eremina AV et al (2016) Characteristics of exosomes and microparticles discovered in human tears. Biomed Khim 62(1):99–106
22. Welch JL, Kaddour H, Schlievert PM et al (2018) Semen exosomes promote transcriptional silencing of HIV-1 by disrupting NF-κB/Sp1/Tat circuitry. J Virol 92:e00731–e00718
23. Taylor DD, Gerçel-Taylor C (2005) Tumour-derived exosomes and their role in cancer-associated T-cell signalling defects. Br J Cancer 92(2):305–311
24. Runz S, Keller S, Rupp C et al (2007) Malignant ascites-derived exosomes of ovarian carcinoma patients contain CD24 and EpCAM. Gynecol Oncol 107(3):563–571
25. Admyre C, Johansson SM, Qazi KR et al (2007) Exosomes with immune modulatory features are present in human breast milk. J Immunol 179(3):1969–1978
26. Reinhardt TA, Lippolis JD, Nonnecke BJ et al (2012) Bovine milk exosome proteome. J Proteomic 75(5):1486–1492

27. Fernández-Llama P, Khositseth S, Gonzales PA et al (2010) Tamm-Horsfall protein and urinary exosome isolation. Kidney Int 77(8):736–742
28. Wu CX, Liu ZF (2018) Proteomic profiling of sweat exosome suggests its involvement in skin immunity. J Invest Dermatol 138(1):89–97
29. Han Y, Jia L, Zheng Y et al (2018) Salivary Exosomes: Emerging roles in systemic disease. Int J Biol Sci 14(6):633–643
30. Livshits MA, Livshts MA, Khomyakova E et al (2015) Isolation of exosomes by differential centrifugation: Theoretical analysis of a commonly used protocol. Sci Rep 5:17319
31. Helwa I, Cai J, Drewry MD et al (2017) A comparative study of serum exosome isolation using differential ultracentrifugation and three commercial reagents. PLoS One 12(1):e0170628
32. Li P, Kaslan M, Lee SH et al (2017) Progress in exosome isolation techniques. Theranostics 7(3):789–804
33. Bunggulawa EJ, Wang W, Yin T et al (2018) Recent advancements in the use of exosomes as drug delivery systems. J Nanobiotechnol 16(1):81
34. Kotton DN, Morrisey EE (2014) Lung regeneration: mechanisms, applications and emerging stem cell populations. Nat Med 20(8):822–832
35. Ionescu L, Byrne RN, van Haaften T et al (2012) Stem cell conditioned medium improves acute lung injury in mice: in vivo evidence for stem cell paracrine action. Am J Physiol Lung Cell Mol Physiol 303(11):L967–L977
36. Kim SY, Burgess JK, Wang Y et al (2016) Atomized human amniotic mesenchymal stromal cells for direct delivery to the airway for treatment of lung injury. J Aerosol Med Pulm Drug Deliv 29(6):514–524
37. Gupta N, Su X, Popov B et al (2007) Intrapulmonary delivery of bone marrow-derived mesenchymal stem cells improves survival and attenuates endotoxin-induced acute lung injury in mice. J Immunol 179(3):1855–1863
38. Antunes MA, Abreu SC, Cruz FF et al (2014) Effects of different mesenchymal stromal cell sources and delivery routes in experimental emphysema. Respir Res 15(1):118
39. Sung DK, Chang YS, Ahn SY et al (2015) Optimal route for human umbilical cord blood-derived mesenchymal stem cell transplantation to protect against neonatal hyperoxic lung injury: Gene expression profiles and histopathology. PLoS One 10(8):e0135574
40. Serrano-Mollar A, Nacher M, Gay-Jordi G et al (2007) Intratracheal transplantation of alveolar type II cells reverses bleomycin-induced lung fibrosis. Am J Respir Crit Care Med 176(12):1261–1268
41. Tibboel J, Keijzer R, Reiss I et al (2013) Intravenous and intratracheal mesenchymal stromal cell injection in a mouse model of pulmonary emphysema. COPD 11(3):310–318
42. Kim YE, Park WS, Sung DK et al (2016) Intratracheal transplantation of mesenchymal stem cells simultaneously attenuates both lung and brain injuries in hyperoxic newborn rats. Pediatr Res 80(3):415–424
43. Monsel A, Zhu Y, Gennai S et al (2015) Therapeutic effects of human mesenchymal stem cell–derived microvesicles in severe pneumonia in mice. Am J Respir Crit Care Med 192(3):324–336
44. Willis GR, Fernandez-Gonzalez A, Anastas J et al (2018) Mesenchymal stromal cell exosomes ameliorate experimental bronchopulmonary dysplasia and restore lung function through macrophage immunomodulation. Am J Respir Crit Care Med 197(1):104–116
45. Lee C, Mitsialis SA, Aslam M et al (2012) Exosomes mediate the cytoprotective action of mesenchymal stromal cells on hypoxia-induced pulmonary hypertension. Circulation 126(22):2601–2611
46. Tan K, Choi H, Jiang X et al (2014) Micro-RNAs in regenerating lungs: an integrative systems biology analysis of murine influenza pneumonia. BMC Genom 15(1):587
47. Vaporidi K, Vergadi E, Kaniaris E et al (2012) Pulmonary microRNA profiling in a mouse model of ventilator-induced lung injury. Am J Physiol Cell Mol Physiol 303(3):L199–L207
48. Sessa R, Hata A (2013) Role of microRNAs in lung development and pulmonary diseases. Pulm Circ 3(2):315–328
49. Zhu Y, Feng X, Abbott J et al (2014) Human mesenchymal stem cell microvesicles for treatment of escherichia coli endotoxin-induced acute lung injury in mice. Stem Cells 32(1):116–125
50. Song Y, Dou H, Li X et al (2017) Exosomal miR-146a contributes to the enhanced therapeutic efficacy of interleukin-1β-primed mesenchymal stem cells against sepsis. Stem Cells 35(5):1208–1221
51. Alexander M, Hu R, Runtsch MC et al (2015) Exosome-delivered microRNAs modulate the inflammatory response to endotoxin. Nat Commun 6(1):7321
52. Huang Y, Crawford M, Higuita-Castro N et al (2012) miR-146a regulates mechanotransduction and pressure-induced inflammation in small airway epithelium. FASEB J 26(8):3351–3364
53. Ibrahim AGE, Cheng K, Marbán E (2014) Exosomes as critical agents of cardiac regeneration triggered by cell therapy. Stem Cell Reports 2(5):606–619
54. Teng X, Chen L, Chen W et al (2015) Mesenchymal stem cell-derived exosomes improve the microenvironment of infarcted myocardium contributing to angiogenesis and anti-inflammation. Cell Physiol Biochem 37(6):2415–2424
55. Khan M, Nickoloff E, Abramova T et al (2015) Embryonic stem cell-derived exosomes promote endogenous repair mechanisms and enhance cardiac function following myocardial infarction. Circ Res 117(1):52–64
56. Zhao Y, Sun X, Cao W et al (2015) Exosomes derived from human umbilical cord mesenchymal stem cells relieve acute myocardial ischemic injury. Stem Cells Int 2015:12

57. Agarwal U, George A, Bhutani S et al (2017) Experimental, systems, and computational approaches to understanding the microRNA-mediated reparative potential of cardiac progenitor cell-derived exosomes from pediatric patients. Circ Res 120(4):701–712
58. Viñas JL, Burger D, Zimpelmann J et al (2016) Transfer of microRNA-486-5p from human endothelial colony forming cell–derived exosomes reduces ischemic kidney injury. Kidney Int 90(6):1238–1250
59. Borges FT, Melo SA, Özdemir BC et al (2013) TGF-β1-containing exosomes from injured epithelial cells activate fibroblasts to initiate tissue regenerative responses and fibrosis. J Am Soc Nephrol 24(3):385–392
60. Tomasoni S, Longaretti L, Rota C et al (2013) Transfer of growth factor receptor mRNA via exosomes unravels the regenerative effect of mesenchymal stem cells. Stem Cells Dev 22(5):772–780
61. Zhou Y, Xu H, Xu W et al (2013) Exosomes released by human umbilical cord mesenchymal stem cells protect against cisplatin-induced renal oxidative stress and apoptosis in vivo and in vitro. Stem Cell Res Ther 4(2):34
62. Jiang Z, Liu Y, Niu X et al (2016) Exosomes secreted by human urine-derived stem cells could prevent kidney complications from type I diabetes in rats. Stem Cell Res Ther 7(1):24
63. Momen-Heravi F, Saha B, Kodys K, Catalano D, Satishchandran A, Szabo G (2015) Increased number of circulating exosomes and their microRNA cargos are potential novel biomarkers in alcoholic hepatitis. J Transl Med. 13(1):261
64. Tan C, Lai R, Wong W et al (2014) Mesenchymal stem cell-derived exosomes promote hepatic regeneration in drug-induced liver injury models. Stem Cell Res Ther 5(3):76
65. Nojima H, Freeman CM, Schuster RM et al (2016) Hepatocyte exosomes mediate liver repair and regeneration via sphingosine-1-phosphate. J Hepatol 64(1):60–68
66. Yan Y, Jiang W, Tan Y et al (2017) HucMSC exosome-derived GPX1 is required for the recovery of hepatic oxidant injury. Mol Ther 25(2):465–479
67. Nong K, Wang W, Niu X et al (2016) Hepatoprotective effect of exosomes from human-induced pluripotent stem cell–derived mesenchymal stromal cells against hepatic ischemia-reperfusion injury in rats. Cytotherapy 18(12):1548–1559
68. Frohlich D, Kuo WP, Fruhbeis C et al (2014) Multifaceted effects of oligodendroglial exosomes on neurons: impact on neuronal firing rate, signal transduction and gene regulation. Philos Trans R Soc B Biol Sci 369(1652):20130510
69. Xin H, Li Y, Buller B et al (2012) Exosome-mediated transfer of miR-133b from multipotent mesenchymal stromal cells to neural cells contributes to neurite outgrowth. Stem Cells 30(7):1556–1564
70. Takeda YS, Xu Q (2015) Neuronal differentiation of human mesenchymal stem cells using exosomes derived from differentiating neuronal cells. PLoS One 10(8):e0135111
71. El Bassit G, Patel RS, Carter G et al (2017) MALAT1 in human adipose stem cells modulates survival and alternative splicing of PKCδII in HT22 cells. Endocrinology 158(1):183–195
72. Mead B, Tomarev S (2017) Bone marrow-derived mesenchymal stem cells-derived exosomes promote survival of retinal ganglion cells through miRNA-dependent mechanisms. Stem Cells Transl Med 6(4):1273–1285
73. Lopez-Verrilli MA, Picou F, Court FA (2013) Schwann cell-derived exosomes enhance axonal regeneration in the peripheral nervous system. Glia 61(11):1795–1806
74. Goncalves MB, Malmqvist T, Clarke E et al (2015) Neuronal RARβ signaling modulates PTEN activity directly in neurons and via exosome transfer in astrocytes to prevent glial scar formation and induce spinal cord regeneration. J Neurosci 35(47):15731–15745
75. Zhang Y, Chopp M, Zhang ZG et al (2017) Systemic administration of cell-free exosomes generated by human bone marrow derived mesenchymal stem cells cultured under 2D and 3D conditions improves functional recovery in rats after traumatic brain injury. Neurochem Int 111:69–81
76. Zhang Y, Chopp M, Liu XS et al (2017) Exosomes derived from mesenchymal stromal cells promote axonal growth of cortical neurons. Mol Neurobiol 54(4):2659–2673
77. Hu L, Wang J, Zhou X et al (2016) Exosomes derived from human adipose mesenchymal stem cells accelerates cutaneous wound healing via optimizing the characteristics of fibroblasts. Sci Rep 6(1):32993
78. Liang X, Zhang L, Wang S (2016) Exosomes secreted by mesenchymal stem cells promote endothelial cell angiogenesis by transferring miR-125a. J Cell Sci 129(11):2182–2189
79. Zhao B, Zhang Y, Han S et al (2017) Exosomes derived from human amniotic epithelial cells accelerate wound healing and inhibit scar formation. J Mol Histol 48(2):121–132
80. Zhang J, Chen C, Hu B et al (2016) Exosomes derived from human endothelial progenitor cells accelerate cutaneous wound healing by promoting angiogenesis through Erk1/2 signaling. Int J Biol Sci 12(12):1472–1487
81. Guo SC, Tao SC, Yin WJ et al (2017) Exosomes derived from platelet-rich plasma promote the re-epithelization of chronic cutaneous wounds via activation of YAP in a diabetic rat model. Theranostics 7(1):81–96
82. Zhang B, Wang M, Gong A et al (2015) HucMSC-exosome mediated-Wnt4 signaling is required for cutaneous wound healing. Stem Cells 33(7):2158–2168
83. Shabbir A, Cox A, Rodriguez-Menocal L et al (2015) Mesenchymal stem cell exosomes induce proliferation and migration of normal and chronic wound

fibroblasts, and enhance angiogenesis in vitro. Stem Cells Dev 24(14):1635–1647
84. Li X, Liu L, Yang J et al (2016) Exosome derived from human umbilical cord mesenchymal stem cell mediates MiR-181c attenuating burn-induced excessive inflammation. EBioMedicine 8:72–82
85. Burns C, Hall ST, Smith R et al (2015) Cytokine levels in late pregnancy: are female infants better protected against inflammation? Front Immunol 6:318
86. Guo SX, Jin YY, Fang Q et al (2015) Beneficial effects of hydrogen-rich saline on early burn-wound progression in rats. PLoS One 10(4):e0124897
87. Zhang B, Wu X, Zhang X et al (2015) Human umbilical cord mesenchymal stem cell exosomes enhance angiogenesis through the Wnt4/β-catenin pathway. Stem Cells Transl Med 4(5):513–522
88. Han K-Y, Tran JA, Chang J-H et al (2017) Potential role of corneal epithelial cell-derived exosomes in corneal wound healing and neovascularization. Sci Rep 7(1):40548
89. Leoni G, Neumann P-A, Kamaly N et al (2015) Annexin A1–containing extracellular vesicles and polymeric nanoparticles promote epithelial wound repair. J Clin Invest 125(3):1215–1227
90. Zhang J, Guan J, Niu X et al (2015) Exosomes released from human induced pluripotent stem cells-derived MSCs facilitate cutaneous wound healing by promoting collagen synthesis and angiogenesis. J Transl Med 13(1):49
91. Rajendran RL, Gangadaran P, Bak SS et al (2017) Extracellular vesicles derived from MSCs activates dermal papilla cell in vitro and promotes hair follicle conversion from telogen to anagen in mice. Sci Rep 7(1):15560
92. Zhou L, Wang H, Jing J et al (2018) Regulation of hair follicle development by exosomes derived from dermal papilla cells. Biochem Biophys Res Commun 500(2):325–332
93. Meel RVD, Fens MHAM, Vader P (2014) Extracellular vesicles as drug delivery systems: Lessons from the liposome field. J Control Release 195:72–85
94. Andaloussi SEL, Mäger I, Breakefield XO et al (2013) Extracellular vesicles: biology and emerging therapeutic opportunities. Nat Rev Drug Discov 12(5):347–357
95. Johnsen KB, Gudbergsson JM, Skov MN et al (2014) A comprehensive overview of exosomes as drug delivery vehicles - endogenous nanocarriers for targeted cancer therapy. Biochim Biophys Acta Rev Cancer 1846(1):75–87
96. Alvarez-Erviti L, Seow Y, Yin H et al (2011) Delivery of siRNA to the mouse brain by systemic injection of targeted exosomes. Nat Biotechnol 29(4):341–345
97. Wahlgren J, Karlson TDL, Brisslert M et al (2012) Plasma exosomes can deliver exogenous short interfering RNA to monocytes and lymphocytes. Nucleic Acids Res 40(17):e130
98. Shtam TA, Varfolomeeva EY, Semenova EV et al (2008) Role of human RAD51 recombinase in the cycle checkpoint and survival of a cell. Cell Tissue Biol 2(5):463–467
99. Shtam TA, Kovalev RA, Varfolomeeva E (2013) Exosomes are natural carriers of exogenous siRNA to human cells in vitro. Cell Commun Signal 11(1):88
100. Banizs A, Huang T, Dryden K et al (2014) In vitro evaluation of endothelial exosomes as carriers for small interfering ribonucleic acid delivery. Int J Nanomed 9(1):4223
101. Bartel DP (2004) MicroRNAs: genomics, biogenesis, mechanism, and function. Cell 116(2):281–297
102. Bartel DP (2009) MicroRNAs: target recognition and regulatory functions. Cell 136(2):215–233
103. Ohno S, Takanashi M, Sudo K et al (2013) Systemically injected exosomes targeted to EGFR deliver antitumor microRNA to breast cancer cells. Mol Ther 21(1):185–191
104. Woodburn JR (1999) The epidermal growth factor receptor and its inhibition in cancer therapy. Pharmacol Ther 82(2–3):241–250
105. Tian T, Zhang H-X, He C-P et al (2018) Surface functionalized exosomes as targeted drug delivery vehicles for cerebral ischemia therapy. Biomaterials 150:137–149
106. Sun D, Zhuang X, Zhang S et al (2013) Exosomes are endogenous nanoparticles that can deliver biological information between cells. Adv Drug Deliv Rev 65(3):342–347
107. Mizrak A, Bolukbasi MF, Ozdener GB et al (2013) Genetically engineered microvesicles carrying suicide mRNA/protein inhibit Schwannoma tumor growth. Mol Ther 21(1):101–108
108. Katakowski M, Buller B, Zheng X et al (2013) Exosomes from marrow stromal cells expressing miR-146b inhibit glioma growth. Cancer Lett 335(1):201–204
109. Torchilin VP (2014) Multifunctional, stimuli-sensitive nanoparticulate systems for drug delivery. Nat Rev Drug Discov 13(11):813–827
110. Petros RA, DeSimone JM (2010) Strategies in the design of nanoparticles for therapeutic applications. Nat Rev Drug Discov 9(8):615–627
111. Upadhyay RK (2014) Drug delivery systems, CNS protection, and the blood brain barrier. Biomed Res Int 2014:869269
112. Lässer C (2015) Exosomes in diagnostic and therapeutic applications: biomarker, vaccine and RNA interference delivery vehicle. Expert Opin Biol Ther 15(1):103–117
113. Chen CC, Liu L, Ma F et al (2016) Elucidation of exosome migration across the blood-brain barrier model in vitro. Cell Mol Bioeng 9(4):509–529
114. Théry C (2011) Exosomes: secreted vesicles and intercellular communications. F1000 Biol Rep 3(15):15
115. Yuan D, Zhao Y, Banks WA et al (2017) Macrophage exosomes as natural nanocarriers for protein delivery to inflamed brain. Biomaterials 142:1–12

116. Ashraf GM, Tabrez S, Jabir NR et al (2015) An overview on global trends in nanotechnological approaches for Alzheimer therapy. Curr Drug Metab 16:719–727
117. Ansari SA, Satar R, Perveen A et al (2017) Current opinion in Alzheimer's disease therapy by nanotechnology-based approaches. Curr Opin Psychiatry 30(2):128–135
118. Sato YT, Umezaki K, Sawada S et al (2016) Engineering hybrid exosomes by membrane fusion with liposomes. Sci Rep 6(1):21933
119. Scheuner D, Eckman C, Jensen M et al (1996) Secreted amyloid β–protein similar to that in the senile plaques of Alzheimer's disease is increased in vivo by the presenilin 1 and 2 and APP mutations linked to familial Alzheimer's disease. Nat Med 2(8):864–870
120. Mawuenyega KG, Sigurdson W, Ovod V et al (2010) Decreased clearance of CNS beta-amyloid in Alzheimer's disease. Science 330(6012):1774
121. Yuyama K, Sun H, Sakai S et al (2014) Decreased amyloid-β pathologies by intracerebral loading of glycosphingolipid-enriched exosomes in Alzheimer model mice. J Biol Chem 289(35):24488–24498
122. Wu DC, Teismann P, Tieu K et al (2003) NADPH oxidase mediates oxidative stress in the 1-methyl-4-phenyl-1,2,3,6-tetrahydropyridine model of Parkinson's disease. Proc Natl Acad Sci 100(10):6145–6150
123. Ebadi M, Srinivasan SK, Baxi MD (1996) Oxidative stress and antioxidant therapy in Parkinson's disease. Prog Neurobiol 48(1):1–19
124. Ambani LM, Van Woert MH, Murphy S (1975) Brain peroxidase and catalase in Parkinson disease. Arch Neurol 32(2):114–118
125. Haney MJ, Klyachko NL, Zhao Y et al (2015) Exosomes as drug delivery vehicles for Parkinson's disease therapy. J Control Release 207:18–30
126. Cooper JM, Wiklander PBO, Nordin JZ et al (2014) Systemic exosomal siRNA delivery reduced alpha-synuclein aggregates in brains of transgenic mice. Mov Disord 29(12):1476–1485
127. Armstrong JPK, Holme MN, Stevens MM (2017) Re-engineering extracellular vesicles as smart nanoscale therapeutics. ACS Nano 11(1):69–83
128. Ingato D, Lee JU, Sim SJ et al (2016) Good things come in small packages: Overcoming challenges to harness extracellular vesicles for therapeutic delivery. J Control Release 241:174–185
129. Webber J, Clayton A (2013) How pure are your vesicles? J Extracell Vesicles 2(1):19861
130. Witwer KW, Buzás EI, Bemis LT et al (2013) Standardization of sample collection, isolation and analysis methods in extracellular vesicle research. J Extracell Vesicles 2(1):20360
131. Théry C, Amigorena S, Raposo G et al (2006) Isolation and Characterization of Exosomes from Cell Culture Supernatants and Biological Fluids. Curr Protoc Cell Biol 30(1):3–22
132. Bobrie A, Colombo M, Krumeich S et al (2012) Diverse subpopulations of vesicles secreted by different intracellular mechanisms are present in exosome preparations obtained by differential ultracentrifugation. J Extracell Vesicles 1(1):18397
133. Alvarez ML, Khosroheidari M, Kanchi Ravi R et al (2012) Comparison of protein, microRNA, and mRNA yields using different methods of urinary exosome isolation for the discovery of kidney disease biomarkers. Kidney Int 82(9):1024–1032
134. Zhang Z, Wang C, Li T et al (2014) Comparison of ultracentrifugation and density gradient separation methods for isolating Tca8113 human tongue cancer cell line-derived exosomes. Oncol Lett 8(4):1701–1706
135. Robbins PD, Morelli AE (2014) Regulation of immune responses by extracellular vesicles. Nat Rev Immunol 14(3):195–208

11 Application of Tissue Engineering and Regenerative Medicine in Maternal-Fetal Medicine

Jong Chul Shin and Hyun Sun Ko

Abstract

A rapid development of ultrasonography has enabled physicians to make earlier prenatal diagnosis of various fetal congenital diseases, in maternal-fetal medicine. Due to the significant mortality and irreversible damage to fetal vital organs during pregnancy, fetal surgeries have been tried in some congenital disease including congenital diaphragmatic hernia, twin-to-twin transfusion syndrome (TTTS), myelomeningocele (MMC), and lower urinary tract obstruction. However, open fetal surgery requires laparotomy followed by hysterotomy, which can cause preterm premature rupture of membrane (pPROM), oligohydramnios, preterm delivery, dehiscence of uterine wall, and other maternal complications during pregnancy. Minimally invasive approach using fetoscopy has been tried, and fetoscopic laser photocoagulation of vascular communications is currently considered as a treatment of choice for TTTS before 26 weeks' gestation. However, more development of surgical instrument and innovative materials using tissue engineering are required to improve outcomes of fetoscopic surgery. Because iatrogenic pPROM is the major challenge after fetoscopic surgery, this review focuses on current development of materials for treatment of spontaneous or iatrogenic pPROM and recent experimental progress of tissue engineering-based technology in prenatal treatment of MMC. Placental tissue is an emerging material for regenerative medicine. This chapter will also review regenerative potential and experiments of placenta and placenta-derived stem cells, as well as prospects of "in utero stem cell therapy."

Keywords

Fetoscopy · Open fetal surgery · Prenatal diagnosis · Preterm premature rupture of membrane · Congenital disease · Maternal-fetal medicine · Fetal surgery · Minimally invasive · Tissue engineering · Placental

11.1 Introduction

11.1.1 Fetal Surgery

Surgical fetal intervention can be justified when the conditions of congenital disease are associated with significant mortality or very severe morbidity if left untreated, during pregnancy, and fetal therapy has demonstrated efficacy in systematic reviews of randomized controlled trials (RCTs), individual RCTs, or "all or none" case series, such as twin-to-twin transfusion syndrome

J. C. Shin (✉) · H. S. Ko
Department of obstetrics and gynecology, Seoul St. Mary's Hospital, College of Medicine, The Catholic University of Korea, Seoul, Korea
e-mail: jcshin@catholic.ac.kr

H. J. Chun et al. (eds.), *Bioinspired Biomaterials*, Advances in Experimental Medicine and Biology 1249, https://doi.org/10.1007/978-981-15-3258-0_11

(TTTS), congenital diaphragmatic hernia, myelomeningocele (MMC), and lower urinary tract obstruction. However, maternal or fetal complications secondary to fetal surgery during pregnancy still should be considered.

11.1.2 Iatrogenic Preterm Premature Rupture of Membrane

The amniotic membrane (AM) is the innermost layer of the placenta and is composed of a single epithelial layer, a dense basement membrane and an acellular compact layer rich in collagen, and underlying fibroblast and spongy layers [14, 32]. Spontaneous healing process after damage of AM is unlikely to occur due to poor vascularity. Therefore, iatrogenic preterm premature rupture of membrane (pPROM) after fetal intervention is one of the big challenges in fetal therapy, because its consequences include oligohydramnios-related pulmonary hypoplasia, chorioamnionitis, and preterm delivery, which can result in considerable mortality and severe morbidities in survivors. The incidence of iatrogenic pPROM after fetal intervention has been reported, up to 15% after ultrasound-guided shunt operation in lower urinary tract obstruction [94], from 9% to 39% after fetoscopic laser surgery [58, 84, 88], and from 33% to 91% after fetoscopic MMC repair [4, 40]. Numerous efforts to treat pPROM have been reported using various sealants and plug materials, including fibrin-based products, gelatin sponge [55, 67], collagen biomatrix [19], blood cryoprecipitates [76], platelets [74], collagen sponges [20], poly-l-lactic acid [71], and decellularized tissue scaffolds [13, 59, 61, 68].

11.2 Experimental and Clinical Progress in the Treatment and Prevention of pPROM

11.2.1 Treatment After Established Membrane Rupture

Established membrane rupture can be diagnosed when clinical symptom of amniotic fluid leakage is evident, such as watery vaginal discharge, decreasing amniotic fluid, or membrane detachment in the ultrasonographic examination. For the treatment of iPROM after fetoscopic umbilical cord ligation in acardiac twin, the amniopatch composed of platelets and cryoprecipitate was firstly described in 1996 [74]. Activation and aggregation of platelets followed by stabilization with cryoprecipitate was proposed as a mechanism of amniopatch. After then, ultrasound-guided injection of amniopatch has been tried in chorioamnion detachment and iatrogenic pPROM after invasive genetic testing or operative fetoscopy [12, 13, 57]. However, intrauterine fetal deaths after the amniopatch procedure have been observed in the past studies, although the exact causes were not proven [13]. It was considered that serotonin, bradykinin, and other factors released by activated platelets can make harmful effect on the fetus. Therefore, the amount of amniopatch has been decreased. In a recent cohort study, amniopatch (approximately 30 mL of platelets followed by 30 mL of cryoprecipitate) within 15 days after iatrogenic pPROM showed 63.2% successful sealing rate, longer gestational age at delivery, and improved perinatal survival, after fetoscopic laser surgery for TTTS [9].

Other treatments to reseal the membranes have been attempted by (a) injecting clotting factors such as thrombin or fibrinogen and other medicines into the hole in the womb to create a patch over the area that is leaking; (b) taking immunological supplements (that may stimulate the body's immune system to mend the area where the seal has broken); and (c) placing a seal with a cervical adapter, over the neck of the womb, to stop fluid leaking out and prevent infection [12]. An immunological stimulant, combination of matrix metalloproteinase (MMP) inhibitors, cytokines, and defensins, showed some benefit in the prolongation of mean gestational age at birth [73], but it was less than a week. Until 2016, there had been insufficient evidence to evaluate sealing procedures or sealing material after pPROM, yet [12]. In 2019, Ahmed et al. reported significant effect of amniopatch (60–80 mL of platelets and 100–150 ml of FFP) in spontaneous pPROM through a randomized controlled trial [57]. Although only 12% of

women with pPROM showed successful sealing of the membrane defect with increase of amniotic fluid, the amniopatch demonstrated significant effect ($p = 0.0144$), because none of the expectant group showed similar sealing and increase of amniotic fluid. The effects of amniopatch have been better in iatrogenic pPROM than in spontaneous pPROM [13]. Because there is no other available option except expectant management or pregnancy termination when membrane of rupture is clinically diagnosed, during the mid-trimester, amniopatch might be worth a try for treatment after pPROM, until the other material or procedure is developed, and demonstrates significant decrease of perinatal mortality after pPROM. However, the safety and efficacy profile about amniopatch needs to be followed in future studies with more cases.

11.2.2 Secondary Prevention Approach of Iatrogenic pPROM

To prevent clinical amniotic fluid leakage after fetoscopic intervention, sealing the iatrogenic membrane defect using a surgical plug, which is composed of collagen, gelatin, or other matrices, has been introduced, before finishing a fetoscopic intervention [20, 55, 59, 65, 67]. Acellular human amnion plug demonstrated similar efficiency in restoring amniotic integrity, compared with collagen matrix foil, and native amniotic scaffolds showed better sealing than polyesterurethane scaffolds in the rabbit model [55]. Human amniotic membrane (hAM) has been used in the treatment of corneal injuries [43, 44], burn injuries, and chronic or non-healing wound [36, 63, 79, 89], because it has low immunogenic, anti-inflammatory, antiscarring, re-epithelization, and non-tumorigenic properties [5, 8, 29, 36, 63, 79, 89]. AM synthesizes and releases cytokines and signaling molecules such as TNF-α, TGF-α, TGF-β, FGF-b, EGF, keratinocyte growth factor, hepatic growth factor, interleukin-4 (IL-4), IL-6, IL-8, natural inhibitors of metalloproteases, β-defensins, and prostaglandins, among others [66]. Decellularized amniotic membrane also has been studied in regeneration of myocardiac infarction [77].

Other materials have been suggested for membrane sealing at the fetoscopic site. Although injectable sealants using poly(ethylene glycol)-based polymer hydrogels which is a mussel-mimetic tissue adhesive, showed efficient, nondisruptive, nontoxic bonding to fetal membranes in an in vitro model [5], it has not been tested in vivo, for restoration of amniotic membrane defect. The other group of the Texas Children's Fetal Center made an in vitro uterine model, to simulate the anatomical relationship of the fetal membranes, uterine wall, and surrounding amniotic fluid [61]. They demonstrated that a lyophilized fetal membrane patch effectively occluded a model of an iatrogenic fetal membrane defect in an aqueous environment. The patch was more effective when used in conjunction with a nanosilica-filled adhesive coacervate. In swine model, hAM promoted fetal membrane healing when secured in the defect site, which was more effective with the bioinspired underwater adhesive, although fetal membranes in swine model showed spontaneous healing [68], within about 20 days after fetoscopic operation.

In our longer period study with swine model (8 weeks), however, there was no complete restoration, but partial restoration of amniotic membrane after iatrogenic pPROM [52]. In our study, a decellularized amniotic membrane (dAM)-derived hydrogel with 3D-printed polycaprolactone framework, which is called "amnion-analogous medical device (AMED)," demonstrated functional restoration of membrane integrity with better preservation of amniotic fluid and normal fetal lung/body weight ratio, compared with no treatment group, in iatrogenic fetal membrane defects after fetoscopy. In addition, when we compared AMED group with a lyophilized fetal membrane patch group, AMED group showed less surgical time and better fetal survival, although both groups induced cellular ingrowth into the defect area and complete healing of the AM. A lyophilized fetal membrane patch group used a commercial amniograft patch, developed for corneal treatment, and adhesive

(TISSEEL Kitl Baxter India, Haryana, India) over the membrane defect.

In a human cohort study undergoing fetoscopic treatment for congenital diaphragmatic hernia, collagen plug sealing of iatrogenic fetal membrane defects after fetoscopic surgery could not reduce the risk of pPROM [20]. In the other human cohort study about fetoscopic laser surgery, which is considered an effective treatment for TTTS, a chorioamniotic plug made of absorbable gelatin sponge did not reduce the risk of iatrogenic pPROM and did not increase the procedure-to-delivery interval [67]. The most significant possible complication associated with sealant use is the stimulation of an inflammatory process, which can lead to preterm uterine activity. Even if a membrane seal is initially successful, the dynamic environment of the amniotic fluid and the activity of uterine musculature will constantly challenge it.

Therefore, further studies with experimental procedure or promising materials are required, before the application in human studies.

11.3 Fetal Surgery and Tissue Engineering in MMC

11.3.1 Rationale of Fetal Surgery in MMC

MMC, the most severe form of spina bifida, characterized by the extrusion of the spinal cord into a sac filled with cerebrospinal fluid, is a candidate congenital disease for fetal therapy, because neurological damage to exposed neural elements by amniotic fluid can be progressed and worsening herniation of hindbrain can result in hydrocephalus, during pregnancy, which can lead to lifelong neurological disabilities [35], including paralysis and bowel and bladder dysfunction. Damage to the spinal cord and peripheral nerves is almost irreversible despite early postnatal surgical repair.

11.3.2 Open Fetal Surgery of MMC

An NIH-sponsored, randomized, controlled, multicenter trial, comparing in utero open surgical repair of the MMC defect to standard postnatal surgery, revealed that open fetal surgery improved neurofunctional outcomes and is now a clinical option for the management of prenatally diagnosed MMC in selected patients [1]. Open fetal surgery requires maternal laparotomy followed by hysterotomy using a uterine stapling device. Then the cystic membrane of the MMC is excised, and the attachments of the meninges to the skin and soft tissues are detached. If possible, native dura is closed over the spinal cord as a first layer, followed by closure of paraspinal myofascial flaps, and then the skin surrounding the lesion is mobilized and closed to complete the repair. When the skin cannot be closed primarily, an acellular human dermis graft is used to complete the closure. However, open fetal surgery showed significant obstetric complications such as preterm delivery, PPROM, placental abruption, and maternal complications.

11.3.3 Fetoscopic Surgery of MMC

Although fetoscopic approaches have been tried as a minimally invasive technique, fetoscopic surgeries have reported higher rates of preterm delivery, pPROM, and technical failure to achieve closure, compared to open fetal surgery, so far [40], while the rate of uterine dehiscence was less after fetoscopic surgery. More minimally invasive techniques for better outcome of fetoscopic surgery are required using a single trocar or at most two small (≤2 mm) trocars [45]. Because prolonged operation time for fetoscopic surgery is considered as a significant factor for obstetric complications and postnatal revision of lesion due to incomplete coverage of MMC defect more frequently occurred in fetoscopic surgery than in open fetal surgery, several studies using scaffold-based coverage of the MMC defect for complete watertight coverage, to make less operation time

with simplified method as an alternative to surgical skin closure, have been reported [6, 17–19, 21, 26, 27, 39, 69, 80, 81, 83, 92, 93]. For the full coverage of MMC, several patches, such as biocellulose patch with or without bilaminar skin substitute [48] and collagen/Teflon patch [31], have been applied in fetoscopic surgery of human MMC cases. However, those patches were fixed by clip or suture. Otherwise, the skin was closed over the patch with a stitch.

11.3.4 Investigation of Tissue Engineering Materials for the Fetal Treatment of MMC

In animal model, several biomaterials using tissue engineering have been developed and studied. The scaffolds investigated in the experiments for the treatment of MMC were naturally derived materials including collagen, alginate, cellulose, or gelatin; synthetic materials including silicone or polypropylene with high-density polyethylene, poly-L-lactic acid, poly-L-lactide-cocaprolactone, and polypropylene glycol; or acellular scaffolds such as small intestinal mucosa biomatrix and acellular dermis. However, most of them required suturing or adhesives for clinical use.

For the application of biomaterials in the fetal MMC therapy, there are several conditions to overcome. Firstly, amniotic fluid in utero makes not only poor visualization for fetoscopic procedures but also limitation in the use of adhesives which is required for the watertight coverage of the defect, instead of suturing of biomaterials. To improve visualization during fetoscopic procedures, a new operation technique which is partial evacuation of amniotic fluid and carbon dioxide insufflation (PACI) has been introduced by Thomas Kohl, in German [46]. Then, in 2015, Belfort et al. at Texas Children's Fetal Center reported a developed PACI after maternal laparotomy and closed the 4 mm uterine port sites with absorbable sutures [3]. Their approach showed the lowest preterm birth rates (36%) in any previously reported cohort of fetal MMC repair [4]. However, there has been no biocompatible adhesive which can secure the material on the defect, in wet condition, yet. Secondly, simplified method, rather than suturing, which can be applied in fetoscopic surgery needs to be developed to decrease operation time. Recently, injectable materials are introduced. Growth factor encapsulated injectable alginate microparticles showed that significant soft tissue coverage of the MMC defect in a rat model [27]. However, it is unclear whether it can be delivered and secured to the defect without adhesive, by ultrasound- or microscope-guided injections, in human utero environment. In addition, safety profile of injectable alginate with growth factor needs to be investigated, especially when microparticles are delivered into the fetal organ, accidentally. The other recent material is reverse thermal gels (RTGs) that can undergo reversible spontaneous phase transition from liquid to physical gel upon temperature change without the need for reactive chemical species (cross-linkers) or outside energy sources (UV stimulation) [78]. It has been evaluated for intraamniotic injection in rat and mice [2, 39, 62, 98, 99]. RTGs are chemically conjugated poly(serinol hexamethylene urea) (PSHU) and poly(N-isopropyl acrylamide) (PNIPAm) which has reverse thermal gelling properties. However, chemical modification of RTG for enhanced adhesive properties is required to improve defect coverage. Thereafter, it needs to be investigated for long-term coverage of defect in utero, with growth factors, in other experimental model with longer gestation. Thirdly, multiple ports or large diameter of uterine port are also associated with the risk of iatrogenic PPROM after fetoscopy. However, if an injectable material using a single or small port can be secured on the defect site, in short time, the risk might be decreased. Lastly, biomaterial and adhesive for fetal surgery need to show plasticity, according to the fetal growth in utero.

11.4 Regenerative Potentials and Experiments of Placental Tissue

Human placenta contributes to the development and nutrition of the offspring and promotes feto-maternal immunotolerance, although most placentas are discarded after birth. They are rich in extracellular matrix, which includes important sources for regenerative medicine such as collagens, laminin, fibronectin, glycoproteins, and growth factors associated with vascular, mesenchymal, parenchymal, and other cell types [60]. In addition, they are high-yield source for the isolation of stem/progenitor cells.

Laminins, a family of large heterotrimeric (alpha, beta, gamma) proteins, are major components of basement membranes. Different commercial laminin preparations isolated from human placenta have been widely used for neuronal cell cultivation and promoting angiogenesis [96]. Extracellular matrix hydrogel from human placenta has been studied in the culture of cardiomyocytes, stem cells, and blood vessel assembly from endothelial cells, and animal model showed potential in therapeutic cardiovascular application [28]. Decellularized placental tissue as scaffolds in tissue engineering demonstrated hepatized potential for hepatic tissue engineering, in an induced acute liver failure sheep model [41]. Wharton's jelly in the umbilical cord also showed promising potential as a scaffold in different tissue defects [38]. Commercial products using decellularized human amniotic membranes are already available (i.e., Acelagraft™ and Biovance™, Celgene Cellular Therapeutics, Morris, New Jersey) for wound healing [54].

As an important source of mesenchymal stem cells (MSCs), placenta has been received attention.

Several studies have isolated and identified MSCs from placental tissues, including the amniotic membrane, the amniotic fluid, the umbilical cord, the chorionic membrane, and the decidua [15, 16, 64]. MSCs renew themselves, and they have characteristics of rapid proliferation and multipotency, including adipogenic, chondrogenic, and osteogenic differentiation potential. MSCs are the most widely explored cell phenotype for therapy due to their regenerative and immune regulatory properties [23]. Because of immunomodulatory effects by suppressing activated pro-inflammatory T cell proliferation and cytokine production, but by increasing in regulatory T cells, MSCs have been applied in clinical trials for GvHD and organ graft rejection, as well as autoimmune diseases [25]. Although a recent Cochrane review found insufficient evidence that MSCs were an effective therapy for GvHD [24], paracrine factors of MSCs and MSC-derived extracellular vesicles are getting more attentions for mediating immunomodulatory and regenerative MSC functions [70]. It is still unclear as to which patients might benefit from MSC therapeutics, yet. Because placenta is a wasting product after delivery, it can be promising source of MSCs, if the safety and efficacy of placenta-derived MSCs is more investigated and proven.

11.5 In Utero Stem Cell Transplantation and Gene Therapy

In utero stem cell transplantation (IUSCT) has been suggested for several genetic disorders and hematopoietic diseases.

MSCs have been proposed as potential in utero stem cell treatments for diseases ranging from severe combined immunodeficiencies (SCID) to osteogenesis imperfecta (OI), which are candidate congenital disorders of pregnancy termination. The unique situations in utero provide rationale for IUSCT [82]. Before the development of immune system to distinguish between autologous and foreign antigens, during fetal life, transplanted foreign cells may be recognized as self, may develop donor-specific immune tolerance, and may not undergo rejection, but proliferate in utero. IUSCT requires less stem cell dosage for fetus, compared with neonates for postnatal treatment. In addition, the same donor cells can be used for postnatal "booster" transplantation, without immunosuppression preventing for rejection [34].

There have been case reports about prenatal MSC infusion, in OI [30, 47, 49]. However, low engraftment levels of donor cells were observed in clinical cases and preclinical studies [33, 34, 91], despite improvement of clinical symptom and bone properties. It is considered that paracrine effects from soluble factors and releasing extracellular vesicles like exosomes and microvesicles, by MSCs, might be responsible for regenerative roles including stimulating endogenous cell proliferation, cell-to-cell communication, and preventing apoptosis of resident cells [7, 42]. An open-label multiple dose multicenter phase I/II trial, which is called "The Boost Brittle Bones Before Birth (BOOSTB4)," is planned to evaluate safety and efficacy of postnatal or prenatal and postnatal infusions of allogeneic fetal liver-derived MSCs for the treatment of severe OI compared with historical and untreated prospective controls [37].

Intrauterine hematopoietic stem cell transplantation (IUHSCT) has been tried in congenital disorders of hematopoietic cells, such as sickle cell anemia, thalassemia, chronic granulomatous disease, hemophilia A, Hurler's syndrome, metachromatic leukodystrophy, and Niemann-Pick disease [95]. IUHSCT in hematopoietically competitive diseases except SCID was not successful in establishing engraftment, in clinical studies. In addition to the competitive barriers, the other reason for the poor engraftment was maternal alloimmunization. Because maternal alloimmunization caused by the IUHSCT with allogenic donor cells can transfer alloantibodies in breast milk and cause fetal adaptive immune response, it has been suggested that maternal donor cells need to be used for IUHSCT [56]. To evaluate the safety, efficacy, and feasibility of IUHSCT approach with maternal donor cells, the University of California, San Francisco (UCSF), in the United States started a phase I clinical trial in fetuses with alpha thalassemia major and other similar variants, in 2017 [10]. Because alpha thalassemia major or hemoglobin Bart's syndrome leads to severe fetal anemia, which requires lifelong transfusions and bone marrow transplantation with immunosuppressive treatment, IUSCT with intrauterine blood transfusion might allow postnatal "booster" transplantation with maternal cells due to the improved tolerance to maternal HCT, even if IUHSCT shows low levels of chimerism.

To avoid immune response from allogenic donor cells, experiments using gene-corrected autologous fetal stem cells have been tried. In a fetal sheep, there was successful cell migration and engraftment in fetal blood and organs, by ultrasound-guided intraperitoneal injection of fetal cells from amniocentesis, after transducing an integrating lentiviral vector [86, 87]. Because the genetic manipulation of the autologous stem cells occurs outside the fetus, it might be able to avoid the risk of germline gene transfer, off-targeting effects, and transfer of the gene therapy to the mother [75]. In hemophilia A, which is the most frequent inheritable defect of the coagulation proteins, in utero FVIII transgene therapy with MSCs as cellular vehicles showed high levels of MSC engraftment and therapeutic benefit, in animal studies [72, 97]. It suggests clinical feasibility and possibility as a better treatment strategy of combining IUSCT with gene therapy than postnatal therapy in several genetic diseases.

However, prior to the application of in utero gene therapy in humans, a number of safety concerns must be investigated more, although the UK Gene Therapy Advisory Council (GTAC) considered that the use of genetically modified stem cells in stem cell transplantation to the fetus was a possibility stating "such ex vivo modification would be unlikely to carry with it any higher risk to the germ line than the trials of postnatal somatic gene therapy which have already been approved" (Gene Therapy Advisory Council 1998).

11.6 Conclusion

Risk of iatrogenic pPROM after fetal surgery is a big challenge in fetal therapy. Because minimally invasive approach using fetoscopy is also required to minimize the risk of pPROM, size and number of fetoscopic ports, as well as operation time, should be decreased. In addition, when a strategy for secondary prevention of iatrogenic pPROM using tissue engineering is further developed, minimally invasive pre-

natal treatment will be more feasible. Therefore, further studies with experimental procedure or promising materials are required, before the application in human studies.

In the prenatal treatment of fetal defect such as MMC, nontoxic, biocompatible, fluid-impermeable, and expansible materials which can secure the defect completely are required for better outcomes of fetoscopic surgery. A biocompatible adhesive, which is applicable in wet condition, should be developed, together. Otherwise, further development and optimization of injectable biomaterials such as RTGs, which can be adhered without glue, might be needed. In addition, stem cell therapy for fetal MMC using bone marrow MSCs and human embryonic stem cells have been studied for intra-amniotic injection [50, 51, 53]. MSCs from amniotic fluid stem cells (AFS) have also shown beneficial effects on the central nervous system, and therapeutic potential of AFS was reported in MMC [15, 16, 22, 64, 85, 90]. Because AFS can be obtained autologously, during pregnancy, by amniocentesis, it might be a feasible candidate for fetal therapy. Future studies need to find the best combination of a candidate material and those stem cells. Placental tissues with abundant immunoregulatory properties are emerging materials for regenerative medicine, as a valuable source of extracellular matrix and stem cells. More than 250 clinical trials employing feto-placental tissue-derived products in advanced cell therapy have been registered for hematology, oncology, acquired neurological conditions or disorders, and so on [11]. In the future, cryopreserved placental tissue can be more likely utilized for cellular therapies and personalized medicine.

References

1. Adzick N, Thom EA, Spong CY et al (2011) A randomized trial of prenatal versus postnatal repair of myelomeningocele. N Engl J Med 364:993–1004
2. Bardill J, Williams SM, Shabeka U et al (2019) An injectable reverse thermal gel for minimally invasive coverage of mouse myelomeningocele. J Surg Res 235:227–236
3. Belfort MA, Whitehead WE, Shamshirsaz AA (2015) Fetoscopic repair of meningomyelocele. Obstet Gynecol 126(4):881–884
4. Belfort MA, Whitehead WE, Shamshirsaz AA et al (2017) Fetoscopic open neural tube defect repair: development and refinement of a two-port, carbon dioxide insufflation technique. Obstet Gynecol 129(4):734–743
5. Bilic G, Brubaker C, Messersmith PB et al (2010) Injectable candidate sealants for fetal membrane repair: bonding and toxicity in vitro. Am J Obstet Gynecol 202(1):85
6. Brown EG, Saadai P, Pivetti CD et al (2014) In utero repair of myelomeningocele with autologous amniotic membrane in the fetal lamb model. J Pediatr Surg 49(1):133–138
7. Caplan AI, Dennis JE (2006) Mesenchymal stem cells as trophic mediators. J Cell Biochem 98(5):1076–1084
8. Castellanos G, Bernabé-García Á, Moraleda JM et al (2017) Amniotic membrane application for the healing of chronic wounds and ulcers. Placenta 59:146–153
9. Chmait RH, Kontopoulos EV, Chon AH et al (2017) Amniopatch treatment of iatrogenic preterm premature rupture of membranes (iPPROM) after fetoscopic laser surgery for twin-twin transfusion syndrome. J Matern Fetal Neonatal Med 30(11):1349–1354
10. Clinical Trials Gov (2017). https://clinicaltrials.gov. Accessed 1 Apr 2019
11. Couto PS, Bersenev A, Verter F (2017) The first decade of advanced cell therapy clinical trials using perinatal cells (2005–2015). Regen Med 12(8):953–968
12. Crowley AE, Grivell RM, Dodd JM (2016) Sealing procedures for preterm prelabour rupture of membranes. Cochrane Database Syst Rev. https://doi.org/10.1002/14651858.CD010218.pub2
13. Deprest J, Emonds MP, Richter J et al (2011) Amniopatch for iatrogenic rupture of the fetal membranes. Prenat Diagn 31:61–66
14. Devlieger R, Millar LK, Bryant-Greenwood G et al (2006) Fetal membrane healing after spontaneous and iatrogenic membrane rupture: a review of current evidence. Am J Obstet Gynecol 195:1512–1520
15. Dionigi B, Ahmed A, Brazzo J et al (2015) Partial or complete coverage of experimental spina bifida by simple intra-amniotic injection of concentrated amniotic mesenchymal stem cells. J Pediatr Surg 50:69–73
16. Dionigi B, Brazzo JA, Ahmed A et al (2015) Transamniotic stem cell therapy (TRASCET) minimizes Chiari-II malformation in experimental spina bifida. J Pediatr Surg 50:1037–1041
17. Eggink AJ, Roelofs LA, Feitz WF et al (2005) In utero repair of an experimental neural tube defect in a chronic sheep model using biomatrices. Fetal Diagn Ther 20:335–340

18. Eggink AJ, Roelofs LA, Lammens MM et al (2006) Histological evaluation of acute covering of an experimental neural tube defect with biomatrices in fetal sheep. Fetal Diagn Ther 21:210–216
19. Eggink AJ, Roelofs LA, Feitz WF et al (2008) Delayed intrauterine repair of an experimental spina bifida with a collagen biomatrix. Pediatr Neurosurg 44:29–35
20. Engels AC, Van Calster B, Richter J et al (2014) Collagen plug sealing of iatrogenic fetal membrane defects after fetoscopic surgery for congenital diaphragmatic hernia. Ultrasound Obstet Gynecol 43(1):54–59
21. Fauza DO, Jennings RW, Teng YD et al (2008) Neural stem cell delivery to the spinal cord in an ovine model of fetal surgery for spina bifida. Surgery 144:367–373
22. Feng C, Graham CD, Connors JP et al (2016) A comparison between placental and amniotic mesenchymal stem cells for transamniotic stem cell therapy (TRASCET) in experimental spina bifida. J Pediatr Surg 51:1010–1013
23. Fierabracci A, Del Fattore A, Luciano R et al (2015) Recent advances in mesenchymal stem cell immunomodulation. The role of microvesicles. Cell Transplant 24(2):133–149
24. Fisher SA, Cutler A, Doree C et al (2019) Mesenchymal stromal cells as treatment or prophylaxis for acute or chronic graft-versus-host disease in haematopoietic stem cell transplant (HSCT) recipients with a haematological condition. Cochrane Syst Rev. https://doi.org/10.1002/14651858.CD009768.pub2
25. Fontaine MJ, Shih H, Schäfer R et al (2016) Unraveling the mesenchymal stromal cells' paracrine immunomodulatory effects. Transfus Med Rev 30(1):37–43
26. Fontecha CG, Peiro JL, Sevilla JJ et al (2011) Fetoscopic coverage of experimental myelomeningocele in sheep using a patch with surgical sealant. Eur J Obstet Gynecol Reprod Biol 156:171–176
27. Farrelly JS, Bianchi AH, Ricciardi AS et al (2019) Alginate microparticles loaded with basic fibroblast growth factor induce tissue coverage in a rat model of myelomeningocele. J Pediatr Surg 54(1):80–85
28. Francis MP, Breathwaite E, Bulysheva AA et al (2017) Human placenta hydrogel reduces scarring in a rat model of cardiac ischemia and enhances cardiomyocyte and stem cell cultures. Acta Biomater 52:92–104
29. Gheorghe A, Pop M, Burcea M et al (2016) New clinical application of amniotic membrane transplant for ocular surface disease. J Med Life 9:177–179
30. Götherström C, Westgren M, Shaw SW et al (2014) Pre- and postnatal transplantation of fetal mesenchymal stem cells in osteogenesis imperfecta: a two-center experience. Stem Cells Transl Med 3(2):255–264
31. Graf K, Kohl T, Neubauer BA et al (2016) Percutaneous minimally invasive fetoscopic surgery for spina bifida aperta. Part III: neurosurgical intervention in the first postnatal year. Ultrasound Obstet Gynecol 47(2):158–161
32. Gratacos E, Sanin-Blair J, Lewi L et al (2006) A histological study of fetoscopic membrane defects to document membrane healing. Placenta 27:452–456
33. Guillot PV, Abass O, Bassett JH et al (2008) Intrauterine transplantation of human fetal mesenchymal stem cells from first-trimester blood repairs bone and reduces fractures in osteogenesis imperfecta mice. Blood 111(3):1717–1725
34. Hayashi S, Peranteau WH, Shaaban AF et al (2002) Complete allogeneic hematopoietic chimerism achieved by a combined strategy of in utero hematopoietic stem cell transplantation and postnatal donor lymphocyte infusion. Blood 100(3):804–812
35. Heffez DS, Aryanpur J, Hutchins GM et al (1990) The paralysis associated with myelomeningocele: clinical and experimental data implicating a preventable spinal cord injury. Neurosurgery 26:987–992
36. Herndon DN, Branski LK (2017) Contemporary methods allowing for safe and convenient use of amniotic membrane as a biologic wound dressing for burns. Ann Plast Surg 78:S9–S10
37. Hill M, Lewis C, Riddington M et al (2019) Stakeholder views and attitudes towards prenatal and postnatal transplantation of fetal mesenchymal stem cells to treat Osteogenesis Imperfecta. Eur J Hum Genet 27:1244–1253
38. Jadalannagari S, Converse G, McFall C et al (2017) Decellularized Wharton's Jelly from human umbilical cord as a novel 3D scaffolding material for tissue engineering applications. PLoS One 12:e0172098
39. Jenkins PM, Laughter MR, Lee DJ et al (2015) A nerve guidance conduit with topographical and biochemical cues: potential application using human neural stem cells. Nanoscale Res Lett 10(1):972
40. Kabagambe SK, Jensen GW, Chen YJ et al (2018) Fetal surgery for Myelomeningocele: a systematic review and meta-analysis of outcomes in Fetoscopic versus open repair. Fetal Diagn Ther 43(3):161–174
41. Kakabadze Z, Kakabadze A, Chakhunashvili D et al (2018) Decellularized human placenta supports hepatic tissue and allows rescue in acute liver failure. Hepatology 67(5):1956–1969
42. Keshtkar S, Azarpira N, Ghahremani MH (2018) Mesenchymal stem cell-derived extracellular vesicles: novel frontiers in regenerative medicine. Stem Cell Res Ther 9(1):63
43. Kim JC, Tseng SC (1995) Transplantation of preserved human amniotic membrane for surface reconstruction in severely damaged rabbit corneas. Cornea 14(5):473–484
44. Kim JS, Kim JC, Na BK et al (2000) Amniotic membrane patching promotes healing and inhibits proteinase activity on wound healing following acute corneal alkali burn. Exp Eye Res 70(3):329–337
45. Klaritsch P, Albert K, Van Mieghem T et al (2009) Instrumental requirements for minimal invasive fetal surgery. BJOG 116:188–197

46. Kohl T, Hering R, Heep A et al (2006) Percutaneous fetoscopic patch coverage of spina bifida aperta in the human--early clinical experience and potential. Fetal Diagn Ther 21(2):185–193
47. Lanfranchi A, Porta F, Chirico G (2009) Stem cells and the frontiers of neonatology. Early Hum Dev 85(10):S15–S18
48. Lapa Pedreira DA, Acacio GL, Gonçalves RT et al (2018) Percutaneous fetoscopic closure of large open spina bifida using a bilaminar skin substitute. Ultrasound Obstet Gynecol 52(4):458–466
49. Le Blanc K, Götherström C, Ringdén O et al (2005) Fetal mesenchymal stem-cell engraftment in bone after in utero transplantation in a patient with severe osteogenesis imperfecta. Transplantation 79(11):1607–1614
50. Lee DH, Kim EY, Park S et al (2006) Reclosure of surgically induced spinal open neural tube defects by the intraamniotic injection of human embryonic stem cells in chick embryos 24 hours after lesion induction. J Neurosurg 105:127–133
51. Lee DH, Park S, Kim EY et al (2004) Enhancement of re-closure capacity by the intra-amniotic injection of human embryonic stem cells in surgically induced spinal open neural tube defects in chick embryos. Neurosci Lett 364:98–100
52. Lee JY, Kim H, Ha DH et al (2018) Amnion-analogous medical device for fetal membrane healing: a preclinical long-term study. Adv Healthc Mater 7(18):e1800673
53. Li H, Gao F, Ma L et al (2012) Therapeutic potential of in utero mesenchymal stem cell (MSCs) transplantation in rat foetuses with spina bifida aperta. J Cell Mol Med 16:1606–1617
54. Lim LS, Poh WY, Riau AK et al (2010) Biological and ultrastructural properties of acelagraft, a freeze-dried-irradiated human amniotic membrane. Arch Ophthalmol 128:1303–1310
55. Luks F, Deprest JA, Peers KH et al (1999) Gelatin sponge plug to seal fetoscopy port sites: technique in ovine and primate models. Am J Obstet Gynecol 81(4):995–996
56. McClain LE, Flake AW (2016) In utero stem cell transplantation and gene therapy: recent progress and the potential for clinical application. Best Pract Res Clin Obstet Gynaecol 31:88–98
57. Maged AM, Kamel HH, Sanad AS et al (2019) The value of amniopatch in pregnancies associated with spontaneous preterm premature rupture of fetal membranes: a randomized controlled trial. J Matern Fetal Neonatal Med 7:1–161
58. Maggio L, Carr SR, Watson-Smith D et al (2015) Iatrogenic preterm premature rupture of membranes after fetoscopic laser ablative surgery. Fetal Diagn Ther 38:29–34
59. Mallik AS, Fichter MA, Rieder S et al (2007) Fetoscopic closure of punctured fetal membranes with acellular human amnion plugs in a rabbit model. Obstet Gynecol 110(5):1121–1129
60. Maltepe E, Fisher SJ (2015) Placenta: the forgotten organ. Annu Rev Cell Dev Biol 31:523–552
61. Mann LK, Papanna R, Moise KJ Jr et al (2012) Fetal membrane patch and biomimetic adhesive coacervates as a sealant for fetoscopic defects. Acta Biomater 8(6):2160–2165
62. Marwan AI, Williams SM, Bardill JR et al (2017) Reverse thermal gel for in utero coverage of spina bifida defects: an innovative bioengineering alternative to open Fetal repair. Macromol Biosci. https://doi.org/10.1002/mabi.201600473
63. Mohammadi AA, Johari HG, Eskandari S (2013) Effect of amniotic membrane on graft take in extremity burns. Burns 39(6):1137–1141
64. Ochiai D, Masuda H, Abe Y et al (2018) Human amniotic fluid stem cells: therapeutic potential for perinatal patients with intractable neurological disease. Keio J Med 67(4):57–66
65. Ochsenbein-Kolble N, Jani J, Lewi L et al (2007) Enhancing sealing of fetal membrane defects using tissue engineered native amniotic scaffolds in the rabbit model. Am J Obstet Gynecol 196(3):263.e1–263.e7
66. Parolini O, Alviano F, Bagnara GP et al (2008) Concise review: isolation and characterization of cells from human term placenta: outcome of the first international workshop on placenta derived stem cells. Stem Cells 26(2):300–311
67. Papanna R, Mann LK, Moise KY et al (2013) Absorbable gelatin plug does not prevent iatrogenic preterm premature rupture of membranes after fetoscopic laser surgery for twin-twin transfusion syndrome. Ultrasound Obstet Gynecol 42(4):456–460
68. Papanna R, Mann LK, Tseng SC et al (2015) Cryopreserved human amniotic membrane and a bioinspired underwater adhesive to seal and promote healing of iatrogenic fetal membrane defect sites. Placenta 36(8):888–894
69. Peiro JL, Fontecha CG, Ruano R et al (2013) Single-access fetal endoscopy (SAFE) for myelomeningocele in sheep model I: amniotic carbon dioxide gas approach. Surg Endosc 27:3835–3840
70. Phinney DG, Pittenger MF (2017) Concise review: MSC-derived exosomes for cell-free therapy. Stem Cells 35(4):851–858
71. Pensabene V, Patel PP, Williams P et al (2015) Repairing fetal membranes with a self-adhesive ultra-thin polymeric film: evaluation in mid-gestational rabbit model. Ann Biomed Eng 43(8):1978–1988
72. Porada CD, Rodman C, Ignacio G et al (2014) Hemophilia a: an ideal disease to correct in utero. Front Pharmacol 5:276
73. Dam P, Laha S, Bhattacharya P et al (2011) Role of amnioseal in premature rupture of membranes. J Obstet Gynaecol India 61(3):296–300
74. Quintero RA, Romero R, Dzieczkowski J et al (1996) Sealing of ruptured amniotic membranes with intra-amniotic platelet-cryoprecipitate plug. Lancet 347:1117

75. Ramachandra DL, Shaw SS, Shangaris P et al (2014) In utero therapy for congenital disorders using amniotic fluid stem cells. Front Pharmacol 5:270
76. Reddy UM, Shah SS, Nemiroff RL et al (2001) In vitro sealing of punctured fetal membranes: potential treatment for midtrimester premature rupture of membranes. Am J Obstet Gynecol 185(5):1090–1093
77. Roy R, Haase T, Ma N et al (2016) Decellularized amniotic membrane attenuates postinfarct left ventricular remodeling. J Surg Res 200(2):409–419
78. Ruel-Gariépy E, Leroux JC (2004) In situ-forming hydrogels-review of temperature-sensitive systems. Eur J Pharm Biopharm 58(2):409–426
79. Ruiz-Cañada C, Bernabé-García Á, Liarte ICL et al (2018) Amniotic membrane stimulates cell migration by modulating transforming growth factor-β signaling. J Tissue Eng Regen Med 12(3):808–820
80. Saadai P, Nout YS, Encinas J et al (2011) Prenatal repair of myelomeningocele with aligned nanofibrous scaffolds – a pilot study in sheep. J Pediatr Surg 46:2279–2283
81. Saadai P, Wang A, Nout YS et al (2013) Human induced pluripotent stem cell-derived neural crest stem cells integrate into the injured spinal cord in the fetal lamb model of myelomeningocele. J Pediatr Surg 48(1):158–163
82. Sagar R, Götherström C, David AL et al (2019) Fetal stem cell transplantation and gene therapy. Best Pract Res Clin Obstet Gynaecol 5:142–153
83. Oliveira RCS, Valente PR, Abou-Jamra RC et al (2007) Biosynthetic cellulose induces the formation of a neoduramater following pre-natal correction of meningomyelocele in fetal sheep. Acta Cir Bras 22:174–181
84. Senat MV, Deprest J, Boulvain M et al (2004) Endoscopic laser surgery versus serial amnioreduction for severe twin-to-twin transfusion syndrome. N Engl J Med 351(2):136–144
85. Shieh HF, Tracy SA, Hong CR et al (2019) Transamniotic stem cell therapy (TRASCET) in a rabbit model of spina bifida. J Pediatr Surg 54(2):293–296
86. Shaw SW, Bollini S, Nader KA et al (2011) Autologous transplantation of amniotic fluid-derived mesenchymal stem cells into sheep fetuses. Cell Transplant 20:1015–1031
87. Shaw SW, Blundell MP, Pipino C et al (2015) Sheep CD34+ amniotic fluid cells have hematopoietic potential and engraft after autologous in utero transplantation. Stem Cell 33:122–132
88. Snowise S, Mann LK, Moise KJ Jr et al (2017) Preterm prelabor rupture of membranes after fetoscopic laser surgery for twin-twin transfusion syndrome. Ultrasound Obstet Gynecol 49(5):607–611
89. Stern M (1913) The grafting of preserved amniotic membrane to burned and ulcerated surfaces, substituting skin grafts: a preliminary report. JAMA 60(13):973–974
90. Turner CG, Pennington EC, Gray FL et al (2013) Intra-amniotic delivery of amniotic-derived neural stem cells in a syngeneic model of spina bifida. Fetal Diagn Ther 34:38–43
91. Vanleene M, Saldanha Z, Cloyd KL et al (2011) Transplantation of human fetal blood stem cells in the osteogenesis imperfecta mouse leads to improvement in multiscale tissue properties. Blood 117(3):1053–1060
92. Watanabe M, Jo J, Radu A (2010) A tissue engineering approach for prenatal closure of myelomeningocele with gelatin sponges incorporating basic fibroblast growth factor. Tissue Eng Part A 16:1645–1655
93. Watanabe M, Li H, Roybal J et al (2011) A tissue engineering approach for prenatal closure of myelomeningocele: comparison of gelatin sponge and microsphere scaffolds and bioactive protein coatings. Tissue Eng Part A 17:1099–1110
94. Welsh A, Agarwal S, Kumar S et al (2003) Fetal cystoscopy in the management of fetal obstructive uropathy: experience in a single European centre. Prenat Diagn 23:1033–1041
95. Westgren M (2006) In utero stem cell transplantation. Semin Reprod Med 24(5):348–357
96. Wondimu Z, Gorfu G, Kawataki T et al (2006) Characterization of commercial laminin preparations from human placenta in comparison to recombinant laminins 2 (alpha2beta1gamma1), 8 (alpha4beta1gamma1), 10 (alpha5beta1gamma1). Matrix Biol 25(2):89–93
97. Yamagami T, Porada C, Chamberlain J et al (2006) Alterations in host immunity following in utero transplantation of human mesenchymal stem cells (MSC). Exp Hematol 34:39–40
98. Yun D, Famili A, Lee YM et al (2014) Biomimetic poly(serinol hexamethylene urea) for promotion of neurite outgrowth and guidance. J Biomater Sci Polym Ed 25(4):354–369
99. Yun D, Lee YM, Laughter MR et al (2015) Substantial differentiation of human neural stem cells into motor neurons on a biomimetic polyurea. Macromol Biosci 15(9):1206–1211

12 Fundamentals and Current Strategies for Peripheral Nerve Repair and Regeneration

Cristiana R. Carvalho, Rui L. Reis, and Joaquim M. Oliveira

Abstract

A body of evidence indicates that peripheral nerves have an extraordinary yet limited capacity to regenerate after an injury. Peripheral nerve injuries have confounded professionals in this field, from neuroscientists to neurologists, plastic surgeons, and the scientific community. Despite all the efforts, full functional recovery is still seldom. The inadequate results attained with the "gold standard" autograft procedure still encourage a dynamic and energetic research around the world for establishing good performing tissue-engineered alternative grafts. Resourcing to nerve guidance conduits, a variety of methods have been experimentally used to bridge peripheral nerve gaps of limited size, up to 30–40 mm in length, in humans. Herein, we aim to summarize the fundamentals related to peripheral nerve anatomy and overview the challenges and scientific evidences related to peripheral nerve injury and repair mechanisms. The most relevant reports dealing with the use of both synthetic and natural-based biomaterials used in tissue engineering strategies when treatment of nerve injuries is envisioned are also discussed in depth, along with the state-of-the-art approaches in this field.

Keywords

Peripheral nerve regeneration · Tissue engineering · Biomaterials

12.1 Introduction

The most significant advances in peripheral nerve repair and regeneration have been achieved over the last years with the improvement of technological tools. However, the study of nerve and its regenerative potential initiated in earlier times, possibly in the ancient Greek period [1]. Nevertheless, the establishment of the basic notions and modern concepts of nerve repair and regeneration were only developed in the twentieth century with the emergence of the neurosurgery field [2].

Peripheral nerve injuries (PNIs) usually involve sensory and motor neurons and frequently

C. R. Carvalho · R. L. Reis · J. M. Oliveira (✉)
3B's Research Group, I3Bs – Research Institute on Biomaterials, Biodegradables and Biomimetics, Headquarters of the European Institute of Excellence on Tissue Engineering and Regenerative Medicine, University of Minho, Guimarães, Portugal

ICVS/3B's – PT Government Associated Laboratory, Guimarães, Portugal

The Discoveries Centre for Regenerative and Precision Medicine, Headquarters at University of Minho, Guimarães, Portugal
e-mail: cristiana.carvalho@i3bs.uminho.pt; rgreis@i3bs.uminho.pt; miguel.oliveira@i3bs.uminho.pt

H. J. Chun et al. (eds.), *Bioinspired Biomaterials*, Advances in Experimental Medicine and Biology 1249, https://doi.org/10.1007/978-981-15-3258-0_12

result in axonal loss and demyelination, depending on the severity of the injury. Under ideal conditions, regeneration of a nerve cable is followed by remyelination, thus allowing a certain degree of sensory and functional recovery to be achieved. In the clinics, PNI repair is based on the knowledge of physiological regenerative processes [3]. However, if no additional strategies are used, functional recovery following an injury remains incomplete. In order to address this tissue regeneration and improve clinical outcomes, the contribution of multidisciplinary fields is required. Interestingly, tissue engineering (TE) has allowed to take impressive steps toward the improvement of functional outcomes, by means of combining areas such as reconstructive microsurgery, transplantation, and biomaterials [4]. Furthermore, the basic triad of TE has an important role in successful nerve regeneration, as the goal remains to develop and fabricate novel nerve guidance conduits (NGCs) built from a particular biomaterial, capable of housing cells and delivering biological and physical molecular cues, enhancing and guiding nerve regeneration [5]. As tubulization and the use of NGCs remain the base for nerve repair, the choice of adequate type(s) of biomaterials is the pillar to achieve the so desired regeneration [6]. In fact, it has been confirmed experimentally that engineered NGCs may also lead to effective nerve repair that was earlier thought to only be restorable using autograft [7].

The topics related to the anatomy of the nervous system as well as on the innate mechanisms related to the natural attempts of tissue regeneration are addressed herein. A comprehensive overview of the biomaterial's approaches being pursuit in nerve regeneration can also be found. Pre-clinical studies comprising natural, synthetic, and endogenous biomaterials have also been extensively explored. Additionally, strategies to achieve nerve repair as well as challenges that need to be overcome are highlighted.

12.1.1 Organization of the Nervous System

In the case of an injury, in order to make an initial assessment/diagnosis and proceed with the appropriate treatment, it is imperative to have plain knowledge of nervous system anatomy. The nervous system is the instrument through which organized vertebrates keep in touch with its internal structures and external surroundings, reacting to changes and adapting to them. This system has a fundamental role in behavior control and can be divided into the central nervous system (CNS) and peripheral nervous system (PNS) [8]. The CNS, composed of the brain and its caudal prolongation, the spinal cord, is connected to the periphery by the PNS [9]. During the embryonic development known as ontogenesis, the CNS emerges from the neural plate of the ectoderm that molds into the neural groove, from which the neural tube results. Subsequently, the neural tube is restructured and gives origin to the brain and spinal cord. This phenomenon is known as neurulation. Two bands of tissue called the neural crest will give origin to the forthcoming PNS that run along the neural tube. These are multi-potent progenitor cells that later form the PNS [10].

At an anatomical level, the CNS consists of the brain and the spinal cord, being both enclosed by three types of meninges [11]. The PNS consists of cranial nerves, spinal nerves and their roots and branches, peripheral nerves, and neuromuscular junctions, in a total of 43 pairs of sensory and motor nerves [12]. Bundles of axons in the PNS are referred to as nerves. These are composed of more than just nervous tissue. They have connective tissue participating in their structure, as well as blood vessels supplying the tissues with nourishment. A neuron consists of a cell body, known as soma, which gives out extensions in PNS, called axons. These are crucial for targeting distant tissues and organs. Axons are coated with myelin sheath membranes, formed by Schwann cells.

Anatomically, each individual axon is firstly protected by a myelin sheath and sheltered by a first layer of collagen and elastic elements, the endoneurium. A group of endoneurium protects axon groups into nerve fascicles, which are sheathed by the perineurium, mainly composed of connective tissue. Finally, several fascicles are gathered together by the epineurium. In the outer layer, the mesoneurium can be found, which also comprises blood vessels supplying oxygen and nutrients to the nerve. Any break or defect in this stratified structure falls out in a programmed and permanent cell death, unless rapidly and meticulously reestablished [13]. Besides myelinated nerve fibers, the PNS contains unmyelinated fibers, with the majority found in the cutaneous nerve, the dorsal roots, and some muscle nerves. Figure 12.1 shows the schematic representation of CNS and PNS in the human body, as well as detailed anatomy of peripheral nerves and neurons.

Myelin is a constant in both PNS and CNS. Myelin found on neurons in the PNS is formed by Schwann cells, while myelin found in the CNS is generated by oligodendrocytes. However, one striking difference can be pointed.

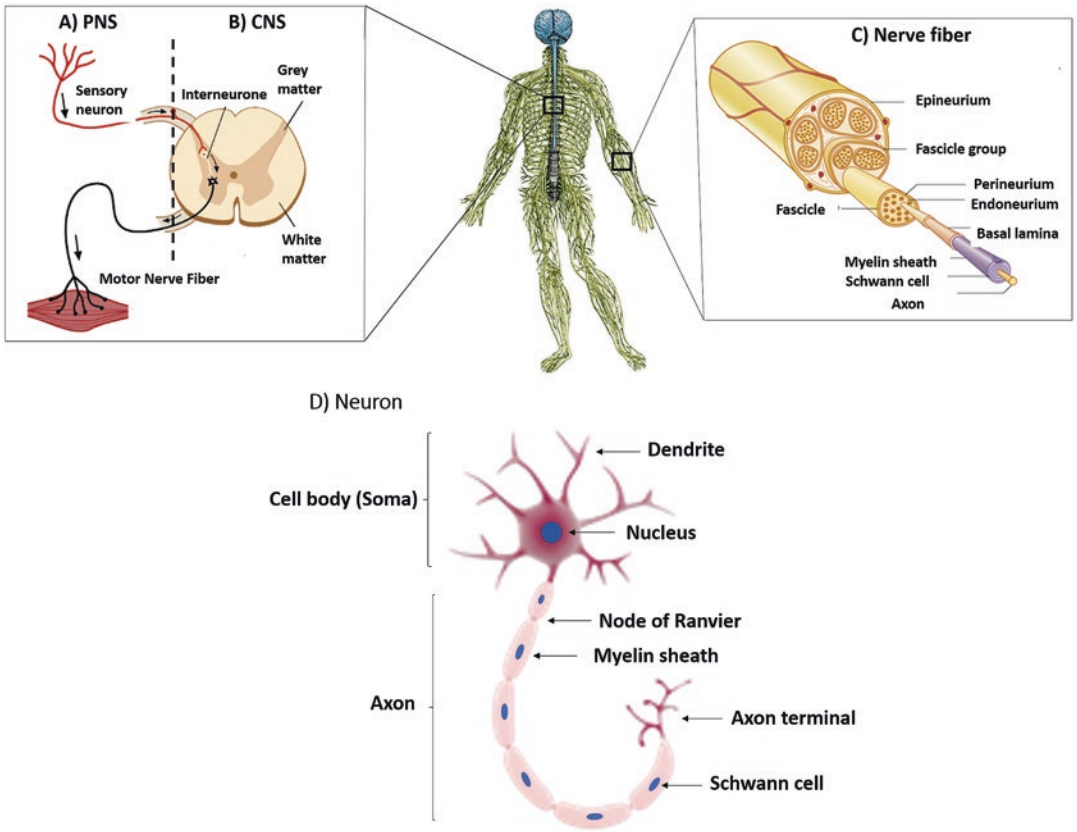

Fig. 12.1 Schematic representation of nervous system anatomy in the human body. The nervous system is divided into CNS (in blue) and PNS (green). (**a**) The PNS is composed of several pairs of nerves, which transmit signals between afferent sensory neurons and efferent motor neurons to the CNS; (**b**) CNS, composed of the brain and spinal cord, which has connections to PNS. In CNS, interneurons receive information from the periphery; (**c**) a peripheral nerve contains many nerve fibers that are held together by connective tissue and bundled into nerve fascicles. The entire nerve is enclosed by connective tissue called epineurium. Individual fascicles are delineated by perineurium. Endoneurium surrounds each nerve fiber; and (**d**) each neuron is composed of a cell body, known as soma, which contains dendrites. The axon, elongating from the cell body, may present myelin sheaths. The spaces between the myelin sheaths are nodes of Ranvier. In the end of the neuron, there is an axon terminal, which releases neurotransmitters from one neuron to another

In one hand, oligodendrocytes and Schwann cells are often compared to each other in terms of function. However, the biggest difference among the two resides in their ability to repair neurons after nerve damage, as Schwann cells promote nerve regeneration and repair, whereas oligodendrocytes inhibit neuron repair after an injury [14].

In terms of purpose, the primary function of the CNS is integration. Conversely, the PNS is mainly a receptor and effector organ that connects the CNS to every part of the body by cranial and spinal nerves and associated ganglia. This connection is made by sensory and motor neurons that conduct impulses to the CNS or the periphery, respectively [15].

12.1.2 General Overview of Peripheral Nerve Injuries

Neurological defects are among the most demanding clinical situations despite decades of research in the neurological field [16]. The reason for this relies in the complexity of the nervous system functions, structure, and anatomy, which makes it more challenging to treat as compared to other tissues in the human body [17]. Opposing to the CNS, the PNS is not protected by a hard bone layer or by the blood-brain barrier, making it much more disposed to traumatisms or any kind of injuries [18]. Therefore, PNIs are considered a huge clinical burden, being the incidence 1 in 1000 individuals per year [19]. The estimated numbers of PNIs range from 300,000 and 360,000 cases per year for Europe and the USA, respectively [20]. In fact, PNIs are associated with $150 billion healthcare expenses per year in the USA alone [15]. These costs are underestimated, since "bed-days" and lack of productivity also account for monetary losses, worldwide. It has been assessed that 25% of patients suffering from traumatic injuries and undergoing surgery do not return to work 1.5 years after the intervention.

This scenario tends to worsen with the increasing world population and respective average lifespan. Considering those, an additional number of injuries tend to appear, and consequently a high number of treatments and surgeries will be required to allow the restoration of the damaged nerves [21]. Although the CNS is vastly protected and therefore less prone to injuries, it has a limited ability to regenerate because of the succeeding scar tissue development which can be created by a vast range of cell types, such as fibroblasts, neuroglia, monocytes, and endothelial cells [22]. In contrast, PNIs are considerably more common, but the peripheral nerves have a greater regeneration potential as compared to the nerves of CNS. This is because PNS glial cells, Schwann cells, adjust to a regenerative phenotype and have the capacity of triggering neuronal regenerative processes, although usually slow and in a partial manner [23]. The regeneration process, however, is dependent on certain factors, such as the lesion size and the quality of the affected nerve, the person's health statues (e.g., diabetic or non-diabetic), age, and, most importantly, the time period from injury to surgical reconstruction. In the case of lengthy time without repair, the distal nerve end and target tissues and organs are chronically denervated, becoming chronically axotomized, which leads to neurons undergoing apoptosis [24].

Given to their exposure, peripheral nerve damages can be caused by many types of events, such as traumatic injuries, complications on surgeries, congenital defects, and war wounds. Concerning the traumatic injuries, they can also vary significantly and include tearing injuries, crushing or smashing, ischemia, and less prevalent types of injury such as thermal, electric shock, and radiation [25]. Compression neuropathies are also ubiquitous among nerve injuries. For instance, carpal tunnel syndrome, the most common compression type of injury, affects 4% of the overall population [26]. A vast range of diseases can also be the root cause of PNIs, as is the case of diabetic peripheral neuropathies [27, 28]. Most of these traumatic events cause neuronal death, demyelination, and axonal degeneration resulting in persistent complaints, such as impaired sensory and motor nerve functionality and radiating neuropathic pain. Disorders concerning the PNS usually have overwhelming and

life-disturbing impacts on patients' daily functions and habits, which are not usually regarded as significant. There is a substantial lack of consideration of the impact of injury on social and emotional well-being, despite their importance to patients. There is, in fact, a strong correlation between PNIs and pain and depression in those patients [29].

Due to the great variety of peripheral nerve traumas, there was a categorization of nerve injuries in main domains, as an attempt to systematize them for the medical and scientific community. Several degrees of injury to peripheral nerves are detailed in Table 12.1, which were firstly described by Seddon [30] and later by Sunderland [31].

The Seddon classification is divided into three categories according to the gravity of the injury: (i) neurapraxia, (ii) axonotmesis, and (iii) neurotmesis. By its turn, Sunderland classification comprises five different categories: first, second, third, fourth, and fifth degree. Seddon classification is more straightforward and therefore the most used. Neurapraxia is the least severe type of injury, and it is not associated with long-term impairments and consequences. The second level, axonotmesis, is related to axon and myelin discontinuity or disruption. The most severe type, neurotmesis, involves the complete disconnection of the nerve, where a gap is formed.

12.1.3 Degeneration and Regeneration Processes Following PNIs

Immediately after injury, the regeneration process of peripheral nerves runs in sequenced phases, and different events occur at different levels on the injury site encompassing both proximal and distal sites (Fig. 12.2a) [32]. In the proximal position, separated axons and cell bodies degenerate via a programmed cell death pathway called chromatolysis [33]. In the distal injury end, a process called Wallerian degeneration occurs 24–48 h after injury, and all nerve components, including the distal axons and adjacent myelin, start to degenerate [34]. The goal of that

Table 12.1 Seddon [30] and Sunderland [31] classification of PNIs

Seddon and Sunderland classification	Process	Sunderland scheme of nerve injury	Neurological deficits	Degree of recovery
Neurapraxia I	Local myelin damage usually secondary to compression	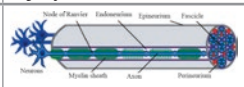	Neuritis, paresthesia	Full recovery
Axonotmesis II, III, IV	Axon severed but endoneurium intact (optimal circumstances for regeneration)	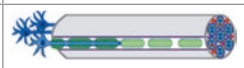	Paresthesia	Full recovery
	Axon discontinuity, endoneurial tube discontinuity, perineurium, and fascicular arrangement preserved		Paresthesia, dysesthesia	Wallerian degeneration, recovery incomplete
	Loss of continuity of axons, endoneurial tubes, perineurium and fasciculi; epineurium intact		Dysesthesia, neuroma	Wallerian degeneration, recovery incomplete
Neurotmesis V	Complete physiologic disruption of the entire nerve trunk	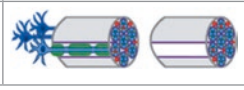	Intractable pain, neuroma	Wallerian degeneration, recovery incomplete

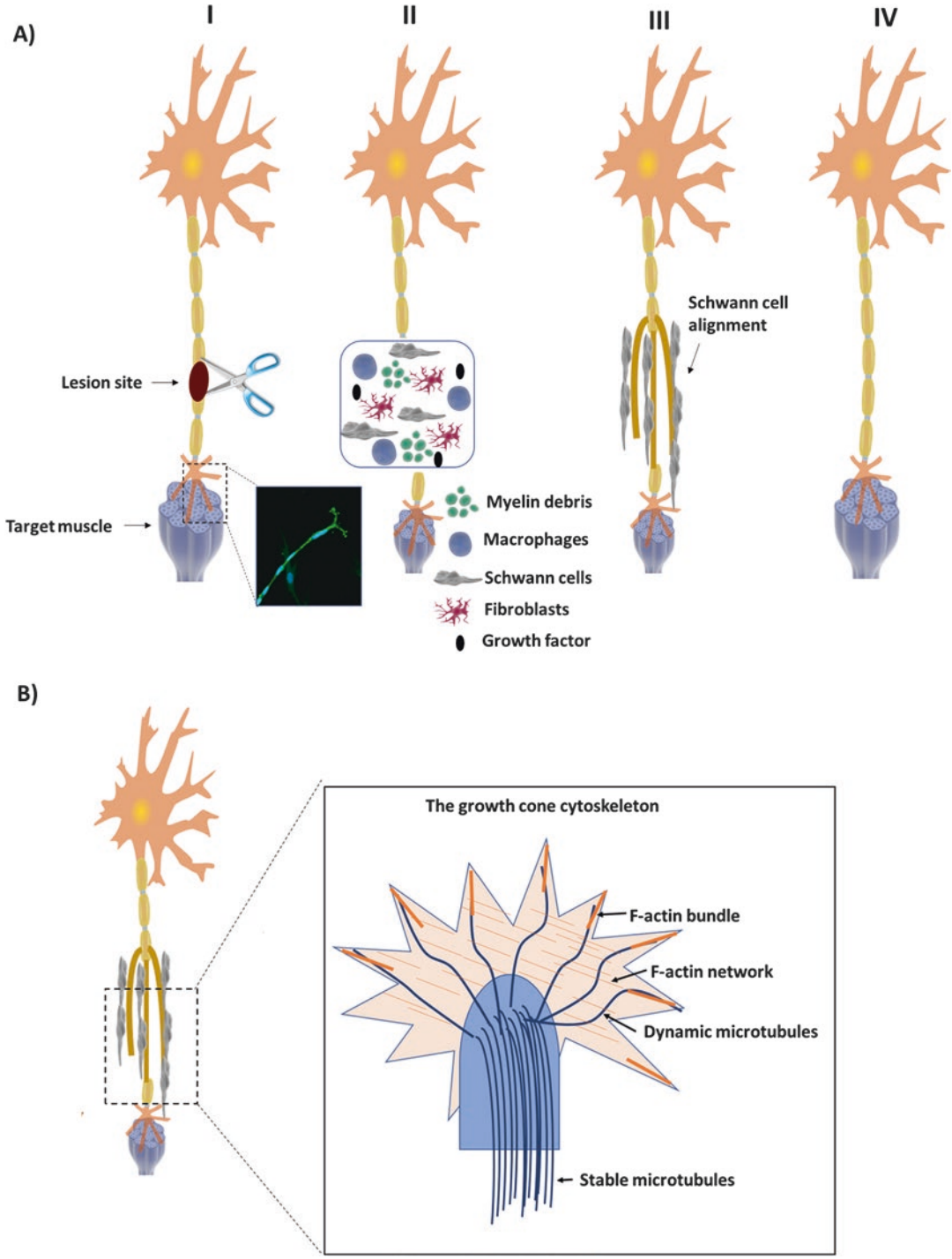

Fig. 12.2 (**a**) Progression of Wallerian degeneration. (I) A single axon with enwrapping myelinating Schwann cells suffers a traumatic injury. (II) The axon breaks, and the distal stump undergoes cellular changes. Distal to the injury, there is a destruction of the remaining intact axon and disintegration of myelin cover, leaving debris behind. Macrophages and Schwann cells, which turned to a pro-regenerative phenotype, accumulate at the lesion site and scavenge the debris. (III) Schwann cells align in the bands of Bungner. These tubes provide a permissive growth environment and guide extending axons toward distal targets. (IV) If the axon is able to traverse the injury gap, the distal target becomes re-enervated, and the neuron becomes fully functional. (**b**) The growth cone is a large actin-supported extension of a regenerating neurite pursuing its corresponding synaptic target. It is responsible for the migration and path finding during neurite extension, in which the lamellipodia and filopodia interact with the adjacent matrix

phenomenon is related to the clearance of undesired debris. Schwann cells phagocytize axonal and myelin debris, until only empty endoneurial tubes remain. Normal nerve function depends on such type of cells, which are the myelinating glial cells of the PNS [35, 36].

After debris removal, Schwann cells fill the empty endoneurial tubes and organize in characteristic bands or tubes of Bungner and by this mean supporting the regrowth of axons. Not only Schwann cells have a crucial role, but also macrophages are recruited to the area releasing growth factors and cytokines. The release of cytokines will stimulate Schwann cells and fibroblast proliferation and are responsible for the axonal regeneration process [37]. Ahead in the process, in the proximal injury end, a growth cone emerges following the path formed by the band of Bungner, which is of fundamental importance for the advance of the regenerating axon [38]. The growth cone can be seen in Fig. 12.2b [39]. In optimal conditions, axonal regeneration is very slow, occurring at a rate of approximately 1 mm/day and demanding at least more than 1 year for muscle re-innervation and initial functional recovery [40].

12.1.3.1 The Role of Schwann Cells in Injury Response

Schwann cells are among the first active components after nerve injury. Finding their embryologic origin in the neural crest, Schwann cells have the capacity to proliferate, produce, and deliver neurotrophic factors, modulate the immune response, myelinate axons, migrate, and adjust their shape and phenotype. This makes them the perfect cells toward intervening in neural repair [41].

Although the degeneration of axons in the distal nerve end starts roughly 2 days after injury, activity of Schwann cells can be distinguished before that, within hours of injury, where Schwann cells undergo a phenotypic change [14]. This phenotypic change will support PNR in several ways. Firstly, they dedifferentiate by means of acquiring a non-myelinating and immature Schwann cell stage phenotype. That stage is characterized by an upregulation of L1, NCAM, p75NTR, and glial fibrillary acidic protein (GFAP). On the other hand, myelin-associated genes are downregulated, which comprise myelin transcription factor Egr2, organizational and mechanical supporting proteins such as protein 0 (P0), myelin basic protein (MBP), and myelin-associated glycoprotein [42]. There is also an upregulation and secretion of a beneficial group of trophic factors, such as nerve growth factor (NGF), brain-derived neurotrophic factor (BDNF), ciliary neurotrophic factor (CNTF), basic fibroblast growth factor (bFGF), vascular endothelial growth factor (VEGF), and pleiotrophin [43]. Furthermore, the expression of cytokines capable of recruiting macrophages is also upregulated, which include tumor necrosis factor (TNF)-α, LIF, interleukin (IL)-1α, IL-1β, and monocyte chemoattractant protein 1 (MCP-1). Schwann cells activate a cell-intrinsic myelin breakdown process, which will destroy myelin by an autophagy process, roughly at the 5th day after injury [23]. This is a key process intimately related to increasing the regenerative potential after injury. In fact, elimination of degenerated myelin is fundamental for repair since PNS myelin holds molecules that inhibit regeneration of severed axons, namely, the myelin-associated glycoprotein [44]. At last, Schwann cells' response to injury also includes the formation of regeneration tracks, known as bands of Bungner. For that, Schwann cells adopt the elongated spindle-shape morphology and line up in columns. To perform such task, they express a variety of adhesion molecules on their surface, such as N-cadherin, L1, and N-CAM. Extracellular matrix (ECM) molecules are also secreted, such as laminin and fibronectin. All the secreted molecules are considered guidance-promoting signaling molecules, important not only during early development but also to create a microenvironment that mediates axon regrowth and guidance, allowing axons to reconnect with their target tissues [45].

Overall, Schwann cells acquire a pro-regenerative phenotype, capable of promoting nerve repair, when there is a conversion of

myelin-Schwann cells to repair Schwann cells. The single protein capable of this transformation is c-Jun, which is rapidly upregulated in the distal nerve end after injury [46].

12.1.4 Strategies for Nerve Repair

Clinically, the straightforward technique to repair minor nerve defects is the end-to-end suture [47]. However, this technique is circumscribed to a maximum gap length ranging from 5 mm to 20 mm, depending on the nerve, since the suture must be done without creating excessive tension in the nerve ends. When the nerve gap length makes end-to-end suture unfeasible, peripheral nerve grafts are the gold standard treatment for nerve restoration. In a technique that dates to Philipeux and Vulpian in 1817 [48], the insertion of a graft section provides a physical and biological scaffolding, over which axonal outgrowth occurs. Grafts can be autologous, known as autografts, or allografts. The use of autografts has inherent disadvantages, such as donor site morbidity and reduced availability [49]. For allografts, the tissue is harvested from another donor, which can increase the risk of disease transmission and immunological response. However, related to allografts, a recent and promising alternative for patients who have exhausted all reconstructive methods is the vascularized composite tissue allotransplantation (VCA) [50]. Furthermore, tacrolimus, one of the immunosuppressant drugs that will accompany the patients for a lifetime when subjected to this procedure, has shown to have positive effects in PNR [51].

However, despite those seemingly good chances of recovery with grafts, incomplete recuperation from PNIs usually can lead to multiple negative consequences, which comprise numbness of affected members, chronic pain, diminishing of sensory and/or motor function, and a disturbing permanent disability of the patients [52]. It is a fact that these outcomes are unsatisfactory for the demands of today's patient lives, since only 25% of patients regain proper motor function and less than 3% recuperate sensation in a full extent [53].

Decellularized nerve conduits are another possibility for nerve repair [54]. In order to avoid the need of immunosuppressive drugs associated with allograft requirements, which make the patient more prone to acquire infection and tumors, the decellularized nerve conduits can eliminate the cellular components that cause immunogenic reactions. However, the native ECM is conserved, along with the basal lamina, and the guiding mechanical cues for axonal growth are maintained. Several methods can be used to decellularize nerves, among them, physical methods such as lyophilization [55], direct pressure, and agitation [56]. Chemical methods have also been attempted and include digestion with alkaline or acidic solutions [57] and detergents [58], together with the action of enzymes such as trypsin and endonucleases [59]. Various studies support the hypothesis that decellularized grafts are among the best options for nerve repair, since they can bridge more than 10–20 mm long gaps in rats [60, 61]. However, as concluded by the authors who performed a 10-year review of the use of allografts for PNR [54], further research is desirable in order to improve and standardize preparation protocols, including recellularization, and advance their effectiveness, therefore being able to substitute the current gold standard, especially in the repair of long nerve defects.

For these reasons, increasing efforts have been made over the last decades in the search for effective alternatives to autografts. Surgical treatment strategies in the case of PNI can be seen in Fig. 12.3.

In an attempt to overcome the limitations of nerve grafting as well as the unsatisfactory outcomes, TE approaches focusing on the development of innovative biocompatible artificial nerve devices to assist innate regeneration processes to reestablish the peripheral nerve have also been reported [62, 63]. TE strategies have been a widely travelled alternative to bridge the nerve gap, and throughout the years, many types of NGCs were proposed, being some of them already approved by the Food and Drug Administration (FDA) [64, 65]. Since mature neurons are not susceptible to mitosis phenom-

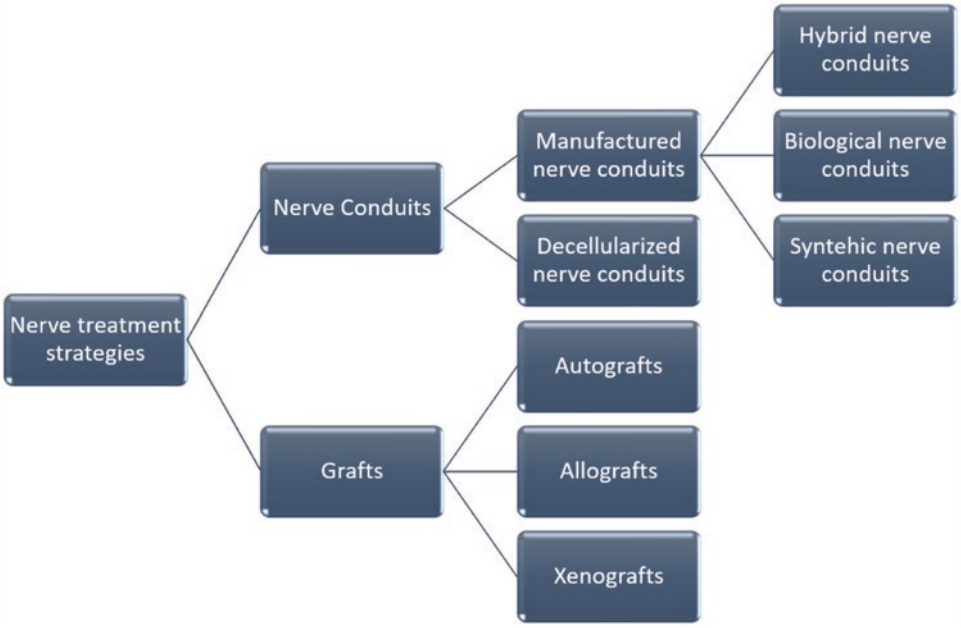

Fig. 12.3 Strategies for nerve repair. In the case of a significant nerve gap formation where end-to-end coaptation is not possible, nerve grafts or engineered NGCs are required to serve as a bridge between the nerve stumps and to support axonal regrowth. In the case of grafts, they can be from the patient herself/himself, known as the autografts. Allografts and xenografts are also a possibility. As an alternative, if the option falls in the NGCs, those can be nerves harvested from the body, which undergo a process of decellularization to avoid immunological reactions, maintaining the ECM for physical support. NGCs can also be manufactured and engineered with biological or synthetic materials, as well as a combination of both

ena, it is crucial to support the regrowth of the existing cell bodies, providing both a protective environment and guiding paths. In this way, it is possible to direct axons from the proximal to the distal site, permitting the proper linking of the damaged synapse connections. In brief, the protection of the injury site and performance as a guidance substrate are the two main reasons why tubulization is used in PNIs.

Engineering a NGC should aim at facilitating cellular spreading and growth of damaged nerve tissues in three dimensions (3D) [66]. In addition, it is crucially important that the material envisioned to be used to construct the NGC is cytocompatible and has pronounced biomechanical properties, and suturability. If an engineered NGC does not present a proper cytocompatibility, it may not contribute to the growth of damaged nerves, but would instead be the reason of acute inflammation and even infection [67]. It must exhibit good biocompatibility with low inflammatory and immunogenic reactions [68]. It must also be biodegradable and ideally degrade in the same rate as nerve regenerates. Otherwise, a quick degradation might trigger an inflammatory response [66, 69]. Regarding the mechanical properties, the NGC should provide sufficient mechanical strength to prevent the NGC rupture during the patient's movements and physically support neural tissue regeneration. Concurrently, the NGC should have appropriate elasticity to be able to lessen tensions in the damaged area [67]. Two other major features that NGCs must possess are related to the suturability, where the suture thread cannot be pulled out of the material when in physical stress [70]. The second feature relates to the ability of a medical device to not calcify when implanted in vivo. Such characteristic must be previously tested and avoided at all costs, since calcification of a conduit would hin-

der regeneration in a great extent. In fact, Carvalho et al. [71] recently reported on a silk fibroin NGC that would or not calcify, according to the method of solvent removal and final surface properties.

Furthermore, the materials used to construct NGCs should prevent the penetration of fibroblasts that will lead to the formation of glial scar tissue around the implant, which could reduce the healing chances [72]. The permeability of a conduit is also an important parameter to consider in the NGC design as both nutrients and oxygen must diffuse into the site of regeneration.

Otherwise, cells inside the conduit, especially if it is a long conduit, will be under a deleterious ischemic environment which can result in cellular hypoxia and lack of proper nutrients. Ideally, electrical conductivity would be preferred for a NGC used in neural TE in order to mimic the electrical properties of nerves and at the same time excite the neuron communication [73]. The parameters to be considered for the design of NGCs are summarized in Table 12.2 [66, 74–81]. In brief, an ideal NGC should be biocompatible, biodegradable, flexible, kink-resistant, compliant, easily suturable, porous, neuroconductive, and with suitable surface and overall mechanical properties [66]. Furthermore, the developed NGC should allow vascularization to occur in the lumen and avoid calcification in vivo.

In the early use of NGCs made of synthetic materials, they were mainly composed of silicon tubes and could only repair injuries up to 10 mm. Some disadvantages on the use of that conduits included total lack of biodegradability, which led to inflammation and chronic foreign body reaction, as well as lack of swelling capacity, which would compress the nerve, thus hindering the regeneration process [83]. In order to overcome such difficulties, biodegradable NGCs have been proposed, some of which are FDA-approved and being currently used in the clinical setting [65]. The FDA-approved NGCs can be seen in Table 12.3 [65].

Table 12.2 Design criteria for the development of NGCs

Ideal properties of NGCs	Detailed description
Biocompatibility	Must be well incorporated in surrounding tissues and not cause inflammatory response [74]
Degradation	Degradation rate should match nerve regeneration rate [75]
Porosity	NGC must allow nutrient and oxygen exchange, limiting scar tissue infiltration [76]
Anisotropy	The NGC conduit itself or the luminal filler should be aligned to provide directional guidance [77]
Adequate protein release	NGC or the luminal filler should provide sustained release of growth factors [78]
Physical fit	Adequate internal diameter not to compress the growing nerve [66]
Cellular support	Must allow the adhesion and proliferation of relevant cell types, such as Schwann cells and endothelial cells [79]
Electrically conducting	Capable of propagating electrical signals [80]
Vascularization	The NGC must allow the vascularization to occur inside the NGCs, to nourish the regenerating tissue [81]
Calcification	The implantable NGC must not calcify in vivo [71]
Suturability	The NGC must withstand a suture being pulled out without breaking the biomaterial [82]

12.1.4.1 Biomaterials

Synthetic Biomaterials

Regarding the synthetic materials, these are still considered very promising since the majority of the FDA-approved NGCs are composed of materials such as Neurotube (Polyglycolic acid, PGA) and Neurolac (poly(L-lactide-co-ε-caprolactone, PLCL). Other synthetic materials widely used in PNR are polylactic acid (PLA), polylactic-co-glycolic (PLGA), polycaprolactone (PCL), and polyhydroxybutyrate (PHB). In brief, synthetic nerve conduits provide higher degree of controllability, better mechanical properties, and poor bioactivity as compared to their natural equiva-

Table 12.3 Approved NGCs used in the clinical setting

Product name	Company	Biomaterial composition	Degradation time
Neuragen®	Integra Neurosciences, NJ, USA	Collagen type I	36–48 months
NeuraWrap™	Integra Neurosciences, NJ, USA	Collagen type I	36–48 months
NeuroMend™	Collagen Matrix, Inc., NJ, USA	Collagen type I	4–8 months
Neuromatrix/ Neuroflex™	Collagen Matrix, Inc., NJ, USA	Collagen type I	4–8 months
Neurotube®	Synovis Micro Companies Alliance, AL, USA	Polyglycolic acid (PGA)	6–12 months
Neurolac™	Polyganics Inc., Netherlands	Poly(D,L-lactide-co-ε-caprolactone (PLCL)	16 months
SaluBridge/ SaluTunnel™	SaluMedica LLC, GA, USA	Polyvinyl alcohol (PVA)	Non-degradable
Axoguard®	Cook Biotech Products, IN, USA	Porcine small intestinal submucosa matrix	N/A
Avance®	AxoGen Corporation, USA	Human nerve allograft	N/A

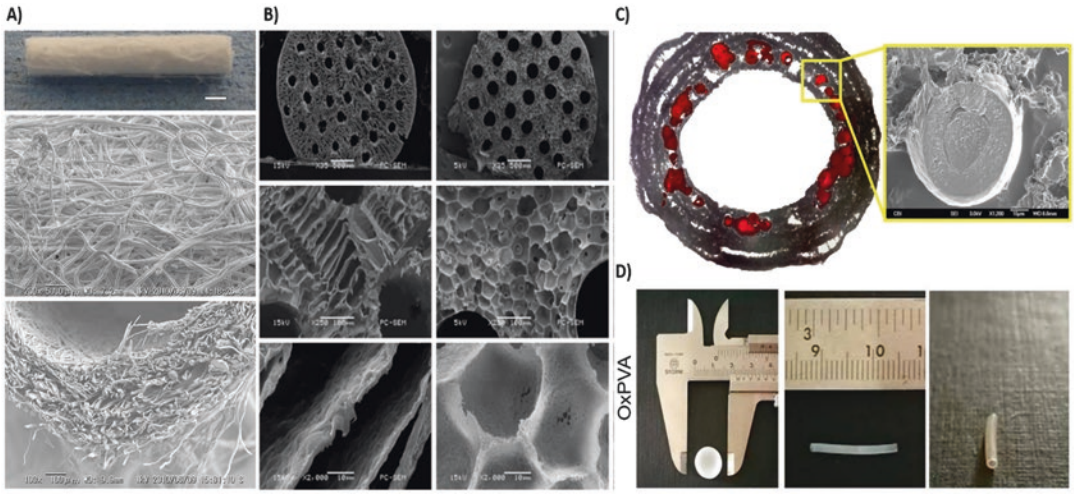

Fig. 12.4 Promising results obtained with synthetic polymers applied to PNR. (**a**) A non-woven polylactic acid (PLA) tube. Scale bar: 1 mm. (**b**) SEM images of the PLLA multi-channel conduits cross section using different magnification. Scale bar: 500, 100, and 10 μm, from top to bottom. (**c**) Scanning electron micrograph of double-walled microsphere following incorporation into PCL nerve guides. (**d**) Gross appearance of disk-shaped and tubular scaffolds made of OxPVA. (**a**–**d**) were reprinted with from [86, 88, 95] and [98], respectively

lents [65]. Moreover, these materials are known for low inflammatory response and effortlessness processing, which means they can be processed in a variety of forms, to enhance nervous tissue growth. However, in spite of the referred positive characteristics of synthetic polymers, a few disadvantages are also reported [84]. The main negative aspects are related to suboptimal biodegradation and possible toxic biodegradation byproducts. These drawbacks block their extended use in the clinics [85]. Figure 12.4 shows some promising results considering synthetic biomaterials applied to PNR. From Table 12.4, it is also possible to find the most recent and relevant reports considering the use of synthetic biomaterials in PNR [86–98].

PLA

PLA has been used as a nerve conduit material in a few studies. Matsumine et al. [86] developed a

Table 12.4 Relevant and recent published works focused on the fabrication of NGC with synthetic biomaterials

Conduit material	Fabrication method	Location, defect size, model	Outcomes	Year, reference
PLA	Non-woven material, melt-blown process	Facial nerve, 7 mm gap, rat	Comparable ability to induce PNR as autologous nerve graft	2014, [86]
	Multi-layer, microbraided, fiber-reinforced conduit	Sciatic nerve, 10 mm gap, rat	Successful regeneration with cables bridging the gap	2009, [87]
PLLA	Low-pressure injection molding and thermal-induced phase separation technique, 33 inner channel NGC	In vitro assays with NSCs	81.1% of NSCs differentiated into neurons	2014, [88]
	Porous PDLLA conduit achieved by dipping method, with micropatterned inner lumen by ion etching. Pre-seeded with Schwann cells	Sciatic nerve, 10 mm gap, rat	Presence of Schwann cells did not affect results; speed of functional recovery was enhanced	2004, [89]
PGA	Neurotube® is fabricated to form a knitted or woven tubular device	Segmental nerve defect, 10 mm gap, rat	Exhibited the poorest results for functional motor recovery in the rat model in comparison to other FDA-approved conduits	2009, [90]
		Facial nerve, 10–30 mm gap, humans	Valid solution for this kind of defect in emergency. Associated with some limitation such as high cost and possible intolerance	2005, [91]
PLGA	PLGA fibrous outer layer produced by electrospinning and containing laminin-coated yarns obtained by double-nozzle electrospinning	In vitro assays with Schwann cells	Significant higher proliferation and elongation of Schwann cells along the inner yarns	2017, [92]
	Two concentric biodegradable PLGA tubes enclosing a NGF reservoir. Solvent casting method	Sciatic nerve, 15 mm gap, rat	Optimal release levels of NGF; improved muscle weight, myelinated nerve growth, and higher target connection	2017, [93]
PCL	3D printed conduit embedded with electrospun aligned nanofibers	In vitro assays with NSCs and primary cortical neurons	Increased average neurite length and directed neurite extension along the fiber	2017, [94]
	PCL conduits were fabricated by dipping and incorporate double-walled PLGA/PLA microspheres encapsulating GDNF	Sciatic nerve, 15 mm gap, rat	GDNF increased tissue formation within the nerve guide lumen and promoted the migration and proliferation of Schwann cells	2010, [95]
PU	Mold casting followed by freeze-drying, producing a porous scaffold	Sciatic nerve, 10 mm gap, rat	Significantly greater efficacy of the PU conduit when compared to the commercial Neurotube®.	2017, [96]
	Electrospun antioxidant PU conduit filled with freeze-dried aligned chitosan-gelatin cryogel	In vitro study with neuro-2a, C2C12, and DRGs.	DRGs demonstrated aligned growth of the neurites along the pores of the cryogel inside the NGCs	2018, [97]
PVA	SaluBridge™, implantable wrap	N/A	No manuscripts have been published regarding this NGC	N/A
	Dipping technique of Oxidized polyvinyl alcohol (OxPVA) hydrogel	Sciatic nerve, 5 mm gap, rat	Axon density in the middle of the conduit significantly higher as compared to autograft	2018, [98]

biodegradable nerve conduit with PLA non-woven fabric and evaluated its nerve regeneration-promoting effect. The conduit made of randomly connected PLA fibers demonstrated a comparable ability as the autograft to induce PNR in the buccal branch of a 7 mm facial nerve defect. Another author developed a biodegradable multi-layer microbraided PLA fiber-reinforced conduit

with outstanding mechanical properties, which revealed to be a promising tool for neuro-regeneration [87].

PLLA

PLLA is the crystalline form of PLA. In a study by Zeng et al. [88], several topographies were achieved in the PLLA conduit using low-pressure injection molding and thermal-induced phase separation, including a nanofibrous microstructure, microspherical pores and nanofibrous pore walls, and a ladder-like microstructure. Of all the topographies experimented, the nanofibrous microstructure allowed the differentiation of neural stem cells (NSCs) into neurons. Also paying a lot of attention to the inner structure of the NGC, others have developed a conduit that consists of a porous poly(D,L-lactic acid) (PDLLA) tubular support structure with a micropatterned inner lumen pre-seeded with Schwann cells [89]. Such device delivered physical, chemical, and biological guidance cues.

PGA

The use of PGA is not very common in PNR field. However, of the clinically available NGCs, PGA has the most rapid degradation rate, and it is FDA-approved (Neurotube®). When testing Neurotube® for facial nerve repair, it was found to be an effective substitute to autologous nerve grafts. However, the authors reported a few limitations to this NGC, which consist in the fact that it can only be used with gaps of less than 30 mm, it is quite costly, and intolerance cases have been reported [91]. When compared to other FDA-approved conduits, Neurotube® achieved the poorest result in terms of nerve regeneration [90].

PLGA

PLGA is one of the most attractive synthetic polymers and broadly used in PNR. This FDA-approved material gives rise to very low inflammatory responses, and its degradation can be easily controlled by altering the ratio of its monomer components. Additionally, PLGA scaffolds have the unique ability of adhering to Schwann cells and directing their growth [99]. A recent study focused on producing a laminin-coated and yarn-encapsulated PLGA NGC [92]. The PLGA fiber yarns were fabricated through a double-nozzle electrospinning system, and then the PLGA fibrous outer layer was collected using a general electrospinning method. The conduit demonstrated adequate mechanical properties as well as promising potential in promoting Schwann cell proliferation and migration. In another study also focused on different topographies [100], it was developed a hybrid-structured nerve conduit which consists of a PLGA microfibrous bundle wrapped in a micro-/nanostructured PLGA membrane. This device demonstrated high capability for guiding nerve cells and promoting cell migration. Many other studies using PLGA were developed, inclusively with conduits capable of releasing NTFs or other neuroprotective molecules such as salidroside and Nectin-like molecule 1 (NECL1) [93, 101, 102].

PCL

PCL is one of the most used polymers in TE [103]. It has been broadly applied in bone [104], cartilage [105], cancer defects [106], and drug delivery applications [107]. It is a biodegradable semicrystalline linear polyester produced by ring-opening polymerization of *e*-caprolactone with a low melting point of around 60 °C. For the biodegradable polyesters mentioned so far, in vivo degradation rate is in the order PCL < PLA < PGA. Due to PCL's very low in vivo degradation rate and high drug permeability, it has been found to be useful in long-term implantable delivery devices [108]. Bearing in mind that polymeric bioabsorbable conduits can be used as drug delivery systems, Salmoria et al. [109] produced PCL conduits by melt extrusion technique, which were loaded with ibuprofen. PCL is also a very attractive polymer for the rapidly emerging and recently popular 3D printing technology. In a study recently published by Lee et al. [94], combination of stereolithography and electrospinning techniques allowed to fabricate a novel 3D biomimetic PCL neural scaffold with tunable porous structure and embedded aligned fibers. The results indicated that PCL fibers greatly increased the average neurite length and directed neurite extension of primary cortical neurons along the

fiber. Quite often, polyesters are blended with other components to make composite NGCs which allows to improve their mechanical properties and control the general features of the NGCs in more detail [95, 110–113].

PU

Created by a water-borne process, PU has recently been applied as the base material for the construction of a novel NGC [96]. The NGC was built through the freeze-drying technique and presented an asymmetric microporous structure that allowed bridging a 10 mm gap in rat sciatic nerve. The results, in terms of nerve regeneration, were remarkable. Inclusively, based on functional recovery and histology findings, the efficacy of PU NGC was superior to that of commercial conduit Neurotube®, to which it was compared. Recently, an antioxidant PU conduit was developed using the electrospinning technique by Singh et al. [97] and further filled with an aligned chitosan-gelatin cryogel filler. The in vitro cellular tests with dorsal root ganglia (DRGs) cultures showed the aligned growth and cellular migration along the pores, indicating that both the outer part of the conduit and the luminal filling are potentially appropriate for PNR.

PVA

PVA is another synthetic polymer used in the construction of NGCs. It is water soluble but non-degradable, being considered non-resorbable. There is currently FDA-approved NGCs made of PVA hydrogels, named SaluBridge™ and SaluTunnel™. However, such devices have not been validated with accessible pre-clinical or clinical studies. It can also be stated that the utilization of nonabsorbable conduits has declined with the recent use of absorbable synthetic grafts [114]. To improve that, Stocco et al. [98] recently manufactured a conduit made of a patented and novel biodegradable hydrogel, oxidized PVA (OxPVA). An in vitro and in vivo battery of tests revealed that OxPVA scaffolds performed very similarly to the autograft group.

Natural-Origin Biomaterials

Natural-origin biopolymers used for the fabrication of NGCs typically have regenerative bioactivity along with appropriate mechanical properties. Natural biomaterials allow for improved communications between cellular components, and the scaffold is also an advantage since cells must be stimulated to proliferate, benefiting tissue regeneration [115]. However, some restrictions are associated with natural-origin biomaterials, such as the batch-to-batch disparities [116]. In the section below, interesting and recent reports using natural-origin biomaterials for PNR applications, from proteins (e.g., silk fibroin and keratin) to polysaccharides (e.g., chitosan and alginate), will be reviewed. Figure 12.5 shows some promising results obtained with natural-origin biomaterials, in particular using silk fibroin, chitosan, and alginate polymers. The significant works considering the use of natural-origin biomaterials in PNR are summarized in Table 12.5 [117–128].

Silk Fibroin

Silk fibroin (SF) is a fibrous protein with remarkable mechanical properties produced by silkworms and spiders [129]. Silk polymers consist of repetitive protein sequences and provide structural roles in nature, such as cocoon formation, nest building, and web creation [130]. With very low immunological response, capacity to be transformed in diverse shapes and matrices, tunable degradation, as well as easily chemically modified, SF has the potential to impact the clinical needs in terms of nerve regeneration [131]. Beyond PNR, SF has been extensively applied in the TERM field with very distinctive applications [132–134].

Carvalho et al. [71] produced tunable enzymatically cross-linked SF NGCs, resourcing to tyrosine groups present in silk structure that are known for allowing the formation of a covalently cross-linked hydrogel. The fact that the process involves an enzymatic cross-linking allows tuning several parameters in the final conduit, i.e., from its mechanical properties to porosity or biological properties.

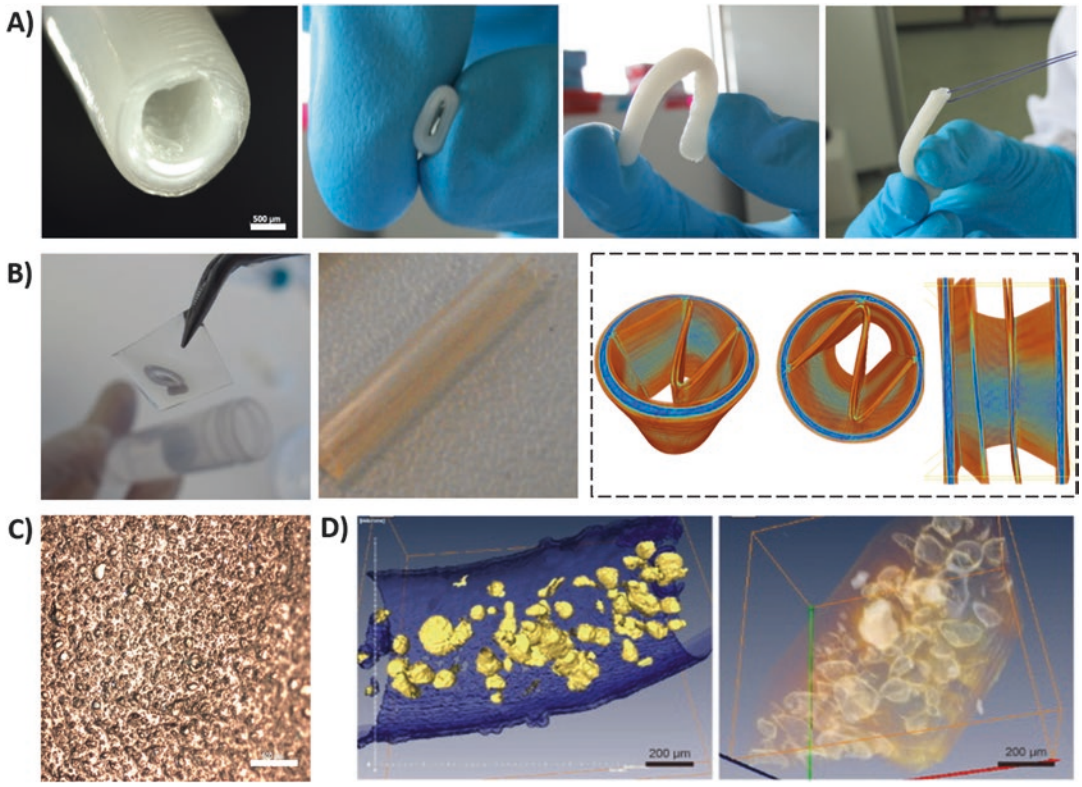

Fig. 12.5 Promising results obtained with natural-origin polymers applied to PNR. (**a**) Example of an enzymatically cross-linked SF nerve guidance conduit developed and patented by Carvalho et al. [71] for application in PNR. The developed NGC presents outstanding mechanical properties, with kinking-resistant capacity and suturability, as can be seen by the images (in that row). (**b**) Images of a 5% of degree of acetylation chitosan membrane, which can be further used as a NGC by rolling up or in a different strategy, as a luminal filler. (**c**) 5% degree of acetylation chitosan membrane incorporating human hair keratin, developed at our research institute. (**d**) Confocal laser microscopy showing macroporous alginate fibers incorporating gelatin particle porogens. Scale bar: 500 µm

One of the advantages of SF relies on the ability to be processed in a variety of shapes. Dinis et al. [135] developed a 3D multi-channel SF conduit through electrospinning system encompassing approximately 12 multi-channel guides of different sizes inside the main conduit, mimicking the native structure of the nerve endoneurium, perineurium, and epineurium. In fact, due to the outstanding properties that several silk NGC have demonstrated after decades of research, there is an active clinical trial (NCT03673449) with SilkBridge. Such device is a biocompatible SF-based matrix that aims at attracting the patients' native cells to regenerate the nerve, i.e., without the need to add cellular components previous to the implantation. The SilkBridge is also being used in digital nerve defects.

Keratin

Keratin protein has been recognized as biomaterial with high potential due to its excellent bioactivity and biocompatibility [136]. Lately, the hair keratin has gained much attention [137, 138], not only because of its properties but because the follicle itself is a bizarrely proliferative organelle that illustrates an extremely arranged regenerative process. Also, the fact that it is potent naturally derived biomaterial, is human-derived, and

Table 12.5 Relevant and recent published works focused on the fabrication of NGC with natural biomaterials

Conduit material	Fabrication method	Defect size, location, model	Outcomes	Year, references
Silk fibroin (SF)	Simple spider silk fibers, from *Nephila edulis* species	In vitro study, co-culture of ADSCs and Schwann cells	Spider silk fibers represent a suitable NGC filler due to cell migration and elongation along the fibers	2018, [117]
	SF and PLLA conduit fabricated by electrospinning	10 mm gap, sciatic nerve defect, rat	The presence of silk augments VEGF secretion, therefore increasing neo-angiogenesis and stimulating nerve regeneration	2018, [118]
	SF conduit with aligned SF filaments in the interior	10 mm gap, sciatic nerve defect, rat	FluoroGold retrograde tracing and histological investigation; SF conduits were able to promote nerve regeneration with results approaching those provoked by the positive control autografts	2018, [119]
	Adsorption of gold nanoparticles onto SF fibers and electrospinning	10 mm gap, sciatic nerve defect, rat	Nerve conduction velocity as well as the compound muscle action potential was improved due to the presence of conductive gold nanoparticles	2018, [120]
Keratin	Human hair keratin hydrogel was injected in a FDA-approved conduit	4 mm gap, tibial nerve defect, mice	Robust nerve regeneration response, in part through activation of Schwann cells. Results similar to autograft	2008, [121]
	Neuragen® collagen conduit filled with keratin hydrogel	10 mm gap, median nerve defect, *Macaca fascicularis*	Confirms earlier findings in studies using rodents; represents off-the-shelf alternative to autograft	2014, [122]
	Double-wall PCL containing GDNF microspheres with a keratin hydrogel	10 mm gap, sciatic nerve defect, rat	Significant increased density of both Schwann cells and axons, resulting in the better quality of the regenerated nerve through the conduit with keratin	2012, [123]
Chitosan	Chitosan nerve guides from Reaxon® with a longitudinal chitosan film as a filler	15 mm gap, sciatic nerve defect, diabetic rat	Supported robust axonal regeneration and functional recovery in healthy animals but also demonstrated to be beneficial for the regeneration process in diabetic rats with relevant blood glucose levels	2016, [124]
	Chitosan film enhanced with MSCs	10 mm gap, sciatic nerve defect, rat	Chitosan film enhanced with MSCs improved functional, electrophysiological, and histomorphometry recovery of transected sciatic nerves	2018, [125]
	Chitosan membranes with different degrees of acetylation	Schwann cell and fibroblast in vitro assays	% of acetylation were found to favor Schwann cell invasion and proliferation, presenting at the same time low fibroblast adhesion	2017, [126]
	Combination of MSCs with a chitosan film	10 mm gap, sciatic nerve defect, rat	MSCs were useful for the injury because of the release of several neurotrophic factors as well as the synergistic effect of chitosan accelerating wound healing by promoting an anti-inflammatory effect	2018, [126]
Alginate	Macroporous alginate fibers produced with a syringe pump	In vitro assays with DRGs	Encapsulation of primary DRGs in macroporous alginate fibers resulted in marked neurite outgrowth over 150 μm	2017, [127]
	3D bioprinting of alginate scaffolds conjugated with single or dual RGD and YIGSR motifs	In vitro assays with Schwann cells and DRGs	Printability, mechanical stability, and neurite outgrowth were assessed with promising results to be used as luminal filler	2019, [128]

possesses cellular interaction sites makes it an attractive protein in TE applications [139].

So far, little has been done concerning the application of hair keratin to PNR. All in vivo work done with keratin in the scope of PNR has been developed under the supervision of the scientist Van Dyke at Wake Forest University [121–123, 140].

Chitin and Chitosan

Chitin and chitosan are two of the most popular natural biopolymers in the TE field, as well as in the area of nerve repair [141]. Chitin is a natural biopolymer normally present in the exoskeletons of arthropods and the shells of crustaceans, being the main sources, in fact, the marine crustaceans such as shrimp and crabs. It is a linear homopolymer composed of N-acetyl-D-glucosamine units that form beta-(1-4)-linkages. The most abundant polysaccharide in nature is cellulose, immediately followed by chitin [142]. On the other hand, chitosan is obtained through the partial deacetylation of chitin. It is a polysaccharide composed of D-glucosamine and N-acetyl-D-glucosamine units linked through beta-(1–4)-glycosidic bonds. Soluble in acidic aqueous media, chitosan is finding applications in many areas, such as food, cosmetics, and biomedical fields [143].

It has early been proved that chitin- and chitosan-based scaffold can allow the attachment, migration, and proliferation of Schwann cells as well as of DRGs, two of the main players in the nerve regeneration process [144–147]. Furthermore, chitosan biomaterials encourage the aligned orientation of Schwann cell and growing axons [148–150], which is a relevant phenomenon in the process of Wallerian degeneration and consequent regeneration. Additionally, chitosan-based NGCs are easily handled, and transparency facilitates surgical manipulation and suturing of the nerve stumps.

Due to the recognized potential of chitosan, a chitosan-based nerve conduit under the name Reaxon® Nerve Guide manufactured by Medovent GmbH (Mainz, Germany), in accordance with the international standard DIN EN ISO 13485, was launched in the market in 2014. These conduits were thoroughly investigated in a report by Haastert-Talini et al. [151], where the referred conduits combined several prerequisites for a clinical acceptance; and the tube with a degree of acetylation of 5% was considered as the most supportive for peripheral nerve regeneration to bridge a 10 mm gap. That conduits were used in a critical sized nerve gap [64] and in type II diabetic Goto-Kakizaki rats [152], confirming their good in vivo performance.

Alginate

Alginate is a broadly used bioresorbable polysaccharide in the food industry, in wound management, or in the TE field. It is a block co-polymer consisting of beta-d-mannuronic acid and alpha-l-guluronic acid, extracted from brown seaweed [153]. It is considered a biocompatible material which has no inhibitory effect on cell proliferation in vitro and induces reduced foreign body reaction when implanted in tissues in vivo [154]. It has been described that calcium ions induce specific associations between alginate chains, consequently forming hydrogels [155]. Using such mechanism, previous studies [156, 157] have shown the possibility to use alginates applied to PNR. Namely, a decomposable freeze-dried alginate gel covered by PGA mesh was employed in a 50 mm gap in a cat sciatic nerve model with positive results [156]. The same authors later examined the interaction between regenerating axons, Schwann cells, and the implanted alginate gel [157], showing that alginate gel provides a good environment for axon outgrowth and Schwann cell migration. In another study [127], macroporous alginate fibers encapsulating primary DRGs were produced by wet spinning an alginate solution containing dispersed gelatin particles. Marked neurite outgrowth was evident over 150 μm, indicating that pores and channels created within the alginate were providing a favorable environment for neurite development. Other studies have focused on using alginate as NGC luminal fillers, with promising results [158–160].

Endogenous Biomaterials/ECM Proteins

Still among the natural-origin biomaterials, ECM endogenous proteins such as collagen, fibrin,

laminin, and hyaluronic acid (HA) have been highly investigated, since they naturally exist in the human body. ECM is a highly organized 3D structure that occupies the intercellular space, providing a physical support to tissue. It fundamentally acts as a natural scaffold by delivering a matrix, where cells can arrange within the connective tissue. Besides delivering the physical support, ECM also provides the chemical setting for adequate cellular behavior in terms of survival, differentiation, and overall fate. Furthermore, Schwann cells express specific integrins, such as $\alpha_1\beta_1$, $\alpha_2\beta_1$, $\alpha_6\beta_1$, $\alpha_6\beta_4$, $\alpha_5\beta_1$, and $\alpha V\beta_3$, that connect to ECM and encourage myelination through their interaction with the basal lamina [161]. The important interaction between ECM molecules and the nervous system can also be inferred from the fact that laminin, fibronectin, and collagen are effectively used as coatings of tissue culture plastics to enhance Schwann cell and DRGs responses, such as adhesion and migration [162].

A few recent publications related to the use of endogenous biomaterials applied to PNR can be found in Table 12.6 [163–173]. Furthermore, Fig. 12.6 summarizes the promising results making use of endogenous biomaterials applied to PNR.

Collagen

Collagen is, within the ECM, probably the major organizational and structural protein of hard and soft tissues. It provides strength, mechanical stability, and structural integrity and plays a crucial biological role in a variety of tissues and organs including the bone, cartilage, tendon, skin, and cornea [174]. To achieve that, collagen is extremely dynamic, undergoing constant modifications to deliver proper physiologic functions [130]. Although collagen offers structure to our bodies, protecting and supporting the soft tissues, collagen is a relatively simple protein, containing a triple-helical structure and the presence of 4-hydroxyproline. Up to this date, 28 collagen types have been acknowledged. The types I, II, III, and V constitute the essential part of collagen in the bone, cartilage, tendon, skin, and muscle. Collagen can be extracted and purified from a variety of sources, typically from bovine and porcine sources. However, in recent years, new sources are being exploited, such as marine-origin residues [175]. The fact that collagen is considered low immunogenic and has good permeability, biocompatibility, and biodegradability makes it a great component for TE scaffolding strategies [176].

Collagen use in PNR approaches is also extensively accepted, as the protein often exhibits cell-binding domains for aiding neuronal and glial cell attachment and migration. In fact, three collagen conduits are commercially available on the market: the FDA-approved NeuraGen® and NeuroFlex®, which are both made of type I collagen, and RevolNerve®, which is made of type I and type III collagens from porcine skin. In a pioneering strategy, Neuromaix® containing collagen-based microstructured 3D longitudinal guidance channels is capable of providing mechanical support to sprouting DRG axons and can offer a shielding niche for nerve cells [177].

Fibrin

In the human body, fibrin is an integral part of the clotting cascade. When the coagulation cascade is triggered after an injury, thrombin activates soluble plasma protein fibrinogen, resulting in the formation of an insoluble fibrin milieu. Fibrin is a protein involved in the formation of the blood clot [178]. It has found application as a sealant glue in neurosurgery for decades, without any reported complications [179]. Furthermore, fibrin plays a critical part in PNR, where longitudinally oriented fibrin cables are formed spontaneously shortly after injury, as a part of the nerve regeneration process, with the intent to direct migration and proliferation of Schwann cells. In fact, the use of fibrin to repair ilioinguinal nerve has shown to have some neuroprotective effect in the injured nerve, where less fibrosis and collagen deposition were found [180].

Fibronectin

Fibronectin, one of the most complex and intriguing proteins, is an abundant soluble con-

Table 12.6 Relevant and recent published works focused on the fabrication of NGC with endogenous biomaterials

Conduit material	Fabrication method	Defect size, location, model	Outcomes	Year, references
Collagen	Oriented collagen tubes with adsorbed bFGF	15 mm, sciatic nerve defect, rat	The presence of bFGF revealed to be beneficial in terms of functional recovery	2017, [163]
	Blend of collagen and chitosan as luminal filler in a PCL conduit	15 mm, sciatic nerve defect, rat	Axonal regeneration and Schwann cell migration, inclusively inducing comparable functional recovery to that of the autograft control group	2018, [164]
Fibrin	Micro-suturing with fibrin glue coaptation	10 mm, sciatic nerve defect, rat	Reduced the operating time and increase the regeneration distance as well as increasing the arborizing axons	2013, [165]
	Epineural repair with fibrin-glue embedded ADSCs	10 mm, sciatic nerve defect, rat	Embedding cellular components in the fibrin glue enhanced regeneration, as immunolabeled cells could be found at the neuronal repair site and near intraneuronal vessels indicating an active participation of ADSCs in the process of nerve angiogenesis	2016, [166]
	3D hierarchically aligned fibrin nanofiber hydrogel through electrospinning and molecular self-assembly and placed it inside chitosan conduits	10 mm, sciatic nerve defect, rat	In vitro, directional cell adhesion and migration of Schwann cells and DRGs was detected. In vivo, results showed that the developed NGC performed similarly to the autologous nerve graft	2017, [167]
Fibronectin	Chitosan conduit enriched with fibronectin	15 mm, sciatic nerve defect, rat	Fibronectin-enriched scaffolds increased muscle re-innervation and the number of myelinated fiber	2017,[169]
	Schwann cells embedded in a matrix of alginate/ fibronectin	10 mm, sciatic nerve defect, rat	Synergistic effect when both Schwann cells and fibronectin were combined with alginate	2003, [168]
Laminin	Laminin-incorporated PLCL nanofibers were produced by electrospinning	In vitro studies with neonatal Schwann cells	Schwann cells expressed bi- and tri-polar elongations due to the presence of laminin	2014, [170]
	Direct injection of laminin in a peroneal nerve crush	Nerve crush defect, rat	Increased axon presence, larger axon diameter, accelerated axon growth and maturity, and advanced motor function recovery	2019, [171]
Hyaluronic acid (HA)	Electrospinning of a blending of HA in PCL	In vitro cells tests with SH-SY5Y human neuroblastoma cell line	PCL/HA 95:5 exhibit the most balanced properties to meet the required specifications for neural cells	2016, [172]
	Single-channel tubular conduits based on hyaluronic acid (HA) with and without poly-l-lactide acid fibers in their lumen were fabricated	In vitro tests with Schwann cells	Impeded the leakage of the cells seeded in their interior and made them impervious to cell invasion from the exterior while allowing transport of nutrients and other molecules needed for cell endurance. The NGC interior tubular surface was completely covered with Schwann cells	2016, [173]

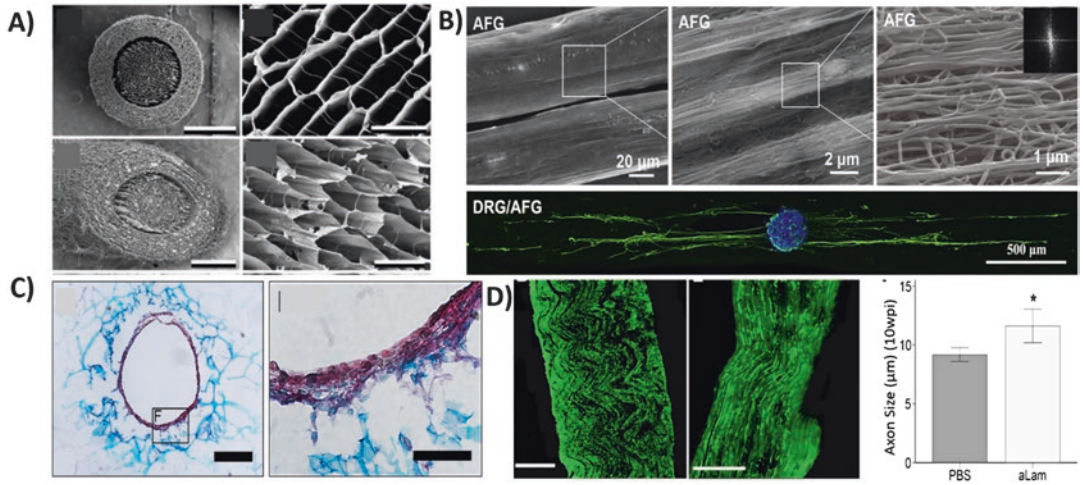

Fig. 12.6 Promising results obtained with natural-origin polymers applied to PNR. (**a**) SEM micrographs of transverse section of the oriented collagen-chitosan filler/PCL sheath scaffold and magnification of the interior of the conduit. (**b**) SEM micrograph of the aligned fibrin hydrogel nanofiber and its magnification. Below, a DRGs where the neurites align along the aligned fibers. (**c**) Transversal cryosections of hyaluronic acid conduits cultured for 10 days with Schwann cells in their lumen, after staining with Harris' hematoxylin, Alcian blue, and picrosirius red. (**d**) Longitudinal section of injured nerve treated with PBS (at left) or laminin (at right), stained with antibodies recognizing NF-h (α-RT97, green). The bar graph illustrates significantly increased axon diameter (μm) with laminin treatment. (**a**–**d**) were reprinted with the permission from [164, 167, 171, 173] respectively

stituent of plasma and other body fluids and part of the insoluble ECM. It also mediates a wide variety of cellular interactions with the ECM and plays important roles in cell adhesion, migration, growth, and differentiation [181]. After extensive characterization, it was found that fibronectin expresses the RGD motif, related to cell adhesion. However, fibronectin has an extensive variety of practical functions other than associate with cell surfaces through integrins. It binds to several biologically important molecules that include heparin, collagen, and fibrin. The potential of including fibronectin for PNR was firstly realized when Whitworth et al. [182] reported a new nerve conduit material consisting of orientated strands of the cell adhesive fibronectin. In a 10 mm nerve defect in rat, the developed NGC produced the highest rate and amount of axonal regeneration, comparable to the one obtained for autografts. Furthermore, increased expression of fibronectin can be found in damaged peripheral nerve during Wallerian degeneration [183].

Laminin

Laminin is a glycoprotein naturally occurring in nerves. It is a component of ECM that plays a decisive part in cell recognition and therefore influences cell migration, differentiation, and axonal growth [184]. Laminin can also be perceived as a fundamental guiding cue, since the growth cone of regenerating axons is attracted to laminin [185]. To make PHBV aligned nanofibers more attractive to neuronal components [186], laminin was adsorbed via electrostatic interactions. Containing both topographic and chemical cues suited for Schwann cell alignment and elongation, the developed NGC was implanted in a critical sized nerve defect in rat, with 12 mm gap, and proved to be suitable for such an application.

Laminin was also added to collagen gels in a gradient of concentrations with interesting effects [187]. For collagen gels without laminin, a typical bimodal response of neurite outgrowth was observed, with increased growth at lower concentrations of collagen gel. However, in the

presence of higher laminin concentrations, the growth became independent of the gel stiffness.

Hyaluronic Acid (HA)

HA is a linear, anionic, non-sulfated glycosaminoglycan that composes the ECM of all living tissues. Being a very versatile polymer, it finds applications in diverse areas. Furthermore, different molecular weights have an impact on the biological performances, being a highly tunable and adaptable polysaccharide [188].

Its use is widely spread in TE applications due to its biocompatibility, biodegradability, and chemical modification easiness. HA is also a very versatile biomaterial, which can be prepared in the form of hydrogels, sponges, cryogels, and injectable hydrogels [189]. Additionally, HA degradation products seem to exert a positive effect in diverse TE areas as they encourage wound healing, tissue restoration, and vascularization [190]. The injection of HA in a nerve defect has proved to be beneficial for nerve regeneration, since HA groups showed an increase in myelinated axon counts, as well as an increase in retrograde flow, necessary for the regenerative process [191]. Furthermore, the advantage of including HA also resides in the fact that it can reduce scar formation after nerve injury [192].

12.1.4.2 The Possibility of Patient-Specific Nerve Repair and NGCs

Personalized TE and regenerative strategies propose a possible solution for contemporary untreatable injuries or illnesses. The use of TE triad offers the possibility of interminable combinations of cells, scaffolds, and growth factors, suggesting endless possibilities to customize diagnostic tools, biomedical devices, as well as the final treatments [193]. Huge efforts are being carried in laboratories throughout the world to personalize the clinical care, catalyzing major advances in the techniques that allow the treatment of serious injuries and chronic diseases [194]. The customization and individualization of medical care carries huge advantages for the patients and the healthcare systems as well. Targeting the treatments to a specific damage of a patient is critical due to innate discrepancies in patient anatomies, injury shapes and gravity, as well as individual genetic and proteomic features [195]. The benefit is clear for the patient, i.e., a tailor-made treatment according to its own organism features. For the hospitals and healthcare systems, the fact that a treatment is 100% suited for that specific patient and will not fail will save time and budget.

Peripheral nerves are tissues with different geometries and shapes, which vary anatomically according to the location within the body. But more importantly, the same nerve may vary from person to person with age, according to their medical condition or type of injury [196]. Furthermore, the process of nerve regeneration and repair itself is a complex biological phenomenon, with vast singularities, that requires an equilibrium at a molecular, cellular, and tissue level [197]. Overall, many advantages are envisioned when using 3D printing for nerve repair and regeneration: (i) fabrication of personalized NGC, (2) concomitant assembly of luminal fillers inside NGCs, (3) 3D bioprinting of cells within a bio-ink or into the NGCs, and (4) establishment of growth factor gradients or pathways [198].

Only recently the hypothesis of patient-specific strategies in nerve regeneration has risen with the development of the 3D printing technology [199]. This was further permitted by the combination of 3D imaging machineries and 3D printing methods. Johnson et al. [199] successfully established the combination of 3D imaging and 3D printing for the design and fabrication of anatomically biomimetic truly patient-specific nerve regeneration strategy. It allowed the fabrication of NGCs with complex anatomical structures and inner biofunctionalization with neurotrophic factors, to create a sensory and a motor pathway (Fig. 12.7a).

Hu et al. [200] explored the 3D printing technology to prepare a bio-conduit with designer

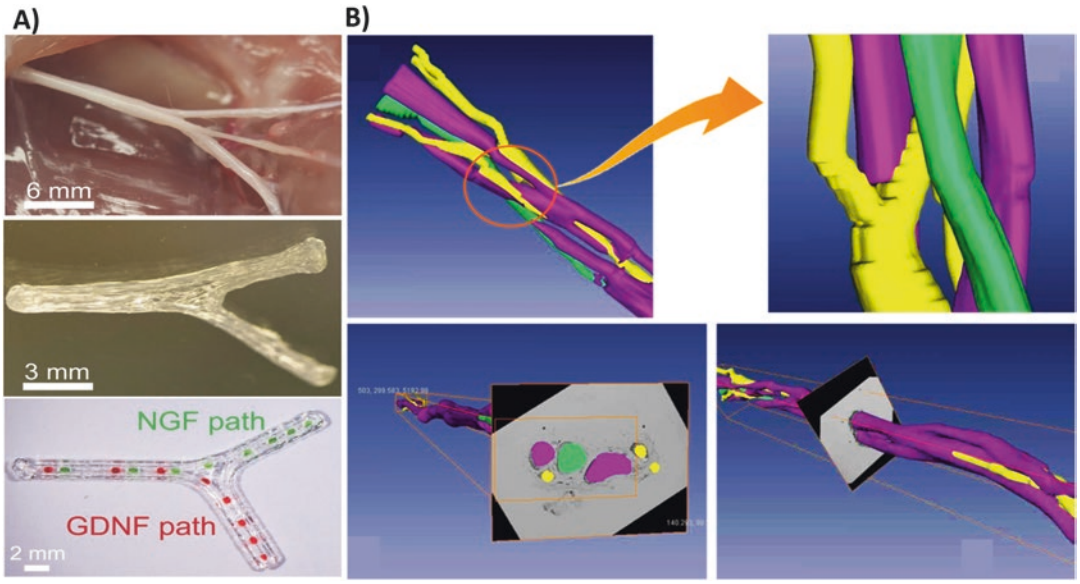

Fig. 12.7 Patient-specific and 3D printing technologies will allow improving the treatment given to patients in the future. (**a**) 3D printed complex nerve pathways from 3D scanned bifurcating nerves. Reprinted with permission from [199]. (**b**) Imaging of a 3D model of median nerve, for further precise reconstruction. (Reprinted with permission from [202], Copyright © 2015, Macmillan Publishers Limited)

structures for PNR, where the chosen polymer, cryoGelMA gel, was cellularized with ADSCs. When implanted in a 10 mm rat sciatic nerve defect, the results were very similar to the autograft in terms of functional recovery. Tao et al. [201] were able to 3D-print an hydrogel conduit with customized size, shape, and structure, providing a physical microenvironment for axonal elongation, where the nanoparticles sustained release a drug to facilitate the nerve regeneration. Zhong et al. [202] described the key technology of 3D peripheral nerve fascicle reconstruction. First, a 3D virtual model of internal fascicles was obtained and successfully applied for 3D reconstruction for the median nerve (Fig. 12.7b).

Exceptional technologies are emerging every day, and 3D printing promises to revolutionize the patient-specific healthcare, namely, in PNR.

12.2 Conclusions

The complex anatomy and physiology of the PNS makes nerve's injury very problematic and extremely difficult to repair. The full recovery is challenging because of the loss of native cues, formation of scar tissue, lack of proper vascularization, and inflammation. The diverse treatments used for nerve repair such as coaptation suturing, grafts, and conduits pose several limitations when trying to recuperate full functionality. Therefore, the development of new NGCs requires a clever combination of the following strategies: (i) the development of new polymer or combination of polymers for better integration with neural native tissue, (ii) addition of topographical structures to intensify neurite alignment and growth, and (iii) biological cues such as growth factors or cellular components.

In what regards the biomaterial choice, there are numerous options to capitalize on different properties of each material. Although many exist and can be used, natural materials are known to be better integrated by host tissue when compared to synthetic ones, more promptly instigating the regenerative mechanisms. The biomaterial availability and cost are also essential parameters to consider. Therefore, and in the author's opinion, SF is probably one of the most versatile biomaterials. It can be processed in a variety of ways and maintain outstanding mechanical properties/suturability and is considered non-immunogenic,

with cheap and easy access as well as natural distribution. This biomaterial can be used to fabricate the conduit itself, as well as anisotropic filling scaffolds in the lumen, in order to be able to treat larger nerve gaps. In addition, several fabrication methods can be used for this biomaterial, including the cross-linking of the tyrosine groups with an enzymatic mediated system or functionalization with growth factors and other molecules of interest. In this context, conductive materials can also be used to intensify the needed neurological transmission and communication.

A brief mention must also be made to the potential of 3D printing for patient-specific nerve reconstructions. The rising of this technology allows to closely reproduce features of the native peripheral nerve, with the aim of possibly replacing autologous nerve grafts. Therefore, the current and future bio-imaging modalities allied with detailed printing will permit the production of patient-specific nerve conduits, revolutionizing the field. As the scientific community makes advances on the fundamental knowledge related to the biological mechanisms behind nerve injury and repair, engineers are able to integrate that knowledge in more complex designs, to better mimic natural nerve regeneration and patient specificity in respect to anatomy and biology requirements.

Acknowledgments This work was supported by Cristiana Carvalho PhD scholarship (Norte-08-5369-FSE-000037). J. M. Oliveira also thanks the FCT for the funds provided under the program Investigador FCT 2015 (IF/01285/2015). The authors are also thankful to the FCT-funded project NanoOptoNerv (ref. PTDC/NAN-MAT/29936/2017). The authors would also like to acknowledge the project "Nano-accelerated nerve regeneration and optogenetic empowering of neuromuscular functionality" (ref. PTDC/NAN-MAT/29936/2017).

References

1. Battiston B, Papalia I, Tos P et al (2009) Peripheral nerve repair and regeneration research: a historical note. Int Rev Neurobiol 87:1–7
2. Belen D, Aciduman A, Er U (2009) History of peripheral nerve repair: may the procedure have been practiced in Hippocratic School? Surg Neurol 72(2):190–193
3. Wu D, Murashov AK (2013) Molecular mechanisms of peripheral nerve regeneration: emerging roles of microRNAs. Front Physiol 4:55–55
4. Geuna S, Tos P, Battiston B (2012) Emerging issues in peripheral nerve repair. Neural Regen Res 7(29):2267–2272
5. Zhang PX, Han N, Kou YH et al (2019) Tissue engineering for the repair of peripheral nerve injury. Neural Regen Res 14(1):51–58
6. Siemionow M, Bozkurt M, Zor F (2010) Regeneration and repair of peripheral nerves with different biomaterials: review. Microsurgery 30(7):574–588
7. Pixley SK, Hopkins TM, Little KJ et al (2016) Evaluation of peripheral nerve regeneration through biomaterial conduits via micro-CT imaging. Laryngoscope Investig Otolaryngol 1(6):185–190
8. Herculano Houzel S (2012) Brain evolution. In: Paxinos G, Mai JK (eds) The human nervous system, 3rd edn. Academic Press, San Diego, pp 2–13
9. Balaji S, Kumar R, Sripriya R et al (2012) Preparation and comparative characterization of keratin–chitosan and keratin–gelatin composite scaffolds for tissue engineering applications. Mater Sci Eng C 32(4):975–982
10. Lobko PI, Ladutjko SI, Bogdanova MI et al (1979) Ganglia formation of the peripheral nervous system. Acta Anat (Basel) 103(4):395–399
11. Payne SL (2019) Central nervous system. In: Atala A, Lenza R, Nerem R, Thomson J (eds) Principles of regenerative medicine, 3rd edn. Academic Press, Boston, pp 1199–1221
12. Birch R (2013) Peripheral nerve injuries: a clinical guide. Springer, London
13. Fricker M, Tolkovsky AM et al (2018) Neuronal cell death. Physiol Rev 98(2):813–880
14. Rotshenker S (2011) Wallerian degeneration: the innate-immune response to traumatic nerve injury. J Neuroinflammation 8:109
15. Grinsell D, Keating CP (2014) Peripheral nerve reconstruction after injury: a review of clinical and experimental therapies. Biomed Res Int 13:1–14
16. López Cebral R, Silva Crreia J, Reis RL (2017) Peripheral nerve injury: current challenges, conventional treatment approaches, and new trends in biomaterials-based regenerative strategies. ACS Biomate Sci Eng 3(12):3098–3122
17. Gaudin R, Knipfer C, Henningsen A et al (2016) Approaches to peripheral nerve repair: Generations of biomaterial conduits yielding to replacing autologous nerve grafts in craniomaxillofacial surgery. Biomed Res Int 2016:1–19
18. Rosso G, Liashkovich I, Gess B et al (2014) Unravelling crucial biomechanical resilience of myelinated peripheral nerve fibres provided by the schwann cell basal lamina and PMP22. Sci Rep 4:7286
19. Zhu S, Ge J, Wang Y et al (2014) A synthetic oxygen carrier-olfactory ensheathing cell composition system for the promotion of sciatic nerve regeneration. Biomaterials 35(5):1450–1461

20. Belkas JS, Shoichet MS, Midha R (2004) Peripheral nerve regeneration through guidance tubes. Neurol Res 26(2):151–160
21. Jaquet JB, Luijsterburg AJ, Kalmijn S et al (2001) Median, ulnar, and combined median-ulnar nerve injuries: functional outcome and return to productivity. J Trauma 51(4):687–692
22. Kawano H, Kimura Kuroda J, Komuta Y et al (2012) Role of the lesion scar in the response to damage and repair of the central nervous system. Cell Tissue Res 349(1):169–180
23. Jessen KR, Mirsky R (2016) The repair schwann cell and its function in regenerating nerves. J Physiol 594(13):3521–3531
24. Dahlin LB (2013) The role of timing in nerve reconstruction. In: Geuna S, Perroteau I, Tos P, Battiston B (eds) International review of neurobiology. vol 109. Academic Press, Malmö, pp 151–164
25. Robinson LR (2000) Traumatic injury to peripheral nerves. Muscle Nerve 23(6):863–873
26. Ghasemi Rad M, Nosair E, Vegh A et al (2014) A handy review of carpal tunnel syndrome: from anatomy to diagnosis and treatment. World J Radiol 6(6):284–300
27. Plastaras CT, Chhatre A, Kotcharian AS (2016) Perioperative upper extremity peripheral nerve traction injuries. Orthop Clin North Am 45(1):47–53
28. Won JC, Park TS (2016) Recent advances in diagnostic strategies for diabetic peripheral neuropathy. Endocrinol Metab (Seoul) 31(2):230–238
29. Wojtkiewicz DM, Saunders J, Domeshek L et al (2015) Social impact of peripheral nerve injuries. Hand (NY) 10(2):161–167
30. Seddon HJ (1943) Three types of nerve injury. Brain 66(4):237–288
31. Sunderland S (1951) A classification of peripheral nerve injuries producing loss of function. Brain 74(4):491–516
32. DeFrancesco LA, Lindborg JA, Niemi JP et al (2015) The neuroimmunology of degeneration and regeneration in the peripheral nervous system. Neuroscience 302:174–203
33. Kiryu Seo S, Kiyama H (2011) The nuclear events guiding successful nerve regeneration. Front Mol Neurosci 4:53
34. Conforti L, Gilley J, Coleman MP (2014) Wallerian degeneration: an emerging axon death pathway linking injury and disease. Nat Rev Neurosci 15(6):394–409
35. Namgung U (2014) The role of schwann cell-axon interaction in peripheral nerve regeneration. Cells Tissues Organs 200(1):6–12
36. Jessen KR, Mirsky R, Lloyd AC (2015) Schwann cells: development and role in nerve repair. Cold Spring Harb Perspect Biol 7(7):1–16
37. Chen P, Piao X, Bonaldo P (2015) Role of macrophages in wallerian degeneration and axonal regeneration after peripheral nerve injury. Acta Neuropathol 130(5):605–618
38. Bearce EA, Erdogan B, Lowery LA (2015) TIPsy tour guides: how microtubule plus-end tracking proteins (+TIPs) facilitate axon guidance. Front Cell Neurosci 9:241
39. Steketee MB, Oboudiyat C, Richard D et al (2014) Regulation of intrinsic axon growth ability at retinal ganglion cell growth cones. Invest Ophthalmol Vis Sci 55(7):4369–4377
40. Fu SY, Gordon T (1997) The cellular and molecular basis of peripheral nerve regeneration. Mol Neurobiol 14(1-2):67–116
41. Bhatheja K, Field J (2006) Schwann cells: origins and role in axonal maintenance and regeneration. Int J Biochem Cell Biol 38(12):1995–1999
42. Jessen KR, Mirsky R (2008) Negative regulation of myelination: relevance for development, injury, and demyelinating disease. Glia 56(14):1552–1565
43. Brushart TM, Aspalter M, Griffin JW et al (2013) Schwann cell phenotype is regulated by axon modality and central-peripheral location, and persists in vitro. Exp Neurol 247:272–281
44. McKerracher L, David S, Jackson LD et al (1994) Identification of myelin-associated glycoprotein as a major myelin-derived inhibitor of neurite growth. Neuron 13(4):805–811
45. Namgung U (2015) The role of Schwann cell-axon interaction in peripheral nerve regeneration. Cells Tissues Organs 200(1):6–12
46. Arthur Farraj PJ, Latouche M, Wilton DK et al (2012) C-Jun reprograms schwann cells of injured nerves to generate a repair cell essential for regeneration. Neuron 75(4):633–647
47. Dahlin LB (2008) Techniques of peripheral nerve repair. Scand J Surg 97(4):310–316
48. Dellon ES, Dellon AL (1993) The first nerve graft, vulpian, and the nineteenth century neural regeneration controversy. J Hand Surg [Am] 18(2):369–372
49. Isaacs J (2010) Treatment of acute peripheral nerve injuries: current concepts. J Hand Surg [Am] 35(3):491–497
50. Suchyta MA, Sabbagh MD, Morsy M et al (2016) Advances in peripheral nerve regeneration as it relates to VCA. Vasc Compos Allotransplant 3(1-2):75–88
51. Fries CA, Tuder DW, Davis MR (2015) Preclinical models in vascularized composite allotransplantation. Curr Transpl Rep 2(3):284–289
52. Vale TA, Symmonds M, Polydefkis M et al (2017) Chronic non-freezing cold injury results in neuropathic pain due to a sensory neuropathy. Brain 140(10):2557–2569
53. Archibald SJ, Shefner J, Krarup C et al (1995) Monkey median nerve repaired by nerve graft or collagen nerve guide tube. J Neurosci 15(5 Pt 2):4109–4123
54. Lovati AB, D'Arrigo D, Odella S et al (2018) Nerve repair using decellularized nerve grafts in rat models. A review of the literature. Front Cell Neurosci 12:427–427

55. Gulati AK (1988) Evaluation of acellular and cellular nerve grafts in repair of rat peripheral nerve. J Neurosurg 68(1):117–123
56. Freytes DO, Badylk SF, Webster TJ et al (2004) Biaxial strength of multilaminated extracellular matrix scaffolds. Biomaterials 25(12):2353–2361
57. De Filippo RE, Yoo JJ, Atala A (2002) Urethral replacement using cell seeded tubularized collagen matrices. J Urol 168(4 Pt 2):1789–1792
58. Woods T, Gratzer PF (2005) Effectiveness of three extraction techniques in the development of a decellularized bone-anterior cruciate ligament-bone graft. Biomaterials 26(35):7339–7349
59. Gamba PG, Conconi MT, Lo Piccolo R et al (2002) Experimental abdominal wall defect repaired with acellular matrix. Pediatr Surg Int 18(5-6):327–331
60. Kim BS, Yoo JJ, Atala A (2004) Peripheral nerve regeneration using acellular nerve grafts. J Biomed Mater Res A 68(2):201–209
61. Lin CH, Hsia K, Ma H et al (2018) In vivo performance of decellularized vascular grafts: a review article. Int J Mol Sci 19(7):1–17
62. Wang EW, Zhang J, Huang JH (2015) Repairing peripheral nerve injury using tissue engineering techniques. Neural Regen Res 10(9):1393–1394
63. Chang W, Shah MB, Lee P et al (2018) Tissue-engineered spiral nerve guidance conduit for peripheral nerve regeneration. Acta Biomater 73:302–311
64. Gonzalez Perez F, Cobianchi S, Geuna S et al (2015) Tubulization with chitosan guides for the repair of long gap peripheral nerve injury in the rat. Microsurgery 35(4):300–308
65. Kehoe S, Zhang XF, Boyd D (2012) FDA approved guidance conduits and wraps for peripheral nerve injury: a review of materials and efficacy. Injury 43(5):553–572
66. De Ruiter GCW, Malessy MJA, Yaszemski MJ et al (2009) Designing ideal conduits for peripheral nerve repair. Neurosurg Focus 26(2):1–9
67. Bueno FR, Shah SB (2008) Implications of tensile loading for the tissue engineering of nerves. Tissue Eng Part B Rev 14(3):219–233
68. Gu X, Ding F, Williams DF (2014) Neural tissue engineering options for peripheral nerve regeneration. Biomaterials 35(24):6143–6156
69. de Luca AC, Lacour SP et al (2014) Extracellular matrix components in peripheral nerve repair: how to affect neural cellular response and nerve regeneration? Neural Regen Res 9(22):1943–1948
70. Belanger K, Schlatter G, Hébraud A et al (2018) A multi-layered nerve guidance conduit design adapted to facilitate surgical implantation. Health Sci Rep 1(12):1–13
71. Carvalho CR, Costa JB, Da Silva MA et al (2018) Tunable enzymatically cross-linked silk fibroin tubular conduits for guided tissue regeneration. Adv Healthc Mater 7(17):1–17
72. Menorca RMG, Fussell TS, Elfar JC (2013) Peripheral nerve trauma: mechanisms of injury and recovery. Hand Clin 29(3):317–330
73. Subramanian A, Krishnan UM, Sethuraman S (2009) Development of biomaterial scaffold for nerve tissue engineering: biomaterial mediated neural regeneration. J Biomed Sci 16(1):108–108
74. Chen YS, Chang JY, Cheng CY et al (2005) An in vivo evaluation of a biodegradable genipin-cross-linked gelatin peripheral nerve guide conduit material. Biomaterials 26(18):3911–3918
75. Yang Y, Zhao Y, Gu Y et al (2009) Degradation behaviors of nerve guidance conduits made up of silk fibroin in vitro and in vivo. Polym Degrad Stab 94(12):2213–2220
76. Wang ML, Rivlin M, Graham JG et al (2019) Peripheral nerve injury, scarring, and recovery. Connect Tissue Res 60(1):3–9
77. Huang C, Ouyang Y, Niu H et al (2015) Nerve guidance conduits from aligned nanofibers: improvement of nerve regeneration through longitudinal nanogrooves on a fiber Surface. ACS Appl Mater Interfaces 7(13):7189–7196
78. Liu C, Wang C, Zhao Q et al (2018) Incorporation and release of dual growth factors for nerve tissue engineering using nanofibrous bicomponent scaffolds. Biomed Mater 13(4):1–18
79. Cattin AL, Burden JJ, Van Emmenis L et al (2015) Macrophage-induced blood vessels guide schwann cell-mediated regeneration of peripheral nerves. Cell 162(5):1127–1139
80. Zhao YH, Niu CM, Shi JQ et al (2018) Novel conductive polypyrrole/silk fibroin scaffold for neural tissue repair. Neural Regen Res 13(8):1455–1464
81. Muangsanit P, Shipley RJ, Phillips JB (2018) Vascularization strategies for peripheral nerve tissue engineering. Anat Rec (Hoboken) 301(10):1657–1667
82. Giannessi E, Coli A, Stornelli MR et al (2014) An autologously generated platelet-rich plasma suturable membrane may enhance peripheral nerve regeneration after neurorraphy in an acute injury model of sciatic nerve neurotmesis. J Reconstr Microsurg 30(9):617–626
83. Stang F, Keilhoff G, Fansa H (2009) Biocompatibility of different nerve tubes. Materials (Basel) 2(4):1480
84. Muheremu A, Ao Q (2015) Past, present, and future of nerve conduits in the treatment of peripheral nerve injury. Biomed Res Int 2015:1–7
85. Nardo T, Irene C, Ruini F et al (2017) Synthetic biomaterial for regenerative medicine applications. In: Orlando G, Remzzi G, Williams DF (eds) Kidney transplantation, bioengineering and regeneration, 1st edn. Academic Press, Turin, pp 901–921
86. Matsumine H, Sasaki R, Yamato M et al (2014) A polylactic acid non-woven nerve conduit for facial nerve regeneration in rats. J Tissue Eng Regen Med 8(6):454–462
87. Lu MC, Huang YT, Lin JH et al (2009) Evaluation of a multi-layer microbraided polylactic acid fiber-reinforced conduit for peripheral nerve regeneration. J Mater Sci Mater Med 20(5):1175–1180

88. Zeng CG, Xiong Y, Quan D et al (2014) Fabrication and evaluation of PLLA multichannel conduits with nanofibrous microstructure for the differentiation of NSCs in vitro. Tissue Eng Part A 20(5–6):1038–1048
89. Rutkowski GE, Miller CA, Jeftinija S et al (2004) Synergistic effects of micropatterned biodegradable conduits and Schwann cells on sciatic nerve regeneration. J Neural Eng 1(3):151–157
90. Shin RH, Friedrich PF, Crum BA et al (2009) Treatment of a segmental nerve defect in the rat with use of bioabsorbable synthetic nerve conduits: a comparison of commercially available conduits. J Bone Joint Surg Am 91(9):2194–2204
91. Navissano M, Malan F, Carnino R et al (2005) Neurotube® for facial nerve repair. Microsurgery 25(4):268–271
92. Wu T, Li D, Wang Y et al (2017) Laminin-coated nerve guidance conduits based on poly(l-lactide-co-glycolide) fibers and yarns for promoting Schwann cells' proliferation and migration. J Mater Chem B 5(17):3186–3194
93. Labroo P, Shea J, Edwards K et al (2017) Novel drug delivering conduit for peripheral nerve regeneration. J Neural Eng 14(6):066011
94. Lee SJ, Nowicki M, Harris B et al (2017) Fabrication of a highly aligned neural scaffold via a table top stereolithography 3D printing and electrospinning. Tissue Eng Part A 23(11-12):491–502
95. Kokai LE, Ghaznavi AM, Marra KG (2010) Incorporation of double-walled microspheres into polymer nerve guides for the sustained delivery of glial cell line-derived neurotrophic factor. Biomaterials 31(8):2313–2322
96. Hsu S, Chang WC, Yen CT (2017) Novel flexible nerve conduits made of water-based biodegradable polyurethane for peripheral nerve regeneration. J Biomed Mater Res Part A 105(5):1383–1392
97. Singh A, Shiekh PA, Das M et al (2018) Aligned chitosan-gelatin cryogel-filled polyurethane nerve guidance channel for neural tissue engineering: fabrication, characterization, and in vitro evaluation. Biomacromolecules 20(2):662–673
98. Stocco E, Barbon S, Lora L et al (2018) Partially oxidized polyvinyl alcohol conduit for peripheral nerve regeneration. Sci Rep 8(1):604–604
99. Wan H, Li DZ, Yang F et al (2007) Research about schwann cells and PLGA implanted to rat transected spinal cord. Zhonghua Wai Ke Za Zhi 45(12):843–846
100. Peng SW, Li CW, Wang GJ et al (2017) Nerve guidance conduit with a hybrid structure of a PLGA microfibrous bundle wrapped in a micro/nanostructured membrane. Int J Nanomedicine 12:421–432
101. Liu H, Lv P, Zhu Y et al (2017) Salidroside promotes peripheral nerve regeneration based on tissue engineering strategy using Schwann cells and PLGA: in vitro and in vivo. Sci Rep 7:1–11
102. Xu F, Zhang K, Lv P et al (2017) NECL1 coated PLGA as favorable conduits for repair of injured peripheral nerve. Mater Sci Eng C 70:1132–1140
103. Tanir TE, Kiziltay A, Malikmammadov E et al (2018) PCL and PCL-based materials in biomedical applications. J Biomater Sci Polym Ed 29(7-9):863–893
104. Wang W, Huang B, Byun JJ et al (2019) Assessment of PCL/carbon material scaffolds for bone regeneration. J Mech Behav Biomed Mater 93:52–60
105. Fu N, Liao J, Lin S et al (2016) PCL-PEG-PCL film promotes cartilage regeneration in vivo. Cell Prolif 49(6):729–739
106. Bala Balakrishnan P, Gardella L, Forouharshad M et al (2018) Star poly(ε-caprolactone)-based electrospun fibers as biocompatible scaffold for doxorubicin with prolonged drug release activity. Colloids Surf B: Biointerfaces 161:488–496
107. Grossen P, Witzigmann D, Sieber S et al (2017) PEG-PCL-based nanomedicines: a biodegradable drug delivery system and its application. J Control Release 260:46–60
108. Pathak VM, Navneet (2017) Review on the current status of polymer degradation: a microbial approach. Bioresour Bioprocess 4(1):15
109. Salmoria GV, Paggi RA, Castro F et al (2016) Development of PCL/Ibuprofen tubes for peripheral nerve regeneration. Procedia CIRP 49:193–198
110. Mobasseri A, Faroni A, Minogue BM et al (2015) Polymer scaffolds with preferential parallel grooves enhance nerve regeneration. Tissue Eng Part A 21(5-6):1152–1162
111. Zhang XF, Coughlan A, O'Shea H et al (2012) Experimental composite guidance conduits for peripheral nerve repair: an evaluation of ion release. Mater Sci Eng C 32(6):1654–1663
112. Wei J, Ao Q, Huang L et al (2018) Constructing conductive conduit with conductive fibrous infilling for peripheral nerve regeneration. Chem Eng J 345:566–577
113. Sun B, Zhou Z, Li D et al (2019) Polypyrrole-coated poly(l-lactic acid-co-ε-caprolactone)/silk fibroin nanofibrous nerve guidance conduit induced nerve regeneration in rat. Mater Sci Eng C Mater Biol Appl 94:190–199
114. Du J, Chen H, Qing L et al (2018) Biomimetic neural scaffolds: a crucial step towards optimal peripheral nerve regeneration. Biomater Sci 6(6):1299–1311
115. Pfister LA, Papaloïzos M, Merkle HP et al (2007) Hydrogel nerve conduits produced from alginate/chitosan complexes. J Biomed Mater Res A 80A(4):932–937
116. Wang ZZ, Sakiyama Elbert SE (2018) Matrices, scaffolds & carriers for cell delivery in nerve regeneration. Exp Neurol 319:1–17
117. Resch A, Wolf S, Radtke C et al (2018) Co-culturing human adipose derived stem cells and schwann cells on spider silk-a new approach as prerequisite for enhanced nerve regeneration. Int J Mol Sci 20(1):71
118. Wang C, Jia Y, Yang W et al (2018) Silk fibroin enhances peripheral nerve regeneration by improving vascularization within nerve conduits. J Biomed Mater Res A 106(7):2070–2077

119. Yang Y, Ding F, Wu J et al (2007) Development and evaluation of silk fibroin-based nerve grafts used for peripheral nerve regeneration. Biomaterials 28(36):5526–5535
120. Das S, Sharma M, Saharia D et al (2015) In vivo studies of silk based gold nano-composite conduits for functional peripheral nerve regeneration. Biomaterials 62:66–75
121. Sierpinski P, Garrett J, Ma J et al (2008) The use of keratin biomaterials derived from human hair for the promotion of rapid regeneration of peripheral nerves. Biomaterials 29(1):118–128
122. Pace LA, Plate JF, Mannava S et al (2014) A human hair keratin hydrogel scaffold enhances median nerve regeneration in nonhuman primates: An electrophysiological and histological study. Tissue Eng Part A 20(3-4):507–517
123. Lin YC, Ramadan M, Van Dyke M et al (2012) Keratin gel filler for peripheral nerve repair in a rodent sciatic nerve injury model. Plast Reconstr Surg 129(1):67–78
124. Meyer C, Stenberg L, Gonzalez Perez F et al (2016) Chitosan-film enhanced chitosan nerve guides for long-distance regeneration of peripheral nerves. Biomaterials 76:33–51
125. Moattari M, Kouchesfehani HM, Kaka G et al (2018) Chitosan-film associated with mesenchymal stem cells enhanced regeneration of peripheral nerves: a rat sciatic nerve model. J Chem Neuroanat 88:46–54
126. Carvalho CR, Silva Correia J, Silva JM et al (2017) Investigation of cell adhesion in chitosan membranes for peripheral nerve regeneration. Mater Sci Eng C Mater Biol Appl 71:1122–1134
127. Lin SC, Wang Y, Wertheim DF et al (2017) Production and in vitro evaluation of macroporous, cell-encapsulating alginate fibres for nerve repair. Mater Sci Eng C Mater Biol Appl 73:653–664
128. Sarker MD, Naghieh S, Ning L et al (2019) Biofabrication of peptide-modified alginate scaffolds: printability, mechanical stability and neurite outgrowth assessments. Bioprinting 2019:1–19
129. Mondal M, Trivedy K, Nirmal Kumar S (2007) The silk proteins, sericin and fibroin in silkworm, Bombyx mori Linn., – a review. Caspian J Env Sci 5(2):63–76
130. Jastrzebska K, Kucharczky K, Dams Kozlowska H et al (2015) Silk as an innovative biomaterial for cancer therapy. Rep Pract Oncol Radiother 20(2):87–98
131. Vepari C, Kaplan DL (2007) Silk as a biomaterial. Prog Polym Sci 32(8-9):991–1007
132. Costa JB, Silva Correia J, Oliveira JM et al (2017) Fast setting silk fibroin bioink for bioprinting of patient-specific memory-shape implants. Adv Healthc Mater 6(22):1701021
133. Ribeiro VP, Sliva Correia J, Goncalves C et al (2018) Rapidly responsive silk fibroin hydrogels as an artificial matrix for the programmed tumor cells death. PLoS One 13(4):1–21
134. Carvalho MR, Maia FR, Reis RL et al (2018) Tuning enzymatically crosslinked silk fibroin hydrogel properties for the development of a colorectal cancer extravasation 3D model on a chip. Global Chall 2(5-6):1–10
135. Dinis TM, Elia R, Vidal G et al (2015) 3D multichannel bi-functionalized silk electrospun conduits for peripheral nerve regeneration. J Mech Behav Biomed Mater 41:43–55
136. Ng K (2016) Human hair keratin templates for biomedical applications. Front Bioeng Biotechnol. Conference Abstract: 10th World Biomaterials Congress. https://doi.org/10.3389/conf.FBIOE.2016.01.01729
137. Ko J, Nguyen LTH, Surendran A et al (2017) Human hair keratin for biocompatible flexible and transient electronic devices. ACS Appl Mater Interfaces 9(49):43004–43012
138. Kan Y, Yanhui L, Batzaya B et al (2018) Visible light crosslinkable human hair keratin hydrogels. Bioeng Transl Med 3(1):37–48
139. Lee HN, Noh KT, Lee SC et al (2014) Human hair keratin and its-based biomaterials for biomedical applications. Tissue Eng Regen Med 11(4):255–265
140. Apel PJ, Garrett JP, Sierpinski P et al (2008) Peripheral nerve regeneration using a keratin-based scaffold: long-term functional and histological outcomes in a mouse model. J Hand Surg [Am] 33(9):1541–1547
141. Bak M, Gutkowska ON, Wagner E et al (2017) The role of chitin and chitosan in peripheral nerve reconstruction. Polim Med 47(1):43–47
142. Muzzarelli RAA (1977) Chitin. Pergamon press, New York, pp 5–44
143. Marguerite R (2006) Chitin and chitosan: properties and applications. Prog Polym Sci 31(7):603–632
144. Freier T, Montenegro R, Shan KH et al (2005) Chitin-based tubes for tissue engineering in the nervous system. Biomaterials 26(22):4624–4632
145. Martin LE, Nieto DM, Nieto SM (2012) Differential adhesiveness and neurite-promoting activity for neural cells of chitosan, gelatin, and poly-L-lysine films. J Biomater Appl 26(7):791–809
146. Wenling C, Duohui J, Jiamou L et al (2005) Effects of the degree of deacetylation on the physicochemical properties and Schwann cell affinity of chitosan films. J Biomater Appl 20(2):157–177
147. Wrobel S, Serra SC, Ribeiro SS et al (2014) In vitro evaluation of cell-seeded chitosan films for peripheral nerve tissue engineering. Tissue Eng Part A 20(17-18):2339–2349
148. Ashleigh C, Narayan B, Minqin Z (2011) Fabrication and cellular compatibility of aligned chitosan–PCL fibers for nerve tissue regeneration. Carbohydr Polym 85(1):149–156
149. Gnavi S, Fornasari BE, Tonda TC et al (2018) In vitro evaluation of gelatin and chitosan electrospun fibres as an artificial guide in peripheral nerve repair: a comparative study. J Tissue Eng Regen Med 12(2):e679–e694
150. Wang W, Itoh S, Konno K et al (2009) Effects of Schwann cell alignment along the oriented electro-

spun chitosan nanofibers on nerve regeneration. J Biomed Mater Res A 91(4):994–1005
151. Haastert TK, Geuna S, Dahlin LB et al (2013) Chitosan tubes of varying degrees of acetylation for bridging peripheral nerve defects. Biomaterials 34(38):9886–9904
152. Stenberg L, Kodama A, Lindwall BC et al (2016) Nerve regeneration in chitosan conduits and in autologous nerve grafts in healthy and in type 2 diabetic Goto-Kakizaki rats. Eur J Neurosci 43(3):463–473
153. Lee KY, Mooney DJ (2012) Alginate: properties and biomedical applications. Prog Polym Sci 37(1):106–126
154. Suzuki Y, Tanihara M, Nishimura Y et al (1999) In vivo evaluation of a novel alginate dressing. J Biomed Mater Res 48(4):522–527
155. Ochbaum G, Davidovich PM, Bitton R (2018) Tuning the mechanical properties of alginate–peptide hydrogels. Soft Matter 14(21):4364–4373
156. Suzuki Y, Tanihara M, Ohnishi K et al (1999) Cat peripheral nerve regeneration across 50 mm gap repaired with a novel nerve guide composed of freeze-dried alginate gel. Neurosci Lett 259(2):75–78
157. Hashimoto T, Suzuki Y, Kitada M et al (2002) Peripheral nerve regeneration through alginate gel: analysis of early outgrowth and late increase in diameter of regenerating axons. Exp Brain Res 146(3):356–368
158. Quigley AF, Bulluss KJ, Kyratzis IL et al (2013) Engineering a multimodal nerve conduit for repair of injured peripheral nerve. J Neural Eng 10(1):016008
159. Naghieh S, Sarker MD, Abelseth E et al (2019) Indirect 3D bioprinting and characterization of alginate scaffolds for potential nerve tissue engineering applications. J Mech Behav Biomed Mater 93:183–193
160. Wu H, Liu J, Fang Q et al (2017) Establishment of nerve growth factor gradients on aligned chitosan-polylactide/alginate fibers for neural tissue engineering applications. Colloids Surf B: Biointerfaces 160:598–609
161. de Luca AC, Lacour SP, Raffoul W et al (2014) Extracellular matrix components in peripheral nerve repair: how to affect neural cellular response and nerve regeneration? Neural Regen Res 9(22):1943–1948
162. Silvan K, Lukas P, Jody V et al (2016) Differential effects of coating materials on viability and migration of schwann cells. Materials (Basel) 9(3):150
163. Fujimaki H, Uchida K, Inoue G et al (2017) Oriented collagen tubes combined with basic fibroblast growth factor promote peripheral nerve regeneration in a 15 mm sciatic nerve defect rat model. J Biomed Mater Res A 105(1):8–14
164. Huang L, Zhu L, Shi X et al (2018) A compound scaffold with uniform longitudinally oriented guidance cues and a porous sheath promotes peripheral nerve regeneration in vivo. Acta Biomater 68:223–236
165. Bhandari PS (2013) Use of fibrin glue in the repair of brachial plexus and peripheral nerve injuries. Indian J Neurotrauma 10(1):30–32
166. Reichenberger MA, Mueller W, Hartmann J et al (2016) ADSCs in a fibrin matrix enhance nerve regeneration after epineural suturing in a rat model. Microsurgery 36(6):491–500
167. Du J, Liu J, Yao S et al (2017) Prompt peripheral nerve regeneration induced by a hierarchically aligned fibrin nanofiber hydrogel. Acta Biomater 55:296–309
168. Mosahebi A, Wiberg M, Terenghi G (2003) Addition of fibronectin to alginate matrix improves peripheral nerve regeneration in tissue-engineered conduits. Tissue Eng 9(2):209–218
169. Gonzalez Perez F, Cobianchi S, Heimann C et al (2017) Stabilization, rolling, and addition of other extracellular matrix proteins to collagen hydrogels improve regeneration in chitosan guides for long peripheral nerve gaps in rats. Neurosurgery 80(3):465–474
170. Kijeńska E, Prabhakaran MP, Swieszkowski W et al (2014) Interaction of Schwann cells with laminin encapsulated PLCL core–shell nanofibers for nerve tissue engineering. Eur Polym J 50:30–38
171. Haggerty AE, Bening MR, Pherribi G et al (2019) Laminin polymer treatment accelerates repair of the crushed peripheral nerve in adult rats. Acta Biomater 86:185–193
172. Entekhabi E, Haghbin NM, Sadeghi A et al (2016) Design and manufacture of neural tissue engineering scaffolds using hyaluronic acid and polycaprolactone nanofibers with controlled porosity. Mater Sci Eng C 69:380–387
173. Vilariño Feltrer G, Martínez Ramos C, Monleón de la Fuente A et al (2016) Schwann-cell cylinders grown inside hyaluronic-acid tubular scaffolds with gradient porosity. Acta Biomater 30:199–211
174. Khan R, Khan MH (2013) Use of collagen as a biomaterial: an update. J Indian Soc Periodontol 17(4):539–542
175. Tiago HS, Joana MS, Ana LPM et al (2014) Marine origin collagens and its potential applications. Mar Drugs 12(12):5881–5901
176. Chanjuan D, Lv Y (2016) Application of collagen scaffold in tissue engineering: recent advances and new perspectives. Polymers 8(2):42
177. Bozkurt A, Claeys KG, Schrading S et al (2017) Clinical and biometrical 12-month follow-up in patients after reconstruction of the sural nerve biopsy defect by the collagen-based nerve guide Neuromaix. Eur J Med Res 22(1):34
178. Litvinov RI, Weisel JW (2016) What is the biological and clinical relevance of fibrin? Semin Thromb Hemost 42(4):333–343
179. Esposito F, Angileri FF, Kruse P et al (2016) Fibrin sealants in dura sealing: a systematic literature review. PLoS One 11(4):e0151533

180. Olcucuoglu E, Kulacoglu H, Ensari CO et al (2011) Fibrin sealant effects on the ilioinguinal nerve. J Investig Surg 24(6):267–272
181. Pankov R, Yamada KM (2002) Fibronectin at a glance. J Cell Sci 115(20):3861–3863
182. Whitworth IH, Brown RA, Doré C et al (1995) Orientated mats of fibronectin as a conduit material for use in peripheral nerve repair. J Hand Surg (Br) 20(4):429–436
183. Chen YS, Hsieh CL, Tsai CC et al (2000) Peripheral nerve regeneration using silicone rubber chambers filled with collagen, laminin and fibronectin. Biomaterials 21(15):1541–1547
184. Liang S, Crutcher KA (1992) Neuronal migration on laminin in vitro. Brain Res Dev Brain Res 66(1):127–132
185. Adams DN, Kao EY, Hypolite CL et al (2005) Growth cones turn and migrate up an immobilized gradient of the laminin IKVAV peptide. J Neurobiol 62(1):134–147
186. Zhang XF, Liu HX, Ortiz LS et al (2018) Laminin-modified and aligned poly(3-hydroxybutyrate-co-3-hydroxyvalerate)/polyethylene oxide nanofibrous nerve conduits promote peripheral nerve regeneration. J Tissue Eng Regen Med 12(1):e627–e636
187. Swindle-Reilly KE, Papke JB, Kutosky HP et al (2012) The impact of laminin on 3D neurite extension in collagen gels. J Neural Eng 9(4):046007
188. Zamboni F, Vieira S, Reis RL et al (2018) The potential of hyaluronic acid in immunoprotection and immunomodulation: chemistry, processing and function. Prog Mater Sci 97:97–122
189. Chircov C, Grumezescu AM, Bejenaru LE (2018) Hyaluronic acid-based scaffolds for tissue engineering. Romanian J Morphol Embryol 59(1):71–76
190. Huang L, Wang Y, Liu H et al (2017) Local injection of high-molecular hyaluronan promotes wound healing in old rats by increasing angiogenesis. Oncotarget 9(9):8241–8252
191. Wang KK, Nemeth IR, Seckel BR et al (1998) Hyaluronic acid enhances peripheral nerve regeneration in vivo. Microsurgery 18(4):270–275
192. Ikeda K, Yamauchi D, Osamura N et al (2003) Hyaluronic acid prevents peripheral nerve adhesion. Br J Plast Surg 56(4):342–347
193. Murphy SV, Atala A (2014) 3D bioprinting of tissues and organs. Nat Biotechnol 32(8):773–785
194. Hamburg MA, Collins FS (2010) The path to personalized medicine. N Engl J Med 363(4):301–304
195. Rengier F, Mehndiratta A, von Tengg KH et al (2010) 3D printing based on imaging data: review of medical applications. Int J Comput Assist Radiol Surg 5(4):335–341
196. Schmidt CE, Leach JB (2003) Neural tissue engineering: strategies for repair and regeneration. Annu Rev Biomed Eng 5:293–347
197. Ji XM, Wang SS, Cai XD et al (2019) Novel miRNA, miR-sc14, promotes Schwann cell proliferation and migration. Neural Regen Res 14(9):1651–1656
198. Petcu EB, Midha R, McColl E et al (2018) 3D printing strategies for peripheral nerve regeneration. Biofabrication 10(3):032001
199. Johnson BN, Lancaster KZ, Zhen G et al (2015) 3D printed anatomical nerve regeneration pathways. Adv Funct Mater 25(39):6205–6217
200. Hu Y, Wu Y, Gou Z et al (2016) 3D-engineering of cellularized conduits for peripheral nerve regeneration. Sci Rep 6:32184
201. Tao J, Zhang J, Du T et al (2019) Rapid 3D printing of functional nanoparticle-enhanced conduits for effective nerve repair. Acta Biomater 90:49–59
202. Zhong Y, Wang L, Dong J et al (2015) Three-dimensional reconstruction of peripheral nerve internal fascicular groups. Sci Rep 5:17168

13 Protein-Based Drug Delivery in Brain Tumor Therapy

Hae Hyun Hwang and Dong Yun Lee

Abstract

Despite the use of active surgeries, radiotherapy, and chemotherapy in clinical practice, brain tumors are still a difficult health problem due to their rapid development and poor prognosis. To treat brain tumors, various nanoparticles can be used to target effective physiological conditions based on continuously changing vascular characteristics and microenvironments to promote effective brain tumor-targeting drug delivery. In addition, a brain tumor-targeting drug delivery system that increases drug accumulation in the brain tumor area and reduces toxicity in the normal brain and peripheral tissues is needed. However, the blood-brain barrier is a big obstacle for drug delivery to the brain. In this chapter, we provide a broad overview of brain drug delivery and current strategies over the last few years. In addition, several questions have been reconsidered, such as whether nanoparticles believed to be delivered to the brain can pass through the blood-brain barrier, whether the drug is delivered to the target site, and what brain tumor treatment is possible.

Keywords

Brain tumor · Drug delivery · Oral administration of protein-based drug · Drug stability

13.1 Introduction

Brain diseases such as central nervous system disorders and brain cancers are the most prevalent and fatal yet untreatable diseases. Brain tumors include a variety of neoplasms that can be classed as either primary or metastatic [30, 85]. Three major types of brain tumors are known by the World Health Organization (WHO) as the classes of gliomas: astrocytomas, oligo-astrocytomas, and oligodendrogliomas [114]. These tumors are classified as subtypes (mainly astrocytomas) and are graded from I to IV, with type IV being the most aggressive, glioblastoma multiforme (GBM) [113].

Malignant astrocytoma constitutes about 50–60% of primary brain tumors [34]. The incidence of brain tumors seems to be increasing, but it is not clear whether this is because of environmental or genetic factors [46]. The standard treatment for brain tumors consists of maximal

H. H. Hwang · D. Y. Lee (✉)
Department of Bioengineering, College of Engineering, and BK21 PLUS Future Biopharmaceutical Human Resource Training and Research Team, Hanyang University, Seoul, Republic of Korea

Institute of Nano Science & Technology (INST), Hanyang University, Seoul, Republic of Korea
e-mail: dongyunlee@hanyang.ac.kr

H. J. Chun et al. (eds.), *Bioinspired Biomaterials*, Advances in Experimental Medicine and Biology 1249, https://doi.org/10.1007/978-981-15-3258-0_13

surgical resection, radiation therapy, and chemotherapy. However, despite ongoing research and new approaches, the prognosis for patients with malignant brain tumors is still very poor [17]. Thus, the median survival rate for GBM patients is 20 weeks with surgical resection or 36 weeks with surgical and radiation therapy, while cytotoxic chemotherapy maximizes survival and increases median survival to 40–50 weeks [9].

Despite the development and progress of anticancer drugs in the past decades, the prognosis of patients with brain cancer has remained almost unchanged [89]. These results imply that it is difficult to avoid the various resistance mechanisms, deliver the therapeutic agents across the blood-brain barrier (BBB), and reach the desired target [41, 52]. In addition, low-molecular-weight chemotherapeutic agents also have the disadvantage that they do not maintain effective steady-state concentrations in glioma cells because of their short blood half-lives [109].

Considering the high incidence of brain tumors and their poor prognosis, much effort has been made to identify the delivery of optimal drugs and valuable systems or anticancer drugs to the central nervous system (CNS). For the tumor to grow, it must develop a vascular network, and the angiogenesis system in the tumor is composed of vasculature with increased permeability due to large endothelial gaps compared to normal vessels [101]. This feature can be used in the anticancer delivery system.

This chapter deals with various approaches for the treatment of primary CNS tumors. In addition, it focuses on the recent discovery of a new strategy for delivering anticancer drugs to the CNS based on efficient targeting protein vectors (antibodies and protein carriers) or nanosystems (colloid carriers) that can cross chemical and biological barriers such as the BBB [7, 16, 58].

13.2 Barriers to Drug Delivery for Brain Tumors

Use of a drug delivery system, one of the therapies used to treat tumor progression in glioma, to reach the tumor site is complicated by many barriers. There are three major barriers to the treatment of brain tumors: the BBB, the blood-brain tumor barrier (BBTB), and the active efflux effect (Fig. 13.1). Specific brain tumor developmental stages require corresponding barrier-targeting treatment strategies.

13.2.1 Blood-Brain Barrier

The blood-brain barrier (BBB) is a diffusion barrier essential for normal functioning of the brain and regulates influx of blood into the brain to maintain homeostasis [20]. Brain capillary endothelial cells (BCECs), tight junctions (TJs), astrocytes (covering up to 90% of brain capillaries), pericytes, neurons, and basement membranes constitute physically rigid brain capillaries in the BBB [52, 99]. Unlike the peripheral microvasculature, BCECs are interconnected by tight junctions with few fenestrations that form a physical barrier to prevent diffusion from blood vessels into the brain. Interendothelial junctions severely limit penetration of water-soluble materials by connecting the endothelial cells to a continuous barrier. In addition, these junctions lead to very high trans-endothelial electrical resistance (TEER) between the blood and brain, significantly limiting the passive diffusion of compounds [3]. The interendothelial junctions are divided into adherence junctions, tight junctions, and gap junctions [64]. Primary control of the permeability of the endothelial barrier is the role of adherence junctions. Tight junctions are important in maintaining the permeability barrier of the epithelial and endothelial cells that regulate tissue homeostasis [69]. Gap junctions composed of six connexin molecules are responsible

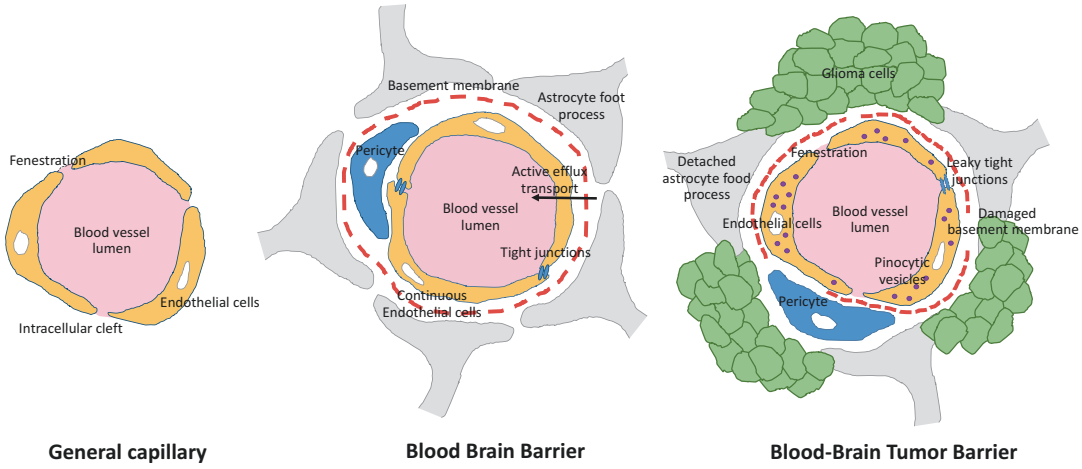

Fig. 13.1 Graphical depiction of the difference structure between normal capillary, BBB, and BBTB

for direct electrical and chemical communication between endothelial cells [42]. Pericytes, astrocytes, and basal membranes form a structure that surrounds the endothelial cells and eventually forms an impermeable BBB. Efflux transporters are located in the BCECs and provide an additional barrier to substances entering the brain (a more detailed description of efflux transporters is given in the next section). Thus, the physical barriers of the BBB significantly limit the accumulation of large molecules such as antibodies and antibody-drug conjugates, as well as small hydrophilic drugs that cannot easily traverse the plasma membranes of capillary endothelial cells [87].

However, the BBB not only has a static structure as mentioned above but also adapts continuously to various physiological changes of the brain [4, 64]. Molecules can cross the BBB by paracellular pathways or transcellular pathways. In the paracellular pathways, ions and solutes pass through the BBB by passive diffusion through a concentration gradient. The transcellular pathways involve various mechanisms such as passive diffusion, transcytosis, and receptor-mediated transcytosis [20]. Physicochemical factors affecting BBB permeability also include molecular weight, charge, surface activity, lipid solubility, and molecular size. [39]. For example, small lipophilic molecules such as carbon dioxide can pass through the BBB by passive diffusion through transcellular pathways. Hydrophilic molecules such as proteins or peptides can enter the brain through specific receptor-mediated transport mechanisms such as glucose transporter-1 (GLUT-1) and insulin transporter, and these transporters are expressed at the luminal and abluminal endothelial cell membranes [79]. Therefore, both physical and biochemical barriers within the BBB significantly limit delivery of remedial agents to the brain, which can limit treatment efficacy.

13.2.2 Blood-Brain Tumor Barrier

Brain tumor cells have a structure similar to that of the BBB in the early stage to match their rapid cell growth and migration rates. When growth of tumor cells reaches a certain level, the BBB structure is damaged, and the blood-brain tumor barrier (BBTB) is created from new blood vessels. The BBTB is located between the brain tumor tissue and the microvessels formed by endothelial cells with highly restrictive barriers [86]. Compared to peripheral tumors, the BBTB has a small pore size and represents a stronger

drug efflux pump, affecting such agents as P-glycoprotein, multidrug-resistant proteins, and breast cancer-resistant proteins [32, 60, 82, 104, 110]. This barrier also limits intercellular transport of most hydrophilic molecules to the tumor tissue. Therefore, the BBTB structure more highly limits drug distribution to brain tumors than to peripheral tumors. For example, Kunal et al. found that the metastatic breast tumor-bearing mouse model showed a lapatinib concentration in lung metastasis that was 5.15 times higher than that in brain metastasis [67]. This result assumes that the BBTB limited drug distribution from the blood to the brain tumor area [10, 38, 41]. Thus, the combination of the BBB and BBTB poses a major barrier to brain tumor drug delivery.

13.2.3 Active Efflux Transporters

Drug efflux receptors are expressed in brain capillary endothelial cells and cancer cells themselves, resulting in brain tumors that are resistant to anticancer drugs [14, 100, 107]. There are various types of efflux transporter systems, all of which belong to the multidrug resistance (MDR) family [106]. Among the MDR family, P-glycoprotein (P-gp, MDR1) is the most important active efflux transporter in drug disposition in the human body [100]. The molecular weight of P-gp is 170 kDa; it is expressed on the apical side of the BBB and actively pumps a variety of anticancer drugs into the systemic circulation [18]. This active transport process is one of the basic mechanisms of CNS anticancer drug resistance. The importance of P-gp in BBB was demonstrated using P-gp knockout mice [1, 111]. Penetration of vinblastine, a chemical analogue of vincristine, into the brain was 7- to 46-fold higher in knockout mice than in wild-type controls [124]. For this reason, many cytotoxic agents that are P-gp substrates cannot reach the tumor cells in the brain parenchyma and have no effect even if the tumor cells do not express P-gp [35, 118]. Furthermore, P-gp has been found in resistant glioblastomas, suggesting that it restricts penetration of anticancer agents into brain tumors despite the leaky nature of the glioma vasculature [6]. Therefore, inhibition of P-gp activity in brain endothelial cells is important for increasing antitumor effects.

13.3 Drug Delivery Strategies in Brain Cancers

As mentioned above, unlike other peripheral tissues, a brain tumor involves many barriers to transmission of anticancer drugs such as the BBB, BBTB, and efflux transporters. However, drug delivery systems for overcoming these problems and treating brain tumors have been actively studied. There are a number of overexpressed receptors and carriers that can act as channels through which the BBB can mediate the transport of certain ligands and cargo, even under intact conditions [102]. The BBB membrane has a negative charge, so it has a high affinity for positively charged compounds and can induce cell internalization. Low-molecular-weight, fat-soluble, and neutral drugs can pass through the BBB via passive diffusion [36]. In a brain tumor, nanoparticles of a certain size or less can pass through the gap between the endothelial cells due to the enhanced permeability and retention (EPR) effect caused by collapse of blood vessels due to solid tumor formation. In addition, drug delivery systems that target specific receptors and specific structures overexpressed in the BBTB, which is a structure independent from the BBB, have been studied.

13.3.1 EPR Effect

As brain tumors develop, they exhibit the EPR effect, though it is much weaker in the brain microenvironment than in peripheral tumors. The EPR effect allows a nanosystem with an appropriate particle size to enter the brain tumor through the microvascular endothelial cleft of the brain tumor. In addition, tumoral masses accumulate macromolecules larger than about 40 kDa in the microenvironment because of poor lymphatic drainage [49, 74, 134]. Nanoparticles use

this feature to target solid tumors. The ideal size range for achieving the benefits of EPR is 10–200 nm. Outside this range, small particles are removed by the kidneys to prevent them from accumulating at the tumor site, and particles larger than this range cannot adequately penetrate the tumor vasculature and interstitial space.

Therefore, some nano-sized drug delivery systems have been developed to use the EPR effect for brain tumor targeting. Huang et al. have developed a tumor-targeting nanoparticle system with passive tumor targeting based on the EPR effect. This system was able to extend the survival time of U87MG tumor-bearing nude mice [49]. There have also been attempts to increase the efficiency of the EPR effect by induction of hypertension, repair of abnormal vascular systems, or targeting of peripheral blood cells [51].

13.3.2 BBTB Targeting Delivery

The blood-brain tumor barrier (BBTB) is located between the microvessels and brain tumor tissues and is formed by highly specialized endothelial cells, limiting paracellular delivery of hydrophilic molecules to tumor cells [86]. The blood tumor barrier structure that grows in the peripheral tissues is generally more permeable than that in the brain [84, 104]. As brain tumors deteriorate, tumor neovascularization becomes more active and the BBB structure becomes damaged, creating a new structure called BBTB. This structure supports the growth of glioma. Abnormality of tumor vasculature increases the permeability of the BBTB, while the cranial microenvironment reduces the permeability of glioma area [112, 133]. Thus, BBTB can limit glioma-targeted transport of chemotherapeutic agents [133].

Therefore, some receptors present on the BBB/BBTB provide an opportunity for glioma-targeted drug delivery at this stage. Several studies proposed a strategy for BBTB targeting based primarily on the receptors expressed at high levels in tumors, such as epidermal growth factor receptors and integrins [128]. The adhesion receptor integrin is overexpressed in the tumor neovasculature and glioblastoma U87MG cells and was identified as a marker of angiogenic blood vessel tissue. The integrin αvβ3 expression is overexpressed in malignant glioma but not in normal brain cells. As ligands for integrins, cyclic arginine-glycine-aspartic acid (RGD) peptides and their analogues have been extensively studied for glioma-targeted drug delivery [11, 63, 73]. Therefore, integrin and RGD interactions are promising drug delivery strategies that target the BBTB. Zhan et al. developed c-RGDyK-modified polyethylene glycol-polyethylenimine nanoparticles (PEG-PEI NPs) for glioma-targeted gene delivery [136]. These NPs showed high binding affinity with U87MG cells and promoted target gene delivery to intracranial glioblastoma in vivo compared to PEG-PEI gene carriers without RGD modification. The therapeutic efficacy of this gene transducer has been demonstrated by significantly prolonging the survival rate of nude mice with intrathecal glioblastoma. These results demonstrated the therapeutic potential of the gene delivery system for the treatment of brain glioma cells using integrin αvβ3 [136]. Zhan et al. reported cyclic RGD peptide-conjugated PEG-PLA micelles for chemotherapy of intracranial glioma. The median time of intracranial U87MG tumor xenograft survival was significantly prolonged after treatment with c(RGDyK)-PEG-PLA-PTX micelles, indicating that the RGD motif is effective in drug delivery targeted to glioblastoma overexpressing integrin αvβ3 [134].

Epidermal growth factor receptor (EGFR) is a transmembrane tyrosine kinase expressed in epithelial cells, mesenchymal cells, and neuronal tissues [116, 131]. Overexpression of EGFR for the BBTB is a promising target for treatment [88]. Epidermal growth factors (EGF) and anti-epidermal growth factor ligand (anti-EGFL) monoclonal antibodies are commonly used EGFR ligands in glioma-targeted therapy. Fondell et al. have adopted EGF to target EGFR and have recently developed a strategy for delivering recently synthesized daunorubicin derivatives to cancer cell nuclei using PEG-stabilized targeted liposomes called “nuclisome-particles” [33]. Tsutsui et al. established a new drug delivery system using hybrid bionanocapsules (BNCs)

coupled with anti-human EGFR antibodies and confirmed the specific delivery of BNCs to brain tumors in in vivo brain tumor animal models [123].

13.3.3 Receptor-Mediated Transcytosis

Many receptors, including the transferrin (Tf) receptor, the nicotinic acetylcholine receptor (nAchR), and the insulin receptor, are overexpressed in the BBB [43, 137]. These receptors specifically bind to corresponding ligands and can cause cellular internalization. Thus, these receptors and their corresponding ligands can be functionalized into the nanoparticle phase to mediate transport through the BBB. Due to the specificity of the interaction between the receptor and ligand, receptor-mediated delivery was the most commonly used and most successful strategy for delivering NPs to the brain via the BBB. The contents of the receptor-mediated transcytosis-related studies will be discussed in more detail in the next section.

13.4 Protein-Based Drug Delivery to Brain Tumors

A variety of proteins and peptides have been studied as promising therapeutic agents for brain pathologies [5, 96] (Table 13.1). Proteins and peptides are present in the entire nervous system with a unique distribution pattern. They have numerous biological actions in the brain, such as controlling the brain's internal environment, controlling cerebral blood flow, controlling the permeability of the BBB to nutrient supply, neurotransmission, neuromodulation, and the various roles of the immune system [22, 96]. This suggests that the diversity of the biological actions of proteins could be used in the treatment of brain and spinal cord disorders. But like all potential neuroleptics, proteins must be transportable from the blood to the brain. Protein nanocarriers are now drawing great interest as drug delivery systems targeting brain tumors [26, 27]. The unique biodegradability and high drug binding capacity of protein drugs indicate them as good alternatives to synthetic polymer nanoparticles. In addition, the available functional groups present in the proteins, such as amino and carboxyl groups, can be derivatized to specific ligands for drug delivery targeted to brain tumors [25, 29].

13.4.1 Transferrin

The transferrin (Tf) receptor, composed of two 90 kDa subunits, is an iron-binding, single plasma glycopeptide that controls the concentration of free iron in biological fluids. Many reports have shown that Tf can target Tf receptors (TfR) that are overexpressed in cancer cells and brain capillary endothelial cells of the BBB, and TfRs have been shown to pass through the BBB and cancer cell membranes [102]. Thus, modification of nanocarriers with Tf is a typical pathway of receptor-mediated delivery, one of the major mechanisms by which various mediators can cross the BBB [94, 95]. In several studies, Tf-modified NPs (Tf-NPs) showed good affinity for endothelial cells of the brain capillaries and could deliver much more cargo to the brain than unmodified NPs. Linuma et al. modified cisplatin (Cis)-liposomes (Tf-Cis-lipo) to enhance transport across bEnd3 cells as a model of the BBB using the TfR [53]. They also identified Tf-Cis-lipo endocytosis through recognition of Tf receptors on the surface of C6 glioma cells. Tf-modified liposomes encapsulating vincristine and tetracene (TFT) have been developed to overcome the multidrug resistance (MDR) that causes glioma treatment failure. Similarly, Tong et al. studied the decoration of artesunate (ART)-loaded liposomes containing Tf-ART-LPs and found that the absorption rate of U87 glioma cells increased from 18.7% for ART-LPs (not modified with Tf) to 59.8% for Tf-ART-LPs [122]. Song et al. conjugated the liposome surface to the Tf via acylation, in which one of the amino groups of Tf coupled with the *N*-hydroxysuccinimide (NHS)

Table 13.1 List of protein- or peptide-modified nanocarriers for the treatment of brain tumor

Material	Modified agents	Drugs	References
Transferrin	Liposome	Tf-Cisplatin-liposome	[53]
		Tf-ART-LPs	[122]
		Tf-PEG-DSPE	[115]
	Monoclonal antibody		[92]
		PDMS-b-PMOXA conjugated to 83-14 mAb	[19]
	Gene	Tf-PEI2-ChA	[23]
	Inorganic NPs	TPGD	[21]
		C-Dots-Tf-DOX	[72]
		Tf-PLCaPZ NPs	[108]
	CPP	Tf3.4 K-CPP2K-liposome	[76]
	Dendrimer	G4-DOX-PEG-Tf-TAM	[71]
Lactoferrin	Tumor-homing peptide	tLyP-1/Lf-NPs	[83]
	Folic acid	Lf/FA/PLGA NPs	[68]
	Polymersome	Lf-PO-DOX/TET	[93]
		Lf_H-NPs	[119]
	Peptide	Urocortin-loaded Lf-NPs	[48]
		S14G-humanin/Lf	[55]
	Magnetic NPs	Lf-M-PAEEPPLLA-NPs	[78]
		Cy5.5-Lf-SPIO micelles	[138]
		Lf-CUR-PDNC	[31]
Albumin	Glucose derivatives	c/m-HSA NPs	[12]
	Folic acid	FA-BSA-SPIO NPs	[127]
	Self-assembled NPs	LMWP-BSA-NPs	[73]
		HSA-Ce6@HSA-RGD NPs	[13]
Peptides	Small peptide	SynB1	[105]
		ANG1005	[120]
		T7-modified dendrimer	[70]
		CDX	[135]
	CPP	AngioPep-2	[126]
	Glycoprotein peptide	RVG29	[50, 75]
		RVG79-modified poly(mannitol-co-PEI) vector	[97]
	Apolipoprotein	ApoA and ApoE	[103, 132]
		Polysorbate 80-coated NPs	[37, 130]
		Polysorbate 60/80	[81]

ART artesunate, *LPs* liposomes, *NP* nanoparticle, *PDMS-b-PMOXA* poly(dimethylsiloxane)-block-poly(2-methyl-2 oxazoline), *mAb* monoclonal antibody, *PEI* polyethyleneimine, *ChA* cholic acid, *TPGD* transferrin-DOX-loaded PEGylated graphene oxide nanoparticles, *DOX* doxorubicin, *C-Dots* carbon-dots, *CaP* calcium phosphate, *PLCaPZ* CaP NP was complexed with zoledronic acid (ZOL), mixed with PEGylated cationic liposomes, *CPP* cell-penetrating peptide, *G4* fourth generation, *TAM* tamoxifen, *Lf* lactoferrin, *FA* folic acid, *PLGA* poly(lactide-co-glycoride), *PO* polymersome, *Lf_H-NPs* PEGylated DOX was converted to Lf, *S14G-humanin* a humanin analogue peptide drug, *PAEEP-PLLA* poly(aminoethyl ethylene phosphate)/poly(L-lactide), *Lf-M-PAEEPPLLA-NPs* OAM-MNP-loaded PAEEP-PLLA NPs modified with Lf, *OAM-MNPs* oleylamine (OAM) coating for Fe3O4 magnetic NPs, *SPIO* superparamagnetic iron oxide, *CUR* curcumin, *PDNC* polydiacetylene nanocarriers, *HAS* human serum albumin, *c-HSA* cationic HSA, *m-HSA* mannose-modified albumin, *BSA* bovine serum albumin, *LMWP* low-molecular-weight protamine, *Ce6* chlorin e6, *RGD* Arg-Gly-Asp, *T7 peptide* HAIYPRH, *RVG29* rabies virus glycoprotein peptide

group of 1,2-distearoyl-sn-glycero-3-phosphoethanolamine (DSPE)-conjugated polyethylene glycol with an active succinimidyl ester (DSPE-PEG-NHS) [115]. Tf-modified liposomes (Tf-PEG-DSPE) can enhance transport through the BBB, increase cellular uptake, and inhibit MDR. Therefore, liposomes accumulated in brain tumors and showed high anticancer efficacy in glioma mice.

Monoclonal anti-transferrin receptor antibody (OX26) is an antibody that can recognize the Tf receptor. Pang et al. conjugated OX26 to the NP for brain-targeted delivery of the peptide NC1900, which is used to treat a neurodegenerative disorder [92]. The concentration of OX26-NP in brain tissue 2 h after intravenous injection was 2.62 times higher than that of unmodified NP. As a result, NC1900-loaded OX26-NP showed the best results for Alzheimer's disease rats, as determined by the water maze learning task using rats with scopolamine-induced learning and memory impairment [92]. In addition, the insulin receptor 83-14 mAb antibody (INSR alpha [83-14]) was about 10 times more effective than the anti-Tf receptor antibody for BBB penetration [15]. Therefore, Dieu et el. conjugated insulin receptor 83-14 mAbs to the NP surface (polymersomes composed of poly(dimethylsiloxane)-*block*-poly(2-methyl-2-oxazoline), PDMS-*b*-PMOXA) for brain target drug delivery. In vitro results showed that brain endothelial cells effectively absorbed modified NPs from insulin receptor 83-14 mAb, which could be inhibited by more than insulin receptor 83-14 mAb use alone [19].

To deliver the gene to glioma cells, Dube et el. developed a new nonviral vector based on low-molecular-weight polyethyleneimine (PEI 2 kDa) modified hydrophobically to cholic acid (ChA) to obtain PEI2-ChA [23]. Condensation of pDNA by the PEI-ChA complex protected the pDNA from enzymatic degradation and promoted absorption of the complex by the cells. Tf was also incorporated into nanopeptides to combine the high gene transfer efficiency of the PEI-ChA nanopeptides with Tf receptor (TfR)-mediated uptake. Tf facilitated the binding of pDNA nanopeptides to Tf receptors on target cells and promoted endocytosis of vesicles, escape of DNA from endosomal compartments, and entered to the nuclei. The size of tumors in the mouse brain treated with Tf-PEI2-ChA nanopeptides was five times smaller than those in the untreated animals.

Inorganic NPs can also be transformed into Tf to enhance brain tumor accumulation. Dong et al. explained that Tf was covalently bound to DOX-loaded PEGylated graphene oxide nanoparticles (TPG) [21]. Modified TPG can pass through the BBB to enhance DOX accumulation and act as dual chemo- and photothermal therapies. Targeted TPGD combination therapy increased the number of neuroblastoma lymphoma cells and prolonged the survival of glioma-bearing mice compared to single DOX or PGD therapy. Carbon dots (C-dots) and quantum-sized carbon NPs, which were smaller than 10 nm, exhibited good water solubility, excellent biocompatibility, excitation wavelength-dependent photoluminescence, and high cell membrane permeability [72]. Thus, the C-Dots-Tf-DOX covalent bond was synthesized by covalently bonding the carboxyl groups of the C-dots to the primary amines of Tf via carbodiimide coupling. C-Dots-Tf-DOX at the 10-nm size was much more cytotoxic than DOX alone, reducing the survival rate by 14–45% in many pediatric brain tumor cells [72]. Another type of inorganic nanoparticle, calcium phosphate NP (CaP NP), was complexed with zoledronic acid (ZOL), mixed with PEGylated cationic liposomes, and then transformed into Tf to generate Tf-PLCaPZ NPs for brain tumor treatment. Sequential treatment with temozolomide (TMZ) and Tf-PLCaPZ NP showed superior therapeutic activity compared to single administration. In the group treated with Tf-PLCaPZ NPs, the tumor size of mice xenotransplanted with U373MG was significantly reduced, but treatment had no effect in the free TMZ group [108].

A dual brain targeting effect was achieved by decorating the nanocarrier surface with Tf combined with other ligands for the purpose of increasing drug accumulation in tumor cells. Liu et al. conjugated Tf and cell-penetrating peptide (CPP) to PEGylated liposomes (Tf-CPP-liposomes) to bind endogenous escaping and per-

meability of CPP with Tf receptors (Tf-Rs) overexpressed in the BBB and glioma cells [76]. A "hand in hand" effect was observed in the Tf3.4 K-CPP2K-liposome and allowed longer PEG chains to nonspecifically mask CPP during blood circulation. The longer PEG chain at the tumor site promotes binding of Tf to the Tf receptor, while the flexible PEG linker is shortened, so that CPP improves cellular internalization through cell adsorption. The CPP portion was concealed by the large volume of the PEG 3.4 k linker of Tf. However, when the Tf3.4 K-CPP3.4 K-liposome was used, CPP could not be sterically hindered, demonstrating its permeation efficiency and significantly increasing normal cell uptake. Thus, to obtain maximum efficacy in target cells, PEG 3.4 k and PEG 2 k were selected to conjugate Tf and CPP with liposomes for the production of Tf-CPP-liposomes. These liposomes had the highest target efficacy for brain microvascular endothelial cells and C6 cell uptake, but absorption into normal cells was scant. Furthermore, Tf-CPP-liposomes were captured in the endosomes of C6 cells, where the complex escaped from the lysosomes and successfully released liposome-confined doxorubicin (DOX) to the cytoplasm. Li et al. conducted double modification of the fourth-generation (G4) DOX-loaded poly(amidoamine) (PAMAM) dendrimer with Tf and tamoxifen (TAM) (G4-DOX-PEG-Tf-TAM). They found that about 7 DOX molecules, over 30 PEG (1000 Da) and PEG (2000 Da) chains, and one Tf group were conjugated on the surface of each G4 PAMAM dendrimer, while 29 TAM molecules were encapsulated into one dendrimer. The result is that TAM inhibited MDR efflux transporters (e.g., P-gp, which is overexpressed in BBB and C6 glioma cells) with Tf receptor-mediated endocytosis to enhance BBB transport and accumulation of DOX in C6 cells. In addition, DOX accumulated in the C6 glioma spheroids and the tumor volume was effectively reduced [71].

13.4.2 Lactoferrin

Similar to transferrin, lactoferrin (Lf) is a mammalian cationic iron-binding globular glycoprotein belonging to the transferrin family and has a molecular weight of about 80 kDa [59]. Lactoferrin has many physiological functions such as defense against infections and severe inflammation. Lactoferrin receptors (LfRs) include low-density lipoprotein receptor-related protein 1 (LRP1) and LRP2, and LfRs induce internalization of Lf into the body. Previous studies have shown that LfRs are highly expressed in the BBB and in glioma cells. The positive charge of Lf promotes electrical attraction between the positively charged Lf-modified drug carrier and negatively charged BBB basement membrane, and this combination is absorbed through LfR-mediated endocytosis. That is, the Lf-modified nanocarrier was transported through the BBB by receptor-mediated transcytosis. Several studies have shown that the BBB permeability of Lf is better than that of transferrin (Tf) [28] because binding between Lf and its receptor is not affected by endogenous Lf. Lactoferrin receptors were not saturated under physiological conditions due to low plasma concentration of endogenous Lf. Conversely, the concentration of the intrinsic Tf in plasma is very high, so TfR is almost saturated under physiological conditions. Therefore, it could be better to use LfR as a target to modify the Lf and transmit it to brain tumors through receptor-mediated transcytosis of BBB.

However, Lf-functionalized nanoparticles for glioma treatment may still be limited because of the high interstitial pressure in cerebral blood vessels and glioma glands with reduced brain function and low efflux system from the blood vessels and low permeability to the glioma parenchyma [54]. Therefore, administering nanocarriers that target both the BBB/BBTB and glioma cells with a tumor penetration-enhancing peptide is a promising platform for antitumor brain drug delivery. For example, Miao et al. reported that lactoferrin was modified with the surface of poly(ethylene glycol)-poly(lactic acid) (PEG-PLA) NPs through a maleimide-mediated cova-

lent bond to induce BBB/BBTB and glioma cell targeting. A tumor-homing peptide, tLyP-1, was also used to mediate BBB penetration through the C-end rule sequence (CendR, R/KXXR/K) and the neuropilin-1 (NRP1) interactions, which induce tissue internalization [83]. Then, tLyP-1 was co-administered with Lf-NPs, which enhanced the accumulation and deep penetration into the glioma parenchyma. In in vitro tests, Lf-NPs showed the most increased cytotoxicity and deep penetration of 3D glioma spheroids in both brain capillary endothelial cells (BCECs) and C6 glioma cells. In vivo, Lf-NPs also exhibited the highest accumulation in the brain tumor area and deep penetration. Due to the specific expression of NRP1 in the endothelial cells of tumor vessels, the distribution of functionalized nanoparticles (Lf-NPs) was reduced in normal brain tissue. In another study, Lf and folic acid (FA) were cross-linked on poly(lactide-co-glycoride) (PLGA) NPs to carry etoposide (ETO, a chemotherapy medication used for glioblastoma) across the BBB and to treat human brain malignant glioblastoma [68]. Lf- and FA-modified PLGA NPs (Lf/FA/PLGA NPs) were infiltrated into human brain microvascular endothelial cells (HBMECs) to inhibit the proliferation of U87MG cells. The antiproliferative effects on the growth of U87MG cells were highest in the Lf/FA/PLGA NP treatment group compared with the other groups. The targeting ability of Lf/FA/PLGA NPs was proved by immunostaining of LfR on HBMECs and FA receptors on U87MG cells through endocytosis.

To create a biodegradable nanoparticle, Pang et al. co-loaded doxorubicin (DOX) and tetradrine (TET) into the Lf-modified polymersomes (PO), Lf-PO-DOX/TET. In vitro, the Lf-PO-DOX/TET NPs were absorbed into cells and exhibited the strongest cytotoxic effect in C6 glioma cells compared with other NP groups. During in vivo imaging analysis, Lf-PO labeled with near-infrared (NIR) dye was absorbed in the brain and accumulated at the tumor site. A pharmacodynamic study demonstrated that the tumor size of the Lf-PO-DOX/TET group was significantly smaller than those of other groups and the median survival time of the Lf-PO-DOX/TET group was longest compared to those of the other therapeutic groups [93]. Jiang et al. modified polymersomes using Lf to stimulate brain accumulation and to be able to administer S14G-humanin (a humanin analogue peptide drug, which has been proved to have an activity 1000-fold more powerful than humanin) to protect the brain from learning and memory damage induced by amyloid β_{25-35}. These results demonstrate that Lf can act as an active BBB target ligand that enhances drug delivery to the brain [55]. Similarly, a dual-target drug delivery system based on bovine serum albumin (BSA) NPs modified using both Lf and mPEG2000 and loaded with DOX was designed and tested for infiltration of the BBB and evaluated for glioma cell targeting properties [119]. PEGylated DOX was converted to Lf (Lf_H-NPs) based on electrostatic interactions between the cationic Lf molecules and negatively charged BSA-NPs (P_{2000}-NPs) at physiological pH. Compared to the other groups, Lf_H-NPs showed strong cytotoxicity and high uptake in both BCEC and C6 cells in vitro. In glioma model rats, the biodistribution of DOX testing showed that the Lf_H-NP group had significantly increased DOX accumulation in the brain compared with other groups, especially at 2 h post-infusion (intravenous, $P < 0.05$). Hu et al. used Lf-NPs to deliver urocortin, a peptide composed of 40 amino acids and highly expressed in the central and peripheral nervous systems, to the brain for treatment of Parkinson's disease (PD) [48]. The results showed that the urocortin-loaded Lf-NP treatment group had significantly attenuated striatum lesions induced by 6-hydroxydopamine (6-OHDA) in rats. In addition, immunohistochemistry and transmitter results demonstrated that treatment with urocortin-loaded Lf-NPs prevented the loss of transmitter contents in the brain, similar to that in normal rats, which means that the behavior of mice from the urocortin-loaded Lf-NP treatment group was significantly better than those in the control and untreated nanoparticle-infused rats.

Magnetic resonance imaging (MRI) is widely used for clinical diagnosis because it is safe to use nanoparticles for diagnostic purposes. In recent years, nano-scale contrast agents have

been developed to improve MRI diagnosis. For this, Lue et al. developed an oleylamine (OAM) coating for Fe_3O_4 magnetic NPs (OAM-MNPs), which were encapsulated in amphipathic poly(aminoethyl ethylene phosphate)/poly(L-lactide) (PAEEP-PLLA) copolymer NPs to diagnose malignant neuroma [78]. The OAM-MNP-contained PAEEP-PLLA NPs (M-PAEEP-PLLA-NPs) were further modified with Lf (Lf-M-PAEEPPLLA-NPs) for brain targeting. The Lf-M-PAEEP-PLLA-NPs showed excellent biocompatibility in cytotoxicity assays and high cell uptake in C6 cells, which indicated that Lf provided active targeting to the brain tumor site. Moreover, a significant enhancement of contrast images was obtained on MRI of Wistar rats in the glioma area in the Lf-M-PAEEPPLLA-NP treatment group. Prussian blue staining in this section also demonstrated retention of Lf-M-PAEEP-PLLA-NPs in brain tumor tissues. Zhou et al. used encapsulated hydrophobic superparamagnetic iron oxide NPs (SPIONs) in polyethylene glycol-*block*-polycaprolactone (PEG-*b*-PCL) and Cy5.5, a near-infrared fluorescent probe, to obtain optical imaging. Then, to target glioma, Lf was used with NPs as a brain MRI contrast agent [138]. The in vivo results showed that Cy5.5-SPION micelles with Lf accumulated efficiently in the C6-induced glioma region and prolonged the intensity persistence in tumor sites over 48 h in MR images compared to non-target groups. The MRI results demonstrated that the glioma margin was clearly distinguished from the fluorescence image, and the mean fluorescence intensity of the tumor was about four times higher than that of normal brain tissue. Therefore, these optical/MRI dual-functional micelles (Cy5.5-Lf-SPIO micelles) can specifically target glioma and provide guidance for surgical resection of glioma prior to and during surgery.

Polydiacetylene nanocarriers (PDNCs) exhibit higher sensitivity and color change depending on temperature and pH due to molecular perturbation [31]. Hydrophobic superparamagnetic iron oxide (SPIO) NPs were used as a nano-substrate for spontaneous assembly of 10, 12-pentacocadylic acid, a diacetylene monomer, on the surface through strong ionic and hydrogen bonds under ultraviolet (UV) irradiation. In addition, curcumin (CUR) was incorporated into the shell between SPIO and polymerized 10, 12-pentacosadiynic acid (PCDA), while self-assembled PCDA micelles were formed. PDNC-modified lactoferrin was used to improve the transport of PDNC across the BBB to track and target gliomas. As a result, improved therapeutic efficacy was obtained using Lf-CUR-PDNC, with improved retention time of the encapsulated CUR, and the number of NPs was four times higher in the brain than in the group treated with free CUR. Recent studies have also shown that lactoferrin not only is a ligand for glioma targeting but also inhibits glioblastoma cell growth. This suggests that lactoferrin may play a role in enhancing the anticancer effect in clinical uses such as temozolomide for the treatment of GBM [2].

13.4.3 Albumin

Albumin nanocarriers have been used as drug delivery systems and were successfully used to target drugs to brain tumors. The biodegradable, nonantigenic, and non-toxic characteristics of human serum albumin (HSA) make it an ideal candidate for tumor targeting [24]. The reason for this is that the secreted protein acidic and rich in cysteine (SPARC) and glycoprotein 60 (gp60), albumin-binding proteins, are highly expressed in human glioma cells. On the other hand, since normal BBB blood vessels have a very low level of albumin protein expression, the passage of natural albumin is difficult [24]. The surface of albumin NPs can be transformed into various ligands for enhanced brain targeting. For example, the surface of albumin can be cationized through the binding of ethylenediamine onto the carboxyl group of albumin, and this is an effective form for brain targeting [61]. Cell surfaces in brain endothelium are maintained with a negative charge at physiological conditions (pH). Therefore, positively charged HSA attached to negatively charged endothelial cells by electro-

static interactions, which led to absorption-mediated transcytosis [77].

Several glucose derivatives, such as mannose, galactose, and 2-deoxyglucose, can pass through the BBB via carrier-mediated delivery. For example, mannose can pass through the BBB via glucose transporter 1 (GLUT1) and GLUT3, and across the brain monolayer endothelial cells [55]. Therefore, Byeon et al. designed nanoparticles to contain naive albumin (human serum albumin, HSA), cationic HSA (c-HSA), or mannose-modified albumin (m-HSA) in doxorubicin (DOX) [12]. In vitro, c/m-HSA NPs showed the most prominent transport across the monolayer of bEnd.3 brain endothelial cells and were also absorbed into U87MG glioblastoma cells and spheroids. In vivo xenografted glioma cell-bearing mice were treated with PBS, free DOX or HSA NPs, and c/m-HSA NPs. Among them, the c/m-HSA NP-treated mice group showed significantly smaller tumor size in the brain than other groups. This improved antitumor efficacy can be explained by dual cationic absorption transformation and glucose transport by the combination of c- and m-HSA. Wang et al. used folic acid (FA), a tumor-specific ligand, to coat bovine serum albumin (BSA)-superparamagnetic iron oxide (SPIO) NPs as a contrast agent for MRI. After confirming intracellular absorption and internalization by glioma U251 cells, FA-BSA-SPIO NPs were labeled with fluorescein isothiocyanate (FITC) for intracellular visualization [127].

However, effective intratumoral penetration is another obstacle that leads to drug resistance and cancer treatment failure due to inadequate drug distribution and intracellular concentrations into the tumor hypoxic area. Lin et al. designed self-assembled NPs through hydrophobic interactions with the domains of albumin by adding hydrophobic drugs such as paclitaxel (PTX) and fenretinide (4-HPR) with a large amount of water [73]. Cleavage of the disulfide bond of albumin allowed the protein to form a linear structure, and additional disulfide bridges were formed to further stabilize the NPs. The combination of the two drugs, PTX and 4-HPR, improved the inter- and intra-molecular interactions with linear albumin, and this structure formed more stable hydrophobic cores. These NPs were further modified by low-molecular-weight protamine (LMWP), one of the cell permeability peptides (CPPs), to produce more potent nanoparticles for glioma cell penetration, because CPPs are often used as adjuvants in tumor invasion. LMWP-BSA-NPs showed 2.5-fold higher cellular uptake in U87MG cells than in unmodified BSA-NP via bEnd.3 monolayers. In addition, LMWP-BSA-NPs penetrated significantly deeper into the U87MG spheroids. Compared with the free drug, the cytotoxicity of LMWP-BSA-NP exhibited the highest antitumor activity, although a weaker inhibitory effect was observed in the PTX or 4-HPR treatment group [73]. Based on a strategy of hydrophobic drug-induced albumin self-assembly, Chen et al. also used PTX to induce aggregation of HSA into theragnostic NPs. Albumin was pre-modified using chlorin e6 (Ce6) and cyclic Arg-Gly-Asp (cRGDyK) peptides. Ce6 is a substance used as a chelating agent for Mn^{2+} to enable dual-modal magnetic resonance and fluorescence imaging, and cRGDyK peptide is a peptide capable of targeting the αvβ3-integrin upregulating endothelial cells of tumor vessels [13]. The result was that significant synergistic cancer cell death was observed using NPs under light irradiation, which means that HSA-Ce6@HSA-RGD NPs were able to target αvβ3-integrin. This signifies that HSA-Ce6@HSA-RGD NPs can be applied by combining photodynamic therapy and chemotherapy for treatment of glioma.

13.4.4 Peptide-Based Drugs for Brain Delivery

Protein ligands have several disadvantages that limit their application, including low stability, high immunogenicity, high molecular weight, and high production costs. To avoid these problems, research on peptide-based ligands, rather than proteins, has received increasing attention. There are two common strategies to generate peptide ligands: protein ligand redesign and selection from a peptide library [38]. Rousselle

et al. have shown that doxorubicin increases brain intake in rats when conjugated to a small peptide (SynB1) compared to doxorubicin alone [105]. AngioPep-2 (TFFYGGSRGKRNNFKTEEY, a cell penetrating peptide) also showed enhanced delivery of small molecules through the BBB via low-density lipoprotein receptor-related protein (LRP1) [126]. ANG1005 (also known as GRN1005) is a conjugate of three molecules of paclitaxel and one molecule of AngioPep-2 peptide and can significantly increase paclitaxel delivery in a rat brain perfusion model [120].

Phage display can select peptides capable of binding to specific receptors or cells. Using this method, the T7 peptide, HAIYPRH, was selected for specificity onto transferrin (Tf) receptors through sequential negative and positive selection [70]. T7 was decorated with peptides onto dendrimers to deliver DNA for genetic treatment of gliomas [65]. Modification with T7 significantly increased cell uptake by BCEC, and gene transfer efficiency could be reduced if Tf was exceeded, which means that the T7-modified dendrimer absorption is mediated by the Tf receptor. The T7-modified dendrimer showed 1.7-fold higher gene expression in the brain, demonstrating that T7 can act as an effective brain-targeting ligand. Rabies virus glycoprotein peptide (RVG29) is derived from a rabies virus glycoprotein capable of binding the nicotinic acetylcholine receptor (nAchR) and can enhance drug delivery to the brain [50, 75]. The apparent permeability coefficients of the RVG79-modified poly(mannitol-co-PEI) vector were 2.23 times higher than those for the vector untreated by RVG [97]. In vivo the RVG-modified vector delivered the GADPH siRNA and BACE1 siRNA to the brain more effectively than the unmodified vector.

Homeobox protein (CDX) is a peptide made from the loop II robe of candoxin and is a ligand capable of binding to nAchR. Although the binding affinity of CDX and nAchR is lower than that of candoxin, it showed significantly improved intake in BCEC cells. After being loaded with paclitaxel, CDX-modified NPs demonstrated a better antitumor effect with a prolonged median survival time of 27 days, which was longer than that for untreated NPs [135].

There are other ligands that can recruit proteins from plasmids to bind to specific receptors. Apolipoproteins (Apo), including ApoA and ApoE, are serum proteins that can be delivered to the brain via low-density lipoprotein (LDL) receptors that are highly expressed in the BBB. Thus, peptides derived from ApoA and ApoE showed the ability to mediate brain transmission of nanoparticles [56, 103, 121, 132]. Polysorbate-80, a nonionic surfactant and emulsifier often used in foods and cosmetics, was able to adsorb ApoE in serum when conjugated to NP, and there have been many studies demonstrating that polysorbate-80-coated NPs can target delivery to the brain [37, 81, 129, 130]. Martins et al. evaluated the efficiency of polysorbate-60 and 80 NPs to enhance brain targeting. The plasma area under the curve (AUC) of NPs coated with polysorbate-60 was 1.18 times higher than that of polysorbate-80-coated NPs; however, in the brain, the number of NPs coated with polysorbate-80 was 1.77 times higher than that coated with polysorbate-60 [81]. This result indicates that polysorbate-80 is a better surfactant for brain targeting. Gao et al. also found that the efficiency of brain targeting of NPs coated with polysorbate-80 was affected by the particle size [37]. Comparisons of polysorbate-80-coated NPs with particle sizes of 70, 170, 220, and 345 nm showed that 70-nm NPs delivered the cargo most effectively to the brain.

13.5 Oral Delivery of Protein-Based Drugs to Brain Tumors

It is still challenging to increase the bioavailability of therapeutic peptides and proteins that are administered orally and deliver them to the target site correctly. However, since they have many advantages, work will continue. Because of their small size and high surface area, nanoparticles used to mediate oral peptide delivery improve the bioavailability of these protein drugs (increase long-term drug exposure compared to intermittent intravenous infusion) [57]. However, biocompatibility through intraoral delivery is almost meaningless due to proteolytic degradation and

gastrointestinal (GI) barriers, as these polymers cannot penetrate the intestinal wall. For example, P-gp expressed in the luminal aspect of the plasma membranes of intestinal epithelial cells prevents P-gp substrate-based chemotherapy from adsorbing in the intestine [45]. Thus, for the past several years, various kinds of microparticles and nanoparticles have been used to modify protein and peptide drugs to overcome intestinal barriers and obtain advanced bioavailability in oral administration.

13.5.1 Current Studies on Oral Delivery of Protein Drugs in Brain Tumors

Paclitaxel is a potent chemotherapeutic agent that has been shown to have therapeutic effects on a variety of solid tumors such as breast cancer, lung cancer, and head and neck cancer [44]. Paclitaxel has also been reported to have antiangiogenic properties, and this property indicates that paclitaxel may be a good candidate for the treatment of brain tumors [8, 40, 98]. However, since paclitaxel is a P-gp substrate [80, 117, 125], it is difficult for orally administered paclitaxel to reach the tumor cells from the parenchyma [45, 62]. Therefore, as inhibition of P-pg activity is essential, Paek et al. studied the combination of P-gp inhibitor HM30181A and paclitaxel to produce oral paclitaxel chemotherapy for brain tumors [90, 91]. They have investigated the therapeutic effects of this combination method in two animal models, a melanoma brain metastasis (MBM) mouse model and an early glioblastoma mouse model. Oral co-administration of HM30181A and paclitaxel showed significant therapeutic effects in both brain tumor models.

13.6 Conclusion and Future Perspectives

This chapter highlights important advances in brain delivery of protein drugs that have been studied in recent years. There are still several limitations on cerebral delivery through administration of peptides and protein drugs. Drug delivery to GBM is difficult because the BBB provides physical and biochemical barriers that limit the penetration of most drugs. However, some strategies show significant potential for improvement in brain intake. Therefore, this approach is still under development, but it will play an increasingly important role in the treatment of central nervous system disorders.

Acknowledgements This study was supported by the Bio & Medical Technology Development Program (NRF-2015M3A9E2030125) and was partially supported by the Creative Materials Discovery Program (NRF-2017M3D1A1039289) through the National Research Foundation (NRF) funded by the Korean government (MSIP & MOHW). Also, this study was partially supported by a grant of the Korea Health Technology R&D project through the Korea Health Industry Development Institute (KHIDI), funded by the Ministry of Health & Welfare, Republic of Korea (grant number: HI18C0453).

References

1. Alfred H, Schinkel, Wagenaar Els, Deemter Liesbeth van, Mol Carla A. A. M, Borst Piet (1995) Absence of the mdr1a P-Glycoprotein in Mice affects tissue distribution and pharmacokinetics of Dexamethasone, Digoxin, and Cyclosporin A. J Clin Investig 96:1698–1699
2. Arcella A, Oliva MA, Staffieri S et al (2015) In vitro and in vivo effect of human lactoferrin on glioblastoma growth. J Neurosurg 123(40):1026–1035
3. Ballabh P, Alex B, Maiken N (2004) The blood–brain barrier: an overview: structure, regulation, and clinical implications. Neurobiol Dis 16(1):1–13
4. Banks WA (2016) From blood–brain barrier to blood–brain interface: new opportunities for CNS drug delivery. Nat Rev Drug Discov 15(4):275
5. Barrett GC, Donald TE (1998) Amino acids and peptides. Cambridge University Press, Cambridge
6. Becker I (1991) The multidrug-resistance gene MDR1 is expressed in human glial tumors. Acta Neuropathol 82(6):516–519
7. Béduneau A, Saulnier P, Benoit JP (2007) Active targeting of brain tumors using nanocarriers. Biomaterials 28(33):4947–4967
8. Belotti D, Vergani V, Drudis T et al (1996) The microtubule-affecting drug paclitaxel has antiangiogenic activity. Clin Cancer Res 2(11):1843–1849
9. Brandes AA, Rigon A, Zampieri P et al (1996) Early chemotherapy and concurrent radio-chemotherapy in high grade glioma. J Neuro-Oncol 30(3):247–255
10. Bronger H, König J, Kopplow K et al (2005) ABCC drug efflux pumps and organic anion uptake trans-

porters in human gliomas and the blood-tumor barrier. Cancer Res 65(24):11419–11428
11. Brooks PC, Richard AC, David AC (1994) Requirement of vascular integrin alpha v beta 3 for angiogenesis. Science 264(5158):569–571
12. Byeon HJ, Lee S, Min SY et al (2016) Doxorubicin-loaded nanoparticles consisted of cationic-and mannose-modified-albumins for dual-targeting in brain tumors. J Control Release 225:301–313
13. Chen Q, Wang X, Wang C et al (2015) Drug-induced self-assembly of modified albumins as nano-theranostics for tumor-targeted combination therapy. ACS Nano 9(5):5223–5233
14. Chu C, Abbara C, Noël-Hudson MS et al (2009) Disposition of everolimus in mdr1a−/1b− mice and after a pre-treatment of lapatinib in Swiss mice. Biochem Pharmacol 77(10):1629–1634
15. Dafang, Wu, Yang Jing, Pardridge William M. (1997) Drug Targeting of a Peptide Radiopharmaceutical through the Primate Blood-Brain Barrier In Vivo with a Monoclonal Antibody to the Human Insulin Receptor. J Clin Investiga 100:1804–1805
16. David, Mathieu, and Fortin David (2007) Chemotherapy and delivery in the treatment of primary brain tumors. Curr Clin Pharmacol 2: 197–198
17. DeAngelis LM (2001) Brain tumors. N Engl J Med 344:114–123
18. Demeule M, Régina A, Jodoin J et al (2002) Drug transport to the brain: key roles for the efflux pump P-glycoprotein in the blood–brain barrier. Vasc Pharmacol 38(6):339–348
19. Dieu LH, Wu D, Paliva CG et al (2014) Polymersomes conjugated to 83-14 monoclonal antibodies: in vitro targeting of brain capillary endothelial cells. Eur J Pharm Biopharm 88(2):316–324
20. Dong XW (2018) Current strategies for brain drug delivery. Theranostics 8:1481–1493
21. Dong H, Jin M, Liu Z et al (2016) In vitro and in vivo brain-targeting chemo-photothermal therapy using graphene oxide conjugated with transferrin for gliomas. Lasers Med Sci 31(6):1123–1131
22. Dorothy T. Krieger, author (1983) Brain peptides: what, where, and why?. Science 222:975–985
23. Dube B, Pandey A, Joshi G et al (2017) Hydrophobically modified polyethylenimine-based ternary complexes for targeting brain tumor: stability, in vitro and in vivo studies. Artif Cells Nanomed Biotechnol 45(8):1685–1698
24. Elzoghby AO, Samy WM, Elgindy NA (2012) Albumin-based nanoparticles as potential controlled release drug delivery systems. J Control Release 157(2):168–182
25. Elzoghby AO, Helmy MW, Samy WM (2013a) Micellar delivery of flutamide via milk protein nanovehicles enhances its anti-tumor efficacy in androgen-dependent prostate cancer rat model. Pharm Res 30(10):2654–2663
26. Elzoghby AO, Saad NI, Helmy MW et al (2013b) Ionically-crosslinked milk protein nanoparticles as flutamide carriers for effective anticancer activity in prostate cancer-bearing rats. Eur J Pharm Biopharm 85(3):444–451
27. Elzoghby AO, Samy WM, Elgindy NA (2015) Swellable floating tablet based on spray-dried casein nanoparticles: near-infrared spectral characterization and floating matrix evaluation. Int J Pharm 491(1–2):113–122
28. Elzoghby AO, Abd-Elwakil MM, Abd-Elsalam K et al (2016a) Natural polymeric nanoparticles for brain-targeting: implications on drug and gene delivery. Curr Pharm Des 22(22):3305–3323
29. Elzoghby AO, Hemasa AL, Freag MS (2016b) Hybrid protein-inorganic nanoparticles: from tumor-targeted drug delivery to cancer imaging. J Control Release 243:303–322
30. Faith G, Davis, and McCarthy Bridget J. (2001) Current epidemiological trends and surveillance issues in brain tumors', Expert Review of Anticancer Therapy 1:395–396
31. Fang JH, Chiu TL, Huang WC et al (2016) Dual-targeting lactoferrin-conjugated polymerized magnetic polydiacetylene-assembled nanocarriers with self-responsive fluorescence/magnetic resonance imaging for in vivo brain tumor therapy. Adv Healthc Mater 5(6):688–695
32. Fattori S, Becherini F, Cianfriglia M et al (2007) Human brain tumors: multidrug-resistance p-glycoprotein expression in tumor cells and intratumoral capillary endothelial cells. Virchows Arch 451(1):81–87
33. Fondell A, Edwards K, Ickenstein LM et al (2010) Nuclisome: a novel concept for radionuclide therapy using targeting liposomes. Eur J Nucl Med Mol Imaging 37(1):114–123
34. Friedman HS, Kerby T, Calvert H (2000) Temozolomide and treatment of malignant glioma. Clin Cancer Res 6(7):2585–2597
35. Gallo JM, Li S, Guo P et al (2003) The effect of p-glycoprotein on paclitaxel brain and brain tumor distribution in mice. Cancer Res 63(16):5114–5117
36. Gao H (2016) Progress and perspectives on targeting nanoparticles for brain drug delivery. Acta Pharm Sin B 6(4):268–286
37. Gao K, Jiang X (2006) Influence of particle size on transport of methotrexate across blood brain barrier by polysorbate 80-coated polybutylcyanoacrylate nanoparticles. Int J Pharm 310(1–2):213–219
38. Gao H, Pang Z, Jiang X (2013) Targeted delivery of nano-therapeutics for major disorders of the central nervous system. Pharm Res 30(10):2485–2498
39. Goyal D, Shuaid S, Mann S et al (2017) Rationally designed peptides and peptidomimetics as inhibitors of amyloid-β (Aβ) aggregation: potential therapeutics of Alzheimer's disease. ACS Comb Sci 19(2):55–80
40. Grant DS, Williams TL, Zahaczewsky M et al (2003) Comparison of antiangiogenic activities using paclitaxel (taxol) and docetaxel (taxotere). Int J Cancer 104(1):121–129

41. Groothuis DR (2000) The blood-brain and blood-tumor barriers: a review of strategies for increasing drug delivery. Neuro-Oncology 2(1):45–59
42. Guerra M, Blázquez JL, Rodríguez EM (2017) Blood–brain barrier and foetal-onset hydrocephalus, with a view on potential novel treatments beyond managing CSF flow. Fluids Barriers CNS 14(1):19
43. Guo L, Ren J, Jiang X (2012) Perspectives on brain-targeting drug delivery systems. Curr Pharm Biotechnol 13(12):2310–2318
44. Hajek R, Vorlicek J, Slavik M (1996) Paclitaxel (Taxol): a review of its antitumor activity in clinical studies Minireview. Neoplasma 43(3):141–154
45. Helgason HH, Kruijtzer CM, Huitema AD et al (2006) Phase II and pharmacological study of oral paclitaxel (Paxoral) plus ciclosporin in anthracycline-pretreated metastatic breast cancer. Br J Cancer 95(7):794–800
46. Hiroko, Ohgaki, and Kleihues Paul (2005) Epidemiology and etiology of gliomas. Acta Neuropathologica 109: 93–94
47. Hobbs SK, Monsky WL, Rk J et al (1998) Regulation of transport pathways in tumor vessels: role of tumor type and microenvironment. Proc Nati Acad Sci 95(8):4607–4612
48. Hu K, Shi Y, Jiang W et al (2011) Lactoferrin conjugated PEG-PLGA nanoparticles for brain delivery: preparation, characterization and efficacy in Parkinson's disease. Int J Pharm 4150(1–2):273–283
49. Huang S, Shao K, Kuang Y et al (2013) Tumor-targeting and microenvironment-responsive smart nanoparticles for combination therapy of antiangiogenesis and apoptosis. ACS Nano 7(3):2860–2871
50. Huo H, Gao Y, Wang Y et al (2015) Polyion complex micelles composed of pegylated polyasparthydrazide derivatives for siRNA delivery to the brain. J Colloid Interface Sci 447:8–15
51. Huynh E, Zheng G (2015) Cancer nanomedicine: addressing the dark side of the enhanced permeability and retention effect. Nanomedicine 10(13):1993–1995
52. Huynh GH, Deen DF, Szoka FC Jr (2006) Barriers to carrier mediated drug and gene delivery to brain tumors. J Control Release 110(2):236–259
53. Iinuma H, Maruyama K, Okinaga K et al (2002) Intracellular targeting therapy of cisplatin-encapsulated transferrin-polyethylene glycol liposome on peritoneal dissemination of gastric cancer. Int J Cancer 99(1):130–137
54. Jain RK (1987) Transport of molecules in the tumor interstitium: a review. Cancer Res 47(12):3039–3051
55. Jiang L, Jiang S, Zhang M et al (2014) Albumin versus other fluids for fluid resuscitation in patients with sepsis: a meta-analysis. PLoS One 9(12):1–21
56. Jose S, Sowmya S, Cinu TA et al (2014) Surface modified PLGA nanoparticles for brain targeting of bacoside-a. Eur J Pharm Sci 63:29–35
57. Joseph A (2007) Overview of the changing paradigm in cancer treatment: Oral chemotherapy. American J Health-System Pharm 64: S4-NaN
58. Juillerat Jeanneret L (2008) The targeted delivery of cancer drugs across the blood–brain barrier: chemical modifications of drugs or drug-nanoparticles? Drug Discov Today 13(23–24):1099–1106
59. Karami Z, Saghatchi Zanjani MR, Rezaee S et al (2019) Neuropharmacokinetic evaluation of lactoferrin-treated indinavir-loaded nanoemulsions: remarkable brain delivery enhancement. Drug Dev Ind Pharm 45(5):736–744
60. Karim R, Palazzo C, Evrard B et al (2016) Nanocarriers for the treatment of glioblastoma multiforme: current state-of-the-art. J Control Release 227:23–37
61. Karimi M, Bahrami S, Ravari SB et al (2016) Albumin nanostructures as advanced drug delivery systems. Expert Opin Drug Deliv 13(11):1609–1623
62. Kemper EM, van Zandbergen AE, Cleypool C et al (2003) Increased penetration of paclitaxel into the brain by inhibition of P-Glycoprotein. Clin Cancer Res 9(7):2849–2855
63. Kim S, Bell K, Mousa SA et al (2000) Regulation of angiogenesis in vivo by ligation of integrin α5β1 with the central cell-binding domain of fibronectin. Am J Pathol 156(4):1345–1362
64. Komarova YA, Kruse K, Mehta D et al (2017) Protein interactions at endothelial junctions and signaling mechanisms regulating endothelial permeability. Circ Res 120(1):179–206
65. Kuang Y, An S, Guo Y et al (2013) T7 peptide-functionalized nanoparticles utilizing RNA interference for glioma dual targeting. Int J Pharm 454(1):11–20
66. Kumar CC, Armstrong L, Yin Z et al (2000) Targeting integrins α v β 3 and α v β 5 for bloking tumor-induced angiogenesis. Adv Exp Med Biol 476:169–180
67. Kunal S, Taskar, Rudraraju Vinay, Mittapalli Rajendar K, Samala Ramakrishna, Thorsheim Helen R, Lockman Julie, Gril Brunilde, Hua Emily, Palmieri Diane, Polli Joseph W, Castellino Stephen, Rubin Stephen D, Lockman Paul R, Steeg Patricia S, and Smith Quentin R. (2012) Lapatinib Distribution in HER2 Overexpressing Experimental Brain Metastases of Breast Cancer. Pharmaceutical Res 29: 770–771
68. Kuo YC, Chen YC (2015) Targeting delivery of etoposide to inhibit the growth of human glioblastoma multiforme using lactoferrin-and folic acid-grafted poly (lactide-co-glycolide) nanoparticles. Int J Pharma 479(1):138–149
69. Lécuyer MA, Saint Laurent O, Larouche S et al (2017) Dual role of ALCAM in neuroinflammation and blood–brain barrier homeostasis. Proc Nati Acad Sci U S A 114(4):E524–E533
70. Lee JH, Engler JA, Collawn JF et al (2001) Receptor mediated uptake of peptides that bind the human transferrin receptor. Eur J Biochem 268(7):2004–2012
71. Li Y, He H, Jia X et al (2012) A dual-targeting nanocarrier based on poly (amidoamine) dendrimers con-

jugated with transferrin and tamoxifen for treating brain gliomas. Biomaterials 33(15):3899–3908
72. Li S, Amat D, Peng Z et al (2016) Transferrin conjugated nontoxic carbon dots for doxorubicin delivery to target pediatric brain tumor cells. Nanoscale 8(37):16662–16669
73. Lin T, Zhao P, Jiang Y et al (2016) Blood–brain-barrier-penetrating albumin nanoparticles for biomimetic drug delivery via albumin-binding protein pathways for antiglioma therapy. ACS Nano 10(11):9999–10012
74. Liu Y, Lu W (2012) Recent advances in brain tumor-targeted nano-drug delivery systems. Expert Opin Drug Deliv 9(6):671–686
75. Liu Y, An S, Li J et al (2016) Brain-targeted co-delivery of therapeutic gene and peptide by multifunctional nanoparticles in Alzheimer's disease mice. Biomaterials 80:33–45
76. Liu C, Liu XN, Wang GL et al (2017) A dual-mediated liposomal drug delivery system targeting the brain: rational construction, integrity evaluation across the blood–brain barrier, and the transporting mechanism to glioma cells. Int J Nanomedicine 12:2407
77. Lu W, Zhaog Y, Tan YZ et al (2005) Cationic albumin-conjugated pegylated nanoparticles as novel drug carrier for brain delivery. J Control Release 107(3):428–448
78. Luo B, Wang S, Rao R et al (2016) Conjugation magnetic PAEEP-PLLA nanoparticles with lactoferrin as a specific targeting MRI contrast agent for detection of brain glioma in rats. Nanoscale Res Lett 11(1):227
79. Mäger I, Meyer AH, Li J et al (2017) Targeting blood-brain-barrier transcytosis–perspectives for drug delivery. Neuropharmacology 120:4–7
80. Martin C, Berridge G, Higgins CF et al (2000) Communication between multiple drug binding sites on P-glycoprotein. Mol Pharm 58(3):624–632
81. Martins SM, Sarmento B, Nunes C et al (2013) Brain targeting effect of camptothecin-loaded solid lipid nanoparticles in rat after intravenous administration. Eur J Pharma Biopharm 85(3):488–502
82. Masanao, Mohri, Nitta Hisashi, and Yamashita Junkoh (2000) Expression of multidrug resistance-associated protein (MRP) in human gliomas. J Neuro-Oncol 49:105–106
83. Miao D, Jiang M, Liu Z et al (2013) Co-administration of dual-targeting nanoparticles with penetration enhancement peptide for antiglioblastoma therapy. Mol Pharm 11(1):90–101
84. Monsky WL, Mouta Carreira C, Tsuzuki Y et al (2002) Role of host microenvironment in angiogenesis and microvascular functions in human breast cancer xenografts: mammary fat pad versus cranial tumors. Clin Cancer Res 8(4):1008–1013
85. Newton HB (1994) Primary brain tumors: review of etiology, diagnosis and treatment. Am Fam Physician 49(4):787–797
86. Ningaraj NS, Rao M, Hashizume K et al (2002) Regulation of blood-brain tumor barrier permeability by calcium-activated potassium channels. J Pharm Exp Ther 301(3):838–851
87. Oberoi RK, Parrish KE, Sio TT et al (2015) Strategies to improve delivery of anticancer drugs across the blood–brain barrier to treat glioblastoma. Neuro-oncol 18(1):27–36
88. Ohgaki H, Kleihues P (2007) Genetic pathways to primary and secondary glioblastoma. Am J Pathol 170(5):1445–1453
89. Omuro AMP, Faivre S, Raymond E (2007) Lessons learned in the development of targeted therapy for malignant gliomas. Mol Cancer Ther 6(7):1909–1919
90. Paek IB, Ji HY, Kim MS et al (2006a) Metabolism of a new p-glycoprotein inhibitor HM-30181 in rats using liquid chromatography/electrospray mass spectrometry. Rapid Commun Mass Spectrom 20(9):1457–1462
91. Paek IB, Ji HY, Kim MS et al (2006b) Simultaneous determination of paclitaxel and a new p-glycoprotein inhibitor HM-30181 in rat plasma by liquid chromatography with tandem mass spectrometry. J Sep Sci 29(5):628–634
92. Pang Z, Lu K, Gao H et al (2008) Preparation and brain delivery property of biodegradable polymersomes conjugated with OX26. J Control Release 128(2):120–127
93. Pang Z, Feng L, Hua R et al (2010) Lactoferrin-conjugated biodegradable polymersome holding doxorubicin and tetrandrine for chemotherapy of glioma rats. Mol Pharm 7(6):1995–2005
94. Pang Z, Gao H, Guo L et al (2011a) Enhanced intracellular delivery and chemotherapy for glioma rats by transferrin-conjugated biodegradable polymersomes loaded with doxorubicin. Bioconjug Chem 22(6):1171–1180
95. Pang Z, Gao H, Yu Y et al (2011b) Brain delivery and cellular internalization mechanisms for transferrin conjugated biodegradable polymersomes. Int J Pharm 415(1–2):284–292
96. Pardridge WM (1991) Peptide drug delivery to the brain. Raven Press, New York
97. Park TE, Singh B, Li H et al (2015) Enhanced BBB permeability of osmotically active poly (mannitol-co-PEI) modified with rabies virus glycoprotein via selective stimulation of caveolar endocytosis for RNAi therapeutics in Alzheimer's disease. Biomaterials 38:61–71
98. Pasquier E, Pourroy B, Camoin L et al (2004) Antiangiogenic activity of paclitaxel is associated with its cytostatic effect, mediated by the initiation but not completion of a mitochondrial apoptotic signaling pathway. Mol Cancer Ther 3(10):1301–1310
99. Pehlivan SB (2013) Nanotechnology-based drug delivery systems for targeting, imaging and diagnosis of neurodegenerative diseases. Pharm Res 30(10):2499–2511

100. Polli JW, Olson KL, Chism JP et al (2009) An unexpected synergist role of p-glycoprotein and breast cancer resistance protein on the central nervous system penetration of the tyrosine kinase inhibitor lapatinib (N-{3-chloro-4-[(3-fluorobenzyl) oxy] phenyl}-6-[5-({[2-(methylsulfonyl) ethyl] amino} methyl)-2-furyl]-4-quinazolinamine; GW572016). Drug Metab Dispos 37(2):439–442
101. Provenzale JM, Mukundan S, Dewhirst M (2005) The role of blood-brain barrier permeability in brain tumor imaging and therapeutics. AJR Am J Roentgenol 185(3):763–767
102. Qian ZM, Li H, Sun H et al (2002) Targeted drug delivery via the transferrin receptor-mediated endocytosis pathway. Pharmacol Rev 54(4):561–587
103. Re F, Cambianica I, Zona C et al (2011) Functionalization of liposomes with ApoE-derived peptides at different density affects cellular uptake and drug transport across a blood-brain barrier model. Nanomedicine 7(5):551–559
104. Roberts WG, Delaat J, Nagane M et al (1998) Host microvasculature influence on tumor vascular morphology and endothelial gene expression. Am J Pathol 153(4):1239–1248
105. Rousselle C, Clair P, Temsamani J et al (2000) New advances in the transport of doxorubicin through the blood-brain barrier by a peptide vector-mediated strategy. Mol Pharmacol 57(4):679–686
106. Salphati L, Lee LB, Pang J et al (2010) Role of p-glycoprotein and breast cancer resistance protein-1 in the brain penetration and brain pharmacodynamic activity of the novel phosphatidylinositol 3-kinase inhibitor GDC-0941. Drug Metab Dispos 38(9):1422–1426
107. Salphati L, Pang J, Plise EG et al (2012) Preclinical assessment of the absorption and disposition of the phosphatidylinositol 3-kinase/mammalian target of rapamycin inhibitor GDC-0980 and prediction of its pharmacokinetics and efficacy in human. Drug Metab Dispos 40(9):1785–1796
108. Salzano G, Zappavigna S, Luce A et al (2016) Transferrin-targeted nanoparticles containing zoledronic acid as a potential tool to inhibit glioblastoma growth. J Biomed Nanotechnol 12(4):811–830
109. Sarin H, Wu H, Hall MD et al (2008) Effective transvascular delivery of nanoparticles across the blood-brain tumor barrier into malignant glioma cells. J Ttransl Med 6(1):80
110. Sarin H, Wu H, Vo HQ et al (2009) Physiologic upper limit of pore size in the blood-tumor barrier of malignant solid tumors. J Transl Med 7(1):51
111. Schinkel AH, Smit JJ, te Riele HP et al (1994) Disruption of the mouse mdr1a P-glycoprotein gene leads to a deficiency in the blood-brain barrier and to increased sensitivity to drugs. Cell 77(4):491–502
112. Schlageter KE, Molnar P, Lapin GD et al (1999) Microvessel organization and structure in experimental brain tumors: microvessel populations with distinctive structural and functional properties. Microvasc Res 58(3):312–328
113. Shai RM, Reichatdt JK, Chen TC (2008) Pharmacogenomics of brain cancer and personalized medicine in malignant gliomas. Future Oncol 4:525–534
114. Sobin LH (1981) The international histological classification of tumours. Bull World Health Organ 59(6):813–819
115. Song XL, Xiao Y, Cheng L et al (2017) Application of multifunctional targeting epirubicin liposomes in the treatment of non-small-cell lung cancer. Int J Nanomedicine 12:7433–7451
116. Spano JP, Fagard R, Soria JC et al (2005) Epidermal growth factor receptor signaling in colorectal cancer: preclinical data and therapeutic perspectives. Ann Oncol 16(2):189–194
117. Sparreboom A, Van Asperen J, Mayer U et al (1997) Limited oral bioavailability and active epithelial excretion of paclitaxel (Taxol) caused by P-glycoprotein in the intestine. PNAS 94(5):2031–2035
118. Stephan, Fellner, Bauer Björn, Miller David S, Schaffrik Martina, Fankhänel Martina, Spru Thilo, Bernhardt Günther, Graeff Claudia, Färber Lothar, Gschaidmeier Harald, Buschauer Armin, and Fricker Gert. 2002. 'Transport of paclitaxel (Taxol) across the blood-brain barrier in vitro and in vivo. J Clin Investig 110: 1309–1310
119. Su Z, Xing L, Chen Y et al (2014) Lactoferrin-modified poly (ethylene glycol)-grafted BSA nanoparticles as a dual-targeting carrier for treating brain gliomas. Mol Pharm 11(6):1823–1834
120. Takasato Y, Rapoport SI, Smith QR (1984) An in situ brain perfusion technique to study cerebrovascular transport in the rat. Am J Phys 247(3):H484–H493
121. Tamaru M, Akita H, Harashima H et al (2014) Application of apolipoprotein E-modified liposomal nanoparticles as a carrier for delivering DNA and nucleic acid in the brain. Int J Nanomedicine 9:4267–4276
122. Tong H, Wang Y, Lu X et al (2015) On the preparation of transferrin modified artesunate nanoliposomes and their glioma-targeting treatment in-vitro and in-vivo. Int J Clin Exp Med 8(12):22045–22052
123. Tsutsui Y, Tomizawa K, Nagita M et al (2007) Development of bionanocapsules targeting brain tumors. J Control Release 122(2):159–164
124. Van Asperen J, Schinkel AH, van Tellingen O et al (1996) Altered pharmacokinetics of vinblastine in Mdr1a P-glycoprotein-deficient mice. J Nati Cancer Inst 88(14):994–999
125. Van Asperen J, Borst P, Beijnen JH et al (1997) Enhanced oral bioavailability of paclitaxel in mice treated with the P-glycoprotein blocker SDZ PSC 833. Br J Cancer 76(9):1181–1183
126. Vlieghe P, Khrestxgatisky M (2012) Medicinal chemistry based approaches and nanotechnology-based systems to improve CNS drug targeting and delivery. Med Res Rev 33(3):457–516
127. Wang X, Tu M, Tian B et al (2016) Synthesis of tumor-targeted folate conjugated fluorescent mag-

netic albumin nanoparticles for enhanced intracellular dual-modal imaging into human brain tumor cells. Anal Biochem 512:8–17
128. Wei X, Chen X, Ying M et al (2014) Brain tumor-targeted drug delivery strategies. Acta Pharm Sin B 4(3):193–201
129. Wilson B, Lavanya Y, Jenita JL et al (2014) Albumin nanoparticles for the delivery of gabapentin: preparation, characterization and pharmacodynamic studies. Int J Pharm 473(1–2):73–79
130. Xin-Hua, Tian, Lin Xiao-Ning, Wei Feng et al (2011) Enhanced brain targeting of temozolomide in polysorbate-80 coated polybutylcyanoacrylate nanoparticles. Int J Nanomed 2011:445–452
131. Yano S, Kondo K, Wadsworth P et al (2003) Distribution and function of EGFR in human tissue and the effect of EGFR tyrosine kinase inhibition. Anticancer Res 23(5A):3639–3650
132. Zensi A, Begley D, Kreuter J et al (2010) Human serum albumin nanoparticles modified with apolipoprotein AI cross the blood-brain barrier and enter the rodent brain. J Drug Target 18(10):842–848
133. Zhan C, Lu W (2012) The blood-brain/tumor barriers: challenges and chances for malignant gliomas targeted drug delivery. Curr Pharma Biotechnol 13(12):2380–2387
134. Zhan C, Gu B, Lu W et al (2010) Cyclic RGD conjugated poly (ethylene glycol)-co-poly (lactic acid) micelle enhances paclitaxel anti-glioblastoma effect. J Control Release 143(1):136–142
135. Zhan C, Li B, Lu W et al (2011) Micelle-based brain-targeted drug delivery enabled by a nicotine acetylcholine receptor ligand. Angew Chem Int Ed Engl 50(24):5482–5485
136. Zhan C, Meng Q, Lu W et al (2012) Cyclic RGD–polyethylene glycol–Polyethylenimine for intracranial glioblastoma-targeted gene delivery. Chem Asian J 7(1):91–96
137. Zhang TT, Li W, Liao W et al (2016) Strategies for transporting nanoparticles across the blood–brain barrier. Biomater Sci 4(2):219–229
138. Zhou Q, Mu K, Yang X et al (2015) Glioma-targeting micelles for optical/magnetic resonance dual-mode imaging. Int J Nanomedicine 10:1805–1818

14 Human Hair: Scaffold Materials for Regenerative Medicine

I-Chun Chen and Jiashing Yu

Abstract

This chapter reviews the studies of keratin-based biomaterials in the past and discusses the advancement of it in recent years. Keratin, as a protein-based biopolymer, possesses excellent biocompatibility and biodegradability. In addition, keratin has abundant disulfide bonds, which result in its unique and tough structure. However, the property also results in dissolubility, which causes difficult process ability. Over the past years, much research utilizes different methodologies to extract keratins. Different kinds of extraction methods affect the characteristics of keratins and give a wide variety of application forms. The features of different methods are discussed and summarized in the following.

Keywords

Keratin · Biomaterial · Tissue engineering · Extraction · Scaffold · Electrospun · Hydrogel

I.-C. Chen · J. Yu (✉)
Department of Chemical Engineering, National Taiwan University, Taipei City, Taiwan
e-mail: jiayu@ntu.edu.tw

14.1 Protein Structure and Characteristics

Keratins are a family of structural proteins characterized by high sulfur content. The most notable feature of keratin different from other natural proteins is the large number of cysteine groups in constitution, resulting in extensive disulfide-bonding formation [1, 2]. Generally, keratin can be sorted into two categories depending on their hardness. Keratins with low disulfide bond density are commonly consisted in epithelial tissues present a more flexible structure, which is called "cytokeratins," while the high disulfide bond density keratins, usually existed in wool, hair, and hooves, construct the tough protective tissues [3, 4].

Because of the cysteine-rich nature, keratins play an important role in supporting construct. Under the sight of a fluorescent microscope, the fiber-like structures spread all over cells. These intermediate filaments, or, namely, cytokeratins, endow cells' stiffness and help in the migration behavior of cells [5–7]; in wools and human hair, different kinds of keratin build up these complicated structures [8, 9]. There are three major groups of keratins in these fibers. Alpha-keratins are the main components of the fiber cortex. They are low in sulfur content and build up the distinct helix structure. Beta-keratins form the outer protective tissue. Gamma-keratins are high in sulfur

H. J. Chun et al. (eds.), *Bioinspired Biomaterials*, Advances in Experimental Medicine and Biology 1249, https://doi.org/10.1007/978-981-15-3258-0_14

content and behave as a disulfide cross-linker bundling the cortical structures together [10].

In addition to the distinctive mechanical properties, the intrinsic bioactivity-related factors make keratin a suitable candidate for biomaterials. These factors can interact with adhesion receptors such as integrins on the cell membranes to regulate cell cycle and organization of the intracellular cytoskeleton. Hence, they promote cell adhesion. The ample cell-binding motifs in keratins such as arginine-glycine-aspartate (RGD), leucine-aspartic acid-valine (LDV), and glutamic acid-aspartic acid-serine (EDS) provide friendly microenvironment for cell adhesion and proliferation [11–13]. According to previous studies, RGD and LDV sequences are also abundant in other proteins such as fibronectin [14]. Keratin-based biomaterials, therefore, could be fabricated into wide-variability applications mimicking the extracellular matrix in native tissues.

14.2 Extraction and Purification Methodologies

14.2.1 Removal of Lipid

The pre-procedure of keratin extraction is the cleaning of dust and removal of lipid on the surface of tissues, especially for wools and hair. First, the tissues are washed several times to remove dust and then are cut down into small pieces or be pulverized to powder form for enhanced performance of keratin extraction. Then, the tissues are immersed in organic solvents to dissolve the grease. For example, Sinkiewicz et al. utilized a Soxhlet apparatus with petroleum ether to remove the lipid of the feather [15]. Yamauchi's group immersed wool in chloroform/methanol (2:1, v/v) for 12 h [16]. Kakkar used Soxhlet's apparatus with hexane and dichloromethane (1:1, v/v) to treat hoof [17]. After draining the organic solvent, the materials are drying and are then prepared as defatting materials for the next step.

14.2.2 Extraction

There are many kinds of extraction methods with different mechanisms as shown in Table 14.1. Generally, extraction methodologies could be classified into two groups: "reductive extraction" and "oxidative extraction." Proteins acquired by reductive methods are named "keratin," while those extracted by oxidative methods are called "keratose" or "oxidative keratin" [3].

14.2.2.1 Reductive Extraction (Urea/2-Mercaptoethanol)

Yamauchi's group developed the reductive method using urea, 2-mercaptoethanol, and sodium dodecyl sulfate (SDS) to extract keratin [16]. The function of urea is the interrupter of hydrogen bonding; it could enhance the dispersion of keratin in solution. 2-Mercaptoethanol is used to break disulfide bonds in keratin. Disulfide bonds would be reduced to thiol groups. However, thiol groups are very active. The disulfide bonds would reform when the extract is dialyzed against DI water. One method to prevent the aggregation of keratin is the addition of SDS, which is usually used in electrophoresis. The SDS would surround the surface of keratin, making them unfolded to prevent aggregation. Nakamura et al. used a similar extraction solution with the addition of thiourea to treat human hair. Their results showed that the protein yield could be effectively increased [18]. Yung-Hao Lin et al. utilized similar chemicals to extract keratin. The SDS-PAGE result is shown in Fig. 14.1 [19]. In Fig. 14.1., the left lane represents the molecular weights of protein standard, and the right lane shows the molecular weight of extracted keratins. The band from 40 to 60 kDa refers to the a-keratins, and the band from 5 to 16 kDa indicates the matrix proteins, while the band larger than 100 kDa represents some coarse and aggregate components.

14.2.2.2 Reductive Extraction (Na_2S)

Kamarudin et al. treated ground chicken feathers with an aqueous solution containing Na_2S (0.5 M) and placed it under 60 °C for 2 h. The acquired solution was further filtered and centrifuged at

Table 14.1 Extraction methods of keratin

Method	Advantages	Disadvantages	References
Urea/2-Mercaptoethanol	Well studied	Environment-toxic, stinky smell	[16, 18, 19]
Na_2S	High yield of keratin, inexpensive	Low purity of product	[20]
L-cysteine	Environment-friendly, low toxicity	Lower content in alpha-keratin yield	[21]
Peracetic acid	Easy handling, inexpensive	Temperature-induced aggregation	[22, 23]

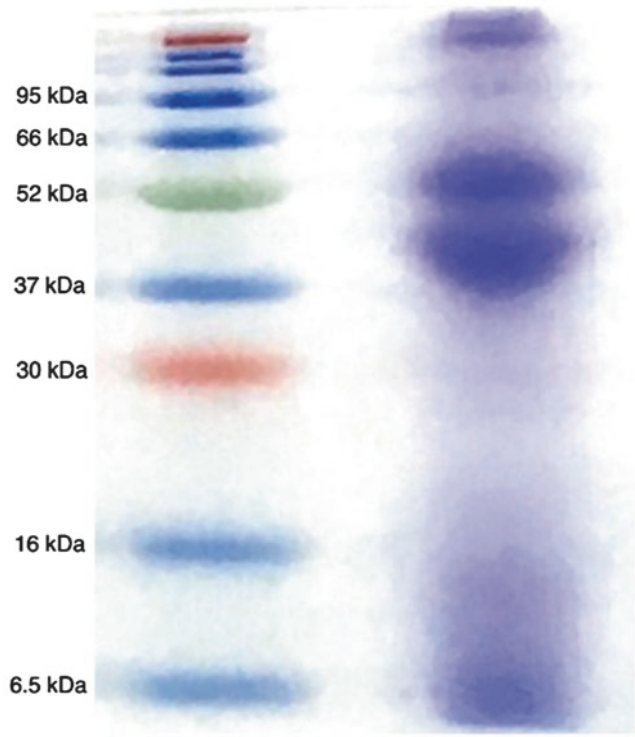

Fig. 14.1 SDS-PAGE shows the characteristic band of a-keratin

10,000 rpm for 5 min. The supernatant was treated with 5 ml HCl (2 M) being added dropwise. The solution was centrifuged at 10,000 rpm, and the sediment was washed with ddH_2O for 3 times. The precipitate was added with 30 ml NaOH (2 M) and then centrifuged again at 10,000 rpm for 5 min. The acquired supernatant was used for further experiments [20]. This study aimed to develop a more efficient way to extract keratins. The result showed that sodium sulfide increases the yield (53%) compared to other reductive reagents such as potassium cyanide and thioglycolic acid (< 30%).

14.2.2.3 Reductive Extraction (L-Cysteine)

K. Wang et al. used L-Cysteine as a reducing agent substituted for 2-mercaptoethanol [21]. Wool fibers were immersed in an aqueous solution containing urea (8 M) and L-cysteine (0.165 M); then pH value was adjusted to 10.5 with NaOH (5 M). The extraction solution was treated by shaking at 75 °C for 5 h. Their study indicates that keratins treated by this method contain more of β-sheet structure and less of α-helix structure. The research team also claims that this method provides a simple, eco-friendly, and economical extraction way compared to other extraction methods.

14.2.2.4 Oxidative Extraction (Peracetic Acid)

Guzman et al. treated human hair with peracetic acid to extract oxidative keratin [22]. The sample was later washed with water to remove oxidants. Then, the treated hair was immersed in a Tris base solution and ultrapure water for the extraction of soluble protein. According to previous studies, the disulfide linkages were irreversibly oxidized to sulfonic and sulfinic groups [22, 24]. These hydrophilic functional groups led to a homogeneous dispersion of oxidative keratin.

14.3 Biomaterial Applications

14.3.1 Sponge Scaffolds

Che-Wei Lin et al. used the freeze-drying technique to fabricate the pristine keratin sponge scaffold. The scaffold possessed interconnected pores and good biocompatibility. The optical appearance of the product is shown in Fig. 14.2 [25]. However, Yung-Hao Lin et al. indicated that the pristine keratin scaffold is too fragile for wide application in tissue engineering. Therefore, they fabricated a keratin scaffold cross-linked with chitosan via an azide functional group. The Live/Dead assay results in Fig. 14.3 showed that the scaffolds displayed excellent biocompatibility. Further cultural differentiation results showed that different ratios of keratin and chitosan would influence the osteogenic differentiation of human adipose-derived stem cells [19]. Hamasaki et al. adapted a protocol combining the particulate-leaching technique and freeze-drying method to fabricate a porous and flexible keratin sponge scaffold. The solution containing keratin and alginate beads was freeze-dried to form a sponge scaffold and then immersed in a solution containing EDTA (0.5 M) for 12 h. Then, the sponge was further immersed in DI water to remove alginate calcium beads and was treated with lyophilization technique again to form a highly interconnected porous sponge. Their result showed that the alginate beads-treated scaffold had more flexible properties compared to the pristine keratin group [26].

14.3.2 Electrospun Scaffolds

Aluigi et al. used keratin extracted from wool fibers by the reductive extraction method with urea (8 M), m-bisulfite (0.5 M), and SDS (0.05 M) to fabricate nanofibers. After the extraction, the keratin solutions were adjusted to specific concentrations. Then, poly- (ethylene oxide) (PEO) powder with a viscosity-average molecular weight of 400,000 g/mol (from Sigma–Aldrich, St. Louis, MO) was added to keratin aqueous solution to obtain the mixing solution. Then, the

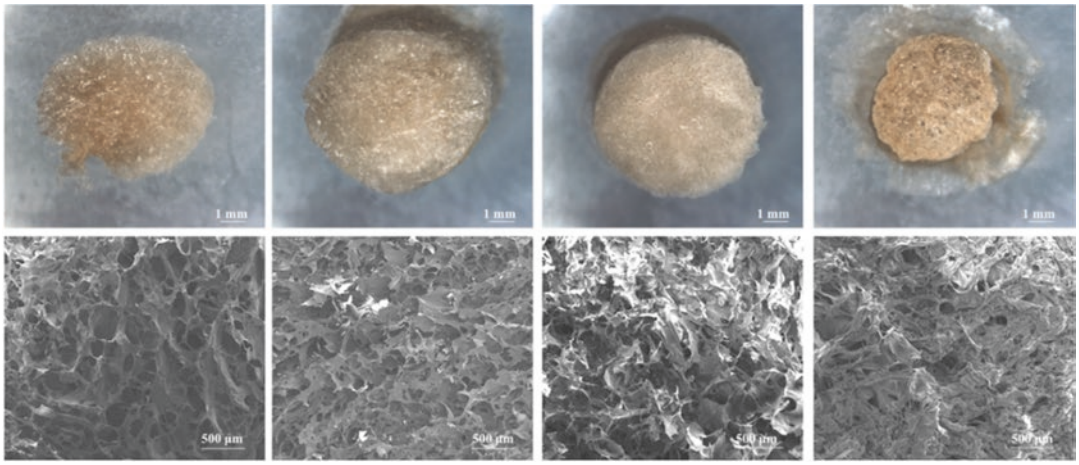

Fig. 14.2 Dissecting and electronic microscopic images of different concentration keratin scaffolds

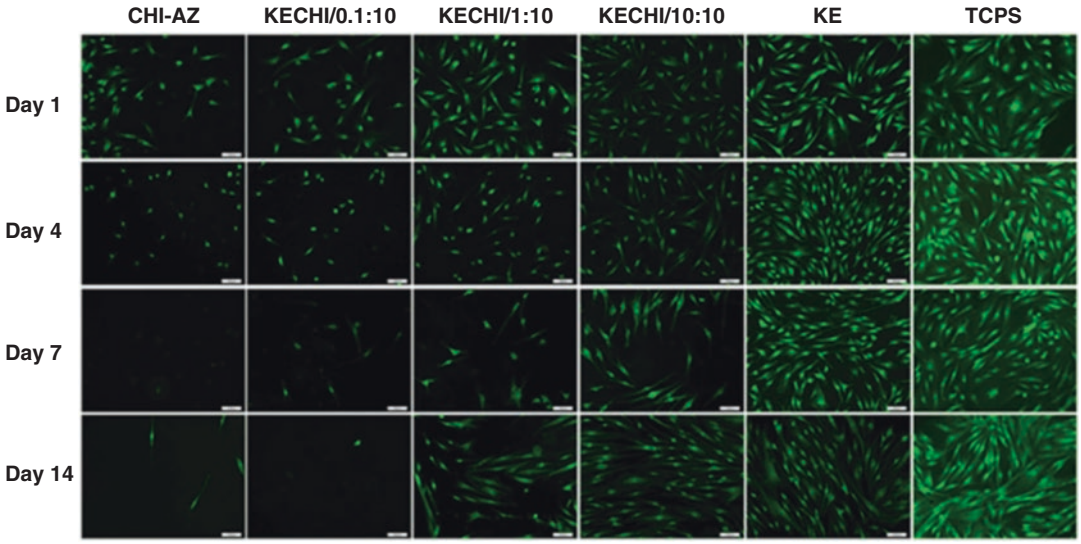

Fig. 14.3 Fluorescence image of cells using LIVE/DEAD assay on days 1, 4, 7, and 14. Live cells fluoresce bright green, whereas dead cells with compromised membranes fluoresce red. Scale = 100 mm

mixing solution was used to fabricate nanofibers with electrospinning technique. The product without defect could be obtained by varying concentrations of polymers. Utilizing the electrospinning technique, different forms of keratin application could be fabricated, including fiber-structure scaffold and planar films [27]. Edwards et al. used keratin obtained by oxidative extraction, mixing it with Poly(e-caprolactone) (PCL) dissolved in trifluoroethanol (TFE) to fabricate nanofibers. The extracted keratin powder was dissolved in DI water, and PCL was dissolved in TFE. Then, a keratin/PCL solution was prepared by mixing keratin with PCL at different ratios. The mixing solution was vortexed until reaching a homogeneous solution. The different concentration ratios of keratin to PCL resulted in variations in physicochemical properties. The nanofiber-constructed membranes showed low cytotoxicity and could be developed into medical applications [28]. Ju Wang et al. also used oxidative keratin and poly (vinyl alcohol) (PVA) to fabricate nanofibers. First, PVA was dissolved in DI water. And then, oxidative keratins were added to the PVA solution to reach different oxidative keratins/PVA mass ratio. With the electrospinning technique, the mixing solution was further turned into nanofibers constructed membrane. The membrane was implanted into animal models. The results showed that the product possessed excellent biocompatibility and biodegradability [29].

14.3.3 Hydrogels

Saul et al. used oxidative keratin extracted by peracetic acid and Tris base solution to fabricate keratose hydrogel. The extracted keratose was rehydrated in phosphate-buffered saline to obtain a 20% solution with or without ciprofloxacin-HCl. The solution was warming overnight at 37 °C to form a viscous hydrogel solution. The hydrogel showed the capability of sustained release of antibiotics and could serve as a platform for controlled drug release [30]. Similar methodologies were conducted by Guzman et al. to combine keratose and BMP-2 for Bone regeneration [23]. Other research used keratin extracted by sulfitolysis method to prepare hydrogel. Silva et al. prepared hybrid hydrogel combining alginate and keratin. The in vitro study showed enhancement of cell adhesion and proliferation, which might be able to serve as applications for tissue regeneration [31]. They claimed the hydrogels exhibit interconnected pores, which can

improve the transport of nutrients and oxygen based on the SEM analysis. Ali's group used the intrinsic property of keratin which is a cysteine-rich protein to fabricate visible light cross-linkable hydrogel. Keratin was blended with PEG-4Nor and cross-linked by the thiol-norbornene reaction. Their research showed that the hydrogel presents good biocompatibility, which can be seen from the Live/Dead assay and phalloidin/DAPI staining. The product could be used for applications in tissue engineering and bioprinting [32]. Barati et al. used tris(2-carboxyethyl) phosphine (TCEP) to extract keratin from chicken feather. The thiol groups of keratin were then further modified to allyl thioether. The modified keratin was capable of being UV cross-linked to hydrogel [33].

14.4 Conclusions and Future Perspectives

Keratin is a naturally abundant protein commonly existing in animal tissues. The huge amounts of keratinous waste from wool production and livestock slaughter industry could be processed into value-added applications. Due to the unique characteristics of disulfide bonding formation, different extraction methodologies can be implemented and can further result in various application forms including sponge scaffolds, electrospun scaffolds and hydrogels, etc. The intrinsic biological activity-related properties of keratin endow itself excellent conditions for developing medical applications such as wound dressing, surgical implants, or drug carriers. However, the weak mechanical strength after the breaking of disulfide bonds requires combining other materials or developing other cross-linking mechanisms to reinforce the structure. Keratin has great potential in bioengineering but still requires comprehensive development of protocols and more in vitro and in vivo experiments to demonstrate its versatile application in the biomedical field.

References

1. Fraser RD, MacRae TP (1985) Intermediate filament structure. Biosci Rep 5(7):573–579
2. Crewther WG, Fraser RD, Lennox FG et al (1965) The chemistry of keratins. Adv Protein Chem 20:191–346
3. Hill P, Brantley H, Van Dyke M (2010) Some properties of keratin biomaterials: kerateines. Biomaterials 31(4):585–593
4. Wang B, Yang W, McKittrick J et al (2016) Keratin: structure, mechanical properties, occurrence in biological organisms, and efforts at bioinspiration. Prog Mater Sci 76:229–318
5. Coulombe PA, Omary MB (2002) 'Hard' and 'soft' principles defining the structure, function and regulation of keratin intermediate filaments. Curr Opin Cell Biol 14(1):110–122
6. Wawersik M, Coulombe PA (2000) Forced expression of keratin 16 alters the adhesion, differentiation, and migration of mouse skin keratinocytes. Mol Biol Cell 11(10):3315–3327
7. Magin TM, Vijayaraj P, Leube RE (2007) Structural and regulatory functions of keratins. Exp Cell Res 313(10):2021–2032
8. Powell BC, Beltrame JS (1994) Characterization of a hair (Wool) keratin intermediate filament gene domain. J Invest Dermatol 102(2):171–177
9. Thibaut S, Barbarat P, Leroy F et al (2007) Human hair keratin network and curvature. Int J Dermatol 46:7–10
10. Sierpinski P, Garrett J, Ma J et al (2008) The use of keratin biomaterials derived from human hair for the promotion of rapid regeneration of peripheral nerves. Biomaterials 29(1):118–128
11. Bellis SL (2011) Advantages of RGD peptides for directing cell association with biomaterials. Biomaterials 32(18):4205–4210
12. Wu YL, Lin CW, Cheng NC et al (2017) Modulation of keratin in adhesion, proliferation, adipogenic, and osteogenic differentiation of porcine adipose-derived stem cells. J Biomed Mater Res B Appl Biomater 105(1):180–192
13. Lin CW, Yang KC, Cheng NC et al (2018) Evaluation of adhesion, proliferation, and differentiation of human adipose-derived stem cells on keratin. J Polym Res 25(2):1–14
14. Wayner EA, Kovach NL (1992) Activation-dependent recognition by hematopoietic-cells of the ldv sequence in the v-region of fibronectin. J Cell Biol 116(2):489–497
15. Sinkiewicz I, Sliwinska A, Staroszczyk H et al (2017) Alternative methods of preparation of soluble keratin from chicken feathers. Waste Biomass Valori 8(4):1043–1048
16. Yamauchi K, Yamauchi A, Kusunoki T et al (1996) Preparation of stable aqueous solution of keratins,

and physiochemical and biodegradational properties of films. J Biomed Mater Res 31(4):439–444
17. Kakkar P, Madhan B, Shanmugam G (2014) Extraction and characterization of keratin from bovine hoof: a potential material for biomedical applications. SpringerPlus 3:596
18. Nakamura A, Arimoto M, Takeuchi K et al (2002) A rapid extraction procedure of human hair proteins and identification of phosphorylated species. Biol Pharm Bull 25(5):569–572
19. Lin YH, Huang KW, Chen SY et al (2017) Keratin/chitosan UV-crosslinked composites promote the osteogenic differentiation of human adipose derived stem cells. J Mater Chem B 5(24):4614–4622
20. Gupta A, Kumar P, Bin Mohd Yunus R et al (2011) Extraction of keratin protein from chicken feather. Chemeca 2011: Engineering a Better World, Sydney Hilton Hotel, NSW, 18–21 September 2011
21. Wang K, Li R, Ma JH et al (2016) Extracting keratin from wool by using L-cysteine. Green Chem 18(2):476–481
22. de Guzman RC, Merrill MR, Richter JR et al (2011) Mechanical and biological properties of keratose biomaterials. Biomaterials 32(32):8205–8217
23. de Guzman RC, Saul JM, Ellenburg MD et al (2013) Bone regeneration with BMP-2 delivered from keratose scaffolds. Biomaterials 34(6):1644–1656
24. Alexander P, Earland C (1950) Structure of wool fibres; isolation of an alpha and beta-protein in wool. Nature 166(4218):396–397
25. Lin CW, Chen YK, Tang KC et al (2019) Keratin scaffolds with human adipose stem cells: physical and biological effects toward wound healing. J Tissue Eng Regen Med 13(6):1044–1058
26. Hamasaki S, Tachibana A, Tada D et al (2008) Fabrication of highly porous keratin sponges by freeze-drying in the presence of calcium alginate beads. Mat Sci Eng C-Bio S 28(8):1250–1254
27. Aluigi A, Varesano A, Montarsolo A et al (2007) Electrospinning of keratin/poly(ethylene oxide) blend nanofibers. J Appl Polym Sci 104(2):863–870
28. Edwards A, Jarvis D, Hopkins T et al (2015) Poly(epsilon-caprolactone)/keratin-based composite nanofibers for biomedical applications. J Biomed Mater Res B Appl Biomater 103(1):21–30
29. Wang J, Hao S, Luo T et al (2017) Keratose/poly (vinyl alcohol) blended nanofibers: fabrication and biocompatibility assessment. Mater Sci Eng C Mater Biol Appl 72:212–219
30. Saul JM, Ellenburg MD, de Guzman RC et al (2011) Keratin hydrogels support the sustained release of bioactive ciprofloxacin. J Biomed Mater Res A 98(4):544–553
31. Silva R, Singh R, Sarker B et al (2014) Hybrid hydrogels based on keratin and alginate for tissue engineering. J Mater Chem B 2(33):5441–5451
32. Yue K, Liu YH, Byambaa B et al (2018) Visible light crosslinkable human hair keratin hydrogels. Bioeng Transl Med 3(1):37–48
33. Barati D, Kader S, Shariati SRP et al (2017) Synthesis and characterization of photo-crosslinkable keratin hydrogels for stem cell encapsulation. Biomacromolecules 18(2):398–412

Correction to: Silk Fibroin Bioinks for Digital Light Processing (DLP) 3D Bioprinting

Soon Hee Kim, Do Yeon Kim, Tae Hyeon Lim, and Chan Hum Park

Correction to:
Chapter 4 in: H. J. Chun et al. (eds.), *Bioinspired Biomaterials*, Advances in Experimental Medicine and Biology 1249, https://doi.org/10.1007/978-981-15-3258-0_4

An earlier version of the chapter was published with an incorrect Acknowledgements text which was corrected as follows:

This work was supported by the National Research Foundation of Korea (NRF) grant funded by the Korea government (MSIP) (grant No.: 2016R1E1A1A01942120), Republic of Korea and by the Hallym University Research Fund.

The updated version of this chapter can be found at https://doi.org/10.1007/978-981-15-3258-0_4

H. J. Chun et al. (eds.), *Bioinspired Biomaterials*, Advances in Experimental Medicine and Biology 1249 , https://doi.org/10.1007/978-981-15-3258-0_15